ACTA TECHNICA

ACADEMIAE SCIENTIARUM HUNGARICAE

REDIGIT: M. MAJOR

TOMUS 86
FASCICULI 1–2

AKADÉMIAI KIADÓ, BUDAPEST 1978

ACTA TECHNICA

Az *Acta Technica* angol, francia, német és orosz nyelven közöl értekezéseket a műszak tudományok köréből.

Az *Acta Technica* változó terjedelmű füzetekben jelenik meg, több füzet alkot egy kötetet.

A közlésre szánt kéziratok a következő címre küldendők:

Acta Technica
1051 Budapest, Münnich Ferenc u. 7.

Ugyanerre a címre küldendő minden szerkesztőségi és kiadóhivatali levelezés.

Megrendelhető a belföld számára az „Akadémiai Kiadó"-nál (1363 Budapest Pf. 24. Bankszámla 215 11448), a külföld számára pedig a „Kultura" Külkereskedelmi Vállalatnál (1389 Budapest 62, P. O. B. 149 Bankszámla: 218-10990) vagy annak külföldi képviseleteinél és bizományosainál.

Die *Acta Technica* veröffentlichen Abhandlungen aus dem Bereiche der technischen Wissenschaften in deutscher, englischer, französischer und russischer Sprache.

Die *Acta Technica* erscheinen in Heften wechselnden Umfanges. Vier Hefte bilden einen Band.

Die zur Veröffentlichung bestimmten Manuskripte sind an folgende Adresse zu senden:

Acta Technica
H-1051 Budapest,
Münnich Ferenc u. 7.
Ungarn

An die gleiche Anschrift ist auch jede für die Schriftleitung und den Verlag bestimmte Korrespondenz zu richten.

Abonnementspreis pro Band: $ 36.00.

Bestellbar bei »Kultura« Außenhandelsunternehmen (H-1389 Budapest 62, P. O. B. 149, Bankkonto Nr. 218-10990) oder seinen Auslandsvertretungen.

ACTA TECHNICA

TOMUS 86

INDEX

ACTA TECHNICA

ACADEMIAE SCIENTIARUM HUNGARICAE

REDIGIT: M. MAJOR

TOMUS 86

AKADÉMIAI KIADÓ, BUDAPEST 1978

E. BÖLCSKEI

1917—1977

Das ungarische wissenschaftliche Leben erlitt einen unersetzbaren Verlust: Elemér BÖLCSKEI, korrespondierendes Mitglied der Ungarischen Akademie der Wissenschaften, leitender Professor des Lehrstuhls für Stahlbetonkonstruktionen der Technischen Universität zu Budapest, Konstrukteur großzügiger Bauwerke, verschied am 16. Juni 1977.

Elemér BÖLCSKEI wurde am 17. November 1917 in Pestszentlőrinc geboren. Die Mittelschulstudien absolvierte er in Budapest, und ließ sich nach deren Beendigung an der Fakultät für Ingenieure der Technischen Universität inskribieren, wo er 1940 das Ingenieursdiplom erwarb.

Noch vor Beendigung seiner Studien an der Universität, hat er im Konstruktionsbüro des Dr.-Ing. István MENYHÁRD eine Stellung angenommen, die er acht Jahre hindurch bekleidete. Während dieser Zeit hatte er reichlich Gelegenheit das hervorragende Wissen seines Meisters kennenzulernen und sich anzueignen. Die hier verbrachte Zeit erwies sich als richtunggebend für seine Tätigkeit und drückte ihren Stempel seinem Lebenswerk auf.

Im Jahre 1947 eröffnete er ein eigenes Konstruktionsbüro, trat aber bereits 1948 in das Institut für Bauwissenschaft und Bauentwurf ein. Gelegent-

lich der Umorganisation dieses Instituts wurde er in das Konstruktionsbüro ÁMTI versetzt und nach dessen Umorganisation wurde er dem Konstruktionsbüro MÉLYÉPTERV, dann dem Konstruktionsbüro UVATERV zugeteilt, wo er Leiter der Abteilung für Brückenbau wurde.

Das Jahr 1955 bedeutete einen wichtigen Wendepunkt im Leben BÖLCSKEIS. Zu dieser Zeit wurde er zum Dozenten am II. Lehrstuhl für Brückenbau der Technischen Universität ernannt. Hier bot sich ihm reichlich Gelegenheit seine als Konstrukteur gesammelten, wertvollen Erfahrungen auf dem Gebiet des Unterrichtes an der Universität zu verwerten. 1956 erwarb er den wissenschaftlichen Grad eines Kandidaten, 1960 den eines Doktors der technischen Wissenschaften.

Im Jahre 1961 wurde er in die Abteilung für Hochschulwesen des Ministeriums für Unterrichtswesen versetzt und noch im selben Jahr zum Professor am II. Lehrstuhl für Brückenbau der Technischen Universität ernannt. Seit 1963 übte er als Leiter des Lehrstuhls für Stahlbetonkonstruktionen wertvolle Lehrtätigkeit aus.

Seine wissenschaftliche Tätigkeit war mannigfaltig. Zahlreiche seiner Abhandlungen befassen sich mit den Problemen des Brückenbaues. Er studierte sehr eingehend und in einer neuen Betrachtungsweise das Problem der Knickung des druckbeanspruchten Stabes. Mehrere Studien widmete er der Anwendung von Schalenkonstruktionen als Fundamente, dem rheologischen Verhalten fester Körper und der Ausgestaltung neuartiger Schalenformen. Besonders hervorzuheben ist sein — mit Mitverfassern geschriebenes — aus fünf Bänden bestehendes, das ganze Gebiet der Stahlbetonkonstruktionen umfassendes Werk „*Vasbetonszerkezetek*" (Stahlbetonkonstruktionen), das nicht nur als Lehrbuch, sondern auch als Fachbuch ein wertvolles Produkt der ungarischen technischen Literatur darstellt.

Die hervorragendsten Ergebnisse seiner wissenschaftlichen Tätigkeit sind die Bestimmung der die Formänderung der Membranschalen beschreibenden partiellen Differentialgleichung zweiter Ordnung und die Behandlung der allgemeinen Schalentheorie mit rechtwinkligen Koordinaten. Diese Arbeiten haben auch internationales Interesse erweckt.

In Anerkennung seiner wertvollen wissenschaftlichen Tätigkeit hat die Ungarische Akademie der Wissenschaften Elemér BÖLCSKEI 1967 zum korrespondierenden Mitglied gewählt.

Außer seiner wissenschaftlichen Betätigung leistete er auch als Konstrukteur vielseitige Arbeit. Er beteiligte sich am Bau mehrerer Brücken in Ungarn und führte auch neuartige konstruktive Lösungen ein. Er entwarf die erste Brücke mit V-Füßen in Ungarn, sowie die erste Spannbetonbrücke. Nach seinen Plänen wurde die größte Stahlbetonbrücke Ungarns, die Talbrücke bei Varasd mit einer Spannweite von nahezu 100 m erbaut. Eine seiner bemerkenswerten Schöpfungen ist die aus vorgefertigten Elementen erbaute fünffeldige

Stahlbetonbalkenbrücke am Bolond út. Er entwarf auch die erste aus Aluminium erbaute Leichtmetallbrücke Europas, bei Szabadszállás.

Auch am öffentlichen Leben beteiligte sich Elemér BÖLCSKEI lebhaft. Er bekleidete in zahlreichen wissenschaftlichen Körperschaften verschiedene Ämter. So war er Mitglied des Wissenschaftlichen Rates des Volksbildungsministeriums, des Ausschusses für Bauwissenschaft und Verkehr, der wissenschaftlichen Qualifizierungskommission der Ungarischen Akademie der Wissenschaften, des Ausschusses für Technische Mechanik, der Fachkommission für Statik und Bemessung des Standardisierungsamtes, sowie des Unterausschusses für das Bauingenieurfach der Justizkommission. Er war auch Redaktionsmitglied zweier Zeitschriften der Abteilung der Technischen Wissenschaften der Ungarischen Akademie der Wissenschaften, namentlich der Zeitschrift „Műszaki Tudomány" (Technische Wissenschaft) und „Acta Technica". Er war auch Mitglied des ungarischen Nationalkomitees des Ass. Int. des Ponts et Charpentes.

Auch an der Ausarbeitung der ungarischen Normen nahm er regen Anteil. Unter seiner Leitung wurden die Grundsätze der auf der Halbwahrscheinlichkeit beruhenden Bemessung, die Normen für den Entwurf von Tragkonstruktionen der Bauwerke und die Richtlinien zur Untersuchung der mit Bauxitbeton ausgeführten Bauwerke ausgearbeitet.

In Anerkennung seiner Tätigkeit hat ihm die Regierung die Titel Arbeitsaktivist, Bestarbeiter, Bestarbeiter des Verkehrswesens, Bestarbeiter des Unterrichtswesens, Bestarbeiter des Bauwesens verliehen.

Leider litt er Jahre hindurch an einer schweren Krankheit. Mit unglaublicher Willenskraft kämpfte er gegen die tückische Krankheit an und arbeitete bis zum letzten Moment seines Lebens. Doch erwiesen sich sein heldenhafter Kampf, alle Versuche der medizinischen Wissenschaften, die sorgenvolle Liebe seiner Familie und Verehrer als nutzlos. Die Krankheit war stärker, er mußte seinen Posten verlassen, auf dem er bis zur letzten Minute ausharrte und auch noch auf seinem Sterbelager den Ingenieurswissenschaften zu dienen bemüht war.

Elemér BÖLCSKEI hat uns für immer verlassen, doch wird das vornehme Beispiel seines kampfreichen Lebens in unserer Erinnerung fortleben und sein Andenken werden Generationen lang seine, mächtige Öffnungen überspannenden, kühnen Brücken und seine hochragenden, schlanken Funktürme bewahren.

P. Csonka

Wissenschaftliche Tätigkeit des Prof. Dr. E. Bölcskei

1. Olaszország útügye a világháború után. (Straßenverhältnisse Italiens nach dem Weltkrieg.) *Technika*, (1940) 146—147
2. A szabadszállási alumíniumhíd. (Die Aluminiumbrücke in Szabadszállás.) *Mélyépítéstudományi Szemle*, **1** (1951) 202—208

3. „V"-lábú szerkezetek. (Konstruktionen mit V-Füßen.) *Mélyépítéstudományi Szemle*, **1** (1951) 342—347
4. Hozzászólás HAVIÁR Győző: „A szabadszállási alumíniumhíd építésénél szerzett tapasztalatok" c. előadásához. (Beitrag zum Vortrag von Győző HAVIÁR: „Beim Bau der Aluminiumbrücke in Szabadszállás gesammelte Erfahrungen".) *MTA VI. Oszt. Közl.* **6** (Veröffentlichungen der 6. Sekt. der Ung. Akad. d. Wiss.) (1953) 279—280
5. Aljuminijevüj most v Szabadszállás. *Acta Techn. Hung.* **5** (1952) 163—182 (Mitverfasser: Gy. HAVIÁR.)
6. Poutres sur pieds en „V". *Acta Techn. Hung.* **4** (1952) 155—168
7. Vastartóval együttdolgozó vasbeton lemezszerkezetek. (Mit Stahlträgern zusammenwirkende Stahlbeton-Plattenkonstruktionen.) *Magyar Építőipar* **1** (1952) 285—288
8. Előrefeszített vasbetonpallós hídszerkezetek. (Brückenkonstruktionen mit vorgespannten Stahlbetonbohlen.) *Mélyépítéstudományi Szemle* **2** (1952) 456—462 (Mitverfasser: A. PETUR)
9. Nagyszilárdságú acélkábel vonórúd. (Zugstab aus hochwertigem Stahlkabel.) *Mélyépítéstudományi Szemle* **2** (1952) 527—531
10. Előrefeszített betonhidak. (Spannbetonbrücken.) *Mérnöki Továbbképző Intézet* (Fortbildungsinstitut für Ingenieure) M. 28, Budapest 1952
11. Előregyártott vasbeton hídszerkezetek. (Vorgefertigte Stahlbeton-Brückenkonstruktionen.) *Mérnöki Továbbképző Intézet* (Fortbildungsinstitut für Ingenieure) M. 28 I—IV. Budapest 1952
12. Deformation des voiles minces. *Acta Techn. Hung.* **5** (1952) 489—506
13. Előregyártott vasbeton hídszerkezetek. (Vorgefertigte Stahlbeton-Brückenkonstruktionen.) *Mélyépítéstudományi Szemle* **3** (1953) 69—77
14. Membránhéjak alakváltozása. (Formänderung der Membranschalen.) *Magyar Építőipar* **2** (1953) 93—100
15. Két pontra felfüggesztett egyenes tengelyű rúd stabilitása. (Stabilität des auf zwei Punkten aufgehängten geradachsigen Stabes.) *Mélyépítéstudományi Szemle* **3** (1953) 433—437
16. Ferdelábú kerethidak. (Rahmenbrücken mit schrägen Stielen.) *Mélyépítéstudományi Szemle* **3** (1953) 488—491
17. Előrefeszített hídszerkezetek. (Spannbeton-Brückenkonstruktionen.) Kapitel im Buch „Spannbetonkonstruktionen" von Imre BÖRÖCZ. Közlekedési Kiadó, Budapest 1953, II. Band 5—28
18. Legnagyobb hazai ívhídunk tervezése. (Entwurf unserer größten Bogenbrücke.) *Mélyépítéstudományi Szemle* **4** (1954) 119—130
19. Die Stabilität des an zwei Punkten aufgehängten Balkens. *Acta Techn. Hung.* **8** (1954) 243—256
20. Teherhordó szerkezetek tervezésére vonatkozó előírások alapelveiről. (Über die Grundsätze der den Entwurf von Tragkonstruktionen betreffenden Vorschriften.) *Mélyépítéstudományi Szemle* **4** (1954) 443—453
21. A Keleti Főcsatorna közúti hídjai. (Die Straßenbrücken des östlichen Hauptkanals.) *Közlekedési Építő* **4** (1954) 172, 189—190
22. An Aluminium Bridge in Hungary. *Light-Metals* (1955) 106—110 (Mitverfasser: Gy. HAVIÁR)
23. Aluminiumbrücke in Szabadszállás (Ungarn). *Bauplanung-Bautechnik* **9** (1955) 191—197
24. Hozzászólás GARAI Tamás: „Statikai fogalmak egységes megnevezéséről és meghatározásáról" c. cikkhez. (Beitrag zur Abhandlung „Über die einheitliche Benennung und Bestimmung statischer Begriffe" von Tamás GARAI.) *Mélyépítéstudományi Szemle* **5** (1955) 313—314
25. Rugalmas anyagú nyomott rúd határteherbírása. (Grenztragfähigkeit des Druckstabes aus elastischem Stoff.) *Mélyépítéstudományi Szemle* **5** (1955) 365—369
26. A nyomott rúd határteherbírása. (Grenztragfähigkeit des Druckstabes.) *Magyar Építőipar* **4** (1955) 432—436
27. A nyomott rúd határteherbírásának kiszámításáról. (Über die Berechnung der Grenztragfähigkeit des Druckstabes.) *MTA VI. Oszt. Közl.* **19** (Veröffentlichungen der VI. Sekt. der Ung. Akad. der Wiss.) (1956) 177—188
28. Külpontosan nyomott négyszög keresztmetszetű farúd határteherbírásának kiszámítása. (Berechnung der Grenztragfähigkeit ausmittig gedrückten Holzstabes mit Rechteckquerschnitt.) *Műszaki Közlemények MÉLYÉPTERV* No. 5 (1955) 3—19
29. A nyomott rúd határteherbírásának kiszámításáról. (Über die Berechnung der Grenztragfähigkeit des gedrückten Stabes.) Vortrag gehalten am Bauwissenschaftlichen Kongress der Ungarischen Akademie der Wissenschaften, am 1. Oktober 1955.

30. A nyomott rúd teherbírása. (Tragfähigkeit des gedrückten Stabes.) *UVATERV Műszaki Fejlesztés* (1955) S. 26
31. Limit Load Capacity of the Compression Bar. *Acta Techn. Hung.* **15** (1956) 19—36
32. Limit Design of Compressed Bars. *Acta Techn. Hung.* **14** (1956) 377—400
33. V-shaped Frames for Supporting Bridges. *Concrete and Constructional Engineering* **60** (1956) 463—469
34. High-tensile Steel Cable Tie-rods. *Építőipari és Közlekedési Műszaki Egyetem Közleményei* (Veröffentlichungen der Technischen Universität für Bauwesen und Verkehr) 1957, 23—29
35. The Limit Load Carrying Capacity of Compression Bar Made of Perfectly Plastic Materials. *Acta Techn. Hung.* **17** (1957) 3—24
36. Újszerű hídfők. (Neuartige Brückenköpfe.) *Mélyépítéstudományi Szemle* **7** (1957) 355—359
37. New-type Abutments of Bridges. *Acta Techn. Hung.* **22** (1958) 135—148
38. A bauxitbeton építményeiről. (Über die Bauwerke aus Bauxitbeton.) *Magyar Építőipar* **7** (1958) (Mitverfasser: K. Szalai)
39. Alapozási héjszerkezetek. (Fundierung mit Schalenkonstruktionen.) *Mélyépítéstudományi Szemle* **9** (1959) 72—73
40. Alapozási héjszerkezetek. (Fundierung mit Schalenkonstruktionen.) *Műszaki Élet*, 1959
41. Hajlított héjak általános elmélete. (Allgemeine Theorie der Biegeschalen.) *Magyar Építőipar* **8** (1959) 494—504
42. Nouveaux types de culées de ponts. *Béton Armé* No. 20 (1959) 33—38
43. Vasbetonhidak. (Stahlbetonbrücken.) Műszaki Kiadó, Budapest 1959. (Mitverfasser: Cs. Láng-Miticzky)
44. Vasbeton Hídszerkezetek. (Stahlbeton-Brückenkonstruktionen.) Kapitel im III. Band des Taschenbuches für Ingenieure. Műszaki Könyvkiadó, Budapest 1959, 1123—1172
45. Application of Shell Structures for Foundations. *Acta Techn. Hung.* **28** (1960) 199—208
46. Tartószerkezetek. (Tragkonstruktionen.) Rezension und Kritik des Werkes des Prof. J. Pelikán. *Felsőoktatási Szemle* **9** (1960) 502—504
47. Kissüllyedésű alapok. (Fundamente mit geringer Setzung.) *Mélyépítéstudományi Szemle* **10** (1960) 166—171 (Mitverfasser: J. Domján)
48. Hajlított héjak általános elmélete. (Allgemeine Theorie gekrümmter Schalen.) *Magyar Építőipar* **9** (1960) 511—514
49. Vasbetonszerkezetek elmélete, méretezése és szerkezeti kialakítása. (Theorie, Bemessung und konstruktive Ausgestaltung von Stahlbetonkonstruktionen.) Rezension und Kritik des Werkes von T. Gyengő und I. Menyhárd) *Mélyépítéstudományi Szemle* **10** (1960) 527—528
50. Allgemeine Theorie der gekrümmten Schalen. *Acta Techn. Hung.* **31** (1960) 391—428
51. Theorie der allgemein gekrümmten Schalen. *IVBH.* 1960, 19—42
52. Csonkakúp héjalapok tervezése. (Entwurf kegelstumpfförmiger Fundamente.) *ÉTI Tudományos Közlemények* **22** (Veröffentlichungen des Instituts für Bauwissenschaften) (Mitverfasser: T. Brajannis—S. Kaliszki)
53. Foundations with Small Settlement. *Acta Techn. Hung.* **33** (1961) 179—194 (Mitverfasser: J. Domján)
54. Lapos héjak elmélete és gyakorlati alkalmazása. (Theorie und praktische Anwendung flacher Schalen.) *ÉKME Tudományos Közleményei* **6** (ÉKME Wissenschaftliche Veröffentlichungen) 1960
55. Szilárdtestek alapvető reológiai tulajdonságairól. (Über die grundlegenden rheologischen Eigenschaften der Festkörper.) *Építés- és Építéstudományi Közlemények* **5** (1961) 3—27.
56. Über die grundlegenden rheologischen Eigenschaften der Festkörper. *Acta Techn. Hung.* **34** (1961) 369—401
57. Alumíniumszerkezetek. (Aluminiumkonstruktionen.) Műszaki Kiadó, Budapest 1962. (Mitverfasser: Z. Buray, Ö. Csellár, A. Domony)
58. Statical Problems of Compression Members. *ÉKME Tudományos Közlemények* **9** (ÉKME Wissenschaftliche Veröffentlichungen), 1963, 291—310
59. Ágas tartók. (Gabelträger.) *Mélyépítéstudományi Szemle* **13** (1963) 16—21
60. A nyomott rúd statikai kérdései. (Die statischen Probleme des druckbeanspruchten Stabes.) *MTA VI. Oszt. Közl.* **34** (Veröffentlichungen der VI. Sekt. der Ung. Akad. der Wiss.) 107—125
61. Térbeli ágas tartók. (Räumliche Gabelträger.) *Mélyépítéstudományi Szemle* **13** (1963) 489—491
62. Stavebné Konstrukcie z hlinika SVTL. Bratislava, 1963, 260 Seiten (Mitverfasser: Z. Buray—Ö. Csellár—A. Domony)

63. Vasbetonépítéstan. Feszített betonszerkezetek. (Stahlbetonbaulehre. Spannbetonkonstruktionen.) Kollegheft. Tankönyvkiadó, Budapest 1963 (Mitverfasser: G. TASSI)
64. Vasbetonépítéstan. Feszített tartók számítása. (Stahlbetonbaulehre. Berechnung vorgespannter Träger.) Kollegheft. Tankönyvkiadó, Budapest 1964, 120 Seiten (Mitverfasser: G. TASSI und T. KLATSMÁNYI)
65. Szerkezettervezés. (Konstruktionsentwurf.) Kollegheft 1965. (Mitverfasser: B. JUHÁSZ)
66. Epoxi-Beton. *Mélyépítéstudományi Szemle* **15** (1965) 277—288 (Mitverfasser: T. KLATSMÁNYI)
67. Vasbetonépítéstan. Hídszerkezetek számítása. (Stahlbetonbaulehre. Berechnung von Brückenkonstruktionen.) Kollegheft. Tankönyvkiadó (Mitverfasser: L. SZERÉMI und T. KLATSMÁNYI)
68. Vasbetonszerkezetek. I. Lemezes szerkezetek, bunkerek, silók. (Stahlbetonkonstruktionen. I. Plattenkonstruktionen, Bunker, Silos.) Kollegheft. Tankönyvkiadó, Budapest 1965. (Mitverfasser: Á. OROSZ)
69. Vasbetonépítéstan. Általános hídépítéstan. Vasbeton hidak. (Stahlbetonbaulehre. Allgemeiner Brückenbau, Stahlbetonbrücken.) Kollegheft. Tankönyvkiadó, Budapest 1964
70. Vasbetonszerkezetek. II. Héjszerkezetek elmélete. (Stahlbetonkonstruktionen. II. Schalenkonstruktionen.) Kollegheft. Tankönyvkiadó, Budapest 1966. (Mitverfasser: Á. OROSZ)
71. Hídépítéstan. I. rész. (Brückenbaulehre I. Teil.) Kollegheft. Tankönyvkiadó, Budapest 1966. (Mitverfasser: T. KLATSMÁNYI)
72. A vasbetonépítés újabb eredményei. (Neuere Ergebnisse des Stahlbetonbaues.) *Magyar Építőipar* **15** (1966) 365—372 (MTI Vortrag)
73. A bauxitcementről és a bauxitbetonról általában. (Über Bauxitzement und Bauxitbeton im allgemeinen.) Fortbildungsinstitut für Ingenieure, Vortrag und Publikation 1966, 26 Seiten
74. Vasbeton adótornyok. (Stahlbeton-Sendetürme.) Fortbildungsinstitut für Ingenieure, Vortrag und Publikation 1966, 28 Seiten
75. Aluminium poradnik. Rozdzial O, Obliczenia na naprezenia graniczne (przyklady) Műszaki Kiadó, Budapest 1967, 917—924
76. Vasbetonszerkezetek oktatása az Építőmérnöki Karon. (Unterricht der Stahlbetonkonstruktionen an der Fakultät für Bauingenieure.) *Magyar Építőipar* **16** (1967) 506—510
77. Bauxitbeton építményekről. (Über Bauxitbetonbauwerke.) *Építés- és Közlekedéstudományi Közlemények* **11** (1967) 3—17
78. Hídépítéstan II. rész. (Brückenbaulehre II. Teil.) Kollegheft. Tankönyvkiadó, Budapest 1967, 310 Seiten (Mitverfasser: F. SZÉPE—T. KLATSMÁNYI)
79. Vasbetonszerkezetek. III. Folyadéktartályok. Különleges vasbetonszerkezetek. (Stahlbetonkonstruktionen III. Flüssigkeitsbehälter. Besondere Stahlbetonkonstruktionen.) Kollegheft. Tankönyvkiadó, Budapest 1967, 128 Seiten (Mitverfasser: Á. OROSZ)
80. V. tervek. Kiegészítés a Vasbetonépítéstan, Hídszerkezetek számítása c. egyetemi jegyzethez. (V. Pläne. Ergänzung zum Kapitel Berechnung der Brückenkonstruktionen des Kollegheftes Stahlbetonbaulehre.) (Mitverfasser: L. SZERÉMI und T. KLATSMÁNYI)
81. A szovjet tudomány főbb eredményei a mérnöki szerkezettan területén. (Die wichtigsten Ergebnisse der sowjetischen Wissenschaft auf dem Gebiet der Konstruktionslehre.) *MTA VI. Oszt. Közl.* (Veröffentlichungen der VI. Sekt. der Ung. Akad. d. Wiss.) **39** (1967) 41—49 (Mitverfasser: P. CSONKA)
82. Méretezés határfeszültségekre. (Bemessung auf Grenzspannungen.) 20. Kapitel des Aluminium Handbuches. Műszaki Kiadó, Budapest 1967, 717—742 Seiten (Chefredakteur: Á. DOMONY)
83. Beton-, Vasbeton- és Feszítettbeton Hidak. (Beton-, Stahlbeton- und Spannbetonbrükken.) Tankönyvkiadó, Budapest 1968, 442 Seiten
84. A magasépítési vasbetonszabályzat új előírásai. (Die neuen Vorschriften der Baunormen für Stahlbetonhochbauten.) *Magyar Építőipar* **17** (1968) 461—467
85. Bauxitbetonépítmények teherbírási tartaléka. I. rész. (Tragfähigkeitsreserve der Bauxitbetonbauten I. Teil.) *Magyar Építőipar* **18** (1969) 465—486 (Mitverfasser: K. SZALAI)
86. Bauxitbeton építmények teherbírási tartaléka II. rész. (Tragfähigkeitsreserve der Bauxitbetonbauten II. Teil.) *Magyar Építőipar* **18** (1969) 635—638
87. Prirucka o Hliniku, 20 Hlinik v doprave c. fejezete. (20. Hlinik v doprave betitteltes Kapitel des Werkes Prirucka o hliniku.) Műszaki Könyvkiadó, Budapest 1969 (Mitverfasser: A. DOMONY)
88. Vasbetonszerkezetek. Feszített tartók. (Stahlbetonkonstruktionen. Spannbeton Träger.) Tankönyvkiadó, Budapest 1970, 308 Seiten (Mitverfasser: G. TASSI)

89. A héjszerkezetek hazai fejlődése. (Entwicklung der Schalenkonstruktionen in Ungarn.) *Magyar Építőipar* **15** (1970) 157—266
90. A gombaszerkezetek a szabályzati előírások tükrében. (Die Pilzkonstruktionen in den Vorschriften der Bauordnung.) *Magyar Építőipar* **19** (1970) 130—318
91. Építményeink biztonsága. (Sicherheit unserer Bauwerke.) *Műszaki Tudomány* **41** (1969) 167—184
92. Dr. Menyhárd István, 1902—1969. (Dr. István Menyhárd, 1902—1969.) *Magyar Építőipar* **18** (1969) 565
93. Építmények teherhordó szerkezeteinek tervezésére vonatkozó szabványsorozat. (Die Planung der Tragkonstruktionen der Bauwerke betreffende Normen.)
94. Menyhárd István élete és munkássága. (István Menyhárds Leben und Werken.) *Műszaki Tudomány* **43** (1970) 35—46
95. Reinforced Concrete Flat Slabs as Reflected by the Various Specifications. *Acta Techn. Hung.* **68** (1970) 265—282
96. Vasbetonszerkezetek nyírási teherbírása. (Schubtragfähigkeit der Stahlbetonkonstruktionen.) *Magyar Építőipar* **19** (1970) 449—458 (Mitverfasser: T. KÁRMÁN)
97. Az Építmények biztonsága; az MSzH Épületek és építmények teherhordó szerkezetei I—II. könyv egy fejezete. (Das Kapitel „Sicherheit der Bauwerke" im Buch I—II. „Tragkonstruktionen der Gebäude und Bauwerke" des Ungarischen Standardisierungsamtes.) Közgazdasági és Jogi Könyvkiadó, Budapest 1970, II. 2067—2085
98. Feszítő huzalok szilárdsági tulajdonságai. (Festigkeitseigenschaften der Spanndrähte.) *Mélyépítéstudományi Szemle* **21** (1971) 145—154 (Mitverfasser: E. MISTÉTH)
99. Vasbetonszerkezetek. Faltartók, Lemezek, Tárolók. (Stahlbetonkonstruktionen. Wandartige träger, Platten, Speicher.) Tankönyvkiadó, Budapest 1972, 336 Seiten (Mitverfasser: Á. OROSZ)
100. A szerkezeti tervezés új szabványelőírásai. (Die neuen Normvorschriften der Konstruktionsplanung.) *Magyar Építőipar* **22** (1973) 65—68
101. Az építmények szerkezeti tervezésének új szabványelőírásai. (Neue Normvorschriften der Konstruktionsplanung von Bauwerken.) *Szabványosítás* **25** (1973) 67—71
102. Designing on the Basis of the Theory of Probability. *Acta Techn. Hung.* **74** (1973) 9—20 (Mitverfasser: E. MISTÉTH)
103. Vasbetonszerkezetek. Héjak. (Stahlbetonkonstruktionen. Schalen.) Tankönyvkiadó, Budapest 1973, 476 Seiten (Mitverfasser: Á. OROSZ)
104. Statikusok Könyve. (Buch für Statiker.) Műszaki Kiadó, Budapest 1974, 610 Seiten (Mitverfasser: E. DULÁCSKA)
105. Forgásfelület alakú membránhéjak alakváltozása. (Formänderung der Rotationsschalen.) *BME Építőanyagok Tanszék Tudományos Közleményei* (Wissenschaftliche Veröffentlichungen des Lehrstuhls für Baustoffe der Technischen Universität in Budapest) Budapest 1975, 7—24
106. Fejnélküli gombafödém. (Pilzdecke ohne Säulenkopf.) *Magyar Építőipar* **23** (1974) 697—701 (Mitverfasser L. SZERÉMI)
107. Redőzött kúphéj. (Gefaltete Kegelschale.) *Mélyépítéstudományi Szemle* **25** (1975) 19—21
108. Membránhéjak hengerkoordinátákban. (Membranschalen in Zylinderkoordinaten.) *Magyar Építőipar* **24** (1975) 385—390
109. Deformation of Membrane Shells of Revolution. *Acta Techn. Hung.* **81** (1975) 3—15
110. Corrugated Conical Shells. *Acta Techn. Hung.* **82** (1976) 1—7
111. Membrane Shells Written in Cylindrical Coordinates. *Acta Techn. Hung.* **82** (1976) 233—244
112. Csuklya alakú héjak (Haubenschalen). *Műszaki Tudomány* **52** (1976) 371—381
113. Haubenschalen. *Acta Techn. Hung.* **84** (1977) 195—205

Acta Technica Academiae Scientiarum Hungaricae, Tomus 86 (1—2), pp. 9—41 (1978)

NONLINEAR STABILITY ANALYSIS OF PSEUDO-CYLINDRICAL SHELLS

R. H. KNAPP*

and

R. SZILÁRD**

[Manuscript received March 30, 1977]

An unconventional geometric configuration is introduced for cylindrical shells. The cylindrical surface has been replaced by an assemblage of flat polyhedral elements. Buckling characteristics of the so-obtained *Pseudo-Cylindrical Concave Polyhedral* (PCCP) shell, subjected to external pressure, is analyzed by means of a finite element approach. To verify the computer results a small scale model test has been carried out. These two independent investigations show excellent agreement. Comparison with the buckling pressure of a "true" cylindrical shell indicates that the proposed modification of the geometrical configuration results in considerably higher buckling resistance. In addition, such a pseudo-cylindrical shell exhibits other desirable structural qualities such as relative ease in fabrication and high insensitivity to initial imperfections. Consequently, it can advantageously be used for various undersea structures.

1. Introduction

Early investigations into the buckling characteristics of axially loaded cylinders have revealed considerable discrepancies between analytical and experimental results [1, 2, 3]. That is, cylindrical shells buckle under approximately one third of the external pressure predicted by the classical linear theory. The reason for this discrepancy is manifold. First, since the flexural rigidity of the cylindrical shell is merely a fraction of its extensional rigidity, even small deviations from the exact cylindrical surface creates intolerably large bending moments. Consequently, the shell seeks a lower strain-energy configuration which involves bending of the middle surface. Thus, the principal cause of the above-mentioned disagreement appears to be small accidental deviations from the perfect cylindrical shape which are almost inevitable in any fabrication procedure. Furthermore, the above-mentioned large discrepancies between analytical and experimental results were partially due to the neglect of the nonlinear terms in the analytical approach. That is, after initial buckling has occurred, inward deflections become large, i.e., not negligible when compared with the initial dimensions of the shell.

* Ronald H. Knapp, Ph.D. Assistant Professor of Mechanical Engineering, University of Hawaii, Honolulu, Hawaii, U.S.A.

** Rudolph Szilárd, Dr.-Ing. Professor of Civil Engineering. Adjunct Professor of Ocean Engineering, University of Hawaii, Honolulu, Hawaii, U.S.A.

Experimental investigations have further revealed that, after initial buckling has occurred, the shell quickly assumes another more stable equilibrium configuration characterized by a polyhedral surface (Fig. 1b). Taking an analytical approach based on the Rayleigh—Ritz energy method, von KÁRMÁN and TSIEN have shown that the small-deflection theory is inadequate to predict the critical load of axially compressed cylindrical shells [4]. Using nonlinear stress-stain relationships, they could verify the experimental results. Their landmark analysis of the postbuckling behavior of cylindrical shells has

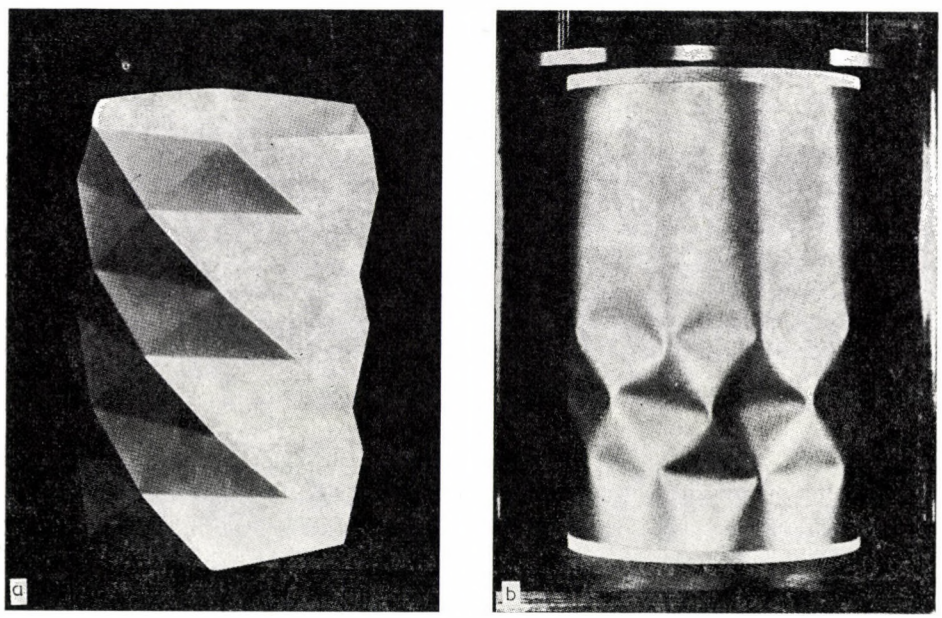

Fig. 1. a) Ideal pseudo-cylindrical concave polyhedral (PCCP) shell; *b*) actual buckled cylinder

shown that from the bifurcation point a secondary equilibrium path drops sharply downward (line AB, Fig. 2) and recovers on a new equilibrium path (line BC, Fig. 2). A minimum occurs in this secondary path which was somewhat less than one third of the bifurcation buckling load and agrees reasonably well with the test results.

During this inextensional large-deformation process, the originally perfect cylindrical surface takes a polyhedral form consisting of predominantly flat triangular subregions. The idealized PCCP shell geometry is shown in Fig. 1a. As MIURA states, two polyhedral postbuckling shapes are possible, i.e., diamond and hexagonal patterns [5, 6, 7]. Since the buckling shapes observed in compression tests of cylindrical shells are predominantly diamond shaped with inward displacements, the name *Pseudo-Cylindrical Concave Polyhedral*

(PCCP) surface, as suggested by MIURA [7], aptly describes such a geometrical configuration. This buckled shape of a cylindrical shell pertinent to the second state of equilibrium (line BC, Fig. 2) can be viewed, however, as a new unfailed structural form which possesses a considerably larger circumferential flexural rigidity than a cylindrical shell of the same overall geometry. For instance, if the amplitude of the concavity of the triangular faces is taken as much as several times the thickness of the shell, its circumferential bending rigidity could be increased approximately ten times over that of a comparable

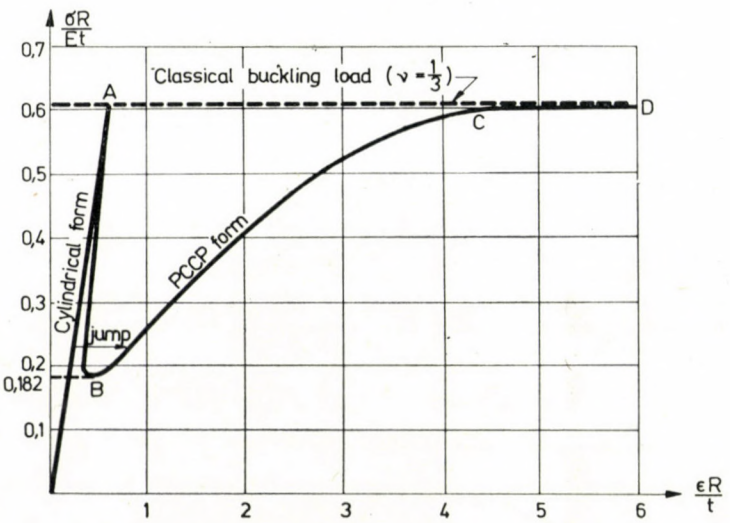

Fig. 2. Axial stress versus unit end shortening

cylindrical shell. Subjecting the PCCP shell to axial compression, a stable load-deformation curve (line BC, Fig. 2) can be achieved, provided that geometry of this pseudo-cylindrical shell remains unchanged; otherwise, the well-known "jump" phenomenon from one buckling mode to the next will take place until the classical buckling load pertinent to the bifurcation point is reached (line CD, Fig. 2). Although the PCCP shell is characterized by inherently high circumferential bending rigidity, axial rigidity is greatly reduced and stiffeners may be required in the axial direction to stabilize its geometry. This can easily be accomplished in many different ways depending on the type of application of such a structure [8].

The aim of the present study is to demonstrate that for such pseudo-cylindrical shells the critical load can be determined with good accuracy. Since the finite element method used in the numerical analysis is highly versatile, it is relatively easy to apply the same approach to other combinations of load, boundary conditions, and overall geometry than those presented here.

2. Notations

A_i Cross sectional area of bar "i".
E Modulus of elasticity.
$\{F\}$ Generalized global force matrix.
F_a Axial load.
I_i In-plane flexural moment of inertia of bar "i".
$[K]$ Global stiffness matrix.
$[K_G]$ Global geometric stiffness matrix.
$[K_t]$ Global tangent stiffness matrix.
$[K]_e$ Element local stiffness matrix.
$[K_g]_e$ Element local geometric stiffness matrix.
k Aspect ratio of rectangular element (Fig. 11).
L_i Length of bar "i".
N Number of elements of the system.
n Number of bars in a framework element.
m Number of components of global force or global displacement matrix.
S Framework element surface area.
t Thickness.
$[T]_e$ Beam element transformation matrix.
u, v Displacement in x, y directions, respectively.
U, U^* Elemental strain energy of the continuum and framework element, respectively.
$\{U\}$ Generalized global displacement matrix.
α_i Angle of inclination of bar "i".
α_y, α_z Rotations of a beam element about the y, z axes, respectively.
β_y, β_z Tensile axial load parameter $= L\sqrt{F_a/EI_{y,z}}$ where F_a = axial tension load
δ Variational operator
$\varepsilon_x, \varepsilon_y, \gamma_{xy}$ In-plane strains.
ε_i Strain in bar "i"
λ_y, λ_z Compressive axial load parameter $= L\sqrt{F_a/EI_{y,z}}$ where F_a = axial compressive load
ν Poisson's ratio
φ_i Bending distortion angle of bar "i".

3. Numerical analysis

3.1. *Nonlinear finite element formulation of instability*

Most shell instability problems, including those we encounter in connection with PCCP shells, cannot be solved analytically. Consequently, a numerical approach must be applied. The finite element method [9], coupled with the use of high-speed digital computers, is a powerful tool for analyzing structures and structural problems of high complexity. Primarily due to its relative simplicity and available large computer program library, the displacement method [10] has been selected for the present analysis. In the matrix-displacement formulation of instability problems using the finite element approach, nonlinearities may occur in various forms. Material nonlinearity is disregarded in this study, and only geometric nonlinearities are assumed to arise in expressing the equilibrium and strain-displacement conditions.

It is apparent that in a *macroscopic* sense the PCCP shell approximates a true cylinder and therefore would be expected to carry loads partially by membrane actions. In a microscopic sense, e.g., within the region of one of the

elementary triangular faces, this shell would appear to respond as a flat plate carrying loads by bending actions. Consequently, both the membrane and bending actions should be considered.[1] In case of large deformations, these actions become coupled and dependent upon the displacement state. To follow the path of deformations, as the compressive load is gradually increased, the undeformed geometrical configuration is taken as the fixed reference state. The task of nonlinear stability analysis involves:

a) selection of suitable finite element type with good convergence characteristics;

b) determination of linear and nonlinear (geometrical) element-stiffness matrices;

c) selection of a stable numerical solution technique; and

d) development of pertinent computer programs.

Before we treat each of these phases of the numerical analysis in detail, let us briefly discuss the fundamentals of the finite element formulation of instability problems.

In the matrix-displacement formulation of buckling, we usually apply the equilibrium method. Let us express first the equilibrium condition of the shell structure in a global reference co-ordinate system (X, Y, Z) (Fig. 3):

$$\{F_{\text{ext}}\} = [K]\{U\} + \{F_G\}\,. \tag{1}$$

This equation relates the generalized external nodal forces, $\{F_{\text{ext}}\}$, and nodal displacements, $\{U\}$. In Eq. (1), $[K]$ is the conventional stiffness matrix of the total system while $\{F_G\}$ represents the geometric force matrix. The matrix $\{F_G\}$ contains terms which are due to both initial forces and nonlinear geometry of deformation. The stiffness matrix of the total structure, $[K]$, also depends upon geometric nonlinearity due to the coupling of element membrane and bending actions.

In order to be able to compile the stiffness $[K]$ for the total structural system, it is required that each element stiffness matrix, $[k]_e$, expressed in its own local co-ordinate system (x, y, z), should first be transformed into the global system. Summing all transformed element stiffness matrices, according to the well-known code number method [13], yields the stiffness properties in the global reference system:

$$[K] = \sum_{e=1}^{N} [T]_e^T\, [k]_e\, [T]_e\,. \tag{2}$$

[1] A detailed stress analysis of the PCCP shell which shows the relationship between these two actions has been carried out [11]. Also, see TANIZAWA and MIURA [12].

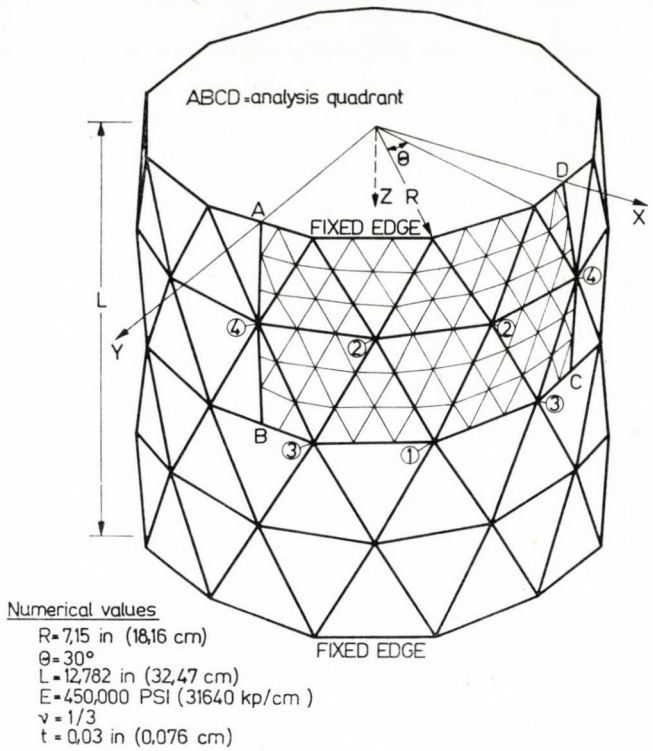

Fig. 3. Finite element model of PCCP shell

The transformation matrix, $[T]_e$, for the beam elements ("building-blocks" of the framework method used to discretize the original continuum) used in the present analysis is given in Table 1.

Equation (1) represents a set of nonlinear algebraic equations. As mentioned earlier, the stiffness matrix, $[K]$, is load dependent, i.e., it is influenced by the presence of the membrane forces, which are (to begin with) unknown. To overcome this difficulty, the so-called *step iteration* method is used which represents a combination of EULER's incremental method and the NEWTON—RAPHSON's iterative procedure (Fig. 4). This mixed procedure consists of applying the EULER incremental method for a limited number of load steps and subsequent corrections with NEWTON—RAPHSON cycling to achieve equilibrium of the nonlinear equations [14]. This combined procedure has the advantage that we can conveniently judge the acceptability of each load increment by the accuracy of the attained equilibrium.

It is evident that the crux of a matrix formulation of shell instability problems is the derivation of an incremental form of Eq. (1) [13]. Operating

Table 1

*Transformation matrix for a beam element**

$$[T]_e = \begin{array}{c} \begin{matrix} 1 & 2 & 3 & 4 & 5 & 6 & 7 & 8 & 9 & 10 & 11 & 12 \end{matrix} \\ \left[\begin{array}{cccc|cccc|cccc|} \multicolumn{3}{c}{[T]\bar{e}} & \multicolumn{3}{c}{[0]} & \multicolumn{3}{c}{[0]} & \multicolumn{3}{c}{[0]} \\ \hline \multicolumn{3}{c}{[0]} & \multicolumn{3}{c}{[T]\bar{e}} & \multicolumn{3}{c}{[0]} & \multicolumn{3}{c}{[0]} \\ \hline \multicolumn{3}{c}{[0]} & \multicolumn{3}{c}{[0]} & \multicolumn{3}{c}{[T]\bar{e}} & \multicolumn{3}{c}{[0]} \\ \hline \multicolumn{3}{c}{[0]} & \multicolumn{3}{c}{[0]} & \multicolumn{3}{c}{[0]} & \multicolumn{3}{c}{[T]\bar{e}} \end{array}\right] \begin{matrix} 1 \\ 2 \\ 3 \\ 4 \\ 5 \\ 6 \\ 7 \\ 8 \\ 9 \\ 10 \\ 11 \\ 12 \end{matrix} \end{array}$$

$$\left[\begin{array}{ccc} C_x & C_y & C_z \\ \hline \dfrac{-C_xC_y\cos\beta - C_z\sin\beta}{\sqrt{C_x^2 + C_y^2}} & \sqrt{C_x^2 + C_y^2}\cos\beta & \dfrac{-C_yC_z\cos\beta + C_x\sin\beta}{\sqrt{C_x^2 + C_y^2}} \\ \hline \dfrac{C_xC_y\sin\beta - C_z\cos\beta}{\sqrt{C_x^2 + C_z^2}} & -\sqrt{C_x^2 + C_z^2}\sin\beta & \dfrac{C_yC_z\sin\beta + C_x\cos\beta}{\sqrt{C_x^2 + C_z^2}} \end{array}\right]$$

$[T]\bar{e}$ for General Orientation

$$\left[\begin{array}{ccc} 0 & C_y & 0 \\ \hline -C_y\cos\beta & 0 & \sin\beta \\ \hline C_y\sin\beta & 0 & \cos\beta \end{array}\right]$$

$[T]\bar{e}$ if local x-Axis is Parallel to global y-Axis

Where $C_x = \dfrac{X_2 - X_1}{L}$; $C_y = \dfrac{Y_2 - Y_1}{L}$; $C_z = \dfrac{Z_2 - Z_1}{L}$; $L = [(X_2 - X_1)^2 + (Y_2 - Y_1)^2 + (Z_2 - Z_1)^2]^{1/2}$

* Refer to Figs 5 and 6

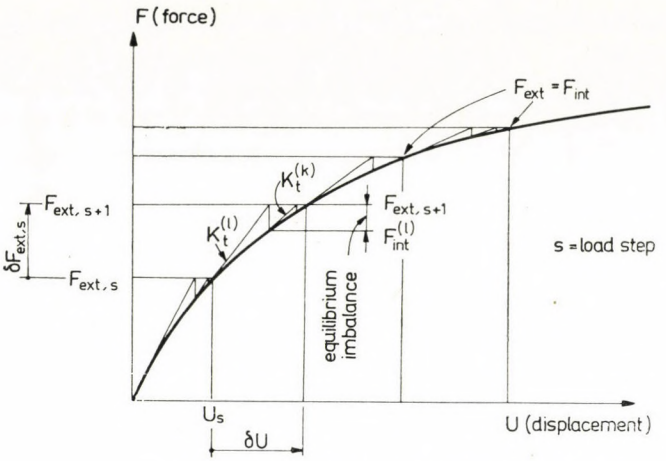

Fig. 4. Step-iteration procedure

on Eq. (1) with the variational operator yields the desired equation of stability:

$$\{\delta F_{\text{ext}}\} = [K]\{\delta U\} + \{\delta F_G\}\,. \tag{3}$$

Reasons for neglecting the variation of $[K]$ in Eq. (3) are given in [8]. Furthermore,

$$\{\delta F_G\} = [K_G]\,\{\delta U\} \tag{4}$$

in which

$$[K_G] = \begin{bmatrix} \dfrac{\partial F_{G1}}{\partial U_1} & \cdots & \dfrac{\partial F_1}{\partial U_m} \\ \vdots & \ddots & \\ \dfrac{\partial F_{Gm}}{\partial U_1} & \cdots & \dfrac{\partial F_{Gm}}{\partial U_m} \end{bmatrix} \tag{5}$$

is the geometric stiffness matrix. Equation (3) can also be written in terms of the so-called *tangent stiffness matrix*, $[K_t]$, based on the apparent analogy with the tangent modulus of elasticity [15]. This relationship is given by:

$$\{\delta F_{\text{ext}}\} = [K_t]\,\{\delta U\} \tag{6}$$

in which

$$[K_t] = [K] + [K_G]\,. \tag{7}$$

Both the structural stiffness matrix, $[K]$, and the geometric stiffness matrix, $[K_G]$, are load and deformation dependent. Explicit expressions for these matrices are given in Tables 2 and 3 for the three-dimensional beam element depicted in Fig. 5 [8, 14].

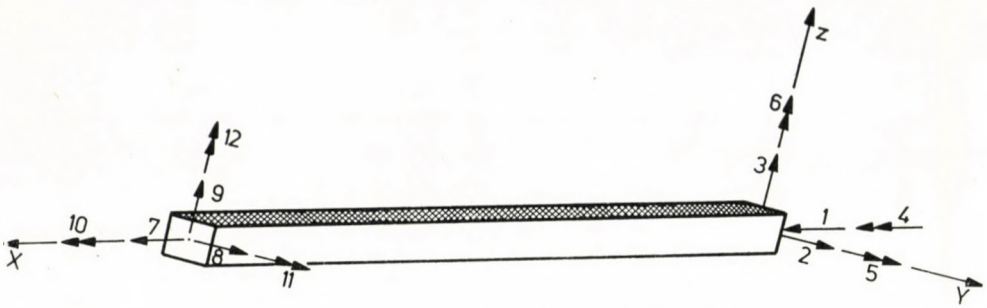

Fig. 5. Element co-ordinate and numbering systems

The numerical solution proceeds in the following manner: Eq. (6) is modified according to the Newton—Raphson scheme

$$[K_t]^{(k)}\{\delta U\}^{(k)} = \{\delta F_{\text{ext}}\}_s + [\{F_{\text{ext}}\}_s - \{F_{\text{int}}\}^{(k)}]. \tag{8}$$

This expression is derived by expanding Eq. (1) into a truncated Taylor's series about a displacement state sufficiently close to the exact solution [8]. The physical meaning of Eq. (8) is clear. The last two terms in square brackets represent the imbalance of internal, $\{F_{\text{int}}\}$, and external, $\{F_{\text{ext}}\}$, forces (Fig. 4). If these terms are neglected, Eq. (8) is equivalent to the simple Euler incremental method in which equilibrium is assumed to be satisfied for each load step. The inclusion of these terms allows a balance between internal and external forces to be achieved for each new load step. For each cycle of iteration, $^{(k)}$, an improved estimate for the values of the displacement state is determined by the recurrence relation:

$$\{U\}^{(k+1)} = \{U\}^{(k)} + \{\delta U\}^{(k)}. \tag{9}$$

For each cycle, the matrices, $[K_t]^{(k)}$ and the matrix representing the vector of the internal stress resultants

$$\{F_{\text{int}}\}^{(k)} = [K_t]^{(k)}\{U\}^{(k)} \tag{10}$$

are re-evaluated in terms of the improved estimate of displacement, $\{U\}^{(k+1)}$. Convergence is achieved when

$$\{U\}^{(k+1)} \simeq \{U\}^{(k)}. \tag{11}$$

3.2 *Determination of element stiffness properties*

There are currently two types of finite elements in use for the solutions of problems in structural mechanics: the framework elements, made of "equivalent" elastic bars, and continuous elements. A preference for the latter has

Table 2

Element

$$[k]_e = \begin{array}{c|cccccc} & 1 & 2 & 3 & 4 & 5 & 6 \\ \hline 1 & k_{11} & 0 & 0 & 0 & 0 & 0 \\ 2 & & k_{22} & 0 & 0 & 0 & \frac{k_{22} \cdot L}{2} \\ 3 & & \text{SYMMETRIC} & k_{33} & 0 & \frac{-k_{22} \cdot L}{2} & 0 \\ 4 & & & & k_{44} & 0 & 0 \\ 5 & & & & & k_{55} & 0 \\ 6 & & & & & & k_{66} \end{array}$$

$$k_{11} = \frac{AE}{L} \qquad k_{44} = \frac{GJ}{L}$$

$$k_{22} = \frac{2EI_z\beta_z^2(\cosh\beta_z - 1)}{[\beta_z \sinh\beta_z - 2(\cosh\beta_z - 1)] \cdot L^3} \qquad k_{55} = \frac{EI_y\beta_y(\beta_y \cosh\beta_y - \sinh\beta_y)}{[\beta_y \sinh\beta_y - 2(\cosh\beta_y - 1)] \cdot L}$$

$$k_{33} = \frac{2EI_y\beta_y^2(\cosh\beta_y - 1)}{[\beta_y \sinh\beta_y - 2(\cosh\beta_y - 1)] \cdot L^3} \qquad k_{66} = \frac{EI_z\beta_z(\beta_z \cosh\beta_z - \sinh\beta_z)}{[\beta_z \sinh\beta_z - 2(\cosh\beta_z - 1)] \cdot L}$$

AXIAL TENSION

$$k_{22} = \frac{2EI_z\lambda_z^2(1 - \cos\lambda_z)}{[2(1 - \cos\lambda_z) - \lambda_z \sin\lambda_z] \cdot L^3}$$

$$k_{33} = \frac{2EI_y\lambda_y^2(1 - \cos\lambda_z)}{[2(1 - \cos\lambda_y) - \lambda_y \sin\lambda_y] \cdot L^3}$$

AXIAL

* Refer to Figure 5 for numbering system and sign convention. See also *Notations*

prevailed in the recent literature. In spite of the popularity of the continuous element, the framework element possesses certain characteristics which makes it competitive. These are:

1. The framework representation of a continuum represents a true elastic structure which may be actually constructed and even experimented with physically. The continuous element is a mathematical abstraction suitable for analysis but not suitable for physical reproduction [16].

2. The derivation of the properties of a framework element are based on the same principles used to derive properties for a continuous element. Also, the framework element has been shown to exhibit good monotonic convergence

*stiffness matrix**

7	8	9	10	11	12	
$-k_{11}$	0	0	0	0	0	1
0	$-k_{22}$	0	0	0	$\frac{k_{22} \cdot L}{2}$	2
0	0	$-k_{33}$	0	$\frac{-k_{33} \cdot L}{2}$	0	3
0	0	0	$-k_{44}$	0	0	4
0	0	$\frac{k_{33} \cdot L}{2}$	0	$k_{33}L^2/2 - k_{55}$	0	5
0	$\frac{-k_{22} \cdot L}{2}$	0	0	0	$k_{22}L^2/2 - k_{66}$	6
k_{11}	0	0	0	0	0	7
	k_{22}	0	0	0	$\frac{-k_{22} \cdot L}{2}$	8
		k_{33}	0	$\frac{k_{33} \cdot L}{2}$	0	9
			k_{44}	0	0	10
				k_{55}	0	11
COMPRESSION				SYMMETRIC	k_{66}	12

$$K_{55} = \frac{EI_y\lambda_y(\sin\lambda_y - \lambda_y\cos\lambda_y)}{[2(1-\cos\lambda_y) - \lambda_y\sin\lambda_y] \cdot L}$$

$$K_{66} = \frac{EI_z\lambda_z(\sin\lambda_z - \lambda_z\cos\lambda_z)}{[2(1-\cos\lambda_z) - \lambda_z\sin\lambda_z] \cdot L}$$

characteristics [17]. In addition, it is important to maintain continuity of displacements and slopes between adjacent edges of elements, especially in instability and large deformation analyses [8, 17, 18]. The framework element inherently possesses edge continuity. Figures 14 through 17 show examples of such problems analyzed with framework elements.

3. The framework element is simple to apply to the solution of structural mechanics problems. If a framework element can be derived for the problem of interest, it is easily used *without modification* of existing space frame programs. Table 4 gives equivalent bar properties for several types of useful *planar* framework elements.

Table 3

Geometric stiffness matrix*

$$[k_G]_e = \begin{array}{c} \begin{array}{cccccccccccc} 1 & 2 & 3 & 4 & 5 & 6 & 7 & 8 & 9 & 10 & 11 & 12 \end{array} \\ \left[\begin{array}{cccccccccccc} [k_G]_{\bar{e}} & & & & & & [k_G]_{\bar{e}} & & & & & \\ & & & & & & & & & & & \\ & & & & & & & & & & & \\ & & & & & & & & & & & \\ & & & & & & & & & & & \\ & & & & & & & & & & & \\ -[k_G]_{\bar{e}} & & & & & & [k_G]_{\bar{e}} & & & & & \\ & & & & & & & & & & & \\ & & & & & & & & & & & \\ & & & & & & & & & & & \\ & & & & & & & & & & & \\ & & & & & & & & & & & \end{array}\right] \end{array} \begin{array}{c} 1 \\ 2 \\ 3 \\ 4 \\ 5 \\ 6 \\ 7 \\ 8 \\ 9 \\ 10 \\ 11 \\ 12 \end{array}$$

$$[k_G]_{\bar{e}} = \frac{AE}{L} \cdot \begin{bmatrix} 0 & \alpha_z & -\alpha_y \\ \alpha_z & \alpha_z^2 + \frac{F_a}{AE} & -\alpha_y\alpha_z \\ -\alpha_y & -\alpha_y\alpha_z & \alpha_y^2 + \frac{F_a}{AE} \end{bmatrix}$$

* Elements not shown are zero. Refer to Fig. 5 for numbering system and sign convention. α_y, α_z are rotations of the beam element about the y and z axes, respectively. F_a is the axial load.

4. The grading of the element mesh can be arbitrary as depicted in Fig. 7.

Because of its basic simplicity, its physical nature and the ease at which it may be implemented, the framework element was selected to study the stability of the PCCP shell. Basically, the framework method consists of replacing a continuum by an assemblage of bars arranged in a definite pattern. Elastic properties of the one-dimensional elements are chosen so as to reproduce the deformations of the original continuum. From the viewpoint of geometry, the framework model may possess some preferred directions (anisotropy). In such case, the elastic properties of the substitute system must be chosen carefully if all types of deformations of the continuum are to be reproduced exactly.

A number of framework element types have appeared in the literature, [16] through [40]. Table 4 summarizes some of the more useful elements suitable for plate and shell analysis.

The present study required merely rectangular and equilateral triangular elements. The required element properties are derived below for in-plane stresses valid for an arbitrary Poisson's ratio by requiring that the strain

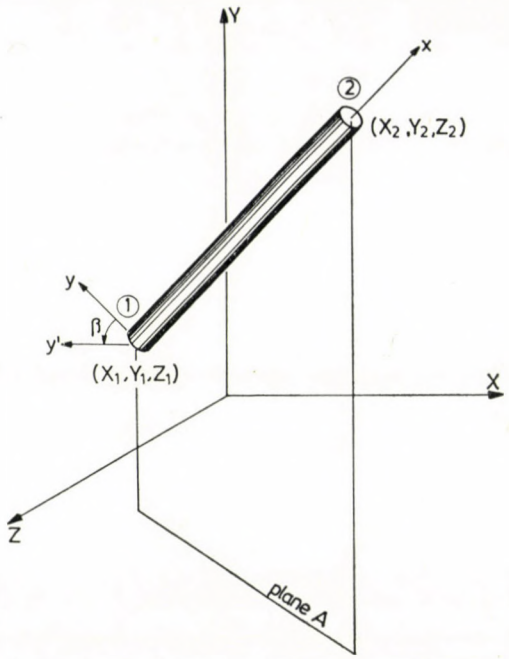

Notes:
1 Plane A is defined by the local x-y axes and must be perpendicular to the global x-z plane
2 The principle beam axis is in the direction of the local y' axis

Fig. 6. Geometry for co-ordinate transformation

energy of the framework cell be the same as the strain energy of the continuum for an arbitrary deformed state.

For an element subject only to in-plane strains, ε_x, ε_y, γ_{xy}, the strain energy of a continuous surface is given by [41]:

$$U = \frac{Et}{2(1-\nu^2)} \left\{ \varepsilon_x^2 + \varepsilon_y^2 + 2\nu\varepsilon_x\varepsilon_y + \frac{(1-\nu)}{2}\gamma_{xy}^2 \right\} S \qquad (12)$$

in which $E =$ modulus of elasticity, $\nu =$ Poisson's ratio, $t =$ thickness and $S =$ elemental area of the plate surface. The elemental area, S, is assumed to be sufficiently small so that the in-plane strains acting over the element are constant.

Considering next that a framework of *rigidly connected* bars are placed along the boundary of the area, S, the strain energy in this bar system is given by:

$$U^* = \frac{1}{2}\sum_{i=1}^{n} A_i EL_i \varepsilon_i^2 + 6\sum_{i=1}^{n} \frac{EI_i \varphi_i^2}{L_i} \qquad (13)$$

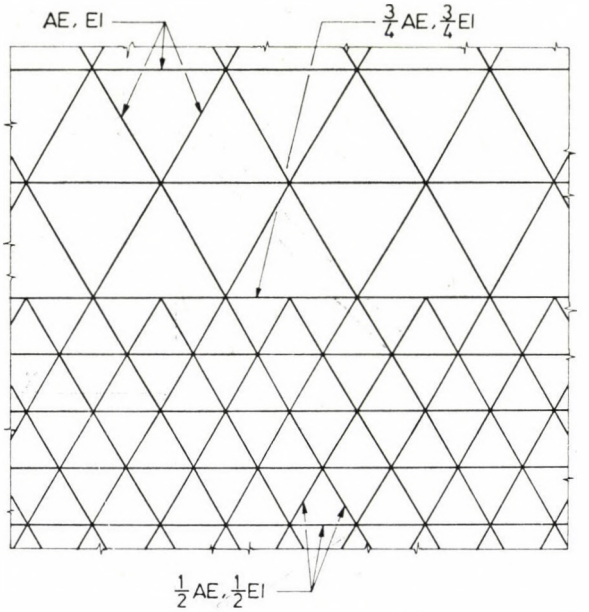

Fig. 7. Grading of framework elements

in which n = number of bars in the framework element, A_iE = axial rigidity of bar "i", ε_i^- = axial strain in bar "i", EI_i = flexural rigidity of bar "i" for bending about a normal to the plane of the element, L_i = length of bar "i" and φ_i = distortion angle of uniform bending of bar "i" (Fig. 8). Since a state of constant strain is assumed to exist over the elemental area, S, the joints of opposite ends of a bar are assumed to rotate through the same angle, φ_i, about a straight line connecting each end.

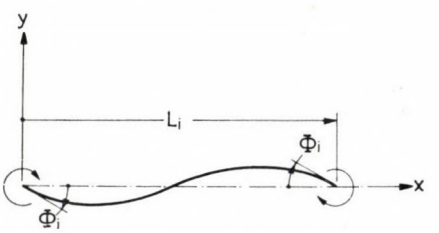

Fig. 8. Uniform bending distortion

The displacements of the joints of a framework element have been determined from the displacement field:

$$u = \varepsilon_x x + \gamma_{xy} y\,, \tag{14}$$

$$v = \varepsilon_y y \tag{15}$$

Table 4.

Properties of planar framework elements with rigid joints

Element type (isolated)	Bar NBR.	Equivalent membrane properties+		Reference	Equivalent transverse bending properties+		Reference
		Axial rigidity (AE)	In-plane flexural rigidity (EI)		Flexural rigidity (EI)	Torsional rigidity (GJ)	
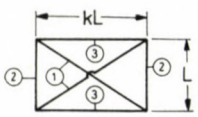 Rectangle	①	$\frac{Lt}{2}\frac{(1+k^2)^{3/2}}{k}\frac{\nu E}{(1-\nu^2)}$	-0-	Eq. (30)	$\frac{Lt^3}{24}\frac{(1+k^2)^{3/2}}{k}\frac{\nu E}{(1-\nu^2)}$	-0-	[28]
	②	$\frac{Lt}{2}\frac{(k^2-\nu)E}{k(1-\nu^2)}$	$\frac{tL^3}{24}\frac{k(1+3\nu)E}{(1-\nu^2)}$		$\frac{Lt^3}{24}\frac{(k^2-\nu)E}{k(1-\nu^2)}$	$\frac{Lt^3}{24}\frac{k(1-3\nu)E}{(1-\nu^2)}$	
	③	$\frac{Lt}{2}\frac{(1-k^2\nu)E}{(1-\nu^2)}$	$\frac{tL^3}{24}\frac{k^2(1+3\nu)E}{(1-\nu^2)}$		$\frac{Lt^3}{24}\frac{(1-k^2\nu)E}{(1-\nu^2)}$	$\frac{Lt^3}{24}\frac{(1-3\nu)E}{(1-\nu^2)}$	
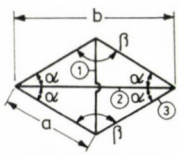 Parallelogram	①	$(\nu=1/3)$ $\frac{9}{8}at\cos\alpha(1-\frac{1}{3}\tan^2\alpha)E$	-0-	[29]	-0-	$\frac{at^3}{12}\frac{(1-4\cos^2\alpha)E}{\cos\alpha(1-\nu^2)}$	[29]
	②	$\frac{9}{8}at\sin\alpha(1-\frac{1}{3}\cot^2\alpha)E$	-0-		$\frac{bt^3\cot\beta}{12}\frac{E}{(1-\nu)}$	$\frac{at^3}{12}\frac{(\sin^2\alpha-\cos^2\alpha-2\nu\sin^2\alpha)E}{\sin\alpha(1-\nu^2)}$	
	③	$\frac{3atE}{16\sin\alpha\cos\alpha}$	-0-		$\frac{at^3\cot\alpha}{24}\frac{E}{(1-\nu)}$	$\frac{at^3\cot\alpha}{24}\frac{(1-\nu\tan^2\alpha)E}{(1-\nu^2)}$	
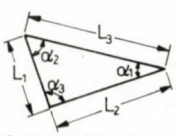 Arbitrary triangle	1-1,2,3	N.A.	N.A.	-	$(\nu=0)$ $\frac{L_1t^3}{24}\frac{\cot\alpha_1E}{(1-\nu^2)}$*	$(\nu=0)$ $\frac{L_1t^3}{24}\frac{\cot\alpha_1E}{(1-\nu^2)}$*	[33]
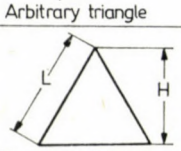 Equilateral triangle	All bars	$\frac{\sqrt{3}Lt}{6}\frac{E}{(1-\nu)}$	$\frac{\sqrt{3}tL}{72}\frac{(1-3\nu)E}{(1-\nu^2)}$	Eq. (22)	$\frac{Ht^3}{36}\frac{E}{(1-\nu)}$	$\frac{Ht^3}{36}\frac{(1-3\nu)E}{(1-\nu^2)}$	[37]

Notes: +t=plate thickness, E=modulus of elasticity, ν=Poisson's ratio.
*ν is arbitrary only for clamped or straight, simply-supported boundaries.

in which u represents a displacement in the x direction, while v denotes a displacement in the y direction. Since the strains are assumed to be constants, these equations satisfy the strain-displacement equations of elasticity [41]:

$$\varepsilon_x = \frac{\partial u}{\partial x},$$

$$\varepsilon_y = \frac{\partial v}{\partial y}, \tag{16}$$

$$\gamma_{xy} = \frac{\partial u}{\partial y} + \frac{\partial v}{\partial x}.$$

If U and U^* are to be compared, a relationship between the normal strains, ε_x, ε_y, γ_{xy}, and the bar strains, ε_i, must be found. A transformation

between these strains has been determined from the relationship of displacements as shown in Fig. 9, which is:

$$\varepsilon_i = \varepsilon_x \cos^2 \alpha_i + \varepsilon_y \sin^2 \alpha_i + \gamma_{xy} \cos \alpha_i \sin \alpha_i \tag{17}$$

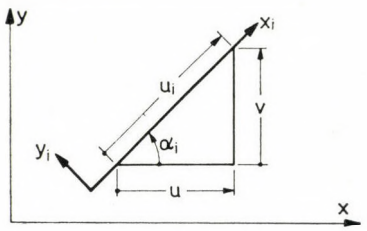

Fig. 9. Transformation of displacements

3.2.1 Equilateral triangle

The geometry of an equilateral triangular element is shown in Table 4 and Fig. 10. For this element, Eq. (17) yields:

$$\begin{aligned} \varepsilon_x &= \varepsilon_1 , \\ \varepsilon_y &= \frac{2}{3}(\varepsilon_2 + \varepsilon_3) - \frac{1}{3}\varepsilon_1 , \\ \gamma_{xy} &= \frac{2}{\sqrt{3}}(\varepsilon_3 - \varepsilon_2) . \end{aligned} \tag{18}$$

These equations are used to transform Eq. (12) into an expression containing bar strains:

$$\begin{aligned} U = {} & \frac{\sqrt{3}\, EtL^2}{36}\left[\frac{5 - 3\nu}{1 - \nu^2}\right]\left\{\sum_{i=1}^{3} \varepsilon_i^2\right\} - \\ & - \frac{\sqrt{3}\, EtL^2}{18}\left[\frac{1 - 3\nu}{1 - \nu^2}\right]\{\varepsilon_1 \varepsilon_2 + \varepsilon_2 \varepsilon_3 + \varepsilon_3 \varepsilon_1\} \end{aligned} \tag{19}$$

The constant strain distortions of this element are shown in Fig. 10. Each bar of the framework cell is assumed to possess additional bending rigidity to resist moments acting in the plane of the element. Furthermore, the bar ends are rigidly connected to each other. Utilizing these assumptions, the distortion angles, φ_1, φ_2, φ_3, have already been derived in previous works [8, 42]. To conserve space, only the pertinent results are given below:

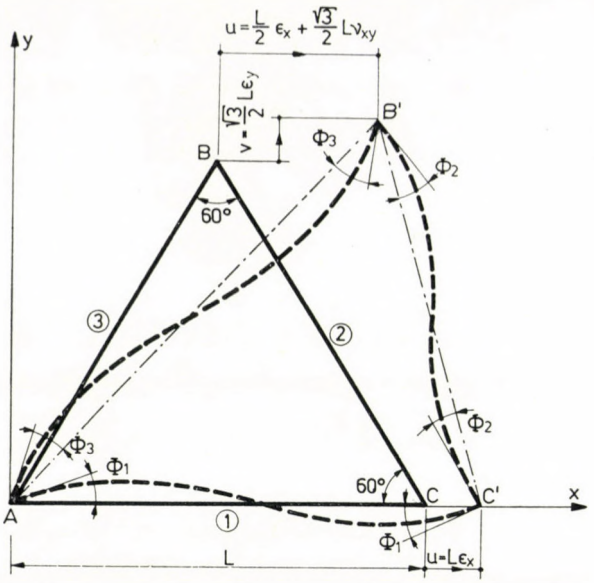

Fig. 10. Constant strain distortion of a triangular framework element

$$\varphi_1 = -\frac{\gamma_{xy}}{2},$$

$$\varphi_2 = \frac{\gamma_{xy}}{4} - \frac{\sqrt{3}}{4}(\varepsilon_x - \varepsilon_y) \tag{20}$$

$$\varphi_3 = \frac{\gamma_{xy}}{4} + \frac{\sqrt{3}}{4}(\varepsilon_x + \varepsilon_y) \ .$$

Equations (13) and (20) give:

$$U^* = \left[\frac{AEL}{2} + \frac{4EI}{L}\right]\left\{\sum_{i=1}^{3}\varepsilon_i^2\right\} - \frac{4EI}{L}\{\varepsilon_1\varepsilon_2 + \varepsilon_2\varepsilon_3 + \varepsilon_3\varepsilon_1\} \ . \tag{21}$$

Due to symmetry, each bar has the same properties.

Comparison of Eqs (19) and (21) shows that the strain energies, U and U^*, are equal if:

$$AE = \frac{\sqrt{3}\,EtL}{6(1-\nu)},$$

$$EI = \frac{\sqrt{3}\,EtL^3(1-3\nu)}{72(1-\nu^2)} \ . \tag{22}$$

Note that these values are valid for an *isolated* element and should be doubled in interior regions, i.e., when two elements are combined.

3.2.2 Rectangle

The geometry of the rectangular element is shown in Table 4 and its constant strain distortion in Fig. 11. Using Eq. (17) we obtain for the rectangular element:

$$\begin{aligned}
\varepsilon_1 &= \left(\frac{k}{r}\right)^2 \varepsilon_x + \left(\frac{1}{r}\right)^2 \varepsilon_y + \left(\frac{k}{r^2}\right) \gamma_{xy}\,, \\
\varepsilon_{1'} &= \left(\frac{k}{r}\right)^2 \varepsilon_x + \left(\frac{1}{r}\right)^2 \varepsilon_y - \left(\frac{k}{r^2}\right) \gamma_{xy}\,, \\
\varepsilon_2 &= \varepsilon_y\,, \\
\varepsilon_3 &= \varepsilon_x\,,
\end{aligned} \tag{23}$$

in which

$$r = \sqrt{1 + k^2}\,. \tag{24}$$

In-plane bending of the bars is a consequence of the shearing strain γ_{xy}. Due to symmetry, the joint rotations, θ, are all equal (Fig. 11). The flexural rigidities of the diagonal members are chosen to be zero. Analysis of the shearing deformations of the frame in Fig. 11 yields:

$$\theta = \gamma_{xy}\left[\frac{EI_2}{EI_2 + EI_3/k}\right]. \tag{25}$$

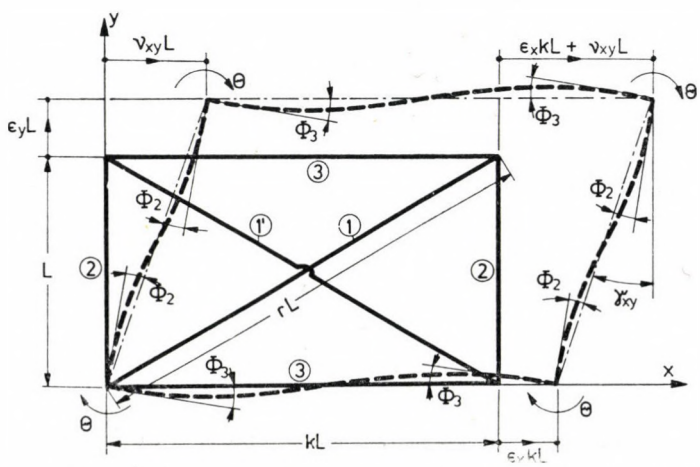

Fig. 11. Constant strain distortion of a rectangular element

This, however, is not a symmetrical result. If the rectangle is oriented in a direction perpendicular to that shown in Fig. 11,

$$\theta_{\perp} = \gamma_{xy}\left[\frac{EI_3/k}{EI_3/k+EI_2}\right]. \tag{26}$$

For a unique solution, such that $\theta = \theta_{\perp}$, we require that

$$EI_2 = EI_3/k\ . \tag{27}$$

Recognizing that $\varphi_3 = \theta$, Fig. 11 reveals that

$$\varphi_2 = \varphi_3 = \frac{\gamma_{xy}}{2}\ . \tag{28}$$

The strain energy in this element is found by combining Eqs (13), (23) and (28):

$$\begin{aligned} U^* = &\left[\frac{A_1\,ELk^4}{r^3} + A_3EkL\right]\varepsilon_x^2 + \left[\frac{A_1\,EL}{r^3} + A_2EL\right]\varepsilon_y^2 + \\ &+ 2\,\frac{A_1EL}{r^3}\,k^2\,\varepsilon_x\,\varepsilon_y + \left[\frac{A_1EL}{r^3}\,k^2 + \frac{6\,EI_2}{r^3}\right]\gamma_{xy}^2\,. \end{aligned} \tag{29}$$

By comparing the coefficients in Eqs (12) and (29), the following rectangular bar properties are obtained:

$$\begin{aligned} A_1E &= \frac{Lt(1+k^2)^{3/2}}{2k}\ \frac{vE}{(1-v^2)}\,, \\ A_2E &= \frac{Lt}{2k}\ \frac{(k^2-v)\,E}{(1-v^2)}\,, \\ A_3E &= \frac{Lt}{2}\ \frac{(1-k^2\,v)\,E}{(1-v^2)}\,, \\ EI_2 &= \frac{L^3\,tk}{24}\ \frac{(1-3v)\,E}{(1-v^2)}\,, \\ EI_3 &= k\cdot EI_2\ . \end{aligned} \tag{30}$$

3.3 *Parametric convergence studies*

The fundamental convergence criterion of a finite element solution is basically the same as for any discrete technique used in numerical stress analysis. That is, it is required that the strain along the finite element boundaries

should approach the strain of the original continuum as the size of framework cells is reduced to the infinitesimal. In order to determine the convergence characteristics of the framework cells used in this investigation, extensive parametric studies have been carried out on pertinent linear and nonlinear problems for which analytical solutions are available.

A cantilever deep-beam problem with a length to depth ratio of two (Fig. 12) has been used as a test problem to establish the convergence characteristics for membrane stiffness coefficients of the equilateral triangular framework element (Fig. 10). The convergence, as Fig. 12 indicates, is monotonic

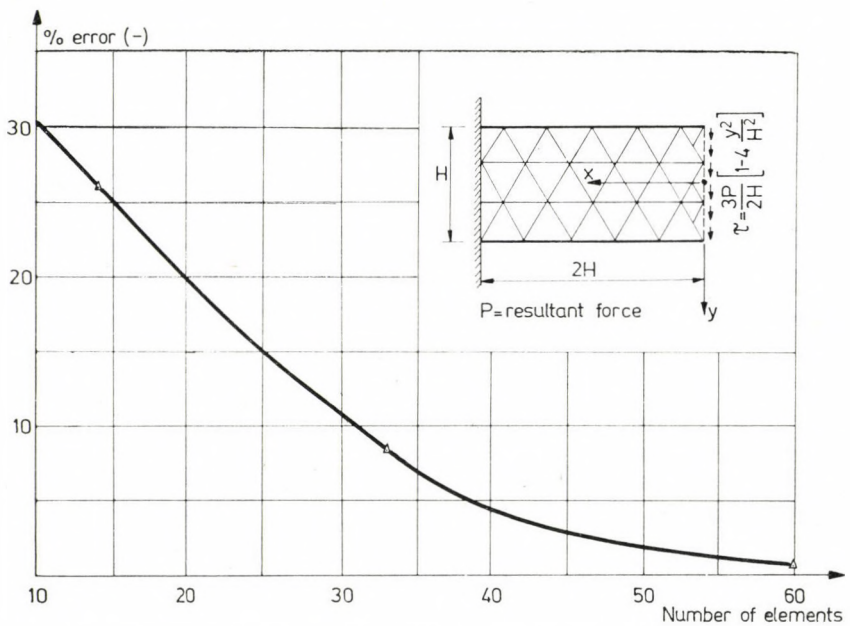

Fig. 12. Convergence characteristics of the membrane part of stiffness coefficients

to the exact solution. Similarly, the linear part of the element bending stiffness coefficients (Table 4) exhibits the very same highly desirable convergence characteristics. In this case, however, a simply supported equilateral plate has been employed as the test problem (Fig. 13).

In investigating buckling of thin shells by means of the finite element method, the nonlinear element stiffness matrices (Table 2 and 3) play a decisive role. Consequently, several test runs have been made to obtain similar information on the element behavior in the geometric nonlinear, elastic regions. Since a relatively extensive literature search has only yielded solutions of problems with rectangular boundary conditions, rectangular framework cells (whose properties are also defined in Table 4) have been used. First, large

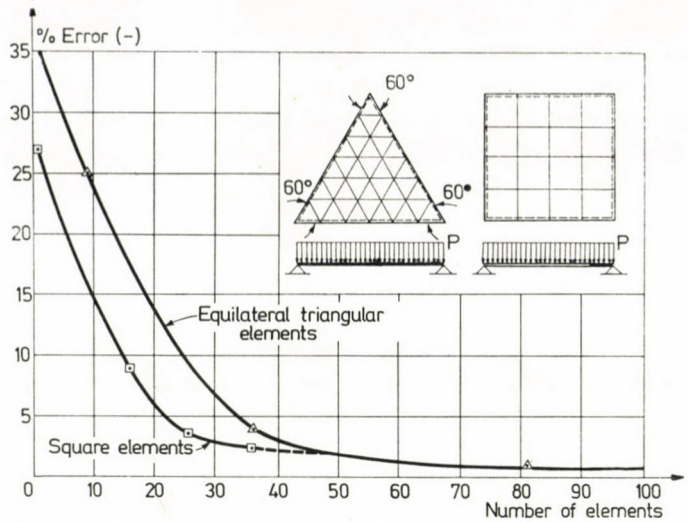

Fig. 13. Convergence characteristics of the bending part of stiffness coefficients

deflections of a laterally loaded square plate with fixed boundary conditions have been computed (Fig. 14). The so-obtained deflection curve shows an excellent agreement with LEVY's analytical solution [43]. Next, in order to test the effect of curvature on the accuracy of the finite element analysis, large deflections of a shallow shell have been computed (Fig. 15). Even with a very coarse subdivision, the results were in close agreement with other, more refined,

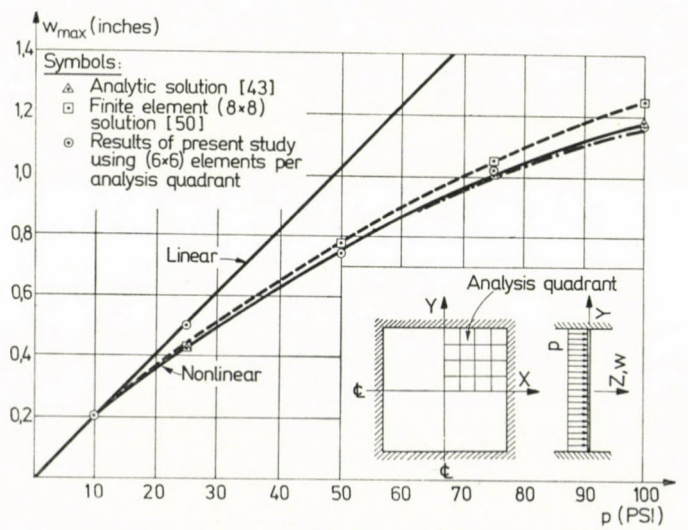

Fig. 14. Large deflection solutions for a square plate

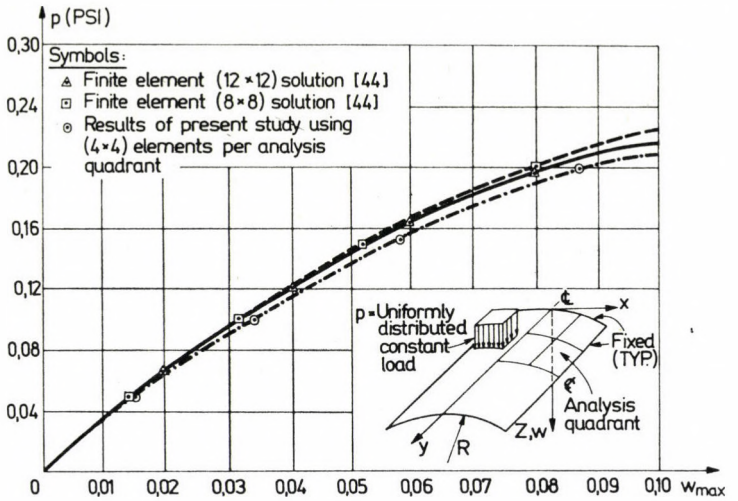

Fig. 15. Large deflection solutions for a shallow cylindrical shell

finite element solutions [44]. The critical buckling load of a simply supported plate subjected to uniformly distributed compressive edge forces, $\bar{n}_x$, has been determined based on a linear analysis using rectangular elements (Fig. 16) [17]. Finally, the buckling load of an elliptical cylinder, subjected to uniform external pressure (Fig. 17), has been determined using rectangular framework cells. For this test problem, buckling occurred when the tangent stiffness

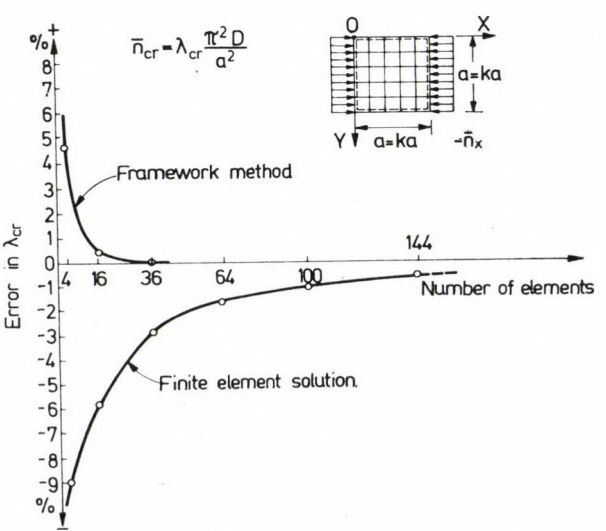

Fig. 16. Comparison of convergence properties in stability analysis [17]

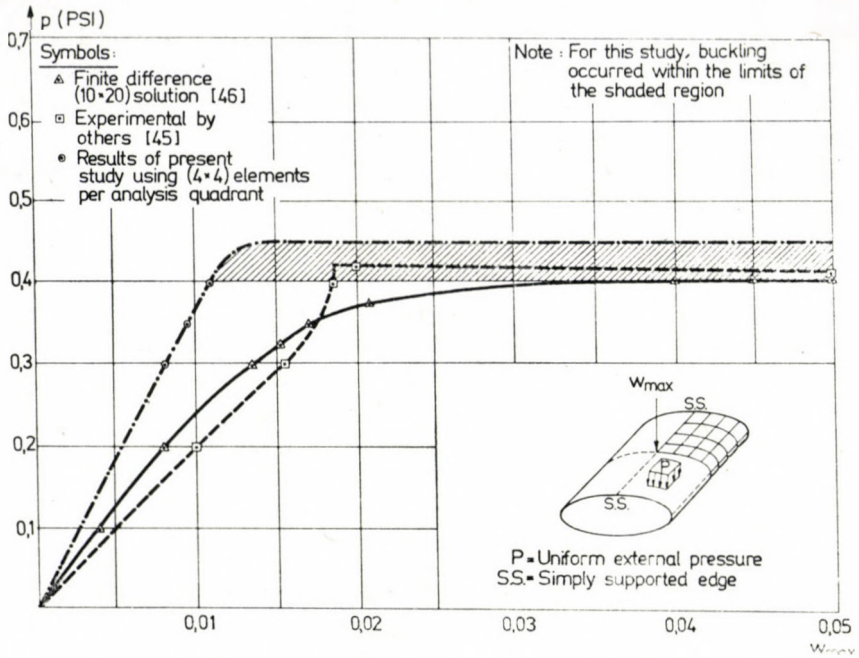

Fig. 17. Nonlinear buckling analysis of an elliptical cylinder

matrix became semi-definite. Since finite load steps have been used in this analysis, we can merely state that the shell has buckled somewhere within the shaded region of Fig. 17. The computation could have been further redefined by introducing smaller load increments. This step, however, has been omitted since relatively good agreement with the experimentally determined buckling load [45] has been achieved. Furthermore, a comparison of the finite element results (based on framework cells) with the finite difference solution of the same problem [46] shows very little discrepancy. Consequently, the required confidence in the numerical procedure used in this study has been established. Finally, it should be mentioned that the buckling, respectively the post-buckling behavior of this elliptical shell resembles, to a certain degree, that of a PCCP shell of similar geometrical configuration; thus, the results of this last test problem can be considered qualitatively quite valuable.

3.4. *Computer program*

As mentioned earlier, for a numerical solution of the nonlinear buckling problems of PCCP shells, the *step iteration* technique, which advantageously combines EULER's incremental and NEWTON—RAPHSON's iterative procedures, has been selected. This decision has primarily been based on the *proven numer-*

ical stability of such a mixed process. In addition, some economical considerations did also favor this approach, i.e., applying merely NEWTON—RAPHSON's method, the required computer time tends to be expensive when large number of degrees of freedom are involved.

The computer program which was utilized in this study is the *Struc*tural *D*esign *L*anguage (STRUDL) program, originally developed at the Massachusetts Institute of Technology, Civil Engineering Laboratory [47]. This program is written in a "dialect" of the FORTRAN computer language, called ICES FORTRAN [48], which is more flexible than FORTRAN IV (for structural analysis). That is, the analyst can use numerous problem oriented "commands". In addition, STRUDL represents a valuable research tool since subroutines, which have been incorporated into this program, include many of the solution algorithms required for finite element analysis [48]. Among other items, STRUDL has the capabilities of nonlinear space frame analysis. Therefore, by introducing finite elements in the form of framework cells this program can be extended, without modification, to cover the general class of thin shells. All computations have been carried out on the IBM 360 computer at the University of Hawaii.

3.5. *Results of the numerical analysis*

The PCCP shell selected for this study is shown in Fig. 3. This shell is characterized by a pattern of equilateral triangles forming twelve circumferential waves and four axial waves of 0.24 inch amplitude. Numerical values defining the geometry of the shell along with its material properties are given in Fig. 3. Since the deformed shell remains symmetrical after buckling has occurred, it was sufficient to model only a one-eighth section of the shell. The above-mentioned symmetry condition requires that the element rotations along lines AB, BC and CD, in addition to the in-plane translations perpendicular to these lines, must be prevented. Each nodal point in the interior domain of the shell has six degrees of freedom, resulting in 311 displacement components. The external pressure is represented by pertinent nodal forces.

Four load step increments (0.2 psi each) have been applied to this discrete model. At each load step, the displacements were found by using one-cycle NEWTON—RAPHSON iteration. It is, of course, possible (or even desirable) to use multiple cycling within each load step.

Since the ends of the PCCP shell under investigation have been restrained in the axial direction, the radial displacements alone can describe the buckling and postbuckling behavior of this structure. This quantity is plotted as a function of the hydrostatic pressure for the joint numbers indicated on the pertinent load-deflection curves in Fig. 18. It appears that up to 0,4 psi hydro-

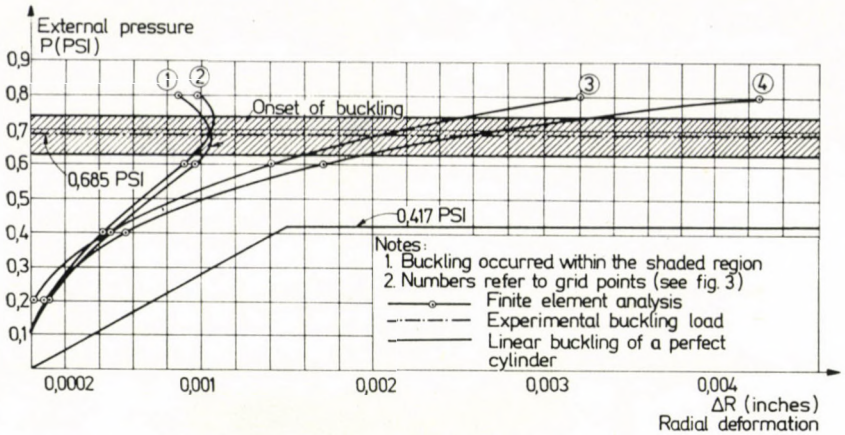

Fig. 18. Results of buckling analysis for PCCP shell shown in Fig. 3

static pressure, the radial displacement components of nodal points are nearly uniform. Beyond this pressure, however, gradual formation of a buckling wave begins to appear. Between 0.6 and 0.8 psi external pressure (indicated by shaded area in Fig. 18) buckling occurs. The load-deformation curves show the gradual formation of a buckling wave up to the point where the curve inverts. The load pertinent to this point is the critical load.

4. Experimental verifications

4.1. *Experimental verification of computer results*

Since, to the writers' knowledge, no analytical stability investigation of PCCP shells has been carried out in the past, it was mandatory to verify the obtained results by a model test. The model used in this experimental approach was fabricated from a rigid-vinyl PVC, manufactured by Union Carbide Company, under the trademark "Bakelite". This material has been selected for the following reasons:

a) It can easily be molded.

b) Its modulus of elasticity is very low in comparison to its tensile strength. (Thus, large deformations are possible without yielding and the same model can be used repeatedly to accumulate a set of data.)

c) The stress-strain curve of "Bakelite" is linearly elastic in the range of interest [8].

A small scale model has been fabricated to conform to the geometrical configuration of a PCCP shell [8]. The fabrication process of the small scale model involved thermal vacuum forming "Bakelite" sheets over a plaster mold

in half sections. Each half shell has then been trimmed to the proper dimensions. Finally, the two halves have been joined with a solvent cement to form the complete PCCP shell model (Fig. 19). The so-obtained model was found to be accurate within 1° on angles and 1% on the radii.

Because of its primary influence on the test results, the modulus of elasticity of the "Bakelite" has been evaluated by separate tensile tests [8] giving $E = 444{,}444$ psi (30,800 kp/cm^2) value. For the lesser significant Poisson's ratio, $\nu = 1/3$ has been used.

Figure 19 shows the test fixtures, which consisted of a center post and two 0.25 in. (0.65 cm) thick aluminum end-plates, machined to match the poly-

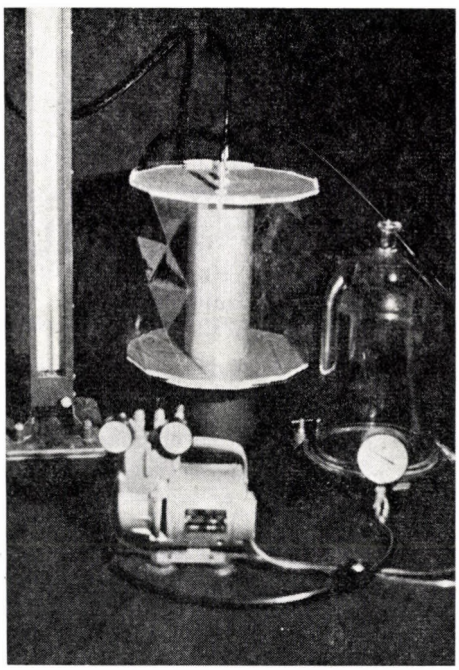

Fig. 19. Model test

hedral boundary of the PCCP shell model. External pressure has been applied by evacuating the air from the interior of the model using a vacuum pump. The level of the vacuum has been measured by a water manometer. Since during buckling the resulting large deformations have considerably decreased the volume of air within the model, the buckling load could be determined with relative ease; i.e. at the time of buckling a dramatic change in the water head could be observed. As Fig. 18 shows, the experimentally determined critical load agrees remarkably well with the results obtained by the finite element

method solution of the problem using framework cells. Similarly, the experimentally determined buckling mode was, for all practical purposes, identical to numerically obtained buckling shape [8].

4.2. *Other pertinent experiments*

Since the PCCP shell is a relatively new structural form, to date, very few analytical or experimental efforts have been carried out. Recently, however, TANIZAWA and MIURA [12] report on two buckling experiments with PCCP shells having 6 and 8 circumferential triangles under external hydro-

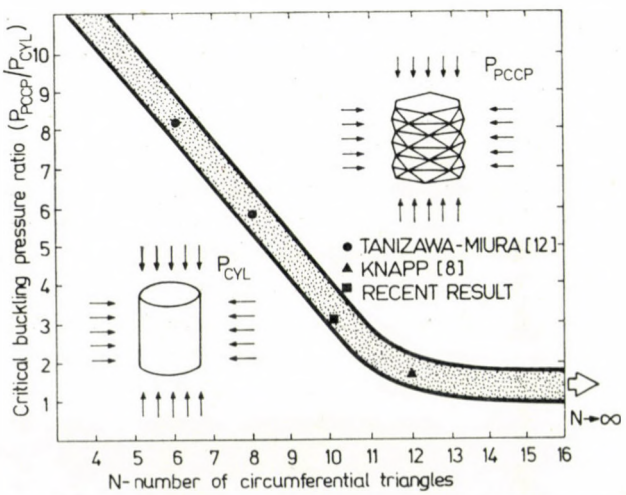

Fig. 20. Buckling tendency of PCCP shells under hydrostatic pressure

static pressure. Although the authors of Ref. [12] have used isosceles triangular faces with $R/t = 104$, and the present effort deals with equilateral triangular faces with $R/t = 238$, it appears to be of interest to compare both results. Figure 20 is a plot of the ratio of buckling pressure for the PCCP shell to that of the comparable "true" cylinder versus the number of circumferential triangular faces, N. A band showing the approximate trend of buckling behavior is plotted in Fig. 20. It is seen that if N is less than 10, buckling pressure ratios become very large. In this case, angles between adjacent triangular faces are large and this results in a significant stiffening effect in the circumferential direction. Also, as N increases, the pressure ratio must approach unity since the PCCP shell approaches the geometry of the perfect cylinder [7]. In view of these results, it appears that PCCP shells offer an improved alternate to the design of cylindrical structures in hydrostatic pressure environments. Additional investigations of the buckling resistance of PCCP shells are in progress.

5. Practial applications

Potential applications of PCCP shells have generally been mentioned by MIURA [7] who proposed their use as large span buildings in architecture, as water reservoirs and as bellows or expansion joints. By the present effort, it has also been demonstrated that the PCCP shell would be well-suited as a structure in the undersea environment where large external pressures govern design. In this case, buckling is usually the primary mode of failure (especially in the shallower depths where the use of economical stress levels require thin-wall shell design), and PCCP shells are apparently more resistant to buckling failure than "true" cylinders having similar geometrical properties. However, this proposed use of PCCP shells is dependent upon the addition of axial rigidity. Although this shell structure possesses large circumferential flexural rigidity, axial rigidity is greatly reduced (path BC, Fig. 2).

A new concept in the design of undersea habitats is depicted in Fig. 21 [49]. Shown in this figure is a PCCP shell which has been modified by the addition of an internal cylinder and radial stiffening rings. The internal cylinder serves the dual role of stiffening the PCCP shell in the axial direction and provides a secondary, "back-up" pressure vessel. The radial stiffening rings provide floor space as well as further restricting radial deformations.

A new structural concept is currently under development which would combine the use of acrylic plastic and the PCCP shell structure to permit the

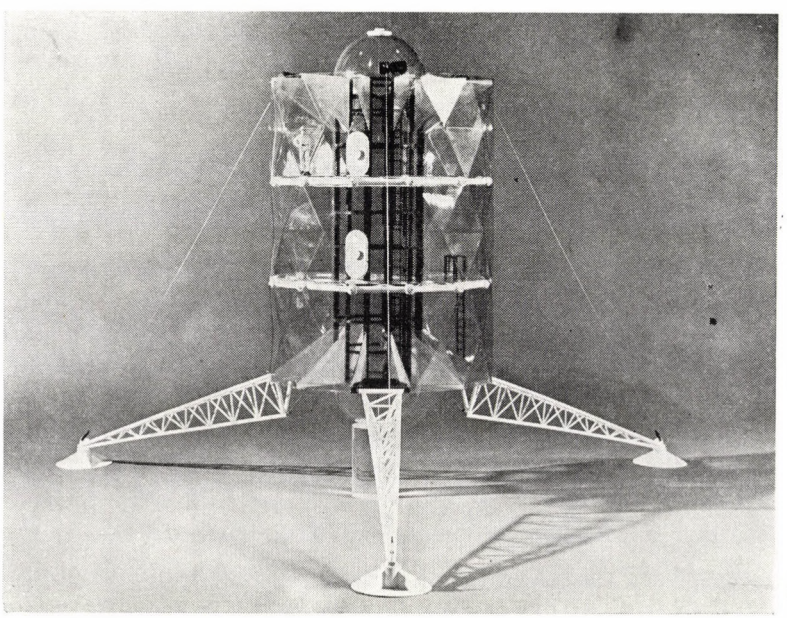

Fig. 21. Undersea habitat

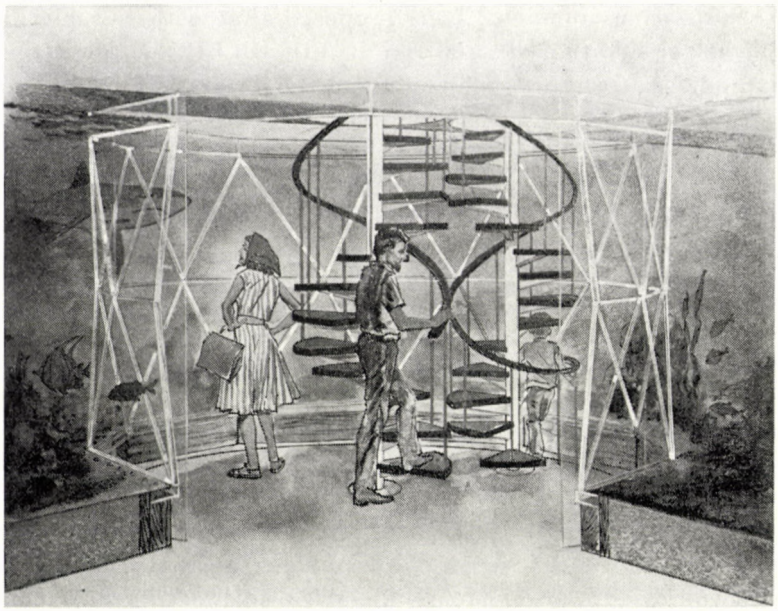

Fig. 22. Acrylic plastic aquarium

construction of high visibility undersea observatories. The PCCP shell surface would be manufactured entirely from acrylic plastic thereby providing the viewer an unrestricted opportunity for visual observation of the marine environment. A 12 ft (3.66 m) diameter, land-based marine aquarium is currently being designed to demonstrate this concept (Fig. 22). The aquarium design is unique in that it represents an inverted approach to the conventional design of aquariums; that is, the observer is located *inside* the acrylic PCCP shell with marine life exhibits on the *outside*. This configuration would give the observer the same experience as being submerged in an actual offshore site. Such structures would be useful for recreation, education and scientific research.

6. Conclusions

Based on a discrete numerical approach, a new type of cylindrical shell structure has been examined under external hydrostatic pressure. It has been demonstrated that the PCCP shell possesses more buckling resistance than a true cylinder having similar overall geometry. Thus, because of its unique structural and geometrical properties, the PCCP shell could be viewed as a new type of "stiffened" cylindrical shell which should function superbly in an ex-

ternal pressurized environment. It is proposed that with suitable modifications, such as the addition of axial rigidity, the PCCP shell ideally could be used as an undersea structure such as a manned habitat or even for submarines. Potential advantages of this concept over the true cylinder include, (1) greater resistance to buckling; (2) large diameter cylinders may be built using modular elements (flat-triangular sheets); (3) greater economy might be realized since special forming operations such as is required to introduce curvature would not be required. Also, this type of structure is inherently less sensitive to manufacturing errors such as out-of-roundness (imperfect circularity of a cylinder). In simple terms, the PCCP shell represents a cylinder which is already greatly out-of-round and small variations in this condition would not markedly affect its structural integrity. Mass production of the modular triangular elements is also possible.

For an actual application of this new structure, a detailed stress analysis must also be carried out. Although the PCCP shell possesses good buckling resistance, the flat triangular plates carry hydrostatic pressure by *membrane* and *bending* stresses. As the size of the triangles is increased, buckling resistance and bending stresses increase simultaneously. Therefore parametric studies should be made to determine the optimum geometry for a specific application. Detailed stress analyses have also been carried out for different PCCP shell geometries [11].

Finally, it should be mentioned that the scope of the present buckling analysis can be further extended by consideration of the nonconservative behavior of the pressure loading. In this case, however, a provision for computing the change in the direction of the loads throughout the deformation process is necessary, especially if large rotations occur.

Acknowledgements

This effort was sponsored by NOAA, Office of Sea Grant, under grant number 04—6—158—44026.

The authors are indebted to Professor KORYO MIURA, University of Tokyo, for his helpful suggestions and his stimulating articles dealing with PCCP shells. Appreciation is also extended to Mr. R. M. KEMPTON for building the model appearing in Fig. 21 and to Mr. Walter UCHIDA for the artist's rendering in Fig. 22.

Dedication

This paper is dedicated to Dr. Eng. Sci. Pál CSONKA, Professor Emeritus, Technical University of Budapest, on the occasion of his 80th birthday in recognition for his numerous contributions to the theory of shell structures and more than half a century of distinguished service to the engineering community.

REFERENCES

1. TIMOSHENKO, S.: Einige Stabilitätsprobleme der Elastizitätstheorie. *Zeitschrift für Mathematik und Physik*, **58** (1910), 337
2. SOUTHWELL, R. V.: On the General Theory of Elastic Stability. *Philosophical Transactions of the Royal Society of London*, Series A, **213** (1914), 187
3. DONNELL, L. H.—WAN, C. C.: Effect of Imperfections on Buckling of Thin Cylinders and Columns under Axial Compression. *Journal of Applied Mechanics*, **17** No. 1, (1950), 73
4. von KÁRMÁN, Th.—TSIEN, H.-S.: The Buckling of Thin Cylindrical Shells under Axial Compression. *Journal of the Aeronautical Science*, **8** (1941), 303
5. MIURA, K.: Inextensional Buckling Deformations of General Cylindrical Shells. *AIAA Journal*, **6** (1968), 966—968
6. MIURA, K.: Concave Polyhedral Shells as New Structural Forms. Proceedings of the 19th Japan National Congress for Applied Mechanics, Science Council of Japan, 1969
7. MIURA, K.: Proposition of Pseudo-Cylindrical Concave Polyhedral Shells. Report No. 442, Institute of Space and Aeronautical Science, University of Tokyo, 1969
8. KNAPP, R. H.: Finite Element Nonlinear Buckling Analysis of a Pseudo-Cylindrical Concave Polyhedral Shell under External Pressure. Doctoral Dissertation, University of Hawaii, 1973
9. ZIENKIEWICZ, O. C.: The Finite Element Method in Engineering Science. McGraw-Hill Publishing Co., London 1971
10. GALLAGHER, R. H.: Finite Element Analysis: Fundamentals. Prentice-Hall, Inc., Englewood Cliffs 1975
11. KNAPP, R. H.: Pseudo-Cylindrical Shells — A New Concept for Undersea Structure Presented at the ASME Winter Annual Meeting, New York, December 5—10, 1976, also, *Journal of Engineering for Industry*, ASME **99** No. 2, (1977) 485—492
12. TANIZAWA, K.—MIURA, K.: Stress Analysis of a Concave Polyhedral Shell. Report No. 523. Institute of Space and Aeronautical Science, University of Tokyo, 1975
13. JENKINS, W. M.: Matrix and Digital Computer Methods in Structural Analysis. McGraw-Hill, London, 1969
14. CONNOR, J. J.—LOGCHER, P. D.—CHAN, S. C. D.: Nonlinear Analysis of Elastic Framed Structures. *Journal of the Structural Division*, ASCE. **94** (1968), 1525—1547
15. DESAI, Ch. S.—ABEL, J. F.: Introduction to the Finite Element Method. Van Nostrand—Reinhold Co., New York 1972
16. HRENNIKOFF, A.: The Finite Element Method in Application to Plane Stress. *Publications of the International Association for Bridge and Structural Engineering*, **28** — II (1968)
17. SZILÁRD, R.: Theory and Analysis of Plates: Classical and Numerical Methods. Prentice-Hall, Inc., Englewood Cliffs 1974
18. HRENNIKOFF, A., et al.: Stability of Plates Using Rectangular Bar Cells. *Publications of the International Association for Bridge and Structural Engineering*, **32** — I (1972)
19. HRENNIKOFF, A.: Plane Stress and Bending of Plates by Method of Articulated Framework. Ph. D. Dissertation, Massachusetts Institute of Technology, 1940
20. HRENNIKOFF, A.: Solution of Problems of Elasticity by the Framework Method. *Journal of Applied Mechanics*, **8** (1941), A-169-175
21. HRENNIKOFF, A.: Framework Method and its Technique for Solving Plane Stress Problems. *Publications of the International Association for Bridge and Structural Engineering*, **9** (1949)
22. MCHENRY, D.: A Lattice Analogy for the Solution of Plane Stress Problems. *J. Inst. Civil Engineering*, **21**, No. 2, (1943—44)
23. SPIERIG, S.: Beitrag zur Lösung von Scheiben-, Platten- und Schalenproblemen mit Hilfe von Gitterrostmodellen. *Abhandlungen der Braunschweigischen Wissenschaftlichen Gesellschaft*, **15** (1963), 133—165
24. CHRISTENSEN, R. M.: Vibration of a 45° Right Triangular Cantilever Plate by a Gridwork Method. *AIAA Journal*, **1** No. 8, (1963)
25. MCCORMICK, C. W.: Plane Stress Analysis. *Journal of the Structural Division*, ASCE, **89** No. ST4, August (1963)
26. LIGHTFOOT, E.: A Grid Framework Analogy for a Laterally Loaded Plate. *International J. Mech.-Sci.*, No. 6, (1964), 201—208
27. RENTON, J. D.: On the Gridwork Analogy for Plates. *J. Mech. Phys., Solids*, **13** (1965), 413—420
28. YETTRAM, Alan L.—HUSAIN, H. M.: Grid-Framework Method for Plates in Flexure. *Journal of the Engineering Mechanics Division*, ASCE, **91** No. EM3, June (1965), 53—64

29. BENARD, E. F.: A Study of the Relationship Between Lattice and Continuous Structures. Doctoral Dissertation, University of Illinois, 1965
30. WALLER, H.: Beitrag zur Berechnung dünner, isotroper, elastischer Platten nach dem Gitterrostverfahren. Dissertation T.-H. Hannover, 1966
31. DIRR, B.: Beitrag zur näherungsweisen Berechnung dünner, isotroper, elastischer Scheiben mit Hilfe von Gitterrostelementen. Dissertation T.-H. Hannover, 1966
32. TEZCAN, S.: Nonlinear Analysis of Thin Plates by Framework Method. *AIAA Journal*, **5** (1967). 1890–1892
33. SALONEN, E.-M.: A Gridwork Method for Plates in Bending. *Acta Polytech. Scand. Civil Eng.* Building Constr. Ser., No. 59, 1969
34. HRENNIKOFF, A.–GANTAYAT, A.: Three-Dimensional Bar Cell for Elastic Stress Analysis. *Journal of the Engineering Mechanics Division*, ASCE, (1970), 313–326
35. OZAKI, M.: Anisotropic Plane Stress Analysis by Equivalent Framework Method. Research Paper No. 43, Building Research Institute, Ministry of Construction, Japanese Government, 1970
36. ZIMMER, A.–GROTH, P.: Elementmethode der Elastostatik-Programmierung und Anwendung. R. Oldenburg Verlag, München–Wien 1970
37. SALONEN, E.-M.: Triangular Framework Model for Plates in Bending. *Journal of Eng. Mech. Div.*, ASCE, **97** No. EM1, (1971), 149–153
38. SMITH, J. H.: Nonlinear Beam and Plate Elements. *Journal of the Structural Division*, ASCE, **98** No. ST3, (1972)
39. HRENNIKOFF, A.–AGRAWAL, K. M.: Superior Rectangular Bar Cells in Plane Stress. Conference on Symmetry, Similarity, and Group Theoretical Methods in Mechanics, Calgary, Canada, Aug. 19–21, 1974
40. BORN, D.: Berechnung von Schalentragwerken mit gekrümmten Gitterrostelementen. Bericht Nr. 72-1, Technische Universität, Braunschweig, 1972
41. TIMOSHENKO. S. P.–GOODIER, J. N.: Theory of Elasticity. McGraw-Hill, New York 1951
42. KNAPP, R. H.: Numerical and Experimental Stability Analysis of a Pseudo-Cylindrical Shell. *Bulletin of the IASS*, No. 59, Vol. XVI-3, Dec., 1975
43. LEVY, S.: Square Plate with Clamped Edges under Normal Pressure Producing Large Deflections. NACA TN 847, Washington, D.C., 1942
44. RODRIGUEZ, A. L.: Finite Element Nonlinear Analysis for Plates and Shallow Shells. Ph. D. Dissertation, Department of Civil Engineering, M.I.T., Cambridge, Mass., 1968
45. YAO, J. C.–JENKINS, W. C.: Buckling of Elliptic Cylinders under Normal Pressure. *AIAA Journal*, **8** (1970), 22–27
46. MARLOWE, M. B.–BROGAN, F. A.: Collapse of Elliptic Cylinders under Uniform External Pressure. *AIAA Journal*, **9** (1971), 2264–2266
47. LOGCHER, R. D.–STURMAN, G. M.: STRUDL– A Computer System for Structural Design. *Journal of the Structural Division*, ASCE, **92** No. ST6, Dec. (1966), 191–212
48. JORDAN, J. C.: ICES: Program Reference Manual. Report R67-50, Dept. of Civil Engineering, Mass. Inst. of Technology, Cambridge, Mass., 1967
49. KNAPP, R. H.: Pressure and Buckling Resisting Cylindrical Undulated Polyhedral Shell Structure. U.S. Patent 4,058,945, Nov. 22, 1977
50. BREBBIA, C.–CONNOR, J. J.: Geometrically Nonlinear Finite Element Analysis. *Journal of Engineering Mechanics Division*, ASCE, April, (1969)

Nichtlineare Stabilitätsuntersuchung von pseudozylindrischen Schalenkonstruktionen. Eine außergewöhnliche geometrische Ausbildung für die Zylinderschalen wurde vorgeschlagen. Die zylindrische Fläche wurde durch eine von flachen Polyedern zusammengesetzte Fläche ersetzt. Die Ausbeulungseigenschaften der auf diese Weise erhaltenen durch äußeren Druck beanspruchten Konkav-Polyeder-Pseudozylinderschale wurde mit Hilfe der Methode der endlichen Elemente untersucht. Zur Kontrolle der Resultate, die mit Hilfe einer Rechenanlage erhalten wurden, wurde ein Modellversuch ausgeführt. Diese beiden, voneinander unabhängig durchgeführten Untersuchungen hatten eine ausgezeichnete Übereinstimmung zur Folge. Eine Gegenüberstellung dem Ausbeulungsdruck einer „echten" Zylinderschale beweist, daß die vorgeschlagene Modifikation der geometrischen Ausbildung eine viel stärkere Ausbeulungsfestigkeit ergibt. Dabei besitzt diese Pseudozylinderschale auch noch andere wünschenswerte konstruktionelle Eigenschaften, sowie eine verhältnismäßig einfache Herstellung und eine erhebliche Unempfindlichkeit gegen Anfangsfehlstellen. Deswegen kann diese Zylinderschalenart vorteilhaft für verschiedene Unterseewerke angewandt werden.

Анализ нелинейной устойчивости ложных бочарных оболочек. В своей работе для анализа бочарных оболочек использую не обычную геометрическую форму. Цилиндрическую поверхность бочарной оболочки авторы замещают поверхностью, образованной из плоских полиэдров. Авторы исследуют свойства вспучивания полученной таким образом ложной бочарной оболочки с конкавной полиэдрической поверхностью, на которую действует внешнее давление, с помощью приближенного метода конечных элементов. Для контроля результатов, полученных с помощью вычислительной машины, выполнены опыты на модели. Эти два исследования, выполненные независимо друг от друга, подтверждены отличным совпадением полученных результатов. На основе сравнения с критическим сжатием на выпучивание действительной бочарной оболочки можно установить, что рекомендованное изменение геометрического оформления в значительной мере повышает прочность в отношении выпучивания. Наряду со сказанными выше такие бочарные облочки обладают еще рядом выгодных свойств как, например, относительно легкая изготовляемость их и большая нечувствительность к начальным неточностям. Следовательно, такие конструкции можно выгодно применять для создания ряда подводных конструкций.

Acta Technica Academiae Scientiarum Hungaricae, Tomus 86 (1—2), pp. 43—53 (1978)

ON THE DESIGN OF A QUADRATIC WEIR WITH SEMI-CUBIC PARABOLA AS THE BASE

K. KESHAVA MURTHY and K. GOPALAKRISHNA PILLAI*

[Manuscript received April 2, 1977]

This paper deals with the design of a quadratic notch, which finds application in the proportionate method of flow measurement in a by-pass, such that the discharge through it is proportional to the square root of the head measured above a certain datum. The weir notch consists of a bottom in the form of a semi cubic parabola of top width '$2W$' and depth 'a' over which a designed curve is fitted. Using the 'slope discharge continuity theorem' the problem is reduced to the determination of an exact solution of the Volterra's integral equation in the Abel's form. It is shown that in this case of the quadratic weir notch, the reference plane or the datum is situated at 5/6 a above the crest of the weir so that the discharge is proportional to the square root of the head measured above the datum.

1. Introduction

The importance of weirs as discharge measuring devices, has been well recognized; what is less known is their application as velocity controlling devices and consequent application as outlet weirs in grit chambers. The discharge through a weir of given shape is a function of h, the head causing flow, e.g. in the case of a rectangular weir the discharge is proportional to $h^{3/2}$; in the case of a triangular weir or V-notch, it is proportional to $h^{5/2}$; in the case of a parabolic weir it is proportional to $h^{7/2}$ etc. The reverse problem of finding the shape of a weir to produce a known head–discharge relationship known as the 'Problem of Proportional Weirs' is more complex. The problem of proportional weirs, apart from having considerable practical applications in several fields like hydraulic engineering, chemical engineering, irrigation and sanitary engineering, is endowed with fundamental and academic interest in hydraulics. The first ever attempt to the design of a proportional weir was made by Oscar VAN PELT STOUT [1] in 1896 when he designed a linear proportional weir. He found out that the curve $y \simeq x^{-1/2}$ where y and x are horizontal and vertical axes respectively, produced a discharge proportional to the linear power of the head. This weir is physically unrealizable as it tends to infinite width at the base. This defect was overcome by SUTRO by providing

* Department of Civil Engineering, Indian Institute of Science, Bangalore 560012, India

a rectangular weir of width $2W$ and depth A as base, over which a designed curve is fitted. This weir is well known as SUTRO weir. The discharge through this weir (for flows above the base) is proportional to the head measured above a reference plane or datum line situated $a/3$ above the crest. It was believed till recently [2, 3] that the datum can be chosen arbitrarily and the choice of the datum at $a/3$ above the crest in the case of the Sutro weir was meant for mathematical convenience. This erroneous notion has mainly been responsible for much of the empiricism and obscurity of this important branch of hydraulics.

COWGILL and BANKS [4, 5] have shown that the equation of the weir producing a discharge $Q = KH^m$, K being a constant, is given by

$$y = \frac{2K}{C_d\,(2g\pi)^{1/2}} \cdot \frac{\Gamma(m+1)}{\Gamma\,(m-1/2)}\, x^{m-3/2}, \quad m > \frac{1}{2}$$

where y and x are the horizontal and vertical axes respectively, g, the acceleration due to gravity and C_d the coefficient of discharge. By putting $m = 3/2$, $5/2$, $7/2$, we get the profiles of the rectangular, triangular and parabolic weirs. It is evident from the above equation that for $m < 3/2$, the profile tends to infinite width at the base, i.e. as $x \to 0$, $y \to \infty$, which is physically unrealizable. Stout's weir is one such case ($m = 1$).

An exact solution for the quadratic weir ($m = 1/2$) earlier attempted by HASZPRA [6] was given by KESHAVA MURTHY [7]. In that, the equation of the weir becomes fastly convergent giving rise to a proportional orifice at depths of flow of $3a$ and above where a is the depth of the rectangular weir base. In this paper another design for the quadratic weir is given which brings down the level of orifice point, thus reducing the height of the proportional orifice.

2. Formulation

The weir is assumed to have a base in the form of a semicubic parabola given by $y' = cx'^{3/2}$ where c is a dimensional constant and y' and x' are the horizontal and vertical axes respectively. Let the equation of the weir above be $y = f(x)$ which has to be determined. The weir is assumed to be symmetrical about the vertical axis, and have a constant coefficient of discharge C_d. The half cross section of the weir is shown in Fig. 1. When the depth of flow is "h" above the y-axis, the discharge through the portion of the weir below the y-axis is

$$q_1 = 2\,C_d \sqrt{2g} \int_0^a y' \sqrt{h + a - x'}\, dx' =$$

$$= 2\,C_d \sqrt{2g} \int_0^a cx'^{3/2} \sqrt{h + a - x'}\, dx' .$$

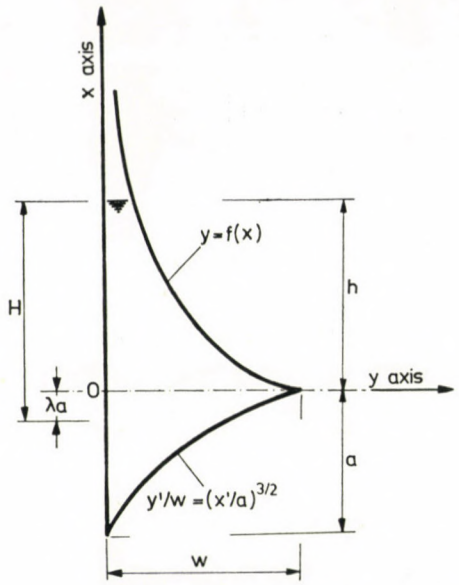

Fig. 1. Definition sketch

After integration we obtain

$$q_1 = Kc\left[\frac{\pi(h+a)^3}{32} - \frac{(ah)^{3/2}}{3} - \frac{(h^2-a^2)}{8}(ah)^{1/2} - \right. \\ \left. - \frac{(h+a)^3}{16}\sin^{-1}\left(\frac{h-a}{h+a}\right)\right] \tag{1}$$

where $K = 2C_d\sqrt{2g}$.

The discharge through the curved portion of the weir above the y-axis is

$$q_2 = K\int_0^h \sqrt{h-x}\,f(x)\,dx\,. \tag{2}$$

The total discharge through the weir is

$$Q = q_1 + q_2 = Kc\left[\frac{\pi(h+a)^3}{32} - \frac{(ah)^{3/2}}{3} - \frac{(h^2-a^2)}{8}(ah)^{1/2} - \right. \\ \left. - \frac{(h+a)^3}{16}\sin^{-1}\left(\frac{h-a}{h+a}\right)\right] + K\int_0 \sqrt{h-x}\,f(x)\,dx\,.$$

We want this to be proportional to $(h+\lambda a)^{1/2}$ where λ is the datum constant. In other words the discharge through the weir is proportional to the square root of the head measured above the reference plane. Therefore,

$$Kc\left[\frac{\pi(h+a)^3}{32}-\frac{(ah)^{3/2}}{3}-\frac{(h^2-a^2)}{8}(ah)^{1/2}-\right.$$
$$\left.-\frac{(h+a)^3}{16}\sin^{-1}\left(\frac{h-a}{h+a}\right)\right]+K\int_0^h\sqrt{h-x}\,f(x)\,dx=b(h+\lambda a)^{1/2} \qquad (3)$$
$$h\geqq 0$$

where b is the proportionality constant which fixes the dimensions of the weir.

3. Mathematical analysis

The Volterra's integral equation of the first kind

$$\int_a^x\frac{f(\xi)}{(x-\xi)^\alpha}\,d\xi=F(x),\quad 0<\alpha<1 \qquad (4)$$

is called the Abel's integral equation, and appears in the solution of equation (3). The solution of this equation under certain conditions [8] is

$$y(x)=\frac{\sin(\alpha\pi)}{\pi}\int_a^x\frac{F'(\xi)}{(x-\xi)^{1-\alpha}}\,d\xi. \qquad (5)$$

In what follows the problem is described in the above form.

The first condition to be satisfied by Eq. (3) is that when $h=0$, there is no flow through the curved portion (continuity of discharge with respect to head). Hence, putting $h=0$ in Eq. (3), we have

$$Kc\left(\frac{\pi a^3}{16}\right)=b\sqrt{\lambda a},$$

i. e.

$$b\sqrt{\lambda}=\frac{\pi WKa}{16} \qquad (6)$$

since $W=ca^{3/2}$.

Differentiating both sides of Eq. (3) with respect to h and rearranging, we have

$$\int_0^h\frac{f(x)}{\sqrt{h-x}}\,dx=\frac{b}{K\sqrt{h+\lambda a}}+\frac{3}{8}c\left[\frac{(10a+6h)}{3}(ah)^{1/2}+\right.$$
$$\left.+(h+a)^2\sin^{-1}\left(\frac{h-a}{h+a}\right)-\frac{\pi}{2}(h+a)^2\right]. \qquad (7)$$

The second condition to be satisfied arises out of the slope discharge continuity theorem [7] requiring the continuity of the derivative of the discharge at

points of discontinuity. Putting $h = 0$ in the right-hand side of Eq. (7), the above condition yields,

$$\frac{b}{\sqrt{\lambda a}} = \frac{3}{8}\pi W K \sqrt{a},$$

i.e.

$$\frac{b}{\sqrt{\lambda}} = \frac{3}{8}\pi W K a. \tag{8}$$

Solving Eqs (6) and (8) for b and λ we have

$$b = \frac{\sqrt{6}}{16}\pi W K a, \tag{9}$$

and

$$\lambda = 1/6.$$

The value of λ fixes the datum or reference plane of the weir from which all heads are reckoned. It is situated at $5a/6$ above the crest of the weir. When the base weir dimensions a and W are known the constant of proportionality is determined from (9).

It is seen that Eq. (7) is in the Abel's form of Eq. (4) and can be solved as in Eq. (5). Here $\alpha = 1/2$. Applying this, we find after some laborious integration and subsequent simplification:

$$y = W\left[\left(1 + \frac{x}{a}\right)^{3/2} - (x/a)^{3/2} - \frac{3}{2}(x/a)^{1/2} - \frac{9}{4}\frac{(x/a)^{1/2}}{(1 + 6x/a)}\right]. \tag{10}$$

The co-ordinates of the various points on the above curve are given in Table 1.

A typical weir (which has been experimented) having $a = 4''$ and $W = 10''$ is shown in Fig. 2.

4. Proportional orifice

An examination of Table 1 reveals a significant fact *viz.*, that the value of the function y very rapidly decreases with x/a and is almost equal to zero for $x/a \geq 1{,}1$ and the value of y/W becomes zero correct to the fourth decimal place for a value of $x/a = 7$. Beyond this we can say that the weir acts like a proportional orifice for all practical purposes. As this weir passes discharges proportional to square root of the head (above a datum) both while acting as a notch as well as an orifice, this weir gives another example of a notch-orifice first proposed by KESHAVA MURTHY [7]. However, before concluding this it is necessary to show that the function is positive throughout the range

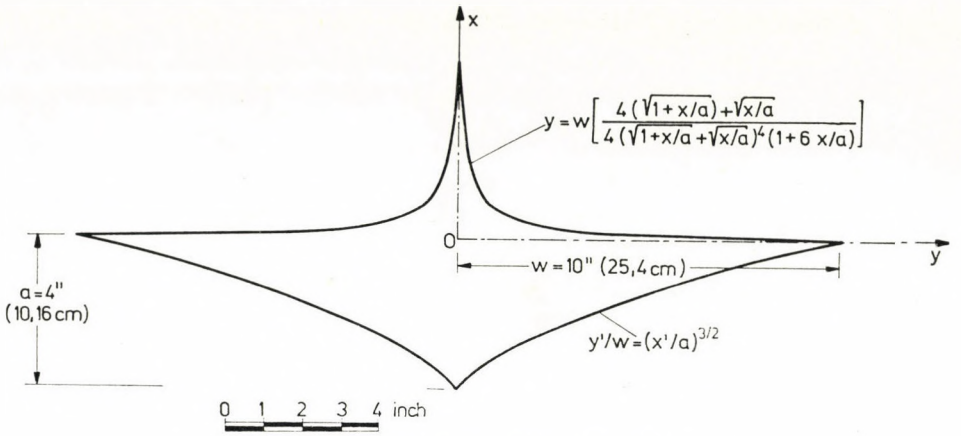

Fig. 2. Semi-cubical quadratic weir

$0 \leq x \leq \infty$ or in other words it does not cross the x-axis. Equation (10) can be put in a more convenient form

$$\frac{y}{W} = \frac{4\left(\sqrt{1+x/a}\right) + \sqrt{x/a}}{4\left(\sqrt{1+x/a} + \sqrt{x/a}\right)^4 (1+6x/a)} \tag{11}$$

when $x = 0$, $y = W$ and when $x \to \infty$, $y \to 0$. Differentiating Eq. (10) or Eq. (11) with respect to x and simplifying, we have

$$\frac{dy}{dx} = -\frac{3W}{8a\sqrt{x/a}} \left[\frac{16(x/a)^{3/2} + 16(x/a)^{1/2} + (1+x/a)(5+34x/a)}{\left(\sqrt{1+x/a}\right)(1+6x/a)^2 \left(\sqrt{1+x/a} + \sqrt{x/a}\right)^4} \right] \tag{12}$$

which is negative for all positive values of x. As the curve starts from $y = W$ at $x = 0$, and since as $x \to \infty$, $y \to 0$ and does not change sign of its slope in $0 \leq x \leq \infty$ it is concluded that $y = f(x)$ is positive and continuously

Table 1

Co-ordinates of the points on $f(x)$ given by Eq. (10)

x/a	y/W	x/a	y/W	x/a	y/W
0,1	0,2030	0,8	0,0108	4,0	0,0003
0,2	0,0962	0,9	0,0086	5,0	0,0002
0,3	0,0562	1,0	0,0070	6,0	0,0001
0,4	0,0363	1,1	0,0058	7,0	0,0000
0,5	0,0252	1,5	0,0030	For all further values of x/a, y/W can be taken as zero, for all practical purposes	
0,6	0,0183	2,0	0,0016		
0,7	0,0139	3,0	0,0007		

decreasing throughout $0 \leq x \leq \infty$. In other words, Eq. (10) gives an approximate solution to the Fredholm integral equation

$$Kc\left[\frac{\pi(h+a)^3}{32} - \frac{(ah)^{3/2}}{3} - \frac{(h^2-a^2)}{8}(ah)^{1/2} - \frac{(h+a)^3}{16}\sin^{-1}\left(\frac{h-a}{h+a}\right)\right] +$$

$$+ K\int_0^{na}\sqrt{h-x}\,f(x)\,dx = b\sqrt{h+\frac{1}{6}a}$$

for $n \geq 1{,}1$. The larger the value of n, closer will be the approximation. However, the accuracy obtained by taking $n = 1{,}1$ is sufficiently good that it does not warrant the taking of higher values of n. Further the practical consideration involved in the cutting of the weir inhibits the taking of too high a value of n. Practically, after $x = 1{,}1a$, weir acts as a "notch of zero width", i.e. a proportional orifice.

5. Example

Suppose it is desired to design a quadratic weir such that it will allow a discharge of about 40 litres/sec at a depth of flow of 55 cm and the minimum depth of flow is 15 cm.

We choose $a = 15$ cm, the effective depth

$$H = h + \frac{1}{6}a = 55 - \frac{5}{6}15 = 42{,}5 \text{ cm}$$

$$b\sqrt{42{,}5} = 40\,,$$

therefore $b = 6{,}137$.

From Eq. (9) $b = (\sqrt{6}/16)\,\pi W \times 2C_d\sqrt{2g}\,a = 6{,}137$

Taking $C_d = 0{,}61$, we get $W = 15{,}75$ cm. Choose $W = 16$ cm.

Therefore $a = 15$ cm, $W = 16$ cm.

6. Experiment

Typical experiments were conducted with one asymmetrical ($a = 6$ in, $W = 6$ in) and two symmetrical ($a = 4$ in, $W = 10$ in; and $a = 6$ in, $W = 6$ in) notches to check the theory. The experimental details are shown in Fig. 3. The weirs were cut in 6,5 mm mild steel plates. The boundary of the weir was carefully marked on the plate by a scratch-awl. The opening was then cut roughly by a do-all machine and then accurately filed to the required shape. The weir had a sharp edge of 1,5 cm with a 45° chamfer. The cutting and filing had to be done with great care at the tips. The weir was fixed at the end of a rectangular channel 18,5 m long, 1,2 m wide and 1,1 m deep with its crest

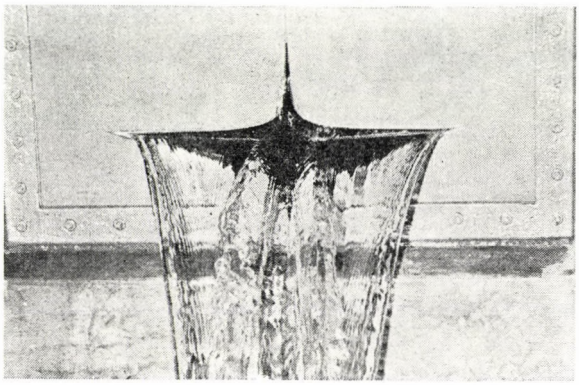

Fig. 3. Quadratic weir discharging at low head as a notch

22,5 cm above the bed of the channel. The water is fed through a head tank measuring 2,25 m × 2,25 m × 1,8 m, to which water is supplied by a pump capable of giving a maximum discharge of 110 litres/sec. The head over the weir was measured with an electronic point gauge having a least count of 0,0025 cm. The discharges were recorded in a tank measuring 4,52 m × × 4,52 m × 1,5 m, through readings in a perspex tube of 2 cm diameter connected to the tank at the bottom at one end (Fig. 4). Proper stilling at the entrance of the tube inside the tank ensured gradual rise without fluctuations.

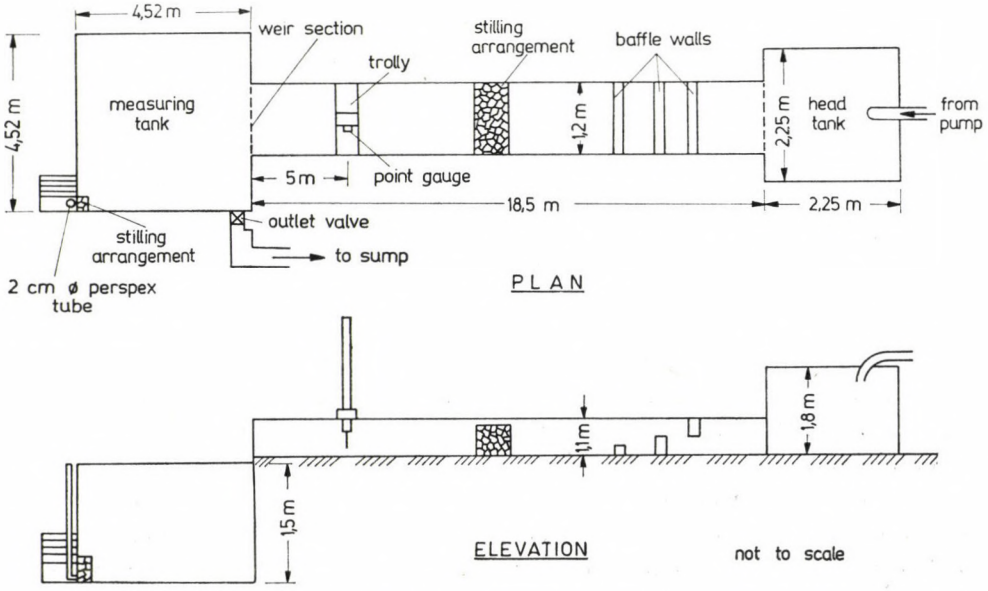

Fig. 4. Experimental set-up

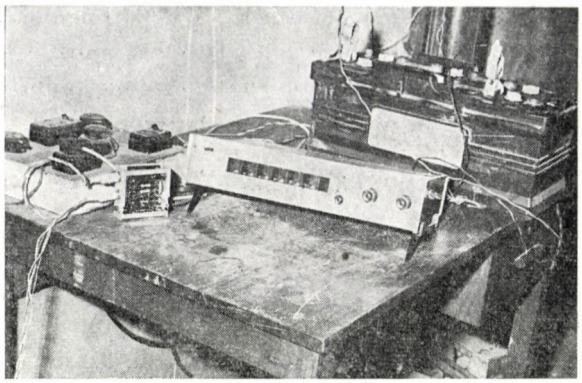

Fig. 5. The electronic timer

The discharge is measured by finding the time taken for the water to raise from one indicator fixed in the perspex tube to another fixed exactly at a distance of 61 cm. The points are connected to the leads of an electronic timer (Fig. 5) through a start and stop electronic mechanism. As soon as the water touches the lower indicator the timer starts, and automatically stops when the water touches the upper indicator. The timer used was an APLAB 15 MHz digital time and frequency counter type IC12 capable of reading 10 microseconds. Each experiment was repeated 3 times to ensure accuracy. At least

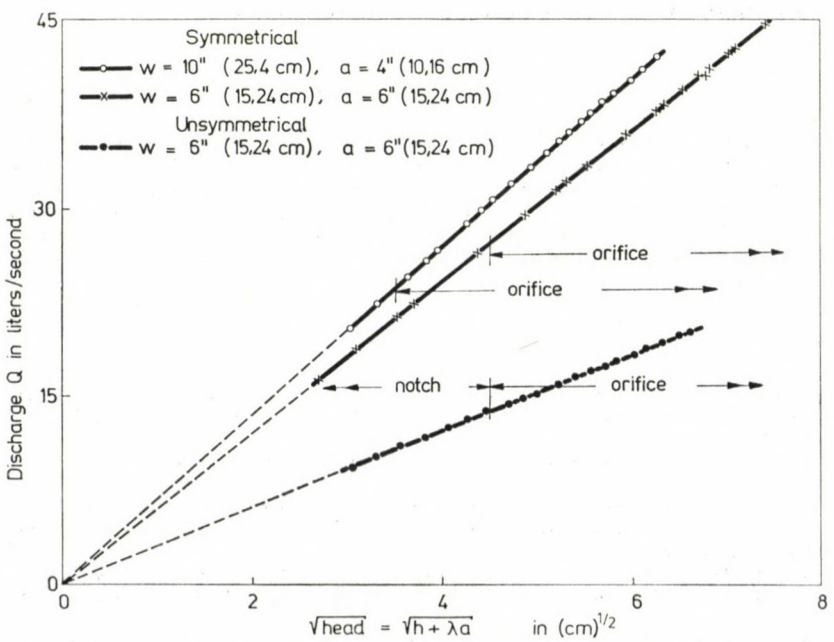

Fig. 6. Graph of discharge versus square root of head

15 minutes were allowed between two sets of experiments to allow for the water level to stabilize. The graph of $h + (1/6)\,a$ is plotted in Fig. 6 for the 3 weirs experimented. The experiments show a remarkable agreement with the theory and show a constant coefficient of discharge of 0,61.

7. Conclusions

In this paper an exact solution to the design of the quadratic weir notch having the base in the form of a semicubic parabola of width $2W$ and depth a and giving a discharge proportional to the square root of the head measured above a datum $5a/6$ above the crest is obtained. An interesting feature of the weir is that its width becomes negligible after $2{,}1a$ above the crest converting the weir into a proportional orifice, thus giving another example for the notch-orifice. This incidentally gives another good approximate solution to a particular integral equation of Fredholm's First Kind. Experiments with one asymmetrical and two symmetrical weirs show a constant coefficient of discharge of 0,61.

The quadratic weir should prove as a sensitive discharge measuring device as 1 per cent error in the measurement of the head would result in only 0,5 per cent error in calculating the discharge as against 1,5 per cent error in the case of a rectangular weir, and 2,5 per cent error in the case of a V-notch. This weir should prove useful as a sensitive discharge measuring device in laboratories, in irrigation, and also in orifice gauging tanks.

Acknowledgements

The authors are thankful to Professor B. V. RANGANATHAM for his encouragement and support, and to Professor N. S. LAKSHMANA RAO for his interest. One of the authors (K. GOPALA-KRISHNA PILLAI) is a recipient of the fellowship of the Ministry of Education, Government of India, under the Quality Improvement Programme. He is grateful to the authorities of the N. S. S. College of Engineering, Kerala for deputing him to the Institute. The authors thank the authorities of the Indian Institute of Science for providing the necessary facilities for conducting this work.

REFERENCES

1. STOUT, O. V. P.: A New Form of Weir Notch. *Trans. Nebraska Eng. Soc.*, **1** (1897) 13
2. REDDICK, H. W.—MILLER, F. H.: Advanced Mathematics for Engineers. John Wiley and Sons, Inc., New York 1957, 174
3. DAVIS, C. V.: Handbook of Applied Hydraulics. McGraw-Hill Book Co., New York 1952, 1106
4. COWGILL, P.: The Mathematics of Weir Forms. *Quart. Appl. Math.*, **2** (1944) 142
5. BANKS, R. B.: A Note on the Generalized Weir Equation. *Northwestern Univ., Paper* HP 0654, November 20, (1954)
6. HASZPRA, O.: The Problem of the Quadratic Weir. *Acta Techn. Hung.* **5** (1965) 121
7. KESHAVA MURTHY, K.: On the Design of Quadratic Weirs. *J. Franklin Inst.* **287** (1969) 159
8. WHITTAKER, E. T.—WATSON, G. N.: A Course in Modern Analysis. London, Cambridge University Press, 1927

Über die Ausbildung eines quadratischen Überfalls mit nach einer kubischen Halbparabel ausgebildeten Wehrschneide. Behandelt wird die Ausbildung eines quadratischen Meßwehrs, das in der Proportionalitätsmethode der Mengenmessung in einer Umlaufleitung Anwendung findet, worin, die Abflußmenge zur Quadratwurzel der über einem Bezugsniveau gemessenen Fallhöhe proportional ist. Der Überfall besteht aus einer Sohle in Form einer kubischen Halbparabel mit einer Schneidenbreite von $2W$ und Tiefe a, worüber eine Kurve entworfen wird. Benutzt man das Theorem der Kontinuität der Gefällenabflußmenge, so wird das Problem zur Ermittelung einer exakten Lösung nach der in der Abelschen Form angegebenen Volterraschen Integralgleichung vereinfacht. Es wird nachgewiesen, daß in diesem Fall des quadratischen Einschnitts das Bezugsniveau sich in einer Höhe von $5/6\,a$ über der Wehrschneide befindet, so daß die Abflußmenge proportional zur Quadratwurzel der über dem Bezugsniveau gemessenen Fallhöhe ist.

Проектирование квадратичного мерного водослива, оформленного в виде параболы полутретей степени. Данная работа занимается проектированием такого квадратичного мерного водослива, который применен при методе пропорциональности измерения количества воды на обходном трубопроводе с таким расчетом, что протекающий расход пропорционален квадратному корню напора, измеряемому над данным уровнем сравнени Данная часть отверстия мерного водослива имеет форму в виде параболы полутретей степени и имеет ширину короны в $2W$ и глубину a, для которой построена огибающая. Применение теоремы сплошности падающего расхода упрощает задачу до строгого решения интегрального уравнения Вольтера, имеющего форму Абеля. Показано, что в данном случае квадратичного мерного водослива относительная плоскость находится на $5/6\,a$ высоты над короной водослива так, что расход является пропорциональным квадратному корню напора над сравнительной поверхностью.

Acta Technica Academiae Scientiarum Hungaricae, Tomus 86 (1—2), pp. 55—77 (1978)

CONTINUUM METHOD OF ANALYSIS FOR DOUBLE LAYER SPACE TRUSSES OF "HEXAGONAL OVER TRIANGULAR" MESH

L. KOLLÁR

DOCTOR OF TECHN. SCI.

[Manuscript received September 22, 1976]

Structural consequences of the instability of one chord plane of a double layer space truss of "hexagonal over triangular" mesh as well as conditions for obtaining a statically determinate truss have been analyzed. Structural characteristics of "grid tubes" providing for torsional stiffness permit to deduce the set of differential equations of a continuum equivalent to the space truss. Equations of boundary conditions as well as the method of computing bar forces from internal forces of the continuum have been presented.

1. Description of the structure

An interesting type of double layer space trusses is one with triangular mesh in the lower chord plane and hexagonal mesh in the upper chord plane (Fig. 1). Triangle corners are under hexagon centres, and are connected by six bars each to the hexagon corners.

This structure is rather aesthetical, it is easy to prefabricate from hexagonal pyramids and straight bars, and lends itself for covering ground plans with 60° or 120° corner angles.

It will now be attempted to clear the structural behaviour of this space truss and to establish equations for the equivalent continuum.

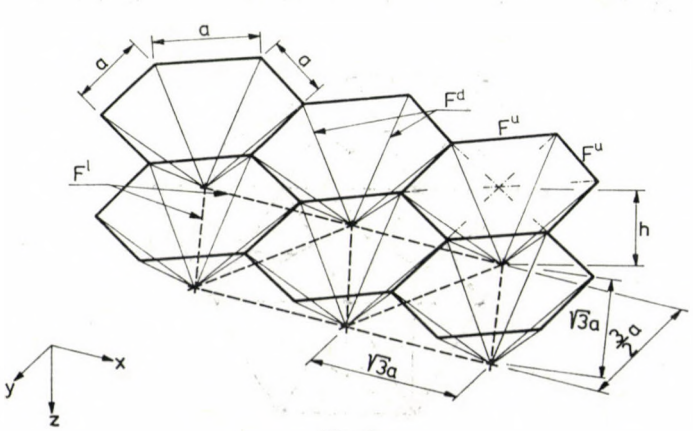

Fig. 1

2. The problem of redundancy

The top chord of the structure, consisting of hexagons, is not rigid in its plane (similarly to space truss in [2]). The problems of the number of supports needed for structural stability (to be statically determinate or indeterminate) and of the relation between the number of redundancies and the number of hexagonal pyramids have to be investigated.

Let us assume first hexagon corners to match edges of the structure (triangle corners being inwards), and hexagon corners at the edge — except those in concave points — to be supported by vertical bars. (In addition, three horizontal supporting bars not passing through one point have to be applied to counteract "rigid-body" motion in horizontal direction.)

The necessary condition for a space truss to be statically determinate is expressed by the known equation

$$r + t = 3c \tag{1}$$

with r bars, t supporting bars and c hinges in the system. For $r + t < 3c$, the structure is unstable, and for $r + t > 3c$, it is hyperstatic.

Applying this condition to the structure consisting of one, two, three etc. pyramids, in this order, we obtain the data compiled in Table 1 (vertical supporting bars are indicated by dots in the ground plans).

Data in Table 1 lead to the following conclusions: Structure a) of a single pyramid is statically determinate. Addition of every new pyramid changes redundancy of the structure depending on how it joins the previous ones. Possible cases have been recapitulated in Table 2.

Thus an illustrative construction rule is given that permits avoiding design of an unstable structure [Table 1, cases b) and c)].

Let us have a look also at the case where the triangle mesh reaches until the edge supports while hexagons lay inside (Fig. 2). The number of redundan-

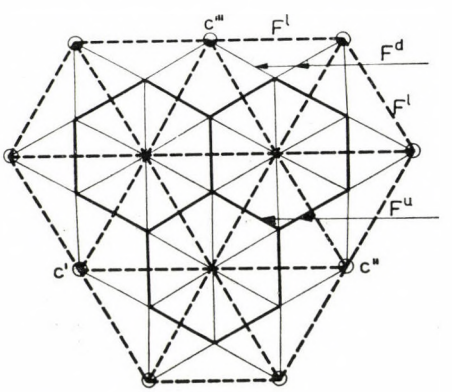

Fig. 2

Table 1

Ground plan	r			t		$r+t$	c		$3c$	Redundancy (instability)
	Upper chord	Diagonal	Lower chord	Vertical	Horizontal		Upper chord	Lower chord		
a, 	6	6	—	6	3	21	6	1	21	determinate
b, 	11	12	1	8	3	35	10	2	36	1× unstable
c, 	16	18	2	10	3	49	14	3	51	2× unstable
d, 	15	18	3	9	3	48	13	3	48	determinate
e, 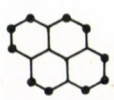	19	24	5	10	3	61	16	4	60	1× redundant
f, 	30	42	12	12	3	99	24	7	93	6× redundant

Table 2

Joining mode	Change in redundancy
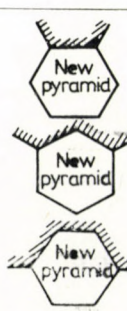	Decrease by 1 Increase by 1 Increase by 3

cies is seen to be higher than in the case where there are no extreme triangles but extreme corners of hexagons are supported (Table 1, case d). Namely all edge nodes but c', c'' and c''' join the inner structure by three bars in a statically determinate manner. Nodes c', c'' and c''', on the straight edge sections join the inner part by four bars each, thus increasing the number of redundancies by 3×1. Besides, nine bars along the edge are "superfluous", increasing the redundancy degree by 9. Number of vertical supporting bars being inaltered, at last the number of redundancies will amount to 12.

3. Structural properties of the space truss

3.1 *Assumptions*

Now a space truss of a mesh consisting of regular triangles and hexagons will be considered. Cross section areas of all upper chord bars are F^u, those of diagonals F^d and of lower zone bars F^l.

A continuum statically equivalent to the space truss is to be established. In case of simpler space trusses [4] this has been a plate with tensile (shear) and bending (torsional) rigidities equal to the corresponding rigidities of the space truss referred to unit width. In the actual case there are two additional complications: on one hand, due to the difference between the lower and the upper chords, the bending (plate-like) forces and reactions are accompanied by an "auxiliary plane force system" in one chord, preventing the equivalent continuum from being a simple plate, and on the other hand, the chord of hexagonal mesh is unstable in itself, involving restrictions for the internal force system.

Deformation due to transverse shear (distorsion in the vertical planes) will be ignored.

3.2 *Structural behaviour of the chords*

The triangular mesh of the lower chord (Fig. 3) has clearly defined equivalent tensile ($A_{11} = A_{22}$) and shear (A_{33}) rigidities [4].

Tensile rigidities in directions x and y:

$$A^l_{11} = A^l_{22} = \frac{3\,EF^l}{4a}\,. \tag{2a}$$

Transversal tensile rigidities:

$$A^l_{12} = A^l_{21} = \frac{EF^l}{4a}\,. \tag{2b}$$

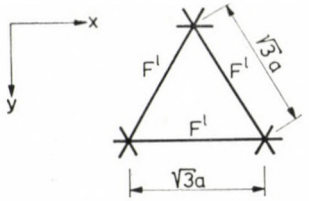

Fig. 3

Shear rigidity:

$$A_{33} = \frac{EF^l}{4a} . \tag{3}$$

Thus, rigidity matrix of the lower chord becomes:

$$\mathbf{A}^l = \begin{bmatrix} A^l_{11} & A^l_{12} & 0 \\ A^l_{12} & A^l_{11} & 0 \\ 0 & 0 & A^l_{33} \end{bmatrix} . \tag{4}$$

Rigidity matrix is interpreted as usual, according to [1]:

$$\mathbf{n} = \mathbf{A}\boldsymbol{\epsilon} \tag{5a}$$

where internal chord forces, summarized in a vector are:

$$\mathbf{n} = \begin{bmatrix} n_x \\ n_y \\ n_{xy} \end{bmatrix} \tag{5b}$$

and strains comprized in a vector:

$$\boldsymbol{\epsilon} = \begin{bmatrix} \varepsilon_x \\ \varepsilon_y \\ \gamma_{xy} \end{bmatrix} . \tag{5c}$$

The hexagonal mesh of the upper chord is unstable: it is able to perform the three deformations in Fig. 4 without resistance.

Deformation in Fig. 4a corresponds to angular distorsion γ_{xy} due to pure shear, hence the hexagonal mesh can take no shear n_{xy}.

Deformation in Fig. 4b is characterized by:

$$\varepsilon_x^{\text{unstab}} = -\varepsilon_y^{\text{unstab}} \tag{6}$$

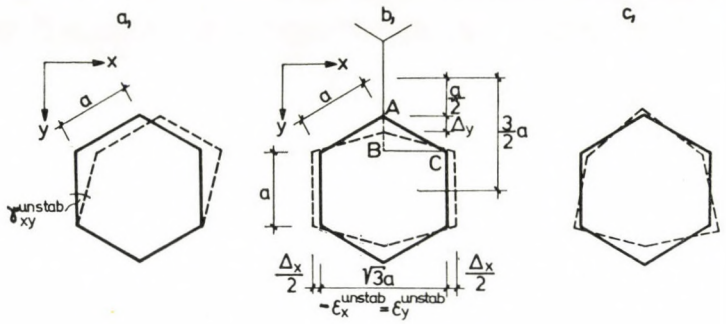

Fig. 4

obvious from the following short deduction. Of a displacement Δ_y of the corner A in direction y referring to a length $3a/2$, converted to unit length, we obtain:

$$\varepsilon_y^{\text{unstab}} = \frac{2\Delta_y}{3a}.$$

The pertaining displacement $\Delta_x/2$ is obtained from the Pythagorean theorem written for the deformed triangle ABC:

$$a^2 = \left(\frac{a}{2} - \Delta_y\right)^2 + \left(\frac{\sqrt{3}}{2}a + \frac{\Delta_x}{2}\right)^2. \tag{7a}$$

Omitting small terms of the second order containing Δ^2 and subtracting the Pythagorean theorem for the original triangle ABC

$$a^2 = \left(\frac{a}{2}\right)^2 + \left(\frac{\sqrt{3}}{2}a\right)^2 \tag{7b}$$

we obtain

$$\Delta_x = \frac{2}{\sqrt{3}}\Delta_y. \tag{8}$$

Since Δ_x has to be referred to the length $\sqrt{3}a$:

$$\varepsilon_x^{\text{unstab}} = -\frac{\Delta_x}{\sqrt{3}a} = -\frac{2\Delta_y}{3a} = -\varepsilon_y^{\text{unstab}}. \tag{9}$$

Consequently, the hexagonal mesh can only withstand hydrostatic compression (or tension), where $n_x = n_y$. This effect is, however, resisted by a clearly defined rigidity of the network, such as:

Hydrostatic tension in a hexagon means a system of forces corresponding to Fig. 5: bar forces developing in all bars are equal to corner forces P. Hence, in the section x–x, one bar force P acts on a length $\sqrt{3}a$, the corresponding

continuum tensile force $n_x = n_y$ is thus:

$$n_x = n_y = \frac{P}{\sqrt{3}a} . \tag{10}$$

All bars elongate by

$$\varepsilon_{\text{bar}} = \frac{P}{EF^u} \tag{11}$$

giving an elongation $\varepsilon_y^{\text{dil}} = \varepsilon_{\text{bar}}$ in both vertical and skew bars. ($\varepsilon_x^{\text{dil}}$ in direction x is certainly of the same value). Thus, the equivalent dilatation tensile rigidity is:

$$A_{\text{dil}}^u = \frac{n_x}{\varepsilon_x^{\text{dil}}} = \frac{n_y}{\varepsilon_y^{\text{dil}}} = \frac{EF^u}{\sqrt{3}a} . \tag{12}$$

Thus, the rigidity matrix of the upper chord referred to the entire elongation vector $\boldsymbol{\epsilon}^u = \boldsymbol{\epsilon}_{\text{unstab}}^u + \boldsymbol{\epsilon}_{\text{dil}}^u$ becomes:

$$\mathbf{A}^u = \begin{bmatrix} \frac{A_{\text{dil}}^u}{2} & \frac{A_{\text{dil}}^u}{2} & 0 \\ \frac{A_{\text{dil}}^u}{2} & \frac{A_{\text{dil}}^u}{2} & 0 \\ 0 & 0 & 0 \end{bmatrix} \tag{13}$$

meeting requirements

$$n_x^u = n_y^u = A_{\text{dil}}^u \frac{\varepsilon_x^u + \varepsilon_y^u}{2} \quad \text{and} \quad n_{xy}^u = 0 .$$

Finally, deformation in Fig. 4c produces no homogeneous deformation field and cannot be related to any internal force. It only increases the instability degree but — as against deformations shown in Figs 4a and b — it imposes no direct restriction upon the force system.

Deformation in Fig. 4c only permits to establish two "quasi-homogeneous" deformation fields shown in Figs 5a, b. Figure 5a shows corners of hexagons A and B to suffer angular distorsions $\pm\beta$ and $\pm\beta/2$, respectively. In the case of Fig. 5b, hexagons C keep undeformed while corners of D undergo angular distorsions $\pm\beta$. For the entire hexagonal mesh in either case: $\varepsilon_x = \varepsilon_y = \gamma_{xy} = 0$.

As against homogeneous deformation fields in Figs 4a, b, these "quasi-homogeneous" deformation fields cannot come about without elongation of bars of the lower chord and of diagonals. Thus, the deformability shown in Fig. 4c is not another form of instability to be directly reckoned with in the system of forces as a restriction.

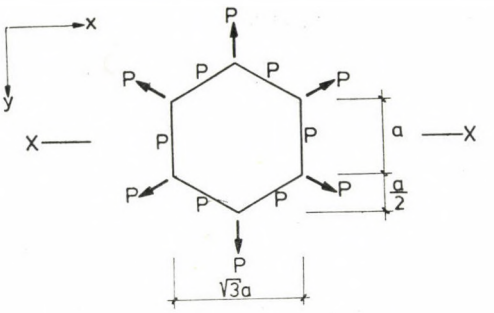

Fig. 5

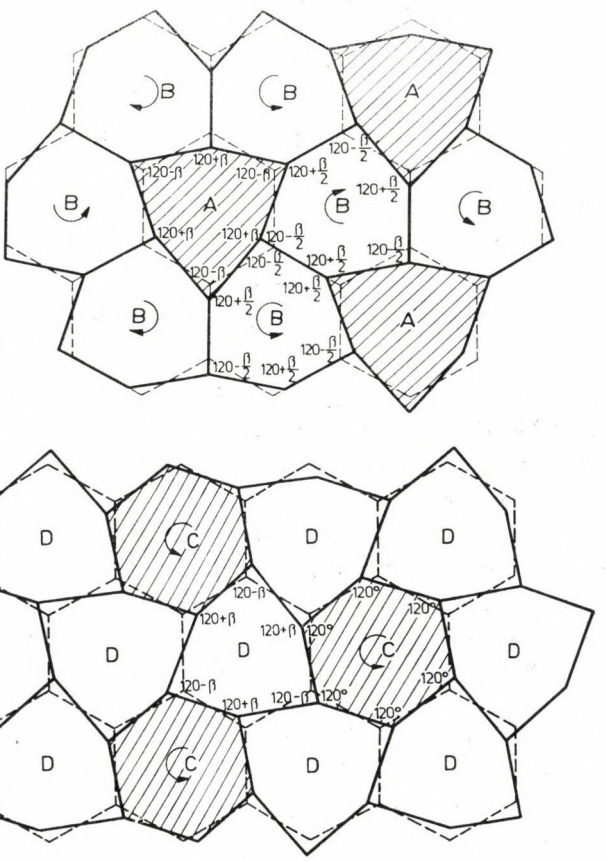

(b)

Fig. 6a, b

3.3 *Structural properties of grid tubes providing for torsional rigidity*

The hexagonal mesh with no shear rigidity cannot take the "other half" of the torque, i.e. the pair of the shear force n_{xy} arising in the lower chord. The lower chord can form "closed tubes" only with the "skew diagonals", thus lending torsion rigidity to the structure. Let us examine these tubes from statical aspects.

Subsequently, deformations of the three tubes will be seen to be compatible, hence to yield deformations of a single continuum.

Figure 7a shows a "grid tube" parallel to one of the lower chord bar directions. Upper chord bars indicated by dotted lines are inexistent. These will be though provisionally inserted but they will be seen not to develop bar forces

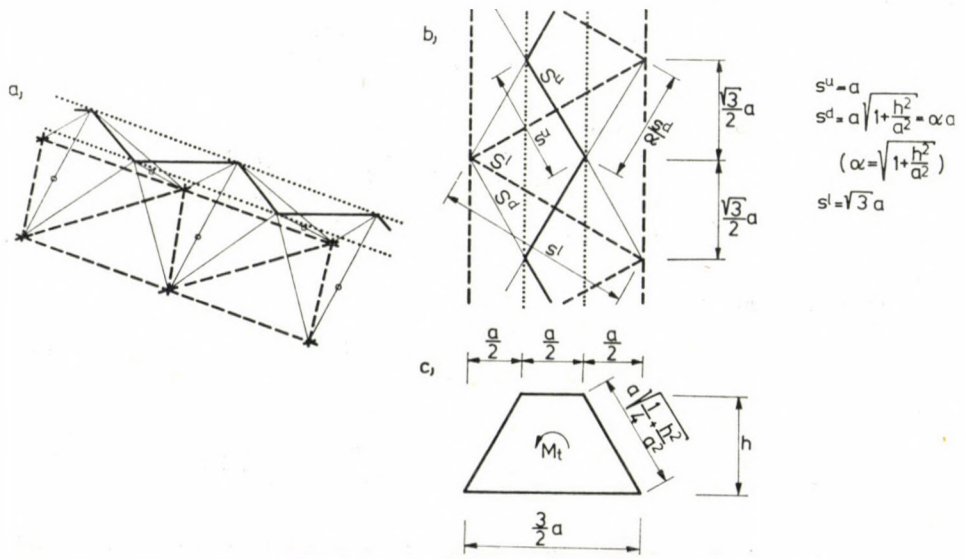

Fig. 7

due to torsion, hence they are superfluous. The same is true for diagonals denoted by *O*. Thereby the tube of trapezoidal cross section seen in Figs 7b, c results. Bar lengths needed later are:

$$s^u = a \tag{14a}$$

$$s^d = a\sqrt{1+\frac{h^2}{a^2}} = \alpha a \tag{14b}$$

where

$$\alpha = \sqrt{1+\frac{h^2}{a^2}} \tag{15}$$

and

$$s^l = \sqrt{3}a \tag{14c}$$

as indicated in the figure.

Similarly to the tube section with solid walls, torque M_t acting on the tube causes a shear flow t [kp/cm] in the cross section, of an intensity according to the Bredt equilibrium equation:

$$t = \frac{M_t}{2F_{\text{trapeze}}} = \frac{M_t}{2ah} . \tag{16}$$

The projections of the forces taken by the diagonal bars on the cross section plane are proportional to the corresponding side lengths of the trapeze, individual bar forces being:

$$S^u = \pm \frac{a}{a/2}\left(t\frac{a}{2}\right) = \pm \frac{M_t}{2h}, \tag{17}$$

$$S^d = \pm \frac{a\sqrt{1+\frac{h^2}{a^2}}}{a\sqrt{\frac{1}{4}+\frac{h^2}{a^2}}}\left(ta\sqrt{\frac{1}{4}+\frac{h^2}{a^2}}\right) = \pm \frac{M_t}{2h}\sqrt{1+\frac{h^2}{a^2}} \tag{18a}$$

or, with notations (15)

$$S^d = \pm \frac{\alpha M_t}{2h} = \pm \alpha S^u \tag{18b}$$

and

$$S^l = \pm \frac{\sqrt{3}a}{3a/2}\left(t\frac{3}{2}a\right) = \pm \frac{\sqrt{3}M_t}{2h} = \pm \sqrt{3}S^u. \tag{19}$$

Analysis of the equilibrium of nodes in direction of the tube axis yields 0 for all chord bar forces lying on the edges of the tube. Similarly, diagonals denoted by O will be inactive bars (Fig. 7a), rightly omitted.

Thereafter, torsional rigidity GI_t of the tube can be determined, defined, as usual, by means of the specific distorsion angle ϑ:

$$GI_t = \frac{M_t}{\vartheta} . \tag{20}$$

Equalizing inner and outer works performed in torsion of a tube length $\sqrt{3}a/2$:

$$\frac{1}{2}M_t\left(\frac{\sqrt{3}a}{2}\vartheta\right) = \frac{1}{2E}\left[\frac{(S^u)^2 s^u}{F^u} + 2\frac{(S^d)^2 s^d}{F^d} + \frac{(S^l)^2 s^l}{F^l}\right] . \tag{21}$$

Expressing ϑ by means of (20), bar forces by (17), (18b) and (19) in terms of M_t, and bar lengths by means of (14a, b, c) in terms of a, yields for GI_t:

$$GI_t = \frac{2\sqrt{3}Eh^2}{\frac{1}{F^u} + \frac{2\alpha^3}{F^d} + \frac{3\sqrt{3}}{F^l}} \tag{22}$$

with α understood as in (15).

3.4 *Torsional rigidity of the space truss*

In knowledge of structural properties of a tube, let us consider the torsional rigidity of a space truss of intersecting tubes of three directions.

First, the torque and the flexural moment developing in the 30° skew section of the torsional tube (hence, in the normal section of a tube in the other direction) will be determined (Fig. 8).

Equilibrium equations yield

$$M_t^{\text{skew}} = \frac{M_t}{2} \tag{23a}$$

and

$$M_b^{\text{skew}} = \frac{\sqrt{3}}{2} M_t \tag{23b}$$

complying with bar forces in the cross section cut as in Fig. 9.

In the following we have to deal with specific internal forces referred to unit width of the structure. In the section normal to the tube axis (Fig. 8) this has the value

$$m_t = \frac{2M_t}{3a} . \tag{24}$$

Length of the skew section being twice that of the normal section, specific moments become:

$$m_t^{\text{skew}} = \frac{m_t}{4} \tag{25a}$$

and

$$m_b^{\text{skew}} = \frac{\sqrt{3}}{4} m_t . \tag{25b}$$

Having these data, the fundamental case of plate torsion will be composed (Fig. 10a).

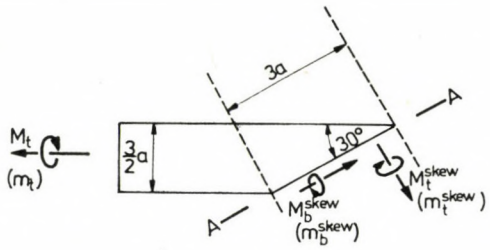

Fig. 8

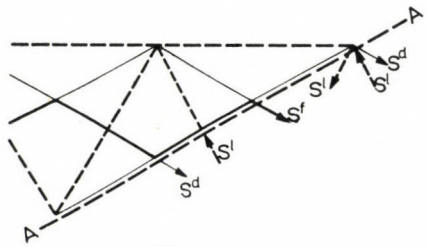

Fig. 9

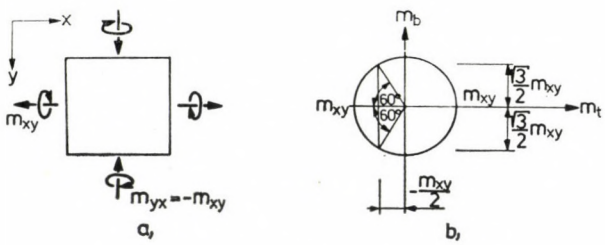

Fig. 10

Now, we know of the tubes of all three directions what moments arise in the sections normal to the two other tubes, due to a specific torque m_t. On the other hand, values of moments arising in the skew sections in Fig. 10a are known to be representable by a Mohr circle (Fig. 10b), thus, moments in sections normal to the other, skew tubes are:

$$m_l^{\text{skew}} = -\frac{m_{xy}}{2} \tag{26a}$$

and

$$m_b^{\text{skew}} = \pm\frac{\sqrt{3}}{2}\, m_{xy}\,. \tag{26b}$$

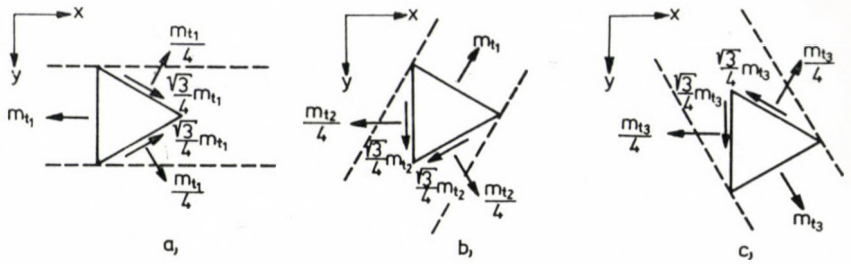

Fig. 11

One normal and two skew sections of tubes of all three directions, with the relevant moments, are shown in Fig. 11. The problem can be stated as to determine torques m_{t1}, m_{t2}, m_{t3} acting on normal tube sections so that these three elementary force systems sum up to that in Fig. 10.

This requirement can be demonstrated to be met for

$$m_{t2} = m_{t3} = -\frac{m_{t1}}{2} \,. \tag{27}$$

Namely then, in the section with the normal x:

$$m_{xy} = \frac{3}{4} m_{t1} \tag{28}$$

and in the skew sections:

$$m_t^{\text{skew}} = -\frac{3}{8} m_{t1} = -\frac{m_{xy}}{2} \tag{29a}$$

and

$$m_b^{\text{skew}} = \pm \frac{3\sqrt{3}}{8} m_{t1} = \pm \frac{\sqrt{3}}{2} m_{xy} \tag{29b}$$

corresponding to Fig. 10b.

Now, deformation of the structure has to be composed of the pure torsion states of the three tubes caused by specific torques m_{t1}, m_{t2}, m_{t3}, respectively. Pure torsion of a tube due to torques on its ends produces in the plate (comprising the tube) a deformation field such as (Fig. 12): in the section normal to the tube axis: $\varkappa_{xy}$, in the section normal to the former: $\varkappa_{yx} = -\varkappa_{xy}$, and in skew sections including an angle φ with the tube cross section

$$\varkappa_{\text{tors}}^{\text{skew}} = \varkappa_{xy} \cos 2\varphi = \varkappa_{xy}(\cos^2 \varphi - \sin^2 \varphi) \tag{30}$$

as seen in the figure, and following from $\varkappa_{xy} = \dfrac{\partial^2 w}{\partial x \, \partial y}$ where w means vertical deflection.

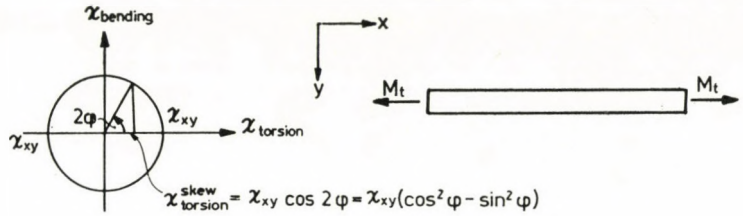

Fig. 12

Accordingly, torsion of the three tubes constituting the structure (Fig. 13) produces a twist in the section with the normal x:

$$\varkappa_{xy} = \frac{M_{t1}}{GI_t} + \frac{M_{t2} + M_{t3}}{GI_t}(\cos^2 60° - \sin^2 60°)\,, \tag{31a}$$

and in the section with the normal y:

$$\varkappa_{yx} = -\frac{M_{t1}}{GI_t} + \frac{M_{t2} + M_{t3}}{GI_t}(\cos^2 30° - \sin^2 30°)\,. \tag{31b}$$

Substituting GI_t from (22) and considering that

$$M_{ti} = \frac{3am_{ti}}{2} \tag{32}$$

and expressing m_{ti} by means of (27) and (28) in terms of m_{xy} yields twist in

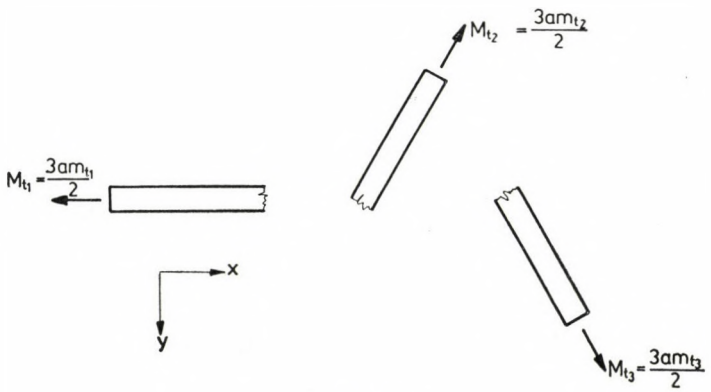

Fig. 13

terms of specific torque m_{xy} acting in the plate:

$$\varkappa_{xy} = -\varkappa_{yx} = \frac{m_{xy}}{B_t} \tag{33}$$

where B_t is the "plate-like" torsional rigidity, half of the torsional rigidity GI of a tube according to (22) referred to unit band width (i.e. divided by $3a/2$):

$$B_t = \frac{1}{2}\frac{GI_t}{\frac{3}{2}a} = \frac{Eh^2}{a}\,\frac{F^l}{\frac{\sqrt{3}\,F^l}{2F^u} + \sqrt{3}\left(1+\frac{h^2}{a^2}\right)^{3/2}\frac{F^l}{F^d} + \frac{9}{2}}\,. \tag{34}$$

By similar reasoning the "tube-like" torsional rigidities furnish bending rigidity $B_t/2$ and transversal bending rigidity $-B_t/2$ in both x and y directions.

4. Deduction of continuum equations

4.1 *Fundamentals*

Equations will be written on the basis of principles in [1], as follows: In the first step the rigidity of the upper chord plane will be taken with its actual value (13), and the rigidity matrix of the lower chord plane (4) will be decomposed into a part consisting of elements proportional to those of the upper plane (I) and the residual part (II). Part I combined with the rigidity matrix of the upper chord plane produces a bending (plate-like) system of forces due to deflection w_1.

This deformation w_1 also includes unstable deformations pertaining to upper chord plane deformations shown in Figs 4a and b. Of course, these unstable deformation parts cannot be directly related to the internal forces, hence, these are not defined by the differential equation proper of the flexural system of forces but by the edge supports (counteracting instability according to item 2), and by the requirement of compatibility. Thus, the unstable part of the deformation cannot unambiguously be determined but by the solution of the set of differential equations of the equivalent continuum taking also boundary conditions into consideration.

The fact that the torsional stiffness is not due to the shearing rigidities of the lower and upper chord planes (this being absent in the upper chord plane) but to "tubes" according to items 3.3 and 3.4, involves another consideration. The rigidities of the lower chord plane should be split suitably in such a way that part I of these rigidities together with those of the upper chord plane give deformations compatible with angular distortion $\gamma^l_{xy,\,\mathrm{tors}}$, computed from the deformation of the tubes. We thus obtain the "plate-like" (bending) part of the inner forces, denoted by 1.

Because of the "residual" rigidity matrix of the lower chord plane, here force excesses II will appear, with no pair in the upper chord plane, hence unbalanced. To restore equilibrium, a complementary plane system of forces 2 has to develop in the lower chord plane as a second, "membrane-like" part of the force system.

4.2 *Splitting suitably the rigidities of the lower chord plane*

The angular distortion due to torsion, $\gamma^l_{xy,\,\mathrm{tors}}$, of the lower chords of the tubes with trapezoidal cross sections can be determined on the base of what has been said in sections 3.3—3.4. If the tubes are submitted to end torques (m_{t1}) only, the shear flow will become, according to (16),

$$t_1 = \frac{\frac{3}{2} a m_{t1}}{2ah} . \tag{36}$$

In case of "plate-like" torsion (i.e. with m_{xy} and m_{yx} both acting), in the three tubes there act, according to (27) and (28), torques $m_{t1} = -2m_{t2} = -2m_{t3} = 4m_{xy}/3$, causing angular distortions [see also (3)] in the first tube:

$$\gamma_{xy,1} = \frac{t_1}{A^l_{33}} = 4 \frac{a}{h} \frac{m_{xy}}{EF^l} , \tag{37a}$$

and in the second and third tubes:

$$\gamma_{\xi\eta,2} = \gamma_{\xi\eta,3} = -2 \frac{a}{h} \frac{m_{xy}}{EF^l} . \tag{37b}$$

These can be summarized according to formula (31a):

$$\gamma^l_{xy,\mathrm{tors}} = 6 \frac{a}{h} \frac{m_{xy}}{EF^l} . \tag{37c}$$

This angular distortion will be compatible with elongations due to bending only if all of them can be computed from bending deflection w_1 by the well-known expression $h^l \cdot L_1 w_1$ [explanation of L_1 given by (40)]. This requires:

$$\gamma^l_{xy,\,\mathrm{tors}} = h^l \cdot 2 \frac{\partial^2 w_1}{\partial x \, \partial y} = h^l \cdot 2\varkappa_{xy} , \tag{38a}$$

h^l being defined in Fig. 14. Taking into account (33), this results in

$$h^l = \frac{3aB_{33}}{hEF^l} = \frac{h}{\frac{F^l}{2\sqrt{3}\,F^u} + \frac{1}{\sqrt{3}} \left(1 + \frac{h^2}{a^2}\right)^{3/2} \frac{F^l}{F^d} + \frac{3}{2}} , \tag{38b}$$

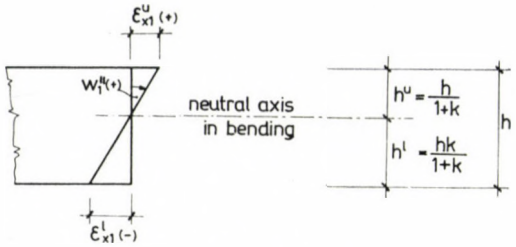

Fig. 14

that determines the required ratio k of stiffness matrices of the upper and lower chord planes $\mathbf{A}_1^u$ and $\mathbf{A}^l$, respectively, defined by the relation

$$\mathbf{A}_1^u = k\mathbf{A}^l. \tag{39a}$$

We thus obtain:

$$k = \frac{h^l}{h - h^l} = \frac{1}{\dfrac{F^l}{2\sqrt{3}\,F^u} + \dfrac{1}{\sqrt{3}}\left(1 + \dfrac{h^2}{a^2}\right)^{2/3}\dfrac{F^l}{F^d} + \dfrac{1}{2}}. \tag{39b}$$

4.3 *Writing the equations*

For the "plate-like" part 1 of the force system, the well-known differential equation of plates in bending [3] can be written, using vector notations

$$L_1 = \begin{bmatrix} \dfrac{\partial^2}{\partial x^2} \\ \dfrac{\partial^2}{\partial y^2} \\ 2\dfrac{\partial^2}{\partial x\,\partial y} \end{bmatrix} \tag{40}$$

and

$$\mathbf{m} = \begin{bmatrix} m_x \\ m_y \\ m_{yx} \end{bmatrix} \tag{41}$$

in the form:

$$L_1^* \mathbf{m} = -p \tag{42}$$

To express moments in terms of bending deflection w_1, the bending rigidity matrix is obtained as the sum of bending matrix $\mathbf{B}_b$ given by tensile matrices $\mathbf{A}^u$ (13) and

$$\mathbf{A}_1^l = \frac{1}{k}\mathbf{A}^u \tag{43}$$

(cf. 39b) according to the formula:

$$\mathbf{B}_b = \frac{h^2}{1+k}\mathbf{A}^u \tag{44}$$

and of torsional matrix containing the rigidities due to the "tube-like" torsional stiffness

$$\mathbf{B}_t = \begin{bmatrix} \frac{B_t}{2} & -\frac{B_t}{2} & 0 \\ -\frac{B_t}{2} & \frac{B_t}{2} & 0 \\ 0 & 0 & \frac{B_t}{2} \end{bmatrix}. \tag{45}$$

Element B_t is defined by (34). Multiplier 1/2 in the last element is needed to compensate factor 2 in the third element of L_1, moments being, in terms of w_1:

$$\mathbf{m} = -(\mathbf{B}_b + \mathbf{B}_t)\, L_1 w_1 \tag{46}$$

which, substituted into (42) yields the equilibrium equation of bent plates in terms of deflection w_1:

$$L_1^*(\mathbf{B}_b + \mathbf{B}_t)\, L_1 w_1 = p. \tag{47}$$

Complementary plane system of forces in the lower chord plane, i.e. part 2 of the force system is obtained by the following consideration.

From among internal forces due to bending deflection w_1, up to now only forces corresponding to lower chord plane rigidity matrix I, $\mathbf{A}_1^l$ (43) and to the "tube-like" torsional rigidity have been considered. These torsional forces mean in fact forces due to lower chord shear rigidity A_{33}^l (3). There remain internal forces still to be considered, determined by the "residual" rigidity matrix II of the lower chord plane as follows:

$$\mathbf{A}_{II}^l = \mathbf{A}^l - (\mathbf{A}_1^l + \mathbf{A}_t^l)\,. \tag{48}$$

where

$$\mathbf{A}_t^l = \begin{bmatrix} 0 & 0 & 0 \\ 0 & 0 & 0 \\ 0 & 0 & A_{33}^l \end{bmatrix}. \tag{49}$$

Deflection w_1 causes strains [1]

$$\epsilon_1^l = -\frac{hk}{1+k} L_1 w_1 \tag{50}$$

in the lower chord plane corresponding to definition (5c), as seen in Fig. 14, generating unbalanced internal forces

$$\mathbf{n}^l_{1\,II} = \mathbf{A}^l_{11}\,\boldsymbol{\epsilon}^l_1 = -\frac{hk}{1+k}\left(\mathbf{A}^l - \frac{1}{k}\,\mathbf{A}^u - \mathbf{A}^l_t\right) L_1 w_1, \tag{51}$$

taking also (48) and (43) into consideration. To restore equilibrium requires a plane stress and strain system

$$\mathbf{n}^l_2 = \mathbf{A}^l \boldsymbol{\epsilon}^l_2\,. \tag{52}$$

Since this system does not cause strains in the upper chord plane, according to Fig. 15 it can be expressed in terms of deflection w_2 it causes [1]:

$$\boldsymbol{\epsilon}^l_2 = -h\mathbf{L}_1 w_2. \tag{53}$$

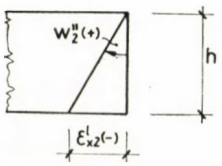

Fig. 15

Equilibrium of force system $(\mathbf{n}^l_{1\,II} + \mathbf{n}^l_2)$ is known to be met by an appropriately chosen stress function Φ such as

$$L_2\Phi = \mathbf{n}^l_{1\,II} + \mathbf{n}^l_2 \tag{54}$$

differential operator L_2 being interpreted as:

$$L_2 = \begin{bmatrix} \dfrac{\partial^2}{\partial y^2} \\ \dfrac{\partial^2}{\partial x^2} \\ -\dfrac{\partial^2}{\partial x\,\partial y} \end{bmatrix}. \tag{55}$$

Thereby equilibrium has been maintained but Φ has still to meet compatibility equation

$$L^*_2 \boldsymbol{\epsilon}^l_2 = 0. \tag{56}$$

Since, in addition to the force system $\mathbf{n}_2^l$, Φ contains also force system $\mathbf{n}_{1\,II}^l$ due to an a priori compatible bending deformation, deformations corresponding to this latter have to be subtracted from deformations expressed by Φ to obtain $\boldsymbol{\epsilon}_2^l$. Based on (52) and (54):

$$\boldsymbol{\epsilon}_2^l = (\mathbf{A}^l)^{-1}\,\mathbf{n}_2^l = (\mathbf{A}^l)^{-1}\,(L_2\,\Phi - \mathbf{n}_{1\,II}^l)\,. \tag{57}$$

Substituted into (56) and taking also (51) into consideration:

$$L_2^*\,(\mathbf{A}^l)^{-1}\left[L_2\,\Phi + \frac{kh}{1+k}\left(\mathbf{A}^l - \frac{1}{k}\,\mathbf{A}^u - \mathbf{A}_t^l\right) L_1\,w_1\right] = 0\,. \tag{58}$$

The coupled differential equations (47) and (58) — together with the boundary conditions — determine functions w_1 and Φ, hence the entire force system. Boundary conditions can, however, be only given for the entire deflection w, sum of bending deflection w_1, and deflection w_2 resulting from the complementary plane force system according to (53):

$$w = w_1 + w_2 \tag{59}$$

Hence, w_1 (or rather, $L_1 w_1$) in both equations has to be expressed by the entire deflection w.

Multiplying both sides of (59) by L_1:

$$L_1 w = L_1 w_1 + L_1 w_2\,. \tag{60}$$

Taking (53), (57) and (51) into consideration:

$$\begin{aligned} L_1 w_2 &= -\frac{1}{h}\,\boldsymbol{\epsilon}_2^l = -\frac{1}{h}\,(\mathbf{A}^l)^{-1}\,(L_2\,\Phi - \mathbf{n}_{1\,II}^l) = \\ &= -\frac{1}{h}\,(\mathbf{A}^l)^{-1}\left[L_2\,\Phi + \frac{kh}{1+k}\left(\mathbf{A}^l - \frac{1}{k}\,\mathbf{A}^u - A_t^l\right) L_1 w_1\right]. \end{aligned} \tag{61}$$

Substituting (61) into (60) and multiplying by $\mathbf{A}^l$ we obtain $L_1 w_1$

$$L_1 w_1 = (1+k)\,(\mathbf{A}^l + \mathbf{A}^u + k\,A_t^l)^{-1}\left(\mathbf{A}^l\,L_1 w + \frac{1}{h}\,L_2\,\Phi\right), \tag{62}$$

that, substituted into (47) and (58), yields the coupled differential equations containing w and Φ:

$$(1+k)\,L_1^*(\mathbf{B}_b + \mathbf{B}_t)\,(\mathbf{A}^l + \mathbf{A}^u + k\mathbf{A}_t^l)^{-1}\left(\mathbf{A}^l L_1 w + \frac{1}{h}\,L_2\,\Phi\right) = p\,, \tag{63a}$$

$$L_2^*(\mathbf{A}^l)^{-1}\Big[L_2\Phi + h(k\mathbf{A}^l - \mathbf{A}^u - k\mathbf{A}_t^l)\,(\mathbf{A}^l + \mathbf{A}^u + k\mathbf{A}_t^l)^{-1}\cdot \cdot\,(\mathbf{A}^l L_1 w + \frac{1}{h}L_2\Phi)\Big] = 0\,. \tag{63b}$$

5. Boundary conditions

Boundary conditions for a simply supported (hinged) edge (parallel to the x axis) are:

zero deflection: $w = 0$ (64a)

zero bending moment normal to the edge: $m_y = 0$ (64b)

zero (horizontal) membrane force in the lower chord normal to the edge: $n^l_{y1\,II} + n^l_{y2} = 0$ (64c)

zero membrane shear force in the lower chord: $n^l_{xy1\,II} + n^l_{xy2} = 0$ (64d)

These also have to be expressed by w and Φ. The moment vector for (64b) will be written using (46) and (42):

$$\mathbf{m} = -(1+k)\,(\mathbf{B}_b + \mathbf{B}_t)\,(\mathbf{A}^l + \mathbf{A}^u + k\mathbf{A}_t^l)^{-1}\left(\mathbf{A}^l L_1 w + \frac{1}{h}L_2\Phi\right). \tag{64b*}$$

Force vector needed for (64c) and (64d) can be directly expressed according to (54) by Φ:

$$n^l_{1\,II} + n^l_2 = L_2\Phi\,. \tag{64c*}$$

Remark on (64d) that, according to (51) and (48), shear component of $\mathbf{n}^l_{1\,II}$ identically equals zero.

Boundary conditions for skew edges can be written by means of formulae of the corresponding rotational transformations.

6. Determination of bar forces from internal forces of the continuum

Continuum internal forces can be converted to bar forces according to the precedings.

Bending moments in both directions are always equal ($m_x = m_y$), hence bar force P arising in the upper chord can be computed by (10) from the normal force

$$n^u_x = -\frac{m_x}{h}\,. \tag{65}$$

In conformity with item 3.4, torque $m_{xy} = -m_{yx}$ has to be decomposed to torques m_{t1}, m_{t2}, m_{t3}, acting on the three tubes, according to (27) and (28), and the resulting bar forces in each tube are given by formulae (17) to (19), considering the relation between M_t acting on an entire tube and the specific torque m_t according to (24).

Bar forces of the complementary plane force system in the lower chord plane, determined by Φ according to (54), can be computed according to [4].

Specific shear forces are given by the relations

$$q_x = \frac{\partial m_x}{\partial x} + \frac{\partial m_{yx}}{\partial y}, \tag{66a}$$

$$q_y = \frac{\partial m_y}{\partial y} - \frac{\partial m_{xy}}{\partial x}, \tag{66b}$$

known from [3].

Bar forces in the diagonals resulting therefrom are to be determined on the grid tube in Fig. 6, according to the well-known methods.

Considering the tube to be parallel with the x axis (Fig. 1), shear force $3aq_x/2$ on a tube width $3a/2$ is taken by two skew grids. Bar forces are

$$S^d = \pm \frac{h}{s^d} \frac{3aq_x}{4} \tag{67}$$

according to the vertical projection equation, with bar length s^d from Eq. (14b).

In the perpendicular direction y, shear force is taken by two bar configurations (Fig. 16): *ac-bc-cd* and *ae-ef-ed*, mirror images to each other. Both are recurrent at spacings $\sqrt{3}a$. Bars *cd* and *ae* lie in the plane *yz* according to

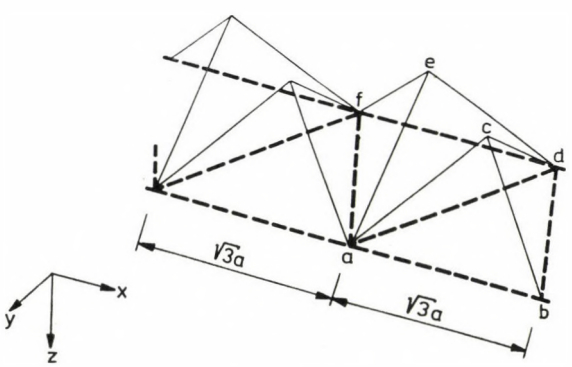

Fig. 16

Fig. 1, hence the share of shear force loading the configuration is borne by them alone, while each bar of bar pairs *ac-cb* and *ef-ed*, symmetric to plane *yz*, supports half as much shear force. Again, from the vertical projection equation:

$$S_{cd} = -S_{ae} = \pm \frac{h}{s^d} \frac{\sqrt{3} a q_y}{2}, \tag{68a}$$

$$S_{ac} = S_{bc} = -S_{ef} = -S_{ed} = \pm \frac{h}{s^d} \frac{\sqrt{3} a q_y}{4}. \tag{68b}$$

REFERENCES

1. Kollár, L.: Continuum Method of Analysis for Double-Layer Space Trusses with Upper and Lower Chord Planes of Different Rigidities. *Acta Techn. Hung.* **76** (1974), 53—63
2. Kollár, L.: Analysis of Double-Layer Space Trusses with Diagonally Square Mesh by the Continuum Method. *Acta Techn. Hung.* **76** (1974), 273—292
3. Timoshenko, S.—Woinowski-Krieger, S.: Theory of Plates and Shells. McGraw-Hill, New York—Toronto—London 1959
4. Wright, D. T.: A Continuum Analysis for Double-Layer Space Frame Shells. *Publ. Int. Ass. Bridge Struct. Eng.* Zürich, **26** (1966)

Untersuchung des zweischichtigen Raumfachwerkes mit »Sechseck über Dreieck«-Netz mittels der Kontinuum-Methode. Zuerst werden die Bedingungen der statischen Bestimmtheit eines zweischichtigen Raumfachwerkes mit „Sechseck über Dreieck"-Netz untersucht, und die statischen Folgen aus der Labilität des Sechseckgurtes klargelegt. Danach werden die statischen Eigenschaften der „Gitterröhre" festgelegt, die eine Torsionssteifigkeit gewährleisten. In deren Kenntnis wird das Differentialgleichungssystem des dem Raumfachwerk gleichwertigen Kontinuums abgeleitet, und schließlich die Aufstellung der Randbedingungen und die Berechnung der Stabkräfte aus den Schnittkräften des Kontinuums dargelegt.

Исследование континуумным методом двухслойной фермы с сеткой «шестиугольник над треугольником». В работе сначала анализируются условия статической определенности двухслойной фермы с сеткой «шестиугольник над треугольником», после чего выясняются статические последствия, вытекающие неустойчивости пояса, состоящего из шестиугольников. В дальнейшем определяются статические характеристики «решетчатых труб», обеспечивающих жесткость на кручение. На основе упомянутых выше выводится система дифференциальных уравнений для континуума, равноценного ферме, и, наконец, иллюстрируются уравнения краевых условий и вычисление стержневых сил на основе усилий разрезов континуума.

Acta Technica Academiae Scientiarum Hungaricae, Tomus 86 (1—2), pp. 79—92 (1978)

ELECTROMAGNETIC WAVE PROPAGATION IN INHOMOGENEOUS MEDIA: METHOD OF INHOMOGENEOUS BASIC MODES

CS. FERENCZ*

[Manuscript received Nov. 23, 1976]

The paper gives a calculation method for electromagnetic wave pattern in a group of inhomogeneous media. It shows that the given pattern may always be executed if the solution exists. It analyses and justifies the most important properties of the method. Based on that it gives a critical analysis of the Appleton—Hartree formula and shows examples of application.

As it is known from earlier papers [1], the inhomogeneous media are to be classified into three basic groups as regards the description of electromagnetic wave propagation. These are:

— quasi-homogeneous media
— (weakly) inhomogeneous media
— strongly inhomogeneous media.

The case of the quasi-homogeneous media is theoretically clear [1, 2, 3]; to complete and systematize the group of dispersion equations, etc., that is, what remains to be done. A general analysis of strongly inhomogeneous media is still open. There exist a lot of methods by special or general claims [2, 3, 4, 5, 6, 7, 8, 9], but a thorough analysis of them [1, 10, 19] shows, that further fundamental investigations are necessary.

In the course of previous investigations a proposition for the solution was made [3, 4, 11] which is generally suitable for analysing the (weakly) inhomogeneous media [1]. One task of this paper is to go over the "method of inhomogeneous basic modes" in details, and to decide precisely the field of applications. For the sake of generality all the investigations will be done for bianisotropic media [1].

Let the solution of Maxwell's equations be of the following monochromatic form:

$$\bar{F} = \bar{F}_0 e^{j(\omega_0 t - \varphi)}$$

where $\bar{F}$ means one of the electromagnetic field vectors ($\bar{E}$ — electric intensity, $\bar{D}$ — electric displacement, $\bar{B}$ — magnetic induction, $\bar{H}$ — magnetic intensity), ω_0 the angular frequency of the signal, t is time, φ is the phase.

From the monochromacy of the signal as a consequence it follows, that in time varying or moving media will be excluded from the present considera-

* Dr. Cs. FERENCZ, Puskin u. 24, H-1088 Budapest, Hungary

tions [1, 2]! To extend the results to such conditions may be the task of further researches. One method is already known [2, 16].

The criteria for the existence of the solution will not be dealt with in this paper, as only after a detailed study of the medium parameter functions and boundary conditions of the given problem may the existence of a solution in the wanted form be decided [2].

As the dispersion equations may justify the existence [12], those solutions will be looked for, which are based on the dispersion equation [17, 18].

In the following the connection between the medium and the electromagnetic wave will be taken as linear, that is, permeability, permittivity, etc. do not depend on the amplitude of the electromagnetic wave. But they may depend on frequency and the direction of propagation.

1. Method of inhomogeneous basic modes

When solving Maxwell's equations, the connection between the components of the electromagnetic fields will be bianisotropic, that is

$$\begin{aligned} \bar{D} &= \epsilon \bar{E} + \varkappa \bar{H} , \\ \bar{B} &= \upsilon \bar{E} + \mu \bar{H} . \end{aligned} \tag{1}$$

It is already known [1], that the use of the following form of Maxwell's equations

$$\begin{aligned} \nabla x \bar{H} &= \varepsilon_0 \frac{\partial \bar{D}}{\partial t} , \\ \nabla x \bar{E} &= - \mu_0 \frac{\partial \bar{D}}{\partial t} , \\ \nabla \bar{B} &= 0, \\ \nabla \bar{D} &= 0 \end{aligned} \tag{2}$$

is sufficient, without any restriction of generality, if only ϵ, $\varkappa$, υ and μ contain all the effects of the medium, and all components of electric currents and charges. ε_0 and μ_0 mean the permittivity and permeability of the vacuum, respectively.

Let the solution of (2) looked for in the form, already reasoned formally [3]

$$\bar{F} = \sum_{i,l} (a_{il} \, e^{-j\varphi_{ai}} \, \bar{F}_{0il}) \, e^{j(\omega_0 t - \varphi_i)} \tag{3}$$

where

$$\sum_{l,l} = \sum_{l=1}^{n} \sum_{l=v,k}$$

$l = v$ is real, k is imaginary; the imaginary components contain the factor j as well $j^2 = -1$;
$i = 1, \ldots, n$; mean the individual inhomogeneous basic modes, which will be precisely defined in the following;
The meaning of a, φ_a, etc. presents itself from Eq. (3).
ω_0 is the angular frequency of the signal; it is constant.

The practical reasons of partitioning shown in (3) may be found in [3] though, but this procedure has the theoretically based reasons as well. It has already been shown [4, 6, 7, 8] in details, that in inhomogeneous media the electromagnetic field is always composed of a sum of more propagating modes, that is, all of them will satisfy Maxwell's equations together. The choice of the modes depends on the method of solution and other aspects of practicality, and in the following an expedient form will be shown.

As φ_{ai} and φ_i may be complex, therefore, if the solution will be sought for "asymptotically" [7, 19], as a solution of the combinations of the Eikonal-equations and transport-equation in the known manner, the result will anyway consist of "inhomogeneous plane waves". In this case the phenomenon will be approximated with an energetically corrected, quasi-homogeneous [1, 2, 7, 19] description. This known way of the solution will not be dealt with in more details in this paper, but a rather general way will be found.

Let the terms (1) and (3) be written into Eq. (2), and as a first step, the time derivation will not be neglected, as will be possible because of those assumptions, made at the beginning. Then Eq. (2) appears in the following form:

$$\sum_{i,l} [\overline{\text{grad}} (\ln a_{il} - j\varphi_{ai}) \times \bar{H}_{il} + \nabla_{tH\text{oil}} \bar{H}_{il} - j\bar{K}_i \times \bar{H}_{il}] =$$

$$= \varepsilon_0 \sum_{i,l} \left[\left(\frac{\partial \epsilon}{\partial t} \bar{E}_{il} + \frac{\partial \varkappa}{\partial t} \bar{H}_{il} \right) + (\epsilon \nabla_{tE\text{oil}} \bar{E}_{il} + \varkappa \nabla_{tH\text{oil}} \bar{H}_{il}) + \right.$$

$$\left. + \left(\epsilon \frac{\partial (\ln a_{il} - j\varphi_{ai})}{\partial t} \bar{E}_{il} + \varkappa \frac{\partial (\ln a_{il} - j\varphi_{ai})}{\partial t} \bar{H}_{il} \right) + j\omega_0 (\epsilon \bar{E}_{il} + \varkappa \bar{H}_{il}) \right]$$

$$\sum_{i,l} [\overline{\text{grad}} (\ln a_{il} - j\varphi_{ai}) \times \bar{E}_{il} + \nabla_{tE\text{oil}} \bar{E}_{il} - j\bar{K}_i \times \bar{E}_{il}] =$$

$$= -\mu_0 \sum_{i,l} \left[\left(\frac{\partial \upsilon}{\partial t} \bar{E}_{il} + \frac{\partial \mu}{\partial t} \bar{H}_{il} \right) + (\upsilon \nabla_{tE\text{oil}} \bar{E}_{il} + \mu \nabla_{tH\text{oil}} \bar{H}_{il}) + \right. \tag{4}$$

$$\left. + \left(\upsilon \frac{\partial (\ln a_{il} - j\varphi_{ai})}{\partial t} \bar{E}_{il} + \mu \frac{\partial (\ln a_{il} - j\varphi_{ai})}{\partial t} \bar{H}_{il} \right) + j\omega_0 (\nu \bar{E}_{il} + \mu \bar{H}_{il}) \right]$$

$$\sum_{i,l} [\overline{\text{grad}\,(\ln a_{il} - j\varphi_{ai})}\,(\epsilon\bar{E}_{ik} + \varkappa\bar{H}_{il}) + (\nabla_\epsilon \bar{E}_{il} + \nabla_\varkappa \bar{H}_{il}) +$$
$$+ (\langle\nabla_{\epsilon il}\bar{E}_{il}\rangle + \langle\nabla_{\varkappa il}\bar{H}_{il}\rangle) - j\bar{K}_i(\epsilon\bar{E}_{il} + \varkappa\bar{H}_{il}] = 0$$

$$\sum_{i,l} [\overline{\text{grad}\,(\ln a_{il} - j\varphi_{ai})}\,(\upsilon\bar{E}_{il} + \mu\bar{H}_{il}) + (\nabla_\upsilon \bar{E}_{il} + \nabla_\mu \bar{H}_{il}) +$$
$$+ (\langle\nabla_{\upsilon il}\bar{E}_{il}\rangle + \langle\nabla_{\mu il}\bar{H}_{il}\rangle) - j\bar{K}_i(\upsilon\bar{E}_{il} + \mu\bar{H}_{il})] = 0\,.$$

The meaning of the new terms in (4) are as follows:

$$\bar{K}_i = \overline{\text{grad}\,\varphi_i};$$

$$\nabla_{TH\text{oil}} = \begin{bmatrix} 0 & -\dfrac{\partial \ln H_{2\text{oil}}}{\partial z} & \dfrac{\partial \ln H_{3\text{oil}}}{\partial y} \\ \dfrac{\partial \ln H_{1\text{oil}}}{\partial z} & 0 & -\dfrac{\partial \ln H_{2\text{oil}}}{\partial x} \\ -\dfrac{\partial \ln H_{1\text{oil}}}{\partial y} & \dfrac{\partial \ln H_{2\text{oil}}}{\partial x} & 0 \end{bmatrix};$$

The meaning of $\nabla_{TE\text{oil}}$ is analogous to $\nabla_{TH\text{oil}}$:

$$\nabla_{tH\text{oil}} = \begin{bmatrix} \dfrac{\partial \ln H_{1\text{oil}}}{\partial t} & 0 & 0 \\ 0 & \dfrac{\partial \ln H_{2\text{oil}}}{\partial t} & 0 \\ 0 & 0 & \dfrac{\partial \ln H_{3\text{oil}}}{\partial t} \end{bmatrix};$$

The meaning of $\nabla_{tE\text{oil}}$ is analogous to $\nabla_{tH\text{oil}}$:

$$\nabla_\varepsilon = \nabla\epsilon,\ \nabla_\mu = \nabla\mu,\ \text{etc.};$$

$$(\nabla_{\varepsilon il})_{jk} = \varepsilon_{jk}\frac{\partial \ln E_{\text{oil}\,k}}{\partial x_j}\ ;$$

and the meaning of $\nabla_{\varkappa il}$, $\nabla_{\nu il}$ and $\nabla_{\mu il}$ is analogous to $\nabla_{\varepsilon il}$;

$$\langle\overline{u}\rangle \equiv u_1 + u_2 + u_3\,.$$

The (4) form of Maxwell's equations will be used in another paper too. Now, however, considering, that a monochromatic solution is wanted, and — therefore — neglecting the time dependence of the medium parameters [1], the solution will have a stationary character. The form of the equations will be the following:

$$\sum_{i,l} [\overline{\text{grad}}\,(\ln a_{il} - j\varphi_{ai}) \times \bar{H}_{il} + \nabla_{TH\text{oil}}\,\bar{H}_{il} - j\bar{K}_i \times \bar{H}_{il}] =$$
$$= \varepsilon_0 \sum_{i,l} j\omega_0\,(\epsilon\bar{E}_{il} + \varkappa\bar{H}_{il})$$

$$\sum_{i,l} [\overline{\text{grad}}\,(\ln a_{il} - j\varphi_{ai}) \times \bar{E}_{il} + \nabla_{TE\text{oil}}\,\bar{E}_{il} - j\bar{K}_i \times \bar{E}_{il}] =$$
$$= -\mu_0 \sum_{i,l} j\omega_0\,(\upsilon\bar{E}_{il} + \mu\bar{H}_{il})$$

$$\sum_{i,l} [\overline{\text{grad}}\,(\ln a_{il} - j\varphi_{ai})\,(\epsilon\bar{E}_{il} + \varkappa\bar{H}_{il}) + (\nabla_\epsilon\,\bar{E}_{il} + \nabla_\varkappa\bar{H}_{il}) +$$
$$+ [\langle\nabla_{\epsilon il}\,\bar{E}_{il}\rangle + \langle\nabla_{\varkappa il}\,\bar{H}_{il}\rangle) - j\bar{K}_i\,(\epsilon\bar{E}_{il} + \varkappa\bar{H}_{il})] = 0 \tag{5}$$

$$\sum_{i,l} [\overline{\text{grad}}\,(\ln a_{il} - j\varphi_{ai})\,(\upsilon\bar{E}_{il} + \mu\bar{H}_{il}) + (\nabla_\upsilon\,\bar{E}_{il} + \nabla_\mu\,\bar{H}_{il}) +$$
$$+ (\langle\nabla_{\upsilon il}\,\bar{E}_{il}\rangle + \langle\nabla_{\mu il}\,\bar{H}_{il}\rangle) - j\bar{K}_i\,(\upsilon\bar{E}_{il} + \mu\bar{H}_{il})] = 0$$

Let φ_i in Eq. (3) be the solution of Maxwell's equations and the dispersion equations valid for the quasi-homogeneous case [1]. Then one arrives at

$$\bar{K}_i = \overline{\text{grad}}\;\varphi_i$$

again, and according to the definitions, the equations of

$$\begin{aligned}
&\bar{K}_i \times \bar{H}_{il} = -\omega_0\,\varepsilon_0\,(\epsilon\bar{E}_{il} + \varkappa\bar{H}_{il})\,,\\
&\bar{K}_i \times \bar{E}_{il} = \omega_0\,\mu_0\,(\upsilon\bar{E}_{il} + \mu\bar{H}_{il})\,,\\
&\bar{K}_i\,(\epsilon\bar{E}_{il} + \varkappa\bar{H}_{il}) = 0\\
&\bar{K}_i\,(\upsilon\bar{E}_{il} + \mu\bar{H}_{il}) = 0
\end{aligned} \tag{6}$$

must be satisfied. After analysing Eq. (3), and reducing the common factors in Eq. (6), one gets

$$\begin{aligned}
&\bar{K}_i \times \bar{H}_{\text{oil}} = -\omega_0\,\varepsilon_0\,(\epsilon\bar{E}_{\text{oil}} + \varkappa\bar{H}_{\text{oil}}),\\
&\bar{K}_i \times \bar{E}_{\text{oil}} = \omega_0\,\mu_0\,(\upsilon\bar{E}_{\text{oil}} + \mu\bar{H}_{\text{oil}})\,,\\
&\bar{K}_i\,(\epsilon\bar{E}_{\text{oil}} + \varkappa\bar{H}_{\text{oil}}) = 0\,,\\
&\bar{K}_i\,(\upsilon\bar{E}_{\text{oil}} + \mu\bar{H}_{\text{oil}}) = 0\,.
\end{aligned} \tag{7}$$

As the last two equations of Eq. (7) will be automatically satisfied, the equations defining φ_i and the $\bar{F}_{\text{oil}}$-s leaving some degree of freedom, are the followings

$$\begin{aligned}
&\bar{K}_i \times H_{\text{oil}} = -\omega_0\,\varepsilon_0\,(\epsilon\bar{E}_{\text{oil}} + \varkappa\bar{H}_{\text{oil}})\\
&\bar{K}_i \times \bar{E}_{\text{oil}} = \omega_0\,\mu_0\,(\upsilon\bar{E}_{\text{oil}} + \mu\bar{H}_{\text{oil}})
\end{aligned} \tag{8}$$

and

$$|\epsilon^{-1}\,(\mathbf{K}_i + \omega_0\,\varepsilon_0\varkappa)\,\mu^{-1}\,(\mathbf{K}_i - \omega_0\mu_0\upsilon) + k_0^2\,\mathbf{1}| = 0 \tag{9}$$

where

$$\mathbf{K}_i = \begin{bmatrix} 0 & -K_{i3} & K_{i2} \\ K_{i3} & 0 & -K_{i1} \\ -K_{i2} & K_{i1} & 0 \end{bmatrix} \text{and} \qquad k_0^2 = \varepsilon_0 \mu_0 \omega_0^2 \,.$$

The functions defined by Eqs (8)—(9) are named in the following "inhomogeneous basic modes". Using these definitions, the terms multiplied by "j" in Eqs (5) — as also for Eqs (6) will be automatically satisfied, as a consequence of this definition — in every equation will automatically fall out. The now failing functions of the total solution wanted in the form (3) can be determined by using the following equations, when Eqs (8)—(9) are already solved:

$$\mathfrak{L}_a = \sum_{i,l} [\overline{\text{grad}\ (\ln a_{il} - j\varphi_{ai})} \times \bar{H}_{il} + \nabla_{THoil} \bar{H}_{il}] = 0 \,, \tag{10/a}$$

$$\mathfrak{L}_b = \sum_{i,l} [\overline{\text{grad}\,(\ln a_{il} - j\varphi_{ai})} \times \bar{E}_{il} + \nabla_{TEoil} \bar{E}_{il}] = 0 \,, \tag{10/b}$$

$$\mathfrak{L}_c = \sum_{i,l} [\overline{\text{grad}\,(\ln a_{il} - j\varphi_{ai})}\,(\epsilon \bar{E}_{il} + \varkappa \bar{H}_{il}) + (\nabla_\varepsilon \bar{E}_{il} + \nabla_\varkappa \bar{H}_{il}) + (\langle \nabla_{\varepsilon il} \bar{E}_{il} \rangle + \langle \nabla_{\varkappa il} \bar{H}_{il} \rangle)] = 0 \,, \tag{10/c}$$

$$\mathfrak{L}_d = \sum_{i,l} [\overline{\text{grad}\,(\ln a_{il} - j\varphi_{ai})}\,(\upsilon \bar{E}_{il} + \mu \bar{H}_{il}) + (\nabla_\upsilon \bar{E}_{il} + \nabla_\mu \bar{H}_{il}) + (\langle \nabla_{\upsilon il} \bar{E}_{il} \rangle + \langle \nabla_{\mu il} \bar{H}_{il} \rangle)] = 0 \,. \tag{10/d}$$

As from Eq. (2) follows the automatic satisfaction of

$$\text{div}\ \bar{D} = 0 \quad \text{and} \quad \text{div}\ \bar{B} = 0$$

in all the cases of the investigations, and as for the last two equations of Eqs (7) will also be automatically satisfied, Eqs (10/c) and (10/d) seem to be negligible. It is really justifiable — as will later be shown — thus it is satisfactory to solve only Eqs (10/a) and (10/b).

One has to add to Eqs (10) perhaps already to Eqs (8)—(9) the complete class of the boundary conditions. This is the way to get the unicity of the solution, that is, to have it in all parameters being fixed.

Examination of existence of the solution must be executed in every case, as according to the Floquet-theorem [12, 18], the satisfaction of Eqs (9), only guarantees the existence of the individual inhomogeneous basic modes and the existence of Eq. (3) does not automatically follow it.

2. Analysis of the solution based on the inhomogeneous basic modes

a) *Statement*

If a solution of the form of

$$\bar{F}_x = \bar{F}_{x0}\, e^{j(\omega_0 t - \varphi_x)}$$

will exist, then it can always be produced with the aid of the inhomogeneous basic modes as well, when properly choosing the free parameters in them.

NB: By reasons of earlier considerations [1, and present paper] it can be seen that it is extraordinarily difficult to give a single dispersion equation for the solutions — thus has not been successful yet. This "sole" solution always means physically an interference picture which is produced as a result of propagating waves. These two causes make the verification of the former statement necessary.

Verification:

It is to be demonstrated, that the partitioning of $\bar{F}_x$ in every case may be executed in the form of

$$\bar{F}_x = \bar{F}_{x0}\, e^{-j\varphi_x}\, e^{j\omega_0 t} = \sum_{i,l} \left(a_{il}\ e^{-j\varphi_{ai}}\, \bar{F}_{0il}\right)\ e^{-j\varphi_i}\ e^{j\omega_0 t} \tag{11}$$

if $\bar{F}_x$ is a solution of Maxwell's equations and $\bar{F}_{il}$ is one of the inhomogeneous basic modes.

It is known, that the partitioning

$$\bar{F}_x = \bar{F}_{x0}\, e^{-j\varphi_x}\ e^{j\omega_0 t} = \sum_{i} \left(\bar{F}_{x0iv} + \bar{F}_{x0ik}\right) e^{-j\varphi_{xi}}\, e^{j\omega_0 t} \tag{12}$$

may be executed, when the components satisfy the 12 equations of Eqs (12), where $\bar{F}_x \rightarrow \bar{E}_x$ and $\bar{H}_x$, that is, they have at least 12 degrees of freedom.

In the recent case, however, $\bar{E}_x$ and $\bar{H}_x$ are not independent, but the solutions belong together with Maxwell's equations. This fact restricts the number of their independent parameters [13, 14, etc.]. Considering the general solutions of Maxwell's equations, the number of the independent parameters may be determined. (In the following, the term "bounded" parameter means parameters, which are specified by the $(\bar{E}_x, \bar{H}_x)$ connection, while "free" parameters are the ones, which are determined by the properties of the medium and boundary conditions of the given problem, but not by the $(\bar{E}_x, \bar{H}_x)$ connection.) Free parameters of the general solution may be (e.g.)

$\bar{A}$ — vector potential

Φ — scalar potential

$\partial\bar{A}/\partial t$ — (e.g. $e^{j(\omega_0 t - \varphi_i)}$) — the from $\bar{A}$ independent factor of the derivative.

Thus, the supposed existing solution of Maxwell's equation — $(\bar{E}_x, \bar{H}_x)$ — may have 4 amplitude-typed and 1 phase-typed, that is 5 *degrees of freedom.* When one assumes solutions of a complex type (rotating polarization, etc.)

the number of degrees of freedom may be *at most* 10, because the two (real and imaginary) parts of the solution are not necessarily connected with each other.

Among the inhomogeneous basic modes appearing in Eq. (11), there must exist *at least two independent* ones, as the (9) dispersion equation is of the second order.

So, concerning the terms in the remaining part of Maxwell's equations — (10) —, the parameters, which may be freely chosen on the right side of Eq. (11) are:

$$a_{il}, \varphi_{ai}$$

and what is really still free in $(\bar{E}_{il}, \bar{H}_{il})$, the solution of Eqs (8)—(9).

Let the number of free parameters in $(\bar{E}_{il}, \bar{H}_{il})$ be determined:

φ_l-s are defined by Eq. (9). The $(\bar{E}_{il}, \bar{H}_{il})$-s belonging to φ_l-s, will be defined by Eqs (8). Taking one equation of Eqs (8), a given $\bar{E}_{\text{oil}}$ uniquely defines a $\bar{H}_{\text{oil}}$ and vice versa. By this three component equations remain concerning E_{oil} or H_{oil}. This is, however, a homogeneous system of equations and Eq. (9) causes one of them to be linearly dependent, so it must be neglected. Therefore, one has two equations for three amplitude components! (That trivial degree of freedom that both sides of an equation may be multiplied by the same factor, was already used when a_{il} was introduced, and also the linearity of medium parameters was used [2].)

Thus, in the inhomogeneous basic modes after solving Eqs (8)—(9)

$$a_{il}, \varphi_{ai}$$

and 1 parameter of $(\bar{E}_{\text{oil}}, \bar{H}_{\text{oil}})$ are still free. As at least two independent basic modes exist, the number of free parameters of the inhomogeneous basic modes are

at least 6,

and

in complex cases (rotating polarization, etc.), this number may reach 10, — meanwhile the l-indices must be kept in mind.

[NB: An analysis of (3) trivially shows, that in the most general cases either

$$a_{iv} \neq a_{ik} \quad \text{and} \quad \varphi_{ai} \text{ common}$$

or

$$\varphi_{aiv} \neq \varphi_{aik} \text{ and } \quad a_{iv} = a_{ik}$$

may be found without the restriction of generality.]

As the number of parameters of the field to be described is 5, or is 10 in a complex case, it now follows, that to all ensembles of inhomogeneous basic modes belong parameters, which are to be chosen freely in suitable number,

that is, the description of Eq. (11) in every case may be used for any existing solution mentioned in the statement.

By this the statement is verified.

[NB: By the use of complex vectors, in the simplest case, when $i_{\max} = 2$, the correspondence is mutually unambiguous. In other cases, because of the number of parameters this will be "levelled up" while the solving procedure is going on, that is, as a condition for the existence of a solution, further conditions may appear. E.g.: it is not certain that an $(\bar{E}_x, \bar{H}_x)$ plane polarized wave may occur, etc.]

b) *Additional comment:*

From the process which can be seen in Chapter 2/a it is trivial, that by those methods of solution, based on dispersion equation as shown in Chapter 1, the statement of 2/a is valid.

Therefore, it is advisable — whenever it is at all possible — to look for solving methods based on a dispersion equation.

c) *Analysis of the divergence equations*

c.1) According to previous works [1], all effects of the medium will be concentrated into $\bar{D}$ and $\bar{H}$, that is, Maxwell's equations take the form of Eq. (2).

In this case, as long as partial derivatives of second order are interchangeable — which for (weakly) inhomogeneous media is valid by definition [1] — one has, that:

$$\operatorname{div}(\operatorname{rot}\bar{H}) = 0 = \varepsilon_0 \operatorname{div}\frac{\partial \bar{D}}{\partial t} = \varepsilon_0 \frac{\partial}{\partial t}(\operatorname{div}\bar{D}) . \tag{13}$$

So the divergence equations will automatically be satisfied, when the rotation equations are satisfied.

c.2) It can be seen trivially, that from Eqs (7), which describes the inhomogeneous basic modes, the last two equations corresponding to the divergence-equations will be fulfilled, when the first two ones are fulfilled.

c.3) Statement: It can be seen from the earlier statement, that in case Eqs (10/a) and (10/b) are fulfilled, the Eqs (10/c) and (10/d) will also be automatically fulfilled. (In this case these equations need not be taken into account.)

Verification: In the case mentioned above the equations have the same form as Eq. (5), namely,

$$\begin{aligned} (\mathfrak{L}_a) \quad & -j\sum_{i,l}\bar{K}_i \times \bar{H}_{il} = \varepsilon_0 \sum_{i,l} j\omega_0 (\epsilon\bar{E}_{il} + \varkappa\bar{H}_{il}) , \\ (\mathfrak{L}_b) \quad & -j\sum_{i,l}\bar{K}_i \times \bar{E}_{il} = -\mu_0 \sum_{i,l} j\omega_0 (\upsilon\bar{E}_{il} + \mu\bar{H}_{il}) , \end{aligned} \tag{14}$$

and

$$(\mathfrak{L}_c) - j \sum_{i,l} \bar{K}_i (\epsilon \bar{E}_{il} + \varkappa \bar{H}_{il}) = 0 ,$$
$$(\mathfrak{L}_d) - j \sum_{i,l} \bar{K}_i (\upsilon \bar{E}_{il} + \mu \bar{H}_{il}) = 0 , \tag{15}$$

where the meaning of $(\mathfrak{L}_\alpha)$ is the same as can be seen in Eqs (10).

If $(\bar{E}_{il}, \bar{H}_{il})$ is an inhomogeneous basic mode, then

$$(\mathfrak{L}_a) = 0$$

and

$$(\mathfrak{L}_b) = 0$$

must be fulfilled to obtain the general solution. (The 6 or 12 equations determine the free parameters, the number of which is ≥ 6 or ≥ 10, respectively. Thus some of the parameters will be settled by the boundary conditions or only the relative value of them will be bound.)

It can be seen from Eq. (14), that the analogous form of that which shows the satisfaction of the divergence-equations in quasi-homogeneous case:

$$\bar{K}_i (\mathfrak{L}_a) - j \sum_{i,l} \bar{K}_i (\bar{K}_i \times \bar{H}_{il}) ,$$

etc., does not exist.

Let the divergence be generated of the first one of Eqs (6) and of Eqs (10/a) (or it can be executed for the second equations in an analogous manner):

$$\operatorname{div} (\bar{K}_i \times \bar{H}_{il}) = \omega_0 \varepsilon_0 \operatorname{div} (\epsilon \bar{E}_{il} + \varkappa \bar{H}_{il}) , \tag{16}$$

and

$$\operatorname{div} (\mathfrak{L}_a) = 0. \tag{17}$$

Eq. (16) may be summarized for all the "i"-s and "l"-s, then

$$\sum_{i,l} \operatorname{div} (\bar{K}_i \times \bar{H}_{il}) = \omega_0 \varepsilon_0 \sum_{i,l} \operatorname{div} (\epsilon \bar{E}_{il} + \varkappa \bar{H}_{il})$$

from which — taken into consideration, that $(\bar{E}_{il}, \bar{H}_{il})$-s are inhomogeneous basic modes

$$- \sum_{i,l} \bar{K}_i \operatorname{rot} \bar{H}_{il} = \omega_0 \varepsilon_0 \operatorname{div} \sum_{i,l} (\epsilon \bar{E}_{il} + \varkappa \bar{H}_{il}) = \omega_0 \varepsilon_0 (\mathfrak{L}_c) \tag{18}$$

can be obtained. When developing rot $\bar{H}_{il}$, Eq. (18) obtains the following form:

$$- \sum_{i,l} \bar{K}_i [\nabla_{THoil} \bar{K}_{il} + \overline{\operatorname{grad}} (\ln a_{il} - j\varphi_{ai}) \times \bar{H}_{il}] = \omega_0 \varepsilon_0 (\mathfrak{L}_c)$$

where it was taken into account, that

$$\bar{K}_i (\bar{K}_i \times \bar{u}) \equiv 0 .$$

The term in the bracket [ ] is the one, which can be found in Eq. (10/a). Using the symbol $(\mathfrak{L}_a)_{il}$ for denoting it, then

$$- \sum_{i,l} \bar{K}_i (\mathfrak{L}_a)_{il} = \omega_0 \varepsilon_0 (\mathfrak{L}_c) \tag{19}$$

Now let Eq. (17) be developed:

$$\operatorname{div} (\mathfrak{L}_a) = \sum_{i,l} [\operatorname{div} (\nabla_{THoil} \bar{H}_{il}) - \overline{\operatorname{grad}} (\ln a_{il} - j\varphi_{ai}) \operatorname{rot} \bar{H}_{il}]. \tag{20}$$

Assuming, that the second partial derivatives of the functions do not only exist but they are continuous, — this may be permitted because of the definition of inhomogeneous media — it follows, that [1]:

$$f''_{x_1 x_2} = f''_{x_2 x_1} \tag{21}$$

and

$$(E_{kil}, H_{kil}) \subset f \quad \text{where} \quad k = 1, 2, 3,$$

then $\operatorname{div} (\nabla_{THoil} \bar{H}_{il})$ may be written in the form

$$\operatorname{div} (\nabla_{THoil} \bar{H}_{il}) = [\overline{\operatorname{grad}} (\ln a_{il} - j\varphi_{ci}) - j\bar{K}_i] \nabla_{THoil} \bar{H}_{il} . \tag{22}$$

Now substituting Eq. (22) and rot $\bar{H}_{il}$ into Eq. (20), it follows, that

$$\operatorname{div} (\mathfrak{L}_a) = \sum_{i,l} [- j\bar{K}_i (\nabla_{THoil} \bar{H}_{il})] + \sum_{i,l} j \overline{\operatorname{grad}} (\ln a_{il} - j\varphi_{ai}) (\bar{K}_i \times \bar{H}_{il}) \tag{23}$$

In the second term of this equation the composite product may be rearranged. Thus, by using the same shortening symbols as above, the new form of Eq. (17) will be:

$$\operatorname{div} (\mathfrak{L}_a) = - j \sum_{i,l} \bar{K}_i (\mathfrak{L}_a)_{il} = 0 . \tag{24}$$

A comparison of Eqs (19) and (24) shows, that if the assumption (21) can be fulfilled, then

$$(\mathfrak{L}_c) = 0 \tag{25}$$

So the statement is verified.

NOTE:

The satisfaction of assumption (21) for (weakly) inhomogeneous media is assured by definition [1] and is congruent with the assumption obtained in

c.1). Therefore, (21) is important when judging the character of inhomogeneity from the point of view of solving the method.

It is important, however, that the assumption (21) will not be fulfilled in case of $1(\bar{r})$ (step function), $\delta(\bar{r})$ (Dirac delta-function) etc. The refraction-reflection laws, the laws of ray tracing methods, etc. belong to this topic. In this case the method shown above may be applied formally [2, 11, 15], but the Eqs (10/c) and (10/d) cannot be neglected! (In this case the formal application needs a further investigation [2, 10].)

3. Additional notices

Consequential on what was mentioned above, two notices must be settled now:

a) *About the Appleton—Hartree equation*

The equation in generally used in space research and geophysics. Let it now be examined keeping in sight the method of solution given in Chapter 1.:

By using the generally used conditions [4, 6]

$$\varepsilon = \varepsilon f(\Theta),$$

where $\Theta = \sphericalangle(\bar{K}, \bar{n}_0)$ and $\bar{n}_0$ is, e.g. a unit vector directed parallel with the static magnetic field vector. Now one has:

$$\left(\frac{\partial \varphi}{\partial x}\right)^2 + \left(\frac{\partial \varphi}{\partial y}\right)^2 + \left(\frac{\partial \varphi}{\partial z}\right)^2 = k_0^2 \, \varepsilon f[\Theta(\overline{\operatorname{grad} \varphi}, \bar{n}_0)] \tag{26}$$

which should correspond to Eq. (9). It would be satisfactory in itself, in quasi-homogeneous cases. For more precise work it would be the base of the asymptotic method [7, 19] or of the precise analysis using the inhomogeneous basic modes. But it can be immediately seen compared with the earlier ones, that Eq. (26) can by no means be originated from Eq. (9), therefore, dispersion equation with such a form does not exist.

Therefore, this equation must not be used in more precise investigations though we are used to it. An analysis of the errors from this point of view is known [15, 21].

b) *Applying the method of inhomogeneous basic modes*

It is impossible to show in this paper a typical application. But the method was used for a detailed analysis of general solution of propagation in inhomogeneous transmission line (one-dimensional wave propagation) [20]. As an illustration of this:

The total current wave — and so the voltage wave as well — can be composed of two travelling and two reflected parts in an interesting case:

$$i(t) = e^{j\omega_0 t - \int \alpha(z_0)\,dx} \left[\left(C_{z1+}\, e^{\int \sqrt{\Delta_1}\,dx} + C_{z2+}\, e^{\int \sqrt{\Delta_2}\,dx} \right) + \left(C_{z1-}\, e^{-\int \sqrt{\Delta_1}\,dx} + \right.\right. \\ \left.\left. + C_{z2-}\, e^{-\int \sqrt{\Delta_2}\,dx} \right) \right] \tag{27}$$

where $\alpha(Z_0)$, Δ_1, Δ_2 depend on the parameter functions of the line; C_{z1+}, C_{z1-}, C_{z2+} and C_{z2-} are constants settled by the boundary conditions. The case of the known exponential line [13, 17] follows from Eq. (27) then and

$$\Delta_1 \equiv \Delta_2 .$$

This special case shows how new and general the solution can be when the method in this paper is used. It can be found in detail in [20].

4. Conclusions

a) The electromagnetic wave propagation in media, which are inhomogeneous, as described in [1], but not strongly inhomogeneous, can be treated by using the method of inhomogeneous basic modes. The method produces the solutions in the form of $\bar{F} = \bar{F}_0 e^{j(\omega_0 t - \varphi)}$ if these exist.

b) The use of the method makes the divergence equations needless as they are fulfilled automatically.

c) It was shown, that there is no dispersion equation (Eikonal equation) which would correspond to the Appleton—Hartree equation, so this is not suitable for precise analysis.

d) Addenda:

d.1. The method is extremely suitable (e.g. with successive approximation, etc.) to solve the types of problems which are transitional between the quasi-homogeneous and inhomogeneous cases.

d.2. The method gives the analyses for developing elementary wave modes, and opens up the way of investigating the wave patterns which are composed of them.

REFERENCES

1. Ferencz, Cs.: Electromagnetic Wave Propagation in Inhomogeneous Media: Strong and Weak Inhomogeneities; *Acta Techn. Hung.* **85** (1977) 433
2. Ferencz, Cs.: Electromagnetic Wave Propagation in Inhomogeneous Linear Media. Thesis submitted for the degree of Candidate of Sciences, Budapest 1970. Library of the Hungarian Academy of Sciences (in Hungarian)
3. Ferencz, Cs.: Wave Propagation in Inhomogeneous Linear Media. *Acta Techn. Hung.* **68** (1970) 215

4. BUDDEN, K. G.: Radio Waves in the Ionosphere. Cambridge at the Univ. Press 1966
5. GINZBURG, V. L.—RUCHADZE, A. A.: Volnü v magnitoaktivnoj plazme. Izd. "Nauka", Moszkva 1970 (in Russian)
6. RATCLIFFE, J. A.: The Magneto-Ionic Theory and its Applications to the Ionosphere. Cambridge at the Univ. Press 1959
7. FELSEN, L. B.: Rays, Modes and Equivalent Networks. *Proc. of the Fourth Coll. on Microwave Comm.*, ET-9, Akadémiai Kiadó, Budapest 1970
8. BRANDSTATTER, J. J.: An Introduction to Waves, Rays and Radiation in Plasma Media. McGraw-Hill Book Co. New York 1963.
9. FERENCZ, Cs.: Wave Propagation in Arbitrary Linear Media. *Acta Techn. Hung.* **71** (1971) 109
10. IDEMEN, M.: The Maxwell's Equations in the Sense of Distributions. *IEEE Trans. on Ant. and Prop.*, *AP*-21, (1973) 736
11. FERENCZ, Cs.—FERENCZ, I.—TARCSAI, Gy.: Refraction Problems and Wave Propagation in Doppler Geodetical Measurements. *Nablj. I. Sz. Z.* **9** (1970) 361
12. ARNAUD, J. A.—SALEH, A. A. M.: Theorems for Bianisotropic Media. *Proc. IEEE*, **60**, (1972) 639
13. SIMONYI, K.: Theoretische Elektrotechnik. VEB Deutsches Verlag der Wissenschaften, Berlin 1968
14. TAMM, I. E.: Basic Theory of Electrodynamics. *Izd. Nauka*, Moscow 1966 (in Russian)
15. DRAHOS, D.—FERENCZ, Cs.—FERENCZ, I.—HORVÁTH, F.—TARCSAI, Gy.: Some Theoretical Contributions Concerning Doppler Geodetical Measurements; Space Research X., 43. North-Holland Publ. Co., Amsterdam 1970
16. FERENCZ, Cs.—TARCSAI, Gy.: Theoretical Explanation of the Solar Limb Effect. *Planet Space Sci.* **19** (1971) 659
17. COLLIN, R. E.: Grundlagen der Mikrowellentechnik. VEB Verlag Technik, Berlin 1973
18. KAMKE, E.: Differentialgleichungen, Lösungsmethoden und Lösungen. Akademische Verlagsgesellschaft Geest & Portig k.-G. Leipzig 1951
19. CHOUDHARY, S.—FELSEN, L. B.: Asymptotic Theory for Inhomogeneous Waves. *IEEE Trans. on Ant. and Prop. AP*-21, (1973) 827
20. ÁRKOS, I. F.: A General Investigation of a Monochromatic Signal Propagating Along an Inhomogeneous Transmission Line., to be published
21. ÁRKOS, I. F.: Refraction Coefficient of Ionosphere. *Híradástechnika*, **21** (1970) 219 (in Hungarian)

Die Ausbreitung elektromagnetischer Wellen in inhomogenen Medien. — II. Das Verfahren der inhomogenen Grundmoden. — Die Arbeit gibt ein Berechnungsverfahren bekannt welches auf eine Klasse des elektromagnetischen Wellenbildes in inhomogenen Medien angewendet werden kann. Es wird nachgewiesen, daß die angegebene Zerlegung immer durchgeführt werden kann, wenn die Lösung existiert. Die wichtigeren Eigenschaften der Methode werden untersucht und bewiesen. Aufgrund deren wird die Appleton–Hartree Formel kritisch untersucht und auf ein Anwendungsbeispiel verwiesen.

Распространение электромагнитных волн в негомогенной среде. II. Метод негомогенных основных модусов. В статье приводится расчетная методика эпюры электромагнитных волн, применимой для одного из классов негомогенных сред. В статье подтверждается, что данное разложение, если существует решение, во всех случаях может быть выполнено. В дальнейшем исследуются и доказываются важнейшие свойства метода. На основе чего критически анализируется формула Аппельтона—Гартре. Далее дается ссылка на пример применения формулы.

Acta Technica Academiae Scientiarum Hungaricae, Tomus 86 (1—2), pp. 93—115 (1978)

DIE BEULUNG VON STAHLBETONSCHALEN

E. DULÁCSKA*

KANDIDAT DER TECHNISCHEN WISSENSCHAFTEN

[Eingegangen am 20 April 1977]

In der vorliegenden Studie dehnt Verfasser die Möglichkeit der Anwendung der Beultheorie elastischer Schalen auf den Bereich der Stahlbetonschalen aus. Es werden hierbei sowohl das Kriechen und die plastischen Eigenschaften des Betons als auch die Risse in der Zugzone des Querschnitts, sowie die Lage und Zahl der Stahleinlagen mitberücksichtigt. Die kritische Last, wie sie sich nach dem hier dazulegenden Verfahren bestimmen läßt, stimmt mit den experimentell ermittelten Resultaten überein.

1. Einleitung

Bei Untersuchung der Stabilität von Schalenkonstruktionen wird die theoretische kritische Last in der Regel durch den Sicherheitskoeffizienten dividiert und das Ergebnis der voraussichtlichen Last gegenübergestellt. Der Sicherheitskoeffizient pflegt hierbei wesentlich höher angesetzt zu werden, als es bei anderweitigen Konstruktionen üblich ist, denn weit stärker als bei diesen setzen bei Schalen zahlreiche Nebenwirkungen die kritische Last herab. Diese Nebenwirkungen sind jedoch noch nicht ausreichend genug geklärt.

Besondere Probleme tauchen bei Stahlbetonschalen auf, da die Steifigkeit des Stahlbetons infolge Auftretens von Rissen abnimmt, mit zunehmender Bewehrung hingegen wächst. So wurde beispielsweise die vergrößerte Steifigkeit der doppelt bewehrten Schale von den Konstrukteuren zwar auch bisher schon wahrgenommen, rechnerisch konnte sie aber nicht erfaßt werden.

Verfasser erscheint es jedoch, daß die Klärung der unterschiedlichen Nebenwirkungen der Beulung von Stahlbetonschalen heute doch schon so weit gediehen ist, daß sie die Grundlage für ein Bemessungsverfahren abgeben kann, welches die erforderliche Sicherheit mit der üblichen Konstruktionsform in Einklang zu bringen vermag. Ein solches Bemessungsverfahren ist um so korrekter, als es die verschiedenen, die Stabilität herabsetzenden Wirkungen einzeln und mit ihren richtigen Werten an ihren Stellen berücksichtigt und deshalb verläßlich ist.

* Dr. E. DULÁCSKA, Ráth Gy. u. 64, H-1122 Budapest, Ungarn

Schreibt man die Gleichgewichts- und Verträglichkeitsgleichungen der geometrisch vollkommenen Schale unter Beschränkung auf kleine Verformungen an, gelangt man zu einer Eigenwertaufgabe. Der kleinste unter den als Lösung dieser Aufgabe hervorgehenden Eigenwerten soll mit n_{kr}^{lin} bezeichnet werden und für die *lineare kritische Druckkraft der Schale* stehen. Die zugehörige Oberflächenlast $p_{\text{kr}}^{\text{lin}}$ sei die *lineare kritische Last der Schale* [1].

Indes haben die Versuchsergebnisse gezeigt, daß die Zylinder- und Kugelschalen bei Lastintensitäten ausbeulten, die wesentlich unter der linearen Last lagen und daß auch die Beulverformung keineswegs gering war. Aus diesem Grunde wurden in die Differentialgleichungen auch die zur Mitberücksichtigung der größeren Deformationen geeigneten nichtlinearen Glieder der Verformung eingeführt. Damit bieten diese Gleichungen die Handhabe dazu, das Verhalten der Schalen auch nach dem dem Eigenwert entsprechenden Verzweigungspunkt weiterzuverfolgen. Die Resultate der Untersuchungen nach der Energiemethode haben folgende Eigenheiten aufgedeckt:

a) Die Tragfähigkeit einer gewissen Gruppe von Schalen nimmt nach Erreichen der linearen kritischen Last zu. Ist die Schale mit einer maximalen Amplitude w_0 vorgebeult, dann hat sie keine kritische Last, vielmehr steigt ihre Tragfähigkeit mit der fortschreitenden Verformung stätig an. Derartige Schalen mit zunehmender Tragfähigkeit sind gegen anfängliche Unvollkommenheiten unempfindlich. Im allgemeinen handelt es sich um Schalen, in denen sich das Kräftespiel nach Erreichen der linearen kritischen Last p_{kr}^{lin} durch Verlagerung der inneren Kräfte so verändert, daß die neue Tragfähigkeitskonfiguration steifer ist als die frühere. Nach den heutigen Erkenntnissen zählen zu den Schalen dieser Art die windschief-viereckigen HP-Schalen sowie einige Schalen mit freien Rändern.

b) Das Verhalten einer anderen Gruppe von Schalen zeigt demgegenüber, daß sich die in Gleichgewicht gehaltene Last mit zunehmender Beulverformung w der geometrisch vollkommenen Schale bis zum Erreichen des Formänderungswertes w_{kr} vermindert, um sich von da ab wieder zu erhöhen.

Die bei w_{kr} in Gleichgewicht gehaltene Kraft bzw. Last soll nach v. KÁRMÁN [2] als untere kritische Kraft bzw. Last n_{kr}^{u} bzw. p_{kr}^{u} bezeichnet werden. Schalen dieser Art — sie werden *Schalen mit abnehmender Tragfähigkeit* genannt — sind im allgemeinen die Zylinder-, die Kegel-, die Kugel- und die sonstigen Kuppelschalen.

Doch auch diese untere kritische Last stimmte mit den experimentell ermittelten Werten nicht überein, da diese bei den Versuchen an Zylinder- und an Kugelschalen zwischen den Werten für die lineare und die untere kritische Last lagen.

Die weiteren Untersuchungen haben ergeben, daß die Zylinder- und die Kugelschalen bei kleineren als den linearen kritischen Lasten deshalb ausbeulen, weil sie mit anfänglichen Unvollkommenheiten (Vorbeulen) behaftet

sind. Die maximale Amplitude der Vorbeule (Ausmittigkeit) soll im weiteren mit w_0 bezeichnet werden. Die Untersuchungen an Schalen, die mit solchen Vorbeulen behaftet sind, haben zu der Feststellung geführt, daß sich die Vorbeule mit wachsender Belastung vergrößert, wogegen sich die Tragfähigkeit nach Erreichen eines Maximums mit zunehmender Verformung verringert. Elastische Schalen beulen de facto beim Erreichen dieses Maximums aus, welches im weiteren als die *obere kritische Kraft* n^0_{kr} bzw. *Last* p^0_{kr} bezeichnet werden wird. Die Zylinder- und die Kugelschalen beulen in Wirklichkeit beim oberen kritischen Last $p^0_{\mathrm{kr}} = \varrho \cdot p^{\mathrm{lin}}_{\mathrm{kr}}$ aus.

Das Verhältnis der oberen zur linearen kritischen Last von radial belasteten Kugel- und von axial gedrückten Zylinderschalen kann aufgrund der Auswertung von Literaturangaben [3, 4, 5, 6, 7, 8, 9, 10, 11, 12] in Abhängigkeit vom Verhältnis w_0/t wie folgt angesetzt werden:

w_0/t	0	0,1	0,2	0,3	0,4	0,5	1,0
$p^0_{\mathrm{kr}}/p^{\mathrm{lin}}_{\mathrm{kr}} = \varrho$	1,0	0,6	0,45	0,35	0,30	0,25	0,20

Im weiteren werden sich die Erörterungen auf die Untersuchung von Schalen mit abnehmender Tragfähigkeit beschränken, weil die Untersuchung der Stabilität von Schalen mit steigender Tragfähigkeit unter Zugrundelegung der linearen kritischen Last ähnlich durchgeführt werden kann wie bei den üblichen Konstruktionen.

2. Die Eigenheiten der Stahlbetonschalen

Die Kennwerte der Formänderung des Schalenbaustoffes, die zur Untersuchung des Beulverhaltens erforderlich sind, können bei Stahlbetonkonstruktionen nicht mit je einer Zahl angegeben werden, weil die Formänderungen von den Rissen, der Bewehrung und auch vom Kriechen des Betons abhängen und somit keine lineare Funktion der Last darstellen. Das macht die eingehendere Behandlung der Formänderungs- und Steifigkeitskennwerte des Stahlbetons erforderlich.

Das Werkstoffmodell der Bewehrung des Stahlbetons kann als ideal elastoplastisch angesehen werden.

Das Spannung-Dehnungs- [$\sigma(\varepsilon)$] -Diagramm des Betons verläuft von Anfang an gekrümmt (Bild 1). Seine Gekrümmtheit ist im Grunde die Folge eines mit der Spannung nicht proportional zunehmenden *(nichtlinearen)* Kriechens, das als Plastizität des Betons berücksichtigt wird. Überdies tritt

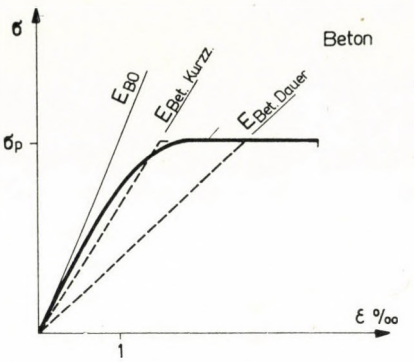

Bild 1. Das Spannungs-Dehnungs- [$\sigma(\varepsilon)$]-Diagramm für Beton

im Beton auch ein langsames, spannungsproportionales *(„lineares")* Kriechen auf, das die Praxis als Kriechen schlechthin kennt. Die Wahl des Formänderungsmoduls E_{Bet} des idealplastischen Werkstoffmodells zur Annäherung der $\sigma(\varepsilon)$-Linie hat sich also danach zu richten, ob es sich um eine dauernd oder um eine kurzfristig wirkende Last handelt. Bei Dauerbelastung entfaltet sich nämlich das Kriechen vollständig, während es bei kurzzeitig wirkender Last (z. B. bei der Probebelastung) nur zum Teil eintritt. Das idealplastische Werkstoffmodell ist somit bei Dauerbelastung durch den *Formänderungsmodul* $E_{\text{Bet. Dauer}}$, bei Kurzbelastung hingegen durch den Formänderungsmodul $E_{\text{Bet. Kurzz.}}$ gekennzeichnet. Unter Dauerlast ist jene zu verstehen, die während der Lebensdauer der Konstruktion mindestens ein Jahr lang wirkt, denn in dieser Zeitspanne vollzieht sich das Kriechen praktisch vollständig.

Bei ganz kurze Zeit wirksamen Belastungen (z. B. bei Schwingungen) kommt es erst gar nicht zum Kriechen, weshalb der Formänderungsmodul E_{Bet} bei Untersuchung solcher Wirkungen dem Anfangselastizitätsmodul E_{Bo} gleichgesetzt werden kann.

Letztlich wird also das Kriechen durch geeignete Wahl des Beton-Formänderungsmoduls E_{Bet} berücksichtigt.

Die Teile des eingerissenen Betonquerschnitts (die zugbeanspruchten Stahleinlagen und die gedrückte Betonzone) gehen in die Berechnung durch Einführung der entsprechenden Formänderungsmoduln als einheitliches idealplastisches Werkstoffmodell ein. Zur gemeinsamen Anwendung der beiden als idealplastisch angesehenen Baustoffe wird angenommen, daß bei Untersuchung der Auswirkungen der Plastizität der volle Querschnitt gleichfalls als idealplastisch angesehen werden kann. In Wirklichkeit hängt der Beginn des Fliessens im Querschnitt nicht nur von den geometrischen Abmessungen, sondern auch vom Gesamtquerschnitt der Stahleinlagen ab. Das aber wird durch die übliche Berechnung der Stahlbetonquerschnitte ohnehin automatisch berücksichtigt.

Der Stahlbeton weicht demnach von den elastischen, homogenen Baustoffen in folgendem ab:

— die gedrückte Zone erleidet ein langsames (lineares) Kriechen,

— sie hat zudem auch plastische Eigenschaften (nichtlineares Kriechen), und überdies

— treten in der Zugzone des Betons Risse auf, wobei sich die Querschnittssteifigkeit verringert und der Querschnitt der Stahleinlagen sowie deren Lage und Qualität zur Geltung kommen.

3. Die Formänderungskennwerte des Betons

3.1. *Der Anfangselastizitätsmodul* (E_{Bo})

Der Anfangselastizitätsmodul E_{Bo} des Betons ist im Grunde für jene Formänderungen kennzeichnend, die unter momentanen Einwirkungen (z. B. Schwingungen) eintreten.

Sein Mittelwert errechnet sich nach der allgemein akzeptierten Formel [13] zu

$$E_{Bo} = 550\,000 \frac{\sigma_p}{150 + \sigma_p} \text{ [kp/cm}^2\text{]} \; . \tag{1}$$

Das σ_p bezeichnet hier die Prismenfestigkeit des Betons, die mit 80 Prozent der Würfelfestigkeit angesetzt werden kann. Es gilt mithin

$$\sigma_p = 0{,}8\sigma_w \; . \tag{2}$$

In der Entwurfsarbeit geht die Streuung des Elastizitätsmoduls mit jener der Materialbeschaffenheit in die Berechnung ein, d. h. das E_{Bo} wird nicht der mittleren Festigkeit, sondern der Nennfestigkeit zugeordnet. Als Nennfestigkeit wird die dem gewünschten Quantile zugehörige Schwellenfestigkeit bezeichnet.

3.2. *Das (lineare) Kriechen*

Die Beulverformung der Betonschale hängt auch vom Kriechen, d. h. der langsamen Verformung des Betons ab. Zwar läßt diese den Wert des Elastizitätsmoduls unverändert, doch kann die durch die Auswirkungen der Anfangsausmittigkeit ausgelöste, mit der Beanspruchungsdauer zunehmende Beulverformung unter der gleichbleibenden Last rechentechnisch durch Reduzierung des E_{Bo}-Wertes berücksichtigt werden.

Der zeitliche Verlauf des linearen Kriechens wird üblicherweise durch die Dischingersche [14] Differentialgleichung

$$d\varepsilon = d\varepsilon_{\text{el}} + d\varepsilon_{\text{Kriechen}} = \frac{1}{E_{B0}} d\sigma + \frac{\sigma}{E_{B0}} d\varphi$$

und durch die in dieser vorkommende Kriechenfunktion

$$\varphi(t) = \frac{\varepsilon_{\text{Kriechen}}(t)}{\varepsilon_{\text{el}}} \tag{3}$$

erfaßt werden.

Der Endwert dieser Kriechenfunktion ist die Endkriechenzahl $\varphi(\infty) = \varphi_0$, die von der Dicke der Konstruktion, von der Menge und Güte des Zements, vom Wasserzementwert sowie vom Feuchtigkeitsgehalt der Luft in der Umgebung der Betonkonstruktion abhängig ist [15]. Unter durchschnittlichen Verhältnissen kann der Wert von φ_0 von der Betonfestigkeitsklasse allein abhängig gemacht werden. Auf dieser Grundlage gilt

$$\varphi_0 = 6 - 2 \log \sigma_{WN}, \tag{4}$$

wenn σ_{WN} die Würfel-Nennfestigkeit des Betons zum Zeitpunkt seiner Belastung in kp/cm², das log hingegen den Briggschen Logarithmus (Basis 10) bezeichnet. Der Ausdruck (4) ergibt für Beton der Festigkeitsklasse BN 250 einen Wert von $\varphi_0 = 1{,}4$, der mit dem für allgemeine Verhältnisse vorgeschriebenen Wert nach DIN 1045/1972 übereinstimmt.

3.3. *Der Formänderungsmodul* (E_{Bet})

Unter genauer Beachtung des linearen Kriechens an bestimmten Konstruktionen bestimmte HUANG deren kritische Last [17]. Die Auswertung seiner Ergebnisse führt zu der Feststellung, daß die Einbeziehung der Kriechwirkung in die Berechnungen durch Reduzierung des E_{Bo}, d. h. also durch den Formänderungsmodul unter Dauerlast $E_{\text{Bet, Dauer}}$ eine geringfügige Näherung zugunsten der Sicherheit darstellt.

Dieser Formänderungsmodul unter Dauerlast errechnet sich nach dem allgemein üblichen Ausdruck [15, 16] zu

$$E_{\text{Bet, Dauer}} = \frac{E_{\text{Bo}}}{1 + \varphi_{\text{o}}} \,. \tag{5}$$

Beansprucht die Last die Konstruktion nur kurzzeitig (etwa nur einige Stunden), dann vollzieht sich das Kriechen nur zu einem geringen Teil [15].

Berücksichtigt man diesen Teil des Kriechens zusammen mit dem erwähnten Ersetzen der $\sigma(\varepsilon)$-Linie durch ein idealplastisches Modell, kann der Kurzzeit-Formänderungsmodul $E_{\text{Bet, Kurzz.}}$ zur Untersuchung der Auswirkungen kurzzeitig anhaltender Beanspruchungen (z. B. Probebelastungen) nach [13] mit 70% des Elastizitätsmoduls E_{Bo} abgesetzt werden. Es gilt daher

$$E_{\text{Bet, Kurzz.}} = 0{,}7\, E_{\text{Bo}}. \tag{6}$$

Im weiteren wird unter $E_{\text{Bet.}}$ stets der jeweils benötigte Wert zu verstehen sein, d. h. bei Untersuchung einer Dauerbelastung wird $E_{\text{Bet}} = E_{\text{Bet, Dauer}}$ sein, während bei Untersuchung einer Kurzzeit-Belastung $E_{\text{Bet}} = E_{\text{Bet, Kurzz,}}$ und bei Untersuchung der Auswirkung von Schwingungen $E_{\text{Bet}} = E_{\text{Bo}}$ gelten.

3.4. *Die Auswirkungen der Plastizität*

Bekanntlich kann die Knickverformung (das Ausknicken) von Stabwerken aus nichtlinear elastischem bzw. plastischem Material unter mittigem Druck nach der Theorie I von ENGESSER untersucht werden, die das gekrümmt verlaufende Spannungs-Dehnungsdiagramm durch dessen Tangente im betreffenden Punkt ersetzt. Bei theoretisch mittiger Druckbeanspruchung von Schalen aus plastischem Material verläuft die Ausknickung ähnlich wie beim geraden Stab [19], die Annahmen der Theorie I von ENGESSER können also auch bei der Berechnung von Schalen angewendet werden.

Bei Untersuchung der Stabilität mittig gedrückter Konstruktionen kann der mit der spezifischen Beanspruchung veränderliche Elastizitätsmodul E (d. h. die Auswirkung des nichtlinearen Kriechens) für die im Schalenbau üblichen Betonqualitäten mit dem Ausdruck

$$E = E_{\text{Bo}}\left[1 - \left(\frac{\sigma}{\sigma_p}\right)^2\right] \tag{7}$$

in die Berechnung einbezogen werden.

Graphisch veranschaulicht diesen Zusammenhang die Kurve 1 des Bildes 2. Die durch die ausmittige Kraft verursachte Deformation wird aber nicht mit dem Elastizitätsmodul E_{Bo}, sondern mit dem Formänderungsmodul $E_{\text{Bet, Kurzz.}}$ berechnet. Durch die diesem Wert entsprechende gestrichelte Linie wird also die in dem Bild aufgetragene Parabel begrenzt. Der Zusammenhang muß indes in den Ausdruck (7) kontinuierlich übergehen, eine Bedingung, die sich durch die Ellipse

$$E = E_{\text{Bet}}\sqrt{1 - \left(\frac{\sigma}{\sigma_p}\right)^2} \tag{8}$$

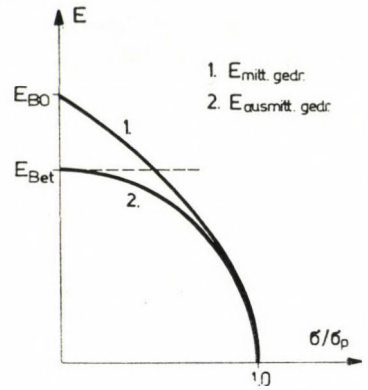

Bild 2. Die Abhängigkeit des Beton-Formänderungsmoduls E vom Verhältnis der durch mittigen Druck geweckten Spannung zur Prismenfestigkeit σ_p

annähern läßt (vgl. die Kurve 2 im Bild 2). Das σ dieser Gleichung bezeichnet die dem elastischen Ausknicken zugehörige Membran-Druckspannung.

Schreibt man die Gleichung (8) auf die Last um, erhält man den Zusammenhang

$$p_{kr,\,pl} = p_{kr,el} \sqrt{\frac{1}{1 + \left(\frac{p_{kr,el}}{p_{pl}}\right)^2}} = p_{kr,el} \cdot \zeta, \tag{9}$$

in dem das $p_{kr,\,pl}$ die auch die plastischen Eigenschaften mit berücksichtigende kritische Last bezeichnet, während $p_{kr,el}$ für die unter Annahme eines linear elastischen Stahlbetons bestimmte obere kritische Last, p_{pl} hingegen für jene Last steht, die die Konstruktion bei der (nicht angewachsenen) Anfangsausmittigkeit w_0 (also ohne Beulung) zu Bruch gehen läßt.

Zur Berechnung der plastischen kritischen Last $p_{kr,\,pl}$ muß also die elastische kritische Last bereits bekannt sein.

4. Die Schalenbeulsteifigkeit des Stahlbeton- und des Betonquerschnitts

Wie bei allen Flächentragwerken aus Beton und Stahlbeton weicht die Wanddicke für gewöhnlich auch bei Schalen von den entwurfsmäßigen Abmessungen ab. Großangelegte Reihenmessungen an ausgeführten Stahlbetonplatten, die vom Budapester Institut für Bauwissenschaft vorgenommen wurden [21, 22], haben bei ihrer Auswertung im Mittel das 1,05fache der entwurfsmäßigen Plattendicke, für die Querschnittabmessungen hingegen einen um 1 cm unter den entwurfsmäßigen Größen liegenden unteren Grenzwert ergeben. Die Knickverformung wird entscheidend durch die durchschnittlichen Quer-

schnittabmessungen bestimmt, und extreme Abweichungen in den Einzelquerschnittabmessungen kommen erst unmittelbar vor dem Bruch zur Geltung. Bei Bestimmung der elastischen kritischen Last kann also die Berechnung der Schalenstabilität die Querschnittabmessungen mit den entwurfsgemäßen Werten ansetzen, das p_{pl} hingegen soll auf Grund der um 1 cm verkleinerten Querschnittshöhe bestimmt werden.

Die Untersuchung der Beulverformung von Stahlbetonschalen bedient sich — im Sinne der Begründung in [23] — des „Schalen-Beulsteifigkeitskennwertes"

$$K = \sqrt{BD}\,, \tag{10}$$

in dem B bzw. D die Biege- bzw. die Dehnsteifigkeit bezeichnen.

Die Steifigkeiten gehen in die Berechnung mit den dem Stadium II der Stahlbetonkonstruktionen entsprechenden Werten, d. h. mit den Kennwerten für die in der Zugzone eingerissenen, linear elastischen Querschnitte ein.

Die Biegesteifigkeit B und die Dehnsteifigkeit D von Stahlbetonkonstruktionen hängen von der Bewehrung und von der Ausmittigkeit der Druckkraft ab, weil die zugbeanspruchte Betonzone mit zunehmender Ausmittigkeit Risse erleidet, wobei ihre Steifigkeit abnimmt.

Betrachtet man die im Bild 3 dargestellten Querschnitte und untersucht man das unter a) aufgetragene Spannungsdiagramm des linear elastischen, ausmittig gedrückten, nicht gerissenen Betonquerschnitts, kann für die Biege- bzw. Dehnsteifigkeit unter Vernachlässigung der Querkontraktionszahl

$$B_{\text{Bet}}^{\text{voll}} = \frac{E_{\text{Bet}}\, t^3}{12} = E_{\text{Bet}}\, J_{\text{Bet}}^{\text{voll}},$$

bzw.

$$D_{\text{Bet}}^{\text{voll}} = E_{\text{Bet}} \cdot t = E_{\text{Bet}}\, F_{\text{Bet}}^{\text{voll}}$$

geschrieben werden. J bezeichnet hier das spezifische Trägheitsmoment, F hingegen die spezifische Fläche.

Ist der Querschnitt bewehrt, erhöht sich der Wert der Steifigkeit K_{Beton} des nicht eingerissenen Querschnitts um den Wert des $E_{St}/E_{\text{Bet}} = n$-fachen Stahlquerschnitts. Das E_{St} bezeichnet den Elastizitätsmodul der Stahlbewehrung. Es gilt somit

$$B_{\text{Stahlb.}}^{\text{voll}} = E_{\text{Bet}}\, J_{\text{Stahlb.}}^{\text{voll}}$$

und

$$D_{\text{Stahlb.}}^{\text{voll}} = E_{\text{Bet}}\, F_{\text{Stahlb.}}^{\text{voll}}$$

Das hochgestellte „voll" bezeichnet hier den Vollquerschnitt ohne Risse, der Index „Stahlb" hingegen die Berücksichtigung der Stahlbewehrung durch die n-fache Betonfläche.

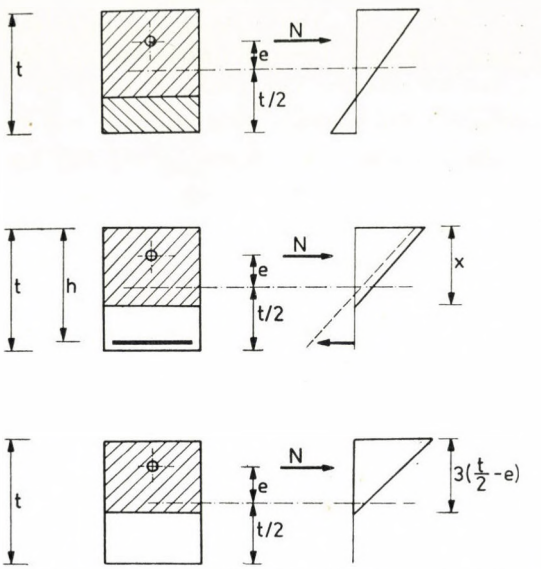

Bild 3. Die Spannungsdiagramme des ausmittig druckbeanspruchten homogenen sowie des Stahlbeton- und des Betonquerschnitts

Treten im Betonquerschnitt Risse auf (s. Bild 3b), vermindern sich seine Schalenbeulsteifigkeits-Kennwerte, wobei das Ausmaß der Reduktion von der Ausmittigkeit der Druckkraft abhängt.

Die Veränderung der Beulsteifigkeits-Kennwerte des Stahlbetonquerschnitts mit dem Parameter $n\mu = 0{,}125$ in Abhängigkeit von der Ausmittigkeit der Druckkraft veranschaulicht Bild 4. Erreicht die Ausmittigkeit die halbe Querschnittshöhe, nähern sich auch die Schalenbeulsteifigkeits-Werte ihren bei der unendlich großen Ausmittigkeit (d. h. bei der reinen Biegung) gültigen Werten

$$B^{\text{riss.}}_{\text{Stahlbet.}} = E_{\text{Bet.}} J^{\text{riss.}}_{\text{Stahlbet.}}$$

$$D^{\text{riss.}}_{\text{Stahlbet.}} = E_{\text{Bet.}} F^{\text{riss.}}_{\text{Stahlbet.}}.$$

Die Werte $B^{\text{riss.}}_{\text{Stahlbet.}}$ und $D^{\text{riss.}}_{\text{Stahlbet.}}$ unterscheiden sich von den Werten $B^{\text{voll}}_{\text{Stahlbet.}}$ und $D^{\text{voll}}_{\text{Stahlbet.}}$ insofern, als in ihnen der aus der Zugzone des Betons resultierende Steifigkeitsanteil nicht mehr enthalten ist.

Die *Schalenbeulsteifigkeits-Kennwerte* des eingerissenen Stahlbetonquerschnitts errechnen sich aus dem Zusammenhang

$$K^{\text{riss.}}_{\text{Stahlbet.}} = E_{\text{Bet.}} \sqrt{F^{\text{riss.}}_{\text{Stahlbet.}} \cdot J^{\text{riss.}}_{\text{Stahlbet.}}}. \tag{11}$$

Mit den Bezeichnungen $x/h = \xi$ und $F_{St}/b \cdot h = \mu$ sowie mit den nach der Stahlbetontheorie [24] errechneten Werten $J^{\text{riss.}}_{\text{Stahlbet.}}$ und $F^{\text{riss.}}_{\text{Stahlbet.}}$ erhält man

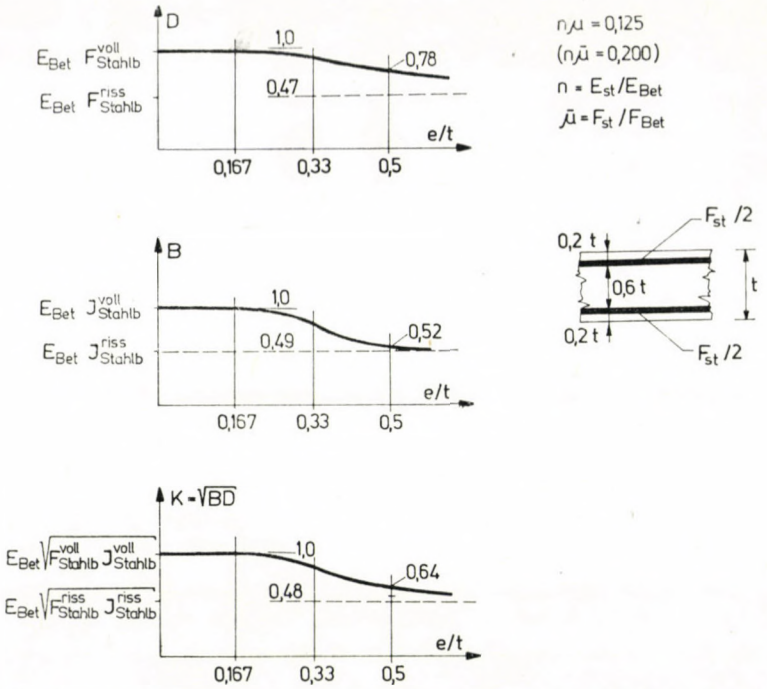

Bild 4. Die Änderungen der Steifigkeiten des Stahlbetonquerschnitts in Abhängigkeit von der Ausmittigkeit w

unter Mitberücksichtigung der Gl. (11) für den spezifischen Wert $K^{\text{riss.}}_{\text{Stahlbet.}}/K^{\text{voll}}_{\text{Bet.}} = \psi$ den Ausdruck

$$\psi = \left(\frac{h}{t}\right)^2 \cdot \left\{12\left[\frac{1}{3}\,\xi^4 + n\mu\left(\xi - \xi^2 + \frac{4}{3}\,\xi^3\right) + n^2\mu^2\,(1 - 2\xi + \xi^2)\right]\right\}^{1/2} . \qquad (12)$$

Das $n = E_{\text{st}}/E_{\text{Bet}}$ steht hier für das Verhältnis der Formänderungsmoduln des Stahls und des Betons.

Die relative Höhe ξ der neutralen Achse liegt dort, wo das statische Moment der zug- und der druckbeanspruchten Querschnitteile gleich Null ist. Aus dieser Bedingung ergibt sich der Zusammenhang

$$\xi = n\mu\left[\sqrt{1 + \frac{2}{n\mu}} - 1\right] . \qquad (13)$$

Bei Stahlbeton-Schalenkonstruktionen kommen zwei Bewehrungsarten, die mittige und die beidseitige Netzbewehrung in Frage.

Bei der mittigen Netzbewehrung gilt, wenn $F_{St}/b = f_{St}$ den Stahleinlagenquerschnitt je Breiteneinheit, h hingegen die nützliche Höhe bezeichnen,

$$h \approx 0{,}4t \quad \text{und} \quad \mu = \frac{f_{st}}{0{,}4t} .$$

Führt man für den auf den gesamten Betonquerschnitt bezogenen Stahlanteil die Bezeichnung $\bar{\mu} = f_{St}/h$ ein, ergibt sich ein $\mu = 2{,}5\ \bar{\mu}$. Mit diesen Werten hat man für den Wert ψ_1 der mittigen Netzbewehrung den Zusammenhang

$$\psi_1 = 0{,}553\left[\frac{1}{3}\xi^4 + 2{,}5n\bar{\mu}\left(\xi - \xi^2 - \frac{4}{3}\xi^3\right) + 6{,}25n^2\bar{\mu}^2(1 - 2\xi + \xi^2)\right]^{1/2} . \quad (14)$$

Für den Fall der *beidseitigen Netzbewehrung* soll die Bewehrung in der gedrückten Betonzone mit einer auf der sicheren Seite liegenden geringfügigen Näherung vernachlässigt werden, weil ihre Mitberücksichtigung die Berechnung komplizieren würde, ohne daß ihre Auswirkungen von Belang wären. Mit dieser Annahme ergibt sich bei der beidseitigen Netzbewehrung ein $h \approx 0{,}8\ t$ und ein $\mu = f_{St}/2\ h = \bar{\mu}/1{,}6$ und somit ein ψ_2-Wert von

$$\psi_2 = 2{,}22\left[\frac{1}{3}\xi^4 + 0{,}625n\bar{\mu}\left(\xi - \xi^2 + \frac{4}{3}\xi^3\right) + 0{,}391n^2\bar{\mu}^2\,(1 - 2\xi + \xi^2)\right]^{1/2} . \quad (15)$$

Tafel 1

$n\bar{\mu}$	0	0,1	0,2	0,3	0,4	0,6	0,8
ψ_1 (mittige Netzbewehrung)	0,00	0,23	0,32	0,43	0,52	0,67	0,79
ψ_2 (beidseitige Netzbewehrung)	0,00	0,32	0,51	0,68	0,83	1,10	1,33

Die für die unterschiedlichen Stahleinlagen-Anteile errechneten ψ_1- und ψ_2-Werte sind in der Tafel 1 zusammengefaßt bzw. im Bild 5 aufgetragen.

Im *unbewehrten Querschnitt* hebt sich die Zugspannung nach dem Auftreten von Rissen auf. Somit müssen die Druckspannungen allein den den Querschnitt beanspruchenden Druckkraft und Biegemoment das Gleichgewicht halten. Hieraus folgt eindeutig, daß unbewehrte Querschnitte Biegemomente nur aufnehmen können, solange die Ausmittigkeit der Kraft e noch innerhalb der Querschnittgrenzlinie liegt.

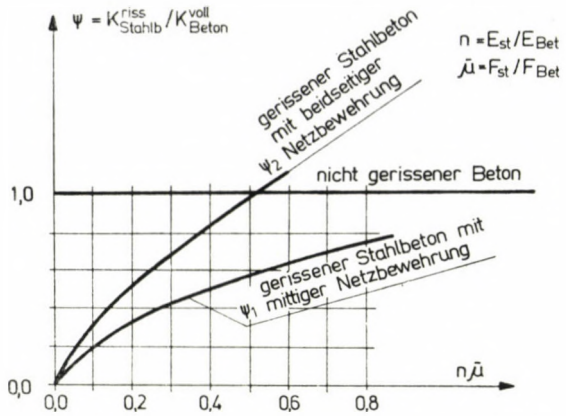

Bild 5. Die Änderung des Faktors ψ zur Berechnung der Beulsteifigkeit der Stahlbetonschale in Abhängigkeit vom Stahlquerschnitt

Im Beton können Risse durch das Schwinden bedingt, d. h. auch ohne Beanspruchung durch eine äußere Last auftreten. Der Querschnitt kann also zugunsten der Sicherheit schon vom Beginn der Beanspruchung durch eine äußere Last an als zugspannungsfrei angesehen werden.

Der Kurve im Bild 3c entsprechend kann die Druckzone des Querschnitts je Breiteneinheit zu

$$F^{riss.}_{Beton} = 3\left(\frac{t}{2} - e\right),$$

seine Dehnsteifigkeit hingegen zu

$$D^{riss.}_{Beton} = E_{Bet} \cdot 3\left(\frac{t}{2} - e\right)$$

errechnet werden. Das e steht hier für die Ausmittigkeit der resultierenden Kraft, auf den Schwerpunkt des ursprünglichen Querschnitts bezogen. (Bei der Beulung ist in den meisten Fällen $e = w$.)

Die Krümmung g der Formänderung kann im allgemeinen aus der Gleichung

$$g = \frac{M}{EJ}$$

berechnet werden.

Beim Querschnitt ohne Zugfestigkeit ist

$$g = \frac{\varepsilon}{x} = \frac{\sigma}{E_{Bet}x} = \frac{2N}{E_{Bet}\left[3\left(\frac{t}{2} - e\right)\right]^2}. \tag{16}$$

Multipliziert man in Gl. (16) Zähler und Nenner mit w, substituiert man den Wert $M = N \cdot e$ und setzt man die beiden g-Zusammenhänge einander gleich, erhält man für die Biegesteifigkeit die Formel

$$B_{\text{Beton}}^{\text{riss.}} = EJ_{\text{Beton}}^{\text{riss.}} = E \cdot 4{,}5e \left(\frac{t}{2} - e\right)^2$$

und somit für den *Schalenbeulsteifigkeits-Kennwert* den Ausdruck

$$K_{\text{Beton}}^{\text{riss.}} = \sqrt{B_{\text{Beton}}^{\text{riss.}} D_{\text{Beton}}^{\text{riss.}}} = E \sqrt{13{,}5e \left(\frac{t}{2} - e\right)^3} \quad . \tag{17}$$

Die Werte der Betonquerschnittssteifigkeiten sind im Bild 6 aufgetragen.

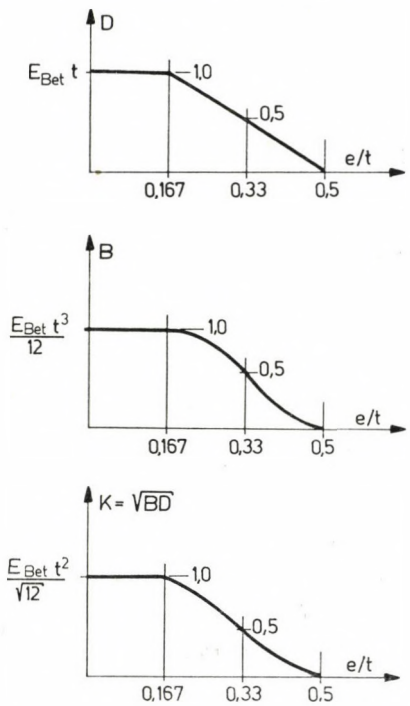

Bild 6. Die Änderung der Steifigkeiten des Betonquerschnitts in Abhängigkeit von der Ausmittigkeit w

5. Die obere kritische Last der elastischen Beton- und Stahlbetonschale

Im Bereich der Beulwellen ändert sich die Ausmittigkeit und damit auch die Beulsteifigkeit der Stahlbetonschale von Stelle zu Stelle. Am entscheidensten beeinflußt die Beulverformung gleichwohl den an der Stelle des größten

Biegemoments gültigen Steifigkeitswert. Da die Steifigkeit an den übrigen Teilen der Beulwelle diesen Wert übersteigt, darf mit einer geringfügigen Vernachlässigung zugunsten der Sicherheit angenommen werden, daß die Steifigkeit der sonst isotropen Stahlbetonschale im ganzen Beulwellenbereich dem an der Stelle des größten Biegemoments gültigen Wert gleichgesetzt werden kann. Sie ist mithin stellenunabhängig, und die Differenzialgleichungen werden konstante Koeffizienten haben. Entsprechend kann die einer Beulverformung w zugeordnete Last p mit der dem w_{max} zugehörigen Schalenbeulsteifigkeit bestimmt werden.

Das Bild 7 veranschaulicht das auf dieser Annahme fußende Verfahren an dem in [1] gelösten Beispiel des Zylinderschalenfeldes aus homogenem elastischem Material. Das Kraft-Beulverformungs-Diagramm der geometrisch

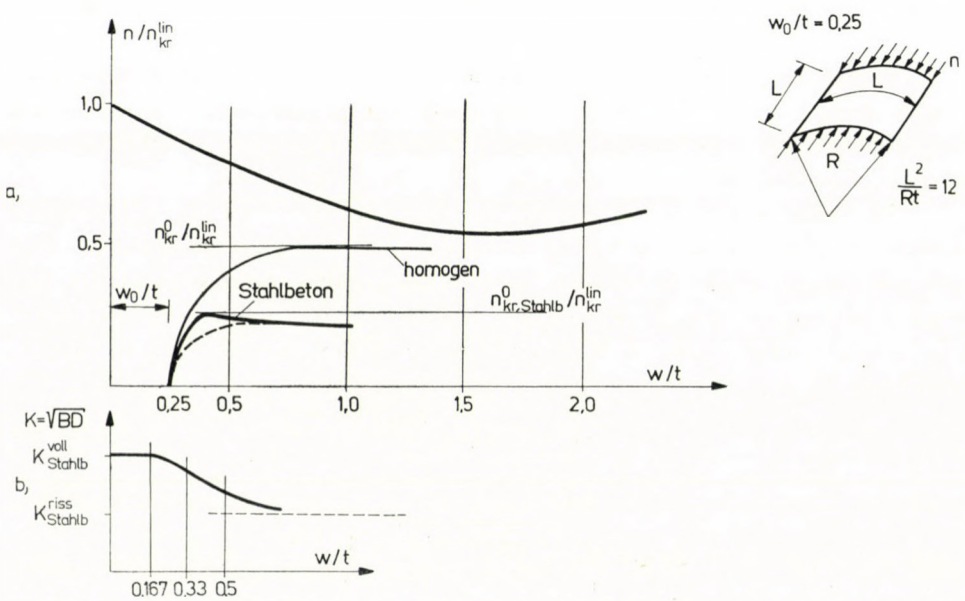

Bild 7. Die Bestimmung der oberen kritischen Last der Beton- und der Stahlbetonschale

vollkommenen Zylinderschale beschreibt die parabelartige, vom Punkt der linearen kritischen Last ausgehende, stark ausgezogene Kurve. Beansprucht die Last die homogene Schale mit einer Ausmittigkeit von $w_0 = 0{,}25t$ (bzw. hat die Vorbeule an der Schale diese Amplitude), dann ändert sich die mit wachsender Last zunehmende Ausmittigkeit w nach [1] nach der in dem Bild dünn ausgezogenen Kurve.

Im Diagramm des Bildes 7b ist der Zusammenhang zwischen der Steifigkeit K des Stahlbetonquerschnitts und der Ausmittigkeit $e = w$ dargestellt.

Die Ordinate jedes einzelnen w-Wertes der Kurve $p(w)$ des homogenen Materials muß im gleichen Verhältnis reduziert werden, in dem sich die Schalenbeulsteifigkeit K gegenüber $K^{\text{voll}}_{\text{Stahlbet.}}$ vermindert. Auf dieser Grundlage ergibt sich für Stahlbeton die im oberen Diagramm des Bildes 7a stark ausgezogene Kurve.

Die Scheitelpunkte dieser Kurven geben die obere kritische Last der elastischen Stahlbetonschale bei der gegebenen Ausmittigkeit an. Sie kann in der Form

$$p^{0}_{kr,el,\,\text{Stahlb.}} = \varrho_{\text{Stahlb.}}\, p^{\text{lin}}_{kr} \tag{18}$$

geschrieben werden.

Setzt man die Schalenbeulsteifigkeit des Stahlbetonquerschnitts vom Anfang an der Steifigkeit $K^{\text{riss}}_{\text{Stahlbet}}$ gleich, erhält man die dünn gestrichelte Kurve des oberen Bildes. Die zugehörige kritische Last liegt, wie ersichtlich, etwas unter dem exakter bestimmten Wert, mit dem Unterschied bleibt man also auf der sicheren Seite.

Bestimmt man die kritische Last der als isotrop angesehenen, über keine Zugfestigkeit verfügenden Betonschale nach dem geschilderten Verfahren mit den Werten $w_{kr} = 2t$ und $p^{u}_{kr} = 0{,}25 p^{\text{lin}}_{kr}$, erhält man die im Bild 8 stark ausgezogene Vollinie.

De facto treten die Risse auf der Betonschale nicht unendlich dicht, sondern in gewissen Abständen voneinander auf. Somit ist auch ihre Steifigkeit um einiges größer als die der Schale ohne jegliche Zugfestigkeit. Deshalb kann statt den aus dem Berechnungsverfahren für die Schale ohne Zugfestigkeit resultierenden exakten Werte die etwas höher liegende Kurve mit der Gleichung

$$\varrho_{\text{Beton}} = \left(1 - \frac{2w_0}{t}\right)^3 \tag{19}$$

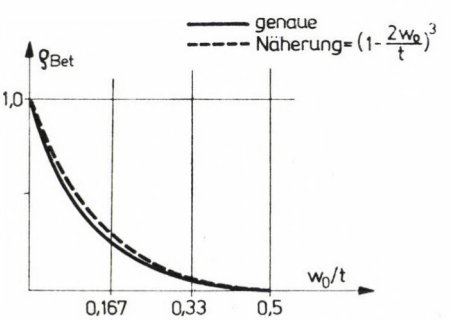

Bild 8. Vergleich des exakten ϱ-Wertes der Betonschale für den Fall dicht gelegener Risse mit dem Näherungswert ϱ bei weniger dicht aufgetretenen Rissen

benutzt werden. Graphisch veranschaulicht diesen Zusammenhang Bild 8. Im allgemeinen Fall kann $\varrho_{\text{Stahlbet.}}$ durch lineare Interpolation nach ψ zwi-

schen den Werten ϱ_{homogen} und ϱ_{Beton} laut folgender Formel ermittelt werden:

$$\varrho_{\text{Stahlbet.}} = \varrho_{\text{Beton}} + \psi\,(\varrho_{\text{homogen}} - \varrho_{\text{Beton}}). \tag{20/a}$$

Bei einem Wert von $w_0/t = 0{,}5$ sinkt die Steifigkeit des Betonquerschnitts auf Null ab. Wie in der Analyse des Beulsteifigkeitskennwerts für den Stahlbetonquerschnitt gezeigt, kann dieser und mit ihm auch die kritische Last der Stahlbetonschale bei Werten von $w_0 > 0{,}5t$ schon mit dem ψ-fachen des Wertes für die homogene Schale angesetzt werden. Im Bereich $w_0 < 0{,}5t$ schmiegt sich die Kurve, die durch den Zusammenhang

$$\varrho_{\text{Stahlb.}} = \left\{1 - 2\frac{w_0}{t} + \sqrt[3]{\psi}\left[\frac{2}{3}\frac{w_0}{t} + \frac{1}{5}\left(\frac{w_0}{t}\right)^2 + \left(\frac{w_0}{t}\right)^3\right]\right\}^3 \tag{20/b}$$

beschrieben wird, an die obere Kurve der homogenen und an die untere Kurve der zylinder-und kugelförmige Betonschale völlig an, während sie im Punkt $w_0/t = 0{,}5$ die ψ-fachen Werte anzeigt (s. Bild 9 und Tabelle 2). In Fällen mit Werten von $w_0 < 0{,}5t$ kann somit die Gl. (20) angewendet werden, wogegen bei Werten von $w_0 > 0{,}5t$ die Anwendung der $\varrho_{\text{Stahlb.}}$-Werte für den Fall $w_0 = 0{,}5t$ erlaubt ist.

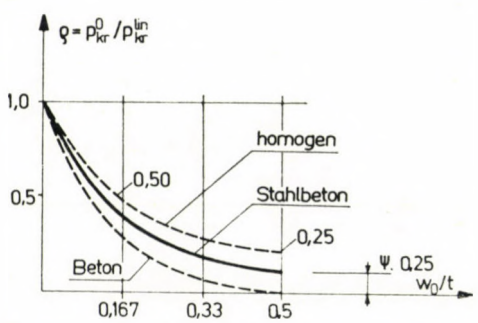

Bild 9. Die ϱ-Werte der homogenen sowie der zylinder- und kugelförmigen Stahlbeton- und der Betonschalen

Bei Kuppelschalen kann der Faktor $\varrho_{\text{Stahlb.}}$ den Wert $\varrho_{\text{hom}} \approx 0{,}6$, der der von der symmetrischen Beulung abzweigenden antimetrischen Beulung zugeordnet ist, nicht überschreiten [25]. Zum ϱ_{hom}-Wert gehört eine Vorbeulamplitude $w_0 = 0{,}125t$, weshalb bei Stahlbeton-Kuppelschalen ein niedrigerer Vorbeulwert als dieser nicht angesetzt werden.

Letztlich errechnet sich die obere kritische Last der elastischen Stahlbetonschale zu

$$p^0_{kr,el,\text{Stahlbet.}} = \varrho_{\text{Stahlb.}} \cdot p^{\text{lin}}_{kr}. \tag{21}$$

Führt man den Quotienten

$$\beta = \frac{\varrho(\psi)}{\varrho(\psi = 1)} \tag{22}$$

ein, kann die obere kritische Last der elastischen Stahlbetonschale statt nach dem Zusammenhang (21) nach der Gleichung

$$p^0_{kr,el,\text{Stahlbet.}} = \beta \cdot p^0_{kr,\,el,\,\text{homogen}} \tag{23}$$

bestimmt werden.

Die β-Werte sind im Bild 10 aufgetragen und in der Tafel 3 zusammengefaßt.

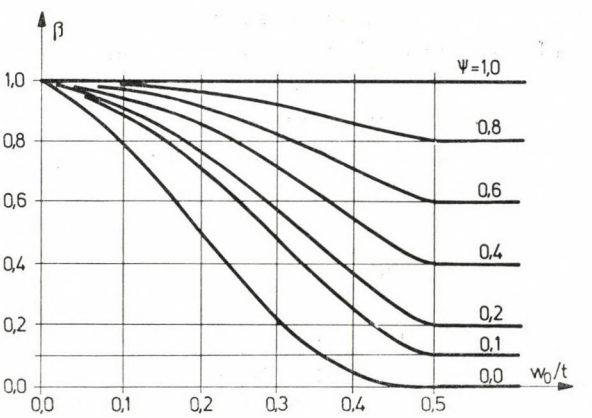

Bild 10. Das Diagram der β-Werte

6. Die obere kritische Last der plastischen Stahlbetonschale

Das plastische Verhalten der Stahlbetonschale kann in die Berechnung mit dem Ausdruck (9) einbezogen werden. Die Zusammenfassung der bisherigen Ausführungen führt letzten Endes zu dem Schluß, daß sich die obere kritische Last bei Berücksichtigung der Eigenschaften der Stahlbetonschale (d. h. der Risse, der Bewehrung, des Kriechens und der Plastizität) nach der Gl.

$$p^0_{kr,\,pl.\,\text{Stahlb.}} = \zeta \cdot p^0_{kr,\,el,\,\text{Stahlb.}} = \zeta \cdot \beta \cdot p^{\text{lin}}_{kr,\,el,\,\text{homogen}} \tag{24}$$

errechnet. In dieser Gleichung bezeichnet das $p^0_{kr,\,pl,\,\text{Stahlb.}}$ die obere kritische Last der auch plastische Eigenschaften aufweisenden Stahlbetonschale.

Tafel 2

ϱ-Faktoren für Beton- und Stahlbetonschalen

ψ \ w_0/t	0,00	0,05	0,10	0,15	0,20	0,25	0,30	0,35	0,40	0,45	0,50
1,00	1,000	0,815	0,660	0,534	0,434	0,359	0,304	0,267	0,246	0,243	0,242
0,90	1,000	0,812	0,655	0,526	0,425	0,348	0,291	0,252	0,229	0,221	0,218
0,80	1,000	0,809	0,649	0,518	0,415	0,336	0,278	0 237	0,212	0,200	0,194
0,70	1,000	0,805	0,642	0,510	0,405	0,324	0,264	0,222	0,194	0,180	1,170
0,60	1,000	0,801	0,635	0,500	0,393	0,311	0,249	0,205	0,175	0,158	0,145
0,50	1,000	0,797	0,628	0,490	0,381	0,297	0,234	0,188	0,156	0,137	0,121
0,40	1,000	0,792	0,619	0,478	0,367	0,281	0,217	0,169	0,136	0,114	0,097
0,30	1,000	0,786	0,608	0,465	0,351	0,263	0,197	0,149	0,114	0,091	0,073
0,25	1,000	0,783	0,602	0,457	0,342	0,253	0,187	0,138	0,103	0,079	0,061
0,20	1,000	0,778	0,596	0,448	0,331	0,242	0,175	0,126	0,091	0,067	0,049
0,15	1,000	0,774	0,587	0,437	0,319	0,229	0,161	0,112	0,078	0,054	0,036
0,10	1,000	0,768	0,578	0,425	0,305	0,213	0,146	0,097	0,063	0,040	0,024
0,05	1,000	0,760	0,563	0,407	0,285	0,193	0,125	0,078	0,045	0,025	0,012
0,00	1,000	0,729	0,512	0,343	0,216	0,125	0,064	0,027	0,008	0,001	0,000

In dieser Tabelle bezeichnen ψ den Faktor zur Berechnung des Stahlbeton-Beulsteifigkeits-Kennwertes, w_0 die Anfangsausmittigkeit und t die Dicke des Stahlbetonquerschnitts

Tafel 3

β-Faktoren für Beton- und Stahlbetonschalen $p^0_{kr,\text{Stahlb.el.}} = \beta \cdot p^0_{kr,\text{hom, el}}$

ψ \ w_0/t	0	0,05	0,1	0,15	0,2	0,25	0,3	0,35	0,4	0,45	0,5
1,0	1,0	1,05	1,0	1,0	1,0	1,0	1,0	1,0	1,0	1,0	1,0
0,9	1,0	0,996	0,992	0,985	0,979	0,969	0,957	0,944	0,931	0,909	0,9
0,8	1,0	0,993	0,983	0,970	0,956	0,936	0,914	0,888	0,862	0,823	0,8
0,7	1,0	0,988	0,973	0,955	0,933	0,903	0,868	0,831	0,789	0,741	0,7
0,6	1,0	0,983	0,962	0,836	0,906	0,966	0,819	0,768	0,650	0,711	0,6
0,5	1,0	0,978	0,952	0,918	0,878	0,827	0,770	0,704	0,634	0,564	0,5
0,4	1,0	0,972	0,938	0,895	0,846	0,783	0,714	0,633	0,553	0,469	0,4
0,3	1,0	0,964	0,921	0,871	0,809	0,733	0,648	0,558	0,463	0,374	0,30
0,25	1,0	0,961	0,912	0,856	0,788	0,705	0,615	0,517	0,419	0,325	0,25
0,2	1,0	0,955	0,903	0,839	0,763	0,674	0,576	0,472	0,370	0,276	0,20
0,15	1,0	0,950	0,889	0,818	0,735	0,638	0,530	0,419	0,317	0,222	0,15
0,1	1,0	0,942	0,876	0,796	0,703	0,593	0,480	0,363	0,256	0,165	0,10
0,05	1,0	0,933	0,853	0,762	0,657	0,538	0,411	0,292	0,183	0,103	0,05
0,00	1,0	0,894	0,776	0,642	0,498	0,348	0,211	0,101	0,033	0,004	0,00

In dieser Tabelle bezeichnen ψ den Faktor zur Berechnung des Stahlbeton-Beulsteifigkeits-Kennwertes, w_0 die Anfangsausmittigkeit und t die Dicke des Stahlbetonquerschnitts

Zur Überprüfung des hier erörterten Verfahrens wurden in [26] die in [27, 28, 29, 30, 31, 32, 33 und 34] publizierten, experimentell ermittelten Beullasten von Stahlbetonschalen nach Gl. (24) auch rechnerisch bestimmt und mit den experimentell festgestellten verglichen. Die Resultate dieser Berechnungen sind in Abhängigkeit von R/t im Bild 11 aufgetragen.

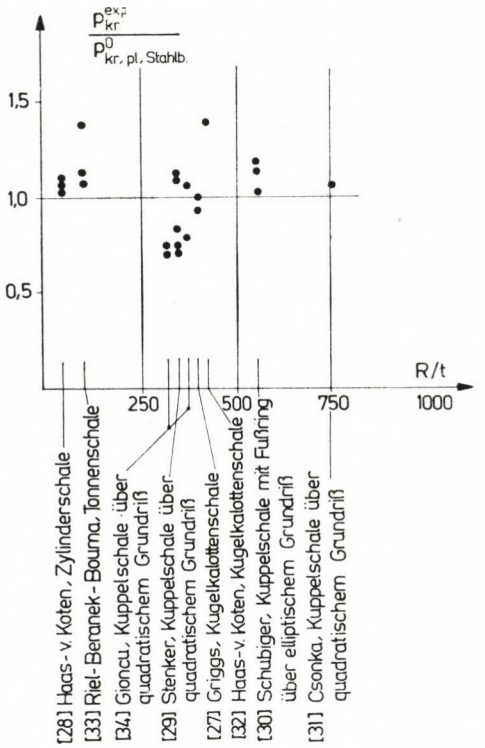

Bild 11. Vergleich der in der Fachliteratur publizierten Versuchsergebnisse mit den nach dem hier beschriebenen Verfahren rechnerisch bestimmten Werten

Der Mittelwert der Quotienten aus den experimentell und den rechnerisch ermittelten kritischen Lasten beträgt 1,02, die Streuung 20%. Das besagt, daß das hier dargelegte Berechnungsverfahren den wirklichen Verhältnissen gut entspricht.

SCHRIFTTUM

1. Wolmir, A. S.: Biegsame Platten und Schalen. Verlag für Bauwesen, Berlin 1962
2. v. Kármán, Th.—Tsien, H. S.: The Buckling of Spherical Shells by External Pressure. *Journ. Aero. Sci.* **7** (1939) 43
3. Almroth, B. O.: Influence of Imperfections and Edge Restraint on the Buckling of Axially Compressed Cylinders. *NASA*-CR-432. (April) 1966

4. THOMPSON, J. M. T.: The Elastic Instability of a Complete Spherical Shell. *Aeronaut. Quart.* **13** (1962) 189—201
5. DONNELL, L. H.—WAN, C. C.: Effect of Imperfections on Buckling of Thin Cylinders and Columns under Axial Compression. *Journ. Appl. Mech.* **17** (1950) 73—83
6. MADSEN, W. A.—HOFF, N. J.: The Snap-through and Postbuckling Equilibrium Behavior of Circular Cylindrical Shells under Axial Load. Standford University Department of Aeronautics and Astronautics. *Report No.* 227 (1965), Stanford, California
7. KOITER, W. T.: The Effect of Axisymmetric Imperfections on the Buckling of Cylindrical Shells under Axial Compression. *Proc. Royal Netherlands Academy of Sciences*, Amsterdam, Series B, **66** (1963) 265—279
8. KOGA, T.—HOFF, N. J.: The Axisymmetric Buckling of Initially Imperfect Complete Spherical Shells. *Intern. Journ. of Solids and Structures*, **5** (1969) 679—697
9. HUTCHINSON, J. W.: Imperfection Sensitivity of Externally Pressurized Spherical Shells. *Journ. Appl. Mech.* **34** (1967) 49—55
10. BUSHNELL, D.: Nonlinear Axisymmetric Behavior of Shells of Revolution. *AIAA Journ.* **5** (1967) 432—439
11. KOITER, W. T.: The Nonlinear Buckling Problem of a Complete Spherical Shell under Uniform External Pressure. I, II, III and IV. *Proc. Kon. Nederl. Acad. Wet.* Series B, **72** (1969) 40—123
12. BUDIANSKY, B.—AMAZIGO, J. C.: Initial Postbuckling Behavior of Cylindrical Shells under External Pressure. *Journ. Math. Phys.* **47** (1968) 223—235
13. Roš, M.: Die materialtechnischen Grundlagen und Probleme des Eisenbetons im Hinblick auf die zukünftige Gestaltung der Stahlbetonbauweise. *EMPA-Bericht*, Nr. 162 (1950)
14. DISCHINGER, F.: Untersuchungen über die Knicksicherheit, die elastische Verformung und das Kriechen des Betons bei Bogenbrücken. *Bauing.* **18** (1937) 604
15. C. E. B. Empfehlungen zur Berechnung und Ausführung von Stahlbetonbauwerken. Deutscher Beton-Verein E. V. 1966
16. MSz (Ung. Norm) 15022/1—71: Statische Bauwerksplanung. Stahlbetonkonstruktionen
17. HUANG, N. C.: Nonlinear Creep Buckling of Some Simple Structures. University of California, San Diego. *Report IRPA*-66-80 (1960)
18. KOLLÁR, L.: A kúszás hatása a szerkezetek kritikus terhére (Die Auswirkungen des Kriechens auf die kritische Last von Konstruktionen *Mélyépítéstud. Szemle* **18** (1968) 472—479
19. BATTERMANN, St. C.: Plastic Stability of Spherical Shells. *Proceedings ASCE* **95** No. EM2, April 1969
20. DULÁCSKA, E.: Praktische Stabilitätsuntersuchung an zentrisch gedrückten Tragwerken aus Material mit veränderlichem Elastizitätsmodul. *Bautechnik* **10** (1972) 340—345
21. SZEPESSZENTGYÖRGYI, O.: ÉMI Tudományos Beszámoló az állandó terhekre vonatkozó ISO előírás kidolgozása c. témáról (Wissenschaftlicher ÉMI-Bericht zum Thema: Ausarbeitung der ISO-Vorschriften über die Dauerbelastungen, ungarisch). Budapest (1966)
22. KORDA, J.—MÓNA, J.: A vasbeton szerkezetek méreteiben mutatkozó tényleges eltérések és azok számításbavétele (Die effektiven Abweichungen in den Abmessungen von Stahlbetonkonstruktionen und ihre Berücksichtigung, ungarisch). *ÉMI-Bericht*, Budapest 1969
23. DULÁCSKA, E.: Der Steifigkeitskennwert der Schalenbeulung. *Acta Techn. Sci. Hung.* **86** (3—4).
24. MIHAILICH, Gy.—PALOTÁS, L.: Vasbetonépítéstan I. A vasbeton szilárdságtana (Stahlbetonbau-Lehre I. Die Stahlbetonfestigkeit, ungarisch). Tankönyvkiadó, Budapest 1964
25. WEINITSCHKE, H. J.: On Asymmetric Buckling of Shallow Spherical Shells. *Journ. Mat. Phys.* **44** (1965) 141—163
26. DULÁCSKA, E.: Beton- és vasbetonhéjak horpadási vizsgálata (Untersuchungen über das Beulverhalten von Beton- und Stahlbetonschalen, ungarisch). *Műszaki Tudomány* **48** (1974) 415—464
27. GRIGGS, H.: Buckling of Reinforced Concrete Shells. *Journ. Eng. Mech. Divis. ASCE* **97** EM. No. 3 (June) (1971) 687—700
28. HAAS, A. M.—van KOTEN, H.: The Stability of Doubly Curved Thin Shells. *RILEM Symposion*, Buenos Aires 1971
29. STENKER, H.: Gesamtbericht von Großversuchen an doppelt gekrümmten Montageschalen für raumabschließende Geschoßdecken. *Wissenschaftl. Zeitschr. Hochschule für Architektur und Bauwesen*, Weimar 1961, 181—202
30. SCHUBIGER, E.: Die Schalenkuppeln im vorgespannten Beton der Kirche Felix und Regula in Zürich. *Schweizerische Bauzeitung* **68** (1950) 223—228

31. CSONKA, P.: Die Verformung und nachträgliche Verstärkung einer kuppelartigen Schale in Ungarn. *Die Bautechnik* **35** (1958) 69
32. HAAS, A. M.—van KOTEN, H.: On the Buckling Behavior of Doubly Curved Shells. *RILEM Symposion*, Buenos Aires 1971
33. RIEL, A. C.—BERANEK, W. J.—BOUMA, A. L.: Tests on Shell Roof Models of Reinforced Mortar. *Proceedings of the Second Symposion on Concrete Shell Roof Constructions* (July 1957, Oslo), Tekniks Ukeblad, Oslo
34. GIONCU, V.: Cercetări experimentale privind stabilitatea cupelelor pe contur pătrat. *St. Cerc. Mec. Apl.* **32** (1973) 641—651

Bezeichnungen

n_{kr}^{lin} bzw. p_{kr}^{lin} — die nach der linearen Beultheorie bestimmbare kritische Kraft bzw. Last,

n_{kr}^{u} bzw. p_{kr}^{u} — die nach der nichtlinearen (Großverformungs-) Beultheorie bestimmbare minimale kritische Last der geometrisch vollkommenen Schale,

n_{kr}^{0} bzw. p_{kr}^{0} — die obere kritische Last, d.h. das Maximum der nach der nichtlinearen Beultheorie bestimmbaren Tragfähigkeit der vorgebeulten Schale,

R — der Schalenkrümmungshalbmesser,

x, y — die Koordinatenachsen. Als Indizes zeigen sie die in Richtung der betreffenden Koordinaten gedeuteten Größen an,

w_0 — die maximale Vorbeulamplitude, d.h. die Anfangsausmittigkeit,

w — die maximale Beulverformungsamplitude,

$w_{0,\text{ungew.}}$ bzw. $w_{0,\text{ber.}}$ — die ungewollte bzw. berechnete Anfangsausmittigkeit,

$K = \sqrt{BD}$ — der Schalen-Beulsteifigkeitskennwert,

B — der Biegesteifigkeitskennwert

D — der Dehnsteifigkeitskennwert,

E — der Elastizitätsmodul

E_{Bo} — der Anfangselastizitätsmodul des Betons

$E_{\text{Bet, Kurzz.}}$ bzw. $E_{\text{Bet, Dauer}}$ — der einer Kurzzeit- bzw. einer Dauerbelastung zugeordnete Formänderungsmodul des Betons,

t — die Schalendicke,

σ_w — die Würfelfestigkeit des Betons,

σ_p — die Prismenfestigkeit des Betons,

φ_0 — die Endkriechzahl,

$p_{kr,\,pl}$ — die obere kritische Last der Beton- oder Stahlbetonschale aus plastischem Beton,

$p_{kr,\,el}$ — die unter Annahme eines linear elastischen Betons bestimmte obere kritische Last der Beton- oder Stahlbetonschale,

$\varrho_{\text{Stahlb.}} = \dfrac{p_{kr,\,el,\,\text{Stahlb.}}^{0}}{p_{kr}^{\text{lin}}}$ — Faktor zur Berechnung der oberen kritischen Last der elastischen Stahlbetonschale,

$\beta = \dfrac{p_{kr,\,el,\,\text{Stahlb.}}^{0}}{p_{kr,\,el,\,\text{homogen}}^{0}}$ — Faktor zur Berechnung der oberen kritischen Last der elastischen Stahlbetonschale,

p_{pl} — jener Lastwert, bei dem die in der Schale auftretende Beanspruchung den Bruchwert erreicht,

ψ — Faktor zur Berechnung der Beulsteifigkeit von Stahlbetonschalen (die Indizes 1 bzw. 2 sind Hinweise auf die ein- bzw. beidseitige Netzbewehrung),

l_x bzw. l_y — die Beulwellenlängen in Richtung x bzw. y,

$n = E_{\text{St}}/E_{\text{Bet}}$ — das Verhältnis des Formänderungsmoduls des Stahls zu jenem des Betons,

μ — der Quotient der spezifischen einseitigen Bewehrung und der nützlichen Höhe,

μ — Verhältnis der beidseitigen Querschnittbewehrung zur Gesamtfläche des Querschnitts.

Buckling of r. c. Shell Structures. The paper extends the possibility for the application of the buckling theory of elastic shell structures over the field of reinforced concrete shells. In doing this, the creep, plastic behaviour, the cracks of the tenson flange of cross

sections and the position and quantity of the reinforcement are taken into account. The critical load to be determined by the worked out method is in good agreement with the results of the experiments.

Устойчивость железобетонных оболочек. В данной работе распространены возможности применения теории устойчивости упругих оболочек для области железобетонных оболочек. При этом учтены ползучесть, эластичные свойства, далее трещинообразование на напряженном поясе сечения бетона, а также положение и количество использованной арматуры. Критическая нагрузка, определяемая при помощи разработанного метода, совпадает с экспериментальными данными.

Acta Technica Academiae Scientiarum Hungaricae, Tomus 86 (1—2), pp. 117—129 (1978)

RHEOLOGISCHE UNTERSUCHUNG DER BODENKONSOLIDATIONSTHEORIE

I. SÁNDOR*

KANDIDAT DER TECHNISCHEN WISSENSCHAFTEN

Behandelt wird die Konsolidationstheorie des porösen, eindimensional verdichtbaren Bodens. Mit Hilfe eines rheologischen Modells wird die partielle Differentialgleichung vierter Ordnung aufgestellt. Dadurch entsteht eine allgemeine Gleichung für die Berücksichtigung des Kriechens, die in der einschlägigen Fachliteratur noch nicht publiziert wurde. Es werden zwei Modelle einander gegenübergestellt, wovon die Florinsche Gleichung (1953) aufgrund von mechanischen Erwägungen abgeleitet werden konnte. Die sich auf die rheologischen Modelle beziehenden Festlegungen werden zusammengefaßt und ergänzt. Zur Lösung der Differentialgleichung werden Methoden der linearen Algebra (und zwar die Rasterlinienmethode) angewandt, die wegen Raummangel hier nicht erörtert werden. Aufgrund von mehreren numerischen Beispielen werden in Zusammenhang mit der Wichtigkeit des Kriechens im Bereich der Konsolidationstheorie der Böden Feststellungen gemacht.

Die Theorie der Bodenkonsolidation ist schon ein halbes Jahrhundert alt. Eines der wichtigsten Probleme der Fundamentenanlagen von Bauten bildet die Ermittelung der Senkung, insbesonders bei bindigen Böden. Der Verlauf der Senkung zieht sich in der Zeit hinaus und dauert auch nach dem Errichten des Bauobjektes. Aus diesen Senkungen können Beschädigungen entstehen. Deshalb ist die Untersuchung der Untergrundsenkungen einer der wichtigsten Bereiche der Bodenmechanik. Eine Reihe von Zeitschriften beschäftigten sich mit der Theorie der Bodenkonsolidation.

TERZAGHI interpretierte den Vorgang der Bodenkonsolidation mit Hilfe des sogenannten rheologischen Modells. Im Bereich der Rheologie ist dieses Modell das sogenannte Kelvin—Voigtsche Modell, welches durch die parallele Verbindung eines Hookeschen und eines Newtonschen Grundmodells hergestellt wird. Seine Bezeichnung ist K||N. Hingegen hat TERZAGHI die Differentialgleichung aufgrund des Hookeschen Modells abgeleitet, d. h., er betrachtete den Boden als elastisch.

Dadurch gab er zwar eine analytische Methode zur Ermittelung der neutralen Spannung, doch stimmte das erhaltene Ergebnis mit dem im Labor gefundenen sog. Kompressionsergebnis in vielen Fällen nicht überein. Auf diese Weise hat sich der Begriff des sekundären Zeiteffekts, bzw. der sekun-

* Dr. I. SÁNDOR, Technische Universität, Budapest

dären Konsolidation entwickelt. Zur Erklärung dieser Erscheinung wurden weitere rheologische Modelle ausgearbeitet.

Einen derartigen Vorschlag brachte THAN im Jahre (1957) durch Anwendung des Maxwellschen Modells $M = H - N$ mit dem Anliegen um das Ergebnis der Reihenschaltung der Hookeschen und Newtonschen Modelle, d. h., den sekundären Zeiteffekt zu berücksichtigen.

GIBSON und LO (1961) betrachten den bindigen Boden als einen Körper $H - K$, welcher als eines der allgemeinsten Modelle betrachtet werden kann.

FLORIN (1953) leitet die Konsolidationstheorie auf rein mechanisch-physikalischer Grundlage ab, die, wenn man sie mit Hilfe eines rheologischen Modells interpretiert, kann als eine Anzahl n des Modells $H - K$ betrachtet werden. Dieses Werk liefert eine völlig analytische Lösung, die zur Bearbeitung auf einer elektronischen Rechenanlage geeignet ist. Es sei noch die Publikation des Symposiums IUTAM (1964) und das Buch von Grenoble und Suklje (1969) erwähnt werden, in welchen schon eine Vielzahl von Konzeptionen zu finden ist.

Einen Fortschritt bilden in diesem Bereich die Werke von VJALOV (1959), weiters von GOLDSTEIN und seinen Mitarbeitern.

Es muß aber bemerkt werden, daß nur ziemlich wenige derartige Werke publiziert werden, die neben den physikalischen Untersuchungen und Laborversuchungen zugleich auch analytische Lösungen liefern.

Vom rheologischen Gesichtspunkt sollte der bindige Boden nach VJALOV als elastisch-viskoser-plastischer Körper betrachtet werden. Diese Eigenschaften können mathematisch gesondert untersucht werden, obgleich in der Wirklichkeit diese Eigenschaften gleichzeitig existieren, nur am Verlauf der Verformung (der Konsolidation) sie veränderlich beteiligt sind. Im ersten Abschnitt gelangt offenbar die elastische Eigenschaft zu einer entscheidenden Rolle, jedoch kann festgestellt werden, daß die Viskosität einen ständigen Einfluß auf den Vorgang ausübt.

Der plastische Einfluß kommt nur im Fall zur Geltung, wo die Spannung eine Grösse σ_0 erreicht, wobei die Bodenkörner sich im Verhältnis zueinander verschieben und die Umwandlung des gebundenen Wassers zu freiem Wasser beginnt. In demselben Vorgang bestehen die elastischen und viskosen Effekte weiter.

Aufgrund des Besagten kann der Anfang des Kriechens, unserer Meinung nach, nicht bestimmt werden; sie ist im wesentlichen ständig vorhanden.

In den rheologischen Untersuchungen, wo die zeitliche Beziehung der Verformung-Spannung und deren Geschwindigkeit behandelt wird, kann man der Erscheinung der sog. Relaxation begegnen; wenn man die zeitabhängige Änderung der Verformung bei konstanter Spannung untersucht, erhält man die Relaxation der Formänderung; untersucht man dagegen die Spannungsänderung bei konstanter Verformung, so spricht man von der

Relaxation der Spannung. Diese beiden Begriffe sind zwar äußerst wichtig, jedoch kann man im Fall von wassergesättigten Böden während des Konsolidationsvorganges von einem derartigem Zustand nicht sprechen. Der Begriff ist jedoch von Wichtigkeit vom Gesichtspunkt der Ermittelung der Kriechfunktion. Damit werden wir uns aber in einem späteren Aufsatz befassen.

Die rheologische Gleichung eines Körpers ist im wesentlichen eine lineare Differentialgleichung mit konstanten Koeffizienten, worin die Verformung und Spannung enthalten sind. Ist eine von den beiden bekannt, so kann die andere ermittelt werden.

Im eindimensionalen Fall erhält man die Gleichung der Bodenkonsolidation wie folgt:

$$-\frac{\partial \varepsilon}{\partial t} = \frac{1 + \varepsilon_{a'}}{\gamma_v} k \frac{\partial^2 u}{\partial z^2} \tag{1}$$

und die Gleichgewichtsgleichung

$$\sigma(z, t) + u(z, t) = q(t) , \tag{2}$$

wo $\varepsilon(t)$ die Verformung,
σ die tatsächliche Spannung
u die neutrale Spannung und
$q(t)$ die Intensität der Belastung
bedeuten.

Die Aufgabe besteht in der Ermittlung der Verformungsgeschwindigkeit aufgrund der obenerwähnten Eigenschaften des Bodens.

Betrachtet man nur das Hookesche Modell, wo

$$\sigma = E\varepsilon ,$$

so, nimmt die Gleichung (1) unter Berücksichtigung der Gleichung (2), die Form

$$\frac{\partial u}{\partial t} - \frac{\partial q(t)}{\partial t} = E \frac{1 + \varepsilon_{a'}}{\gamma_v} k \frac{\partial^2 u}{\partial z^2} \tag{3}$$

an, die die sog. klassische Gleichung ist.

Der Körper, der durch die in dieser Arbeit erwähnten zwei Modelle interpretiert wurde, ist vorstellbar; er besitzt offenbar eine Momentankompression (durch die Federung E_1), und der Effekt des durch die Kennwerte ε_1 und E_{21} charakterisierten viskosen und elastischen Elementes stellt sicher, daß die Größe der Senkung hinter der Belastung zurückbleibt. Dies bestätigt die Theorie von TERZAGHI, d. h., das Eintreffen der Kompression bedingt das Herauspressen des Porenwassers, wozu eine gewisse Zeitdauer erforderlich ist. Der letzte Teil des ersten Modells beginnt in dem Augenblick, wo die Spannung σ_0, d. h., die plastische Streckgrenze erreicht wird, jedoch, im Fall von Böden, ist auch die zur Umlagerung der Körner erforderliche Spannung ein derartiger

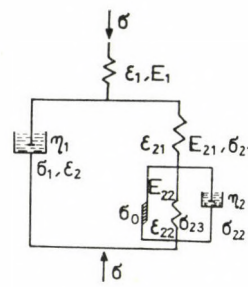

Bild 1

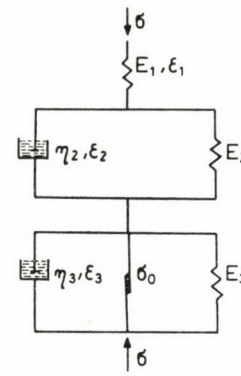

Bild 2

Wert. Es ist offenbar, daß diese Spannung nicht bis zum Bruch (d. h., bis zum Fließen) auswirken muß; die wird durch das mit den Kennwerten ε_2, E_{22} charakterisierte viskose und elastische Element gewährleistet.

Das Terzaghi-Modell ist, wie schon erwähnt wurde, ein Kelvin—Voigtsches Modell, welches keine Momentankompression sichert, und das Bild 3 zeigt, daß in diesem Fall die Vorbedingung, wonach im Augenblick der Belastung das Porenwasser die Last in ihrer Gesamtheit trägt, erfüllt wird.

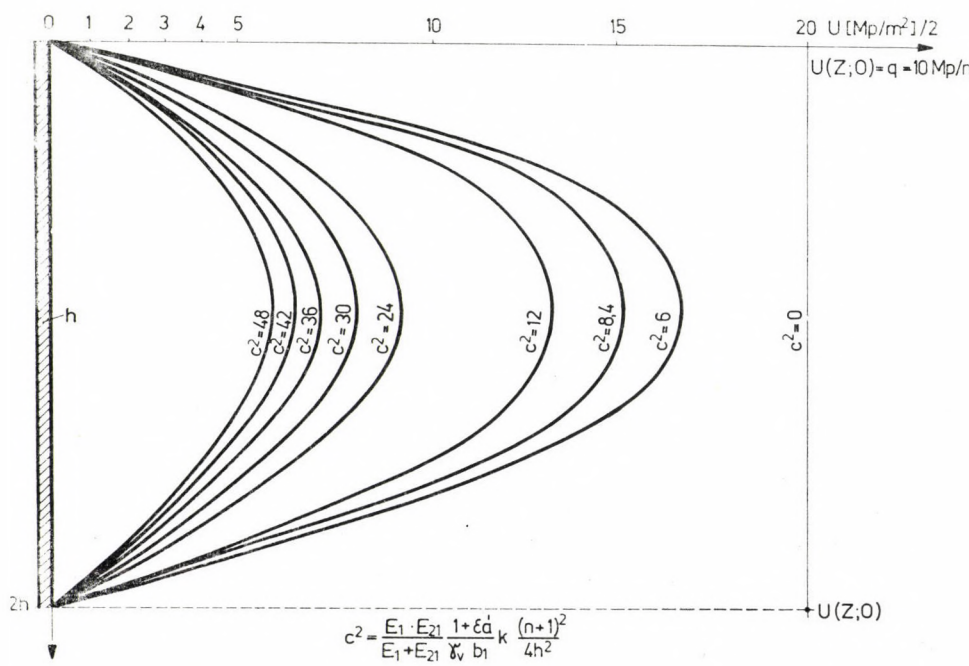

Bild 3

Der größte Mangel des von uns dargestellten Modells ist, daß nach der Entlastung keine bleibende Formänderung bewiesen werden kann, obwohl es offenbar ist, daß im Falle von Böden der größte Teil der Formänderung selbst bei einer kurzen Belastungsdauer bleibend wird.

Hingegen ist es sicher, daß das von uns hergestellte Modell ein genaueres, zuverlässigeres Ergebnis, als die klassische Formel liefert.

1. Nun läßt sich die linke Seite der Gleichung (1) mit Hilfe des auf Bild 1 dargestellten Modells aufschreiben:

$$\sigma = E_1\varepsilon_1, \quad \sigma_1 = \eta_1\dot{\varepsilon}_2, \quad \sigma_{21} = E_{21}\varepsilon_{21}, \quad \sigma_{22} = \eta_2\dot{\varepsilon}_{22}, \quad \sigma_{23} = E_{22}\varepsilon_{22},$$
$$\sigma = \sigma_1 + \sigma_{21} = \sigma_1 + \sigma_0 + \sigma_{22} + \sigma_{23}, \tag{3a}$$
$$\varepsilon = \varepsilon_1 + \varepsilon_2\,,$$
$$\varepsilon_2 = \varepsilon_{21} + \varepsilon_{11}\,\varepsilon_{22}\,.$$

Nach geeigneten Umformungen erhält man die folgende Differentialgleichung

$$\ddot{\varepsilon}\,\frac{\eta_1\eta_2}{E_{21}} + \left(\eta_1 + \eta_2 + \frac{\eta_1 E_{22}}{E_{21}}\right)\dot{\varepsilon} + E_{22}\varepsilon = \frac{\eta_1\eta_2}{E_1E_{21}}\,\ddot{\sigma} +$$
$$+ \left(\frac{\eta_1 + \eta_2}{E_1} + \frac{\eta_1 E_{22}}{E_1E_{21}}\right)\dot{\sigma} + \left(\frac{E_{21} + E_{22}}{E_{21}}\right)\sigma - \sigma_0\,. \tag{4}$$

Führt man die Bezeichnungen

$$\eta_1/E_1 = \gamma_1, \quad \eta_2/E_1 = \gamma_2, \quad \eta_2/E_{21} = \gamma_3, \quad E_{22}/E_{21} = \delta\,, \tag{4a}$$

und

$$\alpha_1 = \frac{\gamma_1(1+\delta) + \gamma_2}{\gamma_1\gamma_3}, \quad \alpha_2 = \frac{E_{22}}{E_1\gamma_1\gamma_3},$$

$$\beta_1 = \frac{1}{E_1}, \quad \beta_2 = \frac{1+\delta}{E_1\gamma_1\gamma_3} \quad \text{und} \quad \beta_3 = -\frac{\sigma_0}{E_1\gamma_1\gamma_3} \tag{4b}$$

ein, so erhält Gleichung (4) die folgende Form:

$$\ddot{\varepsilon} + \alpha_1\dot{\varepsilon} + \alpha_2\varepsilon = \beta_1\ddot{\sigma} + \frac{\alpha_1}{E}\,\dot{\sigma} + \beta_2\sigma + \beta_3 = f(t)\,. \tag{5}$$

Löst man die Gleichung (5) als eine inhomogene lineare Differentialgleichung mit konstanten Koeffizienten unter homogenen Anfangsbedingungen, so erhält man:

$$\varepsilon(t) = e^{\lambda_1 t}\int_0^t \frac{-f(\tau)\,e^{-\lambda_1\tau}}{\lambda_2 - \lambda_1}\,d\tau + e^{\lambda_2 t}\int_0^t \frac{f(\tau)\,e^{-\lambda_2 t}}{\lambda_2 - \lambda_1}\,d\tau\,, \tag{6}$$

wo λ_1 und λ_2 die Wurzel der charakteristischen Gleichung

$$\lambda^2 + \alpha_1\lambda + \beta_2 = 0 \tag{6a}$$

sind, weshalb die Gleichung (6) auch in der folgenden Form aufgeschrieben werden kann:

$$\varepsilon(t) = \frac{1}{\lambda_2 - \lambda_1}\int_0^t [e^{\lambda_2(t-\tau)} - e^{\lambda_1(t-\tau)}]\, f(\tau)\, d\tau \ . \tag{7}$$

Nach Ableitung der Gleichung (7) nach t ergibt sich die folgende Gleichung:

$$\dot{\varepsilon} = \frac{1}{\lambda_2 - \lambda_1}\int_0^t [\lambda_2 e^{\lambda_2(t-\tau)} - \lambda_1 e^{\lambda_1(t-\tau)}]\, f(\tau)\, d\tau \ . \tag{8}$$

Substituiert man (8) in die linke Seite der Gleichung (1), so erhält man:

$$\frac{1}{\lambda_2 - \lambda_1}\int_0^t [\lambda_1 e^{\lambda_1(t-\tau)} - \lambda_2 e^{\lambda_2(t-\tau)}]\, f(\tau)\, d\tau = \frac{1 + \varepsilon_{a'}}{\gamma_v}\, k\, \frac{\partial^2 u}{\partial z^2} . \tag{9}$$

Deriviert man beide Seiten der Gleichung (9), so erhält man:

$$\int_0^t \frac{f(\tau)}{\lambda_2 - \lambda_1}[\lambda_1^2 e^{\lambda_1(t-\tau)} - \lambda_2^2 e^{\lambda_2(t-\tau)}]\, d\tau - f(t) = \frac{1 + \varepsilon_{a'}}{\gamma_v}\, k\, \frac{\partial^3 u}{\partial z^2 \partial t} . \tag{10}$$

Subtrahiert man das λ_1-fache von (9) aus (10), so ergibt sich:

$$-\lambda_2 \int_0^t e^{\lambda_2(t-\tau)} f(\tau)\, d\tau - f(t) = \frac{1 + \varepsilon_{a'}}{\gamma_v}\, k \left[\frac{\partial^3 u}{\partial z^2 \partial t} - \lambda_1 \frac{\partial^2 u}{\partial z^2}\right]. \tag{11}$$

Nach Ableitung der Gleichung (11) nach t:

$$\lambda_2^2 \int_0^t e^{\lambda_2(t-\tau)} f(\tau)\, d\tau - \dot{f}(t) = \frac{1 + \varepsilon_{a'}}{\gamma_v}\, k \left[\frac{\partial^4 u}{\partial z^2 \partial t^2} - \lambda_1 \frac{\partial^3 u}{\partial z^2 \partial t}\right]. \tag{12}$$

Subtrahiert man das λ_2-fache der Gleichung (11) aus der Gleichung (12), so erhält man:

$$\lambda_2 f(t) - f'(t) = \frac{1 + \varepsilon_{a'}}{\gamma_v}\, k \left[\frac{\partial^4 u}{\partial z^2 \partial t} - (\lambda_1 + \lambda_2)\frac{\partial^3 u}{\partial z^2 \partial t} + \lambda_1\lambda_2 \frac{\partial^2 u}{\partial z^2}\right]. \tag{13}$$

Infolge der Gleichung (2) erscheint auf der linken Seite der Gleichung (13) die dritte Ableitung der Funktion $u(z, t)$ nach t. Die zur Lösung der Gleichung (13)

erforderlichen drei Anfangsbedingungen können erhalten werden, wenn $t = 0$ eingesetzt wird. So ergibt sich $u_0 = q$ $(t = 0)$, und die weiteren Bedingungen können aus den Gleichungen (9) und (11) berechnet werden.

Infolge von (2) kann $f(t)$ in der folgenden Form aufgeschrieben werden:

$$f(t) = \beta_1[\ddot{q} - \ddot{u}] + \frac{\alpha_1}{E_1}[\dot{q} - \dot{u}] + \beta_2[q - u] + \beta_3 . \tag{13a}$$

Aufgrund dieses Ausdrucks kann man die Gleichung (13), wie folgt, aufschreiben:

$$\beta_1 \frac{\partial^3 u}{\partial t^2} + \left[\frac{\alpha_1}{E_1} - \beta_1\lambda_2\right]\frac{\partial^2 u}{\partial t^2} + \left[\beta_2 - \frac{\lambda_2\alpha_1}{E_1}\right]\frac{\partial u}{\partial t} - \lambda_2\beta_2 u -$$

$$- \beta_1 \frac{\partial^3 q}{\partial t^3} - \left[\frac{\alpha_1}{E_1} - \beta_1\lambda_2\right]\frac{\partial^2 q}{\partial t^2} - \left[\beta_2 - \frac{\lambda_2\alpha_1}{E_1}\right]\frac{\partial q}{\partial t} + \lambda_2[\beta_2 q + \beta_3] =$$

$$= \frac{1 + \varepsilon a'}{\gamma_v} k\left[\frac{\partial^4 u}{\partial z^2 \partial t^2} - (\lambda_1 + \lambda_2)\frac{\partial^3 u}{\partial z_2 \partial t} + \gamma_1\lambda_2 \frac{\partial^2 u}{\partial z^2}\right]. \tag{14}$$

Gleichung (14) beschreibt die allgemeine Form des Vorganges der Bodenkonsolidation. Untersuchen wir einige der Sonderfälle der Gleichung (14).

1. Nehmen wir an, daß im Modell $H - [N||(H - (Stv||H||N))]$, infolge von $\sigma < \sigma_0$ nur das Modell $H - K$ funktioniert. Dies bedeutet, daß $\varepsilon_{22} = 0$.

Nach entsprechender Neubezifferung der Koeffizienten erhält man aus der Gleichung (5):

$$\dot{\varepsilon} + \alpha_2\alpha_1^{-1}\varepsilon = E_1^{-1}\dot{\sigma} + \beta_2\alpha_1^{-1}\sigma ,$$

oder

$$\dot{\varepsilon} + b_1\varepsilon = b_2\dot{\sigma} + b_3\sigma , \tag{15}$$

wo

$$b_1 = \eta_1^{-1}E_{21}, \quad b_2 = E_1^{-1}, \quad b_3 = (E_1E_{21})^{-1}(E_1 + E_{21})\, b_1.$$

Die Lösung der Gleichung (15) wird:

$$\varepsilon(t) = e^{-b_1 t}\int_0^t (b_2\dot{\sigma} + b_3\sigma)\, e^{b_1\tau}\, d\tau . \tag{15a}$$

Deriviert man diese letzte Gleichung nach t und schreibt man das Ergebnis auf die linke Seite der Gleichung (1), so hat man:

$$-(b_2\dot{\sigma} + b_3\sigma) + b_1 e^{-b_1 t}\int_0^t (b_2\dot{\sigma} + \sigma b_3)\, e^{b_1 t}\, d\tau = \frac{1 + \varepsilon_a'}{\gamma_v} k\frac{\partial^2 u}{\partial z^2} . \tag{16}$$

Deriviert man beide Seiten der Gleichung (16) und addiert man zum Ergebnis das b_1-fache der Gleichung (16), so ergibt sich

$$-b_2\ddot{\sigma} - b_3\dot{\sigma} = \frac{1+\varepsilon_{a'}}{\gamma_v} k\left[\frac{\sigma^3 u}{\partial z^2 \partial t} + b_1 \frac{\partial^2 u}{\partial z^2}\right], \tag{17}$$

oder

$$b_2 \frac{\partial^2 u}{\partial t^2} + b_3 \frac{\partial u}{\partial t} - \left(b_2 \frac{\partial^2 q}{\partial t^2} + b_3 \frac{\partial q}{\partial t}\right) = \frac{1+\varepsilon_{a'}}{\gamma_v} k\left[\frac{\partial^3 u}{\partial z^2 \partial t} + b_1 \frac{\partial^1 u}{\partial z^2}\right]. \tag{18}$$

Die zur Lösung der Gleichung (18) erforderlichen Anfangsbedingungen ergeben sich aus Gleichung (16):

$$\left[b_2 \frac{\partial u}{\partial t} + b_3 u - \left(b_2 \frac{\partial q}{\partial t} + b_3 q\right)\right]_{t=0} = \frac{1+\varepsilon_{a'}}{\gamma_v} k \frac{\partial^2 u}{\partial z^2}\bigg|_{t=0}. \tag{19}$$

und aus der klassischen Bedingung ergibt sich

$$u_0 = q(t=0).$$

2. Aus der Gleichung (18) und offensichtlich auch aus der Gleichung (14) kann der Fall ermittelt werden, wo es keinen rein elastischen Teil gibt, welcher in der klassischen Theorie im allgemeinen (elastische) Momentankompression genannt wird. Dann gilt $E_1 = \infty$, und nach einer kurzen Berechnung erhält man: $b_2 = 0$ und $b_3 = E_{21}^{-1} b_1$,

$$\frac{\partial u}{\partial t} - \frac{\partial q}{\partial t} = E_{21} \frac{1+\varepsilon_{a'}}{\gamma_v b_1} k\left[\frac{\partial^3 u}{\partial z^2 \partial t} + b_1 \frac{\partial_2 u}{\partial z^2}\right] \tag{20}$$

$$u - q = E_{21} \frac{1-\varepsilon_{a'}}{\gamma_v b_1} k \frac{\partial^2 u}{\partial z^2}. \tag{21}$$

Aufgrund der Anfangsbedingung (21) ist einzusehen, daß die Null-Isochronen nicht geradlinig sind. Für verschiedene Werte von b_1 und

$$c^2 = (1+\varepsilon_{a'})\, kE_{21}/b_1\gamma_v \tag{21a}$$

sind Kurven auf Bild 3 dargestellt.

3. Aus Gleichung (18) kann auch der Fall ermittelt werden, wo der Boden durch das Maxwellsche Modell interpretiert wird. Dies ist von besonderer Bedeutung, denn die Größe der Verschiebung kann durch dieses Modell gekennzeichnet werden. In diesem Fall sollte der Wert von E_{21} gleich Null sein.

Dies ist gleichwertig mit $b_1 = 0$. Die Gleichung (16) kann folglich auch in der folgenden Form geschrieben werden:

$$\frac{\partial u}{\partial t} + \frac{E_1}{\eta_1} u + \left(- \frac{\partial q}{\partial t} - \frac{E_1}{\eta_1} q \right) = \frac{1 + \varepsilon_{a'}}{\gamma_v} k \frac{\partial^3 u}{\partial z_2 \partial t} \quad . \tag{22}$$

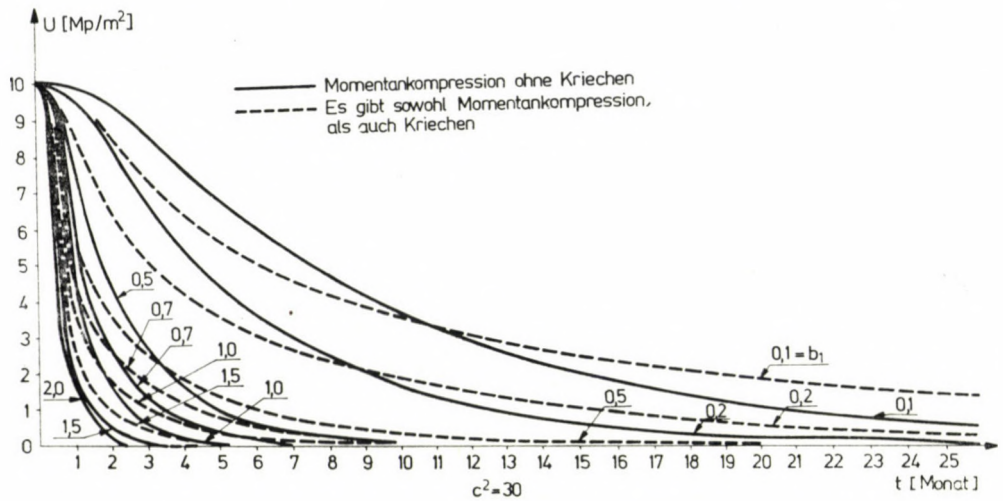

Bild 4

Bei den numerischen Beispielen wird ein Beispiel in Zusammenhang mit Gleichung (18) für q=Konst. vorgeführt.

II. Mit Rücksicht darauf, daß die mechanischen Modelle infolge der Verschiedenheit der Bodenkennwerte veränderlich sind, kann die Gleichung der Konsolidation auch für das im Bild 2 sichtbare Modell aufgestellt werden. Mit den gebrauchten Bezeichnungen kann man schreiben:

$$\sigma = E_1 \varepsilon_1, \quad \sigma = E_2 \varepsilon_2 + \eta_2 \dot{\varepsilon}_2, \quad \sigma = \sigma_0 + E_3 \varepsilon_3 + \eta_3 \dot{\varepsilon}_3, \quad \varepsilon = \sum_{i=1}^{3} \varepsilon_i \tag{22a}$$

Nach Durchführung der entsprechenden Berechnungen kann die letztere Gleichung, wie folgt, geschrieben werden:

$$\varepsilon(t) = \frac{\sigma}{E_1} + \frac{1}{\eta_2} \int_0^t \sigma e^{-\gamma_3 (t-\tau)} \, d\tau + \frac{1}{\eta_3} \int_0^t (\sigma - \sigma_0) \, e^{-\gamma_3 (t-\tau)} \, d\tau \tag{23}$$

und mit Rücksicht auf Gleichung (1):

$$- \frac{\dot{\sigma}}{E_1} - \left(\frac{1}{\eta_2} + \frac{1}{\eta^3} \right) \sigma + \frac{\sigma_0}{\eta_3} + \frac{\gamma_2}{\eta_2} \int_0^t \sigma e^{-\gamma_3 (t-\tau)} \, d\tau +$$

$$+\frac{\gamma_3}{\eta_3}\int_0^t (\sigma-\sigma_0)\, e^{-\gamma_3(t-\tau)}\, d\tau = \frac{1+\varepsilon_{a'}}{\gamma_v}\, k\frac{\partial^2 u}{\partial z^2}, \tag{24}$$

wo

$$\gamma_i = E_i\eta_i^{-1} \qquad (i=2,3) \tag{24a}$$

und

$$\alpha_1 = \eta_2^{-1} + \eta_2^{-}{}_3\ . \tag{24b}$$

Zur Beseitigung der Integral enthaltenden Glieder geht man wie im vorangehenden Fall vor, womit man folgende zwei Gleichungen erhält:

$$-\frac{\ddot{\sigma}}{E_1} - \left(\alpha_1+\frac{\gamma_2}{E_1}\right)\dot{\sigma} - \left(\frac{\gamma_2}{\eta_2}+\frac{\gamma_3}{\eta_3}-\alpha_1\gamma_2\right)\sigma + \frac{\sigma_0}{\eta_3}(\gamma_2-\gamma_3) + \tag{25}$$

$$+\frac{\gamma_3}{\eta_3}(\beta_2-\gamma_2)\int_0^t (\sigma-\sigma_0)\, e^{-\gamma_3(t-\tau)}\, d\tau = \frac{1+\varepsilon_{a'}}{\gamma_v}\, k\left[\frac{\partial^3 u}{\partial z^2\partial t}+\gamma_2\frac{\partial^2 u}{\partial z^2}\right] -$$

$$-\frac{\ddot{\sigma}}{E_1} - \left(\alpha_1+\frac{\gamma_2+\gamma_3}{E_1}\right)\ddot{\sigma} + \left[\frac{\gamma_2}{\eta_2}+\frac{\gamma_3}{\eta_3}-\alpha_1(\gamma_2+\gamma_3)-\frac{\gamma_2\gamma_3}{E_1}\right]\dot{\sigma} =$$

$$= \frac{1+\varepsilon_{a'}}{\gamma_v}\, k\left[\frac{\partial^4 u}{\partial z^2\partial t^2}+(\gamma_2+\gamma_3)\frac{\partial^3 u}{\partial z^2\partial t}+\gamma_2\gamma_3\frac{\partial^2 u}{\partial z^2}\right] \tag{26}$$

Es ist zu bemerken, daß in diesem Fall die der Gleichung (4) entsprechende Gleichung die folgende ist:

$$\ddot{\varepsilon}+(\gamma_2+\gamma_3)\dot{\varepsilon}+\gamma_2\gamma_3\varepsilon = \frac{\ddot{\sigma}}{E_1}+\left(\alpha_1+\frac{\gamma_2+\gamma_3}{E_1}\right)\dot{\sigma}+$$

$$+\left[\frac{\gamma_2}{\eta_2}+\frac{\gamma_3}{\eta_3}-\alpha_1(\gamma_2+\gamma_3)-\frac{\gamma_2\gamma_3}{E_1}\right]\sigma\ . \tag{27}$$

Es ist leicht einzusehen, daß die zwei Gleichungen nicht gleichwertig sind, folglich handelt es sich um einen Körper von verschiedener Qualität:

Auch die Gleichung (26) kann analog zur Gleichung (14) aufgeschrieben werden.

Untersuchen wir jetzt wieder die Sonderfälle.

1. Es sei $\sigma \leq \sigma_0$, weshalb sich auch hier das Modell $H-K$ ergibt. Das dritte Glied der Gleichung (23) ist gleich Null. Berücksichtigt man das in den Berechnungen, so erhält man Ergebnisse, die mit den gefundenen übereinstimmen.

2. Wenn man die Bedingung $E_3 = 0$ aufschreibt, d. h., die Feder ausschaltet, betrachtet man nur ein plastisch-viskoses Element, und in Gleichung (26) ist $\gamma_3 = 0$.

3. Wenn man das viskose Element ausschaltet, d. h., $\eta_3 = 0$, dann werden beide Seiten der Gleichungen (25) und (26) gleich Null. Daraus folgt, daß

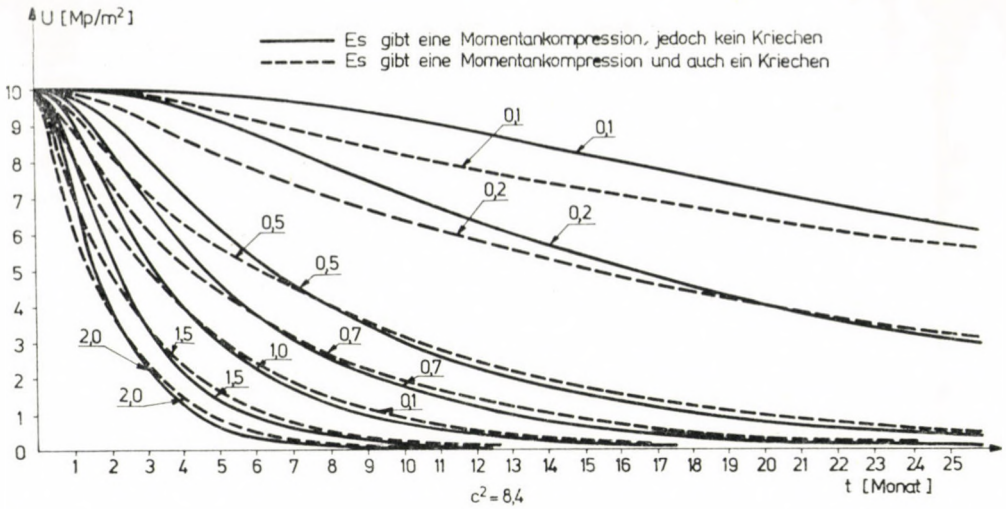

Abb. 5

wenn wir den gleitenden Boden wünschen, dann muß der auch von einer viskosen Erscheinung begleitet werden. Diese Erscheinung tritt im Fall des im Bild 1 dargestellten Modells nicht ein.

Bevor wir auf die Beschreibung der numerischen Beispiele übergehen, machen wir einige Feststellungen im Zusammenhang mit den rheologischen Modellen. Ein Teil derselben ist im Werk von FLORIN (1961) zu finden. Die Ordnungszahl der Differentialgleichung des Verformung-Spannungszustandes ist nicht größer, als die Anzahl der in derselben enthaltenen viskosen Elemente.

In der Differentialgleichung des Verformung-Spannungszustandes ist die Ordnungszahl der Derivierten der Verformung nicht kleiner — und höchstens

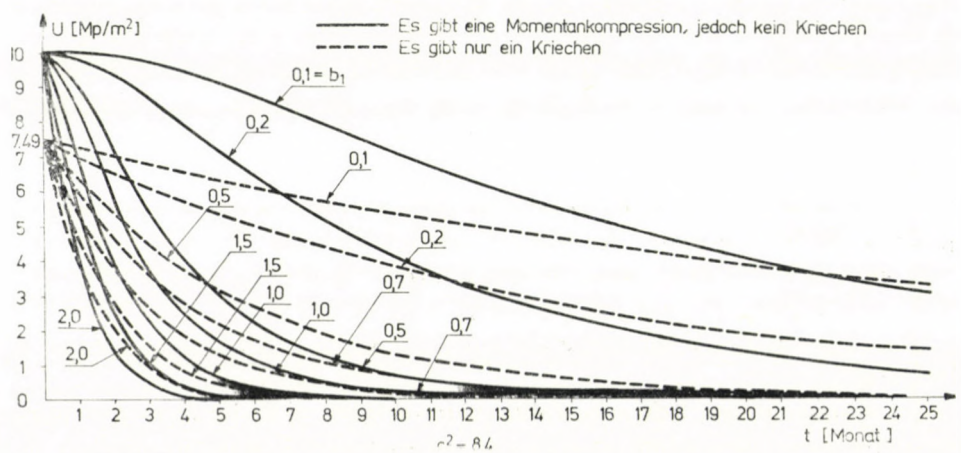

Abb. 6

um 1 größer — als die Ordnungszahl der Derivierten der Spannung. Ist das rheologische Modell viskos-kontinuierlich, so besitzt der Körper keine Momentankompression.

Im Fall von Böden ist ein nicht kontinuierliches elastisches Modell im wesentlichen unvorstellbar, denn in diesem Fall ist die Beziehung Verformung-Spannung nicht eindeutig, und die Verformung ist unbeschränkt. Wenn aber das Modell elastisch-kontinuierlich ist, so wird die Größe der Verformung beschränkt.

In einem komplizierten Modell sollte gleichzeitig mit dem Gleitelement ein viskoses Element beisein.

Bei der Berechnung der numerischen Beispiele haben wir den Vorgang unter der Belastung untersucht.

Mit Hilfe der Formel (21) und des Koeffizienten

$$c^2 = \frac{E_1 E_{21}}{E_1 + E_{21}} k \frac{1 + \varepsilon_{a'}}{\gamma_v b_1} \frac{(n+1)^2}{4h^2} \tag{28}$$

sind die Nullisochronen für die Werte 6, 8.4, 12, 24, 30, 36, 42, 48 ermittelt worden. Das Ergebnis beweist, daß die Nullisochronen nicht geradlinig sind, wenn man nur das langsame Kriechen annimmt.

Auf Bild 4 ist die Lösung der Gleichung (20) für verschiedene b_1-Werte dargestellt. Auch die klassische Gleichung der Konsolidation wurde mit demselben Konsolidationskoeffizienten gelöst um auf den Unterschied hinzuweisen. Es kann festgestellt werden, daß wenn man nur das Kriechen berücksichtigt (und die Momentankompression außer Acht läßt), so schneiden die zur neutralen Spannung gehörigen Kurven die zur klassischen Lösung gehörigen Kurven, u. zw. umso früher, je größer b_1 ist. Es ist zu bemerken, daß sie bei kleinen b_1-Werten nach dem Schnittpunkt hoch über der Kurve der klassischen Lösung bleiben. Das bedeutet, daß die Konsolidation langsamer beendet wird, als es die klassische Methode anzeigt. Schließlich wird die Lösung der Gleichung (18) auf den Bildern (5) und (6) veranschaulicht. Die Lösung wird hier für zwei verschiedene Konsolidationskoeffizienten dargestellt, wobei die Koeffizienten b_2 und b_3 einander gleich sind. Es ist festzustellen, daß infolge der Berücksichtigung des Kriechens neben der Momentankompression nach der Belastung noch eine geraume Zeit lang eine kleinere neutrale Spannung, als im klassischen Fall, sich ergibt, was auf das schnellere Senken hindeutet. Nach einer Weile schneiden sich die beiden Kurven und die weitere Senkung vollzieht sich langsamer.

Anhand dieses Beispiels wollten wir erklären, daß die Berücksichtigung des Kriechens gerechtfertigt ist. In einem späteren Aufsatz werden wir auch für die Gleichung (14) ein numerisches Beispiel anführen.

Die Berechnungen der numerischen Beispiele wurden mit Hilfe von elektronischen Rechenanlagen durchgeführt. Die vorgeführten Gleichungen wurden mit Hilfe der sog. Rasterlinienmethode aufgrund des Aufsatzes von I. SÁNDOR (1972) gelöst, deren Wesen darin besteht, daß in t eine kontinuierliche Lösung sich ergibt, folglich man sich mit der Stabilitätsbedingung nicht beschäftigen muß.

Die Randbedingungen — da sie im Vergleich mit dem klassischen Fall unverändert sind — wurden in der vorliegenden Arbeit nicht behandelt.

SCHRIFTTUM

1. GIBSON, R. E.—LO, K. Y. (1961): A theory of consolidation for soil exhibiting secondary compression. *Acta Polytechnica* (296) 191 Ci. 10.
2. GOLDSTEIN, M.: Reologicseszkije isszledovanija glin i usztojcsivosztyi otkoszov. Dokladü k VI. mezsdunarodnomy kongresszu po mechanike gruntov i fundamentov sztrojeniju. Moszkva (1965)
3. FLORIN, V. A.: Odnomernaja zadacsa uplotnenija zsimajemoj poristoj polzucsej zemljanoj szredü. Iz. AN. SZSZSZR OTN No. 5. (1961) Osznovü mechaniki gruntov. T. II. Moszkva
4. IUTAM Symposium Grenoble (1964)
5. SÁNDOR, I.: Theoretical analysis of consolidation of soil masses with the help of the method of linear algebra. Candidate's dissertation. Budapest 1972. (In Hungarian)
6. SUKLJE, L.: Rheological aspects of soil mechanics. London 1969
7. TERZAGHI, K.: Die Berechnung der Durchlässigkeitsziffer des Tones aus dem Verlauf der hydrodynamischen Spannungserscheinungen. Sitzungsbericht, Akad. Wiss. Wien 1923.
8. TAN TJANG-KIE: Three dimensional theory on the consolidation and flow of the claylayers. *Scientia Sinica* **6** No. 1 (1957)
9. VJALOV, S. S.: Reologicseszkije szvojsztva i nezsusaja szposzobnoszt merzlüh gruntov. Moszkva 1959

Rheological Investigation of the Theory of Soil Consolidation. The theory of consolidation of the one-dimension soil of compressible porosity is dealt with. With the aid of a rheological model the differential equation is established which is a fourth-order partial differential equation. In this way a general equation is yielded which takes the creep into account and which was as yet not to be found in the special literature. Two models are compared and, as a special case of them, the equation is established found by FLORIN (1953) on the basis of mechanical considerations. The statements valid for the rheological models are summarized and completed. For the solution of the partial differential equation the methods of the linear algebra are used, namely the grid-line method which, due to lack of space, is not dealt with. On the basis of several numerical examples statements have been made laying particular stress on creep in the theory of soil consolidation.

Реологическое исследование теории консолидации грунта. Работа занимается (одномерной) теорией консолидации сжимаемого пористого грунта. С помошью реологической модели выводится дифференциальное уравнение, которое представляет собою парциальное дифференциальное уравнение четвертого сморядкаени. С помощью этого уравнения получается общее уравнение (которое ещё не фигурирует в литературе) с учетом медленной деформации. Дается сравнение двух моделей и в качестве специального случая их получается выведенное Флориным (1953) уравнение, которое выведено на основе механического соображения. В дальнейшем дается обобщение известных для реологических моделей определений; после чего автор дополняет эти определения. Для решения дифференциального уравнения применяются методы линейной алгебры, которые в работе не излагаются для экономии места. На основе ряда числовых задач сделаны определения относительно важности медленной деформации в теории консолидации грунтов.

Acta Technica Academiae Scientiarum Hungaricae, Tomus 86 (1—2), pp. 131—145 (1978)

CHARACTERIZATION OF THE SORPTIVE PROPERTIES OF MOIST MATERIAL IN CASE OF MULTICOMPONENT MOISTURE CONTENT

B. PALÁNCZ*

Symbols

D — diffusivity, m^2/h
J, J^* — functionals
H — Hamilton function
M — mean value
N — drying rate, kg moisture (m^2h, kmol moisture/ m^2h
P — total pressure of gas phase, atm.
R — general gas constant, atm m^3/kmol °K
T — absolute temperature, °K
V — total volume, m^3
a — specific surface, m^2/m^3
c — specific heat, kcal/kg °C
f — note for function and coefficient in the objective function
h — adjoint variable
i — enthalpy, kcal/kg
k — mass transfer coefficient, m/h
p — partial pressure, atm.
q_s — heat flux, kcal/m^2h
r_0 — latent heat, kcal/kg
s — co-ordinate, dimensionless
t — temperature, °C
u — moisture content, kg moisture/kg dry material
x — mol fraction in liquid phase,
y — mol fraction in gas phase,
z — co-ordinate, m

Greek letters

α — heat transfer coefficient, kcal/m^2h°C
ε — porosity, m^3/m^3
ϱ — density, kg/m^3
σ — variance
τ — time, h
φ — function for correction,
ψ — saturation curve,
Φ — heat of adsorption and mixing, kcal/kg dry material
ν — parameter
γ — factor of activity

Subscripts

G — gas phase
j — j-th component
kv — convection
kr — critical
L — liquid
na — moist material
p — constant pressure
s — solid surface
v — ending

* B. PALÁNCZ H-1085 Budapest, Salétrom u. 9.

1. Introduction

Relations characterizing the equilibrium state of the sorptive materials are one of the most important terms in the mathematical models of drying.

For one component, the approximation of the experimental data is usually carried out by determining free parameters of a specified function [1]. Although this method is frequently used in practice, it always fails at the processes having strongly transient characters, as the sorptive isotherms are determined in steady state.

In this paper we present a method for characterizing the sorptive multicomponent equilibrium at a specified structure of a mathematical model. In an optimal way, it means, that the tolerance between the experimental values and the theoretical ones given by the model is minimized.

The method based on the control theory, also indicates how adequate the model is, besides the identification of the sufficient function.

2. Characterization of the sorptive properties in case of multicomponent moisture content

Let us define the multicomponent liquid containing no solid phase, as a material having ideal sorptive properties.

In this case the partial pressure of the j-th component just the liquid surface, at the interface is:

$$P_{sj} = \gamma_j x_j P_{j0} \tag{1}$$

where the tension curve of the pure j-th component is

$$P_{j0} = P_{j0}(T_s) \tag{2}$$

and the activity factor of the j-th component is

$$\gamma_j = \gamma_j(T_s, x_j) \ . \tag{3}$$

It means that the partial pressure of the j-th component can be expressed in terms of the temperature and the molfraction of the j-th component in case of ideal sorptive properties.

The most practical characterization of a property can be carried out with the aid of a measure indicating the deviation from the ideal case. It can be proved that moist material has ideal sorptive properties at a certain interval of the moisture content [2]. Accordingly it seems to be advisable to express the partial pressure of the j-th component at the interface in the following

way:

$$\psi_j(u_1, u_2, \ldots, u_{n-1}; t_{na}) = \psi_j^*(x_j; t_{na})\, \varphi_n(u_j) \tag{4}$$

where

$$\psi_j^* \equiv P_{sj}/P \quad \text{and} \quad t_{na} \equiv T_s - 273$$

considering Eq. (4)

$$\psi_j = \psi_j(x_j; t_{na}; u_j) \ ,$$

$$x_j = \frac{u_j/M_j}{\sum_{j=1}^{n} u_j/M_j} \tag{5}$$

in this way x_j and u_j determine the value of the total moisture content $\sum_{j=1}^{n} u_j/M_j$.

It means, that the equilibrium value depends on the temperature, the total moisture content and the partial moisture content of the components.

Considering the importance of wetting depending strongly on the total moisture content, the approximation of Eq. (4) may be said to be physically sufficient.

The functions $\varphi_j(u_j)$ indicate the deviation from the ideal case, so

$$\varphi_j(u_j) = \begin{cases} 1 & \text{if} \quad U_j \geq U_{jkr} \\ < 1 & \text{if} \quad U_j < U_{jkr} \end{cases} \tag{6}$$

Functions are called optimal functions concerning a specified mathematical model if the differences in the values given by the model theoretically and evaluated from measurements experimentally are minimum at a certain interval of time.

3. Mathematical model

Let us choose the so-called one-layer model of the multicomponent drying [3]:

$$-\frac{\mathrm{d}u_j}{\mathrm{d}\tau} = \frac{a}{(1-\varepsilon)\,\varrho_s} N_j, \ j = 1, 2, \ldots, n-1 \, , \tag{7}$$

$$\frac{\mathrm{d}t_{na}}{\mathrm{d}\tau} = \left\{ \frac{a}{(1-\varepsilon)\,\varrho_s} \alpha_{kv} t_G + \sum_{j=1}^{n-1} \left(r_{0j} + c_{pj} t_G - \sum_{i=1}^{n-1} \frac{\partial \Phi_j}{\partial u_i} \right) \cdot \right.$$

$$\cdot \frac{\mathrm{d}u_j}{\mathrm{d}t} - \left[\frac{a}{(1-\varepsilon)\,\varrho_s} \alpha_{kv} + \sum_{j=1}^{n-1} c_{Lj} \frac{\mathrm{d}u_j}{\mathrm{d}t} \right] t_{na} \Bigg\} \cdot$$

$$\cdot \left[c_s + \sum_{j=1}^{n-1} \left(c_{Lj} u_j + \frac{\partial \Phi_j}{\partial t_{na}} \right) \right]^{-1} \, , \tag{8}$$

$$-\frac{P}{RT}\frac{\partial y_j}{\partial s}\frac{K_{Gj}}{D_{jn}} = \sum_{i=1}^{n}\frac{N_j y_j - N_i y_j}{D_{ji}}\,, \qquad (9)$$

$$j = 1, 2, \ldots, n-1$$

$$N_n \equiv 0\ . \qquad (10)$$

The initial conditions are:

$$u_j(0) = u_{j0}, \quad j = 1, 2, \ldots, n-1,$$
$$t_{na}(0) = t_{na0} \qquad (11)$$

The boundary conditions:

$$y_j(\tau)\,|_{s=0} = \psi(u_1, u_2, \ldots, u_{n-1}; t_{na})\ ,$$
$$y_j\,|_{s=1} = y_{Gj}, \quad j = 1, 2, \ldots, n-1\ . \qquad (12)$$

4. The determination of the optimal functions $\varphi_j(u_j)$

It will be proved that optimal $\varphi_j(u_j)$ functions exist respecting the one-layer model and these can be determined unambiguously on the bases of the values of the partial drying rates $N_j(\tau)$ and temperatures $t_{na}(\tau)$ measured experimentally in time.

To prove this existence it is enough to show that optimal $N_j(\tau)$ functions exist, because the relation (9), the equation (4) and the boundary conditions (12) determine the optimal functions $\varphi_j(u_j)$ unambiguously.

It goes without saying that the $N_j = \tilde{N}_j$ does not ensure the satisfying of the condition of the optimality, because generally $t_{na} \neq \tilde{t}_{na}$ in this case.

5. Transforming the problem

This problem of function identification can be transformed into an optimization problem in the following way:

let us minimize

$$J(N_1, N_2, \ldots, N_{n-1}) = \int_0^{\tau_v}\left[(\tilde{t}_{na}(\tau) - t_{na}(\tau))^2 + \sum_{j=1}^{n-1}(\tilde{N}_j(\tau) - N_j(\tau))^2\right]\mathrm{d}\tau \qquad (13)$$

functional, in other words, $N_j(\tau)$ functions minimizing the functional (13) under the conditions (7)—(13) have to be found.

The variables $\tilde{t}_{na}$ and $\tilde{N}_j$ being random ones, the functional itself is a random variable, too. In practice the mean value of these variables can be used, it means $M(\tilde{t}_{na})$ and $M(\tilde{N}_j)$. This is possible, because:

$$M(J) = \int_0^{\tau_v} \left\{ M\left[(\tilde{t}_{na}(\tau) - t_{na}(\tau))^2\right] + \sum_{j=1}^{n-1} M\left[(\tilde{N}_j(\tau) - N_j(\tau))^2\right] \right\} \mathrm{d}\tau =$$

$$= \int_0^{\tau_v} \left\{ M(\tilde{t}_{na}^2) - 2t_{na} M(\tilde{t}_{na}) + t_{na}^2 + \sum_{j=1}^{n-1} \left[M(\tilde{N}_j^2) - 2N_j M(\tilde{N}_j) + N_j^2 \right] \right\} \mathrm{d}\tau$$

considering

$$M(\tilde{t}_{na}^2) = M^2(\tilde{t}_{na}) + \sigma^2 \tilde{t}_{na}$$

and

$$M(\tilde{N}_j^2) = M^2(\tilde{N}_j) + \sigma^2 \tilde{N}_j \ ,$$

so

$$M(J) - \int_0^{\tau_v} \left[\sigma^2 \tilde{t}_{na} + \sum_{j=1}^{n-1} \sigma^2 \tilde{N}_j \right] \mathrm{d}\tau = \int_0^{\tau_v} \left[M(\tilde{t}_{na}(\tau) - t_{na}(\tau))^2 + \right.$$

$$\left. + \sum_{j=1}^{n-1} (M(\tilde{N}_j) - N_j(\tau))^2 \right] \mathrm{d}\tau$$

$$J^* = M(J) - \int_0^{\tau_v} \left[\sigma^2 \tilde{t}_{na} + \sum_{j=1}^{n-1} \sigma^2 \tilde{N}_j \right] \mathrm{d}\tau$$

The integral of the variances of the measured values being independent of the function $N_j(\tau)$, the new functional by using the mean values of the variables differ with a well defined constant from the original one (13).

Obviously, the functionals $M(J)$ and J^* are equivalent in respect to the problem to be solved.

That is why the functional (13) will be considered and for simplicity's sake the sign of the mean value will be omitted. So it is enough to prove the existence of functions $N_j(\tau)$ $j = 1, 2, \ldots, n-1$ minimizing the functional (13).

6. Application of the maximum principle

In order to solve the problem Pontrjagin's maximum principle is used [4]. Let us introduce a new variable:

$$h(\tau) = \int_0^{\tau} \left[\left(\tilde{t}_{na}(\eta) - t_{na}(\eta)\right)^2 + \sum_{j=1}^{n-1} \left(\tilde{N}_j(\eta) - N_j(\eta)\right)^2 \right] \mathrm{d}\tau \ , \tag{14}$$

namely

$$\frac{\mathrm{d}h}{\mathrm{d}\tau} = \left(\tilde{t}_{na}(\tau) - t_{na}(\tau)\right)^2 + \sum_{j=1}^{n-1} \left(\tilde{N}_j(\tau) - N_j(\tau)\right)^2 \tag{15}$$

where

$$h(0) = 0 \ . \tag{16}$$

Considering Eqs (7), (8) and (15) the Hamiltonian of the problem is:

$$H = -\sum_{j=1}^{n-1} z_j \frac{a}{(1-\varepsilon)\,\varrho_s} N_j + z_{na} \frac{a}{(1-\varepsilon)\,\varrho_s} \left\{ \alpha_{kv} t_G - \right.$$
$$\left. - \sum_{j=1}^{n-1} (r_{0j} + c_{pj} t_G)\, N_j - \left[\alpha_{kv} - \sum_{j=1}^{n-1} c_{Lj} N_j \right] t_{na} \right\} \Big/ \left(c_s + \sum_{j=1}^{n-1} c_{Lj} u_j \right) +$$
$$+ z_n \left[(\tilde{t}_{na} - t_{na})^2 + \sum_{j=1}^{n-1} (\tilde{N}_j - N_j)^2 \right] \ . \tag{17}$$

The desorption and other heat effects were neglected.

The necessary condition for the existence of the optimal N_j function is:

$$\frac{\partial H}{\partial N_j} = 0 \quad j = 1, 2, \ldots, n-1 \tag{18}$$

so

$$0 = -z_j \frac{a}{(1-\varepsilon)\,\varrho_s} + z_{na} \frac{a}{(1-\varepsilon)\,\varrho_s} \cdot \left[c_{Lj} t_{na} - (r_{0j} + c_{pj} t_G) \right] \Big/$$
$$\Big/ \left(c_s + \sum_{j=1}^{n-1} c_{Lj} u_j \right) - 2 z_h (\tilde{N}_j - N_j) \ ,$$

therefore

$$N_j = \frac{a}{2(1-\varepsilon)\,\varrho_s} \left[z_j - \frac{c_{Lj} t_{na} - r_{0j} - c_{pj} t_G}{c_s + \sum_{j=1}^{n-1} c_{Lj} u_j} z_{na} \right] + \tilde{N}_j \ , \tag{19}$$
$$j = 1, 2, \ldots, n-1$$

In case of minimization the sufficient condition is:

$$\frac{\partial^2 H}{\partial N_j^2} > 0 \tag{20}$$

because analysing the second variation of the Hamiltonian on the basis of the strong maximum principle [5] in case of maximizing the sufficient condition is:

$$\int_{\tau_1}^{\tau_1 + \Delta\tau} \sum_{k,m} \frac{\partial^2 H}{\partial \Theta_k \partial \Theta_m} (v\bar{\varphi}_k)(v\bar{\varphi}_m)\, \mathrm{d}\tau < 0$$

where

$$h_{k,m} = \frac{\partial^2 H}{\partial \Theta_k \partial \Theta_m} ,$$

so the Hesse matrix must be a negative definite for every τ. In our case

$$\Theta_j = N_j$$

and

$$h_{k,m} = \begin{cases} \dfrac{\partial^2 H}{\partial N_j^2} > 0\,, & k = m = j \\ \dfrac{\partial^2 H}{\partial N_k \partial N_m} = 0 & k \neq m \end{cases}$$

Thus the Hesse matrix must be a positive definite, because of the minimization.

The condition (20) exists, because

$$\frac{\partial^2 H}{\partial N_j^2} = 2 z_h \tag{21}$$

and

$$\frac{\mathrm{d}z_h}{\mathrm{d}\tau} = \frac{\partial H}{\partial h} = 0\,,$$

so

$$z_h(\tau) = \text{const.}$$

In a general form [6]:

$$h = \sum_{j=1}^{n-1} f_j u_j(\tau_v) + f_{na} t_{na}(\tau_v) + f_h h(\tau_v) = h(\tau_v) \tag{22}$$

so

$$z_h(\tau_v) = 1$$

and

$$z_h(\tau) \equiv 1$$

therefore

$$\frac{\partial^2 H}{\partial N_j^2} = 2 > 0 \tag{23}$$

so the condition really exists.

The uniqueness also comes from Eq. (19). In order to determine the functions $N_j(\tau)$ we need the relations for the adjoint variables $z(\tau)$, too,

$$\frac{\mathrm{d}z_j}{\mathrm{d}\tau} = -\frac{\partial H}{\partial u_j}\,, \qquad j = 1, 2, \ldots, n-1 \tag{24}$$

and similarly

$$\frac{\mathrm{d}z_{na}}{\mathrm{d}\tau} = -\frac{\partial H}{\partial t_{na}}\,, \tag{25}$$

so

$$\frac{dz_j}{d\tau} = \frac{z_{na}a}{(1-\varepsilon)\varrho_s}\left\{\alpha_{kv}t_G - \sum_{j=1}^{n-1}(r_{0j} + c_{pj}t_G)N_j - \right.$$

$$\left. - \left[\alpha_{kv} - \sum_{j=1}^{n-1} c_{Lj}N_j\right] t_{na}\right\} \times \frac{c_{Lj}}{\left(c_s + \sum_{j=1}^{n-1} c_{Lj}u_j\right)^2}, \quad j = 1, 2, \ldots, n-1; \quad (26)$$

$$\frac{dz_{na}}{d\tau} = z_{na}\frac{a}{(1-\varepsilon)\varrho_s}\left[\alpha_{kv} - \sum_{j=1}^{n-1} c_{Lj}N_j\right] \Big/ \left(c_s + \sum_{j=1}^{n-1} c_{Lj}u_j\right) - 2(\tilde{t}_{na} - t_{na}) . \quad (27)$$

Boundary conditions for the above equations are:

$$z_j(\tau_v) = 0 \qquad j = 1, 2, \ldots, (n-1) \quad (28)$$

and

$$z_{na}(\tau_v) = 0$$

7. Numerical example

Let us illustrate the application of the algorithm with a numerica example. Considering a system of two components, alcohol–water system, the data are the following.

y_{1G} = 0,01315 kmol alc./kmol total
y_{2G} = 0,0158 kmol alc./kmol total
D_{13} = 0,0476 m²/h
D_{12} = 0,0575 m²/h
D_{23} = 0,106 m²/h
t_G = 67 °C
k_{G1} = 30 m/h
k_{G2} = 35 m/h
$u_{1(0)}$ = 0,5 kg alc./kg dry material
$u_{2(0)}$ = 0,5 kg water/kg dry material
$t_{na(0)}$ = 20 °C
P = 1 atm.
α_{kv} = 30 kcal/m² h °C
c_s = 0,7 kcal/kg °C
$\frac{a}{(1-\varepsilon)\varrho_s}$ = 0,03 m²/kg

In case of two component system equations are:

$$-\frac{du_1}{d\tau} = \frac{a}{(1-\varepsilon)\varrho_s}N_1 ,$$

$$-\frac{du_2}{d\tau} = \frac{a}{(1-\varepsilon)\varrho_s}N_2 , \quad (29)$$

$$\frac{\mathrm{d}t_{na}}{\mathrm{d}\tau} = \frac{a}{(1-\varepsilon)\varrho_s}\,[\alpha_{kv}t_G - (r_{01} + c_{p1}t_G)\cdot N_1 -$$

$$- (r_{02} + c_{p2}t_G)\cdot N_2 - (\alpha_{kv} - c_{L1}N_1 + c_{L2}N_2)\cdot t_{na}]/(c_s + c_{L1}u_1 + c_{L2}u_2)\,, \quad (30)$$

$$N_1 = \tilde{N}_1 + \frac{a}{2(1-\varepsilon)\varrho_s}\left(z_1 - \frac{c_{L1}t_{na} - r_{01} - c_{P1}t_G}{c_s + c_{L1}u_1 + c_{L2}u_2}\,z_{na}\right)\,,$$

$$N_2 = \tilde{N}_2 + \frac{a}{2(1-\varepsilon)\varrho_s}\left(z_2 - \frac{c_{L2}t_{na} - r_{02} - c_{P2}t_G}{c_s + c_{L1}u_1 + c_{L2}u_2}\,z_{na}\right)\,, \quad (31)$$

$$\frac{\mathrm{d}h}{\mathrm{d}\tau} = (\tilde{N}_1 - N_1)^2 + (\tilde{N}_2 - N_2)^2 + (\tilde{t}_{na} - t_{na})^2\,, \quad (32)$$

and

$$\frac{\mathrm{d}z_1}{\mathrm{d}\tau} = \frac{z_{na}a}{(1-\varepsilon)\varrho_s}\{\alpha_{kv}t_G - (r_{01} + c_{P1}t_G)\cdot N_1 - (r_{02} + c_{P2}t_G)\cdot N_2 -$$

$$- [\alpha_{kv} - (c_{L1}N_1 + c_{L2}N_2)]\cdot t_{na}\}\times \frac{c_{L1}}{(c_s + c_{L1}u_1 + c_{L2}u_2)^2}\,, \quad (33)$$

$$\frac{\mathrm{d}z_2}{\mathrm{d}\tau} = \frac{c_{L2}}{c_{L1}}\,\frac{\mathrm{d}z_1}{\mathrm{d}\tau}\,,$$

and

$$\frac{\mathrm{d}z_{na}}{\mathrm{d}\tau} = z_{na}\frac{a}{(1-\varepsilon)\varrho_s}\,[\alpha_{kv} - (c_{L1}N_1 + c_{L2}N_2)]/$$

$$/(c_s + c_{L1}u_1 + c_{L2}u_2) - 2(\tilde{t}_{na} - t_{na}) \quad (34)$$

The so called swinging method [7] was used in order to solve the system. Numerical results are shown by Tables 1—3 and Fig. 1.

Having the optimal values of $N_1(\tau)$ and $N_2(\tau)$ and knowing the prespecified values of y_{1G} and y_{2G}

$$-\frac{\mathrm{d}y_1}{\mathrm{d}s} = \left(\frac{N_1y_2 - N_2y_1}{D_{12}} + \frac{N_1y_3}{D_{13}}\right)\frac{D_{13}RT}{Pk_{G1}}\,,$$

$$-\frac{\mathrm{d}y_2}{\mathrm{d}s} = \left(\frac{N_2y_1 - N_1y_2}{D_{21}} + \frac{N_2y_3}{D_{23}}\right)\frac{D_{23}RT}{Pk_{G2}}\,. \quad (35)$$

Integrating these equations we obtain:

$$y_{1/s=0} = \psi_1(u_1,\ u_2;\ t_{na})$$

and (36)

$$y_{2/s=0} = \psi_2(u_1,\ u_2;\ t_{na})\,,$$

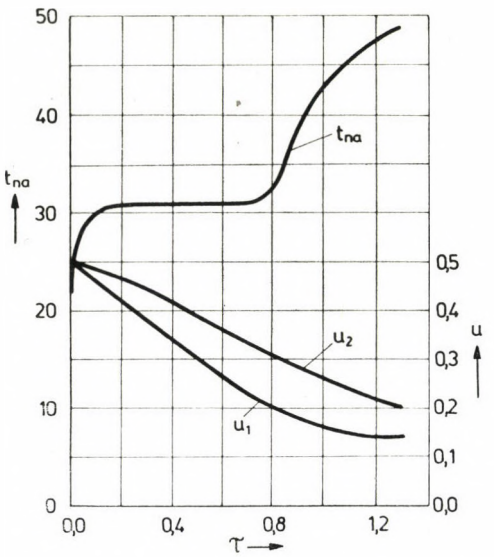

Fig. 1

so the optimal φ functions are

$$\varphi_1(u_1) = \frac{\psi_1(u_1, u_2; t_{na})}{\psi_1^*(t_{na}; x_1)}$$

and (37)

$$\varphi_2(u_2) = \frac{\psi_2(u_1, u_2; t_{na})}{\psi_2^*(t_{na}; x_2)}$$

where ψ_1^* and ψ_2^* can be determined with the aid of the Raoult-law:

$$\psi_1^*(t_{na}; x_1) = \frac{P_1(t_{na})}{P} x_1 \ ,$$

$$\psi_2^*(t_{na}; x_2) = \frac{P_2(t_{na})}{P} x_2 \ . \tag{38}$$

The vapour pressure curve for pure alcohol, respectively, water can be approached by the following relations:

$$\log p_1(t_{na}) = 0{,}0238(t_{na} + 230) - 4{,}35 \tag{39}$$

and

$$\log p_2(t_{na}) = 0{,}622 + \frac{7{,}5 t_{na}}{238 + t_{na}} \tag{40}$$

Table 1

	τ \ i	0	1	2	3	4	5
	0,00	0,0200	0,0008	0,0028	0,0031	0,0032	0,0033
	0,10	0,0200	0,0123	0,0140	0,0145	0,0146	0,0147
	0,20	0,0200	0,0126	0,0138	0,0142	0,0145	0,0146
	0,30	0,0200	0,0118	0,0125	0,0130	0,0132	0,0134
	0,40	0,0200	0,0100	0,0113	0,0117	0,0120	0,0122
	0,50	0,0200	0,0097	0,0100	0,0103	0,0107	0,0110
N_1	0,60	0,0200	0,0084	0,0086	0,0090	0,0094	0,0098
	0,70	0,0200	0,0067	0,0069	0,0074	0,0080	0,0085
	0,80	0,0200	0,0044	0,0052	0,0061	0,0069	0,0074
	0,90	0,0200	0,0012	0,0013	0,0028	0,0037	0,0043
	1,00	0,0200	0,0038	0,0002	0,0017	0,0027	0,0033
	1,10	0,0200	0,0054	0,0008	0,0012	0,0021	0,0026
	1,20	0,0200	0,0052	0,0004	0,0018	0,0024	0,0027
	1,30	0,0200	0,0030	0,0030	0,0030	0,0030	0,0030

	τ \ i	6	7	8	9	10	Measured
	0,00	0,0033	0,0034	0,0034	0,0034	0,0034	0,0035
	1,10	0,0148	0,0149	0,0149	0,0150	0,0150	0,0150
	0,20	0,0147	0,0148	0,0149	0,0150	0,0150	0,0150
	0,30	0,0136	0,0137	0,0138	0,0139	0,0140	0,0140
	0,40	0,0125	0,0126	0,0128	0,0129	0,0129	0,0130
	0,50	0,0113	0,0115	0,0117	0,0118	0,0119	0,0120
N_1	0,60	0,0101	0,0104	0,0106	0,0107	0,0108	0,0110
	0,70	0,0088	0,0091	0,0093	0,0094	0,0095	0,0100
	0,80	0,0078	0,0081	0,0093	0,0085	0,0086	0,0100
	0,90	0,0048	0,0050	0,0052	0,0053	0,0054	0,0074
	1,00	0,0037	0,0039	0,0041	0,0042	0,0042	0,0050
	1,10	0,0029	0,0031	0,0032	0,0032	0,0033	0,0035
	1,20	0,0028	0,0029	0,0030	0,0030	0,0030	0,0030
	1,30	0,0030	0,0030	0,0030	0,0030	0,0030	0,0030

Table 2

	τ \ i	0	1	2	3	4	5
	0,00	0,0200	0,0011	0,0009	0,0012	0,0013	0,0014
	0,10	0,0200	0,0160	0,0177	0,0182	0,0182	0,0184
	0,20	0,0200	0,0181	0,0192	0,0197	0,0200	0,0201
	0,30	0,0200	0,0191	0,0198	0,0203	0,0207	0,0208
	0,40	0,0200	0,0200	0,0204	0,0208	0,0211	0,0214
	0,50	0,0200	0,0207	0,0209	0,0212	0,0216	0,0220
N_2	0,60	0,0200	0,0212	0,0212	0,0216	0,0221	0,0225
	0,70	0,0200	0,0210	0,0211	0,0217	0,0223	0,0228
	0,80	0,0200	0,0193	0,0200	0,0210	0,0218	0,0224
	0,90	0,0200	0,0111	0,0136	0,0151	0,0161	0,0168
	1,00	0,0200	0,0086	0,0122	0,0142	0,0153	0,0159
	1,10	0,0200	0,0075	0,0122	0,0143	0,0153	0,0158
	1,20	0,0200	0,0075	0,0132	0,0147	0,0153	0,0156
	1,30	0,0200	0,0152	0,0152	0,0152	0,0152	0,0152

	τ \ i	6	7	8	9	10	Measured
	0,00	0,0014	0,0015	0,0015	0,0015	0,0015	0,0015
	0,10	0,0185	0,0186	0,0187	0,0187	0,0187	0,0188
	0,20	0,0203	0,0204	0,0204	0,0205	0,0206	0,0206
	0,30	0,0210	0,0211	0,0212	0,0213	0,0214	0,0214
	0,40	0,0217	0,0218	0,0220	0,0221	0,0222	0,0223
	0,50	0,0223	0,0225	0,0227	0,0228	0,0229	0,0230
N_2	0,60	0,0229	0,0231	0,0233	0,0235	0,0236	0,0238
	0,70	0,0232	0,0235	0,0237	0,0238	0,0240	0,0245
	0,80	0,0228	0,0231	0,0233	0,0235	0,0236	0,0251
	0,90	0,0172	0,0175	0,0177	0,0178	0,0179	0,0207
	1,00	0,0163	0,0165	0,0167	0,0168	0,0168	0,0177
	1,10	0,0161	0,0162	0,0163	0,0164	0,0165	0,0167
	1,20	0,0158	0,0159	0,0159	0,0160	0,0160	0,0160
	1,30	0,0152	0,0152	0,0152	0,0152	0,0152	0,0152

Table 3

	τ \ i	1	2	3	4	5	
	0,00	22,00	22,00	22,00	22,00	22,00	
	0,10	24,77	30,24	30,84	31,05	31,05	
	0,20	26,40	29,95	30,99	31,36	31,56	
	0,30	27,33	29,41	30,57	31,09	31,41	
	0,40	27,84	29,06	30,10	30,72	31,17	
	0,50	28,10	28,73	29,55	30,25	30,82	
t_{na}	0,60	28,24	28,41	29,04	29,83	30,55	
	0,70	28,30	27,90	28,55	29,52	30,42	
	0,80	28,33	27,59	28,71	30,02	31,13	
	0,90	28,34	30,45	32,65	34,43	37,73	
	1,00	28,34	34,02	37,55	39,74	41,12	
	1,10	28,35	35,87	40,42	42,80	44,10	
	1,20	28,35	38,87	43,39	45,38	46,39	
	1,30	28,35	44,83	46,99	47,87	48,32	
h		176,61	71,85	38,47	23,38	15,63	

	τ \ i	6	7	8	9	10	Measured
	0,00	22,00	22,00	22,00	22,00	22,00	22,00
	0,10	21,21	31,26	31,30	31,34	31,37	31,74
	0,20	31,71	31,82	31,92	32,00	32,06	32,15
	0,30	31,65	31,85	32,00	32,13	32,23	32,28
	0,40	31,52	31,80	32,02	32,20	32,33	32,40
	0,50	31,29	31,67	31,96	32,19	32,36	32,52
t_{na}	0,60	31,15	31,62	31,98	32,26	32,46	32,64
	0,70	31,15	31,71	32,13	32,44	32,67	32,75
	0,80	31,98	32,60	33,06	33,38	33,62	32,85
	0,90	36,64	37,27	37,71	38,02	38,24	45,69
	1,00	42,00	42,58	42,97	43,24	43,42	46,69
	1,10	44,90	45,38	45,70	45,91	46,05	47,25
	1,20	46,95	47,29	47,51	47,65	47,74	47,86
	1,30	48,56	48,71	48,80	48,86	48,90	48,00
h		11,40	9,01	7,61	6,78	6,26	

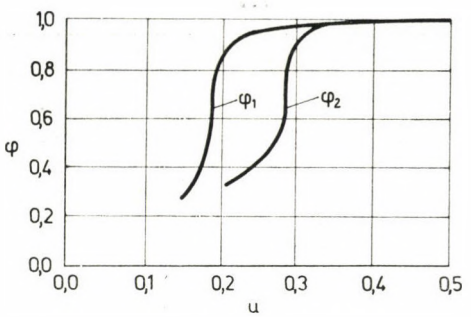

Fig. 2

The functions $\varphi_1(u_1)$ and $\varphi_2(u_2)$ are shown by Fig. 2 and their values are in Table 4.

Table 4

u_1	φ_1	u_2	φ_2
0,500	0,993	0,500	0,998
0,467	0,998	0,486	1,010
0,423	0,996	0,463	1,005
0,380	0,992	0,439	1,002
0,340	0,986	0,414	0,999
0,302	0,988	0,388	1,006
0,268	0,976	0,361	1,007
0,235	0,954	0,334	0,993
0,207	0,899	0,306	0,926
0,188	0,610	0,282	0,626
0,174	0,435	0,263	0,462
0,163	0,355	0,244	0,402
0,154	0,313	0,225	0,366
0,145	0,288	0,207	0,339

REFERENCES

1. GINZBURG, A. S.: Drying in Food Industry (in Hungarian). Műszaki Könyvkiadó, Budapest 1969
2. IMRE, L.: Drying Handbook (in Hungarian). Műszaki Könyvkiadó, Budapest 1975
3. PALÁNCZ, B.—PARTI, M.: Digital Simulation of Multicomponent Drying. *Acta Tech. Hung.* (1975)
4. PONTRJAGIN et al.: The Mathematical Theory of Optimal Processes. Interscience Publishers, Inc., New York 1962
5. FAN, L. T.: Continuous Maximum Principle. John Wiley and Sons. Inc., New York 1973

6. FAN, L. T.—WANG, C. S.: The Discrete Maximum Principle. John Wiley and Sons. Inc., New York 1964
7. KATZ, S.: Best Operating Points for Staged Systems. *Ind. Eng. Chem. Fundamentals*, **1** 226—240

Die Charakterisierung der Sorptionseigenschaften von feuchten Stoffen bei mehrkomponentigem Feuchtigkeitsgehalt. Mit dem in der Arbeit beschriebenen Verfahren können, unter Verwendung der Meßergebnisse, dem einschichtigen Modell der Trocknung am besten angepasste Funktionen gewonnen werden. Die Aufgabe kann auf das Problem einer Funktionsidentifikation zurückgeführt werden, deren Lösung zugleich Antwort auf die Verwendbarkeit des Modells ist.

Характеристика сорбционных свойств влажного материала в случае многокомпонентной влажности. Работа занимается вопросом характеристики сорбционных свойств влажного материала, содержащего многокомпонентную влажность. Приведен такой метод, с помощью которого (при использовании результатов произведенных измерений) можно получить функции, лучше всего подходящие для однослойной модели процесса сушки. Задачу можно свести к задаче идентификации функции, решение которой одновременно дает ответ также в отношении применимости модели.

Acta Technica Academiae Scientiarum Hungaricae, Tomus 86 (1—2), pp. 147—156 (1978)

AN ESTIMATION OF THE MAXIMUM LOADS OF INTERCONNEXIONS

T. TERSZTYÁNSZKY*—G. TUSNÁDY**

[Manuscript received January 1, 1977]

Loads in excess of transmission capacities of tie-lines may cause system disturbances. The paper presents a theoretical method which can be used for determining the probability of maximum loads of random character occurring above a given value. The obtained theoretical values are compared with data measured in practice. The method is suitable for planning the reliability of interconnexions between electrical power systems.

1. Introduction

Co-operation between electric power systems, which enables a more reasonable and efficient utilization of power stations and a better electric power supply to consumers, is realized through intersystem tie-lines. This co-operation results in a continuously varying power flow and it contributes considerably to an economical operation and to the prevention of disturbances. Intersystem tie-lines are particularly useful during disturbances and, at such periods, it is of a decisive importance that an adequate transmission capacity should be available. It is often owing to the latter that the interconnexions are not sufficiently utilized. Interconnexions having the required transmission capacities are especially important when smaller energy systems are linked up with larger ones because the smaller systems, in making use of advantages through power pools (increased block sizes, concentrated power generation), are in need of relatively larger assistance.

It is obvious that, in such cases, the judgment on security requires the knowledge of those maximal loads that may occur on intersystem tie-lines. In this paper a suggestion is made how to estimate power maximums during the given period; these estimations can be used for purposes of planning network and its operation.

2. Loads of interconnexions

Parallel operation of electrical energy systems will make power exchanges possible that result from imbalances of production and consumption. These power exchanges can be divided into the following main groups:

— long-term contractual deliveries ÷ deterministic deliveries,

* T. Tersztyánszky, H-1363 Budapest, P.O.B. 35 (NIM).
** G. Tusnády, H-1153 Budapest, Mezőhegyes u. 42

— occasional power exchanges (inaccuracies of load-frequency regulation; profitable "ad hoc" deliveries; mutual utilization of generating reserves; emergency help, etc.), ÷ deliveries of a casual character.

Long-term contractual deliveries are scheduled in advance and they have, accordingly, daily, weekly, monthly periodicities. Such changes in tendencies depend on specific capabilities, agreements; their maximum values have been pre-established, and on this basis the interconnexions can be dimensioned economically.

The case is different with occasional deliveries of electrical energy, which become necessary partly due to characteristics of the respective systems (so-called uncontrolled power swings), and take place partly as a result of human interventions or even the lack of the latter (complex intersystem effects). The balance of these deliveries can be made zero, by controlling them, e.g. at every quarter-hour, but then some important part of the useful co-operation of energy systems would be lost. Operational advantages (e.g. sudden rise of load curves, emergency help, short-term economical purchases and sales, etc.) would, therefore, require casual deliveries of longer duration. A number of publications have been dealing with casual deliveries statistically and theoretically; some of these publications have examined power swings of short duration [1, 2], while others have dealt with long-term deliveries [3]. These two kinds of analysis differ in their calculated power averages; in one case averages by seconds and minutes are used, in the other hourly averages are calculated. Mathematical procedures used in these publications have in common that stationary statistical characteristics of stochastic processes have been determined separately. In reality, of course, the two kinds of loads emerge jointly.

In respect of deliveries having a random character it is very important to know the maximum loads because they happen to occur just in the presence of emergency help, and may lead to system disturbance if loads exceed the transmission capacities of interconnexions. We intend, therefore, to determine the probable maximum of random power fluctuations.

In our analysis we will try to approach the real situation by considering random loads of long and short durations, respectively, as separate events each; this is followed by a joint analysis of the two kinds of loads, where the resulting load will no longer be seen as independent since short-term power swings are superimposed on loads of long duration.

3. A mathematical model for random changes in electrical loads

Let $\xi(t)$ be the load of an electric system at time t and let Δ be an arbitrary time period. The process of the average loads of length periods Δ may then be described by the process

$$\eta(t) = \frac{1}{\Delta}\int_{t-\Delta/2}^{t+\Delta/2} \xi(t)\,\mathrm{d}t, \qquad \frac{\Delta}{2} \leq t \leq T - \frac{\Delta}{2},$$

or by its discrete version

$$\zeta_i = \eta(i\Delta)\,, \qquad i = 1, 2, \ldots, N\,.$$

Accordingly, the maximal load may be considered to be the random variable

$$Y(T, \Delta) = \max_{\Delta/2 \leq t \leq T - \Delta/2} \eta(t)\,,$$

or

$$Z(N, \Delta) = \max_{1 \leq i \leq N} \zeta_i\,,$$

In case $\xi(t)$ is a stationary Gaussian process with moments

$$E\xi(t) = \mu\,,$$
$$E(\xi(0) - \mu)(\xi(t) - \mu) = B(t)\,,$$

then the distribution of the variables Y, Z is determined by the autocovariance function $B(t)$ and the parameters μ, T, Δ or μ, N, Δ. Now we shall evaluate the distribution of Z, using direct assumptions of the covariences of the process ζ_i. This is a sort of compromise: it would be better first to determine the covariance function $B(t)$ from an appropriate data set and then to proceed with the evaluation of the distribution of Z or Y. This is, however, a rather hard task to do, and we hope that our assumptions on the covariances of the process ζ_i are realistic enough for resulting in usable approximations.

4. The maximum of independent identically distributed random variables

If the random variables $\zeta_1, \zeta_2, \ldots, \zeta_N$ are independent, and identically distributed with distribution function $F(x) = P(\zeta_1 < x)$, then the distribution function of their maximum is the following

$$P(Z < z) = \big(F(z)\big)^N\,. \tag{1}$$

The upper tolerance limit of level ε of the variable Z is the threshold which Z exceeds with probability ε. Let $M = M(N, \varepsilon)$ be the number determined by

$$\left(1 - \frac{1}{M}\right)^N = 1 - \varepsilon\,, \tag{2}$$

and let z_M be determined by

$$F(z_M) = 1 - \frac{1}{M} \; ; \tag{3}$$

then the upper tolerance limit of level ε of Z is z_M.

In Table 1 the upper tolerance limits of the maximum of independent standard normal variables are given for $1 \leqq N \leqq 10^6$, $10^{-4} \leqq \varepsilon \leqq 0{,}9$. In Table 2 the corresponding numbers are given with their approximation

$$\tilde{z}_M = \sqrt{2C_M - \log C_M} \; , \text{ where } C_M = \log \frac{M}{\sqrt{2\pi}} \tag{4}$$

(This approximation is a consequence of the well-known fact that for large z

$$\Phi(z) \sim 1 - \frac{1}{z} \varphi(z) \; ,$$

where

$$\varphi(z) = \frac{1}{\sqrt{2\pi}} e^{-1/2 z^2} \; , \quad \Phi(z) = \int_{-\infty}^{z} \varphi(u) \, du$$

Table 1

Tolerance limits of the maximum of independent standard normal variables

	ε	0,9	0,5	0,33	0,25	0,2	0,1	0,01	0,001	0,0001
$N=$	1	−1,282	0,000	0,431	0,675	0,842	1,282	2,326	3,090	3,719
	2	−0,478	0,545	0,902	1,108	1,251	1,632	2,576	3,290	3,890
	5	0,334	1,128	1,420	1,590	1,710	2,036	2,878	3,540	4,108
	10	0,822	1,498	1,753	1,904	2,014	2,309	3,090	3,719	4,265
	20	1,233	1,826	2,053	2,190	2,287	2,559	3,290	3,890	4,417
	50	1,700	2,204	2,405	2,528	2,616	2,862	3,540	4,108	4,612
	100	2,015	2,462	2,648	2,761	2,844	3,077	3,719	4,265	4,753
	200	2,275	2,701	2,875	2,980	3,057	3,276	3,890	4,417	4,892
	500	2,607	2,992	3,153	3,251	3,322	3,527	4,108	4,612	5,069
	1 000	2,834	3,198	3,350	3,443	3,514	3,705	4,265	4,753	5,199
	2 000	3,050	3,392	3,537	3,626	3,690	3,879	4,417	4,892	5,527
	5 000	3,315	3,636	3,772	3,857	3,919	4,096	4,612	5,069	5,491
	10 000	3,503	3,811	3,941	4,023	4,082	4,252	4,753	5,199	5,612
	20 000	3,685	3,980	4,104	4,181	4,240	4,407	4,892	5,327	5,730
	50 000	3,911	4,190	4,312	4,387	4,440	4,600	5,069	5,491	5,885
	100 000	4,075	4,347	4,462	4,534	4,587	4,743	5,199	5,612	5,998

Table 2

Percentage points of the standard normal distribution

M	z_M	$\tilde{z}_M$	z	M_z	$\tilde{M}_z$
2	0,000	—	2,5	161	142
5	0,842	1,323	2,6	215	191
10	1,282	1,563	2,7	288	259
20	1,645	1,850	2,8	391	353
50	2,054	2,211	2,9	534	487
10^2	2,326	2,463	3,0	741	676
$2 \cdot 10^2$	2,576	2,698	3,1	1 036	948
$5 \cdot 10^2$	2,878	2,987	3,2	1 455	1 342
10^3	3,090	3,192	3,3	2 069	1 915
$2 \cdot 10^3$	3,290	3,386	3,4	2 968	2 759
$5 \cdot 10^3$	3,540	3,629	3,5	4 299	4 010
10^4	3,719	3,804	3,6	6 285	5 833
$2 \cdot 10^4$	3,890	3,972	3,7	9 276	8 710
$5 \cdot 10^4$	4,108	4,184	3,8	13 831	13 015
10^5	4,265	4,339	3,9	20 790	19 631
$2 \cdot 10^5$	4,417	4,489	4,0	31 545	29 887
$5 \cdot 10^5$	4,612	4,680	4,1	48 458	45 930
10^6	4,753	4,820	4,2	75 107	71 251
$2 \cdot 10^6$	4,892	4,957	4,3	117 308	111 580
$5 \cdot 10^6$	5,069	5,132	4,4	184 957	176 396
10^7	5,199	5,261	4,5	294 316	281 520
$2 \cdot 10^7$	5,327	5,388	4,6	473 373	353 583
$5 \cdot 10^7$	5,491	5,551	4,7	768 758	737 807
10^8	5,612	5,670	4,8	1 260 557	1 211 640
$2 \cdot 10^8$	5,730	5,787	4,9	2 086 811	2 008 910
$5 \cdot 10^8$	5,885	5,941	5,0	3 487 967	3 362 848

The inverse M_z of z_M is also given in Table 2 with its approximation $\widetilde{M}_z$. The latter, in turn, are determined by

$$\Phi(z) = 1 - \frac{1}{M_z}, \tag{5}$$

and

$$\widetilde{M}_z = \frac{z}{\varphi(z)} . \tag{6}$$

The function $M = M(N, \varepsilon)$ can be approximated by

$$M = \frac{1}{1 - (1 - \varepsilon)^{1/N}} \sim NE\,, \tag{7}$$

where

$$E = \frac{1}{\log \dfrac{1}{1 - \varepsilon}} = \frac{1}{\varepsilon} - \frac{1}{2} - \frac{\varepsilon}{12} - \frac{\varepsilon^2}{24} - \dots \tag{8}$$

Some values of this function are the following:

ε	0,9	0,5	0,33	0,25	0,2	0,1	0,01	0,001
E	0,435	1,44	2,47	3,48	4,48	9,49	99,5	999,5

For example the upper tolerance limit of level 0,1 of the maximum of 1000 independent standard normal variable is 3,705 according to Table 1. This number may be approximated by the values $z_{9490} = 3{,}7$ or $\tilde{z}_{9490} = 3{,}8$ given in Table 2 for $E(0{,}1) = 9{,}49$.

5. A special form of dependence: equicorrelated variables

As has already been noted, if the joint distribution of variables ζ_1, $\zeta_2, \dots, \zeta_N$ is normal, and their expectation is 0, then the distribution of their maximum depends only on the covariances $E\zeta_i\zeta_j$. Let us assume that

$$E\zeta_i\zeta_j = \begin{cases} 1 & \text{if} \quad i = j\,, \\ \varrho & \text{if} \quad i \neq j\,. \end{cases} \tag{9}$$

In this case (1) is no longer valid, but it is still possible to find a number $\mu = \mu(N, z, \varrho)$ so that

$$p_N(z, \varrho) = P\Big(\max_{1 \leq i \leq N} \zeta_i \leq z\Big) = \big(\Phi(z)\big)^{\mu} \tag{10}$$

holds true (i.e. the probability that the maximum of dependent variables exceeds z equals the probability that the maximum of μ independent variables exceeds the same z).

If (9) holds true, then there are independent standard normal variables $\beta, \gamma_1, \gamma_2, \dots, \gamma_N$ so that

$$\zeta_i = \varrho\beta + \varkappa\gamma_i, \quad i = 1, 2, \dots, N \tag{11}$$

holds true, where $\varkappa = \sqrt{1 - \varrho^2}$. Hence

$$p_N(z, \varrho) = \int_{-\infty}^{\infty} \varphi(t)\, \Phi^N\left(\frac{z - \varrho t}{\varkappa}\right) \mathrm{d}t\,, \tag{12}$$

and the values of this function μ can be determined by numerical integration. If $\varkappa/\varphi = 0{,}6$ (i.e. the standard deviation of the "individual terms" $\varkappa\gamma_i$ is 60% of the standard deviation of the "common term" $\varrho\beta$), then $\varrho = 0{,}8575$. This is the correlation for which the calculation was made, and the results are given in Table 3.

Table 3

The number of independent standard normal variables having the same maximum as N equicorrelated one with $\varrho = 0{,}8575$

	$z = 3$	$z = 4$	$z = 5$
$N =$ 4	3,0257	3,5129	3,7818
16	7,8232	10,7093	13,1451
64	16,5000	27,9983	40,8044
256	30,3231	63,6575	112,8025
1024	48,4094	115,7842	272,0648

6. The matrix-approximation of the covariance function

As we have already seen in the introduction, the loads of the tie-lines have long-term and short-term components. Let us denote them by β and γ, respectively, and let us approximate ζ_i for $i = jm + k$ by the elements of the matrix

$$\alpha_{jk} = \varrho\beta_j + \varkappa\gamma_{jk}\,, \qquad \begin{matrix} j = 0, 1, 2, \ldots, n-1 \\ k = 1, 2, \ldots, m \end{matrix} \tag{13}$$

where the β_j and γ_{jk} are independent standard normal variables, $\varrho^2 + \varkappa^2 = 1$, and $m\Delta$ is the period of long-term effects.

The distribution of the maximum of the variables α_{jk} were determined by the so-called Monte-Carlo method. According to this method the computer generates random numbers by chance and the desired distribution appears as the empirical distribution of the generated numbers. Usually the computer generates random numbers uniformly distributed on the interval [0, 1]. The library routine transforms these random numbers to standard normal ones by taking the sum of 12 of them and then subtracting the constant 6 from the sum.

First we decided to use a more sophisticated method due to Marsaglia, since the former, commonly used routine is not an exact one, e.g. it tends to give emphasis to high values of the normal distribution. Unfortunately, Marsaglia's method presented completely unusable results. The reason for this phenomenon is not clear to us; perhaps the method is sensitive to the distribution of the random numbers used and there is some minor deviation from the desired uniform distribution on the actual computer where the calculations were carried out.

Finally we returned to the standard library routine. Two runs were made, the parameters in the first were

$$n = 100, \quad m = 10, \quad \varrho = 0{,}8575 \tag{14}$$

and 100 matrices were generated. The results are given in Table 4. The second run used the parameters

$$n = 700, \quad m = 70, \quad \varrho = 0{,}8575 \tag{15}$$

Table 4

The S-th largest maximums in 100 matrices $n = 100$, $n = 10$, $\varrho = 0{,}8575$

S	z	M	μ
1	4,09000	43 981	4,40
2	4,05808	38 317	7,66
5	3,89750	19 429	9,71
10	3,72512	9 626	9,63
20	3,50950	4 157	8,31
25	3,43405	3 130	7,82
33	3,37123	2 481	8,27
50	3,22357	1 458	7,29

Table 5

The S-th largest maximums in 10 matrices $n = 700$, $m = 70$, $\varrho = 8575$

S	z	M	μ
1	4,73941	896 160	128,02
2	4,26516	95 334	27,24
3	4,12294	50 757	21,75
4	4,03199	34 257	19,58
5	3,97263	26 615	19,01

and 10 matrices were generated. The results are given in Table 5. In the tables the S-th largest maximum are given for some value of S. Let us denote them by $z = z(s)$. From Table 2 the corresponding $M = M_z$ numbers were determined, then the numbers $\mu = SM/nG$, were calculated, where G is the number of the generated matrices. As it is easy to see, the S-th largest maximum of G blocks of $n\mu$ independent standard normal variables is about $z(S)$. For $z = 4$, $N = 10$ Table 3 gives $\mu = 7{,}5$ which is about the μ-s given in Table 4, but for $z = 4$, $N = 70$ Table 3 gives $\mu = 30$, which is a bit larger then the μ-s given in Table 5 (except the first μ in Table 5 which is unreliable). So we can state that the numerical integration and the Monte Carlo method led to nearly the same results.

Let us note here that the computed works were made by D. SZENDY on an R-40 computer of VEIKI. We are thankful for this collaboration.

7. A comparison of theoretical results with actual data

Let us compare the above theoretical results with the actual maximum occasional power exchange of Hungary's electrical power system. The analysis will be made for loads of hourly averages.

The probability of occurrence that maximum load will exceed the value of a load z is:

$$P(\max_{1 \leq i \leq N} \zeta_i > z) = 1 - \Phi^N(z) \ ,$$

where N is the number of loads. If we want to determine the highest load, which is not exceeded by the maximum with ε probability, then we have to solve the equation

$$\Phi(z) = \sqrt[N]{1 - \varepsilon} \sim 1 - \frac{\varepsilon}{N}$$

for z. Assuming that loads have a normal distribution, Table 2 can be used for determining the value associated with $M = N/\varepsilon$.

A numerical comparison, based on load measurements conducted in 7 years for high-load periods of some 3800 hours per year, is shown in Fig. 1. It should be noted that the reason why the value associated with the probability $\varepsilon = 0{,}0001$ was computed is due to the circumstance that, in American practice, the reliability of intersystem tie-lines ensuring guaranteed deliveries has been taken with 0,9999.

The salient value is an indication that actual maximum values do not always result from loads whose distribution was assumed to be normal for the underlying calculations. It can be said, however, that the method can be used in practice for further purposes, e.g. for the planning of system interconnexions.

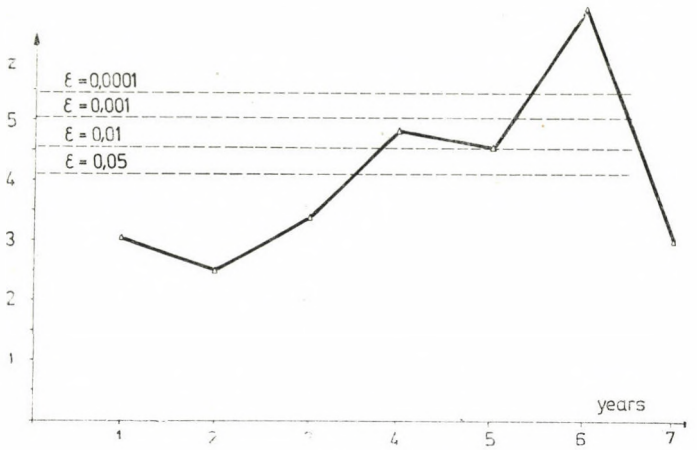

Fig. 1.

REFERENCES

1. ПОРТНОЙ–ТИМЧЕНКО: Учет нерегулярных колебаний мощности — *Электричество* 1968. № 8.
2. ПОРТНОЙ–СОВАЛОВ–ТИМЧЕНКО–КУСТОВ: Вероятные характеристики нерегулярных колебаний — *Электрические Станции* 1976. № 3.
3. ESZTERHÁS–TERSZTYÁNSZKY: Analysis of One-Hour Average Power Flows between Systems with the Probability Theory. *Acta Techn. Hung.* **84** (1977) (3—4)

Abschätzung der maximalen Belastung von Systemverbindungen. Belastungen welche die Übertragungsfähigkeit von Systemverbindungen übersteigen, können Systemstörungen verursachen. Ziel der Arbeit ist es, eine solche theoretische Methode auszuarbeiten und vorzustellen, mit welcher die Wahrscheinlichkeit für das Auftreten eines einen gegebenen Wert übersteigenden Maximums der stochastischen Leistung bestimmt werden kann. Die derart theoretisch erhaltenen Werte werden mit in der Praxis gemessenen Werten verglichen. Das Verfahren ist geeignet, bei der Projektierung der Betriebssicherheit von Verbindungen zwischen elektrischen Energiesystemen angewendet zu werden.

Оценка максимальной загрузки межсистемных связей. Нагрузки, превышающие пропускную способность межсистемных связей могут создать каскадные аварии. Данной работой ставится целью разработка такого теоретического метода и демонстрация его, с помощью которого представляется возможным определить вероятность встречаемости, которая превышает данное значение максимума случайных по характеру нагрузок. Полученные таким образом теоретическим путем данные сравниваются в работе с данными, полученными на практике путем измерения. Предлагаемый метод пригоден для того, чтобы использовать его при проектировании эксплуатационной надежности связей электроэнергетических систем.

Acta Technica Academiae Scientiarum Hungaricae, Tomus 86 (1–2), pp. 157–167 (1978)

DIE BEI DER UNTERSUCHUNG DES BEULVERHALTENS VON SCHALEN IN BETRACHT ZU ZIEHENDE ANFANGSAUSMITTIGKEIT

E. DULÁCSKA*

KANDIDAT DER TECHNISCHEN WISSENSCHAFTEN

[Eingegangen am 20 April 1977]

Der Wert der kritischen Beullast wird durch die Ausmittigkeit der Schalenschnittkräfte erheblich herabgesetzt, weshalb ihrer exakten Berücksichtigung große Bedeutung zukommt. Die vorliegende Studie befaßt sich mit der Bestimmung der durch die ungewollte Anfangsverformung und durch die Randstörungen verursachten Ausmittigkeit.

1. Einleitung

Für die kritische Last p_{kr}, die zum Ausbeulen von Schalen aus elastischem Material führt, kann der Ausdruck

$$p_{kr} = f(E, t, R, w_0)$$

geschrieben werden, in dem E den Elastizitätsmodul, t die Schalendicke, R den Krümmungshalbmesser und w_0 die Anfangsausmittigkeit der Schnittkräfte bezeichnen.

In der vorliegenden Arbeit wird der Versuch unternommen, das Ausmaß jener Anfangsausmittigkeit w_0 zu bestimmen, das in die Berechnung einzubeziehen ist. Seiner richtigen Berücksichtigung kommt große Bedeutung zu, weil die Anfangsausmittigkeit die Neigung der Schale zum Ausbeulen beträchtlich verstärkt und damit die kritische Last erheblich herabsetzt. Da zum Verständnis des Problems die Beulungserscheinungen und die einzelnen Begriffe bekannt sein müssen, soll hier zunächst eine kurze Übersicht über diese gegeben werden.

2. Die Beulung von Schalen aus elastischem Material

Schreibt man die Gleichgewichts- und Verträglichkeitsgleichungen der geometrisch vollkommenen Schale an, gelangt man zu einer Eigenwertauf-

* Dr. E. DULÁCSKA, Ráth Gy. u. 64. H-1122 Budapest Ungarn

gabe. Der kleinste unter den aus ihrer Lösung hervorgehenden Eigenwerten soll mit n_{kr}^{lin} bezeichnet werden und für die lineare kritische Druckkraft der Schale stehen. Die zugehörige Oberflächenlast p_{kr}^{lin} gilt als die kritische lineare Last der Schale.

Die lineare kritische Druckkraft axial gedrückter Zylinderschalen schreibt sich bei Vernachlässigung der Querkontraktion [1] zu

$$n_{kr}^{\text{lin}} = \frac{Et^2}{\sqrt{3}R} \approx 0{,}6\,\frac{Et^2}{R} \,. \tag{1}$$

Die lineare kritische Last der Vollkugelschale unter Außendruck wurde erstmalig von Zoelly bestimmt [1]. Wieder unter Vernachlässigung der Querkontraktion kann diese Last in der Form

$$p_{kr}^{\text{lin}} = \frac{2Et^2}{\sqrt{3}R^2} \approx 1{,}2\,\frac{Et^2}{R^2} \tag{2}$$

geschrieben werden.

Die Versuchsergebnisse haben jedoch gezeigt, daß die Zylinder- und Kugelschalen bei Lastintensitäten ausbeulten, die wesentlich unter den linearen kritischen Lasten lagen und daß auch die Beulverformungen keineswegs gering waren. Aus diesem Grunde wurden in die Differentialgleichungen auch die zur Mitberücksichtigung der größeren Deformationen geeigneten nichtlinearen Glieder der Verformung eingeführt. Das nimmt jedoch den Gleichungen den Charakter von Eigenwertaufgaben. Die Resultate der Untersuchungen nach der Energiemethode haben folgende Eigenheiten aufgedeckt:

a) Die Tragfähigkeit einer gewissen Gruppe von Schalen nimmt nach Erreichen der linearen kritischen Last im Sinne der Kurve I in Bild 1a zu. Ist die Schale mit einer maximalen Amplitude w_0 vorgebeult, dann hat sie keine kritische Last, ihre Tragfähigkeit wächst vielmehr mit der fortschreitenden Verformung stetig an (Kurve II). Derartige Schalen mit zunehmender

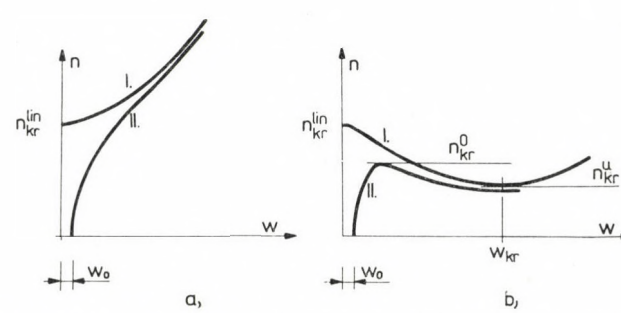

Bild 1. a) Das Verhalten von Schalen mit zunehmender Tragfähigkeit im überkritischen Bereich
b) Das Verhalten von Schalen mit abnehmender Tragfähigkeit im überkritischen Bereich

Tragfähigkeit sind gegen anfängliche Unvollkommenheiten unempfindlich. Im allgemeinen handelt es sich um Schalen, in denen sich das Kräftespiel nach Erreichen des p_{kr}^{lin} durch Umlagerung der inneren Kräfte so verändert, daß die neue Tragfähigkeitskonfiguration steifer ist als die frühere. Nach den heutigen Erkenntnissen zählen zu den Schalen dieser Art die windschief-viereckigen HP-Schalen sowie einige Schalen mit freien Rändern.

b) Das Verhalten einer anderen Gruppe von Schalen zeigt demgegenüber, daß sich die in Gleichgewicht gehaltene Last mit zunehmender Beulverformung w der geometrisch vollkommenen Schale bis zum Erreichen des Formänderungswertes w_{kr} vermindert, um sich von da ab wieder zu erhöhen (s. Bild 1b).

Den Zusammenhang zwischen dieser in Gleichgewicht gehaltenen Last und der Beulverformung w veranschaulicht die Kurve I im Bild 1b. Die bei w_{kr} in Gleichgewicht befindliche Kraft bzw. Last soll mit Th. v. KÁRMÁN [2] als untere kritische Kraft bzw. Last (n_{kr}^{u} bzw. p_{kr}^{u}) bezeichnet werden. Schalen dieser Art — sie werden hier Schalen mit abnehmender Tragfähigkeit genannt — sind im allgemeinen die Zylinder-, die Kegel-, die Kugel- und die sonstigen Kuppelschalen.

Doch auch diese untere kritische Last stimmte mit den experimentell ermittelten Werten nicht überein, da diese bei Versuchen an Zylinder- und Kugelschalen zwischen den Werten für die lineare und die untere kritische Last lagen. Die Abweichungen erhöhten sich nur noch, als die zunehmend exakten Berechnungen für die unteren kritischen Lasten immer niedrigere Werte ergaben.

Gegenwärtig gilt als niedrigster Wert für die Zylinderschale unter Axialdruck nach ALMROTH [3] ein

$$n_{kr}^{u} = 0{,}108\, n_{kr}^{\text{lin}} ,$$

für die radial gedrückte Kugelschale hingegen nach DOSTANOWA-RAJSER [4]

$$p_{kr}^{u} = 0{,}108\, p_{kr}^{\text{lin}} .$$

Die weiteren Untersuchungen haben nachgewiesen, daß die Zylinder- und die Kugelschale bei kleineren als den linearen kritischen Lasten deshalb ausbeulen, weil sie mit anfänglichen Unvollkommenheiten (Vorbeulen) behaftet sind. Die maximale Amplitude der Vorbeule (Anfangsausmittigkeit) soll hier mit w_0 bezeichnet werden. Die Untersuchungen an den mit Vorbeulen behafteten Schalen führten zu der Feststellung, daß sich die Vorbeule mit wachsender Belastung vergrößert, wogegen sich die Tragfähigkeit nach Erreichen eines Maximums mit zunehmender Verformung verringert. Elastische Schalen beulen de facto beim Erreichen dieses Maximums aus, welches im weiteren als die obere kritische Kraft bzw. Last (n_{kr}^{0} bzw. p_{kr}^{0}) bezeichnet wird.

Die Kraft-Verformungs-Kurve der mit Vorbeulen behafteten Zylinder- oder Kugelschale ist im Bild 1b (Kurve II) aufgetragen.

Den Zusammenhang zwischen den oberen kritischen Kräften der Zylinder- und Kugelschalen in Prozenten der linearen kritischen Kräfte einerseits und dem Verhältnis von Vorbeulamplitude zur Schalendicke andererseits veranschaulicht Bild 2 aufgrund einer Auswertung der Ergebnisse von [3, 5, 6, 7, 8, 9, 10, 11 und 12].

Nachgewiesenermaßen setzt die Ausmittigkeit, die durch die abstützungsbedingten Randstörungen verursacht wird, bei Zylinderschalen mit radial starr abgestütztem Rand bzw. bei Kugelkalottenschalen die kritische Kraft ebenso herab wie die Vorbeule, sofern ihre Richtung in die der Beulverformung fällt.

Die Untersuchungen klärten weiterhin [13], daß die Beulung der Kugelkalottenschale, die anfänglich symmetrisch einsetzt, im späteren Verlauf in eine antimetrische Form überspringt. Das hat zur Folge, daß die obere kritische Last selbst bei geometrisch vollkommenen Kugelkalottenschalen das 0,6fache der linearen kritischen Last nicht übersteigen kann.

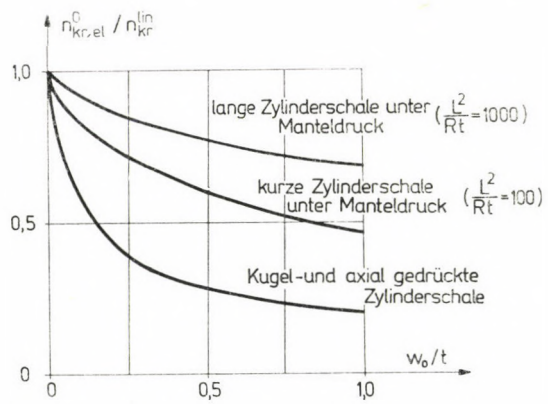

Bild 2. Die Herabsetzung der oberen kritischen Last von Zylinder- und Kugelschalen in Abhängigkeit von der Amplitude w_0 der Anfangsausmittigkeit

2. Die maßgebende Vorbeule (Ausmittigkeit)

Die Anfangsausmittigkeit setzt sich aus zwei Teilen zusammen. Den einen Teil bildet die ungewollte, von der Ungenauigkeit der Ausführung herrührende Ausmittigkeit, deren Amplitude in die Berechnung mit der Bezeichnung $w_{0,\,ungew.}$ einbezogen werden soll.

Den anderen Teil der Anfangsausmittigkeit stellt die rechnerisch erfaßbare Vorbeule dar, die aufgrund der Gesetzmäßigkeiten des Kräftespiels nach der Biegetheorie berechnet werden kann. Sie wird im weiteren mit $w_{0,\,ber.}$ bezeichnet werden.

Daß die Höchstwerte dieser beiden Ausmittigkeiten an der gleichen Stelle auftreten werden, ist wenig wahrscheinlich, weshalb man die Wahrscheinlichkeit des Zusammenfallens der beiden Größen in der Weise berücksichtigen kann, daß man nach den Näherungsregeln der Wahrscheinlichkeitsrechnung die höhere mit ihrem vollen, die niedrigere hingegen mit ihrem halben Wert ansetzt. Als maßgebende Ausmittigkeit (Vorbeule) $w_{0,m}$ ergibt sich mithin der höhere der beiden Werte zu

$$w_{0,m} \geqq \begin{cases} w_{0,\text{ungew.}} + 0{,}5 w_{0,\text{ber.}} \\ 0{,}5 w_{0,\text{ungew.}} + w_{0,\text{ber.}} \end{cases}$$

Die Abweichung der Ausmittigkeiten vom Mittelwert, d. h. die Streuung muß im Sicherheitskoeffizienten berücksichtigt werden.

3. Die ungewollte Ausmittigkeit

Das Bild 3 veranschaulicht nach Versuchen von CLARK, LUNDQUIST, KANEMITSU, BALLERSTEDT, DONNELL und HARRIS und anderen an axial gedrückten Zylindern die der 95%igen Häufigkeit zugehörigen Einhüllenden [1, 3, 5, 6, 7, 12, 13], während im Bild 4 aufgrund einer Zusammenstellung von L. KOLLÁR die in der Literatur [17, 18, 19, 20, 21, 22, 23, 24, 25, 26 und 27] publizierten Ergebnisse von Versuchen an Kugelschalen und die der 95%igen Häufigkeit zugehörigen Einhüllenden dargestellt sind.

Bei beiden Schalen ergibt sich bei einem Verhältnis von $R/t = 1000$ für die obere Einhüllende ein Wert von 0,7, für die untere ein solchen von 0,1, als arithmetisches Mittel somit ein Wert von 0,4. Die Versuchswerte sind jedoch nicht symmetrisch verteilt, denn bei Versuchen an Zylinderschalen lag der Mittelwert um etwa 10% unter dem Durchschnittswert. Der Mittelwert kann also mit 0,36% angesetzt werden.

Betrachtet man die Herabsetzung der kritischen Last in Abhängigkeit von der Ausmittigkeit (Bild 2) und die niedrigeren Ergebnisse aus den Versuchen an axial gedrückten Zylindern und an Kugelschalen in Abhängigkeit vom Verhältnis R/t, erkennt man eindeutig die gleichen Gesetzmäßigkeiten. Das erklärt sich aus der Tatsache, daß Schalen um so weniger genau ausgeführt werden können, je dünner ihre Wand ist.

Die Herabsetzung der Tragfähigkeit von Kugel- und von axial gedrückten Zylinderschalen in Abhängigkeit von der Anfangsausmittigkeit w_0 läßt sich näherungsweise durch die Hyperbel

$$p_{kr}^{0} / p_{kr}^{\text{lin}} = \frac{1}{1 + 6 \dfrac{w_0}{t}} \tag{3}$$

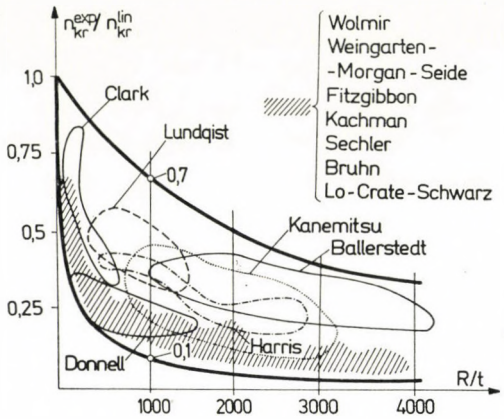

Bild 3. Der Zusammenhang zwischen der experimentell ermittelten kritischen Kraft p_{kr}^{exp} axial gedrückter Zylinderschalen und dem Verhältnis von Krümmungshalbmesser zur Schalendicke R/t

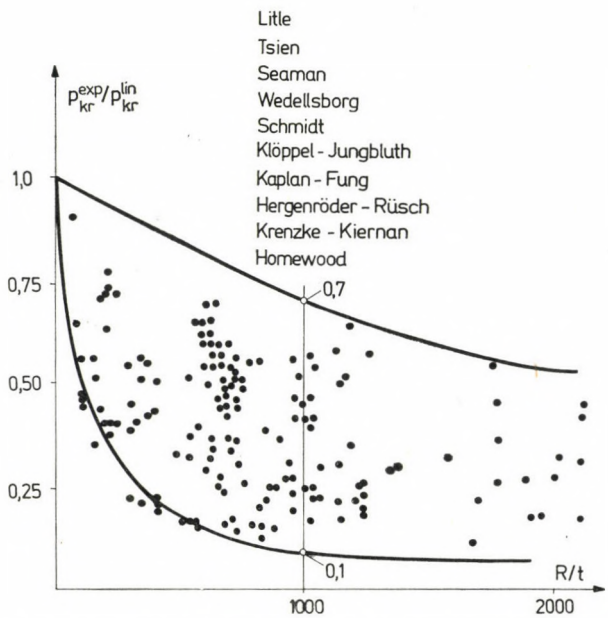

Bild 4. Der Zusammenhang zwischen der experimentell ermittelten kritischen Last p_{kr}^{exp} radial gedrückter Kugel- und Kuppelschalen und dem Verhältnis des Krümmungshalbmessers zur Schalendicke R/t

gemäß Bild 5a beschreiben. Für den Mittelwert der Herabsetzung der experimentell ermittelten kritischen Last in Abhängigkeit vom Verhältnis des Krümmungshalbmessers zur Schalendicke gilt hingegen der im Bild 5b graphisch dargestellte Zusammenhang

$$p_{kr}^{\exp}/p_{kr}^{\text{lin}} = \frac{1}{1 + 1{,}7\dfrac{R}{1000t}} . \tag{4}$$

Aus der Gleichsetzung der beiden Werte ergibt sich der Mittelwert der anzusetzenden ungewollten Ausmittigkeit zu

$$w_0 = \frac{R}{3500} . \tag{5}$$

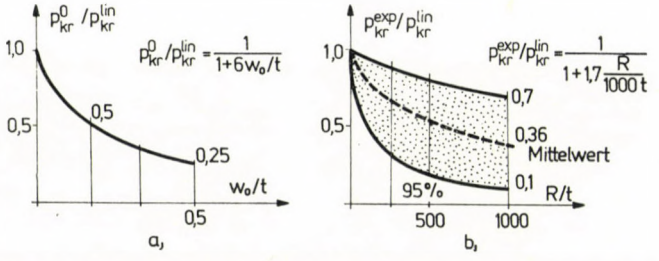

Bild 5. a) Die Änderung der einander näherungsweise gleichgesetzten oberen kritischen Lasten axial gedrückter Zylinder- und radial gedrückter Kugelschalen in Abhängigkeit vom Wert der maximalen Anfangsausmittigkeitsamplitude w_0 b) Der Streuungsbereich der Ergebnisse von Versuchen an Zylinder- und Kugelschalen in Abhängigkeit vom Verhältnis des Krümmungshalbmessers zur Schalendicke R/t

Die ungewollte Ausmittigkeit wurde auch durch Messungen überprüft. An Zylindern mit einem $R/t = 1000$ wurden in der maßgebenden Axialrichtung an den späteren Ausbeulungsstellen ungewollte Ausmittigkeiten gemessen, deren Werte um $R/3000$ schwankten [29]. Der Mittelwert nach Formel (5) erscheint mithin ausreichend verläßlich.

4. Die berechenbare Ausmittigkeit

Der auf rechnerischem Wege erfaßbare Teil der Ausmittigkeit läßt sich durch die exakte Berechnung der Schale nach der Schalenbiegetheorie bestimmen. (Hierbei müssen auch die Ausmittigkeiten berücksichtigt werden, die sich aus Schwingungen ergeben.) Ist die Lösung nach der Biegetheorie nicht

bekannt und die Schale als Membranschale konstruiert, kann die von den Randstörungen herrührende Ausmittigkeit auf Grund der folgenden einfachen Lösungen rechnerisch näherungsweise ermittelt werden:

a) Zunächst soll eine Kuppelschale ohne Seitendruck über quadratischem Grundriß betrachtet werden, deren Randträger nur Schubkräfte aufzunehmen vermögen (vgl. Bild 6a).

In einem Fall sei der Randbogen so dünn, daß er keine Einspannung der Schale gestattet. In diesem Fall erhält man aufgrund der näherungsweisen Berechnung [30] mit dem Schmiegezylinder das maximale positive Biegemoment

$$m_1 = +\frac{pR_2t}{20} \tag{6}$$

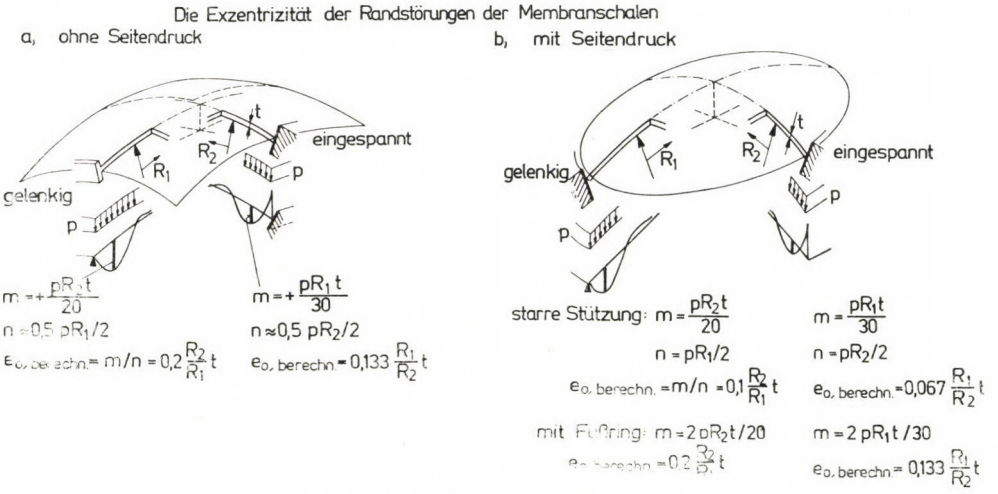

Bild 6. Die Randstörungen an Membranschalen

der Schale in Richtung 1.

Die Membrankraft in Richtung 1 an der Stelle des positiven maximalen Moments errechnet sich zu

$$n_1 \approx 0{,}5\,\frac{pR_1}{2} = \frac{pR_1}{4}, \tag{7}$$

die berechenbare Ausmittigkeit in Richtung 1 also zu

$$w_{0,\,\mathrm{ber.}} = \frac{m_1}{n_1} = 0{,}2\,\frac{R_2}{R_1}\,t\,. \tag{8}$$

In einem anderen Fall sei der Randträger torsionsstarr, so daß er die Schalenplatte einspannt. In diesem Falle beträgt das maximale positive Moment in Richtung 1

$$m_1 = + \frac{pR_2 t}{30} . \tag{9}$$

Die Membrankraft kann aus (7) berechnet werden, die berechenbare Ausmittigkeit in Richtung 1 ergibt sich mithin zu

$$w_{0,\text{ber.}} = \frac{m_1}{n_1} = 0{,}1333 \frac{R_2}{R_1} t . \tag{10}$$

b) Weiterhin sei eine seitlich abgestützte Kuppelschale (Bild 6b), u. zw. zunächst eine mit dem Auflager gelenkig verbundene Konstruktion betrachtet.

Das maximale positive Moment [31] schreibt sich in diesem Falle zu

$$m_1 = + \frac{pR_2 t}{20} . \tag{11}$$

Für die Membrankraft in Richtung 1 gilt, sofern die Last in beiden Richtungen durch gleich große »Bogenwirkungen« getragen wird,

$$n_1 = \frac{pR_1}{2} \tag{12}$$

und somit für die berechenbare Ausmittigkeit in Richtung 1

$$w_{0,\text{ber.}} = \frac{m_1}{n_1} = 0{,}1 \frac{R_2}{R_1} t . \tag{13}$$

Im zweiten Fall soll der Schalenrand starr eingespannt sein. Das positive Moment in Richtung 1 errechnet sich dann zu

$$m_1 = \frac{pR_2 t}{30} . \tag{14}$$

Die Membrankraft kann aus (12) berechnet werden, für die berechenbare Ausmittigkeit in Richtung 1 hat man also

$$w_{0,\text{ber.}} = \frac{m_1}{n_1} = 0{,}067 \frac{R_2}{R_1} t . \tag{15}$$

c) Schließlich sei eine Kuppel betrachtet, die zwar mit einem zur Aufnahme von Seitendruck geeigneten Randring abgestützt, deren Abstützung jedoch wegen der Dehnung des Randringes nicht starr ist (Bild 6b).

Hat der Randring den nötigen Querschnitt und tritt in ihm eine Zugspannung auf, die der Druckspannung in der aufliegenden Schale etwa gleich ist, dann ist der Schalenrand zu einer doppelt so großen Deformation gezwungen wie bei starrer Abstützung, und auch die Biegemomente und die Ausmittigkeiten werden zweifache Werte annehmen.

Bei gelenkiger Abstützung durch einen Randring hat man also für die berechenbare Ausmittigkeit in Richtung 1

$$w_{0,\,\mathrm{ber.}} = 0{,}2\,\frac{R_2}{R_1}\,t \ . \tag{16}$$

Gewährleistet hingegen die Randabstützung eine starre Einspannung, ergibt sich die berechenbare Ausmittigkeit in Richtung 1 zu

$$w_{0,\,\mathrm{ber.}} = 0{,}133\,\frac{R_2}{R_1}\,t \ . \tag{17}$$

Die in den Fällen a), b) und c) der Richtung 2 zugehörigen Ausmittigkeiten können durch Vertauschen der Indizes ermittelt werden. Im Bild 6 sind aus Platzeinsparungsgründen bei den gelenkig eingespannten Rändern nur die Momente in Richtung 1, bei den eingespannten Rändern hingegen jene in Richtung 2 aufgetragen.

Bei einer gegebenen Aufgabe kann also zwischen obigen Fällen interpoliert werden, oder — falls Unsicherheit besteht — kann die Schale für die entsprechenden beiden Extremfälle bemessen werden.

LITERATUR

1. Wolmir, A. S.: Biegsame Platten und Schalen. Verlag für Bauwesen, Berlin 1962
2. v. Kármán, Th.—Tsien, H. S.: The Buckling of Spherical Shells by External Pressure. *Journ. Aero. Sci.* **7** (1939), 43
3. Almroth, B. O.: Influence of Imperfections and Edge Restraint on the Buckling of Axially Compressed Cylinders. *NASA*-CH-432 (April) 1966
4. (Dostanowa, S. H.—Raiser, W. D.) ДОСТАНОВА, С. Х. и РАЙЗЕР, В. Д.: Исследование устойчивости полсгах оболочек положительной кривизны методом локальных вариаций (Stabilitätsuntersuchung flacher Schalen mit positiver Krümmung nach der Methode der lokalen Variation.) *Строит. мех. и расч.* coop. (1973) 34—39
5. Donnell, L. H.—Wan, C. C.: Effect of Imperfections on Buckling of Thin Cylinders and Columns under Axial Compression. *Journ. Appl. Mech.* **17** (1950) 73—78
6. Madsen, W. A.—Hoff, N. J.: The Snap-through and Postbuckling Equilibrium Behavior of Circular Cylindrical Shells and Axial Load. Stanford University Department of Aeronautics and Astronautics *Report No.* 227 (1965) Stanford, California
7. Koiter, W. T.: The Effect of Axisymmetric Imperfections on the Buckling of Cylindrical Shells under Axial Compression. *Proc. Royal Netherlands Academy of Sciences.* Amsterdam. Series B. V. **66** (1963) 265—279
8. Koga, T.—Hoff, N. J.: The Axisymmetric Buckling of Initially Imperfect Complete Spherical Shells. *Intern. Journ. of Solids and Structures.* **5** (1969) 679—697
9. Hutchinson, J. W.: Imperfection Sensitivity of Externally Pressurized Spherical Shells. *Journ. Appl. Mech.* **34** (1967) 49—55

10. Bushnell, D.: Nonlinear Axisymmetric Behavior of Shells of Revolution. *AIAA Journ.* **5** (1967) 432—439
11. Koiter, W. T.: The Nonlinear Buckling Problem of a Complete Spherical Shell under Uniform External Pressure. I, II, III and IV. *Proc. Kon. Nederl. Akad. Wet.* Series B. **72** V. (1969) 40—132
12. Budiansky—Amazigo: Initial Postbuckling Behavior of Cylindrical Shells under External Pressure. *Journ. Math. Phys.* **47** (1968) 223—235
13. Weinitschke, H. J.: On Asymmetric Buckling of Shallow Spherical Shells. *Journ. Math. Phys.* **44** (1965) 141—163
14. Dulácska, E.: On the Critical Load of Shells. Bulletin of the International Association for Shell Structures, No. 39
15. Timoshenko, S. P.—Gere, J. M.: Theory of Elastic Stability. New York, Mac Graw-Hill 1961.
16. Weingarten, V. J.—Morgan, E. J.—Seide, P.: Elastic Stability of Thin-walled Cylindrical and Conical Shells under Axial Compression. *AIAA Journ.* **3** (1965) 500—505
17. Homewood, R. H.—Brine, A. C.—Johnson, A. E. jr.: Experimental Investigations for the Buckling Instability of Monocoque Shells. *Proc. Soc. Experimental Stress Analysis* **18** (1961) 88—96
18. Hergenröder, A.—Rüsch, H.: Recent Findings in the Testing of Models. *Proc. Symp. Shell Research*, Delft, 1961. North Holland Publ. Amsterdam 1961
19. Kaplan, A.—Fung, Y. C.: Nonlinear Theory of the Bending and Buckling of Thin Elastic Shallow Shells. *NACA* TN 3212 (1954)
20. Klöppel, K.—Jungbluth, O.: Beitrag zum Durchschlagproblem dünnwandiger Kugelschalen (Versuche und Bemessungsformeln). *Stahlbau* **22** (1953) 121—130
21. Krenzke, N. A.—Kiernan, T. J.: Elastic Stability of Near-Perfect Shallow Spherical Shells. *AIAA Journ.* **1** (1963) 2855—2857
22. Seaman, L.: The Nature of Buckling in Thin Spherical Shells. Dissertation. Cambridge, Mass. Department of Civil Engineering M.I.T. 1951
23. Tsien, H. S.: A Theory of the Buckling of Thin Shells. *Journ. Aeronaut. Sci.* **9** (1941) 373—384
24. Wedelldborg, B. W.: Critical Buckling Load on Large Spherical Shells. *Proc. ASCE (Journ. Struct. Divis.)* **88** ST. 1 (1962) 111—121
25. Schmidt, H.: Ergebnisse von Beulversuchen mit doppelt gekrümmten Schalenmodellen aus Aluminium. *Proceedings of the Symposium on Shell Research.* (August, 1961, Delft) North Holland Publishing Company, Amsterdam
26. Schubiger, E.: Die Schalenkuppeln im vorgespannten Beton der Kirche Felix und Regula in Zürich. *Schweizerische Bauzeitung* **68** (1950) 223—228
27. Stenker, H.: Gesamtbericht von Großversuchen an doppelt gekrümmten Montageschalen für raumabschließende Geschoßdecken. *Wissenschaftl. Zeitschr. Hochschule für Architektur und Bauwesen*, Weimar 1961, 181—202
28. Bolotin, V. V.: Statisztikai módszerek a szerkezetek mechanikájában (Statistische Methoden in der Mechanik von Konstruktionen). Műszaki Könyvkiadó, Budapest 1970
29. Árbócz, J.: The Effect of General Imperfections on the Buckling of Cylindrical Shells. *Journ. Appl. Mech.* **30** (1969) 28—38
30. Hruban, K.: Transzlációs felületek hajlításelmélete és alkalmazása a csarnoképítésben (Biegetheorie von Translationsflächen und ihre Anwendung im Hallenbau) (ungarisch). *MTA Műsz. Tud. Oszt. Közl.* **11** (1953)
31. Timoshenko, S.—Woinowsky-Krieger, S.: Theory of Plates and Shells. McGraw-Hill, New York 1959

The Initial Eccentricity to be Taken into Account in Investigating Local Buckling of Shell Structures. The eccentricity of the stresses developed in the small wall significantly reduces the magnitude of the critical load causing local buckling of the shell, therefore, it is of great importance of taking exactly into account eccentricities. The paper deals with the determination of the eccentricity caused by initial random waviness and edge disturbances.

Начальная эксцентричность, учитываемая при анализе выпучивания оболочек. Величину критических нагрузок, выпучивающих оболочки, сильно снижает эксцентричность сил разреза оболочек, вследствие чего очень важно точно учитывать имеющиеся эксцентричности. В данной работе рассматривается определение эксцентричности от случайной начальной волнистости и от краевых возмущений.

Acta Technica Academiae Scientiarum Hungaricae, Tomus 86 (1–2), pp. 169–213 (1978)

ELECTROMAGNETIC WAVE PROPAGATION: THE ANALYSIS OF THE GROUP VELOCITY

CS. FERENCZ*

[Manuscript received Nov. 23, 1976]

The paper gives a detailed analysis of energy propagation, the group velocity. It critically investigates the commonly used definition of group velocity. It examines in detail the defineability of average energy with suppositions and consequences. Using the "method of inhomogeneous basic modes", it investigates the group velocity in strictly linear and quasi-linear, dispersive media, deducing the group velocity directly from Maxwell's equations. It shows examples of practice and sees the consequences of the results on an important question of relativistic electrodynamics and propagation of different modes of modulation.

One of the principal tasks of the investigation of the propagation of electromagnetic waves — apart from the determination of the momentary wave pattern — is the study of the propagation of energy (signal, signalling, wave packet, etc.) in the wave picture. Besides the obvious practical importance of this problem we have to remind the reader of its theoretical significance, since the description of energy propagation is intimately connected with the still unresolved problem of the form of the energy-momentum tensor of the electromagnetic fields.

In contrast to the usual derivation we derive the characteristic velocity of energy propagation, i.e. the "group velocity"-$\bar{v}_g$, directly from Maxwell's equations, using the "method of inhomogeneous basic modes" worked out previously [1]. First of all let us examine the usual way to describe the electromagnetic energy and its propagation.

1. Formulation of the problem and the starting point

We derive the energy of the electromagnetic field, like the wave pattern, from Maxwell's equations abstracted from experience, as it was done e.g. [1]

$$\nabla \times \bar{H} = \varepsilon_0 \frac{\partial \bar{D}}{\partial t},$$

* Dr. Cs. Ferencz, Puskin u. 24, H-1088 Budapest, Hungary

$$\nabla \times \bar{E} = -\mu_0 \frac{\partial \bar{B}}{\partial t}, \qquad (1)$$
$$\nabla \bar{B} = 0,$$
$$\nabla \bar{D} = 0.$$

The equation for the energy follows from (1); however, it was actually decided on the basis of experiments that the result of our manipulations is really energy density and energy, respectively. It is well known that if, for the sake of generality,

$$\bar{D} = \epsilon \bar{E} + \varkappa \bar{H}, \qquad (2)$$
$$\bar{B} = \upsilon \bar{E} + \mu \bar{H},$$

where $\bar{E}$ is the electric field, $\bar{B}$ the magnetic induction, $\bar{D}$ the displacement vector, $\bar{H}$ the magnetic field, ϵ, $\varkappa$, υ, μ are the characteristic parameters of the medium (permittivity, etc.), ε_0 and μ_0 the permittivity and the magnetic permeability of the vacuum, resp., $\bar{r}$ the position vector, and t the time then [2]

$$\oint_A (\bar{E} \times \bar{H})\, \mathrm{d}\bar{A} = -\int_V \left(\bar{H} \mu_0 \frac{\partial \bar{B}}{\partial t} + \bar{E} \varepsilon_0 \frac{\partial \bar{D}}{\partial t} \right) \mathrm{d}V. \qquad (3)$$

Here A stands for the surface and V for the volume. It has been shown [5] that (1) can be used for the description of the general case as well.

In what follows let us assume that ϵ, $\varkappa$, υ and μ are independent of the characteristics of the electromagnetic wave — that is, that the medium is strictly linear and stationary in time. Let us assume that it does not move, either (in accordance with the range of validity of the previous investigations [1]). We will separately mention media that are nonlinear in time — in other words, *dispersive* media. Even though in such a way media that show variation with time or that are moving, are excluded from our discussion, we will see that one of the immediate aims of the present investigations is just to find the way to resolve the severe discrepancies that beset the treatment of media which are moving or show time variation.

We do not investigate further the conditions for the existence of a monochromatic solution but, according to [1], assuming that a solution of the form

$$\bar{F} = \bar{F}_0 e^{j(\omega_0 t - \varphi)} = \sum_{i,l} (a_{il}\, e^{-j\varphi_{ai}} \bar{F}_{\mathrm{oil}})\, e^{j(\omega_0 t - \varphi_i)} \qquad (4)$$

exists, where $\bar{F}_0$ and φ are unspecified functions as yet. Here $\bar{F}$ is the sought for electromagnetic field variable ($\bar{E}$, $\bar{D}$, $\bar{B}$, $\bar{H}$), ω_0 is the angular frequency, φ_i the phase functions of the inhomogeneous basic modes and i, running from

1 to n, stands for the individual inhomogeneous basic modes

$$\sum_{i,l} = \sum_{i=1}^{n} \sum_{l=v,k}$$

where $l = v$ denotes the real, and k the imaginary component, with the latter defined, to include the imaginary unit j, where $j^2 = -1$; the meaning of a, φ_a etc. should now be obvious from (4). We cannot deal with the determination of (4) here; we shall just assume familiarity with the method of solution in [1] and with its conditions. Thus, in what follows (4) *is a known solution* of Maxwell's equations [1].

Equation (3) for the energy distribution can also be written in a more detailed form which enables us to analyse which processes contribute to the change of the energy within the volume V, i.e. what is the relation of the individual terms with the energy flowing through surface A

$$\oint_A (\bar{E} \times \bar{H})\, \mathrm{d}\bar{A} = -\int_V \left(\varepsilon_0 \bar{E} \epsilon \frac{\partial \bar{E}}{\partial t} + \varepsilon_0 \bar{E} \varkappa \frac{\partial \bar{H}}{\partial t} + \mu_0 \bar{H} \nu \frac{\partial \bar{E}}{\partial t} + \mu_0 \bar{H} \mu \frac{\partial \bar{H}}{\partial t} \right) \mathrm{d}V. \tag{5}$$

The vector field in the integrand on the left-hand side is usually called the Poynting-vector

$$\bar{S} = \bar{E} \times \bar{H}. \tag{6}$$

Its physical meaning is easily obtained for vacuum, but it is more difficult to obtain for a medium and raises serious problems in moving media [3].

We can see from what was previously mentioned that — as is well known — the propagation of energy is described by means of $\bar{S}$, or rather the variation of $\bar{S}$, as a "detectable, spreading phenomenon". It can be shown from (4), however, that the interpretation of $\bar{S}$ and of its changes entails certain problems of *averaging*, so we have to consider the problem of the possibility of an unambiguous determination of the *average energy*.

2. The usual treatment of group velocity

As at the first glance it seems that the spreading of energy can be traced only by an actual change in $\bar{S}$, the starting point of the usual treatment is that the electromagnetic wave will always possess a beginning and an end [4], and hence in every case (even in the case of "monochromatic" radiation which is made purely hypothetical here) we are dealing with a wave packet. Consequently we can avoid the use of the notion of an average energy, which is a great simplification.

The usual form of the wave packet in a homogeneous medium is

$$\bar{F}(\bar{r}, t) = e^{j(\omega_0 t - \bar{k}_0 \bar{r})} \int_{\bar{k}_0 - \Delta\bar{k}}^{\bar{k}_0 + \Delta\bar{k}} \bar{F}_0(\bar{k}, \bar{k}_0)\, e^{j\left\{(\bar{k} - \bar{k}_0)\left[\left(\frac{\partial\omega}{\partial\bar{k}}\right)_0 t - \bar{r}\right]\right\}} \mathrm{d}\bar{k} \tag{7}$$

where $\bar{k}$ is the wave vector,

$$\begin{aligned} \omega(\bar{k}) &= \omega(\bar{k}_0) + (\bar{k} - \bar{k}_0)\left(\frac{\partial\omega}{\partial\bar{k}}\right)_0 + \ldots \\ \omega(\bar{k}_0) &\equiv \omega_0 \end{aligned} \tag{8}$$

and the spectrum of the wave packet is chosen to be so narrow that the linear approximation (8) will suffice. Then the phase of the "group" described by (7) will be given by $\exp j(\omega_0 t - \bar{k}_0 \bar{r})$ which we can bring in front of the integral. This is formally arbitrary so the choice of the center of the expansion will not be uniquely determined. *The amplitude characterizing the energy propagation in* (7) can be obtained from the propagation of the surfaces corresponding to a constant value of the integral. If $\bar{F}_0(\bar{k}, \bar{k}_0)$ is a slowly varying function, which here is a realistic assumption, then these surfaces will be given by the equation

$$(\bar{k} - \bar{k}_0)\left[\left(\frac{\partial\omega}{\partial\bar{k}}\right)_0 t - \bar{r}\right] = \text{constant} \tag{9}$$

Hence the velocity of the propagation of the surfaces is given by

$$\frac{\mathrm{d}\bar{r}}{\mathrm{d}t} = \left(\frac{\partial\omega}{\partial\bar{k}}\right)_0 = \bar{v}_g\,, \tag{10}$$

the group velocity. We can see that if $\omega(\bar{k}) \sim \bar{k}$, then — as is well known

$$\bar{v}_g = \bar{v}_f\,, \quad \text{where} \quad v_f = \omega_0 \left(\frac{\partial\varphi}{\partial s}\right)^{-1} \tag{11}$$

the phase velocity, and s is the arc length along the phase trajectory.

(The same result can be obtained from the "principle of constant phase" [4], etc.)

This definition in itself is correct, but it leads to a few questions:

— it does not give a general answer to the problem of the velocity of energy propagation within the domain of validity of the phenomenological description, where in the majority of cases we are dealing with continuous and frequently *strictly monochromatic signals;*

— the group velocity is defined through *the form assumed for the solution* and not from Maxwell's equations!

— equation (10) does not give the possibility of a *comparative* study of propagation in many different possible media since the characteristics of the medium enter (10) in an intricate implicit way.

Conclusion: the classical treatment of $\bar{v}_g$ cannot be considered complete and we are forced to consider the problem of determining the energy and describing its propagation directly from Maxwell's equations.

3. The determination of the electromagnetic energy

As follows from the previous sections, in order to start a general and concise analysis of energy propagation we will have to examine the properties of the energy flow (5) and (6) in the case of the solution first of all (4). The range of validity of these solutions is known [1]. A more general investigation (of very inhomogeneous fields, moving or time-varying inhomogeneous fields, etc.) can only be based on the present studies since there are still a number of unsolved questions relating to homogeneous or inhomogeneous cases [2].

As follows from (5), for example, it is not directly $\bar{S}$ that figures in physical measurements but rather the energy passing through a surface ($\bar{A}$ or $\overline{\Delta A}$) in a given length of time (Δt), i.e. the integral of $\bar{S}$. This will then be averaged for a *unit* surface area or for a unit of time. Consequently the result will depend not only on the wave picture but also on the choice of surface and time interval of averaging.

So a question of basic importance is: under what conditions shall we get an average value for the energy which is *independent* of the "measurement" surface and time? Will the result of averaging depend on the *order of averaging* over the surface and time? What are the factors that influence the *uniqueness* of energy averaging?

On the basis of (6), and taking (4) into account, the instantaneous value of the Poynting vector can be written as

$$\bar{s}(\bar{r}, t) = \bar{E}(\bar{r}, t) \times \bar{H}(\bar{r}, t). \tag{12}$$

Using (12) we can give the average energy $\widetilde{W}$ flowing through the surface $\overline{\Delta A}$ in the measurement time Δt ($\sim$ denotes the average value):

$$\widetilde{W} = \frac{1}{\Delta t} \int_{t_1}^{t_2} \left[\int_{\Delta A} \bar{s}(\bar{r}, t) \mathrm{d}\overline{A} \right] \mathrm{d}t. \tag{13}$$

However, the average energy can be obtained in another way as well:

$$\widetilde{W}^0 = \int_{\Delta A} \left[\frac{1}{\Delta t} \int_{t_1}^{t_2} \bar{s}\,(\bar{r}, t)\,\mathrm{d}t \right] \overline{\mathrm{d}A}\ . \tag{14}$$

The questions posed by us can now be formulated in exact terms with the aid of (13) and (14). We can unambiguously speak of an energy and average energy as long as

$$\widetilde{W} = \widetilde{W}^0 \tag{15}$$

and the additional condition, that in a sufficiently small neighbourhood of some $(\bar{r}_0, t_0)$

$$\frac{\partial \widetilde{W}}{\partial(\Delta t)} \cong 0 \quad \text{and} \quad \overline{\operatorname{grad}}_{\Delta A}\, \widetilde{W} = \text{const.} \tag{16}$$

is also imposed, besides the simultaneous fulfilment of the conditions set out by us for the medium and the previous solution. Considering that (4) is a stationary solution [1]

$$\frac{\partial \bar{F}_0}{\partial t} = 0\ . \tag{17}$$

Hence, if the investigation of the energy propagation requires the application of some sort of perturbation, we will require that

$$\frac{\partial \bar{F}_0\,(\text{pert.})}{\partial t} \cong 0 \ll \frac{\partial \bar{F}}{\partial t} \tag{18}$$

be satisfied. (18) will always have to be observed in the subsequent investigations! Then in the calculation of (13) and (14) $\bar{F}_0\,(\text{pert.}) \cong$ const. during the time interval Δt.

Comparison of equations (13)—(17) shows that already at the beginning of such an investigation we are making use of the condition that we should study the possibility of the energy analysis and the conditions of its uniqueness for a stationary monochromatic solution in a medium which is constant in time. So in *every new situation* such or a similar analysis of the energy *should be performed* anew under the new conditions.

3.1. *The analysis of the problem*

Let us carry out our investigations in the orthogonal co-ordinate system with the basis set of unit vectors $(\bar{e}_m, \bar{e}_n, \bar{e}_p)$ and let $k = m, n, p$ (or 1, 2, 3).

Then from (4) the solution that must exist for *physical reasons*

$$\bar{F} = \sum_i \left\{ \sum_k a_i \, F_{0ik} \, \bar{e}_k \sin \left(\omega_{0t} - \varphi_i - \varphi_{ai} + \varphi_{0i\,Fk} \right) \right\} \tag{19}$$

where $(a_i \, F_{0ik})$ and φ_{0iFk} account for the effect of the automatic vanishing of the indices l in the expression of (4). Then (17) is trivially satisfied, and it can be written in the detailed form

$$\frac{\partial a_i \, F_{0ik}}{\partial t} \equiv 0 , \quad \frac{\partial \omega_0}{\partial t} \equiv 0 , \quad \frac{\partial (\varphi_i + \varphi_{ai} - \varphi_{0iFk})}{\partial t} \equiv 0 . \tag{17a}$$

Hence the actual form of (12)

$$\begin{aligned} \bar{s}(\bar{r}, t) = & \sum_i \left[\sum_k a_i \, E_{0ik} \, \bar{e}_k \sin \left(\omega_0 t - \varphi_i - \varphi_{ai} + \varphi_{0i\,Ek} \right) \right] \times \\ & \times \sum_i \left[\sum_k a_i H_{0ik} \, \bar{e}_k \sin \left(\omega_0 t - \varphi_i - \varphi_{ai} + \varphi_{0iHk} \right) \right] = \\ & = \sum_k E_{0k} \, \bar{e}_k \sin \left(\omega_0 t - \varphi - \varphi_{0Ek} \right) \times \\ & \times \sum_k H_{0k} \, \bar{e}_k \sin \left(\omega_0 t - \varphi - \varphi_{0Hk} \right) . \end{aligned} \tag{20}$$

Inspection of (20) shows that the analysis is formally the same for

— *the unimodal* ($i \equiv 1$) case and

— for the general case of the *resultant* field, provided that the necessary conditions [1] are satisfied.

The analysis of the questions posed in (15) and (16) will not give anything *principally new* for the general case of the resultant field expressed as an expansion in *inhomogeneous basic modes*. However, significant details can be clarified concerning the internal motions of the energy, the coupling between the modes, etc., thereby *possibly opening the way* to the definition of "propagating" basic modes (co-moving energy parts) built up of inhomogeneous basic modes on the one hand, and to the further development of the method of solution given in [1] on the other. (The necessity of this was demonstrated in the application of the method to long-distance transmission lines [18].)

According to the above discussion in what follows we will perform the investigations for the general resultant field (and automatically for the one-mode field, of course). Hence we will obtain the result relevant for the investigation of group velocity. A detailed analysis of the multi-mode case will be given elsewhere.

At the same time it is shown by the consideration of (20), as well as of equations (1), (2) and (5) that in the framework of our phenomenological

approach for the existence of $\bar{S}$ or rather (20), it is first of all necessary that all the medium-electromagnetic field interactions according to ϵ, μ, $\varkappa$ and ν *will take place so and with such a speed* that we can speak of $\bar{E}$ and $\bar{H}$, etc. simultaneously. Inclusion of cases *different from this* would require a separate investigation.

Here one should add a further remark: in cases when the "wave-like" solution (4) does not exist or becomes so complicated that the notions of propagation, direction of propagation, etc. become meaningless, it is probable that the analysis of the dispersion of a single wave packet (Section II) will give *at least* as much information as the analysis of some stationary solution.

With this the determination of the range of validity of our investigations is complete.

3.2. *The interchangeability of the order of integrations*

As a first step let us consider equation (20) for $\bar{s}$. For the sake of simplicity let the index $k = 1, 2, 3$ be cyclic, i. e. let $k + 1$ and $k - 1$ be defined for any k (for example, if $k = 3$, then $k + 1 = 1$).

Then

$$\bar{s}(\bar{r}, t) = \bar{E} \times \bar{H} = \sum_k (E_{k+1} H_{k-1} - E_{k-1} H_{k+1}) \bar{e}_k \tag{21}$$

and (20) can be rewritten, using (21), into a form more suitable for the expansion in (13) and (14). Let

$$\psi_0(t) = \omega_0 t - \varphi ,$$

then

$$\begin{aligned} \bar{s}(\bar{r}, t) = \sum_k & [E_{0k+1} H_{0k-1} \sin \varphi_{0Ek+1} \sin \varphi_{0Hk-1} - \\ & - E_{0k-1} H_{0k+1} \sin \varphi_{0Ek-1} \sin \varphi_{0Hk+1}] \bar{e}_k + \\ & + \sum_k \{E_{0k+1} H_{0k-1} \sin [\psi_0(t) + \varphi_{0Ek+1} + \varphi_{0Hk-1}] - \\ & - E_{0k-1} H_{0k+1} \sin [\psi_0(t) + \varphi_{0Ek-1} + \varphi_{0Hk+1}]\} \sin \psi_0(t) \bar{e}_k \end{aligned} \tag{22}$$

that is

$$\bar{s}(\bar{r}, t) = \bar{S}_0 + \bar{s}_*(t) \sin \psi_0(t) \tag{22a}$$

where because of (17a)

$$\frac{\partial \bar{S}_0}{\partial t} \equiv 0 .$$

For a further expansion of (22) we want to completely separate the $\bar{r}$ and t dependences. It is expedient to introduce the short notations

$$E_{0k+1} H_{0k-1} = A_{EH\pm 1} \quad \text{and} \quad E_{0k-1} H_{0k+1} = A_{EH\mp 1},$$

which are time-independent factors. After some trivial steps

$$\bar{s}_*(t)\sin\psi_0(t) = \sum_k \{[A_{EH\mp1}\sin\varphi_{EH\mp1} - A_{EH\pm1}\sin\varphi_{EH\pm1}]\sin\varphi + \\ + [A_{EH\pm1}\sin(\omega_0 t + \Phi_{\pm1}) - A_{EH\mp1}\sin(\omega_0 t + \\ + \Phi_{\mp1})]\sin\omega_0 t\}\,\bar{e}_k = \bar{S}_{*0} + \bar{s}_{**}(t)\sin\omega_0 t \tag{23}$$

where

$$\varphi_{EH\pm1} = \varphi_{0Ek+1} + \varphi_{0Hk-1} - \varphi;$$
$$\varphi_{EH\mp1} = \varphi_{0Ek-1} + \varphi_{0Hk+1} - \varphi;$$
$$\Phi_{\pm1} = \varphi_{EH\pm1} - \varphi; \quad \Phi_{\mp1} = \varphi_{EH\mp1} - \varphi,$$

and

$$\frac{\partial \bar{S}_{*0}}{\partial t_0} = 0 .$$

Consequently

$$\bar{s}(\bar{r},t) = (\bar{S}_0 + \bar{S}_{*0}) + \bar{s}_{**}(t)\sin\omega_0 t = \bar{S}_* + \bar{s}_{**}(t)\sin\omega_0 t = \\ = \bar{S}_* + \bar{s}_{**}(t)\sin\omega_0 t \tag{24}$$

where

$$\partial\bar{S}_*/\partial t = 0 .$$

With the aid of (24) both (13) and (14) can be evaluated. We find that

$$\widetilde{W} = \frac{1}{\Delta t}\int_{\Delta t}\left[\int_{\Delta A}(\bar{S}_* + \bar{s}_{**}(t)\sin\omega_0 t)\,\overline{\mathrm{d}A}\right]\mathrm{d}t = \\ = W_0 + \frac{1}{\Delta t}\int_{\Delta t}\left[\int_{\Delta A}\bar{s}_{**}(t)\,\overline{\mathrm{d}A}\right]\sin\omega_0 t\,\mathrm{d}t \tag{25}$$

and

$$\widetilde{W}^0 = W_0 + \frac{1}{\Delta t}\int_{\Delta t}\left[\int_{\Delta t}\bar{s}_{**}(t)\sin\omega_0\, t\,\mathrm{d}t\right]\overline{\mathrm{d}A} \tag{26}$$

where

$$W_0 = \int_{\Delta A}(\bar{S}_0 + \bar{S}_{*0})\,\overline{\mathrm{d}A}. \tag{27}$$

In order to compare (25) and (26) we have to decompose $\bar{s}_{**}(t)$. Since

$$\bar{s}_{**}(t) = \sum_k [(A_{EH\pm1}\cos\Phi_{\pm1} - A_{EH\mp1}\cos\Phi_{\mp1})\sin\omega_0 t + (A_{EH\pm1}\sin\Phi_{\pm1} - \\ - A_{EH\mp1}\sin\Phi_{\mp1})\cos\omega_0 t]\,\bar{e}_k = \sum_k (\mathcal{A}_{\cos}\sin\omega_0 t + \\ + \mathcal{A}_{\sin}\cos\omega_0 t)\,\bar{e}_k = \overline{\mathcal{A}}_{\cos}\sin\omega_0 t + \overline{\mathcal{A}}_{\sin}\cos\omega_0 t \tag{28}$$

where the notations are self-explanatory. We get that

$$\widetilde{W} = W_0 + \frac{1}{\Delta t}\int_{\Delta t}\left[\left(\int_{\Delta A}\overline{\mathcal{R}}_{\cos}\,\overline{\mathrm{d}A}\right)\sin^2\omega_0 t + \left(\int_{\Delta A}\overline{\mathcal{R}}_{\sin}\,\overline{\mathrm{d}A}\right)\sin\omega_0 t\cos\omega_0 t\right]\mathrm{d}t$$

and

$$\widetilde{W}^0 = W_0 + \frac{1}{\Delta t}\int_{\Delta A}\left[\int_{\Delta t}(\overline{\mathcal{R}}_{\cos}\sin^2\omega_0 t + \overline{\mathcal{R}}_{\sin}\sin\omega_0 t\cos\omega_0 t)\,\mathrm{d}t\right]\overline{\mathrm{d}A}\,.$$

Condition: in all our investigations only those perturbations are allowed, or rather (the sufficiently small) Δt and ΔA are chosen is such a way, that

$$\frac{\partial\left(\int_{\Delta A}\overline{\mathcal{R}}\,\overline{\mathrm{d}A}\right)}{\partial t} \cong 0 \quad \text{and} \quad \frac{\partial\overline{\mathcal{R}}}{\partial t} \cong 0 \tag{29}$$

and also

$$\overline{\mathrm{grad}}\left(\int_{\Delta t}\sin^2\omega_0 t\,\mathrm{d}t\right) \simeq \overline{\mathrm{grad}}\left(\int_{\Delta t}\sin\omega_0 t\cos\omega_0 t\,\mathrm{d}t\right) \cong 0$$

be true. (The lower bounds of Δt and ΔA will be given by the conditions (16) in such a way that $\widetilde{W}$ will be meaningful.]

Let us further have

$$\int_{\Delta t}\sin^2\omega_0 t\,\mathrm{d}t = F_{ss}(t)$$

and

$$\int_{\Delta t}\sin\omega_0 t\cos\omega_0 t\,\mathrm{d}t = F_{sc}(t)\,,$$

and

$$\int_{\Delta A}\overline{\mathcal{R}}_{\cos}\,\overline{\mathrm{d}A} = W_{\cos} \quad \text{and} \quad \int_{\Delta A}\overline{\mathcal{R}}_{\sin}\,\overline{\mathrm{d}A} = W_{\sin}\,.$$

Then it follows from the validity of the set (29) of conditions that the expansion can be continued further, and

$$\widetilde{W} = W_0 + \frac{1}{\Delta t}\int_{\Delta t}W_{\cos}\sin^2\omega_0 t\,\mathrm{d}t + \frac{1}{\Delta t}\int_{\Delta t}W_{\sin}\sin\omega_0 t\cos\omega_0 t\,\mathrm{d}t$$

and

$$\widetilde{W}^0 = W_0 + \frac{1}{\Delta t}\int_{\Delta A}\left[\overline{\mathcal{R}}_{\cos}F_{ss}(t) + \overline{\mathcal{R}}_{\sin}F_{sc}(t)\right]\overline{\mathrm{d}A}\,.$$

Hence, we can see that under the above conditions

$$\widetilde{W} = \widetilde{W}^0 = W_0 + \frac{1}{\Delta t}\left[W_{\cos}F_{ss}(t) + W_{\sin}F_{sc}(t)\right]. \tag{30}$$

With this we have verified that (15) is satisfied under the given circumstances. *At the evaluation of the average energy the result does not depend on the order of the integrations.*

In this discussion we obtained upper bounds for Δt and ΔA (having in mind possible perturbations). However, it can be checked by elementary means that choosing Δt and $\sqrt{\Delta A}$ a negligibly small compared to the periodal time and the wave length, respectively, we can obtain for $\widetilde{W}$ values varying arbitrarily within wide limits. For this reason we have to give for Δt and ΔA lower bounds as well.

3.3. *The analysis of* $\widetilde{W}$

Here our immediate aim is to investigate how the conditions (16) are satisfied; only when these conditions are satisfied can we speak of a constant or unambiguously defined average energy.

a) The investigation of *time dependence.*

In view of the fact that the time dependence is basically periodic even in the periodic case (18), let

$$\Delta t = n\frac{\pi}{\omega_0} + \Delta T \tag{31}$$

where $n = 0, 1, 2, \ldots$ is a non-negative integer and $0 \leqq \Delta T \leqq \pi/\omega_0$. Further, we know that

$$F_{ss}(t) = \frac{\Delta t}{2} - \frac{\sin 2\omega_0 \Delta t}{4\omega_0}$$

and

$$F_{sc}(t) = \frac{1 - \cos 2\omega_0 \Delta t}{4\omega_0}$$

if, without a loss of generality, the integration for the integral Δt is performed for $t(0, \Delta t)$.

Replacing Δt from (31) we see that

$$0 \leqq F_{sc}(\Delta T, n) \leqq \frac{1}{2\omega_0} \tag{32}$$

and

$$\left[\frac{1}{2}\left(n\frac{\pi}{\omega_0} + \Delta T\right) - \frac{1}{2}\,\frac{1}{2\omega_0}\right] \leqq F_{ss}(\Delta T, n) \leqq$$

$$\leqq \left[\frac{1}{2}\left(n\frac{\pi}{\omega_0} + \Delta T\right) + \frac{1}{2}\,\frac{1}{2\omega_0}\right]$$

and furthermore, if $n = 0$ and $\Delta T \ll \pi/\omega_0$, then

$$F_{ss}(\Delta T, 0) \cong 0 \text{ and } F_{sc}(\Delta T, 0) \cong 0 \tag{33}$$

Consequence: the relationships (32) and (33) prove that for a time interval — and it can be analogously proved for a domain of space as well — the "measurable" energy *will depend* on the measurement time (surface), will show fluctuations, and consequently that $\widetilde{W}$ *can be meaningfully defined only as an expectation value* possessing a *certain standard deviation.* The deviation is a function of, for example, Δt. A detailed (measurement) analysis cannot overlook this fact! In our case when the aim is the study of group velocity, statistical analysis is not needed since we are only interested in whether $\widetilde{W}$ can be defined and, if yes, whether it is in an unambiguous relationship with the signal amplitude, provided that the signal amplitude can be defined.

Because of (33) in the following we have to add the extra condition $n \neq 0$. Then, from (31) and (32) and increasing the value of n:

$$\frac{1}{\Delta t} F_{ss}(\Delta T, n) = \frac{1}{2} - \frac{1}{n\frac{\pi}{\omega_0} + \Delta T} \frac{\sin 2\omega_0 \Delta T}{4\omega_0} \cong \frac{1}{2} \tag{34}$$

and

$$\frac{1}{\Delta t} F_{sc}(\Delta T, n) = \frac{1}{n\frac{\pi}{\omega_0} + \Delta T} \frac{1 - \cos 2\omega_0 \Delta T}{4\omega_0} \cong \frac{1}{2n\pi} \ll 1$$

where $n \gg 1$; n is determined by *the accuracy we require.* Hence, we obtained for Δt *a lower limit* as well! The order of the results is a consequence of the way we performed the calculation (concentrating on $\omega_0 t$). If we concentrate on φ instead — which we could have done in view of the structure of $(\omega_0 t - \varphi)$ — then we get *an analogous requirement for* ΔA.

b) The investigation of *the surface dependence.*

We know from (27) and (30) that the surface dependence of $\widetilde{W}$ is contained in the integrals

$$\int_{\Delta A} (\bar{S}_0 + \bar{S}_{*0}) \, \overline{\mathrm{d}A} \, ; \quad \int_{\Delta A} \overline{\mathfrak{H}}_{\cos} \, \overline{\mathrm{d}A} \quad \text{and} \quad \int_{\Delta A} \overline{\mathfrak{H}}_{\sin} \, \overline{\mathrm{d}A} \, .$$

At the detailed analysis of these take W_0 last, and define a surface $\overline{\Delta A}$. Let

$$\overline{\Delta A} = \Delta a_1 \bar{e}_{a1} \times \Delta a_2 \bar{e}_{a2} = \Delta a_1 \Delta a_2 \bar{e}_A \tag{35}$$

where $\bar{e}_{a1}$ and $\bar{e}_{a2}$ are not parallel (and not necessarily perpendicular). Furthermore, we have $\bar{e}_A = \sum_k \xi_k \bar{e}_k$. Also we know that on the basis of (28)

we can use the unambiguous notations $\overline{\mathcal{H}}_{\cos} = \overline{\mathcal{H}}_{\cos\pm} - \overline{\mathcal{H}}_{\cos\mp}$ and $\overline{\mathcal{H}}_{\sin} = \overline{\mathcal{H}}_{\sin\pm} - \overline{\mathcal{H}}_{\sin\mp}$. Then it is enough to study the structure of the terms determining $W_{\cos}$ and $W_{\sin}$ on a single example. So the consideration of

$$\int_{\Delta A} \overline{\mathcal{H}}_{\cos\pm}\, \overline{\mathrm{d}A} = \int_{\Delta A} \sum_k (A_{EH\pm1} \cos \Phi_{\pm1})\, \xi_k\, \mathrm{d}a_1\, \mathrm{d}a_2 \tag{36}$$

will suffice.

Condition: — In order to estimate (36), and considering that we have restrictions for the speed of variation [1] in (4) to begin with, let us assume that it is meaningful to speak about an "amplitude", and $\overline{\Delta A}$ is *only* so large that even for $\overline{\Delta A}_{\max}$

$$\frac{\Delta a_i\, e_{ai}\, \overline{\mathrm{grad}\, A_{EH\pm1}}}{A_{EH\pm1}} \ll 1 \tag{37a}$$

that is, expanding the amplitude along the surface, can be replaced by its value somewhere on the surface.

— If the signal has a (slow) time variation, e.g. because of perturbation, in addition to $(\omega_0 t)$, then we get a condition for $\Delta t_{\max}$ which is analogous to (37a).

— Let us further assume that it is a good approximation to replace the surface $\overline{\Delta A}$ in a small region by a plane, i.e.

$$\frac{\overline{\mathrm{grad}\, \xi_k}}{\xi_k} \ll 1 \tag{37b}$$

In such a way $A_{EH\pm1}$ and ξ_k can be factored out of the integral along ΔA in (36), i.e.

$$\int_{\Delta A} \overline{\mathcal{H}}_{\cos\pm}\, \overline{\mathrm{d}A} \cong \sum_k \xi_k\, A_{EH\pm1} \int_{\Delta a_1}\int_{\Delta a_2} \cos\,(\varphi_{EH\pm1} - \varphi)\mathrm{d}a_1\, \mathrm{d}a_2$$

Furthermore, taking into account the meaning of the variables on the basis of (4), and also (37),

$$\int_{\Delta A} \overline{\mathcal{H}}_{\cos\pm}\, \overline{\mathrm{d}A} \cong \sum_k \xi_k\, A_{EH\pm1} \left[\cos\,(\varphi_{0Ek+1} + \varphi_{0Hk-1}) \int_{\Delta a_1}\int_{\Delta a_2} \cos 2\varphi\, \mathrm{d}a_1\, \mathrm{d}a_2 + \right.$$
$$\left. + \sin\,(\varphi_{0Ek+1} + \varphi_{0Hk-1}) \int_{\Delta a_1}\int_{\Delta a_2} \sin 2\varphi\, \mathrm{d}a_1\, \mathrm{d}a_2 \right] \tag{38}$$

Thereby we obtained a *lower bound for the surface* as well, as compared to the wave length (φ).

Let us have

$$\Delta a_0 \to \varphi\,|_{\Delta a_0} = \pi \quad \text{and} \quad \Delta a_1 \sim \Delta a_2 \gg \Delta a_0 \tag{39}$$

which is analogous to the requirement for time Δt (31). Then it can be verified by elementary means that — analogously to (32)–(38) fluctuates around a small expectation value which is independent of Δa_1 and Δa_2:

$$\int_{\Delta A} \overline{\mathcal{R}}_{\cos \pm} \, \overline{\mathrm{d}A} \cong \sum_{k,q} \xi_k \, A_{EH \pm 1} \frac{\alpha_{\pm q} f_q \, (\varphi_{0E}, \varphi_{0H})}{2 \, \|\varphi\| \, a_1 a_2}$$

where $0 \leq |\alpha_{\pm q}| \leq 1$, and the rest follows self-evidently from (38). This is negligible in comparison with W_0 proportional to the surface, or rather is much smaller than 1 when multiplied by ΔA^{-1}.

c) The *average energy*.

It follows from the previous considerations that

$$\begin{aligned} \widetilde{W} &= W_0 + \frac{1}{\Delta t} F_{ss}(t) W_{\cos} + \frac{1}{\Delta t} F_{sc}(t) W_{\sin} \cong \\ &\cong W_0 + \left[\frac{1}{2} - \mathcal{O}(\Delta t) \right] \mathcal{O}(\Delta A) + \mathcal{O}(\Delta t) \, \mathcal{O}(\Delta A) \cong W_0 \end{aligned} \tag{40}$$

Now we expand $W_0 = \int_{\Delta A} (\bar{S}_0 + \bar{S}_{*0}) \, \overline{dA}$ as was seen in 3.3b and also impose the requirement (39).

The terms characterizing the "creeps" of energy — which would correspond to (32) and (38) — will be neglected here. This can be done as long as the conditions stated above apply. *Remark*: the analysis of these terms characterizing the energy fluctuations is important both from the point of view of measurement technology, and for the investigation of the so-called "reactive power". For our present purposes it was sufficient to prove that it is justifiable to neglect these terms when calculating the average — and *only* here, and from this point of view.

Hence, we can see that

$$\begin{aligned} \int_{\Delta A} \bar{S}_0 \, \overline{\mathrm{d}A} \cong \sum_k \, & (A_{EH \pm 1} \sin \varphi_{0Ek+1} \sin \varphi_{0EHk-1} - \\ & - A_{EH \mp 1} \sin \varphi_{0Ek-1} \sin \varphi_{0Hk+1}) \, \xi_k \, \Delta a_1 \, \Delta a_2 \end{aligned}$$

and

$$\begin{aligned} \int_{\Delta A} \bar{S}_{*0} \, \overline{\mathrm{d}A} \cong \frac{1}{2} \sum_k \, & [\xi_k \, A_{EH \pm 1} \cos \, (\varphi_{0Ek+1} + \varphi_{0Hk-1}) - \\ & - A_{EH \mp 1} \cos \, (\varphi_{0Ek-1} + \varphi_{0Ek+1})] \, \Delta a_1 \, \Delta a_2 \end{aligned}$$

From here, after a few elementary steps it follows that

$$\widetilde{W} \cong \frac{1}{2} \sum_k \xi_k \left[\left[(A_{EH\pm 1} \cos \varphi_{0Ek+1} \cos \varphi_{0Hk-1} - \right. \right. \\ - A_{EH\mp 1} \cos \varphi_{0Ek-1} \cos \varphi_{0Hk+1}) + (A_{EH\pm 1} \sin \varphi_{0Ek+1} \sin \varphi_{0Hk-1} - \\ \left. \left. - A_{EH\mp 1} \sin \varphi_{0Ek-1} \sin \varphi_{0Hk+1}) \right] \Delta a_1 \Delta a_2 \right. . \tag{41}$$

i.e. returning to the customary way of writing $\exp j(\omega_0 t - \varphi)$ seen in (4)

$$\widetilde{W} \cong \frac{1}{2} \overline{\Delta A} \left[(\mathrm{Re}\, \bar{E}_0 \times \mathrm{Re}\, \bar{H}_0) + (\mathrm{Im}\, \bar{E}_0 \times \mathrm{Im}\, \bar{H}_0) \right] \tag{42}$$

On the basis of (42) now we can formally introduce the notions of complex energy and Poynting vector. (The meaning not only of $\widetilde{W}$ but also of the imaginary part of the complex energy, its relationship to the "creeps" of the energy, the *spread* of the average, remain to be checked separately in every case, etc.)

Statement: One can see from (42) that assuming its existence described in terms of inhomogeneous basic modes, and the fulfilment of the additional conditions imposed, *the average energy can be defined and it is determined by the general signal amplitude* ($\bar{F}_0$). Consequently the propagation of the energy can be studied as the propagation of changes in $\bar{F}_0$.

Addenda: — on the basis of (42) we can introduce the average and the complex Poynting vector for the expectation values, i.e. if here the complex conjugate of $\bar{b}$ is denoted by $\bar{b}^*$, it is trivial that

$$\tilde{\mathfrak{S}} \cong \frac{1}{2} \mathrm{Re}\, (\bar{E}_0 \times \bar{H}_0^*) = \frac{1}{2} \mathrm{Re}\, (\bar{E} \times \bar{H}^*) .$$

Let us have

$${}_k\bar{S} = \frac{1}{2} \bar{E} \times \bar{H}^* \qquad \text{and} \qquad {}_kW = \int_{\Delta A} {}_k\bar{S}\, \overline{\mathrm{d}A} , \quad \widetilde{W} = \mathrm{Re}\, {}_kW$$

— All the questions we asked or were led to pose in the course of the investigation, were left open as regards the phenomena outside the range of validity of the assumption made. Further investigations are needed here.

— In cases when the assumptions related to the lower and upper limits of integration are in contradiction with each other, the average energy cannot be defined.

4. A way of giving the group velocity with the aid of the method of inhomogeneous basic modes

We can express the propagation of an infinitesimally small and slow [cf. the previous conditions (17), (18), etc.] change of the amplitude, having accepted the existence of a solution of the form (4), from Maxwell's equations serving as the starting point of the method of inhomogeneous basic modes [1]. Thus in what follows we perturb (modulate) the amplitude in the form $(a_{il} + \delta)$ or $(a_{il} + \delta_i)$, where δ is infinitesimally small.

We shall deal separately with the other possible perturbations (modulations), such as

$(\varphi_{ai} + \delta)$ or $(\varphi_{ai} + \delta_i)$ — phase modulation,

$(\omega_0 + \delta)$ or $(\omega_0 + \delta_i)$ — frequency modulation,

$(\bar{F}_{oil} + \bar{\delta})$ or $(\bar{F}_{oil} + \bar{\delta}_i)$ — polarization modulation.

The original unperturbed solution has the form (4). So, if the perturbation has the form $(a_{i1} + \delta_i)$, then

$$\bar{F}_\delta = \sum_{i,l} (1 + f_{il})\, \bar{F}_{il} = \sum_{i,l} \bar{F}^\delta_{il} = \sum_{i,l} \left[(1 + f_{il})\, a_{il}\, e^{-j\varphi_{ai}}\, \bar{F}_{oil}\right] e^{j(\omega_0 t - \varphi_i)} \tag{43}$$

where

$$f_{il} = \frac{\delta_i}{a_{il}} \ll 1 .$$

Not only the solution (4), but also the perturbed solution (43) must satisfy Maxwell's equations. We will expand Maxwell's equations aiming at the accustomed form in [1]. We take into account that $\ln (1 + f_{i1}) \cong f_{i1}$. So

$$\begin{aligned}
&\sum_{i,l} \left[\overline{\operatorname{grad}\,(\ln a_{il} + f_{il} - j\varphi_{ai})} \times \bar{H}^\delta_{il} + \nabla_{THoil}\, \bar{H}^\delta_{il} - j\bar{K}_i \times \bar{H}^\delta_{il}\right] = \\
&\quad = \varepsilon_0 \sum_{i,l} \left[\left(\frac{\partial \epsilon}{\partial t}\, \bar{E}^\delta_{il} + \frac{\partial \varkappa}{\partial t}\, \bar{H}^\delta_{il}\right) + (\epsilon \nabla_{tEoil}\, \bar{E}^\delta_{il} + \varkappa \nabla_{tHoil}\, \bar{H}^\delta_{il}) + \right. \\
&\quad \left. + \left(\frac{\partial (\ln a_{il} + f_{il} - j\varphi_{ai})}{\partial t} + j\omega_0\right) (\epsilon \bar{E}^\delta_{il} + \varkappa \bar{H}^\delta_{il})\right] \\
&\sum_{i,l} \left[\overline{\operatorname{grad}\,(\ln a_{il} + f_{il} - j\varphi_{ai})} \times \bar{E}^\delta_{il} + \nabla_{TEoil}\, \bar{E}^\delta_{il} - j\bar{K}_i \times \bar{E}^\delta_{il}\right] = \\
&\quad = -\mu_0 \sum_{i,l} \left[\left(\frac{\partial \nu}{\partial t}\, \bar{E}^\delta_{il} + \frac{\partial \mu}{\partial t}\, \bar{H}^\delta_{il}\right) + (\nu \nabla_{tEoil}\, \bar{E}^\delta_{il} + \mu \nabla_{tHoil}\, \bar{H}^\delta_{il}) + \right. \\
&\quad \left. + \left(\frac{\partial (\ln a_{il} + f_{il} - j\varphi_{ai})}{\partial t} + j\omega_0\right) (\nu \bar{E}^\delta_{il} + \mu \bar{H}^\delta_{il})\right]
\end{aligned} \tag{44}$$

$$\sum_{i,l} \left[\overline{\text{grad}\,(\ln a_{il} + f_{il} - j\varphi_{ai})(\epsilon \bar{E}^{\delta}_{il} + \varkappa \bar{H}^{\delta}_{il})} + (\nabla_{\epsilon}\, \bar{E}^{\delta}_{il} + \nabla_{\varkappa}\, \bar{H}^{\delta}_{il}) + \right.$$
$$\left. + (\langle \nabla_{\epsilon il}\, \bar{E}^{\delta}_{il} \rangle + \langle \nabla_{\varkappa il}\, \bar{H}^{\delta}_{il} \rangle) - j\bar{K}_i (\epsilon \bar{E}^{\delta}_{il} + \varkappa \bar{H}^{\delta}_{il}) \right] = 0$$

$$\sum_{i,l} \left[\overline{\text{grad}\,(\ln a_{il} + f_{il} - j\varphi_{ai})(\nu \bar{E}^{\delta}_{il} + \mu \bar{H}^{\delta}_{il})} + (\nabla_{\nu}\, \bar{E}^{\delta}_{il} + \nabla_{\mu}\, \bar{H}^{\delta}_{il}) + \right.$$
$$\left. + (\langle \nabla_{\nu il}\, \bar{E}^{\delta}_{il} \rangle + \langle \nabla_{\mu il}\, \bar{H}^{\delta}_{il} \rangle) - j\bar{K}_i (\nu \bar{E}^{\delta}_{il} + \mu \bar{H}^{\delta}_{il}) \right] = 0\,,$$

where

$K_i = \overline{\text{grad}\,\varphi_i}$;

$$\nabla_{THoil} = \begin{bmatrix} 0 & -\dfrac{\partial \ln H_{2oil}}{\partial z} & \dfrac{\partial \ln H_{3oil}}{\partial y} \\ \dfrac{\partial \ln H_{1oi}}{\partial z} & 0 & -\dfrac{\partial \ln H_{3oil}}{\partial x} \\ -\dfrac{\partial \ln H_{1oil}}{\partial y} & \dfrac{\partial \ln H_{2oil}}{\partial x} & 0 \end{bmatrix};$$

∇_{TEoil} is analogous to ∇_{THoil};

$$\nabla_{tHoil} = \begin{bmatrix} \dfrac{\partial \ln H_{1oil}}{\partial t} & 0 & 0 \\ 0 & \dfrac{\partial \ln H_{2oil}}{\partial t} & 0 \\ 0 & 0 & \dfrac{\partial \ln H_{3oil}}{\partial t} \end{bmatrix}$$

∇_{tEoil} is analogous to ∇_{tHoil};
$\nabla_{\epsilon} = \nabla\epsilon$, $\nabla_{\varkappa} = \nabla\varkappa$, $\nabla_{\nu} = \nabla\nu$ and $\nabla_{\mu} = \nabla\mu$;

$$(\nabla_{\epsilon il})_{jk} = \varepsilon_{jk} \frac{\partial \ln E_{oilk}}{\partial x_j}\,;$$

$\nabla_{\varkappa il}$, $\nabla_{\nu il}$ and $\nabla_{\mu il}$ are, according to their meaning, analogous to $\nabla_{\epsilon il}$;

$$\langle \bar{u} \rangle \equiv u_1 + u_2 + u_3.$$

Furthermore, in what follows we shall be making use of the fact that replacing $f_{il} = 0$ in (44) we get an equation for $\bar{F}_{il}$; and $\bar{F}_{il}$ is a solution of this equation because it is a solution of Maxwell's equations.

4.1. *On the characteristics of the medium*

Before setting out to analyse the ways of solving equation (44), we have to briefly mention the parameters ϵ, $\varkappa$, υ and μ, which characterize the medium.

— We assumed from the start [2, 1] that the energy scale giving rise to the parameters of the medium is orders of magnitude larger than the energy belonging to the monochromatic, low-energy-density signal considered by us. Thus, it follows that ϵ, $\varkappa$, υ and μ are independent of the amplitude of the

signal $\bar{F}_0$, i.e. we are dealing with a media for which linear relationships approximately hold. (If non-linear treatment is needed, it should be attempted by the generalization of the investigation presented here. It is possible to expand the medium parameters in a small environment δ_i of the "point" a_{il} since f_{il} and δ_i are small, etc.)

— The linear media — to which the description by (2) is applicable — can be divided into two large classes: of the *strictly linear media*, and of *dispersive media*.

First we shall consider *strictly linear* media for which

$$\frac{\partial \epsilon}{\partial \omega_0} = \frac{\partial \varkappa}{\partial \omega_0} = \frac{\partial \nu}{\partial \omega_0} = \frac{\partial \mu}{\partial \omega_0} = 0 \tag{45}$$

applies, at least in a sufficiently large neighbourhood of the actual value of ω_0. *Then the parameters of the medium will be independent of all the parameters of the signal* in the frequency range considered.

— We shall separately treat the *dispersive* media for which at least one of the characteristics of medium is dependent on ω_0, e.g.

$$\frac{\partial \epsilon}{\partial \omega_0} \neq 0$$

However, in cases like this we can assert — in view of the well-known derivations [4, 6—8, etc.] for the parameters of dispersive media — that from the point of view of equations (44) it would be conceptually wrong to use the expression

$$\epsilon = \epsilon(\omega_0) \tag{46a}$$

For the signal (43) $\epsilon \neq \epsilon(\omega_0)$, but instead we have to carry out the calculation with a new ϵ^*. The symbol *, unless otherwise stated, will not refer to the complex conjugate! Since we can immediately see from (44) that if f_{il} exists then its time and space derivatives exist as well, i.e.

$$f_{il} = f_{il}(\bar{r}, t),$$

it follows that

$$\epsilon^* = \epsilon(\omega_0, f_{il}) \tag{46}$$

has to be taken into account for the calculation.

Because of (46), first we shall treat only the case (45), then in a separate chapter the case (46), including the interpretation of *linearity* for dispersive media.

4.2. *Group velocity in linear media*

Our present task is to solve equation (44) in a strictly linear media in order to determine f_{il}, or rather the velocity of propagation of f_{il}. We shall utilize the fact that $\sum_{i,l} \bar{F}_{il}$ is a solution obtained with the method of inhomogeneous basic modes, i.e. it satisfies the system of equations [1]:

$$\begin{aligned}
&\bar{K}_i \times \bar{H}_{il} = -\omega_0 \varepsilon_0 (\epsilon \bar{E}_{il} + \varkappa \bar{H}_{il}) \\
&\bar{K}_i \times \bar{E}_{il} = \omega_0 \mu_0 (\nu \bar{E}_{il} + \mu \bar{H}_{il}) \\
&\bar{K}_i (\epsilon \bar{E}_{il} + \varkappa \bar{H}_{il}) = 0 \\
&\bar{K}_i (\nu \bar{E}_{il} + \mu \bar{H}_{il}) = 0
\end{aligned} \tag{47}$$

and

$$\begin{aligned}
&\sum_{i,l} [\overline{\operatorname{grad}} (\ln a_{il} - j\varphi_{ai}) \times \bar{H}_{il} + \nabla_{THoil} \bar{H}_{il}] = 0 \\
&\sum_{i,l} [\overline{\operatorname{grad}} (\ln a_{il} - j\varphi_{ai}) \times \bar{E}_{il} + \nabla_{TEoil} \bar{E}_{il}] = 0 \\
&\sum_{i,l} [\overline{\operatorname{grad}} (\ln a_{il} - j\varphi_{ai})(\epsilon \bar{E}_{il} + \varkappa \bar{H}_{il}) + (\nabla_\epsilon \bar{E}_{il} + \nabla_\varkappa \bar{H}_{il}) + \\
&\qquad + (\langle \nabla_{\epsilon il} \bar{E}_{il} \rangle + \langle \nabla_{\varkappa il} \bar{H}_{il} \rangle)] = 0 \\
&\sum_{i,l} [\overline{\operatorname{grad}} (\ln a_{il} - j\varphi_{ai})(\nu \bar{E}_{il} + \mu \bar{H}_{il}) + (\nabla_\nu \bar{E}_{il} + \nabla_\mu \bar{H}_{il}) + \\
&\qquad + (\langle \nabla_{\nu il} \bar{E}_{il} \rangle + \langle \nabla_{\mu il} \bar{H}_{il} \rangle)] = 0
\end{aligned} \tag{48}$$

separately. We shall also use all the previously mentioned conditions for the medium (strict linearity, no time variation, it is not moving, etc.). We shall exploit that (47) is satisfied by the individual modes one by one. We also know that (4) is a monochromatic, stationary solution.

Using all this (44) can be simplified and rewritten in the following way:

$$\begin{aligned}
&\sum_{i,l} \{f_{il} [\overline{\operatorname{grad}} (\ln a_{il} - j\varphi_{ai}) \times \bar{H}_{il} + \nabla_{THoil} \bar{H}_{il}] + \overline{\operatorname{grad}} f_{il} \times (1 + f_{il}) \bar{H}_{il}\} = \\
&\qquad = \varepsilon_0 \sum_{i,l} (1 + f_{il}) \frac{\partial f_{il}}{\partial t} (\epsilon \bar{E}_{il} + \varkappa \bar{H}_{il}) \\
&\sum_{i,l} \{f_{il} [\overline{\operatorname{grad}} (\ln a_{il} - j\varphi_{ai}) \times \bar{E}_{il} + \nabla_{TEoil} \bar{E}_{il}] + \overline{\operatorname{grad}} f_{il} \times (1 + f_{il}) \bar{E}_{il}\} = \\
&\qquad = -\mu_0 \sum_{i,l} (1 + f_{il}) \frac{\partial f_{il}}{\partial t} (\nu \bar{E}_{il} + \mu \bar{H}_{il}) \\
&\sum_{i,l} \{f_{il} [\overline{\operatorname{grad}} (\ln a_{il} - j\varphi_{ai})(\epsilon \bar{E}_{il} + \varkappa \bar{H}_{il}) + (\nabla_\epsilon \bar{E}_{il} + \nabla_\varkappa \bar{H}_{il}) + \\
&\qquad + (\langle \nabla_{\epsilon il} \bar{E}_{il} \rangle + \langle \nabla_{\varkappa il} \bar{H}_{il} \rangle)] + (1 + f_{il}) \overline{\operatorname{grad}} f_{il} (\epsilon \bar{E}_{il} + \varkappa \bar{H}_{il})\} = 0
\end{aligned} \tag{49}$$

$$\sum_{i,l} \{f_{il}\,[\overline{\mathrm{grad}\,(\ln a_{il} - j\varphi_{ai})}(\nu\bar{E}_{il} + \mu\bar{H}_{il}) + (\nabla_\nu \bar{E}_{il} + \nabla_\mu \bar{H}_{il}) + \\ + (\langle\nabla_{\nu il}\bar{E}_{il}\rangle + \langle\nabla_{\mu il}\bar{H}_{il}\rangle)] + (1 + f_{il})\,\overline{\mathrm{grad}\,f_{il}}(\nu\bar{E}_{il} + \mu\bar{H}_{il})\} = 0 \qquad (49)$$

We can again take into account (47), since

$$\epsilon\bar{E}_{il} + \varkappa\bar{H}_{il} = -\frac{1}{\varepsilon_0\omega_0}\,\bar{K}_i \times \bar{H}_{il}$$

$$\nu\bar{E}_{il} + \mu\bar{H}_{il} = \frac{1}{\mu_0\omega_0}\,\bar{K}_i \times \bar{E}_{il}$$

On the basis of these the (49) equations containing curl and div can be rewritten and f_{i1} obtained in a simpler way. However, even the present form can yield many interesting informations. For instance, we can immediately see that if $\partial f_{il}/\partial t \equiv 0$ or if $\overline{\mathrm{grad}\,f_{il}} \equiv 0$, we essentially get back solution (4).

Now *the group velocity — derived*, in such a way, *directly from Maxwell's equations* — will be given by

$$|v_{gil}| = \left|\frac{\partial f_{il}}{\partial t}\right| \Big/ |\overline{\mathrm{grad}\,f_{il}}| \qquad (50)$$

since here we perturbed a_{il}. (Interesting results can be rapidly obtained, if the inhomogeneity of ϵ, etc. is chosen in such a way that we are led to well-known types of differential equations [18].)

Since this method of analysis is as still unaccustomed, in the following let us consider the *concrete* results of a few simpler, but important cases.

4.3. *The group velocity in a linear, homogeneous medium*

Since the medium is homogeneous

$$\nabla_\varepsilon = \nabla_\varkappa = \nabla_\nu = \nabla_\mu = 0$$

and in a homogeneous medium the basic signal (4) is stationary, too, since it is monochromatic, etc. [1]. (The signal is stationary, i.e. $\nabla_{tEoil} = 0$, etc. hold; from which $\nabla_{tHoil} = 0$, etc. follow in this case.) Thus, after a few vector-algebraic transformations, we get

$$\sum_{i,l} (1 + f_{il})\,\overline{\mathrm{grad}\,f_{il}} \times \bar{H}_{il} = -\frac{1}{\omega_0}\sum_{i,l}(1 + f_{il})\,\frac{\partial f_{il}}{\partial t}\,\bar{K}_i \times \bar{H}_{il}$$

$$\sum_{i,l} (1 + f_{il})\,\overline{\mathrm{grad}\,f_{il}} \times \bar{E}_{il} = -\frac{1}{\omega_0}\sum_{i,l}(1 + f_{il})\,\frac{\partial f_{il}}{\partial t}\,\bar{K}_i \times \bar{E}_{il} \qquad (51)$$

$$\sum_{i,l} [(1 + f_{il})\,\overline{\mathrm{grad}\,f_{il}} \times \bar{H}_{il}]\,\bar{K}_i = 0$$

$$\sum_{i,l} [(1 + f_{il})\,\overline{\mathrm{grad}\,f_{il}} \times \bar{E}_{il}]\,\bar{K}_i = 0$$

for an arbitrary *bianisotropic* case! Furthermore, we know that $f_{il} \ll 1$. Hence (51) will very accurately satisfy the following equations

$$\begin{aligned}
&\sum_{i,l} \overline{\operatorname{grad} f_{il}} \times \bar{H}_{il} = -\sum_{i,l} \frac{\partial f_{il}}{\partial t} \frac{\bar{K}_i}{\omega_0} \times \bar{H}_{il} \\
&\sum_{i,l} \overline{\operatorname{grad} f_{il}} \times \bar{E}_{il} = \sum_{i,l} \frac{\partial f_{il}}{\partial t} \frac{\bar{K}_i}{\omega_0} \times \bar{E}_{il} \\
&\sum_{i,l} (\overline{\operatorname{grad} f_{il}} \times \bar{H}_{il}) \bar{K}_i = 0 \\
&\sum_{i,l} (\overline{\operatorname{grad} f_{il}} \times \bar{E}_{il}) \bar{K}_i = 0
\end{aligned} \tag{52}$$

Since $(\bar{E}_{il}, \bar{H}_{il})$ are known existing, non-trivial solutions of Maxwell's equations we know [1] that, for instance

$$\bar{E}_{il} = -\frac{1}{\varepsilon_0 \omega_0} \epsilon^{-1} (\mathbf{K}_i + \omega_0 \varepsilon_0 \varkappa) \bar{H}_{il} = \alpha_{il} \bar{H}_{il}$$

where

$$\mathbf{K}_i \bar{u} = \bar{K}_i \times \bar{u} \quad \text{and} \quad \alpha_i \neq 1. \text{ So } \bar{E}_{il} \nparallel \bar{H}_{il}, \text{ etc.}$$

With this it has become possible to determine v_g in any concrete case. (We cannot go further in the general formulation since the "coupling" between the inhomogeneous basic modes depends on the particular conditions prevalent in a concrete problem.)

Taking into account the boundary conditions as well, we obtain *the complete wave picture, including the perturbation*, and from this in the given — homogeneous — case (ranging from propagation in free space to wave guides) the velocity of the propagation of energy in the monochromatic signal under consideration.

Special cases:

a) In the homogeneous case the inhomogeneous basic modes usually mean orthogonal, *independently propagating modes* (see, for example [7]). Assuming this, we obtain from (52) for the independently propagating modes, and for the single-mode signal ($i = 1$) that because of

$$\bar{E}_{il} \nparallel \bar{H}_{il}, \ \overline{\operatorname{grad} f_{il}} \parallel \bar{K}_i \,, \tag{53}$$

and the equations are the same for both values of l, since $\bar{K}_i$ is the same, independently of l. So $f_{iv} \equiv f_{ik} \equiv f_i$, or $f_{ik} = 0$.

From this we obtain

$$\overline{\text{grad}}\, f_i + \frac{\bar{K}_i}{\omega_0} \frac{\partial f_i}{\partial t} = 0 \tag{54}$$

Consequently,

$$\frac{\overline{\text{grad}}\, f_i}{\left(-\frac{\partial f_i}{\partial t}\right)} = \frac{\bar{K}_i}{\omega_0}, \quad \text{and} \quad \frac{|\overline{\text{grad}}\, f_i|}{\left(\frac{\partial f_i}{\partial t}\right)} = \frac{K_i}{\omega_0}$$

i.e., in this case

$$v_{gi} \equiv v_{fi} \quad \text{and} \quad \bar{v}_{gi} \parallel \bar{v}_{fi} \tag{55}$$

where

$$v_{fi} = \frac{\omega_0}{K_i}, \quad \text{and} \quad \bar{v}_{fi} \parallel \bar{K}_i \ .$$

b) For a single, separately propagating mode ($i \equiv 1$) (55) will result without any further conditions needed.

Statement.

The phase and group velocity *are the same* in a monochromatic plane wave even in a bianisotropic case!

4.4. *A comment on propagation in moving media*

The statement closing section 4.3 is of basic, conceptual relevance in investigations concerning the propagation of electromagnetic waves in moving media.

It is well known, and not a hitherto solved, problem that the phase velocity of a monochromatic plane wave propagating in a *homogeneous, moving* medium does *not follow*, even in the simplest possible case ($\boldsymbol{\epsilon} = \varepsilon \mathbf{l}$, $\boldsymbol{\varkappa} = \boldsymbol{\upsilon} = \mathbf{0}$, $\mu = 1$) *Einstein's relationship for the transformation of velocity* [9—12].

To absolve this discrepancy, numerous attempts have been made based on the analysis of energy-momentum tensor belonging to this specific physical phenomenon, according to which *in this case the phase velocity is not equal to the group velocity*, $v_g \neq v_f$ [12—14].

In other investigations [15—17], however, the treatment starts out from Maxwell's equations and *bianisotropic* medium characteristics, formally including a "velocity parameter" as well, are introduced; the moving medium is considered as equivalent to a "standing" bianisotropic medium. For example:

If in a system (K') co-moving with the medium in the direction $+x$ with velocity v

$$\bar{D}' = \varepsilon \bar{E}' \quad \text{and} \quad \bar{B}' = \bar{H}'$$

then in the laboratory system (K)

$$\bar{D} = \varepsilon \mathbf{A}\bar{E} + \mathbf{B}\bar{H} \quad \text{and} \quad \bar{B} = \mathbf{A}\bar{H} - \mathbf{B}\bar{E} \tag{56}$$

where

$$\mathbf{A} = \begin{bmatrix} 1 & 0 & 0 \\ 0 & A & 0 \\ 0 & 0 & A \end{bmatrix}, \quad \mathbf{B} = \begin{bmatrix} 0 & 0 & 0 \\ 0 & 0 & -B \\ 0 & B & 0 \end{bmatrix};$$

$$A = \frac{1 - v^2/c^2}{1 - \varepsilon v^2/c^2}; \qquad B = \frac{v}{c} \frac{\varepsilon - 1}{1 - \varepsilon v^2/c^2},$$

and C is the velocity of light in vacuum. At the same time the relationships $\bar{E}$ ($\bar{E}'$), etc., formally disappear from the treatment. In this way not only the Doppler-effect, etc. are caused to disappear — or, rather, their inclusion will be qualified as arbitrary, as we have pointed out earlier [5] — but also, *by necessity, a discrepancy* with the investigations based on the energy-momentum tensor *will arise.*

The reason for this is that the bianisotropic medium parameters, obtained according to (56), or in an analogous manner in other cases, are *independent* of the signal parameters, giving a *strictly linear, bianisotropic relationship.*

Then from (55) it surely follows that $v_g \equiv v_f$!

Statement:

In the case of moving media the present investigation makes the already known problem more emphatic arising because of the transformation properties of the phase and group velocities. Its solution is of basic importance, and cannot be achieved without taking into account the — on the basis of the foregoing obviously geometrical — peculiarities of the wave pattern. (The dissolution of this discrepancy will be presented in another paper.)

4.5. *Addenda*

a) There is another way, based on (44), of describing the propagation of an infinitesimal perturbation of a signal propagating in a homogeneous medium, in the case of a single monochromatic plane wave (a simple propagating mode).

Let, for example, ε and μ be the parameters of the medium. Then the propagation of an infinitesimal perturbation across the signal can be obtained as follows:

The basic solution satisfies the dispersion equation

$$K^2 = k_0^2 \varepsilon \mu$$

where $k_0^2 = \omega_0^2 \varepsilon_0 \mu_0$. Consequently, the group velocity which refers to the propagation of some infinitesimal perturbation of the signal, can be obtained from the following equation:

$$\begin{aligned} \nabla_{TH0}\bar{H} &= \varepsilon_0 \varepsilon \nabla_{tE0}\bar{E} \\ \nabla_{TE0}\bar{E} &= -\mu_0 \mu \nabla_{tH0}\bar{H} \\ \langle \nabla_\mu \bar{H} \rangle &= 0 \\ \langle \nabla_\varepsilon \bar{E} \rangle &= 0 \end{aligned} \tag{57}$$

paying due attention to the boundary conditions! (For other cases similar equations can be written down.) Hence, for the propagation in direction x, for example the equation

$$\frac{\partial H_0}{\partial x} = -k_0 \sqrt{\varepsilon\mu}\, \frac{\partial H_0}{\partial t} \tag{58}$$

describes the propagation of the perturbation, i.e. — naturally — we arrived at the special case of (54). For the investigation of fluctuations of the polarization, etc., (57) is often useful.

b) On the basis of the foregoing the investigations can be extended. It is expedient, for example, to examine the group velocity in a few inhomogeneous cases describable by periodic or power functions, and also for a few important boundary conditions (wave guides). It is also important to keep in mind that the propagation of the infinitesimal perturbation across the entire interference pattern is the *resultant* of propagations in the inhomogeneous basic modes. So determining the propagation of infinitesimal perturbations in the individual inhomogeneous basic modes is not the *goal*, it is only a *useful means*.

5. Group velocity in dispersive media

Also in this case we shall start out from equations (44). However, we shall take into account that the medium parameters in (44) are given by (46), while they figure with their "basic values" (46a) in equations (47) and (48)!

Since the present treatment is, from many points of view, basically new, for the sake of a more detailed presentation, for clarity, and in order to facilitate a comparison of the final results, we shall restrict ourselves to the study of the case with a *single propagating mode*. Besides we know that, analogously to what we have seen in section 4, the results can be generalized.

Making use of the method and of the results of the present investigation, we are able to tackle such problems as the build-up of the *wave front* in dis-

persive media, the process of the *formation of the beam*, etc. These equations are of basic importance in many cases (whistler propagation path studies, laser-beam propagation, etc.).

5.1. *The equations in the dispersive case*

According to the foregoing, after a few expedient transformations our equations will take the following form:

$$\sum_{i,l}\{f_{il}[\overline{\mathrm{grad}}\,(\ln a_{il}-j\varphi_{ai})\times\bar{H}_{il}+\nabla_{THoil}\bar{H}_{il}]+[\overline{\mathrm{grad}}\,f_{il}-j\bar{K}_i]\times$$
$$\times\bar{H}_{il}(1+f_{il})\}=\varepsilon_0\sum_{i,l}(1+f_{il})\left[\left(\frac{\partial\epsilon^*}{\partial t}\bar{E}_{il}+\frac{\partial\varkappa^*}{\partial t}\bar{H}_{il}\right)+\right.$$
$$\left.+\left(\frac{\partial f_{il}}{\partial t}+j\omega_0\right)(\epsilon^*\bar{E}_{il}+\varkappa^*\bar{H}_{il})\right]$$

$$\sum_{i,l}\{f_{il}[\overline{\mathrm{grad}}\,(\ln a_{il}-j\varphi_{ai})\times\bar{E}_{il}+\nabla_{TEoil}\bar{E}_{il}]+[\overline{\mathrm{grad}}\,f_{il}-j\bar{K}_i]\times$$
$$\times\bar{E}_{il}(1+f_{il})\}=-\mu_0\sum_{i,l}(1+f_{il})\left[\left(\frac{\partial\nu^*}{\partial t}\bar{E}_{il}+\frac{\partial\mu^*}{\partial t}\bar{H}_{il}\right)+\right.$$
$$\left.+\left(\frac{\partial f_{il}}{\partial t}+j\omega_0\right)(\nu^*\bar{E}_{il}+\mu^*\bar{H}_{il})\right] \tag{59}$$

$$\sum_{i,l}\{[\overline{\mathrm{grad}}\,(\ln a_{il}-j\varphi_{ai})+\overline{\mathrm{grad}}\,f_{il}-j\bar{K}_i](\epsilon^*\bar{E}_{il}+\varkappa^*\bar{H}_{il})(1+f_{il})+$$
$$+[(\nabla_{\varepsilon *}\bar{E}_{il}+\nabla_{\varkappa *}\bar{H}_{il})+(\langle\nabla^*_{\varepsilon il}\bar{E}_{il}\rangle+\langle\nabla^*_{\varkappa il}\bar{H}_{il}\rangle)](1+f_{il})\}=0$$

$$\sum_{i,l}\{[\overline{\mathrm{grad}}\,(\ln a_{il}-j\varphi_{ai})+\overline{\mathrm{grad}}\,f_{il}-j\bar{K}_i[\,](\nu^*\bar{E}_{il}+\mu^*\bar{H}_{il})(1+f_{il})+$$
$$+[(\nabla_{\nu *}\bar{E}_{il}+\nabla_{\mu *}\bar{H}_{il})+(\langle\nabla^*_{\nu il}\bar{E}_{il}\rangle+\langle\nabla^*_{\mu il}\bar{H}_{il}\rangle)](1+f_{il})\}=0$$

where the meaning of * is explained in (46). We can examine the group velocity in those cases which are interesting or important in practice if we know the * medium parameters to be used in the respective cases, based on Eqs (59).

a) In what follows we will be interested in the single-mode (homogeneous) case. Then from (59) it follows that

$$(\overline{\mathrm{grad}}\,f-j\bar{K})\times\bar{H}=\varepsilon_0\left[\left(\frac{\partial\epsilon^*}{\partial t}\bar{E}+\frac{\partial\varkappa^*}{\partial t}\bar{H}\right)+\left(\frac{\partial f}{\partial t}+j\omega_0\right)(\epsilon^*\bar{E}+\varkappa^*\bar{H})\right]$$

$$(\overline{\mathrm{grad}}\,f-j\bar{K})\times\bar{E}=-\mu_0\left[\left(\frac{\partial\nu^*}{\partial t}\bar{E}+\frac{\partial\mu^*}{\partial t}\bar{H}\right)+\left(\frac{\partial f}{\partial t}+j\omega_0\right)(\nu^*\bar{E}+\mu^*\bar{H})\right]$$

$$[(\overline{\mathrm{grad}}\,f-j\bar{K})+\overline{\mathrm{grad}}\,(\ln a-j\varphi_a)](\epsilon^*\bar{E}+\varkappa^*\bar{H})=0 \tag{60}$$

$$[(\overline{\mathrm{grad}}\,f-j\bar{K})+\overline{\mathrm{grad}}\,(\ln a-j\varphi_a)](\nu^*\bar{E}+\mu^*\bar{H})=0$$

We can see that first of all the analysis of the * medium characteristics has to be performed since we cannot go further without their knowledge.

Assuming that the relationships $\partial\epsilon^*/\partial t = 0$, etc., hold, and considering that for a stationary, homogeneous solution $\overline{\text{grad}}\,(\ln a - j\varphi_a) = 0$, it becomes apparent that the second two equations are automatically satisfied. So

$$\begin{aligned}(\overline{\text{grad}} f - j\bar{K}) \times \bar{H} &= \varepsilon_0 \left(\frac{\partial f}{\partial t} + j\omega_0\right)(\epsilon^* \bar{E} + \varkappa^* \bar{H}) \\ (\overline{\text{grad}} f - j\bar{K}) \times \bar{E} &= -\mu_0 \left(\frac{\partial f}{\partial t} + j\omega_0\right)(\nu^* \bar{E} + \mu^* \bar{H})\end{aligned} \tag{61}$$

Let us further have

$$\begin{aligned}\omega_f &= f' + j\omega_0\,; \\ f' &= \partial f / \partial t; \\ \mathbf{K}_f \bar{u} &= (\overline{\text{grad}} f - j\bar{K}) \times \bar{u} = (\mathfrak{F} - j\mathbf{K})\bar{u}\,.\end{aligned} \tag{62}$$

Then (61) can be transformed in the usual way [5], and expanded according to $\bar{E}$ or $\bar{H}$. The expansions for $\bar{E}$ is as follows

$$[(\mathbf{K}_f - \varepsilon_0 \omega_f \varkappa^*)\mu^{*-1}(\mathbf{K}_f + \mu_0 \omega_f \nu^*) + \varepsilon_0 \mu_0 \omega_f^2 \epsilon^*]\bar{E} = 0 \tag{63}$$

The formula for $\bar{H}$ is equivalent and does not yield anything new [5].

It is *important* to notice, however, that no dispersion equation corresponds to (63). Though $\bar{E}$ and $\bar{H}$ are not equal to zero, they are solutions corresponding to the eigenvalue of a different dispersion equation. So for us $\bar{E}$ is given, and any statement about the tensor in [ ] should be made by keeping this in mind.

For this reason we shall further rewrite (63) and take into account what are the original dispersion equations of which $\bar{E}$ (and analogously $\bar{H}$) is the solution. Further we take into account that f and the variations of f are very small quantities, so their products, being small in the second order, can be neglected. Then:

$$\begin{aligned}\{j[(\mathbf{K} + \omega_0 \varepsilon_0 \varkappa^*)\mu^{*-1}(\mathfrak{F} + \mu_0 f' \nu^*) - k_0 \sqrt{\varepsilon_0 \mu_0}\, f' \epsilon^*] + \\ + j[(\mathfrak{F} - \varepsilon_0 f' \varkappa^*)\mu^{*-1}(\mathbf{K} - \omega_0 \mu_0 \nu^*) - k_0 \sqrt{\varepsilon_0 \mu_0}\, f' \epsilon^*] + \\ + [(\mathbf{K} + \omega_0 \varepsilon_0 \varkappa^*)\mu^{*-1}(\mathbf{K} - \omega_0 \mu_0 \nu^*) + k_0^2 \epsilon^*]\}\bar{E} = 0\end{aligned} \tag{64}$$

With this equation, just as it happened at the previous steps, we have arrived at a form the meaningful discussion of which requires the accurate knowledge of the medium characteristics denoted by symbols with *.

b) Before coming to this point, as a check, let us regard the solution of (64) in the *non-dispersive* case. Then $\epsilon^* = \epsilon$, etc. Furthermore, let us multiply the equation with $\frac{\omega_0}{-f'}$, which is *not equal to either zero or* ∞. Then

$$\left[(\mathbf{K} + \omega_0 \varepsilon_0 \varkappa)\mu^{-1}\left(\omega_0 \frac{\mathfrak{F}}{-f'} - \omega_0 \mu_0 \nu\right) + \right.$$
$$\left. + \left(\omega_0 \frac{\mathfrak{F}}{-f'} + \omega_0 \varepsilon_0 \varkappa\right)\mu^{-1}(\mathbf{K} - \omega_0 \mu_0 \nu) + 2 k_0^2 \epsilon\right] \bar{E} = 0 \tag{65}$$

Knowing that the $\bar{E}$ is the previous solution which belongs to equation [5]

$$\left[(\mathbf{K} + \omega_0 \varepsilon_0 \varkappa)\mu^{-1}(\mathbf{K} - \omega_0 \mu_0 \nu) + k_0^2 \epsilon\right] \bar{E} = 0$$

with the resulting eigenvalues $\bar{K}$ and φ, (65) will be satisfied for any $\bar{E}$ only if

$$\omega_0 \left(\frac{\mathfrak{F}}{-f'}\right) = \mathbf{K} \tag{66}$$

a statement identical to (54).

5.2. *Perturbed medium characteristics*

We shall not attempt a general discussion in this paper. We will rather choose three examples which seem to us either suggestive or important.

a) Simple approximations for the *neutral gas* and *for the isotropic, ionized gas*:

— A simple approximation for the neutral gas:

As is usual, we assume that $\varkappa = \upsilon = \mathbf{0}$, $\mu = \mathbf{1}$, and $\epsilon = \varepsilon \mathbf{1}$, where $\varepsilon = n^2$ and n is the refractive index. In this case the gas is usually not considered dispersive. Hence

$$\frac{\partial \varepsilon}{\partial \omega_0} \equiv 0$$

and as a consequence

$$\varepsilon^* \equiv \varepsilon \,. \tag{67}$$

— A simple approximation for the isotropic, ionized gas:

The actual behaviour of the medium parameters will be disregarded here, too; instead, taking over the known results [6, etc.] we assume that $\varkappa = \upsilon = \mathbf{0}$, $\mu = \mathbf{1}$, and $\epsilon = \varepsilon \mathbf{1}$, where

$$\varepsilon \leq 1, \text{ i.e. } \varepsilon = 1 - e$$

Since $e \cong \omega_p^2/\omega_0^2$, where ω_p is the plasma frequency (cf. [4, 6] etc.), (62) is known as well:

$$\varepsilon^* = 1 - \frac{\omega_p^2}{(\omega_0 - jf')^2} \cong \varepsilon - j2\,e\,\frac{f'}{\omega_0}\,. \tag{68}$$

— These simple approximations only serve the purpose of comparison. An accurate analysis of the medium characteristics will reveal more interesting relationships.

b) An accurate analysis for the *neutral gas*:

It is known that for a simple neutral gas $\varkappa = \upsilon = 0$, $\mu = 1$. In order to obtain the permittivity we start out from the equation of motion for the polarization. It is well known that

$$m\frac{\mathrm{d}\bar{v}}{\mathrm{d}t} = -a\bar{r} + q\bar{E}$$

where m is the mass of the particle, $\bar{v}$ the velocity, and a is the constant of the elastic restoring force (we consider only small displacements), and q is the charge. Thus,

$$\frac{\mathrm{d}^2\bar{r}}{\mathrm{d}t^2} + \frac{a}{m}\bar{r} = \frac{q}{m}\bar{E} \tag{69}$$

and we are interested only in solutions stationary in time. Putting in $\bar{E} = \bar{E}_0 e^{j\omega_0 t}$

$$\bar{r} = \bar{A}e^{j\sqrt{\frac{a}{m}}\,t} + \frac{q}{m}\bar{E}_0\frac{1}{\frac{a}{m} - \omega_0^2}e^{j\omega_0 t}$$

where (since the state is stationary) it is justified to accept the solution $\bar{A} \equiv 0$, as it is usually done. Hence, since $\bar{D} = \frac{1}{\varepsilon_0}\int^t \bar{J}\,\mathrm{d}t + \bar{E}$ [5], it follows that

$$\bar{D} = \left[1 + \frac{1}{\varepsilon_0}\,\frac{q^2 N}{a - m\omega_0^2}\right]\bar{E}_0\,e^{j\omega_0 t}$$

where $\bar{J}$ is the current density, and N the particle density. Consequently,

$$\varepsilon = 1 + \frac{q^2 N}{\varepsilon_0 m}\,\frac{1}{\frac{a}{m} - \omega_0^2}\,. \tag{70}$$

An important remark: as long as $\omega_0^2 \ll a/m$, we can write

$$\varepsilon \cong 1 + \frac{q^2 N}{\varepsilon_0 a} = \text{constant} . \tag{70a}$$

However, in the neighbourhood of and above the resonance, the medium will be dispersive. Then if, for instance, $\omega_0^2 \gg a/m$, we have

$$\varepsilon \cong 1 - \frac{q^2 N}{\varepsilon_0 m} \frac{1}{\omega_0^2} . \tag{70b}$$

For this reason, in the *general* case in a neutral gas $\varepsilon^* \neq \varepsilon$!

When determining the perturbed ε^*, we carry out the calculation with the excitation field $\bar{E}^* = (1+f)\bar{E}_0 e^{j\omega_0 t}$. We shall seek for the solution of (69) in the form suggested by the equations (61) and (62), i.e. in $\bar{r}^*$ we replace

$$\bar{A} = 0 \quad \text{and} \quad \omega_0 \to \omega_0^* = \omega_0 \left(1 + \frac{f'}{j\omega_0}\right).$$

One can verify that a stationary solution of the equation

$$\frac{\mathrm{d}^2 \bar{r}^*}{\mathrm{d}t^2} + \frac{a}{m} \bar{r}^* = \frac{q}{m} \bar{E}^*$$

is

$$\bar{r}^* = \frac{q}{m} \frac{(1+f)\,\bar{E}_0}{\dfrac{a}{m} - \omega_0^2 \left(1 + \dfrac{f'}{j\omega_0}\right)^2} e^{j\omega_0 t}$$

provided

$$\begin{aligned} \frac{\partial \omega_0^*}{\partial t} &= 0 , \\ \frac{\partial \omega_0^*}{\partial t} &= -jf'' \cong 0 \end{aligned} \tag{71}$$

according to the assumptions made earlier. (Quantities that are small in second order are neglected here.)

So we find that linearity in the dispersive case (in the given example) does not mean a *complete* lack of dependence on the parameters of the signal, but rather, *besides the dependence* on the frequency (ω_0^*), understood in a general sense, the fulfilment of the equation (71)! In such a case the dispersive, neutral gas *is still linear*.

Thus,

$$\varepsilon^* = 1 + \frac{q^2 N}{\varepsilon_0 m} \frac{1}{\frac{a}{m} - \omega_0^2 \left(1 + \frac{f'}{j\omega_0}\right)^2} \tag{72}$$

Making use of (70) and (72) we are going to analyse the behaviour of v_g in a neutral gas.

An important remark: In a more accurate investigation we *cannot* neglect *either* the internal losses, *or* the effect of the many components of the gas, *neither can we* employ (at least without further justification — for such an analysis see the last remark of 3.1) the condition $\bar{A} = 0$.

c) The analysis of the *anisotropic plasma*:

We know that in the anisotropic plasma $\varkappa = \upsilon = \mathbf{0}$, and $\mu = \mathbf{1}$, and that the permittivity ϵ behaves as in [6, 7]. Furthermore we have

$$\bar{D} = \epsilon \bar{E} = \frac{1}{\varepsilon_0} \int^t \bar{J}\, \mathrm{d}t + \bar{E} = \frac{1}{\varepsilon_0} \int^t \sigma \bar{E}\, \mathrm{d}t + \bar{E}$$

where σ is the conductivity tensor [5].

— The non-perturbed permittivity:

In the usual way [6, 7], in a tempered plasma, neglecting the collision terms, and taking into account that the mass of the positive particles is orders of magnitude larger than that of the negative particles (electrons): $m_+ \gg m_-$, and that the magnetic field causing the anisotropy can be taken as constant when compared to the signal, i.e.

$$\frac{\partial \bar{B}_0}{\partial t} \cong 0 \ll \frac{\partial \bar{F}}{\partial t}$$

then the equation of motion which in this simple case has to be written down for the electrons only, becomes

$$m \frac{\mathrm{d}\bar{v}}{\mathrm{d}t} = q(\bar{E} + \bar{v} \times \bar{B}_0)$$

where $\bar{E} = \bar{E}_0 e^{j\omega_0 t}$ and we are looking for *stationary solutions only*. Therefore, $\bar{v} = \bar{v}_0 e^{j\omega_0 t}$, $\mathrm{d}\bar{v}/\mathrm{d}t = j\omega_0 \bar{v}$ is assumed. (The concluding remark of 5.2b applies here, too.) Let us further have

$$-\frac{q}{m} \bar{B}_0 \times \bar{v} = \bar{\omega}_b \times \bar{v} = \Omega_B \bar{v}$$

So,

$$(j\omega_0 \mathbf{1} - \mathbf{\Omega}_B)\bar{v} = \frac{q}{m}\bar{E}$$

and

$$\bar{J} = \frac{q^2 N}{m}(j\omega_0 \mathbf{1} - \mathbf{\Omega}_B)^{-1}\bar{E} = qN\bar{v}.$$

The co-ordinate system is chosen as it most frequently is [2–8] done in the literature: $\bar{B}_0(0, 0, B_0)$. Then

$$\bar{J} = \frac{q^2 N}{m}\begin{bmatrix} j\omega_0 & -\omega_b & 0 \\ \omega_b & j\omega_0 & 0 \\ 0 & 0 & j\omega_0 \end{bmatrix}^{-1}\bar{E} = \frac{q^2 N}{m}\mathbf{I}^{-1}\bar{E}. \tag{73}$$

Carrying out the expansion of (73), and taking into account on the basis of the foregoing that

$$\varepsilon_0 \frac{\partial \bar{D}}{\partial t} = \bar{J} + j\omega_0\varepsilon_0\bar{E} = \varepsilon_0 \frac{\partial \boldsymbol{\epsilon}\bar{E}}{\partial t}$$

we obtain that

$$\bar{J} + j\omega_0\varepsilon_0\bar{E} = j\omega_0\varepsilon_0\boldsymbol{\epsilon}\bar{E} = \left| j\omega_0\varepsilon_0 \begin{bmatrix} \varepsilon_\perp & -j\varepsilon_x & 0 \\ j\varepsilon_x & \varepsilon_\perp & 0 \\ 0 & 0 & \varepsilon_{||} \end{bmatrix}\bar{E} \right. \tag{74}$$

where under the conditions imposed

$$\varepsilon_\perp = 1 - \frac{\alpha^2}{1-\beta^2}, \qquad \alpha^2 = \frac{\omega_p^2}{\omega_0^2} = \frac{q^2 N}{\varepsilon_0 m}\frac{1}{\omega_0^2},$$

$$\varepsilon_{||} = 1 - \alpha^2, \qquad \beta = \frac{\omega_b}{\omega_0} = \frac{qB_0}{m\omega_0},$$

$$\varepsilon_x = \frac{\alpha^2\beta}{1-\beta^2}.$$

We can see that $\boldsymbol{\epsilon} = \boldsymbol{\epsilon}(\omega_0)$, the medium is anisotropic and dispersive.

— The perturbed permittivity:

We follow a procedure completely analogous to the previous one, now for the case of the excitation $\bar{E}^* = (1+f)\bar{E}_0 e^{j\omega_0 t}$. The equation to be solved is then

$$\left(\frac{\mathrm{d}}{\mathrm{d}t}\mathbf{1} - \mathbf{\Omega}_B\right)\bar{v}^* = \frac{q}{m}\bar{E}^* \tag{75}$$

Let us take into account that

$$\frac{\mathrm{d}\bar{E}^*}{\mathrm{d}t} \simeq j\omega_0\left(1 + \frac{f'}{j\omega_0}\right)\bar{E}^* = j\omega_0^*\bar{E}^*$$

and also some of the partial results for the non-perturbed case. On this basis let us *seek for the solution with the operator change*

$$\frac{\mathrm{d}}{\mathrm{d}t} \to j\omega_0^* \tag{76}$$

i.e., with the assumption $\bar{v}^* = \bar{v}_0^* e^{j\omega_0 t}$ being aware of the fact that $\bar{v}^*$ will not be a constant, just as $(1+f)\bar{E}_0$. This can be done if the equation

$$\left(\frac{\mathrm{d}}{\mathrm{d}t}\,\mathbf{1} - \mathbf{\Omega}_B\right)\bar{v}^* = \frac{q}{m}(1+f)\bar{E}_0 e^{j\omega_0 t} \tag{77}$$

is satisfied, with $\bar{v}_0^* = \dfrac{q}{m}(j\omega_0^*\mathbf{1} - \mathbf{\Omega}_B)^{-1}(1+f)\bar{E}_0$. Hence

$$\mathbf{I}^{*-1} = \frac{1}{j\omega_0^*(\omega_b^2 - \omega_0^{*2})}\begin{bmatrix} -\omega_0^{*2} & -j\omega_0^*\omega_b & 0 \\ j\omega_0^*\omega_b & -\omega_0^{*2} & 0 \\ 0 & 0 & \omega_b^2 - \omega_0^{*2} \end{bmatrix}. \tag{78}$$

Making use of these we can check if

$$\bar{v}^* = \frac{q}{m}\mathbf{I}^{*-1}(1+f)\,\bar{E}_0\,e^{j\omega_0 t} \tag{79}$$

is a solution of the original equation (75). After replacing and expanding

$$\frac{\partial \mathbf{I}^{*-1}}{\partial t} + (j\omega_0^*\,\mathbf{1} - \mathbf{\Omega}_B)\mathbf{I}^{*-1} = \mathbf{1} \tag{80}$$

one can see from (78) that in $\mathbf{I}^{*-1}$ the only time-dependent quantity is ω_0^*, and from (71), in accordance with our previous assumptions, $\partial\omega_0^*/\partial t \cong 0$. Remember that among the initial conditions of the present analysis we also had $f \ll 1$, and $f' \ll \omega_0$.

Statement: the anisotropic (homogeneous) plasma can be regarded as a linearly dispersive medium as long as the approximation

$$\frac{\partial \mathbf{I}^{*-1}}{\partial t} \cong 0 \tag{81a}$$

can be used in the equation (80). *This is the condition of linearity*!

In this case, in turn, (80) becomes the identity of $\mathbf{I}^*\mathbf{I}^{*-1} = \mathbf{1}$, and consequently (79) *is a solution for* (75).

Hence, $\boldsymbol{\epsilon}^*$ is formally identical to $\boldsymbol{\epsilon}$ given by (74), provided we perform the replacement $\omega_0 \to \omega_0^* = \omega_0(1 + f'/j\omega_0)$.

$$\boldsymbol{\epsilon}^* = \boldsymbol{\epsilon}(\omega_0 \to \omega_0^*) \tag{81b}$$

d) *Remark*: In this section, besides determining $\boldsymbol{\epsilon}^*$, we have managed to find an objective criterion by which one can judge whether, and to what extent, the medium characteristics dependent on the parameters describing the time variation of the signal can be regarded as linear.

5.3. *The group velocity in dispersive cases*

Utilizing the medium parameters determined in section 5.2 let us consider v_g in a case which is also important from the practical point of view: for a monochromatic, single-mode signal. (The result obtained here can easily be generalized in any sense we like: for another kind of homogeneous medium, inhomogeneous media, dispersive transmission line, etc.)

In the Section 5.2 we shall considered the case for which $\boldsymbol{\varkappa} = \boldsymbol{\upsilon} = \mathbf{0}$, $\boldsymbol{\mu} = \mathbf{1}$, i.e. $\boldsymbol{\varkappa}^* = \boldsymbol{\upsilon}^* = \mathbf{0}$ and $\boldsymbol{\mu}^* = \mathbf{1}$ are simultaneously valid. From here the new form of equation (64), making use of (65a):

$$\left[\mathbf{K}\mathfrak{F} + \mathfrak{F}\mathbf{K} - 2\,k_0^2 \frac{f'}{\omega_0}\boldsymbol{\epsilon}^* - jk_0^2(\boldsymbol{\epsilon}^* - \boldsymbol{\epsilon})\right]\bar{E} = 0 \tag{82}$$

Taking into account that $k_0^2 = \omega_0^2/c^2$, using self-evident short forms and considering that the way of writing $\mathbf{K} = k_0\mathfrak{K}$ is both permitted and expedient [1, 5], let

$$\mathfrak{K}\mathfrak{F} + \mathfrak{F}\mathfrak{K} = \mathbf{k}_{KF}\,.$$

Hence (82), and if

$$\mathbf{A}_\varepsilon = 2(-f')\,\boldsymbol{\epsilon}^* - j\omega_0(\boldsymbol{\epsilon}^* - \boldsymbol{\epsilon})$$

then the equation

$$\left(\mathbf{k}_{KF} + \frac{1}{c}\mathbf{A}_\varepsilon\right)\bar{E} = 0 \tag{83}$$

where $\bar{E}$ is the known monochromatic (plane wave) basic solution of Maxwell's equation, determines the group velocity in cases of interest for us.

a) Comparison of *the neutral and of the isotropic, ionized gas:*

In this example we shall utilize the relationship (67) and (68) for a further expansion of (83). Because the medium is *isotropic*, we can take, without the loss of generality, a signal with

$$\bar{K} = K\tilde{i}, \quad \text{and} \quad K = k_0\sqrt{\varepsilon} = \omega_0\frac{\sqrt{\varepsilon}}{c}$$

propagating in direction x. We know that the form of the solution is $\bar{E}(0, E_y, E_z)$

— For a neutral gas (67) is also satisfied. Hence (83), rewritten in a more useful form

$$\left[\left(\frac{\mathbf{K}}{\omega_0}\,\frac{\mathfrak{F}}{(-f')}+\frac{\mathfrak{F}}{(-f')}\,\frac{\mathbf{K}}{\omega_0}\right)+2\frac{\varepsilon}{c^2}\,\mathbf{1}\right]\bar{E}=0$$

From here it follows that

$$\frac{\varepsilon}{c^2}E_x=0$$

which is trivially satisfied. Since $E_y \neq 0$, $E_z \neq 0$, the correct solution will be

$$\frac{K}{\omega_0}\,\frac{(\partial f_l/\partial x)}{(-\partial f_l/\partial t)}=\frac{\varepsilon}{c^2} \tag{84}$$

i.e.

$$v_g=\frac{c}{\sqrt{\varepsilon}} \tag{84a}$$

For the isotropic case it can be verified by elementary means, that, generally, the vectors $\bar{K}$ and $\overline{\text{grad}\, f}$ are parallel.

— For the isotropic, ionized gas we use (68) for the expansion. Then

$$\left[\left(\frac{\mathbf{K}}{\omega_0}\,\frac{\mathfrak{F}}{(-f')}+\frac{\mathfrak{F}}{(-f')}\,\frac{\mathbf{K}}{\omega_0}\right)+\frac{2}{c^2}\right]\bar{E}=0$$

Hence

$$\frac{K}{\omega_0}\,\frac{(\partial f/\partial x)}{(-\partial f_l/\partial t)}=\frac{1}{c^2} \tag{85}$$

i.e.

$$v_g=c\sqrt{\varepsilon} \tag{85a}$$

— Making use of the fact that $\bar{K}$ and $\overline{\text{grad}\, f}$ are parallel, from (82) we can gain a common expression for the two types of gases. Then the notations

$$K/\omega_0=1/v_f=\sqrt{\varepsilon}/c \quad \text{and} \quad F_l(-f')=1/v_g$$

will already be used in the course of the derivation. Then the equation of condition from (82)

$$v_g=\frac{\sqrt{\varepsilon}}{\varepsilon^*-j\,\dfrac{\omega_0}{f'}\,\dfrac{\varepsilon^*-\varepsilon}{2}}\,c \tag{86}$$

Since we are studying a monochromatic signal and f' is very small, we can take into account the inequality $f'/\omega_0 \ll 1$, if necessary.

Hence for a neutral gas [see Eq. (67)]

$$v_g = c\frac{1}{\sqrt{\varepsilon}}$$

and for the isotropic plasma [see Eq. (68)]

$$v_g = c\sqrt{\varepsilon}$$

As a check for vacuum

$$v_g = c$$

Statement: One can see from the previous results that the comparative study of different media can very easily and lucidly be performed with our method.

b) A detailed study of the *neutral gas:*

As shown by the relationships (70) and (72), isotropy is preserved. Hence, also in this case we can study the propagation in direction x, where

$$\mathfrak{K}_2 = \mathfrak{K}_3 = E_1 = 0$$

and

$$\mathfrak{K}_1 = \mathfrak{K} = \sqrt{\varepsilon}$$

Then the form of (83), introducing the notation $\boldsymbol{\epsilon}^* - \boldsymbol{\epsilon} = \mathbf{e}^*$:

$$\left\{\sqrt{\varepsilon}\begin{bmatrix} 0 & \mathfrak{F}_2 & \mathfrak{F}_3 \\ \mathfrak{F}_2 & -2\mathfrak{F}_1 & 0 \\ \mathfrak{F}_3 & 0 & -2\mathfrak{F}_1 \end{bmatrix} + \frac{1}{c}\left[2(-f')\boldsymbol{\epsilon}^* - j\omega_0\mathbf{e}^*\right]\right\}\begin{bmatrix} 0 \\ E_2 \\ E_3 \end{bmatrix} = 0 \qquad (87)$$

Let us consider the general values ε and ε^* "intermediate" between the regimes $\omega_0^2 \ll a/m$, and $\omega_0^2 \lesssim a/m$. Then $\mathbf{A}_\varepsilon$ can be determined:

$$\mathbf{A}_\varepsilon = \frac{\mathbf{1}}{c}\left[2(-f')\,\varepsilon^* - j\omega_0\,e^*\right].$$

Furthermore, in order to avoid the discontinuity of $\varepsilon = 1 + e$ [see (70)] let us *assume* that ω_0 and ω_0^* are sufficiently far from the point of resonance. Then it is justifiable to use (70) and losses due to internal friction, etc., can be neglected. (In our case this is not a principal restriction, it is made just for the sake of computational convenience.) Then in the expansion of $\mathbf{A}_\varepsilon$ we have

$$\frac{2j}{\dfrac{a}{m\omega_0^2} - 1}\frac{f'^2}{\omega_0} \cong 0$$

since it is small in second order compared to 1.

Thus on the basis of (70) and (72)

$$e^* \cong -2j\omega_0 f' \frac{e}{\frac{a}{m} - \omega_0^2},$$

$$\varepsilon^* \cong \varepsilon + e^*$$

Hence

$$\mathbf{A}_\varepsilon = \frac{\mathbf{1}}{c} A = \frac{\mathbf{1}}{c}\left[2(-f')\varepsilon + 2j\omega_0 f' \frac{\varepsilon - 1}{\frac{a}{m} - \omega_0^2}(j\omega_0 + 2f')\right].$$

Using the value of $\mathbf{A}_\varepsilon$ obtained above we can expand (87):

$$\begin{bmatrix} \frac{A}{c\sqrt{\varepsilon}} & \mathfrak{F}_2 & \mathfrak{F}_3 \\ \mathfrak{F}_2 & \frac{A}{c\sqrt{\varepsilon}} - 2\mathfrak{F}_1 & 0 \\ \mathfrak{F}_3 & 0 & \frac{A}{c\sqrt{\varepsilon}} - 2\mathfrak{F}_1 \end{bmatrix} \begin{bmatrix} 0 \\ E_2 \\ E_3 \end{bmatrix} = 0 \tag{88}$$

From (88) it can be seen in an elementary way that

$$\mathfrak{F}_2 = \mathfrak{F}_3 = 0, \text{ i.e. } \overline{\mathfrak{F}} \| \overline{K}$$

Furthermore

$$\frac{A}{c\sqrt{\varepsilon}} - 2\mathfrak{F}_1 = 0 \tag{89}$$

(89) can be expanded to gain v_g, and under the conditions stated earlier

$$v_g = \frac{1}{\sqrt{\varepsilon} - \frac{\varepsilon - 1}{\sqrt{\varepsilon}} \frac{j\omega_0}{\frac{a}{m} - \omega_0^2}(j\omega_0 + 2f')}. \tag{90}$$

An important remark: *we can see* from (90) that *generally* $v_g \neq v_f$ is even in the simplest media, so we can count on the occurrence of the most unexpected phenomena in propagation!

For the discussion of (90) we shall introduce the notations

$$\omega_p^2 = \frac{q^2 N}{\varepsilon_0 m}, \quad \text{and} \quad \omega_D^2 = \frac{a}{m}. \tag{91}$$

Furthermore, we know that $v_f = c\sqrt{\varepsilon}$.

— If we are very far from the resonance then

$$\omega_0^2 \ll \omega_D^2$$

and

$$v_g \cong v_f \frac{1}{1 + \frac{\omega_0^2}{\omega_D^2} \frac{\omega_p^2}{\omega_p^2 + \omega_D^2}} \cong v_f \tag{91a}$$

— If we are still far away from the resonance, but the second term in the denominator depending on the ratio ω_D/ω_p can no longer be neglected then

$$v_g \cong v_f \frac{1}{1 + \frac{\omega_0^2}{\omega_D^2} \frac{\omega_p^2}{\omega_p^2 + \omega_D^2}} \neq v_f \tag{91b}$$

— At last, if we are approaching the resonance to the extent permitted by our previous conditions then

$$v_g \cong v_f \frac{1}{1 + \frac{\omega_0^2}{\omega_D^2 - \omega_0^2} \frac{\omega_p^2}{\omega_p^2 + \omega_D^2 - \omega_0^2}} \neq v_f \tag{91c}$$

c) *An analysis of the anisotropic plasma*:

Since previously we chose a co-ordinate system for which $\bar{B}_0(0, 0, B_0)$, we can choose, without loss of generality, the solution

$$\mathbf{K} = \begin{bmatrix} 0 & -K_3 & 0 \\ K_3 & 0 & -K_1 \\ 0 & K_1 & 0 \end{bmatrix}$$

Then (83) becomes

$$\left\{ c\mathcal{H}\left(\frac{\mathcal{F}}{-f'}\right) + c\left(\frac{\mathcal{F}}{-f'}\right)\mathcal{H} + \left[2\epsilon^* - j\frac{\omega_0}{(-f')}(\epsilon^* - \epsilon)\right]\right\} \bar{E} = 0 \ . \tag{92}$$

First of all let us carry out the analysis of the components of ϵ^* one by one, having made the corresponding approximations:

$$\varepsilon_\perp^* \cong 1 - \frac{\alpha^2}{1 - \beta^2}\left(1 - 2\frac{f'}{j\omega_0}\frac{1}{1 - \beta^2}\right) = \varepsilon_\perp + e_\perp^* \ ,$$

$$\varepsilon_{\|}^{*} \cong 1 - \alpha^2 \left(1 - 2\frac{f'}{j\omega_0}\right) = \varepsilon_{\|} + e_{\|}^{*} \,, \tag{93}$$

$$\varepsilon_x^{*} \cong \varepsilon_x \left(1 - \frac{f'}{j\omega_0} \frac{3 - \beta^2}{1 - \beta^2}\right) = \varepsilon_x - e_x^{*} \,.$$

Making use of (93) one can verify that

$$\boldsymbol{\epsilon}^{*} - \boldsymbol{\epsilon} = \mathbf{e}^{*} = \begin{bmatrix} e_{\perp}^{*} & je_x^{*} & 0 \\ -je_x^{*} & e_{\perp}^{*} & 0 \\ 0 & 0 & e_{\|}^{*} \end{bmatrix} \sim f' \,. \tag{94}$$

Hence $\mathbf{A}_{\varepsilon}$ can be given as

$$\mathbf{A}_{\varepsilon} = (-2f') \begin{bmatrix} \left(1 - e_{\perp} \dfrac{\beta^2}{1 - \beta^2}\right) & j\varepsilon_x \dfrac{2}{1 - \beta^2} & 0 \\ -j\varepsilon_x \dfrac{2}{1 - \beta^2} & \left(1 - e_{\perp} \dfrac{\beta^2}{1 - \beta^2}\right) & 0 \\ 0 & 0 & 1 \end{bmatrix} = (-2f')\,\mathbf{a}_{\varepsilon} \,. \tag{95}$$

If the plasma is isotropic ($B_0 \equiv 0$), then $\mathbf{A}_{\varepsilon iz} = (-2f')\mathbf{1}$. For this case it can briefly be shown that we get back the results (85) and (85a).

Therefore in our case *the equation determining the group velocity* is:

$$\left\{\frac{c}{2}\frac{1}{(-f')}\begin{bmatrix} -2\mathcal{H}_3\mathcal{F}_3 & \mathcal{H}_1\mathcal{F}_2 & (\mathcal{H}_1\mathcal{F}_3 + \mathcal{H}_3\mathcal{F}_1) \\ \mathcal{H}_1\mathcal{F}_2 & -2(\mathcal{H}_3\mathcal{F}_3 + \mathcal{H}_1\mathcal{F}_1) & \mathcal{H}_3\mathcal{F}_2 \\ (\mathcal{H}_1\mathcal{F}_3 + \mathcal{H}_3\mathcal{F}_1) & \mathcal{H}_3\mathcal{F}_2 & -2\mathcal{H}_1\mathcal{F}_1 \end{bmatrix} + \mathbf{a}_{\varepsilon}\right\}\begin{bmatrix} E_1 \\ E_2 \\ E_3 \end{bmatrix} = 0 \tag{96}$$

Hence, taking a known solution $\bar{E}$ in the anisotropic plasma with the corresponding $\bar{K}(K_1, 0, K_3)$ (cf. [6—8]), and substituting it into (96), we can obtain and discuss the equations for the components. From these one obtains the "energy propagation factor" $\bar{\mathcal{F}}/(-f')$ for a given direction of propagation, and also

$$v_g = |-f'|/|\mathcal{F}| \,.$$

These results will be of basic importance, for example in the discussion of the propagation path of the whistlers, and in many other investigations in space research, astronomy or engineering.

5.4. *Summary*

The method suggested for the determination of v_g has been successful in dispersive cases as well, and we have shown a practical application of the method achieving some new results at the same time.

6. The propagation of other types of perturbation

In the introduction to Section 4 we have briefly outlined that the stationary solution can be perturbed in the following ways

$$(a_{il} + \delta_i); \quad (\varphi_{ai} + \delta_i); \quad (\omega_0 + \delta_i), \quad \text{and} \quad (\bar{F}_{oil} + \bar{\delta}_i)$$

On the basis of Section 3 we gave an argument as to why we carried out the investigation for perturbing v_g according to $(a_{il} + \delta_i)$. Now we shall briefly examine the behaviour of the other types of perturbation as well. This is particularly important from the point of view of propagation of different kinds of modulation!

Our basic expression is equation (43). The other elementary "modulations" will be examined by comparison with this.

6.1. *Phase perturbation*

In this case the perturbed factor takes the form

$$e^{-j(\varphi_{ai}+\delta_i)} = e^{-j\varphi_{ai}\left(1+\frac{\delta_i}{\varphi_{ai}}\right)} \cong \left[\left(1 + \frac{\delta_i}{\varphi_{ai}}\right) e\right]^{-j\varphi_{ai}}$$

since $\delta_i/\varphi_{ai} \ll 1$. Hence

$$e^{-j(\varphi_{ai}+\delta_i)} \cong (1 - j\delta_i)\, e^{-j\varphi_{ai}}$$

Consequently the phase modulation (perturbation) can be *treated analogously with the amplitude perturbation* if the replacement

$$f_i \to (-j\delta_i) \tag{97}$$

is performed. It propagates in the same manner.

6.2. *Perturbation of the polarization*

In this case the perturbed factor is

$$(\bar{F}_{oil} + \bar{\delta}_i) = F_{oil}(\bar{e}_{oil} + f_{il}\bar{e}_{\delta i})$$

Let us have

$$\bar{e}_{\delta i} = \mathbf{T}_{\delta i}\bar{e}_{\text{oil}}, \quad \text{i.e.}$$

$$\mathbf{f}_{il} = f_{il}\mathbf{T}_{\delta i}$$

Thus,

$$\bar{F}_{\delta} = \sum_{i,l} (\mathbf{1} + \mathbf{f}_{il})\,\bar{F}_{il}. \tag{98}$$

To evaluate (98) let us discuss the single-mode solution of $\bar{F}_{\delta} = (\mathbf{1} + f\mathbf{T}_{\delta})\,\bar{F}_1$. The operations to be performed on $\bar{F}$ are, after putting it into Maxwell's equations, curl, div and $\partial/\partial t$. These can both be studied for $\bar{F}_1$ and $f\mathbf{T}_{\delta}\bar{F}_1$.

Having done the details, one can see that the equations fall into *two independent* parts, and hence

$$\mathbf{T}_{\delta}\bar{F}_1 = \bar{F}_2 \tag{99}$$

is the *independent solution* corresponding to the same φ, but with a different polarization. Consequently

$$\bar{F}_{\delta} = \bar{F}_1 + f\bar{F}_2$$

Consequently, in the case of polarization modulation the perturbation gives rise to a *new mode*, and the group velocities of the basic signal and the new component are *not necessarily equal.*

For this reason in the case of polarization modulation one has to be prepared for the side-effects (disturbances) in the propagation.

6.3. *Frequency perturbation*

In this case the perturbed factor is

$$e^{j(\omega_0+\delta_i)t} \cong (1 + j\delta_i t)\,e^{j\omega_0 t} \tag{100}$$

rewritten in the usual way; (100) can be dealt with using the previous results only if besides $\delta_i \ll \omega_0$, the condition

$$\delta_i t \ll 1 \tag{101}$$

is fulfilled as well. If this condition is satisfied, we can take over the previous results.

However, generally speaking, (101) because of the presence of t, is not valid.

Because of this, the frequency modulation is fundamentally different from the cases considered earlier. *Its propagation has to be separately analysed*, taking the signal as non-monochromatic.

Addendum:

Let us attempt to find, *with the aid of special restrictions*, the possible range of validity of our previous results picking out, in the strictly monochromatic case, those perturbations which strictly and rapidly converge to zero.

Keeping in mind the foregoing we can say that if our results are applicable under special restrictions then — perhaps with δ_i that are small *in second order* — we can define the tensor

$$\mathfrak{D} = jt\Delta$$

where there is a correspondence $\Delta \to \overline{\text{grad}}\ \delta \times \ldots$

In the non-dispersive case then, for example, the relationship

$$\frac{K}{\omega_0} = \frac{|\overline{\text{grad}}\ \delta|}{|-\delta'|} \tag{102}$$

has to be valid. However, in our case

$$\frac{\mathbf{K}}{\omega_0} = \frac{\mathfrak{D}}{(-d')} \tag{103}$$

where $(-d') = (-jt)(\delta' + \delta/t)$. Hence, in turn, since from (103)

$$\frac{K}{\omega_0} = \frac{|\overline{\text{grad}}\ \delta|}{|-\delta' - \delta/t|} \tag{104}$$

follows, for (102) to be valid, the

$$\delta \ll \delta' t \tag{105}$$

additional condition has to be observed.

Hence our previous results are applicable, if simultaneously the conditions

$$\begin{aligned} &\delta \ll \omega_0, \\ &\delta t \ll 1, \\ &\delta \ll \delta' t \end{aligned} \tag{106}$$

are satisfied.

However, the perturbation δ, as we have previously seen, is a function of position and time. Since it is a perturbation, the initial value (δ_0) of δ is certainly zero, and because it is very small, varying slowly in space and time,

it can *generally* be approximated by a series expansion, such as

$$\delta(t)_{\bar{r}} \sim \delta_{0\bar{r}} + \delta'_{\bar{r}}\, t \sim \delta'_{\bar{r}}\, t \tag{107}$$

(105) and (107) cannot be valid *at the same time.*

Important:

A detailed investigation would perhaps lead to the discovery of a class of perturbation $\delta(\bar{r}, t)$ for which our previous results are applicable also in the case of frequency modulation. *However, generally speaking* the frequency perturbation behaves *in a way fundamentally different* from other types of perturbation.

It seems that from the energetical point of view the frequency is a non-perturbable *attribute* of the electromagnetic signal! (The investigations can be carried further in this direction as well.)

6.4. *Generally speaking* the result we have obtained is that the amplitude and phase modulation mean modulation of the same mode while polarization and frequency modulation are accompanied with the appearance of one or many (perhaps infinitely many) new modes.

As far as propagation is concerned, phase modulation is the counterpart of amplitude modulation, and not that of frequency modulation! For telecommunication practice this is a principal result.

7. Summary and consequences

7.1. We have established that the usual description of group velocity in the monochromatic case is not really good, neither is it practicable.

It has been found that the customary description of group velocity does not give it directly from Maxwell's equations, but ties it to the assumed form of solution.

We have found that the usual description is not well-suited for a wide-range comparative analysis, neither can it be regarded as complete.

7.2. We have studied the question of the interpretability of an average energy for an electromagnetic wave propagating in vacuum, or in a medium, respectively, assuming that the signal can be described by the method of inhomogeneous basic modes and that other conditions adopted by us are fulfilled. Then:

We have obtained restrictions for the size and velocity for the perturbation of the signal.

We have given a method for the investigation of the resultant, and the single-mode, field. We have briefly considered what would be the consequences

of an analysis of a description based on the decomposition into inhomogeneous basic modes — and have shown the way to finding the "propagating fundamental modes".

In the calculation of the average energy, we have obtained a lower and upper bound for the surface area and the time interval of averaging.

We have verified that, even in the "classical" case, the average energy can only be defined as an expectation value possessing a certain mean standard deviation! We found that the definability and the mean deviation of the average value depend on the area of the measurement surface and on the measurement time. This has important consequences, both for theory and for measurement technology. Further, development of the present investigation into a fully statistical description is desirable.

We proved that the value of the average energy does not depend on the order of integrations over space and time, respectively.

We proved that it is possible to define an average energy, and average energy density, independently of the measurement time and surface, i.e. uniquely.

We have proved that in this case the average energy is unambiguously determined by the general (total — $\bar{F}_0$) signal amplitude.

We have found a way to investigate the energy fluctuation, "creeps" (reactive power) in more complicated cases as well.

We have proved that in such a case a complex Poynting vector, complex average energy, etc. can be defined, the real part of which is the actual average energy, etc.

7.3. We have studied the group velocity in strictly linear media:

We have given a method for the determination of v_g from Maxwell's equations in the general case, provided that the assumptions made are valid. (Special care and circumspection are needed when carrying the results for the group velocity over to such cases when the propagation vector of the phase, and hence of the propagation vector of the perturbation, is complex, i.e. it does not correspond to pure propagation [18].)

We have given a method for the determination of v_g in the homogeneous case for multi-mode signals as well.

As a special case, we found for single-mode, homogeneous signals, and for homogeneous signals composed of independently propagating modes, that for a monochromatic plane wave, even in the bianisotropic case, $v_g \equiv v_f$ and $\bar{v}_g \parallel \bar{v}_f$.

Brief comparison with investigations of moving, homogeneous media showed that

— the non-Einsteinian transformation of the phase velocity represents a discrepancy which is very important and is of basic significance,

— the only way to the dissolution of this discrepancy lies in some sort of geometrical analysis.

7.4. We have studied the group velocity in dispersive media:

We have given the general method of the determination of v_g from Maxwell's equations. In the homogeneous case it was possible to describe the energy propagation factor determining the group velocity by an equation similar to the dispersion equation which determines the propagation vector ($\overline{K} = \overline{\text{grad}\, \varphi}$).

We verified that in the non-dispersive case these equations give the results of the investigations in 7.3.

We have determined the perturbed medium characteristics:

— in a simple approximation for the neutral gas and the isotropic plasma,

— in a more accurate approximation for the neutral gas,

— for the anisotropic plasma.

Herewith, we have also shown a general method for the determination of the perturbed medium characteristics.

We have given accurate conditions for the linearity of a dispersive medium.

We have given the general equation for v_g in the homogeneous dispersive case, if $\boldsymbol{\varkappa} = \boldsymbol{\upsilon} = \mathbf{0}$ and $\boldsymbol{\mu} = \mathbf{1}$, and if the permittivity is an arbitrary isotropic or anisotropic medium characteristic.

We have carried out a comparative analysis of the cases of the simple, neutral gas and the isotropic plasma. We have shown how the solution $v_g = c/\sqrt{\varepsilon}$ changes into the solution $v_g = c\sqrt{\varepsilon}$, while $v_f = c/\sqrt{\varepsilon}$ remains unaltered.

We verified that the method is highly suitable both for a comparative study, and for the determination of the sought value of $\overline{v}_g$.

For the more accurately described isotropic, neutral gas we analysed in detail the connection between $\overline{v}_g$ and $\overline{v}_f$. We have given conditions for the fulfilment of $v_g \cong v_f$, and in other cases described the character of the deviation. We verified that $\overline{v}_g \parallel \overline{v}_f$ is generally true, but $v_g \neq v_f$.

We have considered in detail the determination of v_g for the anisotropic plasma and given the method of determination, and the principal areas of application.

7.5. We have investigated the character of the perturbation of phase, polarization, and frequency, respectively, in comparison with the perturbation of amplitude. We have listed the cases in which the disturbances in propagation can be expected to be either large, or dissimilar to those seen in the monochromatic case. We have made suggestions for general applications in telecommunication or engineering.

Acknowledgement

I wish to express my gratitude for Prof. F. KÁROLYHÁZY for valuable remarks and advice.

REFERENCES

1. FERENCZ, Cs.: Electromagnetic Wave Propagation in Inhomogeneous Media: Method of Inhomogeneous Basic Modes. *Acta Techn. Hung.* **86** (1978) 79
2. SIMONYI, K.: Theoretische Elektrotechnik. VEB Deutsches Verlag der Wissenschaften, Berlin 1968
3. TAMM, I. E.: Basic Theory of Electrodynamics. Izd. Nauka. Moscow 1966 (in Russian)
4. BRANDSTATTER, J. J.: An Introduction to Waves, Rays and Radiation in Plasma Media. McGraw-Hill Book Co., New York 1963
5. FERENCZ, Cs.: Electromagnetic Wave Propagation in Inhomogeneous Media: Strong and Weak Inhomogeneities. *Acta Techn. Hung.* **85** (1977) 433
6. BUDDEN, K. G.: Radio Waves in the Ionosphere. Cambridge at the Univ. Press, 1966
7. ALLIS, W. P.—BUCHSBAUM, S. J.—BERS, A.: Waves in Anisotropic Plasmas. M.I.T. Press, Cambridge, Mass. 1963
8. FERENCZ, Cs.: Electromagnetic Wave Propagation in Inhomogeneous Linear Media. Thesis submitted for the degree of Candidate of Sciences, Budapest 1970. Library of the Hungarian Academy of Sciences (in Hungarian)
9. NOVOBÁTZKY, K.: The Theory of Relativity (in Hungarian). Tankönyvkiadó, Budapest 1951
10. MARX, G.: Das Elektromagnetische Feld in bewegten, anisotropen Medien. *Acta Phys. Hung.* 3 (1953) 75
11. SYNGE, J. L.: Relativity, the Special Theory. North-Holland Publ. Co., Amsterdam 1965
12. v. LAUE, M.: Die Relativitätstheorie, I. Fr. Vieweg & Sohn, Braunschweig 1955
13. OTT, H.: Zum Energie-Impulstensor der Maxwell-Minkowskischen Elektrodynamik. *Annalen der Phys.* (6), **11** (1952) 33
14. BECK, F.: Die Allgemeingültigkeit des Trägheitsgesetzes der Energie in der Plankschen Fassung. *Zeitschrift für Phys.* **134** (1953) 136
15. LINDELL, I. V.: On the Definiteness on the Constitutive Parameters of a Moving Anisotropic Medium. *Proc. IEEE* **60** (1972) 638
16. KONG, J. A.—CHENG, D. K.: Modified Reciprocity Theorem for Bianisotropic Media. *Proc. IEEE* **117** (1970) 349
17. CENSOR, D.: First-Order Propagation in Moving Media. *IEEE Trans. on Micr. Theory and Techn. MIT*-16 (1968) 565
18. ÁRKOS, I. F.: A General Investigation of a Monochromatic Signal Propagating Along an Inhomogeneous Transmission Line., to be published.

Elektromagnetische Wellenausbreitung: Analyse der Gruppengeschwindigkeit. Die Arbeit bringt die eingehende Analyse der Ausbreitung der Energie, und der Gruppengeschwindigkeit. Die übliche Definition der Gruppengeschwindigkeit wird kritisch untersucht. Die Definierbarkeit der Durchschnittsenergie, deren Bedingungen und Konsequenzen werden eingehend analysiert. Aufgrund dieses, unter Verwendung auch des „Verfahrens der inhomogenen Grundmoden" wird die Gruppengeschwindigkeit in streng linearen und in als linear zu betrachtenden dispersiven Medien untersucht, wobei die Gruppengeschwindigkeit direkt aus den Maxwellschen Gleichungen abgeleitet wird. Anwendungsbeispiele werden gezeigt und die theoretischen Folgerungen aus den Ergebnissen für eine wichtige Frage der relativistischen Elektrodynamik sowie für die Verbreitung der verschiedenen Modulationsmoden werden untersucht.

Распространение электромагнитных волн: Анализ групповой скорости. В статье дается детальный анализ распространения энергии, групповой скорости. Критически исследуется обычную дефиницию групповой скорости. Детально анализируется толкуемость средней энергии, далее ее условия и последствия. На основе сказанного выше, при использовании также «метода негомогенных основных модусов» детально исследуется групповая скорость в строго линеарной и считаемой линеарной диспензивной среде, выведя групповую скорость непосредственно из уравнений Максвелла. Иллюстрируются примеры применения, далее исследуются принципиальные последствия полученных результатов по одному важному вопросу релятивистической электродинамики и на распространение различных образов модуляции.

Acta Technica Academiae Scientiarum Hungaricae, Tomus 86 (1 – 2), pp. 215 – 229 (1978)

ELASTIC PROPERTIES OF THE REINFORCED EARTH

I. SZALATKAY*

[Manuscript received April 27, 1977]

Reinforced earth is a composite material made up of soil layers and steel strips placed on each other. Mechanical characterization of this material can be achieved by two conventional methods: one is the theory of plasticity, the other is the theory of elasticity. Accordingly, the structural design methods can be classified as bearing capacity oriented and as deformation specifications oriented. Bearing capacity is calculated from the known plastic behaviour of the reinforced earth, while the deformation or strain of the reinforced earth retaining walls and slabs can be calculated from the elastic properties of the material. Estimation of the elastic constants requires the knowledge of the elastic parameters of the soil and steel, and the geometry of the reinforcement. From the constants of the transversally anisotropic material the tilting of the reinforced earth wall and the settlement of the reinforced earth slabs are computable.

1. Introduction

Since the introduction of Henry VIDAL's invention, the reinforced earth, more than a decade has passed (VIDAL, H., 1966). During this short period it has been used in retaining walls or abutments in some developed countries (France, Japan, the USA and Spain), its economic and technological advantages have been proved and up to now more than 1000 such structures have been put into operation. The structure, its elements and theory received coverage in the Hungarian literature as well (KÉZDI, 1966; SCHARLE, SZALATKAY, 1976 and 1977) and the first steps have been taken to spread it in Hungary.

During this period the theory of reinforced earth retaining structures has developed in many ways. The first procedures, resulting in bulky designs, were refined into methods representing the static and kinematic behavior better and ensuring reasonable safety. Theoretical investigations have been launched into the mechanical and economic problems of reinforced earth slabs (reinforcement placed in the subsoil under foundations) (SCHLOSSER, 1974; LEE et al., 1975). Although the latter have a primarily theoretical significance at least at present, they have contributed to our knowledge of the mechanical behavior of the reinforced earth material and pointed out its wide application

* I. SZALATKAY, H-1114 Budapest, Bukarest u. 3.

possibilities. Numerous other investigations (i.e. seismic, corrosion, etc.) carried out on this topic, aimed at the utilization of the potential benefits of this composite material on even more fields.

This paper deals with the elastic characterization of reinforced earth and reinforced earth structures and their design on the basis of the theory of plasticity or load bearing capacity. Through this an attempt is made to formulate a design method based on the permissible deformation specifications, i.e. on the specified magnitude of tilting for reinforced earth retaining walls and on the maximum amount of settlement tolerated for reinforced earth slabs, finding ever wider use in the civil engineering practice.

2. Bearing capacity design for structures made of reinforced earth by the theory of plasticity

That reinforcement boosts the ultimate failure load of an earth mass can be proven both experimentally and theoretically (SCHLOSSER, 1972). Figure 1 shows the results of a triaxial test performed on a reinforced sample. The diagram shows that the thin aluminium disks placed in the cylindrical sample at a given separation (2 centimeters) produce a large increase (400 per

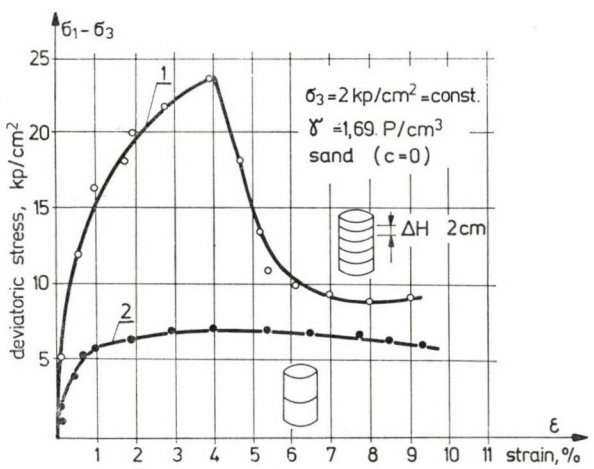

Fig. 1. Increased strength of the reinforced earth sample (SCHLOSSER, 1972); *1* — reinforced; *2*— nonreinforced

cent in the given example) in the soil material's shear strength (or breaking resistance). The magnitude of this increase depends on the deviatoric stress. SCHLOSSER supports his experimental results with physical considerations and

proves that reinforcement in the horizontal direction gives the soil material a vertical, so called anisotropic cohesion by virtue of the friction between the granular soil and the reinforcement.

Three researchers base their stability investigations of the reinforced earth walls on this frictional effect. SCHLOSSER (1972), LEE et al. (1973) and BACOT (1975) assumed that the stability criteria are fulfilled if the strips

— cannot be pulled out of the soil mass,

— will not fail as a consequence of tension stress.

All of them had performed model testing and through the study of the failure modes they proposed a failure mechanism, as shown in Fig. 2. A parabolic, a simple and a double broken-plane potential sliding surface in the rein-

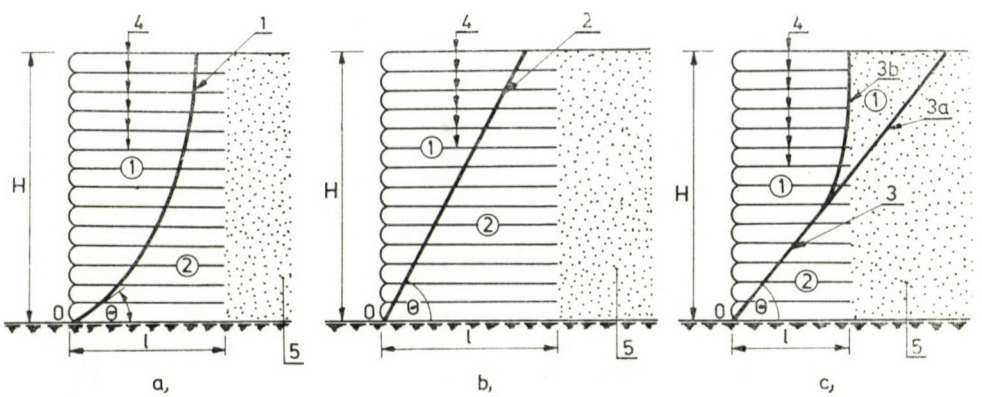

Fig. 2. Failure surfaces inside the reinforced earth wall; a — SCHLOSSER, b — LEE et al. c — BACOT; *1* — parabola, *2* — plane, *3* — double failure surface (parabola and plane), *4* — strips, *5* — backfill

forced earth zone is proposed by SCHLOSSER, LEE and BACOT, respectively. They assumed that the reinforced mass left of the sliding surface tends to slide downwards, but it is anchored back to the fixed *passive* zone by the strips. Friction resistance between the soil and the strips in the *active* zone does not allow the strips to be pulled out, so the whole system remains in a static equilibrium, provided the friction resistance between the soil and the strips is sufficiently large. If this friction resistance is exceeded or the strips break the wall loses its stability and collapses.

Beside the theory based on the principle of anchorage, there is another theory that starts out from the plastic deformations in the reinforced earth. By this approach the whole mass of the wall is supposed to move as a solid, monolithic body, with no sliding surfaces inside it and therefore no anchorag-

ing effect taking place (see for example KÉZDI, 1966; SMITH and BRANSBY, 1976). Figure 3 shows this hypothetical kinematic behavior of the reinforced retaining wall, or abutment. According to this theory, the reinforcement and the soil mass in the wall work together from a physical point of view and suffer a shearing or tilting deformation under the influence of the horizontal component of the backfill load. Therefore every horizontal plane moves forward somewhat, while point *O* remains in its original position. The validity of the designing procedure based on this concept of collapse was proved earlier (SZALATKAY, 1976), moreover the economically most advantageous structural dimensions are given by this method.

All of the design methods were analyzed and compared and their deficiencies were discussed recently (SCHARLE and SZALATKAY, 1976). Herein only

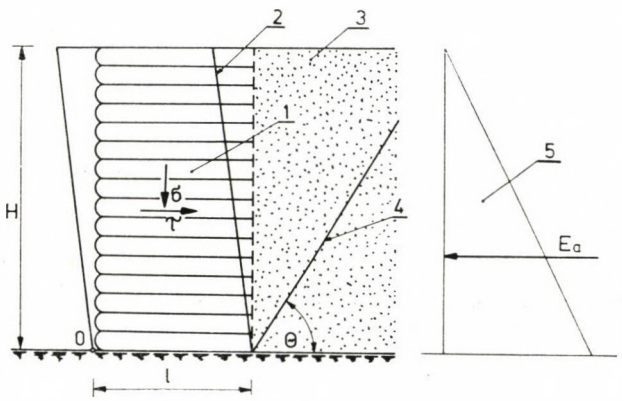

Fig. 3. Failure mood of the reinforced earth wall by KÉZDI (1966) and SMITH — BRANSBY (1976); *1* — reinforcement, 2 — deformation line, *3* — backfill, 4 — failure surface, *5* — backfill pressure

the deficiency of the bearing capacity-based design approach is mentioned, i.e. there is no way to know what the deformation of the reinforced earth retaining wall will be, even if we are convinced of the stability by selecting an appropriate value of the safety factor. This statement is similarly true for the reinforced earth slabs, LEE et al. (1975/1 and 1975/2) showed how the thin steel strips laid in the subsoil in layers under a strip load increase the bearing capacity of the original soil. The load-settlement curves obtained from their tests were compared and supported by theoretical investigations. They published a design method based on their considerations. Their results indicate not only an increase in bearing capacity, but an essential decrease in settlements. Figure 4 illustrates the test set-up, the pertinent data and shows a typical load-settlement curve. Their calculations are based on the break-

ing mechanism shown. Two zones are assumed to form in the subsoil during loading. Zone 1 is fixed, while zone 2 moves together with the foundation. The boundary lines of the two zones connect the points of the τ_{zx} shearing stress maxima in the horizontal planes. Failure (or relative displacement between the two zones) is prevented by the strips laid across the boundary lines and having the desired tension strength. Hence the design method reduces to the prevention of the tensile breaking and slippage of the strips, just as in the case of the retaining wall, so the main task is to solve the bearing capacity problem of an anchored structure.

Similar conclusions result from LEE's design approach of reinforced earth slabs. As their deformation or settlement must be controlled, the capability to estimate these is even more important.

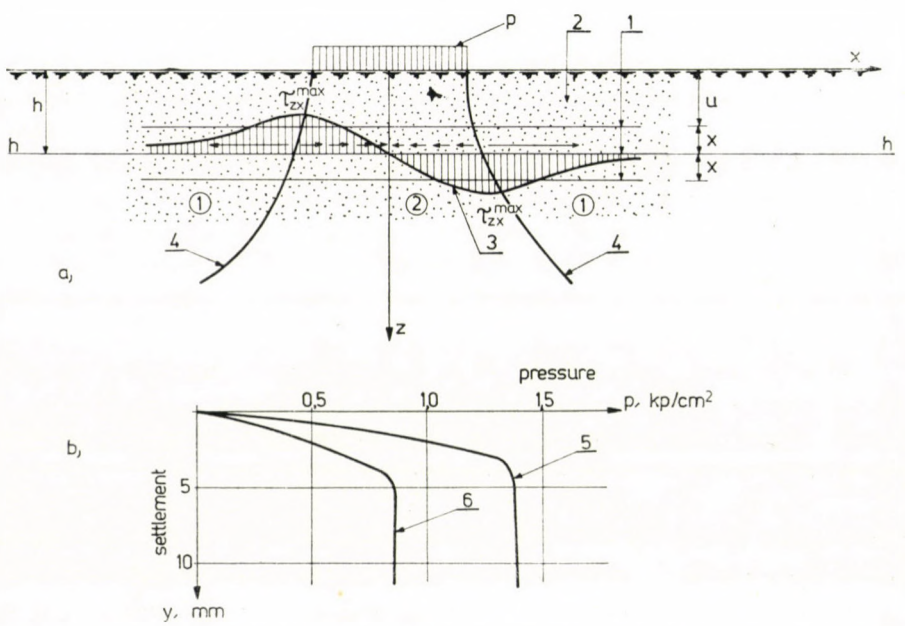

Fig. 4. Failure mood of the reinforced earth slabs. *a* — breaking mechanism; *b* — load-settlement curve. *1* — Horizontal planes of the reinforcement; *2* — soil; *3* — diagram of the shearing stress; *4* — failure surfaces; *5* — load-settlement curve for the reinforced earth; *6* — load-settlement curve the for non-reinforced earth

At the same time a clear trend can be observed in the civil engineering practice according to which both earth work structures and foundations are preferably designed for permissible deformations rather than for bearing capacity only.

This paper attempts to develop a calculation method for the deformations of reinforced earth retaining walls and reinforced earth slabs through the characterization of the elastic response of the reinforced earth material.

3. Calculation of the elastic parameters of the reinforced earth mass

The triaxial test set-up seen in Fig. 1 is well suited to measure the beneficial effects of reinforcement on the soil's breaking resistance as well as on its rigidity. The reinforced sample's stress-strain curve is steeper than that of the non-reinforced one, the difference can be expressed with Young's modulus, or the modulus of elasticity. The initial value is about three times higher for the strengthened material than for the sample made of soil only.

Estimation of the elastic parameters for the reinforced earth, however, is much more complicated than its laboratory measurement, because of its anisotropic elastic response. Starting from identical physical and almost identical geometric assumptions, HARRISON and GERRARD (1972) and HERRMANN et al. (1976) deducted the elastic constants of the transversally anisotropic continuum. The former authors' reinforcement model consists of metal sheets, while the latter's so-called "unit cell" contains a steel strip in the middle of the soil prism, with vertical and horizontal spacing dimensions corresponding to the conditions obtaining in an in situ wall. This difference in the initial assumptions means, however, no difference in the results because as it will be seen later, the reinforcing systems (sheets, or strips) can easily be transformed into each other.

Without going into the details of the derivation, the basic assumptions and the resulting expressions are presented below. It is assumed that

— the two component materials, that is the soil and the steel, are homogeneous and isotropic from a mechanical point of view;

— the two component materials are linearly elastic and therefore their behavior can be described by two pairs of parameters, the Young's modulus E_{st} and E_{so} and the Poisson-ratio ν_{st} and ν_{so} for the steel and soil, respectively;

— along the contact surfaces of the soil and steel no relative displacement can occur as the soil particles adhere perfectly to the strips, through friction resistance;

— the composite material of reinforced earth is transversally anisotropic from a mechanical point of view.

Supposing an elastic and linear response in the stress-strain relationship of a soil material is rather a course approximation. The third assumption is also an approximation, though less far fetched, while the last one follows from the first three.

Figure 5 specifies the geometric and physical characteristics of the basic reinforced earth element. From our assumptions it follows that all of the

strains for the soil, the steel and for the composite material are equal in all directions. So, for example, strain ε_h for the reinforced earth is equal to the strains ε_{st}^h and ε_{so}^h for the steel and soil respectively, in the same h direction, or

$$\varepsilon_h \equiv \varepsilon_{st}^h \equiv \varepsilon_{so}^h \tag{1}$$

For all of the six strains of the reinforced earth and its component materials an equation, similar to equation (1) can be written along the axes, h, h and v. This procedure leads to six equations, from which, through substitution of the geometric and elastic parameters all of the elastic constants of the composite material can be defined. Two of the main axes in the horizontal direction are marked by h, referring to the axial symmetricity of the physical

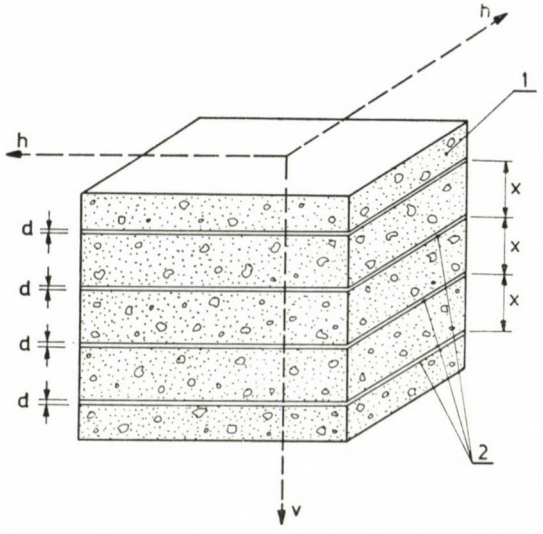

Fig. 5. Sketch of the reinforced earth element; *1* — soil, *2* — reinforcing sheets

constants, resulting from the axially symmetric arrangement of the two elements.

Let us introduce the geometric constant t, characterizing the reinforcing density, or the quantity of steel in the soil:

$$t = \frac{x - d}{x} \tag{2}$$

where x is the vertical distance between two reinforcement planes (or the thickness of the soil layers) and d is the thickness of the steel sheets. The

value of t approaches zero as the quantity of steel increases and is unity when there is no reinforcing material.

The elastic parameters of the reinforced earth in the principal directions are as follows

$$\nu_h = \frac{\dfrac{(1-t)\,E_{so}\nu_{so}}{1-\nu_{so}^2} + \dfrac{tE_{st}\nu_{st}}{1-\nu_{st}^2}}{\dfrac{(1-t)\,E_{so}}{1-\nu_{so}^2} + \dfrac{tE_{st}}{1-\nu_{st}^2}} \tag{3}$$

$$\nu_{hv} = (1-\nu_h)\left[\frac{(1-t)\,\nu_{so}}{1-\nu_{so}} + \frac{t\nu_{st}}{1-\nu_{st}}\right], \tag{4}$$

$$E_h = (1-\nu_h^2)\left[\frac{(1-t)\,E_{so}}{1-\nu_{so}^2} + \frac{tE_{st}}{1-\nu_{st}^2}\right], \tag{5}$$

$$\frac{1}{E_v} = \frac{1-t}{E_{so}}\left(1 - \frac{2\nu_{so}^2}{1-\nu_{so}}\right) + \frac{t}{E_{st}}\left(1 - \frac{2\nu_{st}^2}{1-\nu_{st}}\right) + \frac{2\nu_{hv}^2}{(1-\nu_h)\,E_h}, \tag{6}$$

$$G_h = \frac{E_h}{2(1-\nu_h)}, \tag{7}$$

$$\frac{1}{G_v} = \frac{2(1-t)(1+\nu_{so})}{E_{so}} + \frac{2t(1+\nu_{st})}{E_{st}}. \tag{8}$$

The seven equations express seven different elastic parameters, of which only five are independent. Anyone of the five can be calculated and the other two can be expressed with them, because of the geometrical symmetry and the isovolumetry during shearing strain.

Now, as we have all of the elastic constants, the strains produced by any state of stress can be determined numerically from the physical equations, as follows:

$$\varepsilon_h^c = \frac{1}{E_h} \cdot \sigma_h - \frac{\nu_h}{E_h} \cdot \sigma_h - \frac{\nu_{vh}}{E_v}\sigma_v, \tag{9}$$

$$\varepsilon_h^c = \frac{1}{E_h}\sigma_h - \frac{\nu_{vh}}{E_v}\sigma_v - \frac{\nu_h}{E_h}\sigma_h, \tag{10}$$

$$\varepsilon_v^c = \frac{1}{E_v}\sigma_v - \frac{\nu_{vh}}{E_h}\sigma_h - \frac{\nu_{vh}}{E_h}\sigma_h, \tag{11}$$

$$\gamma_{hv}^c = \frac{\tau_{hv}}{G}, \tag{12}$$

$$\gamma_{hv}^{c} = \frac{\tau_{hv}}{G_v}, \tag{13}$$

$$\gamma_{hh}^{c} = \frac{\tau_{hh}}{G_h}. \tag{14}$$

It is seen immediately that without subscripts these equations reduce to the physical equations of an isotropic material.

Since the forms of the static equations are unchanged all the expressions needed to solve any continuum mechanics problem of reinforced earth structures are now at hand.

To summarize the important geometric and physical quantities for the calculation of the elastic constants of reinforced earth are

— density t of the reinforcement;
— the two elastic parameters for the steel (E_{st}, ν_{st});
— the two elastic constants for the soil (E_{so}, ν_{so}).

4. Plane deformation problems for reinforced earth structures

To clarify things we have worked out two numerical examples, but first the reinforced earth unit cell mentioned in the previous section must be brought into correlation with the real world. This would force us to regard it as a three dimensional isotropic continuum. As, however, the problems below are plane strain ones, we can solve them with the formulas developed earlier for the transversally anisotropic material.

Figure 6 shows the characteristics of the steel strips. The strips (or ties) of w width and d_{vt} thickness are placed into the soil at a separation of s and x horizontally and vertically, respectively. It is easy to prove that the physical properties in the laying direction are not changed if the strips are substituted with sheets having the same cross sectional area. This means that the strips, placed at a separation of x, have to be spread continuously in the horizontal plane and a new, equivalent, or "theoretical" sheet thickness has to be calculated from the dimensional parameters of w, d_{vt} and s. The condition of the cross sectional equality is expressed as

$$ds = wd_{vt}, \tag{15}$$

from which

$$d = \frac{wd_{vt}}{s}. \tag{15a}$$

Having estimated the theoretical sheet thickness d, Eq. (2) can be used to calculate the geometric constant t for use in equations (3) through (14).

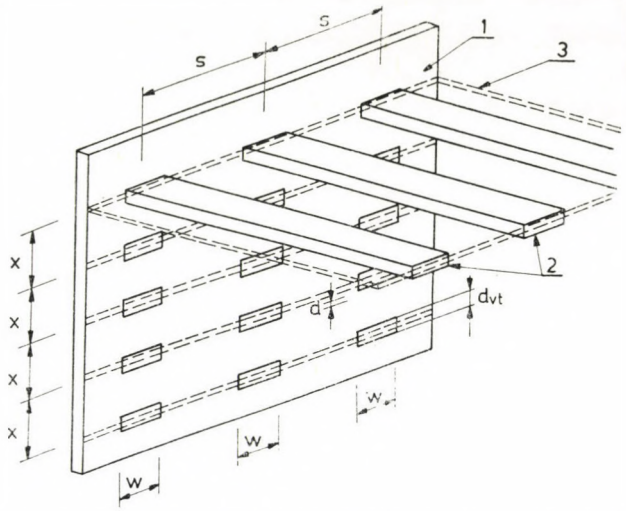

Fig. 6. Estimation of the "theoretical" strip thickness; *1* — face of the wall; *2* — strips; *3* — equivalent sheet

Because of the plane nature of the deformations, strains ε_h, γ_{vh}, and γ_{hh} are zero in (10), (13) and (14), thus we get a simpler set of equations. As there are no strains in the vertical plane perpendicular to the strips (as follows from the plane strain condition) deformations in a retaining wall and settlements under a strip load can be readily calculated.

After these considerations let us examine the case of the reinforced earth retaining wall. It was proved earlier by model testing that the horizontal component of the backfill load produces a shear strain inside the wall in the vertical plane, parallel to the strips (SMITH and BRANSBY, 1976; SZALATKAY, 1976). This horizontal backfill pressure can vary from a passive load to an active one, producing a wall tilt. If we know how the earth pressure ratio K varies in terms of the wall tilting α, we can express it as $K(\alpha_0)$ earth pressure function. We assume that the specified or allowed α_0 tilting is constant along the height of the wall, as defined by the function $K = K(\alpha)$ (Fig. 7). Assuming further that the behavior of the reinforced earth can be described with the elastic parameters derived in the previous sections, the width of the wall (or the length of the ties) can be conveniently estimated.

Now, we can proceed with the derivation through the help of the work theorems known from stress analysis.

$$W_i = W_e \tag{16}$$

means that the internal deflection work, performed by the shear strain inside the wall equals the external work W_e of the backfill pressure. Consequently,

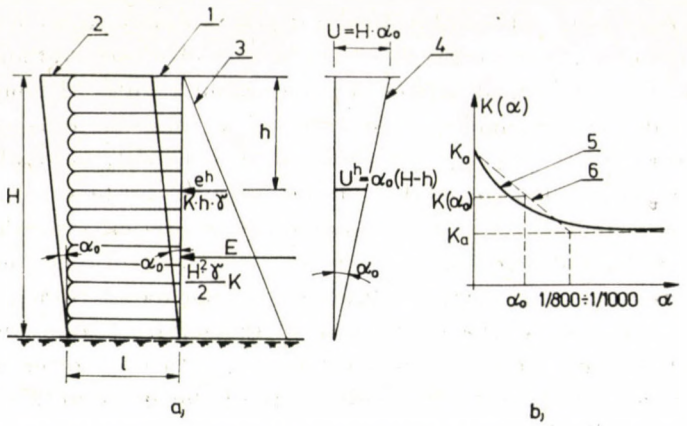

Fig. 7. Estimation of the deformation in the reinforced earth retaining wall. *a* — Sketch of the wall displacement; *1* — the reinforced earth retaining wall; *2* — deformation line; *3* — backfill pressure; *4* — displacement originated from the wall-tilting; *b* — calculation of the earth pressure, *5* — exact curve for $K = K(\alpha)$ function; *6* — approximate straight line

the two quantities can be expressed as

$$W_e = \frac{1}{2} l \int_0^H \frac{\tau_h^2}{G_r} dh \tag{17}$$

and

$$W_e = \frac{1}{2} \int_0^H h\gamma K(\alpha_0) \frac{\alpha_0(H-h)}{2} \tag{18}$$

where l is the width of the wall, τ_h is the shear stress in any horizontal plane at height h, H is the height of the wall, γ is the density of the soil and $K(\alpha_0)$ is the earth pressure coefficient, dependent on α_0, the permissible tilting of the wall. τ_h, the shearing stress, can be expressed as

$$\tau_h = \frac{E^h}{l} = \frac{h^2\gamma}{2l} K(\alpha_0) \tag{19}$$

After rearrangement of (17) through (20), the necessary length of the ties can be obtained:

$$l = \frac{3}{10} H^2 \frac{K(\alpha_0)\gamma}{G_r \alpha_0} . \tag{20}$$

The maximum value of $K(\alpha_0)$ corresponds to the coefficient of earth pressure at rest, when $\alpha_0 = 0$. In this case

$$K_0 = 1 - \sin \Phi . \tag{21}$$

The only snag is that (20) does not give a usable result for $\alpha_0 = 0$ (because the denominator becomes zero). It is very probable that at about $\alpha_0 = 1/800$ the active state is reached in most of the granular soils. Although no experimental results are available on this subject at present, it is supposed that $K(\alpha_0)$ is linear in the $0 < \alpha_0 < 1/1000$ range, with only a small error.

The G_v shear modulus of the reinforced earth can be calculated from the theory discussed above. Having estimated the theoretical strip thickness d and t, the reinforcing density of steel, from (16/a) and (2), the only unknown physical quantity, the shear modulus G_v, is calculated from (8). The latter consists of two terms; the first includes the elastic parameters of the soil (E_{so}, ν_{so}), the second those of the steel (E_{st}, ν_{st}). In both terms the value of t is almost zero. Assuming $t = 0$ results in the following simplification:

$$\frac{1}{G_v} \cong \frac{2(1 + \nu_{so})}{E_{so}} \cong \frac{1}{G_{so}} . \tag{22}$$

Note that only the soil's elastic constants are in the expression. This does not mean at all that the wall could stand up without reinforcement. Rather, the case is that strengthening takes place indirectly, the reinforcing strips cause the wall to deform in a way that consumes much more energy than it would without reinforcement.

Estimating the elastic constants of the reinforced earth may be helpful for the calculation of the settlement under a strip foundation. The loading and reinforcing system shown in Fig. 4 can be modeled as a three-layered subsoil, shown in Fig. 8. Layers 1 and 3 have the original soil's physical properties. Between these there is the layer 2, having reinforcement of thickness

$$v = nx \tag{23}$$

where n is the number of reinforcement planes in the subsoil. This middle layer has the elastic parameters calculated as shown in the previous sections. Layer 1 is of thickness u, while layer 3 reaches the bottom of the soilbox.

The physical parameters of the layers can be determined in a straightforward way. The physical behaviour of the upper and lower layers can be characterized by Young's modulus E_{so} and the Poisson ratio ν_{so}. Layer 2, situated in between, having a thickness of v, is more rigid, its physical properties in all directions can be calculated from (3) through (8). Equations (9) through (14) are useful to estimate the elastic response to the load applied on the surface.

Calculating the settlement only in a plane perpendicular to the axis of a strip load means a certain amount of simplification, too, but it is still a much more complicated case than that of the retaining wall. The shear strain γ_{hv} is,

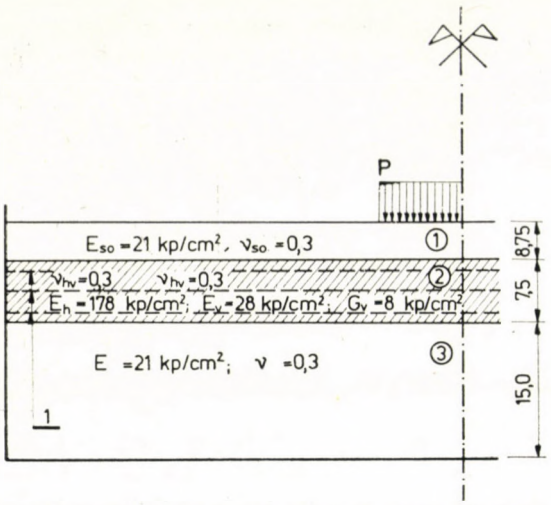

Fig. 8. The three-layered subsoil system in the case of reinforced earth; *1* — reinforcement planes

in fact, not the only one; vertical and horizontal normal strains, ε_v and ε_h, also occur in that plane. This means that all of the five independent variables (E_h, E_v, G_h, ν_{vh} and G_v) found in (9), (10) and (12) must also be determined.

Even in the knowledge of the physical parameters and the equations the settlements under the reinforced earth slabs cannot be calculated as easily as could be done in the case of the retaining wall (from a closed mathematical expression), but by applying the finite-element method for the estimation it becomes a routine task for a computer.

Such an example is shown in Fig. 4. LEE's experimental results (1975) were used for comparison and one of his loading and reinforcing systems was used in our example. The dimensions of his soilbox are shown in Fig. 8. As seen, the ties are modeled by aluminium foil strips. Altogether 17 such strips were placed in 3 horizontal planes, spaced $x = 25$ mm apart. The geometrical arrangement and the physical parameters are also indicated in Fig. 8.

Figure 9 shows the final result of the comparison, including two curves obtained by LEE and two straight lines estimated by the finite element method, for which a computer program was worked out in the Hungarian Institute for Building Science. The small difference of the experimental and theoretical data shows that the considerations and the estimation method of the physical properties of the reinforced earth are valid and reasonably accurate and that the elastic theory should be introduced as a useful technique for the design of reinforced earth structures.

At the end of this paper let us refer to the assumption made in the introduction about the linearity of the stress-strain characteristics of soil, as the

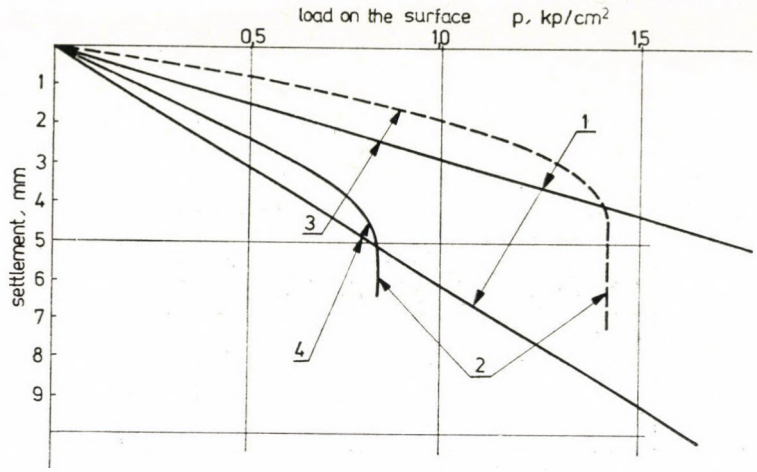

Fig. 9. Comparison of LEE's experimental and ÉTI's calculation data; *1* — estimated results; *2* — experimental curve; *3* — reinforced; *4* — nonreinforced

crudest of the approximations. Though this problem exceeds the frame of this work, yet, as the soil parameters have an important role in the accuracy of the deformation estimation, the question cannot be avoided.

Elastic behavior of the soil can be characterized on several accuracy levels, depending on the requirements and on the calculation methods available. The least exact, but fastest method is the use of the tabular data published in handbooks on soil mechanics. Different triaxial tests may give low or high accuracy during the estimation of Young's modulus and the Poisson ratio of soils. In connection with the approximation method, BALLA's study (1967) can be mentioned. Higher accuracy is reached by the testing method reported by CHANG and DUNCAN (1970), DOMATSCHUK and WADE (1969). The latter two take the nonlinearity and the effect of the initial stress state into consideration, but this complicates the calculation procedure so much, that only a computer can successfully crunch through it.

According to these principles given in this paper it can be said that the accuracy of any calculation depends essentially on the accuracy of the soil parameters, e.i. E_{s0}, ν_{s0}, or $K = K(\alpha_0)$, the whole static behavior of these sorts of structures, however, can only be verified or determined by a new calculating model based on some in situ experimental measurements.

REFERENCES

1. BACOT, I.—LAREAL, P.: Comportement à la rupture de soutenements realises en terre armée. *Proc. of the 1st Baltic Conf. on Soil Mech. and Found. Eng.*, Gdansk, 1975, in French.
2. BALLA, Á.: Estimation of the Elastic Modulus of Soils. *Scientific Publications of the Technical University*, Budapest 1963, No. 5.

3. Domatschuk, L.—Wade, N. H.: A Study of Bulk and Shear Moduli of a Sand. *Journa of the Soil Mechanics and Foundation Division*, ASCE, No. SM2 (March, 1972)
4. Duncan, J. M.—Chang, C. Y.: Nonlinear Analysis of Stress and Strain in Soils. *Journal of the Soil Mech. and Found. Division*, ASCE, Vol. **96** No. SM5 (Sept., 1970)
5. Harrison, W. J.—Gerrard, C. M.: Elastic Theory to Reinforced Earth. *Journal of the Soil Mechanics and Foundation Div*, ASCE, SM12 (Dec., 1972)
6. Herrmann, L. R.—Romstad, K. M.—Shen, C. K.: Integrated Study of Reinforced Earth. I.: Theoretical Formulation. *Journal of the Geotechnical Eng. Div.*, ASCE, GT6 (June, 1976)
7. Kézdi, Á.: New Earth Retaining Structures. *Scientific Review of Civil Engineering*, Dec., 1966, in Hungarian
8. Kézdi, Á.: Stability of Rigid Structures. General Report of Session II of the 5th European Conf. on Soil Mech. and Found. Eng. Madrid 1972
9. Lee, K. L.—Adams, B. D.—Vagnernon, I. I.: Reinforced Earth Retaining Walls. *Journal of the Soil Mechanics and Foundation Div.*, ASCE, SM10 (Oct., 1973) 745—764
10. Lee, K. L.—Bingquet, I.: Bearing Capacity Tests on Reinforced Earth Slabs. *Journal of the Geotechnical Eng. Div.*, ASCE, GT12 (Dec., 1975) 1241—1255
11. Lee, K. L.—Bingquet, I.: Bearing Capacity Analysis of Reinforced Earth Slabs. *Journal of the Geotechnical Eng. Div.*, ASCE, GT12 (Dec., 1975) 1257—1276
12. Scharle, P.—Szalatkay, I.: Stability Problems of Reinforced Earth Wall. *Építési Kutatás Fejlesztés* (Developing of Building Research) Nr. 1 (1976), in Hungarian
13. Scharle, P.—Szalatkay, I.: Utilization and Mechanical Behavior of Reinforced Earth Walls. *Scientific Review of Civil Engineering*, under publication, in Hungarian
14. Schlosser, F.—Long, T. H.: Recent Results in French Research on Reinforced Earth. *Journal of the Construction Div.*, ASCE, Vol. **100** No. CO3 (September, 1974) 223—237
15. Schlosser, F.: Reinforced Earth, Research and Realization. *Laboratoire des Ponts et Chaussees, Bull.* Liaison L.P.C. 62. (Dec., 1972) 79—92, in French
16. Smith, A. K. C.—Bransby, P. L.: The Failure of Reinforced Earth Walls by Overturning. *Geotechnique*, (June, 1976) No. 2, 376—381
17. Szalatkay, I.: The Reinforced Earth Retaining Wall and Its Mechanical Behavior. *Proc. 5th Conf. on Soil Mechanics and Found. Eng.*, Budapest 1976

Die Elastizitätseigenschaften des stahlverstärkten Bodens. Der stahlverstärkte Boden ist eine Verbundkonstruktion, die aus abwechselnd übereinander gelagerten Stahlbändern und Bodenschichten besteht. Seine mechanische Untersuchung kann mittels zweier traditioneller Methoden der Festigkeitslehre — der Plastizitätslehre und der Elastizitätslehre — durchgeführt werden. In analoger Weise können auch die Festigkeitsbemessungen der stahlverstärkten Bodenkonstruktionen klassifiziert werden. Sobald das anisotrope plastische Verhalten des stahlverstärkten Bodens geklärt ist, kann auch die Grenztragfähigkeit der stahlverstärkten Bodenkonstruktionen bestimmt werden. Mit Hilfe der anisotropen Elastizitätscharakteristika kann auch die Formänderung der Konstruktionen berechnet werden. Die Konstanten der Elastizitätslehre können aufgrund der Angaben über die Festigkeitsparameter der Einlagen und des Bodens, der Einlagenabmessungen und der Angaben über die Auslegung der Einlagen bestimmt werden. Mit den Konstanten des in Querrichtung anisotropen Materials können sowohl die Neigung der stahlverstärkten Bodenstützmauer, als auch die im verstärkten Grund auftretende Senkung berechnet werden.

Характеристики упругости армированного грунта. Армированный грунт представляет собою комбинированный конструкционный материал, который состоит из размещенных попеременно друг над другом металлических лент и слоев грунта. Механическое испытание такого конструкционного материала производится с помощью двух обычных методов теории сопротивления материалов (теории пластичности и теории упругости). При помощи этого метода можно аналоговым способом классифицировать также динамический расчет армированных грунтовых конструкций. Поскольку выяснено поведение с точки зрения анизотропной теории пластичности армированного грунта, то представляется возможным определить предельно допустимую нагрузку армированных грунтовых конструкций. С помошью анизотропных характеристик теории упругости можно производить расчет деформацию конструкций. Определение постоянных теории упругости производят на основе параметров по теории сопротивления материалов, действительных для армирования и грунта, а также данных по размерам арматуры и по шагу арматуры. С помощью полученных постоянных материала, который в поперечном направлении ведет себя анизотропно, представляется возможным произвести расчет как угла откоса армированной грунтовой опорной стены, так и погружения укрепленного армированием грунта.

INDEX

Printed in Hungary

A kiadásért felel az Akadémiai Kiadó igazgatója — Műszaki szerkesztő: Zacsik Annamária

A kézirat nyomdába érkezett: 1977. XII. 19. — Terjedelem: 21,0 (A/5) ív, 85 ábra

78.5296 Akadémiai Nyomda, Budapest — Felelős vezető: Bernát György

ERRATA

In the paper "Paraboloid Shells with Vertical Director Line" published by P. Csonka *(Acta Techn. Hung.* **84** (1977), 207 – 220) the right form of Eq. (3) is

$$6\,\frac{ha^2}{b^2}\cdot\frac{y^2}{x^4}\cdot\frac{\partial^2 F}{\partial y^2}+8\,\frac{ha^2}{b^2}\cdot\frac{y}{x^3}\cdot\frac{\partial^2 F}{\partial x\cdot\partial y}+2\,\frac{ha^2}{b^2}\cdot\frac{1}{x^2}\cdot\frac{\partial^2 F}{\partial x^2}+\bar{p}=0\,.$$

Accordingly, Table 2 should be corrected as follows:

$\bar{b}_{mn}=x^m y^n$	F_{mn}
y^2	$-\dfrac{b^2}{100ha^2}\,\dfrac{(a^{-5}-a_1^{-5})(x^{-10}-a_1^{-10})-(a^{-10}-a_1^{-10})(x^{-5}-a_1^{-5})}{a^{-10}a_1^{-5}-a^{-5}a_1^{-10}}\,x^4y^2$
$\dfrac{y^2}{x}$	$-\dfrac{b^2}{72ha^2}\,\dfrac{(a^{-4}-a_1^{-4})(x^{-9}-a_1^{-9})-(a^{-9}-a_1^{-9})(x^{-4}-a_1^{-4})}{a^{-9}a_1^{-4}-a^{-4}a_1^{-9}}\,x^3y^2$
$\dfrac{y^2}{x^2}$	$-\dfrac{b^2}{48ha^2}\,\dfrac{(a^{-3}-a_1^{-3})(x^{-8}-a_1^{-8})-(a^{-8}-a_1^{-8})(x^{-3}-a_1^{-3})}{a^{-8}a_1^{-3}-a^{-3}a_1^{-8}}\,x^2y^2$
$\dfrac{y^2}{x^3}$	$-\dfrac{b^2}{28ha^2}\,\dfrac{(a^{-2}-a_1^{-2})(x^{-7}-a_1^{-7})-(a^{-7}-a_1^{-7})(x^{-2}-a_1^{-2})}{a^{-7}a_1^{-2}-a^{-2}a_1^{-7}}\,xy^2$
$\dfrac{y^2}{x^4}$	$-\dfrac{b^2}{12ha^2}\,\dfrac{(a^{-1}-a_1^{-1})(x^{-6}-a_1^{-6})-(a^{-6}-a_1^{-6})(x^{-1}-a_1^{-1})}{a^{-6}a_1^{-1}-a^{-1}a_1^{-6}}\,y^2$
$\dfrac{y^2}{x^5}$	$-\dfrac{b^2}{10ha^2}\left(-\dfrac{x^{-5}-a_1^5}{a^5-a_1^5}\,a^5\ln a-\dfrac{a^5-x^5}{a^5-a_1^5}\,a_1^5\ln a_1+x^5\ln x\right)\,x^{-6}y^2$
$\dfrac{y^2}{x^6}$	$+\dfrac{b^2}{8ha^2}\,\dfrac{(a-a_1)(x^{-4}-a_1^{-4})-(a^{-4}-a_1^{-4})(x-a_1)}{a^{-4}a_1-aa_1^{-4}}\,x^{-2}y^2$
y^4	$-\dfrac{b^2}{224ha^2}\,\dfrac{(a^{-7}-a_1^{-7})(x^{-16}-a_1^{-16})-(a^{-16}-a_1^{-16})(x^{-7}-a_1^{-7})}{a^{-16}a_1^{-7}-a^{-7}a_1^{-16}}\,x^4y^4$
$\dfrac{y^4}{x}$	$-\dfrac{b^2}{180ha^2}\,\dfrac{(a^{-6}-a_1^{-6})(x^{-15}-a_1^{-15})-(a^{-15}-a_1^{-15})(x^{-6}-a_1^{-6})}{a^{-15}a_1^{-6}-a^{-6}a_1^{-15}}\,x^3y^4$
$\dfrac{y^4}{x^2}$	$-\dfrac{b^2}{140ha^2}\,\dfrac{(s^{-5}-a_1^{-5})(x^{-14}-a_1^{-14})-(a^{-14}-a_1^{-14})(x^{-5}-a_1^{-5})}{a^{-14}a_1^{-5}-a^{-5}a_1^{-14}}\,x^2y^4$
$\dfrac{y^4}{x^3}$	$-\dfrac{b^2}{104ha^2}\,\dfrac{(a^{-4}-a_1^{-4})(x^{-13}-a_1^{-13})-(a^{-13}-a_1^{-13})(x^{-4}-a_1^{-4})}{a^{-13}a_1^{-4}-a^{-4}a_1^{-13}}\,xy^4$
$\dfrac{y^4}{x^4}$	$-\dfrac{b^2}{72ha^2}\,\dfrac{(a^{-3}-a_1^{-3})(x^{-12}-a_1^{-12})-(a^{-12}-a_1^{-12})(x^{-3}-a_1^{-3})}{a^{-12}a_1^{-3}-a^{-3}a_1^{-12}}\,y^4$
$\dfrac{y^4}{x^5}$	$-\dfrac{b^2}{44ha^2}\,\dfrac{(a^{-2}-a_1^{-2})(x^{-11}-a_1^{-11})-(a^{-11}-a_1^{-11})(x^{-2}-a_1^{-2})}{a^{-11}a_1^{-2}-a^{-2}a_1^{-11}}\,x^{-1}y^4$
$\dfrac{y^4}{x^6}$	$-\dfrac{b^2}{20ha^2}\,\dfrac{(a^{-1}-a_1^{-1})(x^{-10}-a_1^{-10})-(a^{-10}-a_1^{-10})(x^{-1}-a_1^{-1})}{a^{-10}a_1^{-1}-a^{-1}a_1^{-10}}\,x^{-2}y^4$

Lightweight Construction

by Gy. Sebestyén

Lightweight constructions occupy a most important place among modern building techniques. This book summarizes the information of lightweight construction dealing among other topics with the main solutions of building structures, production technologies, and the consequences of lightweight construction on heating, ventilation and air conditioning. No summarizing work similar to this has been published up to the present time neither in Hungarian nor any other language. The large number of drawings provide orientation on the various trends of developments in this field.

In English · Approx. 400 pages · Cloth

A co-edition — distributed in the socialist countries by KULTURA, Budapest, ISBN 963 05 1109 6; in all other countries by GEORGE GODWIN, London

AKADÉMIAI KIADÓ
Budapest

GEORGE GODWIN
London

F. Kovács

Hochfrequenzanwendungen von Halbleiter-Bauelementen

Die in der Nachrichtentechnik gebräuchlichen verschiedenen Hochfrequenzkreise werden in Hinblick auf die Funktion der Halbleiter-Bauelemente besprochen. Die Ausführungen über diese Bauelemente für Hochfrequenz berühren im einzelnen ihre Herstellungstechnologien, Konstruktion, elektrischen Parameter, Ersatzschaltungen, ihren Anwendungsbereich sowie die durch ihre Anwendung bedingten besonderen Probleme. Das Buch behandelt die für die praktische Anwendung wesentlichen Hochfrequenzkreise, die Breitbandverstärker und die Selektivverstärker, die Oszillatoren, Vervielfacher und Mischkreise. Besondere Beachtung verdienen jene Teile des Buches, in welchen die Breitbandverstärker mit Leitungsformator und die Extremhochfrequenzverstärker besprochen werden.

In deutscher Sprache – Etwa 370 Seiten – 17 × 25 cm – Ganzleinen

Eine Gemeinschaftsausgabe – vertrieben in den sozialistischen Ländern von KULTURA, Budapest, ISBN 963 05 1252 1; in allen anderen Ländern von FRANZIS VERLAG, München

Akadémiai Kiadó

FRANZIS VERLAG, München

Budapest

Kósa, Zoltán
KENZO TANGE

Die japanische Baukunst — mit seinen charakteristischen Formen und Farben — hat immer Bewunderung ausgelöst. In letzter Zeit faßt in Japan immer mehr die moderne Baukunst Fuß; daneben besteht aber auch die herkömmliche, charakteristische Architektur des fernen Ostens weiterhin. Kenzo Tange ist einer der größten Meister dieser neuen Baukunst. Das Buch Zoltán Kósas zeigt vor allem, wie die Werke des heute vierundsechzigjährigen Meisters entstanden, welche Schöpfungen ihnen vorausgingen und wie aus einem, in althergebrachter Tradition herangewachsenem Japaner, ein modernen Architekt unserer Tage wurde. Seine Gemeindebauten, seine Städtpläne sind nicht nur für Fachleute aufschlußreich, sondern auch für Studenten und Laien von Interesse.

In deutscher Sprache — Etwa 100 Seiten, mit 65 Abbildungen — 21 × 23 cm — Ganzleinen
ISBN 963 05 1516 4

AKADÉMIAI KIADÓ, Budapest
Verlag der Ungarischen Akademie der Wissenschaften

Acta Techn. Hung. **86** (1978), pp. 9—41

KNAPP, R. H.—SZILÁRD, R.: *Nonlinear Stability Analysis of Pseudo-Cylindrical Shells*

An unconventional geometric configuration is introduced for cylindrical shells. The cylindrical surface has been replaced by an assemblage of flat polyhedral elements. Buckling characteristics of the so-obtained *Pseudo-Cylindrical ConcavePolyhedral* (PCCP) shell, subjected to external pressure, is analyzed by means of a finite element approach. To verify the computer results a small scale model test has been carried out. These two independent investigations show excellent agreement. Comparison with the buckling pressure of a "true" cylindrical shell indicates that the proposed modification of the geometrical configuration results in considerably higher buckling resistance. In addition, such a pseudo-cylindrical shell exhibits other desirable structural qualities such as relative ease in fabrication and high insensitivity to initial imperfections. Consequently, it can advantageously be used for various undersea structures.

Acta Techn. Hung. **86** (1978), pp. 43—53

KESHAVA MURTHY, K.—GOPALAKRISHNA PILLAI, K.: *On the Design of a Quadratic Weir with Semi-Cubic Parabola as the Base*

This paper deals with the design of a quadratic notch, which finds application in the proportionate method of flow measurement in a by-pass, such that the discharge through it is proportional to the square root of the head measured above a certain datum. The weir notch consists of a bottom in the form of a semi cubic parabola of top width '2W' and depth 'a' over which a designed curve is fitted. Using the 'slope discharge continuity theorem' the problem is reduced to the determination of an exact solution of the Volterra's integral equation in the Abel's form. It is shown that in this case of the quadratic weir notch, the reference plane or the datum is situated at 5/6 *a* above the crest of the weir so that the discharge is proportional to the square root of the head measured above the datum.

Acta Techn. Hung. **86** (1978), pp. 55—75

KOLLÁR, L.: *Continuum Method of Analysis for Double Layer Space Trusses of "Hexagonal Over Triangular" Mesh*

Structural consequences of the instability of one chord plane of a double layer space truss of "hexagonal over triangular" mesh as well as conditions for obtaining a statically determinate truss have been analyzed. Structural characteristics of "grid tubes" providing for torsional stiffness permit to deduce the set of differential equations of a continuum equivalent to the space truss. Equations of boundary conditions as well as the method of computing bar forces from internal forces of the continuum have been presented.

Acta Techn. Hung. **86** (1978), pp. 79—92

FERENCZ, CS.: *Electromagnetic Wave Propagation in Inhomogeneous Media: Method of Inhomogeneous Basic Modes*

The paper gives a calculation method for electromagnetic wave pattern in a group of inhomogeneous media. It shows that the given pattern may always be executed if the solution exists. It analyses and justifies the most important properties of the method. Based on that it gives a critical analysis of the Appleton—Hartree formula and shows examples of application.

Acta Techn. Hung. **86** (1978), pp. 93—115

DULÁCSKA, E.: *Buckling of r. c. Shell Structures*

The paper extends the possibility for the application of the indentation theory of elastic shell structures over the field of reinforced concrete shells. In doing this, the creep, plastic behaviour, the cracks of the tenson flange of cross sections and the position and quantity of the reinforcement are taken into account. The critical load to be determined by the worked out method is in good agreement with the results of the experiments.

Acta Techn. Hung. **86** (1978), pp. 117—129

SÁNDOR, I.: *Rheological Investigation of the Theory of Soil Consolidation*

The theory of consolidation of the one-dimension soil of compressible porosity is dealt with. With the aid of a rheological model the differential equation is established which is a fourt-order partial differential equation. In this way a general equation is yielded which takes the creep into account and which was as yet not to be found in the special literature. Two models are compared and, as a special case of them, the equation is established found by FLORIN (1953) on the basis of mechanical considerations. The statements valid for the rheological models are summarized and completed. For the solution of the partial differential equation the methods of the linear algebra are used, namely the grid-line method which, due to lack of space, is not dealt with on the basis of several numerical examples statements have been made laying particular stress on creep in the theory of soil consolidation.

Acta Techn. Hung. **86** (1978), pp. 147—156

TERSZTYÁNSZKY, T.—TUSNÁDY, G.: *An Estimation of the Maximum Loads of Interconnexions*

Loads in excess of transmission capacities of tie-lines may cause system disturbances. The paper presents a theoretical method which can be used for determining the probability of maximum loads of random character occurring above a given value. The obtained theoretical values are compared with data measured in practice. The method is suitable for planning the reliability of interconnexions between electrical power systems.

Acta Techn. Hung. **86** (1978), pp. 157—167

DULÁCSKA, E.: *The Initial Eccentricity to be Taken into Account in Investigating Local Buckling of Shell Structures*

The eccentricity of the stresses developed in the small wall significantly reduces the magnitude of the critical load causing local buckling of the shell, therefore, it is of great importance of taking exactly into account eccentricities. The paper deals with the determination of the eccentricity caused by initial random waviness and edge disturbances.

Acta Techn. Hung. **86** (1978), pp. 169—213

FERENCZ, CS.: *Electromagnetic Wave Propagation: The Analysis of the Group Velocity*

The paper gives a detailed analysis of energy propagation, the group velocity. It critically investigates the commonly used definition of group velocity. It examines in detail the defineability of average energy with suppositions and consequences. Using the "method of inhomogeneous basic modes", it investigates the group velocity in strictly linear and quasi-linear, dispersive media, deducing the group velocity directly from Maxwell's equations. It shows examples of practice and sees the consequences of the results on an important question of relativistic electrodynamics and propagation of different modes of modulation.

Acta Techn. Hung. **86** (1978), pp. 215—229

SZALATKAY, I.: *Elastic Properties of the Reinforced Earth*

Reinforced earth is a composite material made up of soil layers and steel strips placed on each other. Mechanical characterization of this material can be achieved by two conventional methods: one is the theory of plasticity, the other is the theory of elasticity. Accordingly, the structural design methods can be classified as bearing capacity oriented and as deformation specifications oriented. Bearing capacity is calculated from the known plastic behaviour of the reinforced earth, while the deformation or strain of the reinforced earth retaining walls and slabs can be calculated from the elastic properties of the material. Estimation of the elastic constants requires the knowledge of the elastic parameters of the soil and steel, and the geometry of the reinforcement. From the constants of the transversally anisotropic material the tilting of the reinforced earth wall and the settlement of the reinforced earth slabs are computable.

The *Acta Technica* publish papers on technical subjects in English, French, German and Russian.

The *Acta Technica* appear in parts of varying size, making up one volume.

Manuscripts should be addressed to

Acta Technica
H-1051 Budapest
Münnich Ferenc u. 7.
Hungary

Correspondence with the editors and publishers should be sent to the same address.

Subscription rate: $ 36.00 a volume.

Orders may be placed with "Kultura" Foreign Trading Company (H-1389 Budapest 62, P. O. B. 149. Account No. 218-10990) or its representatives abroad.

Les *Acta Technica* paraisent en français, allemand, anglais et russe et publient des travaux du domaine des sciences techniques.

Les *Acta Technica* sont publiés sous forme de fascicules qui seront réunis en volumes.

On est prié d'envoyer les manuscrits destinés à la rédaction à l'adresse suivante:

Acta Technica
H-1051 Budapest
Münnich Ferenc u. 7.
Hongrie

Toute correspondance doit être envoyée à cette même adresse.

Le prix de l'abonnement: $ 36.00 par volume.

On peut s'abonner à l'Entreprise du Commerce Extérieur «Kultura» (H-1389 Budapest 62, P. O. B. 149. Compte courant No. 218-10990) on chez représentants à l'étranger.

«*Acta Technica*» публикуют трактаты из области технических наук на русском, немецком, английском и французском языках.

«*Acta Technica*» выходят отдельными выпусками разного объема. Несколько выпусков составляют один том.

Предназначенные для публикации рускописи следует направлять по адресу:

Acta Technica
H-1051 Budapest
Münnich Ferenc u. 7.
Венгрия

По этому же адресу направлять всякую корреспонденцию для редакции и администрации.

Подписная цена — $ 36.00 за том. Заказы принимает предприятие по внешней торговле «Kultura» (H-1389 Budapest 62, P. O. B. 149 Текущий счет № 218-10990) или его заграничные представительства и уполномоченные.

Reviews of the Hungarian Academy of Sciences are obtainable at the following addresses:

AUSTRALIA
C.B.D. LIBRARY AND SUBSCRIPTION SERVICE, Box 4886, G.P.O. *Sydney N.S.W. 2001*
COSMOS BOOKSHOP, 135 Ackland Street, *St. Kilda (Melbourne), Victoria 3182*

AUSTRIA
GLOBUS, Höchstädtplatz 4, *1200 Wien* XX

BELGIUM
OFFICE INTERNATIONAL DE LIBRAIRIE, 30 Avenue Marnix, *1050 Bruxelles*
LIBRAIRIE DU MONDE ENTIER, 162 Rue du Midi, *1000 Bruxelles*

BULGARIA
HEMUS, Bulvar Ruszki 6, *Sofia*

CANADA
PANNONIA BOOKS, P.O. Box 1017, Postal Station "B", *Toronto, Ontario M5T 2T8*

CHINA
CNPICOR, Periodical Department, P.O. Box 50, *Peking*

CZECHOSLOVAKIA
MAD'ARSKÁ KULTURA, Národní třida 22, *115 66 Praha*
PNS DOVOZ TISKU, Vinohrádská 46, *Praha 2*
PNS DOVOZ TLAČE, *Bratislava 2*

DENMARK
EJNAR MUNKSGAARD, Norregade 6, *1165 Copenhagen*

FINLAND
AKATEEMINEN KIRJAKAUPPA, P.O. Box 128, *SF-00101 Helsinki 10*

FRANCE
EUROPERIODIQUES S. A., 31 Avenue de Versailles, *78170 La Celle St. Cloud*
LIBRAIRIE LAVOISIER, 11 rue Lavoisier, *75008 Paris*
OFFICE INTERNATIONAL DE DOCUMENTATION ET LIBRAIRIE, 38 rue Gay-Lussac, *75240 Paris Cedex 05*

GERMAN DEMOCRATIC REPUBLIC
HAUS DER UNGARISCHEN KULTUR, Karl-Liebknecht-Strasse 9, *DDR-102 Berlin*
DEUTSCHE POST ZEITUNGSVERTRIEBSAMT, Strasse der Pariser Kommüne 3—4, *DDR-104 Berlin*

GERMAN FEDERAL REPUBLIC
KUNST UND WISSEN ERICH BIEBER, Postfach 46, *7000 Stuttgart 1*

GREAT BRITAIN
BLACKWELL'S PERIODICALS DIVISION, Hythe Bridge Street, *Oxford OX1 2ET*
BUMPUS, HALDANE AND MAXWELL LTD., Cower Works, *Olney, Bucks MK46 4BN*
COLLET'S HOLDINGS LTD., Denington Estate, *Wellingborough, Northants NN8 2QT*
W.M. DAWSON AND SONS LTD., Cannon House, *Folkestone, Kent CT19 5EE*
H. K. LEWIS AND CO., 136 Gower Street, *London WC1E 6BS*

GREECE
KOSTARAKIS BROTHERS, International Booksellers, 2 Hippokratous Street, *Athens-143*

HOLLAND
MEULENHOFF-BRUNA B.V., Beulingstraat 2, *Amsterdam*
MARTINUS NIJHOFF B.V., Lange Voorhout 9—11, *Den Haag*
SWETS SUBSCRIPTION SERVICE, 347b Heereweg, *Lisse*

INDIA
ALLIED PUBLISHING PRIVATE LTD., 13/14 Asaf Ali Road, *New Delhi 110001*
150 B-6 Mount Road, *Madras 600002*
INTERNATIONAL BOOK HOUSE PVT. LTD., Madame Cama Road, *Bombay 400039*
THE STATE TRADING CORPORATION OF INDIA LTD., Books Import Division, Chandralok 36 Janpath, *New Delhi 110001*

ITALY
EUGENIO CARLUCCI, P.O. Box 252, *70100 Bari*
INTERSCIENTIA, Via Mazzé 28, *10149 Torino*
LIBRERIA COMMISSIONARIA SANSONI, Via Lamarmora 45, *50121 Firenze*
SANTO VANASIA, Via M. Macchi 58, *20124 Milano*
D. E. A., Via Lima 28, *00198 Roma*

JAPAN
KINOKUNIYA BOOK-STORE CO. LTD., 17-7 Shinjuku-ku 3 chome, Shinjuku-ku, *Tokyo 160-91*
MARUZEN COMPANY LTD., Book Department, P.O. Box 5056 Tokyo International, *Tokyo 100-31*
NAUKA LTD. IMPORT DEPARTMENT, 2-30-19 Minami Ikebukuro, Toshima-ku, *Tokyo 171*

KOREA
CHULPANMUL, *Phenjan*

NORWAY
TANUM-CAMMERMEYER, Karl Johansgatan 41—43, *1000 Oslo*

POLAND
WĘGIERSKI INSTYTUT KULTURY, Marszałkowska 80, *Warszawa*
CKP I W ul. Towarowa 28 *00-958 Warsaw*

ROMANIA
D. E. P., *Bucureşti*
ROMLIBRI, Str. Biserica Amzei 7, *Bucureşti*

SOVIET UNION
SOJUZPETCHATJ — IMPORT, *Moscow* and the post offices in each town
MEZHDUNARODNAYA KNIGA, *Moscow G-200*

SPAIN
DIAZ DE SANTOS, Lagasca 95, *Madrid 6*

SWEDEN
ALMQVIST AND WIKSELL, Gamla Brogatan 26, *101 20 Stockholm*
GUMPERTS UNIVERSITETSBOKHANDEL AB Box 346, *401 25 Göteborg 1*

SWITZERLAND
KARGER LIBRI AG, Petersgraben 31, *4011 Basel*

USA
EBSCO SUBSCRIPTION SERVICES, P.O. Box 1943, *Birmingham, Alabama 65201*
F. W. FAXON COMPANY, INC., 15 Southwest Park, *Westwood, Mass, 02090*
THE MOORE-COTTRELL SUBSCRIPTION AGENCIES, *North Cohocton, N. Y. 14838*
READ-MORE PUBLICATIONS, INC., 140 Cedar Street, *New York, N. Y. 10003*
STECHERT-MACMILLAN, INC., 7250 Westfield Avenue, *Pennsauken* N. J. 08110

VIETNAM
XUNHASABA, 32, Hai Ba Trung, *Hanoi*

YUGOSLAVIA
JUGOSLAVENSKA KNJIGA, Terazije 27, *Beograd*
FORUM, Vojvode Mišića 11, *21000 Novi Sad*

15. VIII. 1978 HU ISSN 0001—7035 Index: 26.025

ACTA TECHNICA

ACADEMIAE SCIENTIARUM HUNGARICAE

REDIGIT: M. MAJOR

TOMUS 86
FASCICULI 3—4

AKADÉMIAI KIADÓ, BUDAPEST 1978

ACTA TECHNICA

Az *Acta Technica* angol, francia, német és orosz nyelven közöl értekezéseket a műszaki tudományok köréből.

Az *Acta Technica* változó terjedelmű füzetekben jelenik meg, több füzet alkot egy kötetet.

A közlésre szánt kéziratok a következő címre küldendők:

Acta Technica
1051 Budapest, Münnich Ferenc u. 7.

Ugyanerre a címre küldendő minden szerkesztőségi és kiadóhivatali levelezés.

Megrendelhető a belföld számára az „Akadémiai Kiadó"-nál (1363 Budapest Pf. 24. Bankszámla 215 11448), a külföld számára pedig a „Kultura" Külkereskedelmi Vállalatnál (1389 Budapest 62, P. O. B. 149 Bankszámla: 218-10990) vagy annak külföldi képviseleteinél és bizományosainál.

Die *Acta Technica* veröffentlichen Abhandlungen aus dem Bereiche der technischen Wissenschaften in deutscher, englischer, französischer und russischer Sprache.

Die *Acta Technica* erscheinen in Heften wechselnden Umfanges. Vier Hefte bilden einen Band.

Die zur Veröffentlichung bestimmten Manuskripte sind an folgende Adresse zu senden:

Acta Technica
H-1051 Budapest,
Münnich Ferenc u. 7.
Ungarn

An die gleiche Anschrift ist auch jede für die Schriftleitung und den Verlag bestimmte Korrespondenz zu richten.

Abonnementspreis pro Band: $ 36.00.

Bestellbar bei »Kultura« Außenhandelsunternehmen (H-1389 Budapest 62, P. O. B. 149 Bankkonto Nr. 218-10990) oder seinen Auslandsvertretungen.

IN MEMORIAM PROFESSOR GY. MIHAILICH

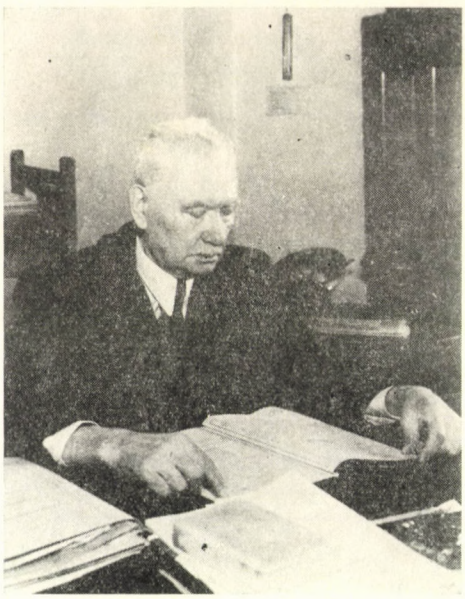

"Non omnis moriar . . ."

Diese Zeilen sollen dem Andenken des vor einem Jahrhundert geborenen Gelehrten, Prof. Győző MIHAILICH, Mitglied der Ungarischen Akademie der Wissenschaften gewidmet sein, den seine Fachkenntnisse, seine technische Erfindungsgabe, seine Entschlossenheit und sein sicheres Urteilsvermögen zu einem der größten ungarischen Ingenieure erhoben. Seine markante Person bestimmte ihn während langer Jahrzehnte zur leitenden Persönlichkeit der ungarischen Ingenieurgesellschaft. Sein Name war weit über die Grenzen Ungarns bekannt und geachtet.

GYŐZŐ MIHAILICH wurde 1877 in Temesrékás, einer kleinen Ortschaft des Banats, als Sohn des Gemeindenotars geboren. Das Gymnasium absolvierte er im Herzen der ungarischen Tiefebene, in Kecskemét, von wo er nach Budapest kam und 1899 an der Technischen Universität das Ingenieurdiplom erwarb. Hier erlangte er in rascher Reihenfolge als Assistent am Lehrstuhl des berühmten Professors ANTAL KHERNDL den wissenschaftlichen Grad eines Doktors der technischen Wissenschaften, den Titel eines Privatdozenten und wurde kurz danach als Lehrbeauftragter mit dem Vortrag des Gegenstandes Stahlbetonkonstruktionen betraut. Im Jahre 1916 wurde ihm der Titel eines außerordentlichen Universitätsprofessors verliehen und 1920 wurde er zum öffentlichen ordentlichen Professor an dem damals errichteten II. Lehrstuhl für

Brückenbau ernannt. Diesen Arbeitskreis versah er 37 Jahren lang, bis zu seiner in 1957 erfolgten Pensionierung. Inzwischen bekleidete er mehrmals das Amt eines Dekans der Fakultät für Ingenieure und war zweimal auch Rektor der Technischen Universität.

Seine Aufmerksamkeit galt bereits zu Beginn seiner Laufbahn der damals noch in ihren Anfängen befindlichen und in Ungarn wenig bekannten Stahlbetonbauweise. Sein erster Plan, den er noch als Student der Universität ausarbeitete und der, die konstruktive Lösung einer Stahlbetonbalkenbrücke zum Gegenstand hatte, wurde an der Pariser Weltausstellung von 1900 mit einer Belobungsurkunde ausgezeichnet. Von nun an befaßte er sich noch eingehender mit der Entwicklung des ungarischen Stahlbetonbauwesens und leistete zusammen mit Prof. Dr. Szilárd Zielinszki bahnbrechende Arbeit auf diesem Gebiet.

Seine ersten wissenschaftlichen Aufsätze waren auch den zeitgemäßen Fragen des Stahlbetonbaues gewidmet. In der Wochenzeitschrift des Ungarischen Ingenieur- und Architektenverbandes behandelte er in zahlreichen Aufsätzen die bedeutendsten Schöpfungen des ausländischen Stahlbetonbaues und in der Zeitschrift *Beton und Eisen* schrieb er einen Aufsatz über die von ihm geplante Stahlbeton-Balkenbrücke über die Bega in Temesvár, die seinerzeit die größte Spannweite von Brücken dieser Art aufwies. Dieses Werk errang auch in den ausländischen Fachkreisen allgemeine Anerkennung. Dieser Erfolg förderte die Entwicklung des Stahlbetonbaues in Ungarn in so hohem Maße, daß auf diesem Gebiet zahlreiche, weit größere Länder übertroffen wurden.

Sein Name als Konstrukteur ist mit einer ganzen Reihe großer Schöpfungen verbunden. Außer der bereits erwähnten Bega-Brücke in Temesvár ist die Theiß-Brücke in Szolnok zu nennen (Zeitschrift des Ungarischen Ingenieur- und Architektenvereins, 1912) die die erste Stahlbrücke in Ungarn mit Strebenfachwerk war. Die Fahrbahnplatte dieser Brücke wurde in Stahlbeton ausgeführt und stellt eine vollauf neue Konstruktion dar. Er entwarf auch die Pläne der Stahlbetonbrücken über die Flüße Sebes Körös in Berekböszörmény (1910) und Fekete Körös bei Temeshida (1912). Nach seinen Plänen wurde die Margit-Brücke in Budapest verstärkt und verbreitert (1929). Er beteiligte sich am Wettbewerb der Planung der Budapester Árpád-Brücke und gewann mit Prof. János Kossalka den I. und II. Preis. Er beteiligte sich auch am Wettbewerb der Planung der Budapester Petőfi-Brücke und errang den II. Preis.

Er entwarf auch den Getreidespeicher im Freihafen von Csepel (*Beton und Eisen*, 1929), wo in Ungarn erstmalig eine Pilzdecke und Gleitschalung Anwendung fanden. An seinen Namen knüpft sich auch der Entwurf der Stahlkonstruktion der Autobusgarage in der Szabó József-Gasse in Budapest (*Die Bautechnik*, 1931), die eine neuartige, aus Rahmenträgern und aus zwischen diese gesenkten Oberlichtstreifen bestehende Konstruktion ist.

Eines der bedeutendsten Produkte seiner wissenschaftlichen Tätigkeit ist das 1922 ausgegebene Lehrbuch *Stahlbetonkonstruktionen*, das der Ungarische Ingenieur- und Architektenverein mit der goldenen Medaille auszeichnete. Gestützt auf reiche Versuchsergebnisse befaßte sich der Autor in diesem Werk mit den verschiedenen zeitgemäßen Problemen des Stahlbetonbaues, mit ihrer Lösung, ja mit bis dahin unbekannten Lösungen. Das Buch war jahrzehntenlang das einzige Lehrbuch bzw. Handbuch, das den am Stahlbetonbau interessierten Kreisen zur Verfügung stand. So war es ein langentbehrtes Werk, von größter Bedeutung.

Das dem Lehrstuhl angeschlossene Forschungsinstitut leistete ausgedehnte Forschungsarbeiten. Die bedeutendsten dieser auch von der Wissenschaftlichen Széchenyi Gesellschaft unterstützten Versuche bezogen sich auf die mit Siliziumstahl bewehrten T-Träger. Über die Ergebnisse dieser Versuche berichtete Prof. MIHAILICH am in 1932 abgehaltenen Kongreß der Internationalen Vereinigung für Brückenbau und Hochbau als Abgesandter der ungarischen Regierung, sowie in seiner Eigenschaft als Vizepräsident eines Unterausschußes des Kongresses. Mit seienen Versuchen hat er nachgewiesen, daß die Schubbewehrung der Balken der üblichen Bewehrung gegenüber ohne Gefährdung der Sicherheit wesentlich vermindert werden kann. Später führte er im Anschluß an diese Versuchsreihe Untersuchungen von, mit Flußstahl- und Stahlbewehrung versehenen, mit Portland- und Bauxitzement angefertigten T-Trägern durch (*Anyagvizsgálók Közlönye*, 1934). In seiner Antrittsvorlesung an der Akademie der Wissenschaften befaßte er sich mit dem Einfluß der Wärmewirkungen auf die Festigkeit der Bauxitbetone (*Matematikai és Természettudományi Értesítő*, 1926). Seine diesbezüglichen Versuche waren für die Festigkeitseigenschaften des Bauxitbetons von grundlegender Bedeutung. Sehr wertvoll erwiesen sich auch die Versuche, die er zwecks Ermittlung der Eigenschaften der ungarischen Zemente vornahm (*Acta Techn. Hung.*, 1952). Diese befaßten sich vornehmlich mit dem Schwinden der Betone, sowie mit der Wirkung der Dampfbehandlung und der Haftung der Bewehrungsstähle an den Beton. Zahlreiche seiner Aufsätze sind der stets fortschreitenden Entwicklung des Stahlbetonbaues bzw. ihren künftigen Entwicklungsmöglichkeiten gewidmet.

Nach seiner 1957 — in seinem 80. Lebensjahr — erfolgten Pensionierung setzte er seine literarische Tätigkeit fort. Zu dieser Zeit verfaßte er das Werk "*Geschichte des ungarischen Brückenbaues im 19. und 20. Jahrhundert*", dann unter Mitwirkung seines Mitarbeiters Prof. LÁSZLÓ PALOTÁS das Buch "*Stahlbetonlehre*". Die Ausgabe seines mit seinem Mitarbeiter GYŐZŐ HAVIÁR verfaßten Buches "*Anfänge des Stahlbetonbaues und die ersten Stahlbetonbauten in Ungarn*" konnte er leider nicht mehr erleben.

Neben seiner Lehr- und Forschungstätigkeit spielte er auch im öffentlichen Leben eine bedeutende Rolle. Jahre hindurch war er Präsident und

Leiter der Budapester Ingenieurskammer, dann Direktor des von ihm angeregten Fortbildungsinstituts für Ingenieure. In seiner Eigenschaft als Präsident des Stahlbetonausschusses nahm er lebhaften Anteil an der Arbeit des Ungarischen Ingenieur- und Architektenvereins, sowie an jener des Vereins der Ungarischen Werkstoffprüfer. Unter seiner Leitung wurde unter anderen 1931 die neue Stahlbetonvorschrift angefertigt.

In Anerkennung seiner umfassenden fachmännischen und wissenschaftlichen Tätigkeit wurde er 1933 zum korrespondierenden und 1949 zum ordentlichen Mitglied der Ungarischen Akademie der Wissenschaften gewählt. Im Rahmen der Akademie bekleidete er jahrelang die Stellung eines Präsidenten der Sektion für technische Wissenschaften, beteiligte sich eingehend an den Arbeiten der verschiedenen Ausschüsse der Akademie, vornehmlich an der des Hauptausschußes für Bauwissenschaften, deren Präsident er während eines Jahrzehntes war. In Würdigung seiner Tätigkeit wurde er zum Ehrenpräsidenten des Hauptausschußes gewählt.

Sowohl die ungarische Regierung, als auch die ungarischen und ausländischen Universitäten würdigten seine Tätigkeit durch Verleihung von hohen Auszeichnungen. 1938 wurde Prof. MIHAILICH das Komturkreuz des Ungarischen Republik verliehen. 1948 erhielt er die höchste ungarische Auszeichnung, den goldenen Grad des Kossuth-Preises. 1950 wurde er mit dem Verdienstorden III. Klasse der Ungarischen Volksrepublik ausgezeichnet. Der Präsidialrat der Ungarischen Volksrepublik verlieh Prof. MIHAILICH im Jahre 1957 den Verdienstorden der Roten Fahne und 1962 den Orden der Arbeit. Anläßlich seines 80. und 85. Geburtstages wurden ihm, sowohl seitens der Technischen Universität für Bau- und Verkehrswissenschaften feierliche Ehrungen zuteil, aber auch ausländische Fachkreise würdigten seine Schöpfungen mit großer Anerkennung. Bei dieser Gelegenheit würdigten die Fachzeitschriften: "*Die Bautechnik*" und "*Beton- und Stahlbetonbau*" eingehend die Verdienste, die Prof. MIHAILICH auf dem Gebiet der Entwicklung des Stahlbetonbaues erwarb.

Die Budapester Technische Universität zeichnete Prof. MIHAILICH 1948 für seine wertvolle wissenschaftliche Tätigkeit mit der Verleihung des wissenschaftlichen Grades eines Dr. E. h. aus. Derselbe Titel wurde ihm 1954 von der Dresdner Technischen Universität zugesprochen. Das diesbezügliche Diplom überreichte ihm feierlich eine Abordnung der Dresdner Technischen Universität, an deren Spitze der Rektor der Universität stand.

Anläßlich der hundersten Jahreswende des Geburtstages des hervorragenden Gelehrten, Professors und ungarischen Ingenieurs gedenken wir seiner in tiefer Ehrfuhrt. Zwar verließ er uns, doch wird sein an Schöpfungen reiches Leben stets als ein edles Beispiel einer hervorragenden Persönlichkeit dienen. Seine kühnen Brückenkonstruktionen großer Spannweiten, seine hochragenden, stolzen Bauwerke werden zahlreiche Generationen hindurch den Ruf und die

unvergänglichen Verdienste des gelehrten Professors verkünden. Seinen hochsinnigen Geist werden seine Tätigkeit immer bezeugen. Das Andenken an seine markannte Persönlichkeit, die ein langes Menschenleben hindurch dem Unterricht der jungen Ingenieurgeneration und der Fortentwicklung der ungarischen technischen Wissenschaften diente, wird nicht erlöschen.

GYŐZŐ MIHAILICH ist verschieden, doch als Unsterblicher in das Pantheon der großen ungarischen Ingenieure eingezogen.

P. Csonka

Acta Technica Academiae Scientiarum Hungaricae, Tomus 86 (3—4), pp. 237—269 (1978)

A LOGIC THEORY OF HAZARDS AND ITS APPLICATION TO COMBUSTION PROCESSES

K. POLINSZKY

MEMBER OF THE HUNG. AC. OF SCI.

BÁTOR B.—GY. FÁY—J. FÜLÖP—R. TŐRÖS

[Manuscript received: 26 June 1975]

The aim of the present paper is to introduce a theory of hazards, and an actual application thereof. This theory describes the idea of hazards by logic rather than by an algebraic quantity. The introduction informs on how to model the hazards of any actually operating plant. As an application of the theory of hazards, a study on combustion processes using the method of stationary thermal conditons will be described. Then, on this basis the coefficients of combustion process hazards are determined. With these factors known, the hazards of all the elementary events feasible in the area associated with the combustion processes will be theoretically calculated, by taking into full account the preconditons of hazards.

Introduction

In 1972, one of the major scientific organizations of the United States, the Institute of Electrical and Electronics Engineers (IEEE) had elaborated in a methodical manner [1] a logical procedure for the studies on hazards, applicable for the facilities of nuclear energy production. This method is based on the observation that the factors making an equipment (nuclear reactors, steam boiler, pressure vessel, etc.) hazardous can rather be described by a collection of yes-or-no statements, than by differential equations, continuous and analytical functions, or similar means preferred in mathematical physics.

It was recognized, furthermore, that the hazards of an equipment cannot be calculated in that sense, for example, as its strength, operational temperature, or pressure is usually determined, designed, and dimensioned. The hazards of an equipment are far more estimated than calculated.

The hazards of an equipment considered hazardous in practice are represented by a two-valued physical quantity, if it is expressed in the terminology of physical description. These two values are the two logical values of a proposition or statement: the "yes" and the "no", or the "true" and the "false".

It was nuclear reactor engineering, in the elaboration of which, as in publicly known, some of the top mathematical authorities of the world like J. von NEUMANN and G. BIRKHOFF [2] have also participated, where it was recognized for the first time that the parameters involved and most essential

from the aspect of hazards would greatly differ from other physical quantities characteristic of reactors. This difference is expressed by the fact that the characteristics used to describe the hazards are correlated in quite another way than the physical properties. Here, for example, pressure and volume are never multiplied with each other (although this product would undoubtedly characterize the hazards, among others, in one way or another), but the factors of exposure to danger are "conjugated".

Such a factor may be the temperature increase in the equipment

$$\Delta T > 0,$$

while another one might be represented by the increaded concentration of the fuel:

$$\Delta C > 0.$$

The joint effect of the above two factors can be described by the expression

$$(\Delta T > 0) \wedge (\Delta C > 0)$$

where $\wedge$ is the symbol of the logical conjunction and it means "and" or "et".

The effect of the factors of hazards may be simultaneous or alternative. The simultaneous effect of these factors can be described by their conjunction, while that of the alternative factors (jointly considered in logics, but not necessarily jointly encountered) by their disjunction. In the previous example, the fact that at least one of the temperature and concentration of an equipment has greatly increased, may be described by the following logical expression:

$$(\Delta T > 0) \vee (\Delta C > 0)$$

which is the disjunction of the two factors (the two events $\Delta T > 0$ and $\Delta C > 0$). This is another peculiar operation in mathematical logics, quite different from those usually performed with numbers, as addition, multiplication, etc.

The factors of hazards may be implied by each other. For example, an increased concentration may cause temperature increase. In such cases the following expression may be written:

$$(\Delta C > 0) \Rightarrow (\Delta T > 0).$$

This is a relation between the hazard factors, resembling from several aspects the relation "being larger than" in connection with numbers, such as asymmetrical, transitive, etc. The coefficients of exposure to hazards have their reverse expressions as well. Thus the reverse of $\Delta T > 0$ is

$$\Delta T \leq 0.$$

It is easy to realize that the reverse of

$$(\Delta T > 0) \wedge (\Delta C > 0)$$

is

$$(\Delta T \leq 0) \vee (\Delta C \leq 0).$$

Verbally, the reverse of increasing both temperature and concentration is that at least one of them will not increase. The individual chapters of mathematical logics deal with the regularities of the "and", "or", "if — then", "no", etc. operations and relations. These can be described and used in the same exact way as, for example, the four operations of arithmetic. The paragraphs below summarize the formal basic knowledge made use of in the logic theory of the factors of hazards. These, by the way, coincide with the operations of the so-called "event algebra" employed in probability theory and with those of the "proposition algebra", the other concretization of Boole algebra widely used in computation engineering.

To sum up, the concept of hazard factor covers the following ideas:

(1) If p is a physical quantity and Δp a change in p, then the statement (event, relation)

$$\Delta p > 0$$

is a hazard factor.

(2) The reverse of a hazard factor is again a hazard factor, that is, if then the statement (event, relation)

$$\Delta p \leq 0$$

is again a hazard factor.

(3) If a and b are hazard factors then the events

$$a \wedge b, \text{ and } a \vee b$$

futhermore, a' and b'
are similarly hazard factors; here

$a \wedge b$ is the conjunction of a and b,
$a \vee b$ means the disjunction of a and b, and
a' (b') represents the reverse of a resp. (b).

The mathematical definition of conjunction, disjunction, and reverse, respectively, is given below.

To begin with, two events hazard factor are considered equal if they are mutually implied by each other or, in the form of an expression:

We say $a = b$, if $a > b$ and $b > a$

Attention: Here the term "and" cannot be replaced by the symbol $\wedge$, since $a > b$ and $b >$ are not hazard factors anylonger, only statements about them.

In order to define the fundamental equations of the hazard factors two more auxiliary notions have to be introduced: the absolute hazardous and the absolute harmless events (hazard factors). The former, denoted by I. means every event that is implied by any event together with its denial, such as

$$(\Delta T > 0) \vee (\Delta T \leq 0)$$

since out of a hazard factor and of its reverse at least one has to be hazardous (in the above example $\Delta T > 0$ is really dangerous although, when freezing $\Delta T \leq 0$ will become the actually hazardous event).

A fundamental feature of the logical theory of hazards is that the absolute dangerous events are not distinguished. Thus the absolute hazardous event

$$(\Delta C > 0) \vee (\Delta C \leq 0)$$

is considered to be equal to $(\Delta T > 0) \vee (\Delta T \leq 0)$ above, although the two cannot be said to be mutually implied.

On this basis the absolute dangerous event can now be discussed as denoted by a single letter symbol, say I. An absolute harmless event, on the other hand, is which brings about every and any other event together with its reverse, as

$$(\Delta T > 0) \wedge (\Delta T \leq 0).$$

Although this never takes place, but if it ever would, we could arrive at the conclusion that, among others, $\Delta T > 0$ and, of course, $\Delta T \leq 0$. In other words, the $(\Delta T > 0)$ statement, together with its reverse, would follow from an absolute harmless event. Just as in the case of the absolute hazardous events, here again only one absolute harmless event may exist, denoted by 0. It might be said that absolute hazardous is the event which always takes place, while absolute harmless is which never occurs. This clarifies the basic concept of the logic of hazards and, accordingly, the fundamental rules of the logic of exposure to hazards may now be set up.

The first two rules assure that the grouping of the hazard factors is irrelevant whenever more than two such factors are dealt with either simultaneously or alternatively:

$$(L_1) \quad a \wedge (b \wedge c) = (a \wedge b) \wedge c$$

$$(L_2) \quad a \vee (b \vee c) = (a \vee b) \vee c$$

L_1 and L_2 are the associative laws of the hazard factors.

The second two rules express the indifference of the order of the hazard factors in the case of their conjunctions and disjunctions:

$$(L_3) \quad a \wedge b = b \wedge a,$$

$$(L_4) \quad a \vee b = b \vee a.$$

The third two rules describe how the factors of danger surpass each other. If factor "a" may be spoken about in connection with "b", both simultaneously and alternatively, then "a" will be the decisive factor in the following sense:

$$(L_5) \quad a \wedge (b \vee a) = a,$$

$$(L_6) \quad a \vee (b \wedge a) = a.$$

These are the superiority laws of hazards.

The fourth pair of rules describe the formal relation of the coffecients of hazards to their respective reverse:

$$(L_7) \quad a \wedge a' = 0,$$

$$(L_8) \quad a \vee a' = I.$$

This includes by stipulation, that only one opposite hazard factor pertains to every hazard factor and that only a finite number of hazard factor exist.

By means of laws L_1—L_8 it is easy to show that the following two pairs of rules, are also valid:

$$(L_9) \quad a \wedge (b \vee c) = (a \wedge b) \vee (a \wedge c),$$

$$(L_{10}) \quad a \vee (b \wedge c) = (a \vee b) \wedge (a \vee c).$$

the distributive laws of hazards, and

$$(L_{11}) \quad (a \wedge b)' = a' \vee b',$$

$$(L_{12}) \quad (a \vee b)' = a' \wedge b'$$

the De Morgan law of exposure to danger.

The logic theory of hazards can readily be elaborated on this algebraic basis as will be shown later on.

Now a few words on the evaluation of the coefficients of hazards, as this has not even been touched upon yet. In other words, it has not been mentioned wether the event expressed by the hazard factor would actually occur or not?

From now on the danger value of the hazard factor (or event) x will be denoted by the symbol $v(x)$.

Let us assume only two possibilities: event x will either take place or not.

If x occurs then its danger value is 1, so we write

$$v(x) = 1.$$

If, on the other hand, x does not occur then

$$v(x) = 0$$

is written, and the danger value of the hazard factor (or event) x is said to be 0.

Clearly, the danger value of an absolute harmless event is 0, while that of an absolute dangerous one equals 1, that is,

$$v(0) = 0, \qquad v(I) = 1.$$

Another assumption on the value of hazards is that

$$v(x') = 1 - v(x),$$
$$v(x \vee y) + v(x \wedge y) = v(x) + v(y).$$

If a number $v(x)$ between 0 and 1 is assigned to every x event, and if in the case of $x \neq 0$ we have

$$v(x) \neq 0$$

then a quantitative theory of hazards can be elaborated. For example, if the events x and y turn a to be in the relationship

$$v(x) > v(y)$$

then it might be said that x is more dangerous than y. Thus, a theory can be developed in this direction as well.

Application of the theory

1. *Examination of the combustion process*

In order to illustrate what has been said so far, let us now take an actual example whereby all the principal notions of the theory may be clearly presented.

The example will be based on a combustion chamber model, in the form elaborated by VULIS [4] and his Hungarian followers [5], [6].

The method of the stationary thermal conditions was established by VULIS [4] in the early fifties. Essentially, the method determines relationship between data characteristic of the firing. This requires certain assumptions, of course, and the latter determine both the validity and structure of said relationships and the number as well as character of the physical properties taken into consideration. In recent years our Institute has worked out a diagram technique for the VULIS method, in the very first phase of the research only for the simplest, although in practice, already a quite promising case.

The research work involved the participation of ANDRÁS BÉKÉSSY, and the results were reported on in a brief publication [5] [6]. The present paper mainly deals with the problems of stability.

In the following paragraphs, starting out from a simplified, so-called null-dimension model of the combustion process, a practicable calculation technique will be elaborated, whose formalism can be applied for even the models of more sophisticated combustion processes. However, the reduction itself will not be illustrated in detail but only by a suitable model example, so the possibility of involving other secondary features of the combustion process, as well as, to the discussion will not be dealt with, either, as the essentials of the method to be presented, designed by VULIS as referred to above, can readily be understood even on the basis of the simplest model.

Let us take a vessel Fig. 1, to which a gas mixture is introduced at a certain rate.

Immediately after its introduction to the reaction area the compound will there be uniformly mixed so an homogeneous distribution will develop in the entire space. The condition of the gas leaving the vessel corresponds to the same. In a unit time a G amount of mixture enters the vessel combustion chamber with concentration c_0, and the same quantity will leave it, but with concentration c. The gas entering the combustion chamber is characterized by two data: temperature T_0 and by the stoichiometric concentration c_0, while the characteristics of the outlet gas are T and c.

Since in a unit time a G amount of mixture enters the combustion chamber with concentration c_0, and the same quantity will leave it but with concentration c, the material transformation per unit time will be

$$G(c_0 - c).$$

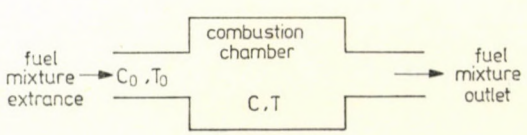

Fig. 1

If a first order reaction rate mass effect law is assumed then the following mass balance can be written:

$$G(c_0 - c) = G_k k_0 \exp(-E/RT) \cdot c \tag{2}$$

where G_k is the weight of the mixture always present in the combustion chamber (firing extensity),
k_0 is the "pre-exponential coefficient" of the reaction rate constant,
E means the activation energy,
R is the ideal gas constant, and
G represents the "firing intensity".

If the symbols

$$\Theta = \frac{RT}{E},$$

$$\tau = \frac{G}{k_0 G_k} = \left(\frac{1}{\tau_{\pi k}}\right), \tag{3}$$

are introduced, from (2) we obtain

$$\frac{c_0 - c}{c} = \frac{1}{\tau} e^{-1/\Theta} \tag{4}$$

Similarly to the mass balance the thermal equilibrium, too, may be expressed by assuming that the chemical reaction takes place under isolated conditions and, therefore, the heat thus produced will increase the enthalpy. If the specific heat pertaining to the constant pressure is considered as being constant, the heat released in the unit time will be

$$Q_{\mathrm{I}} = G(c_0 - c)q \tag{5}$$

where q is the reaction heat per unit weight. The enthalpy increase of the mixture will amount to

$$Q_{\mathrm{II}} = Gc_p(T - T_0). \tag{6}$$

Thus the thermal balance by (5) and (6) will be expressed by

$$G(c_0 - c)\, q = Gc_p(T - T_0). \tag{7}$$

If the expression

$$\frac{c_p}{c_0 q} \frac{E}{R} = \frac{1}{\vartheta} \tag{8}$$

is now introduced, we obtain

$$\frac{c_0 - c}{c_0} = \frac{1}{\vartheta}(\Theta - \Theta_0). \tag{9}$$

It can easily be seen that heat production and dissipation specify two different functions $c(\theta)$ according to (4) and (9). If now the new variable

$$\varphi = \frac{c_0 - c}{c_0} \tag{10}$$

is introduced then (6) and (9) may be written in a simplified form, and from (6) we obtain

$$\varphi(1 - \varphi) = \tau \exp\left(-\frac{1}{\theta}\right),$$

that is,

$$\varphi = \frac{1}{1 + \tau^{-1} e^{1/\Theta}} \tag{11}$$

This is called, as it has been obtained by the transformation of the heat production equation (4), the transformed heat production function, or briefly the emission function. Similarly, from (10) we obtain

$$\varphi = \frac{1}{\vartheta}(\theta - \theta_0) \tag{12}$$

and $\varphi(\theta,\theta_0,\vartheta)$ is known as the transformed heat dissipation or, briefly, the absorption function.

Now let us study the features of these functions and find out what physical conclusions might be arrived at therefrom.

First let us discuss the physical meaning of the quantities involved, then the relationship derived thereby and, finally, the stationary thermal conditions with, however, the relationships referred to always taken into full account.

Parameters G, G_k, c_0, and q are known to be given by the fuel and the equipment. G is the fuel flow, G_k means the weight of the fuel in the combustion chamber c_0 represents the initial stochiometric concentration of the fuel entering the combustion chamber and q, as the specific reaction heat, is the material characteristic of the fuel.

In addition, the description of the physical process involves, the basic quantities k_0, E, c_p, R, T, and c as well, whereof k_0, E, and c_p are material characteristics, denoting the reaction rate constant, the activation energy, and the specific heat at a constant pressure, while c and T are the state determinants of the combustion process. R is a universal constant. Thus, the complete combustion process is characterized by ten data:

$$T_0,\ c_0,\ k_0,\ E,\ c_p,\ G,\ G_k,\ T,\ c, \text{ and } q. \tag{13}$$

Five new quantities have been introduced earlier by transformations (5), (8), and (10):

$$\theta_0,\ \vartheta,\ \tau,\ \theta,\ \varphi. \tag{14}$$

These, according to (5), (8) and (10), are in the following relations to the ten data of (13):

$$\begin{aligned}
\theta_0 &= \frac{RT_0}{E}, \\
\vartheta &= \frac{c_0 q}{c_p} \cdot \frac{R}{E}, \\
\tau &= \frac{1G}{k_0 G_k}, \\
\theta &= \frac{RT}{E}, \\
\varphi &= \frac{c_0 - c}{c_0},
\end{aligned} \tag{15}$$

whereof only the last two depend on the state determinants T, c, so the first three are called transformed parameters, while θ and φ are known as transformed state determinants. By the way, transformation (15) is often referred to as similarity transformation. The data thus transformed are dimensionless n character, and yield two equations under stationary conditions:

$$\varphi = \frac{1}{1 + \tau e^{1/\theta}}, \tag{16}$$

$$\varphi = \frac{1}{\vartheta}(\theta - \theta_0). \tag{17}$$

Value pairs φ, θ, satisfying these two equations, represent the intersection points of the emission and absorption functions. Equations (16) and (17) involving the above five quantities determine two data. Thus if θ_0, ϑ, and τ are specified, then φ and θ can be calculated from (16) and (17). And since the expression under (16) is transcendent, both the easiest way of its solution and discussion is to do it graphically.

The best review is feasible by specifying two of the θ_0, ϑ, and τ parameters and varying the third one, then studying the development of the intersection point and combustion conditions as the function of it. Accordingly, the following cases may be encountered:

(a) θ_0, ϑ fixed, τ variable, (18)

(b) θ_0, τ fixed, ϑ variable, (19)

(c) ϑ, τ fixed, θ_0 changing. (20)

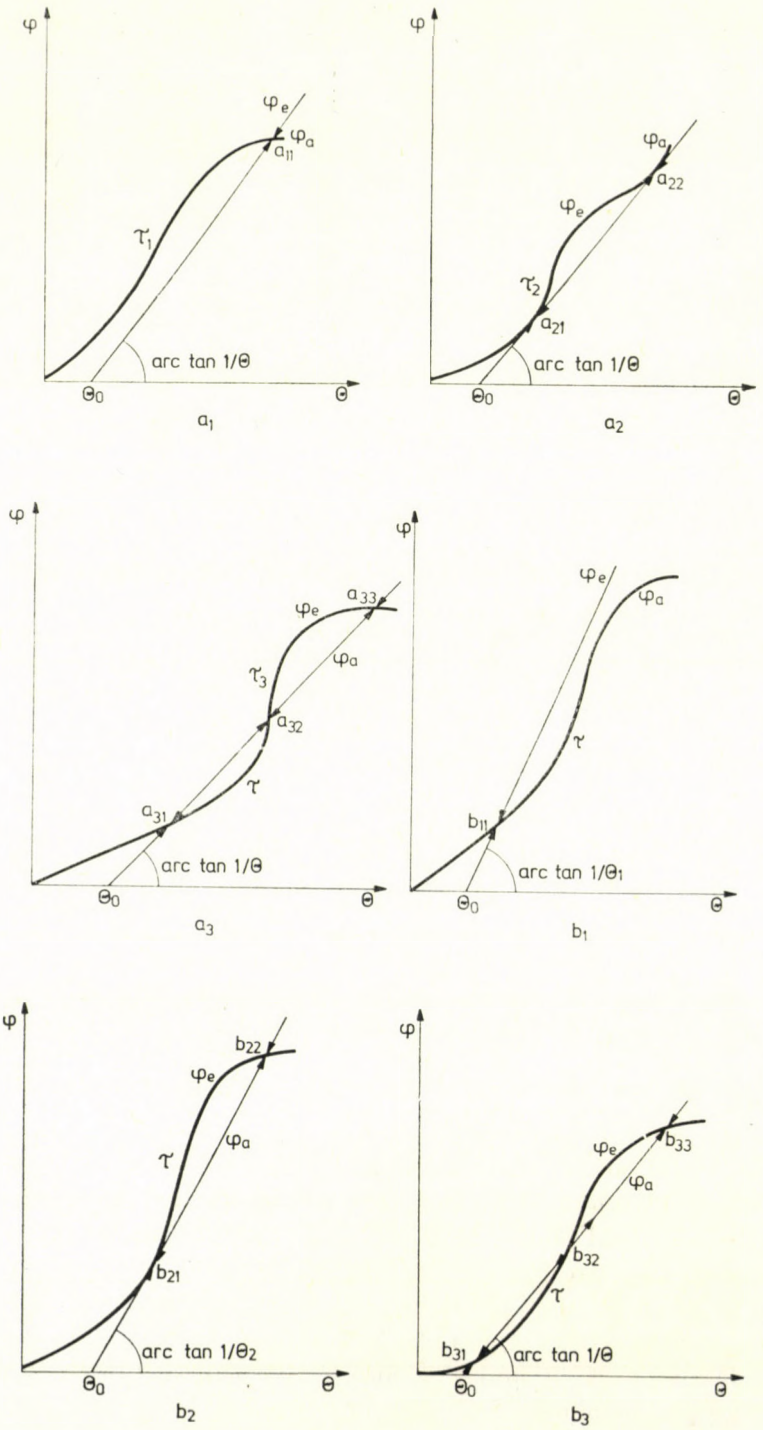
φ
φe
φa
a11
τ1
arc tan 1/Θ
Θ0
Θ
a1
φ
φa
a22
φe
τ2
a21
arc tan 1/Θ
Θ0
Θ
a2
φ
a33
φe
φa
τ3
a32
τ
a31
arc tan 1/Θ
Θ0
Θ
a3
φ
φe
φa
τ
b11
arc tan 1/Θ1
Θ0
Θ
b1
φ
b22
φe
φa
τ
b21
arc tan 1/Θ2
Θ0
Θ
b2
φ
φe
b33
φa
b32
τ
b31
arc tan 1/Θ
Θ0
Θ
b3

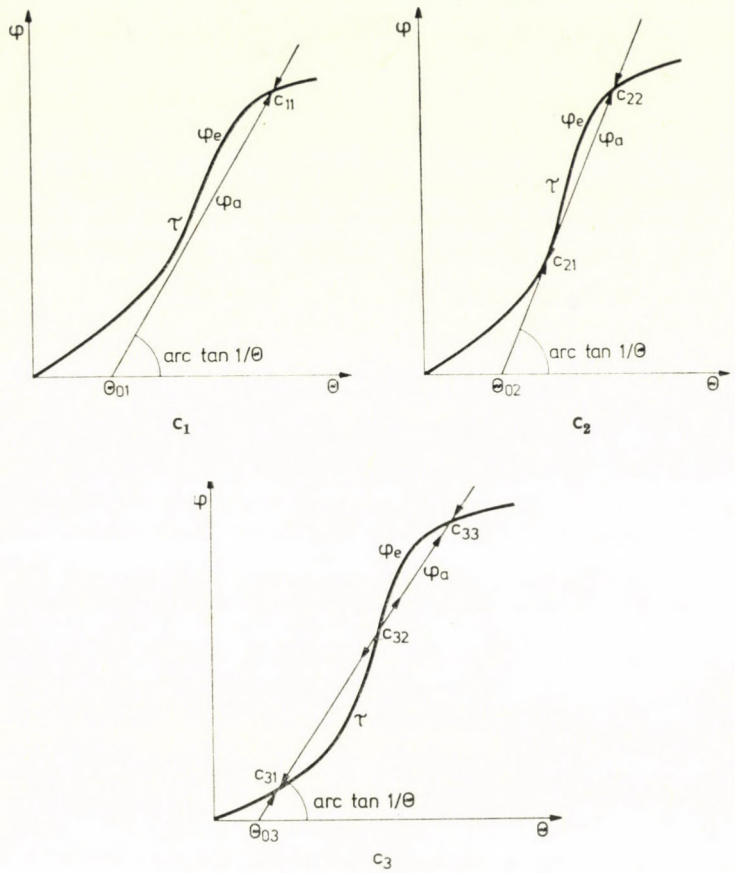

Fig. 2. Thermal condition types possible in practice

Theoretically, the number of intersections may be one, two, or three, in each case. It is not certain at all, on the other hand, whether at a joint fixed parameter pair value any of the three cases may be arrived at merely by changing the third parameter (this will happen only in case a_3 of the attached figures, see below).

Taking into consideration the possible number of points of intersection, a total of 9 cases will be feasible (Table I). In Table I all the states have been indicated where the number of the points of intersection is one, two, or three (singular, double, and triple states, respectively). The conditions corresponding to these 9 cases are illustrated in Figures 2/a_1, a_2, a_3; b_1, b_2, b_3; c_1, c_2, c_3. Symbols for the points of intersection include a letter symbol referring to the principal cases (*a*), (*b*) and (*c*) of (18) to (20), a first index applying to sub-cases 1., 2. and 3. of Table I, and a second index increasing with the similarly increasing ordinate values.

Table I

Cases	Fixed parameters	Variable parameters	No of the points of intersection (feasible stationary states) — "multiplicity"	Symbol of the points of intersection
a_1	θ_0, ϑ	τ	singular 1	a_{11}
a_2	θ_0, ϑ	τ	duble 2	a_{21} a_{22}
a_3	θ_0, ϑ	τ	triple 3	a_{31} a_{32} a_{33}
b_1	θ_0, τ	ϑ	singular 1	b_{11}
b_2	θ_0, τ	ϑ	duble 2	b_{21} b_{22}
b_3	θ_0, τ	ϑ	triple 3	b_{31} b_{32} b_{33}
c_1	ϑ, τ	θ_0	singular 1	c_{11}
c_2	ϑ, τ	θ_0	duble 2	c_{21} c_{22}
c_3	ϑ, τ	θ_0	triple 3	c_{31} c_{32} c_{33}

Fig. 2 reveals that two points of intersection are possibly only of at least one thereof is a tangent point.

Now let us study the physical states represented by the 9 possible points of intersection (a_{11} . . . c_{33}).

Obviously, a precondition of stability is to have a lower or higher emission function value when increasing or decreasing the temperature of the system than that of absorptions respectively, as this would mean that the heat absorbed within a unit volume per unit time would be greater or smaller, respectively, than the heat actually produced or, in other words, that the temperature of the system should attempt to decrease or increase, again respectively, that is, to restore its original value.

Left-side metastable (instable from the left, stable from the right) is the state where absorption exceeds emission upon either an increase or a decrease of the temperature, while right-side metastable (instable from the right and stable from the left) is any condition under which the emission would exceed absorption at a temperature increase and decrease alike.

In Fig. 2 the stable states are symbolized by arrows directed to the appropriate point, while the instable conditions by those following opposite directions from that point. The left and right-side metastable states are shown by connection-oriented arrows pointing to the left and right, respectively. These

arrows reveal, at the same time, the reaction trend of the system upon the effect of minor perturbations.

Following the discussion of the stable state conditions, let us now examine the so-called critical states. A stationary state, or the point representing such a state, is called critical if its state characteristics (or φ and θ co-ordinates) are not continuous functions of the parameters θ_0, ϑ, and τ.

Fig. 2. shows that all metastable states or tangent points, and only those are critical. Point a_{21}, for example, is critical because by any arbitrarily small variation of 2, line φ_a with parameters θ_0 will cease to touch the new emission curve whereby θ_{a21} will not be a continuous function of τ, anymore, since in the case of fixed θ_0, ϑ it is undefined for $\tau + \Delta\tau$ however small $\Delta\tau$ is.

Let us now examine a left-side metastable state, meaning that by decreasing either θ_0, ϑ or $1/\tau$ the double state will be transformed into a singular one, since the reduction of θ_0 would make φ_a shift to the left, parallel to itself, whereas an increased $1/\vartheta$ will make the straight line rotate anti-clockwise around θ_0, and an increase of τ^{-1} will cause the displacement of curve φ_e to the right. Thus φ_a and φ_e will not touch anylonger, in any of the three cases, no new intersection will be created and, therefore, actually a double to singular transition will occur.

Now what does this transition mean from physical aspects?

A reduction of θ_0 obviously means a cool-off for the mixture entering the system, that of ϑ a decrease of at least one of c_0 or q, according to (15), that is, a reduction of the thermal power of the mixture introduced, whereas a reduction of $1/\tau$ would lead, according to (3), to an increased rate of the mixture blown in. In our approach however, these three moments mean exactly the "blow-out" of the fire. It is, therefore, fully justified to call this leftside metastable state as the extinction point, since with the above phenomenon the existing state would be transformed into a state of a lesser temperature and lesser concentration variations

$$\varphi = \frac{c_0 - c}{c_0}$$

that is, oxidation would slow down (this is why a candle will keep on glowing after extinction).

The right-side metastable state can be interpreted in a similar way, but characterized by exactly the opposite moments. If the sytem is in this state (the right-side metastable state of a double case), then, upon any arbitrarily small temperature increase, the state would correspond to the only one possible c_{11} form. If, on the other hand, temperature θ_0 is slightly reduced, then, since the state is of the left-side stable type, no significant change will take place, but the system will attempt to return to its original condition. This phenomenon of ignition is well known: everyday experiences show that firing simply must

have a phase that will change over into a state of radically higher temperature when the temperature of the mixture feed is increased even to only an arbitrarily small degree (flash point). The same changeover will be experienced upon the increase of ϑ or $1/\tau$. The latter means that a reduction of the blast rate may lead to flash-up. According to another everyday experience, if the fire of barbecue place "does not want to start burning", we start blowing it and, if the blow is intensive, enough, flame-up will always follow.

Based on the above findings, it may be stated that the notions of metastable and critical conditions are equivalent, and that the left-side metastable conditions represent extinction points, while the right-side ones flash-up or ignition point cases, as such events will lead to increased ϑ and $1/\tau$ parameters, that is, to instability.

2. *Coefficients of hazards in the combustion process*

The reason why the combustion chamber model had to be discussed in such detail was to prove that the factors promoting the development of hazards would accumulate in only three theoretical values: θ_0, ϑ, and τ. Increasing any of them would transform the point of intersection of the heat production and thermal absorption curves into a tangent point, whereby a critical condition might be achieved.

From a practical viewpoint, therefore, the hazard factors will be those on which parameters θ, ϑ, and τ depend in a measurable and physically known way.

These are, as has been pointed out above, the physical quantities

$$T_0,\ c_0,\ G,\ k_0,\ E,\ c_p,\ q,\ \text{and}\ G_k$$

wherefrom the hazard factors are obtained by creating events of the

$$\Delta p > 0 \quad \text{or}$$

$$\Delta p < 0$$

form. An adequate discussion may be assumed in one of two schemes. It might be agreed that, for example, if a physical quantity p is reducing instead of increasing any of the hazard factors θ_0, ϑ and τ then p should be replaced by $1/p$ as in the case of k_0, E, or c_p. As another convention, however, instead of e.g. the event

$$\Delta \frac{1}{k_0} > 0$$

we may deal with the hazard factor

$$\Delta k < 0.$$

Hereafter the present paper will accept the latter.

Accordingly, the hazard factors of the Vulis combustion chamber will be

$$\Delta T_0 > 0,\ \Delta c_0 > 0,\ \Delta G > 0,\ \Delta k_0 > 0,\ \Delta E < 0,$$
$$\Delta c_p < 0,\ \Delta q > 0,\ \Delta G_k > 0.$$

These events represent a complete event system in the following sense. If they are denoted by $e_1, e_2, \ldots e_8$, then it might be said that the absolute dangerous situation will only occur if at least one of the above events takes place:

$$I \Rightarrow e_1 \vee e_2 \vee e_3 \vee e_4 \vee e_5 \vee e_6 \vee e_7 \vee e_8$$

or briefly

$$I \Rightarrow \bigvee_{i=1}^{8} e_i$$

and, separately for each $e_i (i = 1, \ldots 8)$:

$$e_i \Rightarrow I.$$

By means of this complete event system each element of the event scheme associated with the system in question (here the Vulis combustion chamber) can be readily obtained.

It is to be noted here that the literature usually adds to the complete event system idea the fact that the members (elements) of such a system exclude each other mutually. In our work such a system of events is known as a normalized event system whose elements are connected to create 8-member conjunctions consisting of the above $e_1, e_2, \ldots e_8$ events and their $e_1', e_2', \ldots e_8'$ opposites, in which each element or its reverse may occur only once. These conjunctions are regarded as elementary events.

Such an elementary event is, for example,

$$e_1' \wedge e_2' \wedge e_3 \wedge e_4 \wedge e_5 \wedge e_6 \wedge e_7' \wedge e_8$$

or, in an abbreviated form:

$$e_1' e_2' e_3 e_4 e_5 e_6 e_7' e_8$$

In our example this means that

$$\Delta T_0 \leq 0,\ \Delta c_0 \leq 0,\ \Delta G > 0,\ \Delta k_0 < 0,\ \Delta E < 0,$$
$$\Delta c_p < 0,\ \Delta q \leq 0,\ \Delta G_k = 0.$$

In other words, the firing system was affected by a disturbation in which five of the eight parameters, except temperature, concentration, and firing extensity, had been dangerously changed. Similarly, in the course of the

$$e_1 \wedge e_2 \wedge e_3 \wedge e_4 \wedge e_5 \wedge e_6 \wedge e_7 \wedge e_8$$

elementary event all the parameters have been modified to a dangerous degree, while the elementary event

$$e_1' \wedge e_2' \wedge e_3' \wedge e_4' \wedge e_5' \wedge e_6' \wedge e_7' \wedge e_8'$$

has been developed without any of the parameters having been changed to hazards.

Thus, the event scheme associated with the Vulis firing system may be said to have an 8-dimensional character, as the events in the combustion chamber are described by 8 variables. So it is easy to see that in the Vulis space the number of elementary events is $2^8 = 256$.

3. *Calculation of the hazardous states*

Certainly not all of the elementary events should be considered as hazardous. One of the fundamental duties of the theory of hazards is exactly to supply a method whereby it could be determined under the known conditions of hazards which of the elementary events would prove to be hazardous, and which not.

In order to illustrate the above statement, let us now deal with the conditions of hazards which are similarly statements but, in turn, of a character by means of which the hazards of the individual events might be assessed.

A typical example on the conditions of hazards may be found in the IEEE standard referred to in the Introduction of this paper (1), which is the generally accepted "2/3 condition". This means that in a threedimensional space of events an elementary event will be regarded to be dangerous if at least two of the three hazard factors vary in a dangerous way. Naturally, some other (simpler or more sophisticated) conditions of danger are also considered in practice. The condition of hazards we have the intention to discuss here is of the so-called

"all/one"

type. This means that an elementary event is regarded hazardous, if all the parameters increasing at least by one of the theoretical parameters θ_0, ϑ, and τ change dangerously.

This stipulation, rather complex at the first glance, is actually quite plausible and is often used in the theory of hazards.

In order to bring the "all/one" condition into mathematical form, let us consider the dependence of the parameters θ_0, ϑ, and τ on $T_0 \ldots G_k$ in the case of the Vulis model. From the aspects of the theory of hazards, this is summarized in the following Table:

Table II

Coefficients (events) of hazards	e_1	e_2	e_3	e_4	e_5	e_6	e_7	e_8
Physical-chemical parameters	T_0	c_0	G	$1/k_0$	$1/E$	$1/c_p$	q	$1/G_k$
Theoretical parameters								
θ_0	+				+			
ϑ		+			+	+	+	
τ			+	+				+

In this table the cross sign means that the physical-chemical parameter in that column will increase the theoretical fuel engineering parameter in the corresponding row.

Based on what has been so far said, all the disturbations and danger values can readily be determined now. The relevant calculation results are summarized in Table III.

Thus, for example, T_0 will increase θ_0 but not ϑ, $1/k_0$ is increasing τ, etc. It should not be forgotten that, from the aspects of the theory of hazards, only the increasing coefficients of θ_0, ϑ, and τ are interesting. Table III shows for example, that disturbation.

$$e_1' \wedge e_2 \wedge e_3 \wedge e_4 \wedge e_5' \wedge e_6' \wedge e_7 \wedge e_8' = D_{114}$$

is not dangerous, as it means that

$$c_0,\ G,\ 1/k_0,\ q, \text{ and } 1/G_k$$

have increased, but none of these five parameters include a group in which all the increasing factors of any of θ_0, ϑ or τ would occur since, for instance, those of θ_0 are e_1 and e_5, but e_1 cannot be found in D_{114}.

Similarly, the increasing factors of ϑ are e_2, *et*, e_6 and e_7, but only e_2 and e_7 can be discovered in D_{114}. Finally, the increasing factors of τ are e_3, e_4 and e_8, but D_{114} has no e_8.

A few words on the numbering of the disturbations. The total of 256 disturbations actually feasible are best numbered in such a manner that a conclusion should be arrived at from this numbering to the disturbation proper.

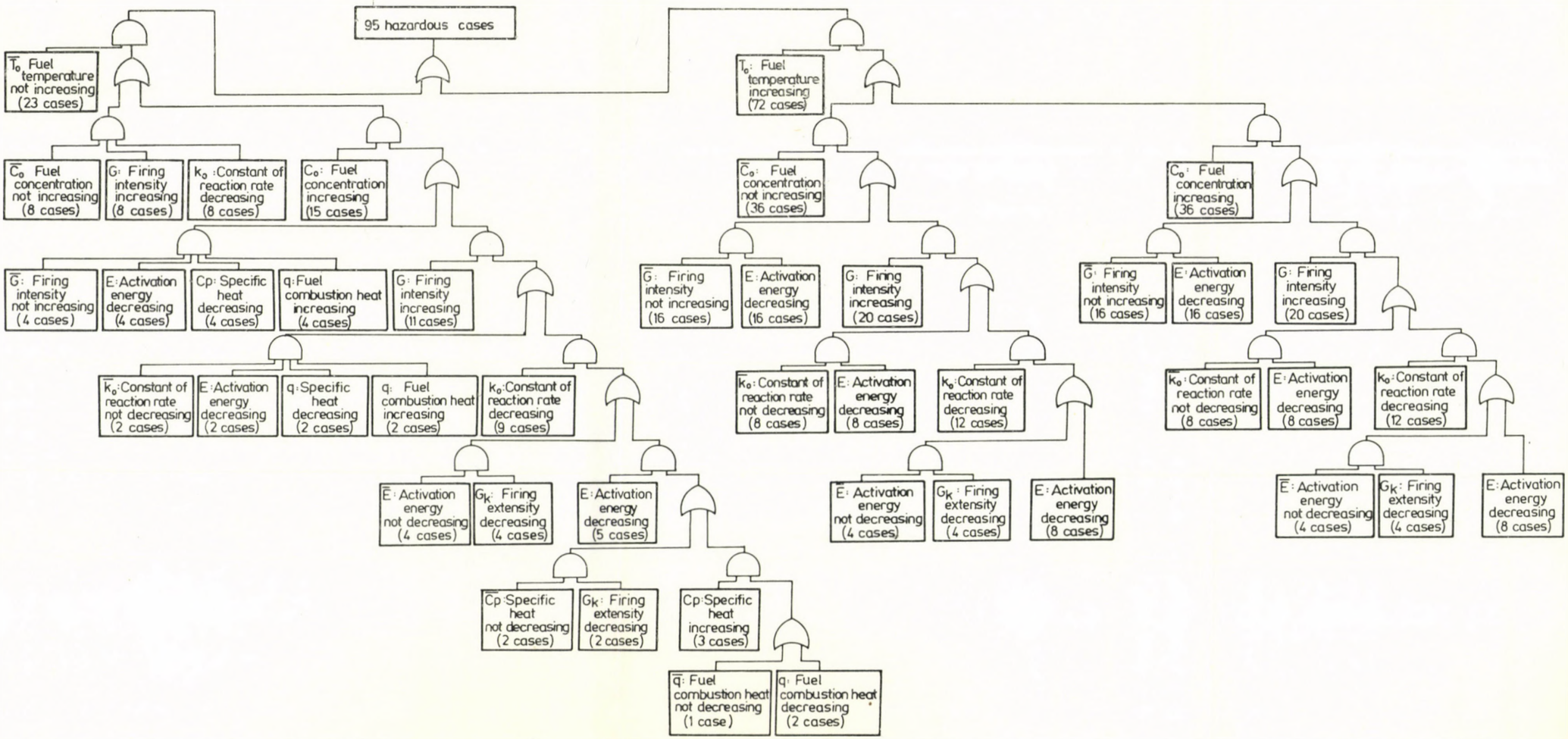
95 hazardous cases
$\overline{T_o}$ Fuel temperature not increasing (23 cases)
T_o: Fuel temperature increasing (72 cases)
$\overline{C_o}$ Fuel concentration not increasing (8 cases)
G: Firing intensity increasing (8 cases)
k_o :Constant of reaction rate decreasing (8 cases)
C_o: Fuel concentration increasing (15 cases)
$\overline{C_o}$: Fuel concentration not increasing (36 cases)
C_o: Fuel concentration increasing (36 cases)
$\overline{G}$: Firing intensity not increasing (4 cases)
E: Activation energy decreasing (4 cases)
Cp: Specific heat decreasing (4 cases)
q: Fuel combustion heat increasing (4 cases)
G: Firing intensity increasing (11 cases)
$\overline{G}$: Firing intensity not increasing (16 cases)
E: Activation energy decreasing (16 cases)
G: Firing intensity increasing (20 cases)
$\overline{G}$: Firing intensity not increasing (16 cases)
E: Activation energy decreasing (16 cases)
G: Firing intensity increasing (20 cases)
$\overline{k_o}$: Constant of reaction rate not decreasing (2 cases)
E: Activation energy decreasing (2 cases)
q: Specific heat decreasing (2 cases)
q: Fuel combustion heat increasing (2 cases)
k_o: Constant of reaction rate decreasing (9 cases)
$\overline{k_o}$: Constant of reaction rate not decreasing (8 cases)
E: Activation energy decreasing (8 cases)
k_o: Constant of reaction rate decreasing (12 cases)
$\overline{k_o}$: Constant of reaction rate not decreasing (8 cases)
E: Activation energy decreasing (8 cases)
k_o: Constant of reaction rate decreasing (12 cases)
$\overline{E}$: Activation energy not decreasing (4 cases)
G_k: Firing extensity decreasing (4 cases)
E: Activation energy decreasing (5 cases)
$\overline{E}$: Activation energy not decreasing (4 cases)
G_k: Firing extensity decreasing (4 cases)
E: Activation energy decreasing (8 cases)
$\overline{E}$: Activation energy not decreasing (4 cases)
G_k: Firing extensity decreasing (4 cases)
E: Activation energy decreasing (8 cases)
$\overline{Cp}$: Specific heat not decreasing (2 cases)
G_k: Firing extensity decreasing (2 cases)
Cp: Specific heat increasing (3 cases)
$\overline{q}$: Fuel combustion heat not decreasing (1 case)
q: Fuel combustion heat decreasing (2 cases)

Fig. 3

The so-called binary coding is the most suitable for this purpose. This is based on ordering to the events $e_1, e_2, \ldots e_8$ to the numbers

$$128 = 2^7, 64 = 2^6, 32 = 2^5, 16 = 2^4, 8 = 2^3,$$
$$4 = 2^2, 2 = 2^1, \text{ and } 1 = 2_0$$

and then multiply them by 1 or 0, according to whether the event itself, or its reverse plays a role in the disturbation. The products thus obtained are added up, and the result will be the serial or code number of the disturbation in question. For instance, in the above example the events

$$e_2, e_3 \quad \text{and} \quad e_7, e_4$$

are involved without, however, their reciprocals (the others are present reversed.)

Thus, the code will be

$$2^{8-2} \cdot 1 + 2^{8-3} \cdot 1 + 2^{8-4} \cdot 1 + 2^{8-7} \cdot 1 =$$
$$= 64 + 32 + 16 + 2 = 114$$

In a more detailed form, the code of the

$$e_1' \wedge e_2 \wedge e_3 \wedge e_4 \wedge e_5' \wedge e_6' \wedge e_7 \wedge e_8'$$

disturbation will be

$$2^{8-1} \cdot 0 + 2^{8-2} \cdot 1 + 2^{8-3} \cdot 1 + 2^{8-4} \cdot 1 + 2^{8-5} \cdot 0 +$$
$$+ 2^{8-6} \cdot 0 + 2^{8-7} \cdot 1 + 2^{8-8} \cdot 0 = 114.$$

Generally, a disturbation may be specified in an n-dimensional space of events by the following formula:

$$e_1^{\varepsilon_1} e_2^{\varepsilon_2} e_3^{\varepsilon_3} \ldots e_n^{\varepsilon_n}, \text{ where } \varepsilon_1 = 0 \text{ or } 1, \text{ and}$$

$$\begin{aligned} e_i^0 &= e_i, \\ e_i^1 &= e_i. \end{aligned} \qquad (i = 1, 2, \ldots, n)$$

In a still more concise form, the general form of disturbation may be written as

$$\bigwedge_{i=1}^{n} e_1^{\varepsilon_i}$$

while the serial number of the disturbation can be expressed, in general, as

$$2^{n-1} \cdot \varepsilon_1' + 2^{n-2} \cdot \varepsilon_2' + 2^{n-3} \cdot \varepsilon_3' + \ldots + 2^{n-n} \cdot \varepsilon_n'$$

where

$$\varepsilon_1' = 1 - \varepsilon_1, \qquad (i = 1, 2, \ldots, n)$$

Thus, again still more concisely, the serial number of disturbation

$$\bigwedge_{i=1}^{n} e^{\varepsilon_i}$$

will be

$$\sum_{i=1}^{n} 2^{n-i}\, \varepsilon_i' .$$

Let us see by way of an example, disturbation No 77:

$$77 = 64 + 8 + 4 + 1 = 2^{8-2} + 2^{8-5} + 2^{8-6} + 2^{8-8}$$

and since this resolution is clearly unique thus the events

$$2, 5, 6 \text{ and } 8$$

are contained by disturbation No 77 unreversed and the others reversed. Thus, we obtain

$$\mathrm{D}_{77} = e_1' \wedge e_2 \wedge e_3' \wedge e_4' \wedge e_5 \wedge e_6 \wedge e_7' \wedge e_8$$

which means that

$$\Delta T_0 \leq 0,\ \Delta c_0 > 0,\ \Delta G \leq 0,\ \Delta 1/k_0 \leq 0,\ (\Delta k_0 \geq 0),$$
$$\Delta 1/E > 0,\ (\Delta E < 0),\ \Delta 1/c_p > 0,\ (\Delta c_p < 0),$$
$$\Delta q \leq 0,\ \Delta 1/G_k > 0,\ (\Delta G_k < 0\}.$$

This is such a disturbation of the parameters, when

- the fuel temperature does not increase (T_0),
- the fuel concentration is increasing (c_0),
- firing intensity does not increase (G),
- the reaction rate constant will not decrease (k_0),
- the activation energy is decreasing (E),
- the specific heat at a constant pressure will decrease (c_p),
- combustion heat does not increase (q'), and
- the firing extensity (G_k) is decreasing.

Table III tells that this is not a hazardous disturbation as θ_0 does not increase through T_0, neither does ϑ by q, nor τ by either G or k_0.

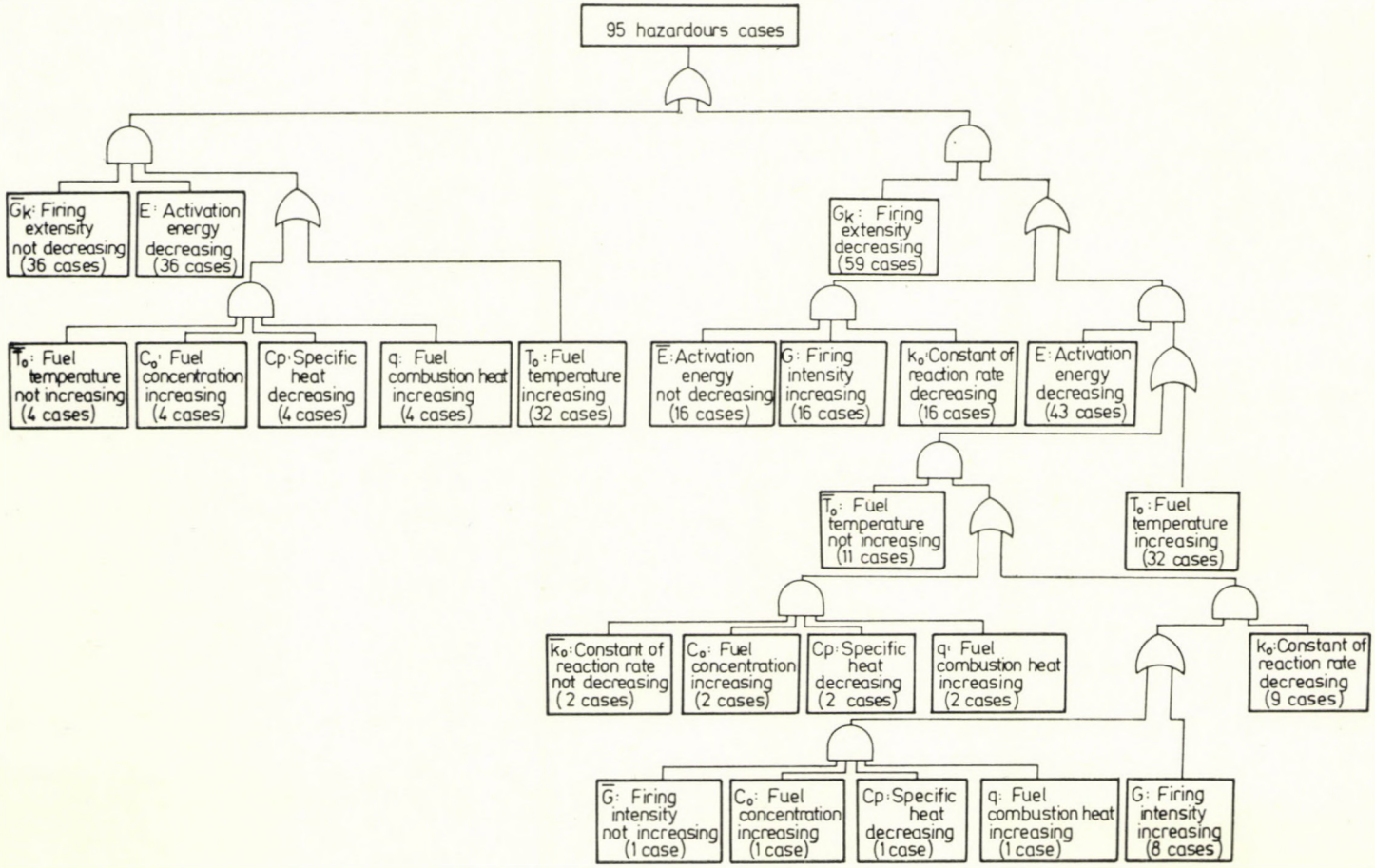
95 hazardours cases
$\bar{G}_k$: Firing extensity not decreasing (36 cases)
E: Activation energy decreasing (36 cases)
$\bar{T}_o$: Fuel temperature not increasing (4 cases)
C_o: Fuel concentration increasing (4 cases)
Cp: Specific heat decreasing (4 cases)
q: Fuel combustion heat increasing (4 cases)
T_o: Fuel temperature increasing (32 cases)
G_k: Firing extensity decreasing (59 cases)
$\bar{E}$: Activation energy not decreasing (16 cases)
G: Firing intensity increasing (16 cases)
k_o: Constant of reaction rate decreasing (16 cases)
E: Activation energy decreasing (43 cases)
$\bar{T}_o$: Fuel temperature not increasing (11 cases)
T_o: Fuel temperature increasing (32 cases)
$\bar{k}_o$: Constant of reaction rate not decreasing (2 cases)
C_o: Fuel concentration increasing (2 cases)
Cp: Specific heat decreasing (2 cases)
q: Fuel combustion heat increasing (2 cases)
k_o: Constant of reaction rate decreasing (9 cases)
$\bar{G}$: Firing intensity not increasing (1 case)
C_o: Fuel concentration increasing (1 case)
Cp: Specific heat decreasing (1 case)
q: Fuel combustion heat increasing (1 case)
G: Firing intensity increasing (8 cases)

Fig. 4

Table III

Dangerous disturbations

Sering № Serial	T_0 Temperature	c_0 Concentration	G Firing	k_0 Reaction rate constant	E Activation energy	c_p Specific heat	q Combustion heat	G_k Firing extensity	Hazards
0	No increase	No increase	No increase	No decrease	No decrease	No decrease	No increase	No decrease	Harmless
1	No increase	No increase	No increase	No decrease	No decrease	No decrease	No increase	Decreasing	Harmless
2	No increase	No increase	No increase	No decrease	No decrease	No decrease	Increasing	No decrease	Harmless
3	No increase	No increase	No increase	No decrease	No decrease	No decrease	Increasing	Decreasing	Harmless
4	No increase	No increase	No increase	No decrease	No decrease	Decreasing	No increase	No decrease	Harmless
5	No increase	No increase	No increase	No decrease	No decrease	Decreasing	No increase	Decreasing	Harmless
6	No increase	No increase	No increase	No decrease	No decrease	Decreasing	Increasing	No decrease	Harmless
7	No increase	No increase	No increase	No decrease	No decrease	Decreasing	Increasing	Decreasing	Harmless
8	No increase	No increase	No increase	No decrease	No decrease	Decreasing	Increasing	Decreasing	Harmless
9	No increase	No increase	No increase	No decrease	Decreasing	No decrease	No increase	Decreasing	Harmless
10	No increase	No increase	No increase	No decrease	Decreasing	No decrease	Increasing	No decrease	Harmless
11	No increase	No increase	No increase	No decrease	Decreasing	No decrease	Increasing	Decreasing	Harmless
12	No increase	No increase	No increase	No decrease	Decreasing	Decreasing	No increase	No decrease	Harmless
13	No increase	No increase	No increase	No decrease	Decreasing	Decreasing	No increase	Decreasing	Harmless
14	No increase	No increase	No increase	No decrease	Decreasing	Decreasing	Increasing	No decrease	Harmless
15	No increase	No increase	No increase	No decrease	Decreasing	Decreasing	Increasing	Decreasing	Harmless
16	No increase	No increase	No increase	Decreasing	No decrease	No decrease	No increase	No decrease	Harmless
17	No increase	No increase	No increase	Decreasing	No decrease	No decrease	No increase	Decreasing	Harmless
18	No increase	No increase	No increase	Decreasing	No decrease	No decrease	Increasing	No decrease	Harmless
19	No increase	No increase	No increase	Decreasing	No decrease	No decrease	Increasing	Decreasing	Harmless
20	No increase	No increase	No increase	Decreasing	No decrease	Decreasing	No increase	No decrease	Harmless
21	No increase	No increase	No increase	Decreasing	No decrease	Decreasing	No increase	No decrease	Harmless
22	No increase	No increase	No increase	Decreasing	No decrease	Decreasing	Increasing	No decrease	Harmless

23	No increase	No increase	No increase	Decreasing	No decrease	Decreasing	Increasing	Decreasing	Harmless
24	No increase	No increase	No increase	Decreasing	Decreasing	No decrease	No increase	No decrease	Harmless
25	No increase	No increase	No increase	Decreasing	Decreasing	No decrease	No increase	Decreasing	Harmless
26	No increase	No increase	No increase	Decreasing	Decreasing	No decrease	Increasing	No decrease	Harmless
27	No increase	No increase	No increase	Decreasing	Decreasing	No decrease	Increasing	Decreasing	Harmless
28	No increase	No increase	No increase	Decreasing	Decreasing	Decreasing	No increase	No decrease	Harmless
29	No increase	No increase	No increase	Decreasi g	Decreasing	Decreasing	No increase	Decreasing	Harmless
30	No increase	No increase	No increase	Decreasi g	Decreasing	Decreasing	Increasing	No decrease	Harmless
31	No increase	No increase	No increase	Decreasing	Decreasing	Decreasing	Increasing	Decreasing	Harmless
32	No increase	No increase	Increasing	No decrease	No decrease	No decrease	No increase	No decrease	Harmless
33	No increase	No increase	Increasing	No decrease	No decrease	No decrease	No increase	Decreasing	Harmless
34	No increase	No increase	Increasing	No decrease	No decrease	No decrease	Increasing	No decrease	Harmless
35	No increase	No increase	Increasing	No decrease	No decrease	No decrease	Increasing	Decreasing	Harmless
36	No increase	No increase	Increasing	No decrease	No decrease	Decreasing	No increase	No decrease	Harmless
37	No increase	No increase	Increasing	No decrease	No decrease	Decreasing	No increase	Decreasing	Harmless
38	No increase	No increase	Increasing	No decrease	No decrease	Decreasing	Increasing	No decrease	Harmless
39	No increase	No increase	Increasing	No decrease	No decrease	Decreasing	Increasing	Decreasing	Harmless
40	No increase	No increase	Increasing	No decrease	Decreasing	No decrease	No increase	No decrease	Harmless
41	No increase	No increase	Increasing	No decrease	Decreasing	No decrease	No increase	Decreasing	Harmless
42	No increase	No increase	Increasing	No decrease	Decreasing	No decrease	Increasing	No decrease	Harmless
43	No increase	No increase	Increasing	No decrease	Decreasing	No decrease	Increasing	Decreasing	Harmless
44	No increase	No increase	Increasing	No decrease	Decreasing	Decreasing	No increase	No decrease	Harmless
45	No increase	No increase	Increasing	No decrease	Decreasing	Decreasing	No increase	Decreasing	Harmless
46	No increase	No increase	Increasing	No decrease	Decreasing	Decreasing	Increasing	No decrease	Harmless
47	No increase	No increase	Increasing	Decreasing	No decrease	No decrease	No increase	No decrease	Harmless
48	No increase	No increase	Increasing	Decreasing	No decrease	No decrease	No increase	No decrease	Harmless
49	No increase	No increase	Increasing	Decreasing	No decrease	No decrease	No increase	Decreasing	Hazardous

Table III (continued)

Sering N° Serial	T_0 Temperature	c_0 Concentration	G Firing	k_0 Reaction rate constant	E Activation energy	c_p Specific heat	q Combustion heat	G_k Firing extensity	Hazards
50	No increase	No increase	Increasing	Decreasing	No decresae	No decraese	Increasing	No decrease	Harmless
51	No increase	No increase	Increasing	Decreasing	No decrease	No decrease	Increasing	Decreasing	Hazardous
52	No increase	No increase	Increasing	Decreasing	No decrease	Decreasing	No increase	No decrease	Harmless
53	No increase	No increase	Increasing	Decreasing	No decrease	Decreasing	No increase	Decreasing	Hazardous
54	No increase	No increase	Increasing	Decreasing	No decrease	Decreasing	Increasing	No decrease	Harmless
55	No increase	No increase	Increasing	Decreasing	No decrease	Decreasing	Increasing	Decreasing	Hazardous
56	No increase	No increase	Increasing	Decreasing	Decreasing	No decrease	No decrease	No decrease	Harmless
57	No increase	No increase	Increasing	Decreasing	Decreasing	No decrease	No increase	Decreasing	Hazardous
58	No increase	No increase	Increasing	Decreasing	Decreasing	No decrease	Increasing	No decrease	Harmless
59	No increase	No increase	Increasing	Decreasing	Decreasing	No decrease	Increasing	Decreasing	Hazardous
60	No increase	No increase	Increasing	Decreasing	Decreasing	Decreasing	No increase	No decrease	Harmless
61	No increase	No increase	Increasing	Decreasing	Decreasing	Decreasing	No increase	Decreasing	Hazardous
62	No increase	No increase	Increasing	Decreasing	Decreasing	Decreasing	Increasing	No decrease	Harmless
63	No increase	No increase	Increasing	Decreasing	Decreasing	Decreasing	Increasing	Decreasing	Hazardous
64	No increase	Increasing	No increase	No decrease	No decrease	No decrease	No increase	No decrease	Harmless
65	No increase	Increasing	No increase	No decrease	No decrease	No decrease	No increase	Decreasing	Harmless
66	No increase	Increasing	No increase	No decrease	No decrease	No decrease	Increasing	No decrease	Harmless
67	No increase	Increasing	No increase	No decrease	No decrease	No decrease	Increasing	Decreasing	Harmless
68	No increase	Increasing	No increase	No decrease	No decrease	Decreasing	No increase	No decrease	Harmless
69	No increase	Increasing	No increase	No decrease	No decrease	Decreasing	No increase	Decreasing	Harmless
70	No increase	Increasing	No increase	No decrease	No decrease	Decreasing	Increasing	No decrease	Harmless
71	No increase	Increasing	No increase	No decrease	No decrease	Decreasing	Increasing	Decreasing	Harmless
72	No increase	Increasing	No increase	No decrease	Decreasing	No decrease	No increase	No decrease	Harmless
73	No increase	Increasing	No increase	No decrease	Decreasing	No decrease	No increase	Decreasing	Harmless

74	No increase	Increasing	No increase	No decrease	Decreasing	No decrease	Increasing	No decrease	Harmless
75	No increase	Increasing	No increase	No decrease	Decreasing	No decrease	Increasing	Decreasing	Harmless
76	No increase	Increasing	No increase	No decrease	Decreasing	Decreasing	No increase	No decrease	Harmless
77	No increase	Increasing	No increase	No decrease	Decreasing	Decreasing	No increase	Decreasing	Harmless
78	No increase	Increasing	No increase	No decrease	Decreasing	Decreasing	Increasing	No decrease	Hazardous
79	No increase	Increasing	No increase	No decrease	Decreasing	Decreasing	Increasing	Decreasing	Hazardous
80	No increase	Increasing	No increase	Decreasing	No decrease	No decrease	No increase	No decrease	Harmless
81	No increase	Increasing	No increase	Decreasing	No decrease	No decrease	No increase	Decreasing	Harmless
82	No increase	Increasing	No increase	Decreasing	No decrease	No decrease	Increasing	No decrease	Harmless
83	No increase	Increasing	No increase	Decreasing	No decrease	No decrease	Increasing	Decreasing	Harmless
84	No increase	Increasing	No increase	Decreasing	No decrease	Decreasing	No increase	No decrease	Harmless
85	No increase	éncreasing	No increase	Decreasing	No decrease	Decreasing	No increase	Decreasing	Harmless
86	No increase	Increasing	No increase	Decreasing	No decrease	Decreasing	Increasing	No decrease	Harmless
87	No increase	Increasing	No increase	Decreasing	No decrease	Decreasing	Increasing	Decreasing	Harmless
88	No increase	Increasing	No increase	Decreasing	Decreasing	No decrease	No increase	No decrease	Harmless
89	No increase	Increasing	No increase	Decreasing	Decreasing	No decrease	Increasing	Decreasing	Harmless
90	No increase	Increasing	No increase	Decreasing	Decreasing	No decrease	Increasing	No decrease	Harmless
91	No increase	Increasing	No increase	Decreasing	Decreasing	No decrease	Increasing	Decreasing	Harmless
92	No increase	Increasing	No increase	Decreasing	Decreasing	Decreasing	No increase	No decrease	Harmless
93	No increase	Increasing	No increase	Decreasing	Decreasing	Decreasing	No increase	Decreasing	Harmless
94	No increase	Increasing	No increase	Decreasing	Decreasing	Decreasing	Increasing	No decrease	Hazardous
95	No increase	Increasing	No increase	No decrease	Decreasing	Decreasing	Increasing	Decreasing	Hazardous
96	No increase	Increasing	Increasing	No decrease	No decrease	No decrease	No increase	No decrease	Harmless
97	No increase	Increasing	Increasing	No decrease	No decrease	No decrease	No increase	Decreasing	Harmless
98	No increase	Increasing	Increasing	No decrease	No decrease	No decrease	Increasing	No decrease	Harmless
99	No increase	Increasing	Increasing	No decrease	No decrease	No decrease	Increasing	Decreasing	Harmless
100	No increase	Increasing	Increasing	No decrease	No decrease	Decreasing	No increase	No decrease	Harmless

Table III (continued)

Sering N« Serial	T_0 Temperature	c_0 Concentration	G Firing	k_0 Reaction rate constant	E Activation energy	c_p Specific heat	q Combustion heat	G_k Firing extensity	Hazards
101	No increase	Increasing	Increasing	No decrease	Decreasing	Decreasing	No incerease	Decreasing	Harmless
102	No increase	Increasing	Increasing	No decrease	No decrease	Decreasing	Increasing	No decrease	Harmless
103	No increase	Increasing	Increasing	No decrease	No decrease	Decreasing	Increasing	Decreasing	Harmless
104	No increase	Increasing	Increasing	No decrease	Decreasing	No decrease	No increasing	No decrease	Harmless
105	No increase	Increasing	Increasing	No decrease	Decreasing	No decrease	No increase	Decreasing	Harmless
106	No increase	Increasing	Increasing	No decrease	Decreasing	No decrease	Increasing	No decrease	Harmless
107	No increase	Increasing	Increasing	No decrease	Decreasing	No decrease	Increasing	Decreasing	Harmless
108	No increase	Increasing	Increasing	No decrease	Decreasing	Decreasing	No increase	No decrease	Harmless
109	No increase	Increasing	Increasing	No decrease	Decreasing	Decreasing	No increase	No decrease	Harmless
110	No increase	Increasing	Increasing	No decrease	Decreasiúg	Decreasing	Increasing	No decrease	Hazardous
111	No increase	Increasing	Increasing	No decrease	Decreasing	Decreasing	Increasing	Decreasing	Hazardous
112	No increase	éncreasing	Increasing	Decreasing	No decrease	No decrease	No increase	No decrease	Harmless
113	No increase	Increasing	Increasing	Decreasing	No decrease	No decrease	No increase	Decreasing	Hazardous
114	No increase	Increasing	Increasing	Decreasing	No decrease	No decrease	Increasing	No decrease	Harmless
115	No increase	Increasing	Increasing	Decreasing	No decrease	No decrease	Increasing	Decreasing	Hazardous
116	No increase	Increasing	Increasing	Decreasing	No decrease	Decreasing	No increase	No decrease	Harmless
117	No increase	Increasing	Increasing	Decreasing	No decrease	Decreasing	No increase	Decreasing	Hazardous
118	No increase	Increasing	Increasing	Decreasi g	No decrease	Decreasing	Increasing	No decrease	Harmless
119	No increase	Increasing	Increasing	Decreasing	No decrease	Decreasing	Increasing	Decreasing	Hazardous
120	No increase	Increasing	Increasing	Decreasing	Decreasing	No decrease	No increase	No decrease	Harmless
121	No increase	Increasing	Increasing	Decreasing	Decreasing	No decrease	No increase	Decreasing	Hazardous
122	No increase	Increasing	Increasing	Decreasing	Decreasing	No decrease	Increasing	No decrease	Harmless
123	No increase	Increasing	Increasing	Decreasing	Decreasing	No decrease	Increasing	Decreasing	Hazardous
124	No increase	Increasing	Increasing	Decreasing	Decreasing	Decreasing	No increase	Decreasing	Harmless

125	No increase	Increasing	Increasing	Decreasing	Decreasing	Decreasing	No increase	Decreasing	Hazardous
126	No increase	Increasing	Increasing	Decreasing	Decreasing	Decreasing	Increasing	No decrease	Hazardous
127	No increase	Increasing	Increasing	Decreasing	Decreasing	Decreasing	Increasing	Decreasing	Hazardous
128	Increasing	No increase	No increase	No decrease	No decrease	No decrease	No increase	No decrease	Harmless
129	Increasing	No increase	No increase	No decrease	No decrease	No decrease	No increase	Decreasing	Harmless
130	Increasing	No increase	No increase	No decrease	No decrease	No decrease	Increasing	No decrease	Harmless
131	Increasing	No increase	No increase	No decrease	No decrease	No decrease	Increasing	Decreasing	Harmless
132	Increasing	No increase	No increase	No decrease	No decrease	Decreasing	No increase	No decrease	Harmless
133	Increasing	No increase	No increase	No decrease	No decrease	Decreasing	No increase	Decreasing	Harmless
134	Increasing	No increase	No increase	No decrease	No decrease	Decreasing	Increasing	No decrease	Harmless
135	Increasing	No increase	No increase	No decrease	No decrease	Decreasing	Increasing	Decreasing	Harmless
136	Increasing	No increase	No increase	No decrease	Decreasing	No decrease	No increase	No decrease	Hardous
137	Increasing	No increase	No increase	No decrease	Decreasing	No decrease	No increase	Decreasing	Hardous
138	Increasing	No increase	No increase	No decrease	Decreasing	No decrease	Increasing	No decrease	Hardous
139	Increasing	No increase	No increase	No decrease	Decreasing	No decrease	Increasing	Decreasing	Hazardous
140	Increasing	No increase	No increase	No decrease	Decreasing	Decreasing	No increase	No decrease	Hazardous
141	Increasing	No increase	No increase	No decrease	Decreasing	Decreasing	No increase	Decreasing	Hazardous
142	Increasing	No increase	No increase	No decrease	Decreasing	Decreasing	Increasing	No decrease	Hazardous
143	Increasing	No increase	No increase	No decrease	Decreasing	Decreasing	Increasing	Decreasing	Hazardous
144	Increasing	No increase	No increase	Decreasing	No decrease	No decrease	No increase	No decrease	Harmless
145	Increasing	No increase	No increase	Decreasing	No decrease	No decrease	No increase	Decreasing	Harmless
146	Increasing	No increase	No increase	Decreasing	No decrease	No decrease	Increasing	No decrease	Harmless
147	Increasing	No increase	No increase	Decreasing	No decrease	No decrease	Increasing	Decreasing	Harmless
148	Increasing	No increase	No increase	Decreasing	No decrease	Decreasing	No increase	No decrease	Harmless
149	Increasing	No increase	No increase	Decreasing	No decrease	Decreasing	No increase	Decreasing	Harmless
150	Increasing	No increase	No increase	Decreasing	No decrease	Decreasing	Increasing	No decrease	Harmless
151	Increasing	No increase	No increase	Decreasing	No decrease	Decreasing	Increasing	Decreasing	Harmless

Table III (continued)

Sering № Serial	T_0 Temperature	c_0 Concentration	G Firing	k_0 Reaction rate constant	E Activation energy	c_p Specific heat	q Combustion heat	G_k Firing extensity	Hazards
152	Increasing	No increase	No increase	Decreasing	Decreasing	No decrease	No increase	No decrease	Hazardous
153	Increasing	No increase	No increase	Decreasing	Decreasing	No decrease	No increase	Decreasing	Hazardous
154	Increasing	No increase	No increase	Decreasing	Decreasing	No decrease	Increasing	No decrease	Hazardous
155	Increasing	No increase	No increase	Decreasing	Decreasing	No decrease	Increasing	Decreasing	Hazardous
156	Increasing	No increase	No increase	Decreasing	Decreasing	Decreasing	No increase	No decrease	Hazardous
157	Increasing	No increase	No increase	Decreasing	Decreasing	Decreasing	No increase	Decreasing	Hazardous
158	Increasing	No increase	No increase	Decreasing	Decreasing	Decreasing	Increasing	No decrease	Hazardous
159	Increasing	No increase	No increase	Decreasing	Decreasing	Decreasing	Increasing	Decreasing	Hazardous
160	Increasing	No increase	Increasing	No decrease	No decrease	No decrease	No increase	No decrease	Harmless
161	Increasing	No increase	Increasing	No decrease	No decrease	No decrease	No increase	Decreasing	Harmless
162	Increasing	No increase	Increasing	No decrease	No decrease	No decrease	Increasing	No decrease	Harmless
163	Increasing	No increase	Increasing	No decrease	No decrease	No decrease	Increasing	Decreasing	Harmless
164	Increasing	No increase	Increasing	No decrease	No decrease	Decreasing	No increase	No decrease	Harmless
165	Increasing	No increase	Increasing	No decrease	No decrease	Decreasing	No increase	Decreasing	Harmless
166	Increasing	No increase	Increasing	No decrease	No decrease	Decreasing	Increasing	No decrease	Harmless
167	Increasing	No increase	Increasing	No decrease	No decrease	Decreasing	Increasing	Decreasing	Harmless
168	Increasing	No increase	Increasing	No decrease	Decreasing	No decrease	No increase	No decrease	Hazardous
169	Increasing	No increase	Increasing	No decrease	Decreasing	No decrease	No increase	Decreasing	Hazardous
170	Increasing	No increase	Increasing	No decrease	Decreasing	No decrease	Increasing	No decrease	Hazardous
171	Increasing	No increase	Increasing	No decrease	Decreasing	No decrease	Increasing	Decreasing	Hazardous
172	Increasing	No increase	Increasing	No decrease	Decreasing	Decreasing	No increase	No decrease	Hazardous
173	Increasing	No increase	Increasing	No decrease	Decreasing	Decreasing	No increase	Decreasing	Hazardous
174	Increasing	No increase	Increasing	No decrease	Decreasing	Decreasing	Increasing	No decrease	Hazardous
175	Increasing	No increase	Increasing	No decrease	Decreasing	Decreasing	Increasing	Decreasing	Hazardous

176	Increasing	No increase	Increasing	Decreasing	No decrease	No decrease	No increase	No decrease	Harmless
177	Increasing	No increase	Increasing	Decreasing	No decrease	No decrease	No increase	Decreasing	Hazardous
178	Increasing	No increase	Increasing	Decreasing	No decrease	No decrease	Increasing	No decrease	Harmless
179	Increasing	No increase	Increasing	Decreasing	No decrease	No decrease	Increasing	Decreasing	Hazardous
180	Increasing	No increase	Increasing	Decreasing	No decrease	Decreasing	No increase	No decrease	Harmless
181	Increasing	No increase	Increasing	Decreasing	No decrease	Decreasing	No increase	Decreasing	Hazardous
182	Increasing	No increase	Increasing	Decreasing	No decrease	Decreasing	Increasing	No decrease	Harmless
183	Increasing	No increase	Increasing	Decreasing	No decrease	Decreasing	Increasing	Decreasing	Hazardous
184	Increasing	No increase	Increasing	Decreasing	Decreasing	No decrease	No increase	No decrease	Hazardous
185	Increasing	No increase	Increasing	Decreasing	Decreasing	No decrease	No increase	Decreasing	Hazardous
186	Increasing	No increase	Increasing	Decreasing	Decreasing	No decrease	Increasing	No decrease	Hazardous
187	Increasing	No increase	Increasing	Decreasing	Decreasing	No decrease	Increasing	Decreasing	Hazardous
188	Increasing	No increase	Increasing	Decreasing	Decreasing	Decreasing	No increase	No decrase	Hazardous
189	Increasing	No increase	Increasing	Decreasing	Uecreasing	Decreasing	No increase	Decreasing	Hazardous
190	Increasing	No increase	Increasing	Decreasing	Decreasing	Decreasing	Increasing	No decrease	Hazardous
191	Increasing	No increase	Increasing	Decreasing	Decreasing	Decreasing	Increasing	Decreasing	Hazardous
192	Increasing	Increasing	No increase	No decrease	No decrease	No decrease	No increase	No decrease	Harmless
193	Increasing	Increasing	No increase	No decrease	No decrease	No decrease	No increase	Decreasing	Harmless
194	Increasing	Increasing	No increase	No decrease	No decrease	No decrease	Increasing	No decrease	Harmless
195	Increasing	Increasing	No increase	No decrease	No decrease	No decrease	Increasing	Decreasing	Harmless
196	Increasing	Increasing	No increase	No decrease	No decrease	Decreasing	No increase	No decrease	Harmless
197	Increasing	Increasing	No increase	No decrease	No decrease	Decreasing	No increase	Decreasing	Harmless
198	Increasing	Increasing	No increase	No decrease	No decrease	Decreasing	Increasing	No decrease	Harmless
199	Increasing	Increasing	No increase	No decrease	No decrease	Decreasing	Increasing	Decreasing	Harmless
200	Increasing	Increasing	No increase	No decrease	Decreasing	No decrease	No increase	No decrease	Hazardous
201	Increasing	Increasing	No increase	No decrease	Decreasing	No decrease	No increase	Decreasing	Hazardous
202	Increasing	Increasing	No increase	No decrease	Decreasing	No decrease	Increasing	No decrease	Hazardous

Table III (continued)

Sering № Serial	T_0 Temperature	c_0 Concentration	G Firing	k_0 Reaction rate constant	E Activation energy	c_p Specific heat q	Combustion heat	G_k Firing extensity	Hazards
203	Increasing	Increasing	No increase	No decrease	Decreasing	No decrease	Increasing	Decreasing	Hazardous
204	Increasing	Increasing	No increase	No decrease	Decreasing	Decreasing	No increase	No decrease	Hazardous
205	Increasing	Increasing	No increase	No decrease	Decreasing	Decreasing	No increase	Decreasing	Hazardous
206	Increasing	Increasing	No increase	No decrease	Decreasing	Decreasing	Increasing	No decrease	Hazardous
207	Increasing	Increasing	No increase	No decrease	Decreasing	Decreasing	Increasing	Decreasing	Hazardous
208	Increasing	Increasing	No increase	Decreasing	No decrease	No decrease	No increase	No decrease	Harmless
209	Increasing	Increasing	No increase	Decreasing	No decrease	No decrease	No increase	Decreasing	Harmless
210	Increasing	Increasing	No increase	Decreasing	No decrease	No decrease	Increasing	No decrease	Harmless
211	Increasing	Increasing	No increase	Decreasing	No decrease	No decrease	Increasing	Decreasing	Harmless
212	Increasing	Increasing	No increase	Decreasing	No decrease	Decreasing	No increase	No decrease	Harmless
213	Increasing	Increasing	No increase	Decreasing	No decrease	Decreasing	No increase	Decreasing	Harmless
214	Increasing	Increasing	No increase	Decreasing	No decrease	Decreasing	Increasing	No decrease	Harmless
215	Increasing	Increasing	No increase	Decreasing	No decrease	Decreasing	Increasing	Decreasing	Harmless
216	Increasing	Increasing	No increase	Decreasing	Decreasing	No decrease	No increase	No decrease	Hazardous
217	Increasing	Increasing	No increase	Decreasing	Decreasing	No decrease	No increase	Decreasing	Hazardous
218	Increasing	Increasing	No increase	Decreasing	Decreasing	No decrease	No increase	No decrease	Hazardous
219	Increasing	Increasing	No increase	Decreasing	Decreasing	No decrease	Increasing	Decreasing	Hazardous
220	Increasing	Increasing	No increase	Decreasing	Decreasing	Decreasing	No increase	No decrease	Hazardous
221	Increasing	Increasing	No increase	Decreasing	Decreasing	Decreasing	No increase	Decreasing	Hazardous
222	Increasing	Increasing	No increase	Decreasing	Decreasing	Decreasing	Increasing	No decrease	Hazardous
223	Increasing	Increasing	No increase	Decreasing	Decreasing	Decreasing	Increasing	Decreasing	Hazardous
224	Increasing	Increasing	Increasing	No decrease	No decrease	No decrease	No increase	No decrease	Harmless
225	Increasing	Increasing	Increasing	No decrease	No decrease	No decrease	No increase	No decrease	Harmless
226	Increasing	Increasing	Increasing	No decrease	No decrease	No decrease	Increasing	Decreasing	Harmless

227	Increasing	Increasing	Increasing	No decrease	No decrease	No decrease	Increasing	No decrease	Harmless
228	Increasing	Increasing	Increasing	No decrease	No decrease	Decreasing	No increase	No decrease	Harmless
229	Increasing	Increasing	Increasing	No decrease	No decrease	Decreasing	No increase	Decreasing	Harmless
230	Increasing	Increasing	Increasing	No decrease	No decrease	Decreasing	Increasing	No decrease	Harmless
231	Increasing	Increasing	Increasing	No decrease	No decrease	Decreasing	Increasing	Decreasing	Harmless
232	Increasing	Increasing	Increasing	Decreasing	Decreasing	No decrease	No increase	No decrease	Hazardous
233	Increasing	Increasing	Increasing	Decreasing	Decreasing	No decrease	No increase	Decreasing	Hazardous
234	Increasing	Increasing	Increasing	Decreasing	Decreasing	No decrease	Increasing	No decrease	Hazardous
235	Increasing	Increasing	Increasing	Decreasing	Decreasing	No decrease	Increasing	Decreasing	Hazardous
236	Increasing	Increasing	Increasing	Decreasing	Decreasing	Decreasing	No increase	No decrease	Hazardous
237	Increasing	Increasing	Increasing	Decreasing	Decreasing	Decreasing	No increase	Decreasing	Hazardous
238	Increasing	Increasing	Increasing	Decreasing	Decreasing	Decreasing	Increasing	No decrease	Hazardous
239	Increasing	Increasing	Increasing	Decreasing	Decreasing	Decreasing	Increasing	Decreasing	Hazardous
240	Increasing	Increasing	Increasing	Decreasing	No decrease	Decreasing	No increase	No decrease	Harmless
241	Increasing	Increasing	Increasing	Decreasing	No decrease	Decreasing	No increase	Decreasing	Hazardous
242	Increasing	Increasing	Increasing	Decreasing	No decrease	Decreasing	Increasing	No decrease	Harmless
243	Increasing	Increasing	Increasing	Decreasing	No decrease	Decreasing	Increasing	Decreasing	Hazardous
244	Increasing	Increasing	Increasing	Decreasing	No decrease	Decreasing	No increase	No decrease	Harmless
245	Increasing	Increasing	Increasing	Decreasing	No decrease	Decreasing	No increase	Decreasing	Hazardous
246	Increasing	Increasing	Increasing	Decreasing	No decrease	Decreasing	Increasing	No decrease	Harmless
247	Increasing	Increasing	Increasing	Decreasing	No decrease	Decreasing	Increasing	Decreasing	Hazardous
248	Increasing	Increasing	Increasing	Decreasing	Decreasing	No decrease	No increase	No decrease	Hazardous
249	Increasing	Increasing	Increasing	Decreasing	Decreasing	No decrease	No increase	Decreasing	Hazardous
250	Increasing	Increasing	Increasing	Decreasing	Decreasing	No decrease	Increasing	No decrease	Hazardous
251	Increasing	Increasing	Increasing	Decreasing	Decreasing	No decrease	Increasing	Decreasing	Hazardous
252	Increasing	Increasing	Increasing	Decreasing	Decreasing	Decreasing	No increase	No decrease	Hazardous
253	Increasing	Increasing	Increasing	Decreasing	Decreasing	Decreasing	No increase	Decreasing	Hazardous
254	Increasing	Increasing	Increasing	Decreasing	Decreasing	Decreasing	Increasing	No decrease	Hazardous
255	Increasing	Increasing	Increasing	Decreasing	Decreasing	Decreasing	Increasing	Decreasing	Hazardous

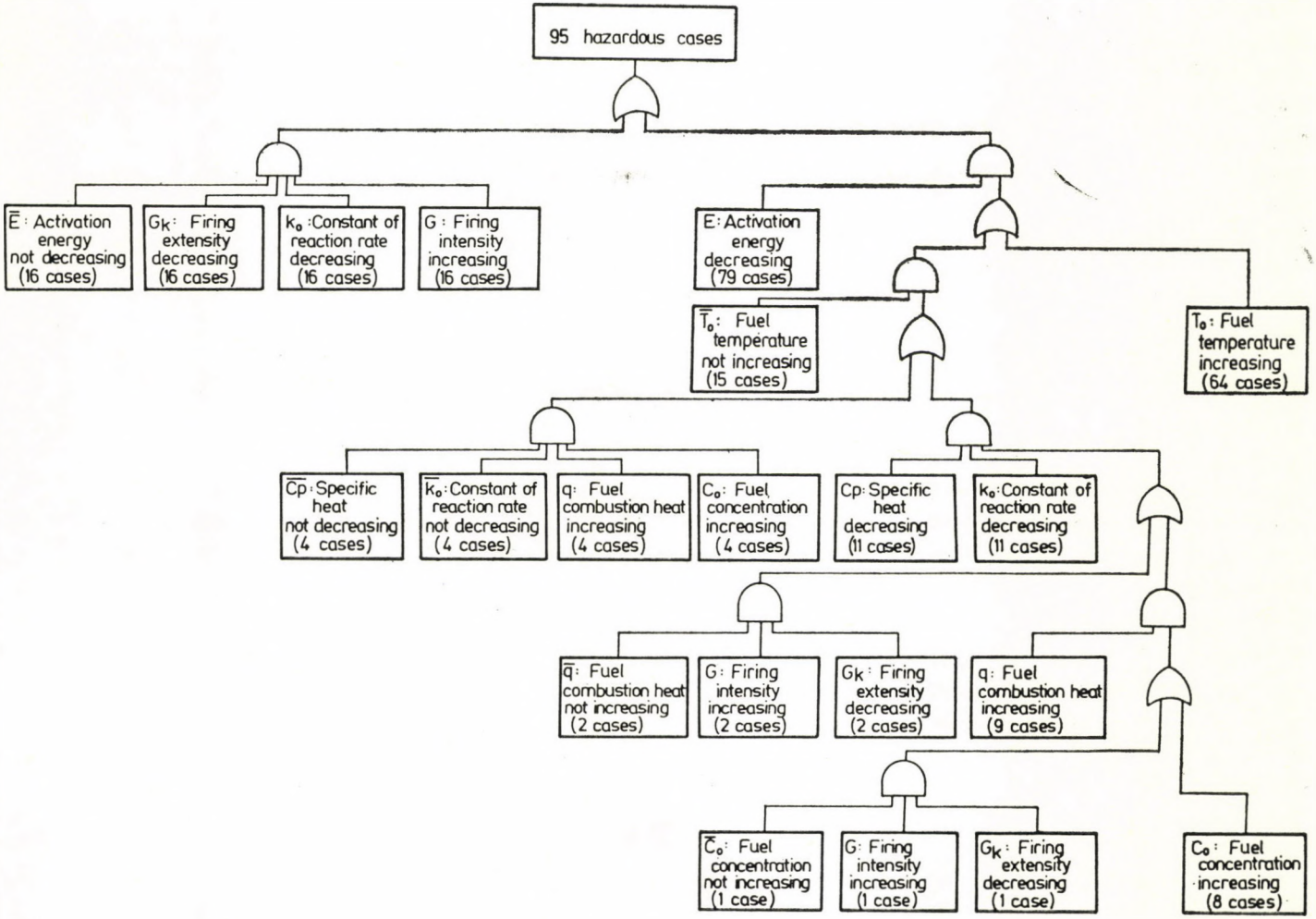
95 hazardous cases
$\overline{E}$: Activation energy not decreasing (16 cases)
G_k: Firing extensity decreasing (16 cases)
k_o: Constant of reaction rate decreasing (16 cases)
G: Firing intensity increasing (16 cases)
E: Activation energy decreasing (79 cases)
$\overline{T_o}$: Fuel temperature not increasing (15 cases)
T_o: Fuel temperature increasing (64 cases)
$\overline{Cp}$: Specific heat not decreasing (4 cases)
$\overline{k_o}$: Constant of reaction rate not decreasing (4 cases)
q: Fuel combustion heat increasing (4 cases)
C_o: Fuel concentration increasing (4 cases)
Cp: Specific heat decreasing (11 cases)
k_o: Constant of reaction rate decreasing (11 cases)
$\overline{q}$: Fuel combustion heat not increasing (2 cases)
G: Firing intensity increasing (2 cases)
G_k: Firing extensity decreasing (2 cases)
q: Fuel combustion heat increasing (9 cases)
$\overline{C_o}$: Fuel concentration not increasing (1 case)
G: Firing intensity increasing (1 case)
G_k: Firing extensity decreasing (1 case)
C_o: Fuel concentration increasing (8 cases)

Fig. 5

Interestingly, however, that disturbation No 78 is already quite dangerous:

$$D_{78} = e_1' \wedge e_2 \wedge e_3' \wedge e_4' \wedge e_5 \wedge e_6 \wedge e_7 \wedge e_8'$$

as here ϑ is definitely increasing through all of its variables (increasing factors), that is, e_2, e_5, e_6 and e_7.

The hazardous character of disturbation D_{79}, for example, can be similarly seen.

REFERENCES

1. IEEE: General Principles for Reliability Analysis of Nuclear Power Generating Station Protection Systems — *ANSI IEEE* N. 41. 4 Std 352, 1972
2. Birkhoff, G.: Lattices in Applied Mathematics — *Proc. of Symp. in Pure Mathematics*, **2,** 155—184
3. Vilenkin, N. J.: Kombinatorika — Műszaki Könyvkiadó, Budapest 1971 (in Hungarian)
4. Vulis, A. A.:Teplovoy rezhim gorenya — Moscow 1954
   Vulis, A. A.: Thermal Conditions of Combustion — Manuscript translation from Russian. OMKDK 1961 (in Hungarian)
5. Fáy, Gy., and Zhelev, B.: Examination of the Combustion Process by the Method of Stationary Thermal Conditions — *Magyar Kémiai Folyóirat*, **69,** (1963) 348 (in Hungarian)
6. Békéssy, A., and Fáy, Gy.: Fuel Engineering Representation Theory — *Magyar Kémiai Folyóirat*, **69,** (1963) 355 (in Hungarian)
7. Fáy, Gy.: Bulletin of the Fuel Engineering Research Institute 1962, p. 429 (in Hungarian)

Logische Theorie der Gefährlichkeit und ihre Anwendung auf Verbrennungsvorgänge. Ziel der vorliegenden Arbeit ist Besprechung der Theorie der Gefährlichkeit und Vorführung einer Anwendung. Statt durch eine algebraische Größe wird der Begriff der Gefährlichkeit durch eine logische Größe beschrieben. Die Einführung in die Arbeit informiert über die Modellierung der Gefährlichkeit eines beliebigen funktionierenden Betriebes. Als Anwendung der Gefährlichkeitstheorie werden die Verbrennungsvorgänge nach der Methode der stationären Wärmezustände untersucht. Aufgrund dessen werden die Gefährlichkeitsfaktoren des Verbrennungsvorganges ermittelt. Im Besitz der Faktoren werden für sämtliche in Betracht kommende elementare Ereignisse des vom Standpunkt der Gefährlichkeit den Verbrennungsvorgängen zugeordneten Ereignisfeldes, die Gefährlichkeiten, unter Berücksichtigung der Gefährlichkeitsbedingungen, theoretisch berechnet.

Логическая теория опасности и ее применение для процессов горения. Данным сообщением ставится цель ознакомления с теорией опасности и демонстрировать один из вариантов ее применения. Теория опасности понятие опасности описывает вместо алгебраического количества с помощью логического количества. Вводная часть сообщения дает информацию относительно моделирования опасности любого работающего производственного предприятия. В качестве применения теории опасности дается исследовани процессов горения методом стационарных тепловых состояний. На основе чего определяются коэффициенты опасности процесса горения. При использовании указанных выше коэффициентов теоретическим путем вычисляется опасность всех элементарных событий, которые могут придти в расчет на основа учета условий опасности пространтсв опасности, приданных к процессам горения с точки зрения осапности.

Acta Technica Academiae Scientiarum Hungaricae, Tomus 86 (3—4), pp. 271—285 (1978)

SURVEY OF SOME VARIATIONAL THEOREMS IN ELASTOSTATICS

J. BARTA*

DOCTOR OF TECHN. SCI.

[Manuscript recevied 6 October, 1977]

Variational theorems will be examined to show whether these are minimal theorems at the same time. The proofs will be carried out by applying the influence numbers as is usual in the theory of structures. A numerically elaborated example elucidates the application of the different theorems.

In this paper, the theorems which are to be surveyed, are numbered from I to VIII. Each of these theorems is a variational theorem, in addition, I, II, III, IV, VI and VIII are minimal theorems. In I and II, the admissible variables are restricted to stresses which satisfy equilibrium conditions (first restriction). In III and IV, the admissible variables are restricted to displacements (second restriction). From the two restrictions, V, VI, VII and VIII are free. But V and VII are not minimal theorems.

I is already due to L. F. MÉNABREA and A. CASTIGLIANO [1]. II is a generalization of I. In the literature, II is called the theorem of minimum complementary energy, [2]. IV is a generalization of III. In the literature, IV is called the theorem of minimum potential energy, [3]. V is due to E. REISSNER, [4]. VII is a generalization of V, and VIII is that of VI. Formulation and proof of VI, VII and VIII will be given in the present paper.

The following usual assumptions can be accepted: Frictionless joints and rigid supports prevent the body from moving. The supporting forces do not work. The body and its support are statically determinate or statically indeterminate, and free from initial stresses. It is assumed that only statical effects arise, that is, neither dynamical nor thermal effects take place. The material of the body is homogeneous or heterogeneous, and isotropic or anisotropic. We assume the linear elasticity and the validity of principle of superposition.

In the present paper, two kinds of external forces ase distinguished, namely the prescribed external forces (in other words: active forces) and the supporting forces, also two kinds of displacements, namely, the prescribed displacements and the free displacements.

* Prof. Dr. Ing. J. BARTA, József körút 35, H-1085 Budapest, Hungary

Notations

U strain energy as a homogeneous quadratic function of the internal forces (stress components). For ex., in the case of axial loaded prismatic bar, $U = S^2l/(2EF)$ where S is the force in the bar, l the length of the bar, EF the modulus of rigidity.

V strain energy as a homogeneous quadratic function of the displacements (strain components). For ex., in the case of an axial loaded prismatic bar, $V = e^2EF/(2l)$ where e is the elongation of the bar.

W strain energy as a homogeneous quadratic function which is homogeneous linear, with respect both to the internal forces (stress components) and to the displacements (strain components. For ex., in the case of an axial loaded prismatic bar, $W = Se/2$.

L_d virtual work of those external forces for application points for which the displacements are prescribed.

L_p virtual work of those external forces which are prescribed.

Six theorems

Theorem I: If the state of stress and displacement is caused by prescribed external forces, but not by prescribed displacements, then among all states of stress which conform to the prescribed external forces and satisfy the equilibrium conditions, the actual stresses are such as to minimize the expression

$$U. \tag{1}$$

Theorem II: Among all states of stress and displacement which conform to the prescribed external forces and satisfy the equilibrium conditions, the actual stresses are such as to minimize the expression

$$U - L_d\,. \tag{2}$$

Theorem III: If the state of stress and displacement is caused by prescribed displacements, but not by prescribed external forces, then among all states of displacement which conform to the prescribed displacements, the actual displacements are such as to minimize the expression

$$V. \tag{3}$$

Theorem IV: Among all states of stress and displacement which conform to the prescribed displacements, the actual displacements are such as to minimize the expression

$$V - L_p\,. \tag{4}$$

Theorem V: Among all states of stress and displacement which conform to the prescribed displacements, the actual stresses and displacements are such as to make the first variation of the expression

$$U - 2W + L_p \tag{5}$$

vanish.

Theorem VI: Among all states of stress and displacement which conform to the prescribed displacements and to the prescribed external forces, and satisfy the equilibrium condition, the actual stresses and displacements are such as to minimize the expression

$$U + 2V - 2W - L_p \,. \tag{6}$$

Proof of the theorem VI

When proving, let the body (beam, frame, truss, plate, etc.) be characterized by the influence numbers

$$\begin{array}{l} a_{11}, \ldots, a_{1k}, \quad a_{1(k+1)}, \ldots, a_{1n}, \\ \ldots\ldots\ldots\ldots\ldots\ldots\ldots\ldots\ldots \\ a_{k1}, \ldots, a_{kk}, \quad a_{k(k+1)}, \ldots, a_{kn}, \\ a_{(k+1)1}, \ldots, a_{(k+1)k}, \quad a_{(k+1)(k+1)}, \ldots, a_{1(k+1)n}, \\ \ldots\ldots\ldots\ldots\ldots\ldots\ldots\ldots\ldots \\ a_{n1}, \ldots, a_{nk}, \quad a_{n(k+1)}, \ldots, a_{nn} \end{array} \tag{7}$$

and let the numbering

$$i = 1, 2, \ldots, k, k+1, k+2, \ldots, n \tag{8}$$

be chosen as follows:

$P_1, P_2, \ldots, P_k$ are those external forces for application points for which the displacements are prescribed.

$P_{k+1}, P_{k+2}, \ldots, P_n$ are those external forces which are prescribed.

i also denotes the direction of the external force, (Fig. 1).

$\mathbf{d}_i$ is the displacement vector of the application point of P_i, (Fig. 1).

d_i is the component of $\mathbf{d}_i$ in direction i, (Fig. 1).

a_{ij} is the influence number, that is, the value of d_i, if $\mathbf{d}_i$ will be produced by an unit external force P_j.

In order to elucidate the numbering (8), let us consider the two-dimensional case shown in Fig. 2. The body, its supports, the external forces of 28 units, of 45 units and of 36 units, the displacements of 0,03 units and of 0,07 units are given. We can introduce the numbering as shown in Fig. 3. Thus now in expressions U, V, W, L_d, L_P, the quantities

$$\begin{array}{lllll} P_1, & P_2, & P_3 = 28, & P_4 = 45, & P_5 = 36, \\ d_1 = 0{,}03, & d = 0{,}07, & d_3, & d_4, & d_5, \end{array}$$

occur. From among these, d_1, d_2, P_3, P_4, P_5 are given, P_1, P_2, d_3, d_4, d_5 are unknown. In the three-dimensional case, the numbering can be carried out in a similar manner.

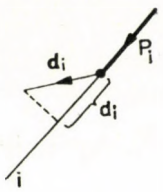

Fig. 1

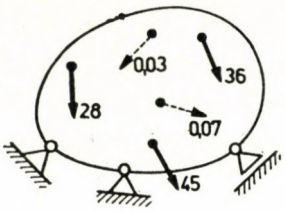

Fig. 2

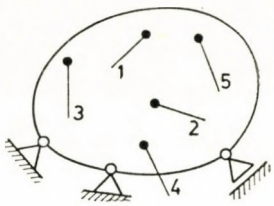

Fig. 3

The determinant of the influence numbers (7) takes the form

$$D = \begin{vmatrix} a_{11} \dots a_{1n} \\ \dots\dots\dots \\ a_{n1} \dots a_{nn} \end{vmatrix}. \tag{9}$$

Let Δ denote the reciprocal determinant of D, that is,

$$\Delta = \begin{vmatrix} D_{11} \dots D_{1n} \\ \dots\dots\dots \\ D_{n1} \dots D_{nn} \end{vmatrix} \tag{10}$$

where D_{11}, D_{12}, ..., D_{1n} are the minors of D. According to well known properties of the influence numbers, for the actual external forces and displacements, we have the equations

$$\left.\begin{aligned} &a_{11} P_1 + \dots + a_{1n} P_n = d_1, \\ &\dots\dots\dots\dots\dots\dots\dots\dots \\ &a_{n1} P_n + \dots + a_{nn} P_n = d_n \end{aligned}\right\} \tag{11}$$

$$\left.\begin{aligned} &\frac{D_{11}}{D} d_1 + \dots + \frac{D_{1n}}{D} d_n = P_1, \\ &\dots\dots\dots\dots\dots\dots\dots\dots \\ &\frac{D_{n1}}{D} d_1 + \dots + \frac{D_{nn}}{D} d_n = P_n \end{aligned}\right\} \tag{12}$$

and the ascertainment A: Both the determinant (9) and the determinant (10) are symmetrical and positive definite.

Using the definitions of U, V, W, L_d, L_p and the formulae (11) and (12), we can write

$$U = \frac{1}{2}\left[P_1(a_{11} P_1 + \dots + a_{1n} P_n) + \dots + P_n(a_{n1} P_1 + \dots + a_{nn} P_n)\right], \tag{13}$$

$$V = \frac{1}{2}\left[d_1(D_{11} d_1 + \dots + D_{1n} d_n) + \dots + d_n(D_{n1} d_1 + \dots + D_{nn} d)\right]/D, \tag{14}$$

$$W = \frac{1}{2}(P_1 d_1 + \ldots + P_n d_n), \tag{15}$$

$$L_d = P_1 d_1 + \ldots + P_k d_k, \tag{16}$$

$$L_p = P_{k+1} d_{k+1} + \ldots + P_n d_n. \tag{17}$$

Introducing the notation

$$\Omega = U + 2V - 2W - L_P \tag{18}$$

and taking into account the expressions (13), ..., (17), we can see that Ω is a function of

$$P_1, P_2, \ldots, P_k, d_{k+1}, d_{k+2}, \ldots d_n.$$

Thus, the minimum problem of this function is in question. Applying both formula (18) and equations (13), ..., (17), we obtain the partial derivatives

$$\begin{aligned}
&\frac{\partial \Omega}{\partial P_1} = a_{11} P_1 + \ldots + a_{1n} P_n - d_1, \\
&\ldots\ldots\ldots\ldots\ldots\ldots\ldots\ldots \\
&\frac{\partial \Omega}{\partial P_k} = a_{k1} P_1 + \ldots + a_{kn} P_n - d_k, \\
&\frac{\partial \Omega}{\partial d_{k+1}} = \frac{2}{D}(D_{(k+1)1} d_1 + \ldots + D_{(k+1)n} d_n) - 2 P_{k+1}, \\
&\ldots\ldots\ldots\ldots\ldots\ldots\ldots\ldots\ldots\ldots\ldots\ldots \\
&\frac{\partial \Omega}{\partial d_n} = \frac{2}{D}(D_{n1} d_1 + \ldots + D_{nn} d_n) - 2 P_n
\end{aligned} \tag{19}$$

In consequence of equations (11) and (12), for the actual external forces and displacements, the right sides of equations (19) vanish (ascertainment B). We also obtain the second derivatives

$$\frac{\partial^2 \Omega}{\partial P_1^2} = a_{11}, \quad \frac{\partial^2 \Omega}{\partial P_1 \partial P_2} = a_{12}, \ldots, \quad \frac{\partial^2 \Omega}{\partial P_1 \partial d_{k+1}} = 0, \ldots, \quad \frac{\partial^2 \Omega}{\partial d_n^2} = 2D_{nn}/D.$$

Therefore, the determinant of the minimum problem in question takes the form

$$\begin{vmatrix}
a_{11} & \ldots & a_{1k} & 0 & \ldots & 0 \\
\ldots & \ldots & \ldots & \ldots & \ldots & \ldots \\
a_{k1} & \ldots & a_{kk} & 0 & \ldots & 0 \\
0 & \ldots & 0 & 2D_{(k+1)(k+1)}/D & \ldots & 2D_{(k+1)n}/D \\
\ldots & \ldots & \ldots & \ldots & \ldots & \ldots \\
0 & \ldots & 0 & 2D_{n(k+1)}/D & \ldots & 2D_{nn}/D
\end{vmatrix}. \tag{20}$$

It follows from the ascertainment A that the determinant (20) is positive definite (ascertainment C). The ascertainment B and C demonstrate that the conditions of minimum are fulfilled. With this, theorem VI is proved.

Remarks. — The method by means of which we have proved theorem VI, is based on applying the influence numbers (7), since during the proof, we have considered a structural body as beam, frame, truss, plate, etc. The same method is appropriate also for proving the theorems I, II, ..., V. In the literature [2, 3, 4, 6] where a continuous body is considered, the usual method of proof is based on applying the displacement-stress relations

$$\partial u/\partial x = [\sigma_x - \mu(\sigma_x + \sigma_y)]/E, \quad \ldots, \quad \partial v/\partial z + \partial w/\partial y = \tau_{yz}/G, \quad \ldots$$

The two methods have essentially the same train of thought. — In the above presented proof of theorem VI, equations (19) have the scheme

$$\begin{aligned}
&\ldots = \ldots - d_1,\\
&\ldots\ldots\ldots\ldots\\
&\ldots = \ldots - d,\\
&\ldots = \ldots - 2P_{k+1},\\
&\ldots\ldots\ldots\ldots\ldots\\
&\ldots = \ldots - 2P_n.
\end{aligned}$$

In a very similar and here not presented proof of theorem V, the corresponding equations have the scheme

$$\begin{aligned}
&\ldots = \ldots - d_1,\\
&\ldots\ldots\ldots\ldots\\
&\ldots = \ldots - d_k,\\
&\ldots = 0,\\
&\ldots\ldots\ldots\\
&\ldots = 0.
\end{aligned}$$

The two schemes show that theorem VI needs the phrase "and to the prescribed external forces and satisfy the equilibrium condition", but theorem V does not. — As is well known from the theory of structures, the above definition of the influence number a_{ij} also remains valid if P_j denotes a moment, and $\mathbf{d}_i$ a rotation vector.

Example

The elastic body shown in Fig. 4 is composed of three prismatic parts. The quantities $l_1 = 3$, $l_2 = 5$, $l_3 = 4$, $E_1F_1 = 15\,000$, $E_2F_2 = 5000$, $E_3F_3 = 10\,000$ are given. The ends of the body are fixed. $P_A = 14$ is the prescribed external force, $d_B = 0{,}01$ is the prescribed displacement.

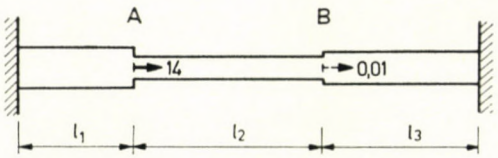

Fig. 4

Using these data and the definitions of U, V, W, L_d, L_P, we werite

$$U = \frac{S_1^2\, 3}{2 \cdot 15\,000} + \frac{S_2^2\, 5}{2 \cdot 5000} + \frac{S_3^2\, 4}{2 \cdot 10\,000},$$

$$V = \frac{d_A^2\, 15\,000}{2 \cdot 3} + \frac{(0{,}01 - d_A)^2\, 5000}{2 \cdot 5} + \frac{(-0{,}01)^2\, 10\,000}{2 \cdot 4},$$

$$W = \frac{S_1\, d_A}{2} + \frac{S_2\,(0{,}01 - d_A)}{2} + \frac{S_3\,(-0{,}01)}{2},$$

that is

$$U = 0{,}0001\, S_1^2 + 0{,}0005\, S_2^2 + 0{,}0002\, S_3^2, \tag{21}$$

$$V = 3000\, d_A^2 - 10\, d_A + 0{,}175, \tag{22}$$

$$W = 0{,}5 S_1\, d_A - 0{,}5\, S_2\, d_A + 0{,}005\, S_2 - 0{,}005\, S_3 \tag{23}$$

and

$$L_d = 0{,}01\, P_B, \tag{24}$$

$$L_p = 14\, d_A. \tag{25}$$

Let us apply *theorem V*. Expression (5) has to be scrutinized. To do this, we introduce the notation

$$\Phi = U - 2W + L_P.$$

Inserting here (21), . . ., (25), the equation

$$\Phi = 0{,}0001\, S_1^2 + 0{,}0005\, S_2^2 + 0{,}0002\, S_3^2 - \\ - S_1\, d_A + S_2\, d_A - 0{,}01\, S_2 + 0{,}01\, S_3 + 14\, d_A$$

arises. As can be seen, Φ is a function of S_1, S_2, S_3 and d_A. From the vanishing of the first variation, the equations

$$\frac{\partial \Phi}{\partial S_1} = 0{,}0002\, S_1 - d_A = 0,$$

$$\frac{\partial \Phi}{\partial S_2} = 0{,}001\, S_2 + d_A - 0{,}01 = 0,$$

$$\frac{\partial \Phi}{\partial S_3} = 0{,}0004\, S_3 + 0{,}01 = 0,$$

$$\frac{\partial \Phi}{\partial d_A} = -S_1 + S_2 + 14 = 0 \tag{26}$$

follow. From these *four* equations, we compute the *four* unknowns S_1, S_2, S_3, d_A and obtain the result

$$S_1 = 20,\ S_2 = 6,\ S_3 = -25,\ d_A = 0{,}004. \tag{27}$$

Thus the actual stresses and displacements are such that equations (27) hold. That in this case, there is no minimum, will be indicated as follows.

$$\frac{\partial^2 \Phi}{\partial S_1^2} = 0{,}0002\,,\quad \frac{\partial^2 \Phi}{\partial S_1 \partial S_2} = 0,\frac{\partial^2 \Phi}{\partial S_2^2} = 0{,}001,\ \ldots$$

are the second partial derivatives, and these yield the determinants

$$D_1 = 0{,}0002,$$

$$D_2 = \begin{vmatrix} 0{,}0002 & 0 \\ 0 & 0{,}001 \end{vmatrix} = 2 \cdot 10^{-7},$$

$$D_3 = \begin{vmatrix} 0{,}0002 & 0 & 0 \\ 0 & 0{,}001 & 0 \\ 0 & 0 & 0{,}0004 \end{vmatrix} = 8 \cdot 10^{-11},$$

$$D_4 = \begin{vmatrix} 0{,}0002 & 0 & 0 & -1 \\ 0 & 0{,}001 & 0 & 1 \\ 0 & 0 & 0{,}0004 & 0 \\ -1 & 1 & 0 & 0 \end{vmatrix} = -48 \cdot 10^{-8}.$$

Not each of these determinants is positive or zero. Thus there is no minimum in this case. With this, it is shown that theorem V is not a minimal theorem.

Now, let us apply *theorem VI*. In order to scrutinize expression (6), the notation

$$\Psi = U + 2V - 2W - L_P$$

will be used. From this and from (21), . . ., (25), the equation

$$\begin{aligned} \Psi = {} & 0{,}0001\, S_1^2 + 0{,}0005\, S_2^2 + 0{,}0002\, S_3^2 + \\ & + 6000\, d_A^2 - 20\, d_A + 0{,}35 - \\ & - S_1 d_A + S_2 d_A - 0{,}01\, S_2 + 0{,}01\, S_3 - 14\, d_A \end{aligned}$$

ensues. Let us not forget that according to theorem VI, the quantities S_1, S_2, S_3, d_A have to be conformed not only to the prescribed displacements but also to the prescribed external forces (equilibrium). This means that in the present case, we have to substitute $S_2 = S_1 - 14$ and $S_3 = S_1 - 14 - P_B$. Therefore, we write

$$\Psi = 0{,}0001\, S_1 + 0{,}0005(S_1 - 14)^2 + 0{,}0002(S_1 - 14 - P_B)^2 + \\ + 6000\, d_A^2 - 0{,}48\, d_A - 0{,}01\, P_B + 0{,}35\,.$$

As can be seen, Ψ is a function of S_1, d_A and P_B. The vanishing of the first variation claims the equations

$$\frac{\partial \Psi}{\partial S_1} = 0{,}0016\, S_1 - 0{,}0004\, P_B - 0{,}0196 = 0,$$

$$\frac{\partial \Psi}{\partial d_A} = 12\,000\, d_A - 48 = 0,$$

$$\frac{\partial \Psi}{\partial P_B} = -0{,}0004\, S_1 + 0{,}0004\, P_B - 0{,}0046 = 0. \tag{28}$$

From these *three* equations, we compute the *three* unknowns S_A, d_A, P_B and obtain the result

$$S_1 = 20,\ d_A = 0{,}004,\ P_B = 31. \tag{29}$$

Thus, the actual stresses and displacements are such that equations (29) hold. Of course, (29) does not contradict (27). That in this case, there is a minimum, will be indicated as follows. The second partial derivatives

$$\frac{\partial^2 \Psi}{\partial S_1^2} = 0{,}0016\,, \quad \frac{\partial^2 \Psi}{\partial S_1\, \partial d_A} = 0, \quad \frac{\partial^2 \Psi}{\partial d_A^2} = 12\,000\,, \ldots$$

yield the determinants

$$D_1 = 0{,}0016,$$

$$D_2 = \begin{vmatrix} 0{,}0016 & 0 \\ 0 & 12\,000 \end{vmatrix} = 19{,}2,$$

$$D_3 = \begin{vmatrix} 0{,}0016 & 0 & -0{,}0004 \\ 0 & 12\,000 & 0 \\ -0{,}0004 & 0 & 0{,}0004 \end{vmatrix} = 0{,}00576.$$

Each of these determinants is positive. Thus, the computation shows that for the quantities (29), the expression (6) assumes its minimum value. This result was already to be expected by virtue of theorem VI.

Two further theorems

U, V, W, L_d, L_P are functions defined at the beginning of the present paper. We have seen that by applying theorem V, the expression

$$U - 2W + L_p,$$

and by applying theorem VI, the expression

$$U + 2V - 2W - L_P$$

is to be subjected to a variational procedure. Now, it is natural to ask whether it might not be possible to chose five constants

$$p, q, r, s, t \tag{30}$$

so that a similar variational procedure be applied to the expression

$$pU + qV + rW + sL_d + tL_P.$$

This question is answered in the two following theorems.

Theorem VII: If the constants p, q, r, s, t fulfil the conditions

$$p + \frac{r}{2} + s = 0, \quad q + \frac{r}{2} + t = 0 \tag{31}$$

then among all states of stress and displacement which conform to the prescribed displacements and to the prescribed external forces, and satisfy the equilibrium condition, the actual stresses and displacements are such as to make the first variation of expression

$$pU + qV + rW + sL_d + tL_P \tag{32}$$

vanish.

Theorem VIII: If the constants p, q, r, s, t fulfil both the conditions

$$p + \frac{r}{2} + s = 0, \quad q + \frac{r}{2} + t = 0 \tag{33}$$

and the conditions

$$p \geqq 0, \quad q \geqq 0 \tag{34}$$

then among all states of stress and displacement which conform to the prescribed displacements and to the prescribed external forces and satisfy the equilibrium condition, the actual stresses and displacements are such as to minimize the expression

$$pU + qV + rW + sL_d + tL_P. \tag{35}$$

Proof of theorems VII and VIII

Here, the same course of reasoning will be followed as by the proof of theorem VI. Equations (11), ..., (17) hold also here. Instead of (18),

$$\Omega = pU + qV + rW + sL_d + tL_P \tag{36}$$

will be written. Equations (19) assume the form

$$\begin{aligned}
&\frac{\partial \Omega}{\partial P_1} = p(a_{11} P_1 + \ldots + a_{1n} P_n) + \left(\frac{r}{2} + s\right) d_1 , \\
&\ldots\ldots\ldots\ldots\ldots\ldots\ldots\ldots\ldots\ldots\ldots\ldots \\
&\frac{\partial \Omega}{\partial P_k} = p(a_{k1} P_1 + \ldots + a_{kn} P_n) + \left(\frac{r}{2} + s\right) d_k , \\
&\frac{\partial \Omega}{\partial d_{k+1}} = \frac{q}{D}(D_{(k+1)1} d_1 + \ldots + D_{(k+1)n} d_n) + \left(\frac{r}{2} + t\right) P_{k+1} , \\
&\ldots\ldots\ldots\ldots\ldots\ldots\ldots\ldots\ldots\ldots\ldots\ldots\ldots\ldots\ldots\ldots \\
&\frac{\partial \Omega}{\partial d_n} = \frac{q}{D}(D_{n1} d_1 + \ldots + D_{nn} d_n) + \left(\frac{r}{2} + t\right) P_n .
\end{aligned} \tag{37}$$

The determinant (20) assumes the form

$$\begin{vmatrix}
pa_{11} & \ldots & pa_{1k} & 0 & \ldots & 0 \\
\ldots & \ldots & \ldots & \ldots & \ldots & \ldots \\
pa_{k1} & \ldots & pa_{kk} & 0 & \ldots & 0 \\
0 & \ldots & 0 & qD_{k+1)(k+1)}/D & \ldots & qD_{(k+1)n}/D \\
\ldots & \ldots & \ldots & \ldots & \ldots & \ldots \\
0 & \ldots & 0 & qD_{n(k+1)}/D & \ldots & qD_{nn}/D
\end{vmatrix} . \tag{38}$$

By applying the above ascertainments A, B and C to (37) and (38), we can see that both theorem VII and theorem VIII are proved.

Continuation of the example

Theorems VII and VIII permit a certain liberty in choosing the constants p, q, r, s, t because in VII only the condition (31), in VIII only the conditions (32) and (33) are to be fulfilled. By making use of this liberty, one endeavours to choose such constants p, q, r, s, t which facilitate the numerical computation. This idea will be employed in what follows.

Let us apply *theorem VII*. We shall choose

$$p = 0,\ q = 1,\ r = -2,\ s = 1,\ t = 0. \tag{39}$$

By this choice, condition (31) is fulfiled. Expression (32) now has the form

$$V - 2W + L_d. \tag{40}$$

In order to scrutinize expression (40), we introduce the notation

$$\Lambda = V - 2W + L_d.$$

After inserting (21), . . ., (25) we obtain the function

$$\begin{aligned}\Lambda = {} & 3000\, d_A^2 - 10\, d_A + 0{,}175 - \\ & - S_1 d_A + S_2 d_A - 0{,}01\, S_2 + 0{,}01\, S_3 + \\ & + 0{,}01\, P_B.\end{aligned}$$

Since according to theorem VII, the quantities S_1, S_2, S_3, d_A, P_B have to be conformed not only to the prescribed displacements but also to the prescribed external forces, we substitute $S_2 = S_1 - 14$ and $S_3 = S_1 - 14 - P_B$, and obtain

$$\Lambda = 3000\, d_A^2 - 24\, d_A + 0{,}175.$$

As can be seen, Λ is a function of d_A. From the vanishing of the first variation,

$$\frac{d\Omega}{dd_A} = 6000\, d_A - 24 = 0 \tag{41}$$

follows. From this *single* equation, we can compute the *single* unknown d_A and obtain the result

$$d_A = 0{,}004. \tag{42}$$

Thus, the actual stresses and displacements are such that equation (42) holds.

By applying *theorem VIII*, the choice

$$p = 1,\ q = 0,\ r = 0,\ s = -1,\ t = 0$$

yields theorems I and II, and the choice

$$p = 0,\ q = 1,\ r = 0,\ s = 0,\ t = -1$$

yields theorems III and IV. Although the application of theorems I, II, III and IV is already presented in several text-books, yet for entirety's sake, let also the theorems I, II, III and IV be applied to the simple structure shown in Fig. 4. Since the application of I, II, III and IV will be carried out in the very same manner as that of V, VI and VII, we content ourselves with the following concise presentation.

If the state of stress and displacement is caused only by $P_A = 14$, and *theorem I* will be applied:

$$\begin{aligned} U &= 0{,}0001\, S_1^2 + 0{,}0005\, S_2^2 + 0{,}0002\, S_3^2 = \\ &= 0{,}0001\, S_1^2 + 0{,}0005(S_1 - 14)^2 + 0{,}0002(S_1 - 14)^2, \\ \frac{dU}{dS_1} &= 0{,}0016\, S_1 - 0{,}0196 = 0\,. \\ S_1 &= 12{,}25. \end{aligned} \tag{43}$$

If the state of stress and displacement is caused by $P_A = 14$ and $d_B = 0{,}01$, and *theorem II* will be applied:

$$\begin{aligned} U &= 0{,}0001\, S_1^2 + 0{,}0005\, S_2^2 + 0{,}0002\, S_3^2 = \\ &= 0{,}0001\, S_1^2 + 0{,}0005(S_1 - 14)^2 + 0{,}0002(S_1 - 14 - P_B)^2, \\ L_d &= 0{,}01\, P_B\,, \\ \frac{\partial}{\partial S_1}(U - L_d) &= 0{,}0016\, S_1 - 0{,}0004\, P_B - 0{,}0196 = 0, \\ \frac{\partial}{\partial P_B}(U - L_d) &= -0{,}0004\, S_1 + 0{,}0004\, P_B - 0{,}0004 = 0. \\ S_1 &= 20,\ P_B = 31. \end{aligned} \tag{44}$$

If the state of stress and displacement is caused only by $d_B = 0{,}01$, and *theorem III* will be applied:

$$\begin{aligned} V &= 3000\, d_A^2 - 10\, d_A^2 + 0{,}175 \\ \frac{dV}{dd_A} &= 6000\, d_A - 10 = 0\,, \\ d_A &= \frac{1}{600}\,. \end{aligned} \tag{45}$$

If the state of stress and displacement is caused by $P_A = 14$ and $d_B = 0{,}01$, and *theorem IV* will be applied:

$$V = 3000\, d_A^2 - 10\, d_A + 0{,}175,$$
$$L_p = 14\, d_A,$$
$$\frac{d}{dd_A}(V - L_p) = 6000\, d_A - 24 = 0,$$
$$d_A = 0{,}004. \tag{46}$$

Of course, (43), (44), (45), (46) are not in contradiction with (27), (28), (29).

Retrospection

The problem, the solving of which the variational theorems will often be applied, is the following: Determine the stresses and displacements of an elastic body in equilibrium when at certain points the displacements, and at certain points the external forces are prescribed.

Such a problem was treated in the above example. For solving, the surveyed theorems were applied. As is well known, the theory of linear-elastic structures leads to linear algebraic equations. Also in the above example, the computation led to linear algebraic equations with more or less unknowns: four in (26), three in (28), two in (44), one in (41). The unknowns were not always the same quantities. Thus, by applying different theorems, the magnitude of computing work may be different. For this reason, one endeavours to choose, from time to time, one of the suitable theorems.

In the above example, a very simple structure (Fig. 4) was considered. Of course in practice, more complicated structures occur, but a very simple structure was sufficient to explain the application of theorems.

REFERENCES

1. MÉNABRÉA, L. F.: Nouveau principe sur la distribution des tensions dans les systèmes élastiques. *C. R.*, tome **46,** Paris (1858), p. 1056. — CASTIGLIANO, A.: Théorie de l'équilibre des systèmes élastiques et ses applications. Turin, 1879, p. 30.
2. See for ex SOKOLNIKOFF, I. S.: Mathematical Theory of Elasticity. First edition. 1946, p. 286
3. Ibidem p. 281
4. REISSNER, E.: On a Variational Theorem in Elasticity. *Journal of Mathematics and Physics.* **29,** (1950) 90—95
5. See for ex. *Handbuch der Physik.* Bd. **6,** Berlin 1927, p. 73
6. BALDACCI, R. F.: Metodi variazionali nella teoria delle strutture. Rendiconti del corso di perfezionamento, vol **8,** Libreria Editrice Politecnica, Milano 1958. — Further theorems and literature are told over in paper TONTI, E.: Vaariational Principles in Elastostatics. *Meccanica*, vol. II, no. 4 (1967), Tamburini Editore, Milano.

Übersicht einiger Variationssätze in der Elastostatik. Es wird untersucht, welche von den Variationssätzen zugleich Minimalsätze sind. Zum Beweis der Sätze wird statt der üblichen Spannungsanalyse die Einflußwertmethode verwendet. Der Verfasser arbeitet Zahlenbeispiele aus um zu zeigen, daß man in konreten Fällen bald den einen, bald den anderen von den Sätzen anwenden soll, wenn möglichst wenig Berechnungsarbeit aufgewendet soll.

Рассмотрение нескольких вариационных положений теории упругости. Автор исследует, что которые из положений являются положениями-минимум. Доказательство положений вместо обычно применяемого анализа напряжений выполняется автором с помощью значений воздействий, применяемых в теории несущих конструкций. С помощью разработанных цифровых примеров автор указывает на то, что среди имеющихся в распоряжений в каждом отдельном случае следует выбирать для использования то положение, которое требует меньших по объему вычислительных работ.

Acta Technica Academiae Scientiarum Hungaricae, Tomus 86 (3—4), pp. 287—300 (1978)

PLASTIZITÄTSMECHANISCHE UNTERSUCHUNG DES SPANBILDUNGSVORGANGES

H. WEBER* — J. LEOPOLD**

[Eingegangen: 30. März 1977]

Im Beitrag wird ein Modell zur Berechnung der Spannungen an der Spanfläche eines Schneidwerkzeuges vorgestellt. Grundlage der Untersuchungen ist die Gleitlinientheorie. Die von LEE und SHAFFER bekannten Gleitlinienfelder wurden hinsichtlich des Reibwertes, des möglichen Spanwinkels und der Berücksichtigung einer realen Schneidkantenrundung erweitert. Einige Ergebnisse von numerischen Berechnungen werden diskutiert. Daraus wird der große Einfluß des Schneidkantenradius auf die Spannungsverteilung ersichtlich.

1. Einleitung

Von den Forschungsergebnissen der Fertigungstechnik wird zunehmend erwartet, daß sowohl Maßnahmen zur Reduzierung der Fertigungskosten, der eingesetzten Energie und des Materialverbrauches abgeleitet werden als auch den ständig steigenden Forderungen nach Erhöhung der Qualität der Erzeugnisse Rechnung getragen wird. Die Qualität und damit die Gebrauchsgüte von bearbeiteten Teilen hängt entscheidend von der Oberflächenbeschaffenheit ab. So wirkt sich der nach der spanenden Bearbeitung veränderte Zustand der Oberflächenschicht, d. h. die in ihr verbleibenden Spannungen, die Stärke der verfestigten Schicht und die eingetretenen Gefügeveränderungen auf die mechanischen Eigenschaften des Bauteiles und damit auf dessen Lebensdauer sowie Zuverlässigkeit aus [1].

Zum anderen erfordert die ständig steigende Erhöhung der Arbeitsgeschwindigkeiten der Maschinen eine verstärkte Automatisierung der Bearbeitungsvorgänge. Die Tatsache, daß die Kenntnisse über die Fertigungsverfahren größtenteils empirisch gewonnen wurden und phänomenologischen Charakter tragen wirkt sich erschwerend auf die Bildung eines möglichst viele Seiten des Spanbildungsvorganges beschreibenden Modells aus. Weiterhin hat eine Verbesserung der Modellbildung ebenso großen Einfluß auf die bessere

* Prof. Dr.-Ing. habil. Horst WEBER. Rektor — Technische Hochschule Karl-Marx-Stadt.

** Dr. Ing. Jürgen LEOPOLD. Wissenschaftlicher Oberassistent, Technische Hochschule Karl-Marx-Stadt, Sektion Fertigungsprozeß und Fertigungsmittel.

Acta Technica Academiae Scientiarum Hungaricae 86, 1978

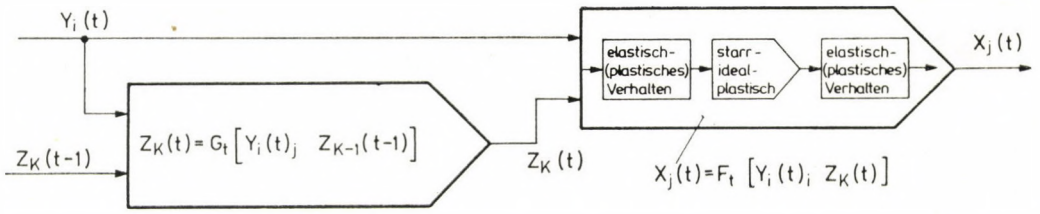

EINGANGSGRÖßEN $Y_i(t)$

i	$Y_i(t)$
1	Werkstückgeometrie
2	Schnittgeschwindigkeit
3	Vorschub
4	Schnittiefe
5	Kühlung, Schmierung
6	Statische und dynamische Steife des Systems Maschine - Werkzeug - Werkstück
7	Werkstoff des Werkstückes
8	Werkstoff des Werkzeuges

ZUSTANDSGRÖßEN $Z_K(t-1)$

K	$Z_K(t-1)$
1	Globale Materialkennwerte E-Modul Poissonzahl Schubfließgrenze Viskosität
2	Geometrie des Werkzeuges Schneidenrundung Aufbauschneide Freiflächenverschleiß
3	Versetzungsdichte
4	Eigenspannungsverteilung
5	Verfestigung

AUSGANGSGRÖßEN $X_j(t)$

j	$X_j(t)$
1	Kräfte
2	Spanstauchung
3	Energie
4	Oberfläche - Gestalt - Beschaffenheit - Verhalten
7	Spanablaufgeschwindigkeit
8	Kontaktlänge
9	Temperatur

Bild. 1. Kenngrößen im Prozeß der Spanbildung

Beherrschung von Meßaufgaben in komplizierten Fertigungssystemen. Nach Einschätzung des VII. IMEKO-Kongresses [2] wird die Gewinnung größerer a-priori-Kenntnisse über das zu steuernde Modell immer noch unterschätzt. Hinzu kommt, daß seitens der CIRP [3] eine Prognostizierung der Zukunft der Fertigungstechnik ergab, daß um 1985 mit einer vollständigen on-line-Automatisierung und Optimierung kompletter Fertigungsbetriebe zu rechnen ist.

2. Methoden der Modellbildung des Spanbildungsvorganges

Bild 1 zeigt wesentliche Kenngrößen im Prozeß der Spanbildung. Unter den Eingangsgrößen $Yl(x)$ dienen Schnittgeschwindigkeit, Vorschub und Schnittiefe als steuerbare Prozeßgrößen. Meßgrössen zur Charakterisierung der Spanhsóff2étеqees aus. Historisch gesehen und auf eine einfache praktische Handhabung ausgerichtet, dominiert die technologische Modellbildung. Hierzu gehören die Schnittkraftgieichungen nach KRONENBERG und KIENZLE sowie die Berechnung des Standzeitverhaltens nach TAYLOR. Gegenwärtig werden Erweiterungen z. B. für Probleme der Feinbearbeitung vorgenommen, sowie Schnittwertspeicher für eine Vielzahl von Werkstoff Werkzeugpaarungen und unterschiedliche Schnittbedingungen angewendet [4]. Grundlegende Erkenntnisse zum Elementarvorgang sind durch Änderungen des Modells nach dieser Methods nicht mehr möglich. Lediglich die Verfahren zum Aufstellen der nötigen Richtwerte haben sich den modernen technischen Möglichkeiten und mathematischen Verfahren angepaßt [5].

Eine genauere Beschreibung der im Zerspanungsprozeß ablaufenden Vorgänge gewinnt man durch eine breitere Anwendung naturwissenschaftlich-mathematischer Erkenntnisse.

Zu den Verfahren der elementaren Theorie, die Lösungen über Gleichgewichtsbedingungen ermitteln, gehören Gleitlinienmodelle. Hierbei kann zwischen jenen Modellen unterschieden werden, die den realen Spanbildungsvorgang experimentell (z. B. mittels Visioplastizität, Moiréverfahren) untersuchen und solchen, die vereinfachte Gleitlinienfelder unter Beachtung gültiger Randbedingungen zu Hilfe nehmen. Zweckmodelle haben den Vorteil, zu praktisch verwendbaren analytischen Beziehungen zu gelangen, die für eine Steuerung des Vorganges von großer Wichtigkeit sind.

In jüngster Zeit wurde der Spanbildungsvorgang mit Hilfe von Extremalprinzipen modelliert, die auf Energiebetrachtungen basieren. Es läßt sich zeigen, daS die Gleitlinienlösung stets eine gute Näherung darstellt [6].

Eine Einbeziehung des viskosen Materialverhaltens im Gesamtbereich der Spanbildung (Globale-Fließmodelle) bzw. lediglich zur Beschreibung der Fließschicht an der Spanunterseite (lokale-Fließmodelle) erweitert den Gültigkeitsbereich der Spanmodelle. Der gegenwärtige Stand der Modellierung des

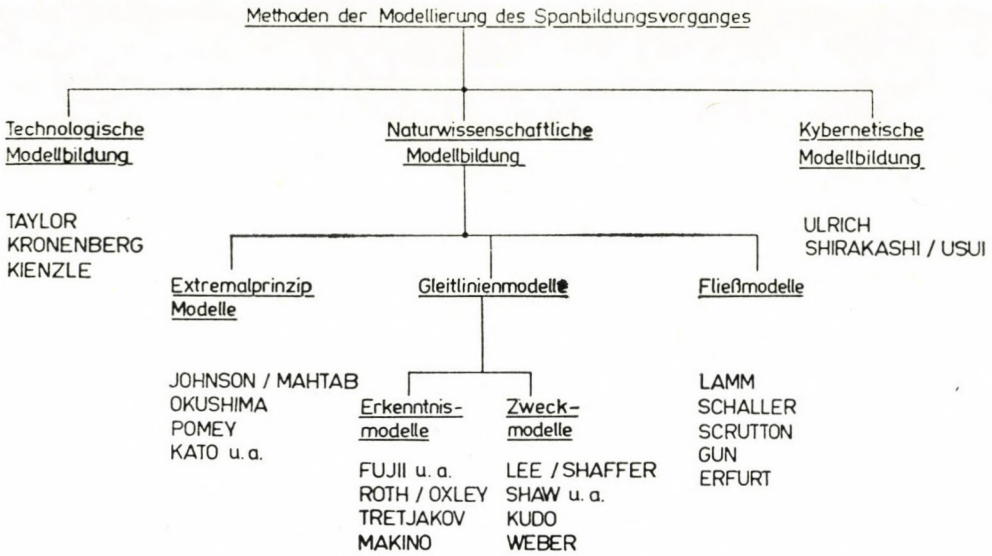

Bild. 2. Methoden der Modellierung des Spanbildungsvorganges

Vorganges der Spanbildung zum Zwecke einer Steuerung bzw. Regelung beruht größtenteils auf Faustformeln für Kräfte und Temperaturen. Diese statischen Beziehungen werden "dynamisiert", indem Vorschub bzw. Schnittiefe zu Zeitfunktionen werden. Neuerdings werden Simulationsmethoden angewendet, die Werkstoffprüfung unter Zerspanungsbedingungen und numerische Modellberechnungen in wechselseitiger Abhängigkeit vornehmen.

Bild 2 zeigt eine Übersicht zu Methoden der Modellierung des Spanbildungsvorganges.

3. Gleitlinienmodell des Zerspanungsvorganges

Aus der vorangegangenen Übersicht von Methoden zur Beschreibung des Zerspanungsvorganges ist ersichtlich, daß eine allgemeine Theorie der Spanbildung noch aussteht. Sowohl der theoretische Entwicklungsstand von Mechanik, Mathematik und Physik als auch die Forderung nach möglichst einfachen und praktisch leicht anwendbaren Ergebnissen zwingen zu Annahmen und größeren Einschränkungen.

Wie das Moirèbild einer Spanwurzel (Bild 3) zeigt, konzentrieren sich die Deformationen im wesentlichen auf einen schmalen Bereich in unmittelbarer Nähe der Scherlinie. Hinzu kommt, daß beim quasistatischen Prozeß (stationärem Spanen) kein Wechsel von Be- und Entlastung vorliegt, so daß im Gebiet uneingeschränkten plastischen Fließens starr-ideal-plastisches Materialverhalten eine gute Näherung ist. Dies gestattet es, unter Vernach-

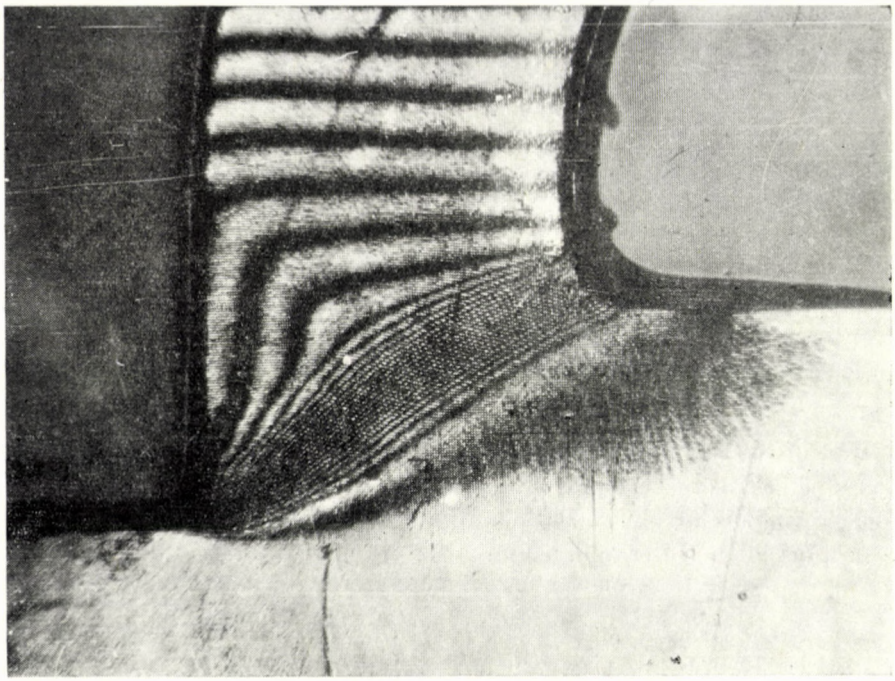

Bild. 3. Moiréaufnahme einer Spanwurzel

lässigung elastischer bzw. viskoser Anteile die MISES'sche Spannungs-Deformationsbeziehung Gl. (3) zu benutzen. Da gleichzeitig in diesem Bereich die Deformationsgeschwindigkeiten sehr groß sind (von NAUMANN [7] wurden beim Zerspanen einer superplastischen Pb-Sn-Legierung $|\dot{\varepsilon}| \approx 3 \cdot 10^{-1}\,\mathrm{s}^{-1}$ ermittelt) wird die MISES'sche Fließbedingung (Gl. 2) im gesamten plastischen Gebiet als gültig angesehen. Nach WEBER [8] ist es gerechtfertigt, unter gewissen Zerspanungsbedingungen (z. B. für Spanungsverhältnisse $4 \leq a|s \leq 20$) einen ebenen Deformationszustand vorauszusetzen.

Im weiteren wird ausgegangen von den Bedingungen des statischen Kräftegleichgewichtes

$$\frac{\partial \sigma_{1i}}{\partial x_1} + \frac{\partial \sigma_{2i}}{\partial x_2} + \frac{\partial \sigma_{3i}}{\partial x_3} = 0, \quad i = 1, 2, 3 \tag{1}$$

der Fließbedingungen von MISES

$$\begin{aligned} I_2 - K^2 \text{ mit } I_2 &= \frac{1}{2} \sum_{i,j=1}^{3} \overline{\sigma}_{ii}^2 \\ \overline{\sigma}_{ii} &= \sigma_{ij} - \sigma_m \, \delta_{ij} \\ \sigma_m &= \frac{1}{2} \sum_{i,j=1}^{3} \sigma_{ij} \end{aligned} \tag{2}$$

und dem Stoffgesetz

$$\bar{\sigma}_{ij} = \frac{K \cdot \dot{\varepsilon}_{ij}}{\sqrt{\dot{I}_2}} \quad \text{mit} \quad \dot{I}_2 = \frac{1}{2} \sum_{i,j=1}^{3} \dot{\varepsilon}_{ij}^2 . \tag{3}$$

Entsprechend unserer eingangs getroffenen Annahme wird der ebene Deformationszustand betrachtet.

Für die Spannungen wird angesetzt

$$\sigma_{11} = p + k \cdot \sin 2\vartheta, \tag{4.1}$$

$$\sigma_{22} = p - k \cdot \sin 2\vartheta, \tag{4.2}$$

$$\sigma_{12} = -k \cdot \cos 2\vartheta \tag{4.3}$$

mit der Mittelspannung $p(x,y) = p = (1/2)(\sigma_{11} + \sigma_{22})$ und dem Winkel $\vartheta(x, y) = \vartheta$, den die Tangente an eine erste Gleitlinie im Punkt $P(x, y)$ mit der positiven y-Achse bildet. Dann sind $p(x, y)$ und $\vartheta(x, y)$ Lösungen des quasilinearen partiellen Differntialgleichungssystems.

$$\frac{\partial P}{\partial x} + 2K \left(\frac{\partial \vartheta}{\partial x} \cos 2\vartheta + \frac{\partial \vartheta}{\partial y} \sin 2\vartheta \right) = 0 , \tag{5.1}$$

$$\frac{\partial P}{\partial y} + 2K \left(\frac{\partial \vartheta}{\partial x} \sin 2\vartheta - \frac{\partial \vartheta}{\partial y} \cos 2\vartheta \right) = 0 . \tag{5.2}$$

Die Gleichungen (5) wurden unter der Voraussetzung abgeleitet, daß die Fließschubspannung k im gesamten Gebiet des uneingeschränkten plastischen Fließens konstant ist.

Soll der Einfluß der im realen Zerspanungsvorgang wirkenden Verfestigung berücksichtigt werden, muß eine von CHRISTOPHERSEN [9] vorgenommene und von PALMER/OXLEY [10] vollständig auf die Zerspanung angewendete veränderliche Fließschubspannung $k = k(x, y)$ berücksichtigt werden. Neuerdings wurden aus experimentellen Untersuchungen des Zerspanungsvorganges mittels der Methode der Visioplastizität von MAKINO [11] Gleitlinienfelder und Spannungsverteilungen berechnet. Über einen Zusammenhang zwischen der Änderung der Gleichgewichtskomponenten von Materialteilchen gemäß der Geiringer-Gleichungen und den Komponenten des Versetzungschichtetensors berichten WENG/PHILLIPS [12].

Sind geeignete Randbedingungen gegeben, dann können Lösungen für die Gleichungen (5) gefunden werden und es ist möglich, die Spannungsverteilung für dieses Problem des ebenen plastischen Fließens zu ermitteln. Hierbei sind bereits bekannte Methoden der Analysis anwendbar.

Bild 4 zeigt die für die weiteren Ableitungen nötigen Definitionen. Daraus wird deutlich, daß die Schubspannung in den Punkten I bzw. II ihren Maximal-

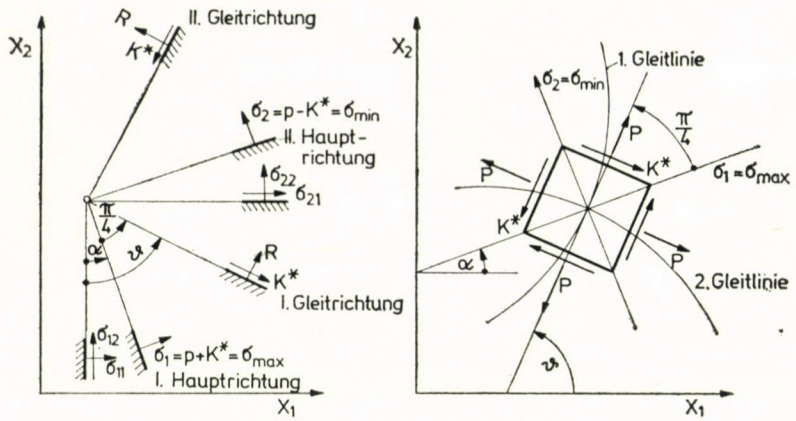

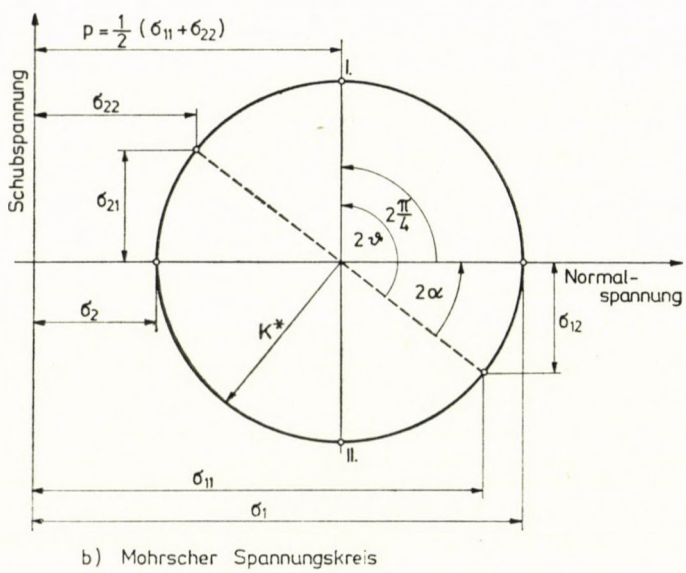

Bild. 4. Definitionen in der physikalischen Ebene und Spannungsebene

wert erreicht und betragsmäßig gleich der Schubfließgrenze k ist. Die im Bild 4 eingezeichneten Strecken I-P bzw. II-P repräsentieren die beiden Gleitrichtungen. Eine Gleitlinie ist eine Kurve, die in jedem ihrer Punkte den gleichen Neigungswinkel wie die Richtung der entsprechenden Gleitrichtung besitzt. Sie sind Hauptschubspannungslinien, längs deren die Schubspannung konstant ist.

Die Gleitlinienmethode ist weit entwickelt und liefert mit Werten der Praxis relativ gut übereinstimmende Integralgrößen. Daher scheint es zweck-

mäßig, trotz der eingangs erwähnten Einschränkungen, die Gleitlinienmethode zur Untersuchung des Zerspanungsvorganges anzuwenden. LEE/SHAFFER [13] wendeten sie erstmals auf den Spanbildungsvorgang an. Sie gingen davon aus, daß die Scherebene gleichzeitig Gleitebene ist. Damit ergab sich, beginnend von der Scherebene (vgl. Bild 5a) ein Feld konstanter Spannungen. Praktische Untersuchungen zeigten deutliche Abweichungen von der Theorie. Insbesondere führen große Reibwinkel und kleine bzw. negative Spanwinkel zu großen bzw. unendlichen Werten für die Schnittkräfte. Durch Berücksichtigung einer Aufbauschneide an der Schneidkante und dem Einfügen eines in P_0 — zentrierten Fächers konnten gewisse Schwierigkeiten beseitigt werden.

Die von WEBER [8] vorgenommene Erweiterung der Lösungen von LEE/SHAFFER [13] erfolgte so, daß alle möglichen Reibwerte $\mu = \sigma_{12}/\sigma_{11}$ im Bereich $0 \leq \mu \leq 1$ auf der Spanfläche für jeden möglichen Spanwinkel $-90° = \gamma = +90°$ auftreten können. In (8) werden Gleitlinienfelder entwickelt, die diesen erweiterten Bedingungen entsprechen.

Für theoretisch scharfe Werkzeuge zeigt Bild 6 diese Felder. Bereits nach kurzer Schnittzeit zeigt die Schneide eine Schneidkantenrundung sowie Freiflächenverschleiß. Deshalb sind erweiterte Gleitlinien- und Geschwindigkeitsfelder nötig. Messungen von SMEJCAL [14] zeigten u. a. eine konkave Krümmung der Scherlinie im Bereich der Schneidkante. Hinzu kommt, daß jedes im Eingriff befindliche Werkzeug einen Schneidkantenradius aufweist. Das Gleitlinienfeld nach Bild 5 befriedigt alle diese Forderungen.

Der Span gleitet über der Spanfläche des Werkzeuges innerhalb der Kontaktlänge $1_k = \overline{0 - P_k}$. In P_k und M_1 soll Spannungsfreiheit herrschen. Die Linie $P_k - M_1$ gibt die Richtung der größten Hauptspannung an. Das Gleitlinienfeld $P_k - M_1 - P_{M1} - P_k$ ist ein Gebiet konstanten Zustandes (Bild 5a). Diesem plastischen Feld konstanter Spannungen schließt sich ein zentrierter Fächer mit dem Mittelpunkt in M_1 und dem Öffnungswinkel Θ an (Bild 5b). Der Teil $\overline{M_1 - P_{1,1}}$ des Fächers ist der gerade Teil der Scherlinie. Ihm folgt über den Schneidkantenradius der gekrümmte Teil der Scherlinie $\widehat{P_{1,1} - P_{1,N}}$.

Die Randgleitlinien $\widehat{P_{M,1} - P_{1,1}}$ und $\widehat{P_{1,1} - P_{1,N}}$ grenzen ein allgemeines HENCKY-PRANDTL-Netz gekrümmter Gleitlinien ab.

In [8] werden auch Näherungslösungen für die Schnittkräfte, aus den Spannungsverhältnissen längs der Scherfläche abgeleitet. Für die Schnittkraft F_S und die Drangkraft F_D gilt:

$$F = -k \cdot b \cdot h \, [\cot \Phi + (1 - 2\Theta)], \tag{6.1}$$

$$F = +k \cdot b \cdot h \, [(1 - 2\Theta) \cot \Phi - 1]. \tag{6.2}$$

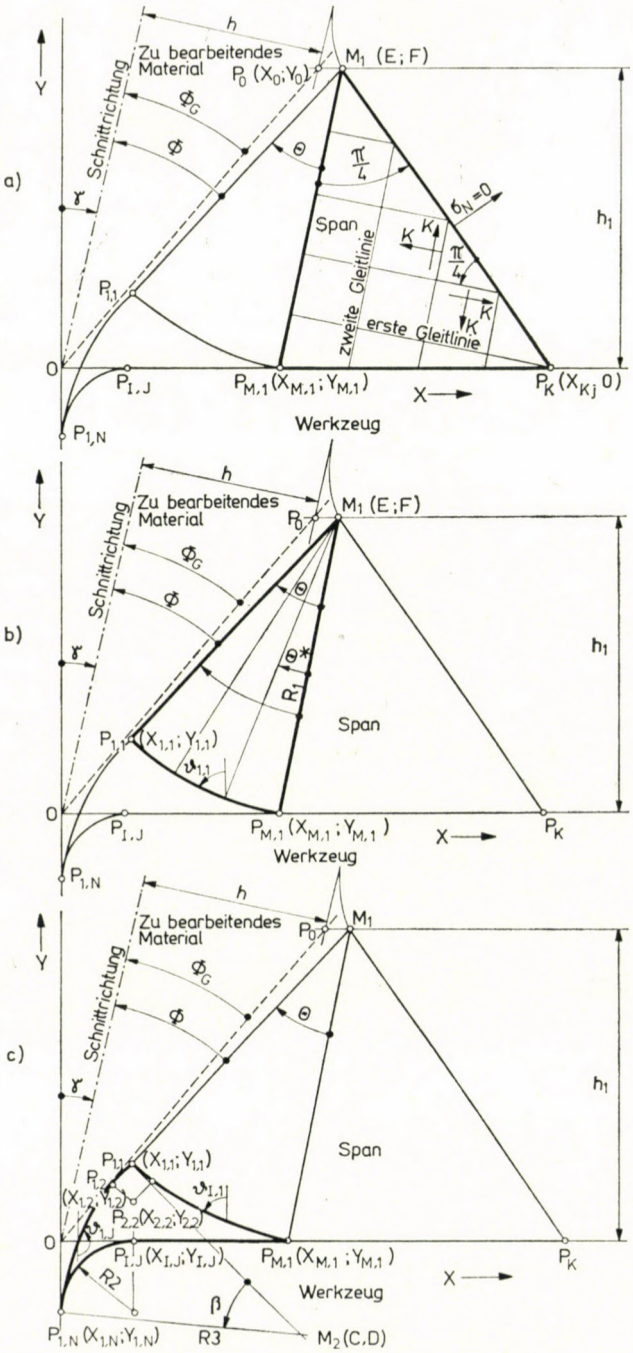

Bild. 5. **Erweitertes Gleitlinienfeld für einen negativen zentrierten Fächer und Schneidkantenrundung**

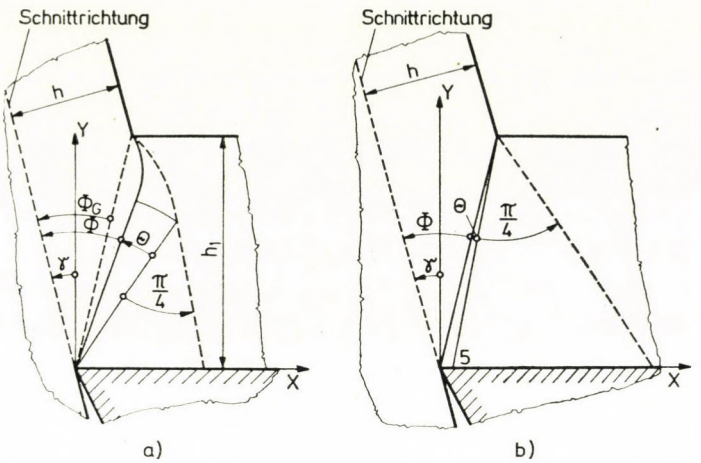

Bild. 6. Spanbildungsmodelle für theoretisch scharfe Werkzeuge

Zusammen mit der Spanstauchung

$$\frac{h_1}{h} = \cos\gamma \cdot \cot\Phi + \sin\gamma \tag{7}$$

steht ein System von drei Gleichungen zur Verfügung, mit dem aus einer Messung von F_S, F_D und h_1/h der Scherwinkel Φ, der Fächeröffnungswinkel Θ sowie die Schubfließgrenze k bestimmt werden können.

Wie Untersuchungen in [8] zeigten, strebt die Schubfließgrenze für große Spanungsdicken und hohen Verformungsgeschwindigkeiten einem Grenzwert zu. Dieser ist materialabhängig.

Zum Beispiel werden für *C* 15 das $K_{\text{Grenz}} = 44$ kp/mm² und für *C* 60 das $K_{\text{Grenz}} = 65$ kp/mm² ermittelt. Es wird angenommen, daß diese Grenzwerte den Belastungen in der Scherebene entsprechen.

Mit Hilfe dieser Schubspannungskorrektur ist es möglich, über die Gleichungen (6)–(7) einen mittleren wirkenden Spanwinkel γ_w einen wirkenden Scherwinkel Φ_w und Öffnungswinkel Θ_w zu berechnen. Sie sind der Ausgangspunkt für die Konstruktion des Gleitlinienfeldes oberhalb der Spanfläche.

4. Numerische Berechnung des Gleitlinienfeldes nahe der Schneidkantenrundgung

Nahe der Schneidkante wird das Werkzeug am stärksten mechanisch belastet. Damit ist das plastische Gebiet $P_{1,1} - P_{1,N} - P_{M,1} - P_{1,1}$ von besonderem Interesse. Infolge der Krümmung der Scherlinie zwischen $\overset{\frown}{P_{1,1} - P_{1,N}}$

handelt es sich hierbei um ein verallgemeinertes HENCKY-PRANDTL-Netz gekrümmter Gleitlinien. Das zu bestimmende Gleitlinienfeld wird begrenzt durch die erste Gleitlinie $\overset{\frown}{P_{M,1} - P_{1,1}}$ (Kreisbogen), durch den gekrümmten Teil der Scherlinie $\overset{\frown}{P_{1,1} - P_{1,N}}$ (zweite Gleitlinie) sowie durch die Spanfläche des Werkzeuges, bestehend aus den Bogen der Schneidkantenrundung mit dem Radius R_2 und dem sich anschließenden geraden Teil bis zum Punkt $P_{M,1}$.

Zweckmäßigerweise werden zuerst alle dimensionslosen Variablen des Spannungszustandes $\omega_{I,1}$ und $\vartheta_{I,1}$ entlang der Randgleitlinie $P_{M,1} - P_{1,1}$ bestimmt, und anschließend die $\omega_{1,J}$ bzw. $\vartheta_{1,J}$ entlang des gekrümmten Teiles der Scherlinie. In $P_{M,1}$ gilt nach [8] $p = -k$ und damit für $\omega_{I,1} = -05$. Der Winkel $\vartheta_{M,1}$ der ersten Gleitlinie in $P_{M,1}$ ergibt sich zu

$$\vartheta_{M.1} - \gamma_w - \Theta_w - \Phi_w + \frac{\pi}{2} . \tag{8}$$

Da für den negativ zentrierten Fächer $M_1 - P_{1,1} - P_{M,1} - M_1$ die Randgleitlinie $\overset{\frown}{P_{1,1} - P_{M,1}}$ ein Kreisbogen ist, erhält man bei äquidistanter Änderung des Fächeröffnungswinkels Θ für den Neigungswinkel $\vartheta_{I,1}$

$$\vartheta_{I,1} = \vartheta_{M,1}' + \frac{M - I}{M - 1}\Theta, \quad I - 1, 2, \ldots, M. \tag{9}$$

Nach einem Satz von HENCKY folgt für $\omega_{I,1}$

$$\omega_{I,1} = \omega_{I+1,1} + \vartheta_{I,1} - \vartheta_{I+1,1} . \tag{10}$$

Vom Punkt $P_{M,1}$ beginnend werden die $\omega_{I,1}$ und $\vartheta_{I,1}$ entlang der ersten Gleitlinie bis $P_{1,1}$ berechnet und von dort analog die $\omega_{1,J}$ bzw. $\vartheta_{1,J}$ bis $P_{1,N}$. Zur Konstruktion des Gleitlinienfeldes im Innern dieser Randgleitlinien wird die Sekantenmethode benutzt (Bild 7).

Jedes Bogenstück wird durch eine Sehne ersetzt, deren Neigung das Mittel der Endneigung ist. Unter Nutzung der Orthogonalitätsbedingungen der Gleitlinien folgt für die Koordinaten von $P_{I,J}$:

$$X_{I,J} = \frac{Y_{I-1,J} - Y_{I,J-1} \mp X_{I-1,J} \cot \vartheta^*_{I,J} + X_{I,J-1} \tan \vartheta^*_{I,J}}{\cot \vartheta^*_{I,J} + \tan \vartheta^*_{I,J}} , \tag{11}$$

$$Y_{I,J} = Y_{I-1,J} + \frac{X_{I-1,J} - X_{I,J}}{\tan \vartheta^*_{I,J}} , \tag{12}$$

$$\vartheta^*_{J,J} = \frac{1}{2}(\vartheta_{I,J} + \vartheta_{I-1,J}) . \tag{13}$$

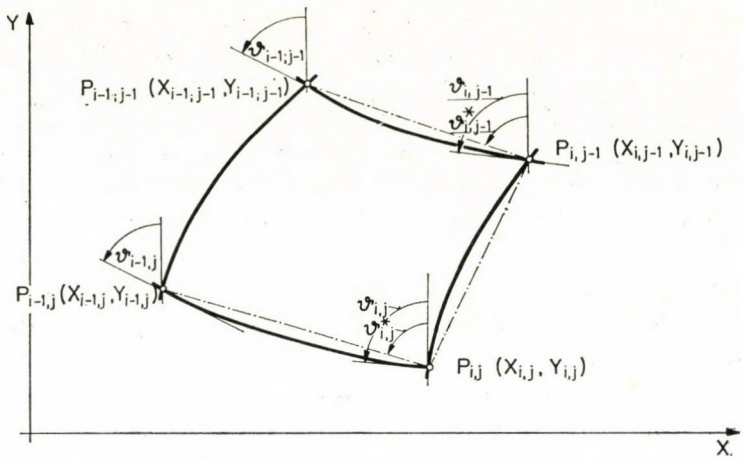

Bild. 7 Approximationsmodel zur näherungsweisen Berechnung innerer Punkte des Gleitlinienfeldes

Die Reihenfolge, in der diese Punkte berechnet werden, ist beliebig. Praktisch hat es sich als günstig erwiesen, erst alle Punkte einer Gleitlinie zu berechnen, bevor die nächste folgt. Die Berechnung wird abgebrochen, wenn die Spanfläche am Werkzeug erreicht bzw. gerade unterschritten wurde.

Mit Hilfe des ersten HENCKY'schen Satzes kann der Neigungswinkel der durch den Punkt $P_{1,J}$ gehenden ersten Gleitlinie zu

$$\vartheta_{I,J} = \vartheta_{I-1,J} + \vartheta_{I-1,J} - \vartheta_{I-1,\,J-1} \tag{14}$$

bestimmt werden.

Für $\omega_{I,1}$ erhält man

$$\omega_{I,1} = \omega_{I-1,J} - \vartheta_{I-1,J} + \vartheta_{I,J}\,. \tag{15}$$

Die Normal- bzw. Schubspannungen im Punkt $P_{I,J}$ sind:

$$\sigma_{11}(I, J) = k \cdot \omega_{I,J} + k \cdot \sin 2\vartheta_{I,J}\,, \tag{16.1}$$

$$\sigma_{22}(\mathrm{I}, J) = k \cdot \omega_{I,J} - k \cdot \sin 2\vartheta_{I,J}\,, \tag{16.2}$$

$$\sigma_{12}(I, J) = -\mathrm{k} \cdot \cos 2\vartheta_{I.J}\,. \tag{16.3}$$

Mit einem auf dieser Grundlage erstellten FORTRAN-Programm [15] wurde u. a. die Spannungsverteilung im Bereich des Fächers für drei verschiedene Schneidkantenradien berechnet. Wie aus Bild 8 ersichtlich, hat der Schneidkantenradius einen besonders großen Einfluß auf die Normalspannung σ_{11} (äußere Normalspannung auf der Spanfläche). Dies deutet darauf hin, daß ein

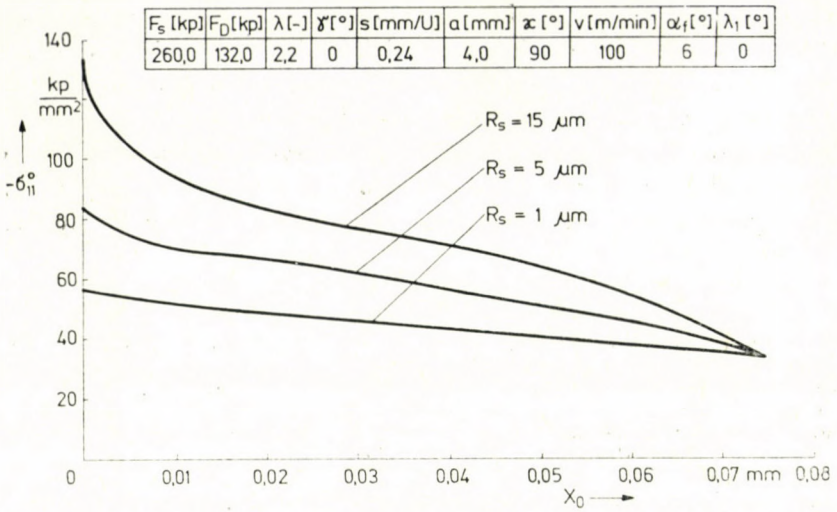

Bild. 8. Abhängigkeit der Normalspannung σ_{11} vom Schneidkantenradius R_S im Berech des Fächers

sich vergrößernder Schneidkantenradius im Bearbeitungsprozeß nicht nur unmittelbar in Schneidkantenspitze höhere Werkzeugbelastungen hervorruft, sondern im gesamten Bereich des Fächers. Eine Erweiterung der Untersuchungen auf den Bereich der Freifläche ist möglich.

5. Zusammenfassung

Die beschriebene Methode der Modellierung des Spanbildungsvorganges mittels Gleitlinien kann in analoger Weise auf die Berechnung der Spanungsverteilung entlang der Freifläche erweitert werden. Derartige Berechnungen würden es gestatten, die Belastungen der Freifläche zu ermitteln sowie Aussagen über zu erwartende Verfestigungstiefen an gespanten Oberflächen zu treffen.

Da bei jedem realen Spanbildungsvorgang die Schneide gerundet ist, ist im Bereich der Schneidenrundung ein negativ zentrierter Fächer vorhanden. Die Stauzone kann sowohl im "festen" als auch im plastischen Zustand vorhanden sein. Dieser, Zustand wird durch die Temperatur in der unmittelbaren Umgebung der Schneide sowie durch die Werkstoff-Schneidstoff-Paarung bestimmt. Damit ist die Stauzone der Keim für eine Aufbauschneidenbildung. Eine Aufbauschneide kann sich bei allen Spanwinkeln bilden. Ihre Größe ist vom Spanwinkel abhängig.

Die Voraussetzung starr-ideal-plastischen Werkstoffverhaltens zwischen $P_{M,1}$ und P_K muß als eine grobe Näherung angesehen werden, wie Vergleiche

zwischen den nach diesem Modell berechneten Kontaktlängen l_K und Versuchen zeigen. Zum anderen müssen die sich in der Fließschicht an der Spanunterseite bzw. Freifläche abspielenden Vorgänge ausgeklammert werden und getrennten Untersuchungen vorbehalten bleiben.

Der exakten Bestimmung der Größe des Schneidkantenradius muß große Aufmerksamkeit geschenkt werden. Änderungen im Bereich von $1 \leqq R_S \leqq$ $\leqq 15$ μm ergaben stark veränderte Spanungsverläufe entlang der Spanfläche.

SCHRIFTTUM

1. KACZMAREK, J.: Hauptentwicklungsrichtungen der Fertigungstechnik *WZ der TH Karl-Marx-Stadt*, **16,** (1974), 1, 5—20
2. HOFMANN, D.: Bericht vom Rundtischgespräch "Meßtheorie während des VII. IMEKO-Kongreß in London 1976" msr **19,** (1976), 10, 328
3. MERCHANT, M. E.: Long-range Trends in the Automation of Machine Tools and Manufacturing 16. MTDR-UMIST, Manchester, Konferenz vom 10. — 12. 9. 1975
4. SATA, T.—FUJITA, N.—HIRAMATSU, Y.—KOKUBO, K.—TAKEYAMA, H.: The Present Stage and Future of the Machinability Data Service in Japan Fourteen. *International Machine Tool Design and Research Conference Manchester* 12. — 14. September 1973
5. JACOBS, H.—J.: Primärdatengewinnung für Fräsoptimierung durch Richtwertmaschine *Annals of the CIRP* **25,** (1976) 1, 403—406
6. LEOPOLD, J.—TOTZAUER, W.: Unveröffentlichter Forschungsbericht TH Karl-Marx-Stadt, Sektion FPM 1975
7. NAUMANN, J.: Beitrag zur experimentellen Untersuchung plastischer Fließvorgänge mit dem Moirèverfahren Diss. TH Karl-Marx-Stadt 1973
8. WEBER, H.: Mechanik der Spanbildung. *WZ der THK* **11,** (1969), 5. 597—629
9. CHRISTOPHERSEN, D. G.— OXLEY, P. L. B.—PALMER, W. B.: Orthogonal Cutting of work-Hardening Material *Engineering* **186,** (1958), 113
10. PALMER, W. B.—OXLEY, P. L. B.: Mechanics of Orthogonal Maching Proc. *Instn. Mech. Engrs.* **173,** (1959), 24, 623—638
11. MAKINO, R.: Spannungs- und Dehnungsverteilung beim langsamen Fileßspannen *Seimisu Kikai* **39,** (1973), 3, 318—325
12. WENG, GEORG, J.— PHILLIPS, ARIS: On the Kinematics of Continuous Distribution of Dislocations in Plasticity *Int. J. Engng.* Sci. **14,** (1976), 65—73
13. LEE, E., H.— SHAFFER, B. W.: The Theory of Plasticity Applied to a Problem of Machining. *Journal of Applied Mechanics* **73,** (1951), 405—413
14. SMEJKAL, E.: Schnitkraft und Spanbildung — über einige plastizitätsmechanische Zusammenhänge beim Spanen im freien Schnitt Diss. TH Karl-Jarx-Stadt, 1969
15. LEOPOLD, J.—ARNOLD, W.: Zur numerischen Berechnung von Gleitlinienfeldern bei der Zerspanung *WZ der THK* **19,** (1977), 1, 145—152
16. TOTZAUER, W.: Forschungsbericht 1976, THK, sektion FPM

An Investigation of Chip Forming Based on the Theory of Elasticity. The paper presents a model for calculating the stresses on the cutting surface of a cutting tool based on the theory of sliding lines. The sliding line fields known since LEE and SHAFFER, are extended as for the coefficient of friction, the possible chip angle and a realistic cutting edge radius. Some results of numerical calculations are discussed; they show the great influence of the cutting edge radius on the stress distribution.

Исследование механизма пластичности процесса образования напряжения. Вданной работе приведена модель для вычисления напряжений на напряженной поверхности режущего инструмента. В качестве основы исследований служит теория линии скольжения. Поля линии скольжения LEE и SHAFFER расширены в отношении показателя трения, возможного угла напряжения и с учетом реального округления режущей кромки. Приведено обсуждение некоторых результатов числовых вычислений. На основе чего установливается большое воздействие радиуса режущей кромки на распределение напряжений.

Acta Technica Academiae Scientiarum Hungaricae, Tomus 86 (3—4), pp. 301—316 (1978)

SIMPLE, DISCRETE MODELS OF THE ELASTIC SUBGRADE

S. KALISZKY*

DR. TECHN. SCI.

[Manuscript received 8 September, 1977]

Paper presents the pyramid and the shear models of subgrade which both can be used for the numerical analysis of elastically supported structures and the subgrade, as well. Containing two independent parameters the shear model is quite general, since as special cases the Winkler—Zimmermann and the pyramid models are also included in it. The application of the two discrete models is illustrated by a numerical example.

1. Introduction

The investigation of the interaction between the supporting continuum and the structure is an important problem of technical mechanics. At these problems, however, the exact elastic analysis of the continuum (in the following subgrade) yields in very complicated calculation [1, 2] therefore in the practice the use of such models has become general which result in relatively simple analytical solutions or can form a basis for numerical computations.

The models elaborated by WINKLER—ZIMMERMANN [3, 4] PASTERNAK [5], FILONENKO-BORODITS [6] and VLASOV [7] replace the subgrade by a single layer of elastic elements (e.g. springs); therefore they lead to relatively simple analytical solutions but can not provide any informations about the stress and strain distribution of the subgrade. Using numerical methods as the finite element method a complete analysis of the structure and the subgrade can be carried out but it needs very large computations.

In order to eliminate these deficiencies and to overtake these difficulties, respectively, the application of such discrete models may be useful in the practice which are between the "one-layer" models and the finite element model both in respect to accuracy and computational work. Such discrete models are the *pyramid model* applied for analytical solutions by KANDAUROV [8] and later extended for numerical investigations [9, 10] and the *shear model* published first in [11]. In this paper both the pyramid and the shear model will be reviewed and with the aim of comparison the results of numerical examples will be also presented.

* Prof. Dr. S. KALISZKY, Delej u. 25. 1089 Budapest, Hungary.

2. The pyramid model

The pyramid model of subgrade consists of smooth prismatical elements which only transmit normal stresses on their contact surfaces to each other. Every second layer of the elements is shiffted horizontally in such a manner that a force acting on the boundary of the subgrade spreads away in a triangular region as in case of a stone-wall or a pyramid (Fig. 1/a). Having n layers the pressure is distributed to the depth $H = nb$ on the breadth $L = na$. Because of the pressure the elements in the region A are deformed and, as a consequence of it, the stressless elements in the regions B undertake rigid body motion. Consequently, the effect of a force extends to the distance $L = na$ on the boundary of the subgrade.

Applying a unit vertical force at the point k of the boundary the resultant vertical forces s^0_{ij} arising in the elements can be calculated from the recurrent formula (Fig. 1/b):

$$s^0_{1j} = \delta, \text{ where } \delta = \begin{cases} 1, \text{ if j } = \text{k}, \\ 0, \text{ if } j \neq \text{k} \end{cases} \tag{1}$$

$$s^0_{ij} = \frac{1}{2}\left(s^0_{i-1,j-1} + s^0_{i-1,j}\right). \tag{2}$$

The results up to $n = 6$ layers are illustrated in Fig. 2. Having a system of vertical contact pressures acting on the boundary the normal forces s_{ij} arising in the elements can be uniquely determined by using formula (1) and (2) and the principle of superposition.

Let us suppose that the subgrade is of homogeneous and linear elastic material. Then the elastic properties of each element with the edges a, b and c can be characterised by the same single parameter k which is the force acting in the direction z and causing a unit strain in the same direction ($\varepsilon_z = 1$). In case of plane stress ($\sigma_y = 0$) and plane strain ($\varepsilon_y = 0$), respectively:

$$k = E\,\frac{ac}{b} = E\frac{nac}{H}, \tag{3}$$

$$k = \frac{\mathrm{E}}{1 - \nu^2}\,\frac{ac}{b} = \frac{E}{1 - \nu^2}\,\frac{nac}{H}. \tag{4}$$

Here E is the Young's modulus and ν is the Poisson's ratio of the material.

Considering the unit force acting at the point k of the boundary the vertical displacement in the point l of the boundary can be calculated from the formula:

$$v_{kl} = \frac{1}{2}\sum\sum s^{0k}_{ij}\, s^{0l}_{ij}. \tag{5}$$

Here s_{ij}^{0k} and s_{ij}^{0l} are the forces of the elements caused by the unit boundary forces acting at the point k and l, respectively. In formula (5) the summarization extends for all the elements where none of s_{ij}^{0k} and s_{ij}^{0l} is equal to zero. Depending on the number of layers applied the influence coefficients v_{kl} are

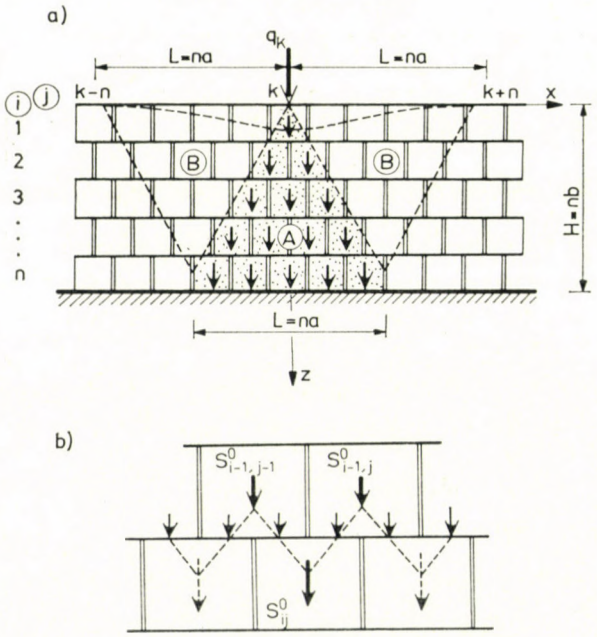

Fig. 1

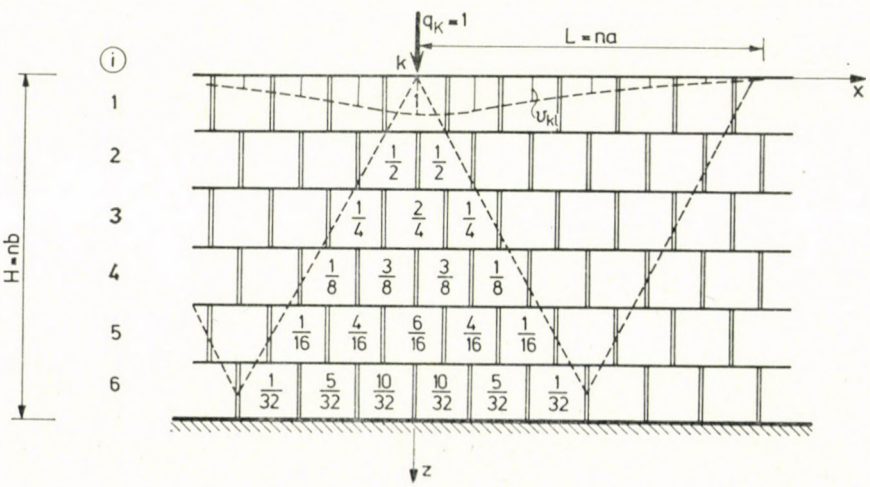

Fig. 2

given in Table I. As we shall see in Section 4. having these influence coefficients and the forces s_{ij}^0 the complete elastic analysis of a supported structure and the subgrade can be carried out.

Table I

Pyramid model

Number of layers applied (n)	Enlarged vertical displacements caused by a unit force (kv_{kl})								
	The point of displacement(l)								
	1	2	3	4	5	6	7	8	9
1	1								
2	$\frac{6}{4}$	$\frac{1}{4}$							
3	$\frac{30}{16}$	$\frac{8}{16}$	$\frac{1}{16}$						
4	$\frac{140}{64}$	$\frac{47}{64}$	$\frac{10}{64}$	$\frac{1}{64}$					
5	$\frac{630}{256}$	$\frac{244}{256}$	$\frac{68}{256}$	$\frac{12}{256}$	$\frac{1}{256}$				
6	$\frac{2772}{1024}$	$\frac{1186}{1024}$	$\frac{392}{1024}$	$\frac{93}{1024}$	$\frac{14}{1024}$	$\frac{1}{1024}$			
7	$\frac{12012}{4096}$	$\frac{5536}{4096}$	$\frac{2063}{4096}$	$\frac{592}{4096}$	$\frac{122}{4096}$	$\frac{16}{4096}$	$\frac{1}{4096}$		
8	$\frac{51480}{16384}$	$\frac{25147}{16384}$	$\frac{10254}{16384}$	$\frac{3369}{16384}$	$\frac{852}{16384}$	$\frac{155}{16384}$	$\frac{18}{16384}$	$\frac{1}{16384}$	
9	$\frac{218790}{65536}$	$\frac{112028}{65536}$	$\frac{49024}{65536}$	$\frac{18004}{65536}$	$\frac{5228}{65536}$	$\frac{1180}{65536}$	$\frac{192}{65536}$	$\frac{20}{65536}$	$\frac{1}{65536}$

3. The shear model

3.1. *Description of the model*

The shear model of subgrade consists of prismatical elements which can only transmit normal stresses on their horizontal contact surfaces to each other, on the vertical surfaces, however, in a prescribed manner shear stresses can also arise (Fig. 3/a). The elements construct a rectangular mesh thus, in this model the shear stresses are destined for the distribution of the pressure in the subgrade. It is supposed that a certain proportion (2α) of the force acting on the top of an element is transmitted by shear to the two neighbouring elements, while the reminder part ($\beta = 1 - 2\alpha$) of the force loads the supporting element. The neighbouring elements fully transmit their forces to their supporting elements by normal stresses i.e. no shear forces develop between the further elements.

Having n layers the pressure is distributed to the depth $H = nb$ on the breadth $L' = 2na$. Because of the pressure the elements in the region A are deformed and as a consequence of it the stressless elements in the regions B undertake rigid body motion. Consequently, the effect of a force extends to the distance $L = na$ on the boundary of the subgrade.

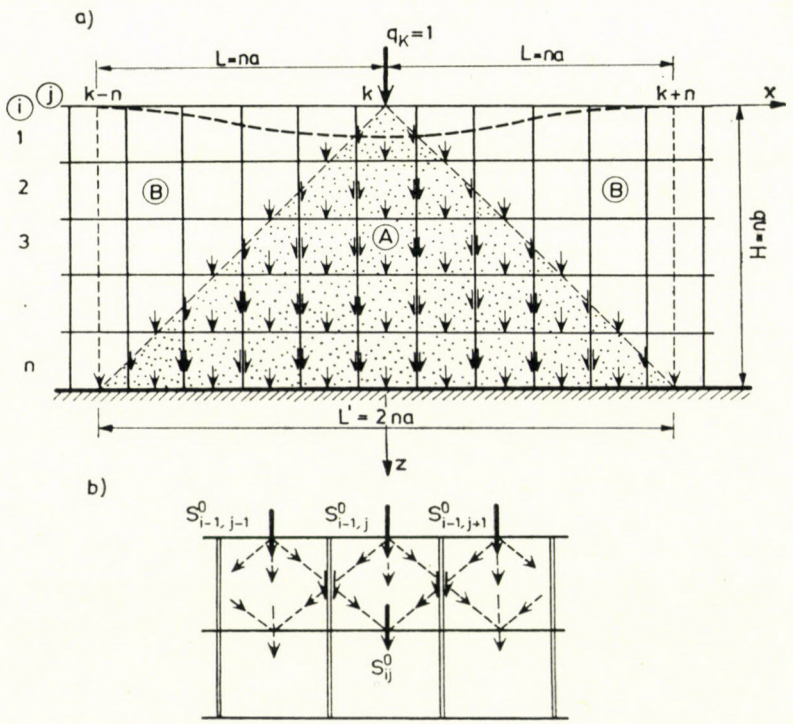

Fig. 3

Applying a unit vertical force at the point k of the boundary the vertical forces s^0_{ij} acting on the top of the elements can be calculated from the recurrent formula (Fig. 3/b):

$$s^0_{1j} = \delta, \text{ where } \delta = \begin{cases} 1, \text{ if } j = \text{k}, \\ 0, \text{ if } j \neq \text{k}. \end{cases} \tag{6}$$

$$s^0_{ij} = (1 - 2\alpha)\, s^0_{i-1,j} + \alpha\,(s^0_{i-1,j-1} + s^0_{i-1,j+1}). \tag{7}$$

The results in terms of α and $\beta = (1 - 2\alpha)$ up to $n = 6$ layers are given in Fig. 4.

Let us suppose that the subgrade is of homogeneous and linear elastic material. Then, neglecting the shear deformations and assuming that the vertical pressure in an element does not vary the elastic deformation of each element can be characterized by the same single parameter given by formula

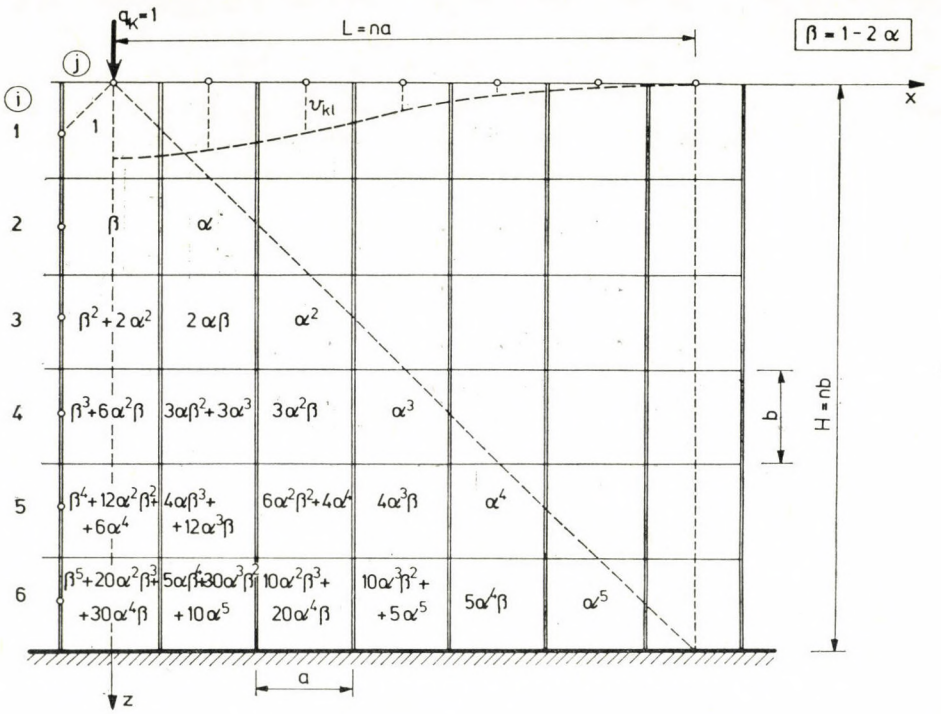

Fig. 4

(3) and (4). In order to be able to compare the results calculated by the use of different number of layers it may be useful to introduce a parameter which does not contain the number of layers. This parameter is in the state of plane stress and plane strain, respectively:

$$\bar{k} = \frac{k}{n} = E\frac{ac}{H} \tag{3a}$$

and

$$\bar{k} = \frac{k}{n} = \frac{E}{1-\nu^2}\,\frac{ac}{H}\,. \tag{4a}$$

One has to notice that the behaviour of the shear model is strongly influenced by the parameter α, too, but since the shear deformation are neg-

lected this parameter only plays a role in the distribution of the pressure as it will be illustrated later. By all means one can state, that the shear model is of two parameters since the behaviour of the subgrade can be described by two independent parameters (k and α).

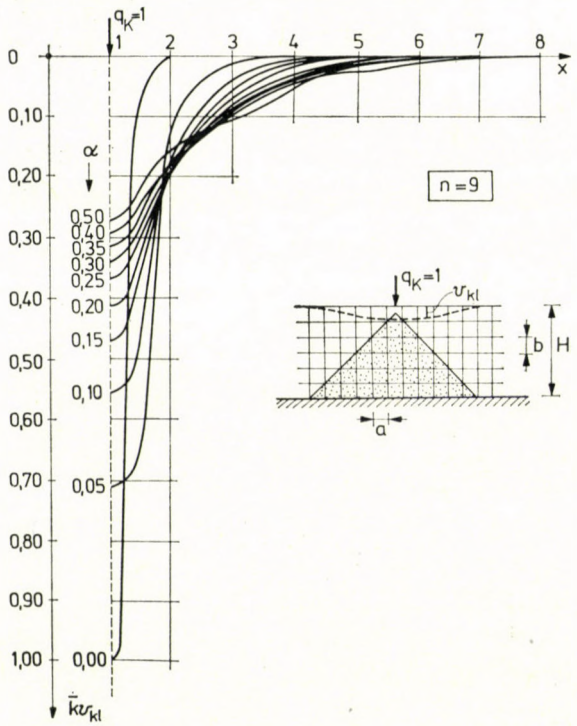

Fig. 5

Considering a unit force acting at the point k of the boundary the vertical displacement in the point l of the boundary can be calculated from the formula:

$$v_{kl} = \frac{1}{\bar{k}} \sum_{i=1}^{n} s_{il}^{0k}. \tag{8}$$

Here s_{il}^{0k} denotes the forces of the elements in the column $j = l$ caused by the unit force acting at the point $j = k$ of the boundary. The distribution of the influence coefficient v_{kl} for different values of α and n are illustrated in Fig. 5. and 6. and are given in Table II. and III. As we shall see later having these influence coefficients and the forces s_{ij}^{0} the complete elastic analysis of a supported structure and the subgrade can be carried out.

Table II

Shear model $\alpha = 0{,}25$

Number of layers applied (n)	Enlarged vertical displacements caused by a unit force ($\bar{k}v_{kl}$)								
	The point of displacement (l)								
	1	2	3	4	5	6	7	8	9
1	1								
3	0,625000	0,166667	0,020833						
5	0,492180	0,190625	0,053125	0,009375	0,000781				
7	0,418945	0,193080	0,071952	0,020647	0,004255	0,000558	0,000035		
9	0,370941	0,189935	0,083116	0,030250	0,008863	0,002000	0,000326	0,000034	0,000002

Table III

Shear model $n = 9$

α	Enlarged vertical displacements caused by a unit force ($\bar{k}v_{kl}$)								
	The point of displacement (l)								
	1	2	3	4	5	6	7	8	9
0,50	0,273437	0,162326	0,105902	0,049479	0,029513	0,009548	0,005208	0,000868	0,000434
0,40	0,296512	0,177618	0,096861	0,047090	0,020161	0,007282	0,002185	0,000473	0,000073
0,35	0,316103	0,182049	0,093893	0,042540	0,016528	0,005321	0,001348	0,000243	0,000025
0,30	0,340268	0,186287	0,089609	0,036956	0,012717	0,003507	0,000729	0,000102	0,000007
0,25	0,370941	0,189935	0,083116	0,030250	0,008863	0,002000	0,000326	0,000034	0,000002
0,20	0,411635	0,191899	0,073506	0,022450	0,005288	0,000920	0,000109	0,000008	0,000000
0,15	0,469122	0,189407	0,059261	0,014006	0,002437	0,000302	0,000025	0,000001	0,000000
0,10	0,557847	0,174986	0,039220	0,006215	0,000696	0,000054	0,000003	0,000000	0,000000
0,05	0,710445	0,128582	0,014963	0,001168	0,000062	0,000002	0,000000	0,000000	0,000000
0,00	1	0	0	0	0	0	0	0	0

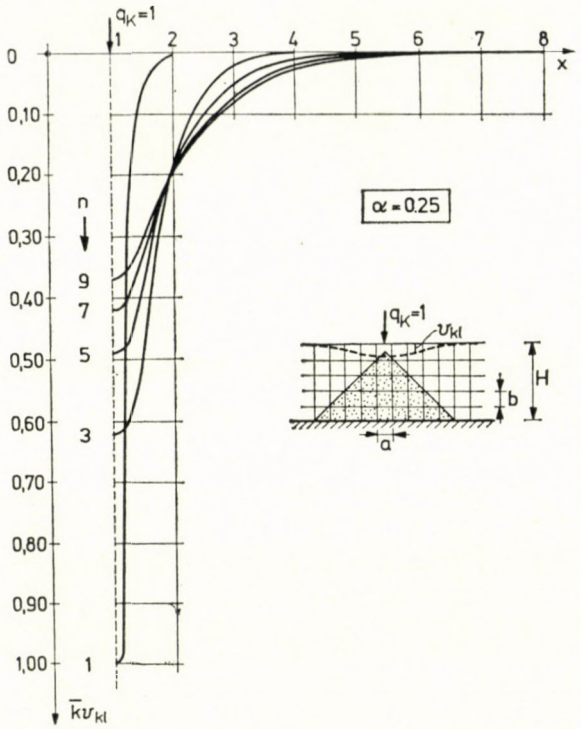

Fig. 6

3.2. *The role of the parameter* α

The parameter α of the shear model has an important role, since by its choice one can influence the pressure distribution in the subgrade. At the pyramid model there is not such a possibility since after assuming the mesh of the model the pressure distribution is uniquely determined by Eqs (1) and (2). Thus, the shear model is more general than the pyramid model, its behaviour can be controlled by the suitable choice of two parameters.

The parameter α can vary between 0 and 0,50 In case of $\alpha = 0$ there is no interaction between the neighbouring elements, therefore a force acting on the boundary of the subgrade is only carried by the elements lying on the vertical line of the force, in question. Thus, this special case corresponds to the Winkler-Zimmermann-model of subgrade. In the other extreme case ($\alpha = 0{,}50$) the elements transmit all their loads by shear forces to the neighbouring elements. As a consequence of it the pressure distribution of the subgrade belonging to a unit load and presented in Table IV. is very extreme (the normal force is equal to zero in every second element) and therefore the curve

Table IV

Shear model $\alpha = 0{,}50$

i	Force distribution in the subgrade corresponding to a unit load								
	1	2	3	4	5	6	7	8	9
1	1								
2	0	0,5							
3	0,5	0	0,250						
4	0	0,374	0	0,125					
5	0,375	0	0,250	0	0,0625				
6	0	0,3125	0	0,15625	0	0,03125			
7	0,3125	0	0,234375	0	0,09375	0	0,015625		
8	0	0,273438	0	0,164062	0	0,054688	0	0,007812	
9	0,273438	0	0,218750	0	0,109375	0	0,03125	0	0,003906

of displacements illustrated in Fig. 5 is also irregular. It is evident that such a subgrade which corresponds to the value $\alpha = 0{,}50$ does not exsist in the reality, therefore this case has no practical importance.

A particular attention should be paid to the case, when $\alpha = 0{,}25$. It is easy to prove that in such a case between the forces s_{ij}^{0p} and s_{ij}^{0s} belonging to the pyramid and the shear model, respectively there is the simple relationship

$$s_{(2i-1)j}^{0p} = s_{ij}^{0s}, \tag{9}$$

that means that the forces arising in each second layer of the pyramid model are equal to the forces of the shear model. Besides, it can be also proved that applying the same number of layers (n) the influence coefficients v_{kl}^{p} and v_{kl}^{s} of the pyramid and the shear model are identical:

$$v_{kl}^{p} = v_{kl}^{s}. \tag{10}$$

It means that when $\alpha = 0{,}25$ from the point of view of the supported structure the shear model yields in identical results with the pyramid model. *Thus, the pyramid model can be considered as a sepcial case of the shear model.* Because of the difference expressed by Eq. (9) the stress distributions of the subgrade obtained by the two models are not identical, still the discrepancy is not very significant.

It is to be seen from Fig. 5. that the parameter α has a significant influence on the distribution of the displacements of the boundary caused by a unit load. At lower values of α the displacements are larger below the load but departing from it they rapidly diminish, while at higher values of α the distribution of the displacements is more equal. At a given problem the value of α should be assumed corresponding to the actual behaviour of the subgrade on the ground of theoretical considerations or experiments. The detailed discussion of this question is beyond the scope of this paper. Further on a simple formula will be only presented which can enlighten the physical meaning of the different discrete models, in question. This formula has been deduced on the condition that the vertical displacements of the middle points of the vertical contact surfaces of two neighbouring elements should be equal. Then, introducing some simplifications the following relationship between the parameter α, the Young's modulus E, the shear modulus G and the size a and b of the elements applied can be obtained (Fig. 7.):

$$\alpha = \frac{1}{2\left(1 + \frac{aE}{bG}\right)}. \tag{11}$$

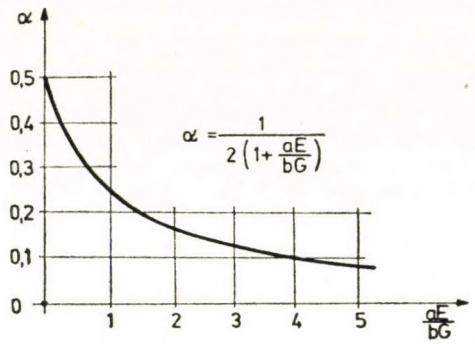

Fig. 7

One can see, that

if $G/E \to 0$,	then	$\alpha \to 0$,
if $G/E \to \infty$,	then	$\alpha \to 0{,}50$,
if $bG/aE = 1$,	then	$\alpha = 0{,}25$.

Accordingly, the Winkler-Zimmermann-model corresponds to a subgrade with zero shear stiffness ($G = 0$), while in case of $\alpha = 0{,}50$ the subgrade is of infinitely large shear stiffness ($G \to \infty$) or of zero compressional stiffness ($E \to 0$). According to the third case above the pyramid model describes correctly the behaviour of the subgrade in that case when the size of the elements applied are assumed corresponding to the ratio: $b/a = E/G$. It means, that at the pyramid model the mesh of the subgrade can not be assumed optionally, on the one hand, and it provides with some idea, on the other hand, for the suitable choice of the size of the elements at a given subgrade [9, 10].

At the shear model the ratio b/a can be assumed optionally and then using formula (11) the parameter α can be calculated.

4. The numerical analysis of the structure and the subgrade

4.1. *The procedure of computation*

The two models presented are suitable to the numerical analysis of an elastically supported elastic structure and the subgrade. The procedure of the computation at both models is the same and can be carried out as below.

Let us consider an elastic plane structure resting on an elastic subgrade. As it is usual at numerical computations let us assume along the part of the structure being in contact with the subgrade N joints in equal distance a. We suppose that the subgrade and the structure only at these joints are in connection and here only normal forces can be developed equaly in compres-

sion and in tension. Then, starting from the depth H of the subgrade we assume the thickness (b) and the number (n) of the layers, respectively and calculate the coefficient k and parameter α. From these at the application of any model the influence coefficients v_{kl} can be determined and the *flexibility matrix* **F** of size $N \times N$ of the subgrade can be constructed. Inverting **F** one can get the *stiffness matrix* **K** of the subgrade. For example at the pyramid model in case of $n = 3$ and $N = 8$ these matrices are as below:

$$\mathbf{F} = \frac{1}{k}\begin{bmatrix} \frac{30}{16} & \frac{8}{16} & \frac{1}{16} & 0 & 0 & 0 & 0 & 0 \\ \frac{8}{16} & \frac{30}{16} & \frac{8}{16} & \frac{1}{16} & 0 & 0 & 0 & 0 \\ \frac{1}{16} & \frac{8}{16} & \frac{30}{16} & \frac{8}{16} & \frac{1}{16} & 0 & 0 & 0 \\ 0 & \frac{1}{16} & \frac{8}{16} & \frac{30}{16} & \frac{8}{16} & \frac{1}{16} & 0 & 0 \\ 0 & 0 & \frac{1}{16} & \frac{8}{16} & \frac{30}{16} & \frac{8}{16} & \frac{1}{16} & 0 \\ 0 & 0 & 0 & \frac{1}{16} & \frac{8}{16} & \frac{30}{16} & \frac{8}{16} & \frac{1}{16} \\ 0 & 0 & 0 & 0 & \frac{1}{16} & \frac{8}{16} & \frac{30}{16} & \frac{8}{16} \\ 0 & 0 & 0 & 0 & 0 & \frac{1}{16} & \frac{8}{16} & \frac{30}{16} \end{bmatrix}$$

$$\mathbf{K} = \mathrm{k}\begin{bmatrix} ,57512 & -,15964 & ,02364 & -,00082 & -,00062 & ,00020 & -,00003 & ,00000 \\ -,15964 & ,61943 & -,16620 & ,02387 & -,00065 & -,00068 & ,00021 & -,00003 \\ ,02364 & -,16620 & ,62040 & -,16624 & ,02384 & -,00064 & -,00068 & ,00020 \\ -,00082 & ,02387 & -,16624 & ,62040 & -,16624 & ,02384 & -,00065 & -,00062 \\ -,00062 & -,00065 & ,02384 & -,16624 & ,62040 & -,16624 & ,02387 & -,00082 \\ ,00020 & -,00068 & -,00064 & ,02384 & -,16624 & ,62040 & -,16620 & ,02364 \\ -,00003 & ,00021 & -,00068 & -,00065 & ,02387 & -,16620 & ,61943 & -,15964 \\ ,00000 & -,00003 & ,00020 & -,00062 & -,00082 & ,02364 & -,15964 & ,57512 \end{bmatrix}$$

The **F** and **K** matrix of the subgrade can be incorporated in the flexibility and stiffness matrix of the structure, respectively and then, by the use of the force and the displacement method, respectively the analysis of the structure can be carried out. As a result of this calculation beside the stresses and

strains of the structure the contact forces q and the vertical displacements v of the boundary of the subgrade can be also obtained and finally, by the use of the formula of the s_{ij}^0 forces the distribution of the vertical normal stresses (σ_z) can be determined. Thus it can be stated, that the pyramid and the shear models are more advanced than e.q. the Winkler-Zimmermann or Pasternak models since by means of simple calculation they provide with approximate informations about the stress and strain field of the whole subgrade. Finally, it should be noticed, that because of its regular, rectangular mesh, the shear model is more suitable for numerical computations than the pyramid model.

4.2. *Numerical example*

The application of the shear model and the influence of the parameter α on the results will be illustrated by a simple numerical example shown in Fig. 8.

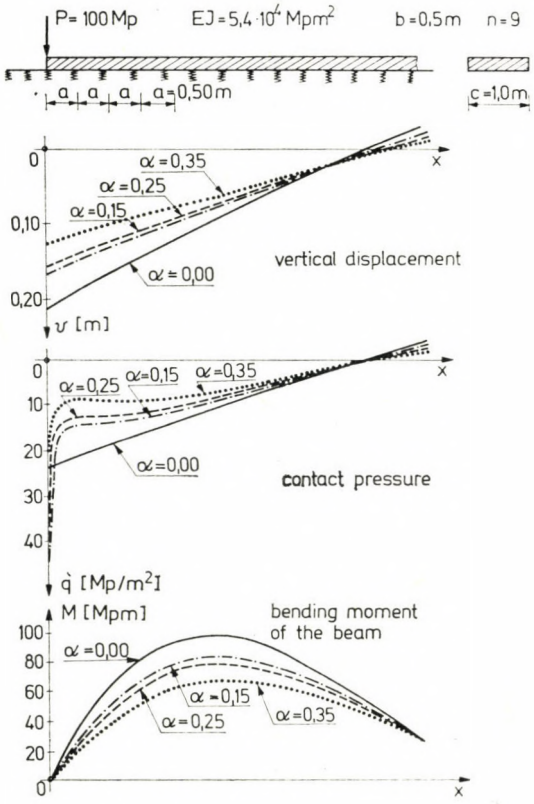

Fig. 8

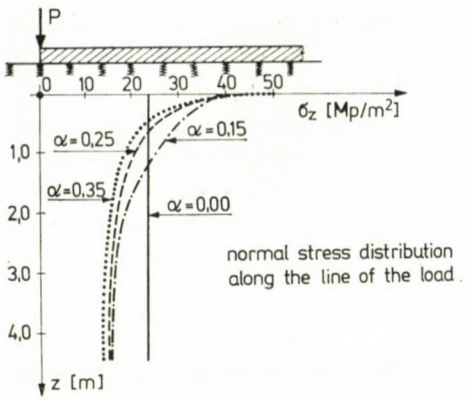

Fig. 9

The elastically supported infinitely long beam loaded by a force at its free end has the flexural stiffnes $EJ = 5{,}4 \cdot 10^4$ Mpm², and the width $c = 1{,}0$ m, while the subgrade is characterised by the Young's modulus $E_s = 1000$ Mp/m², the Poisson's ratio $\nu_s = 0$ (for the calculation of $\bar{k}$) and the depth $H = 4{,}5$ m. The size of the elements applied is $a = b = 0{,}5$ m, consequently the number of layers is $n = 9$.

The displacements and bending moments of the beam and the distribution of contact pressures and the normal stresses σ_z along the line of the load are illustrated in Figs 8. and 9. It can be seen that the parameter α has an important influence on the results of calculation. The results of the Winkler-Zimmermann-model especially show a great difference compared with the results of the cases $\alpha = 0{,}15-0{,}25$ which presumably are near to the actual behaviour of the subgrade. It refers to the well known deficiency and the bounds of application of the Winkler-Zimmermann model.

5. Conclusions

Two discrete models has been presented which both are suitable for the numerical analysis of elastically supported structures and the subgrade.

The pyramid model known already from the literature yields in simple calculations its deficiency is, however, that the behaviour of the subgrade is characterized by a single parameter and therefore the distribution of the pressure can be only influenced by the choice of the size of the applied elements. The shear model proposed in the paper contains two independent parameters and therefore eliminates this deficiency. This model can be considered as the generalization of the known simple discrete models of subgrade since as special cases the Winkler—Zimmermann and the pyramid models are also included in it.

In a previous paper it has been already shown [10] that the pyramid model is suitable for the investigation of inhomogeneous and plastic subgrade, too, and by the use of it space problems and subgrades bounded by a vertical plane can be also analysed. Such generalization of the shear model is also possible. It has been also proved that on the ground of both discrete models statically admissible stress fields of the subgrade can be constructed and those can be used for the limit analysis and optimal design of plastic structures resting on plastic subgrade. The results of these investigations will be published elsewhere.

REFERENCES

1. Boussinesq, J.: Application des potentiels a l'Etude de l'Equilibre et du Mouvement des Solides elastiques. Paris 1885
2. Flamant: *Compt. Rend.* **114,** p. 1465, 1892 Paris
3. Winkler, M.: Die Lehre von der Elastizität und Festigkeit. Prag 1867
4. Zimermann, H.: Die Berechnung des Eisenbahn-Oberbaues. 2. Aufl. Wilhelm Ernst und Sohn. Berlin 1930
5. Pasternak, P. L.: Osznovi novogo metoda raszcseta fundamentov na uprugom osznovanii pri pomosi dvich koefficientov poszteli. Gossztroizdat, Moszkva 1964
6. Filonenko-Borodits M. M.: Prosztejsaja model uprugovo osznovania szposzobnaja raszpredeljat nagruzki. Szb. Trudov. MEMIIT 53
7. Vlaszov V. Z.—Leontjev N. N.: Balki, pliti, obolocski na uprugom osznovanii. Gosztroizdat Moszkva 1960
8. Kandaurov I.: K teorii raszpredelenia naprozsenij b zernisztom gruntovom osznovanii. 1960
9. Kaliszky, S.—Galaskó Gy.: A New Model of the Elastic Subgrade (in Hungarian) *Mélyépítéstudományi Szemle* **25,** (1975) 298—305
10. Kaliszky, S.—Galaskó Gy.: Numerical Applications of the Pyramid Model of Subgrade. *Periodica Polytechnica* 1977
11. Kaliszky, S.: Simple, Discrete Models of the Elastic Subgrade (in Hungarian). *Építés-Építészettudomány* **9** (1977), 155—174

Einfache diskrete Modelle der elastischen Unterlage. Die Abhandlung beschreibt die Pyramiden- und Schubmodelle, die zur numerischen Untersuchung von Konstruktionen auf elastischer Unterlage benutzt werden können. Das zwei freie Parameter enthaltende Schubmodell ist allgemeiner, da es als Sonderfall auch das Winkler-Zimmermannsche und das Pyramidelmodell is sich enthält. Die Anwendung der beiden diskreten Modelle wird durch ein numerisches Beispiel erklärt.

Простые, дискретные модели упругого основания. Статья излагает пиранидная и касатульная модели применяюшчиеся численным решением конструкции лежающи на упругих основанниях. Касательная модель является больше обшой, потомущчто содержит специальный случайем и модель Винклерфициммермана, и пирамидная модель. Применение двух дискретних модели рассчотривается численныч причерач.

Acta Technica Academiae Scientiarum Hungaricae, Tomus 86 (3—4), pp. 317—329 (1978)

REMARKS ON THE CALCULATION OF THE TOOTH FRICTION LOSSES OF GEARS

L. HUSZTHY*

[Manuscript received February 6, 1975]

Numerous books and papers have dealt with the tooth friction losses of gear pairs. In the basically equivalent formulae deduced by different authors the coefficient of friction is a mean value determined by some experiment. The present paper aims at a more accurate definition of the "mean" friction coefficient and at clarifying the conditions under which the relation for tooth friction are valid.

Symbols

a = center distance
d_1, d_2 = diameter of pinion and gear rolling circle, resp.
e_1, e_2 = contact section length from pitch point to addendum circle
i = gear ratio
k, l = length of section corresponding to double contact on the line of action
r_1, r_2 = radius of rolling circle of pinion and of gear
t = pitch
t_a = base pitch
u_1, u_2 = length of single-pair contact on line of action
v = peripheral velocity at the pitch point
v_1, v_2 = circumferential velocity components on the tooth profile of pinion and gear, respectively, at the point of contact
v_a = mean sliding velocity between teeth
v_r = $v_1 - v_2$ = relative sliding velocity between teeth
v_s = $v_1 + v_2$ so-called transportation velocity
z_1, z_2 = number of teeth of pinion and gear
x, y = coordinates
A, E end points of contact section
E_1, E_2 end points of single pair contact section
C = pitch point
F_n = tooth force in normal direction
M = moment
P = power
W_0 = tooth friction work per unit time
W_a = tooth friction work per base pitch on contact line
W_k = tooth friction work per time of contact of one teeth pair
α = pressure angle
ε = contact ratio
ζ = viscosity of lubricate
η = efficiency
μ = coefficient of friction
τ = time
ω_1, ω_2 = angular velocity of pinion and gear

* Dr. L. HUSZTHY, Miskolc

Introduction

Gear pairs are practically dimensioned according to several principles depending on the purpose of the gearbox, under what operating conditions they are expected to operate. In the very extensive literature are found those dimensioning methods which provide long life, high strength (against breaking and surface damage), possibility of hydrodynamical lubrication, quiet, noiseless operation etc. and possibly to aim at securing the combined realization of several favourable characteristics [2, 3, 11, 12, 14].

In the application of gears the efficiency is *generally* of no particular significance. With gears made from suitable material, accurately machined and assembled, in well maintained gearboxes, the percentage of tooth friction losses of one gear pair is in general negligible, as compared to the transmitted power (0, 2, . . .1,5%).

Nevertheless there are cases when the tooth friction loss is of importance or when it causes tooth damage.

In "Die Tragfähigkeit der Zahnräder" THOMAS [12] remarks: "Because of the low sliding velocity at very low speeds dry friction should be anticipated and therefore shorter life — aprox. half of that for medium speeds . . at very high speeds also dry friction occurs because of the lubricant being thrown out. Such gears tend to overheat ans sieze already at small loads."

In his "Gear Handbook" DUDLEY [3] attracts attention to the fact that " . . . if the power must be transmitted with the smallest possible energy loss . . . sliding must be kept at the smallest value possible; . . . an accelerating drive is the most sensitive to friction between teeth". Furthermore: "With an accelerating drive the higher efficiency may have increased importance; there have been cases when because of the high friction and unsufficient lubrication self-locking has occurred". (With a high coefficient of friction the resultant of the tooth force at normal direction and the friction force, acting on the driven gear, at the beginning part of contact strongly deviates from the direction of the tooth normal towards the axis of the driven gear, thus, the transmitted torque is greatly reduced; with an accelerating drive, in the entering section of the engagement at the foot part of the driving gear a hollow, at the addendum part of the diven gear a bulge forms [13], with a corresponding braking effect).

In the transmission of large powers the tooth friction loss can amount to a high value, if not percentually, but absolutely, and in that case reduction of friction is certainly useful [11].

From the point of view of friction loss evacuation it is essential to know the value of tooth friction loss anyhow and to reduce it if possible [11].

In the following some remarks will be made in connection with the calculation of the tooth friction losses of spur gears.

It is assumed that accurately manufactured and assembled gears are dealt with.

1. On the tooth friction in general

The instantaneous value of the tooth friction power of mating gears is

$$P = \mu F_n |v_r| \,. \tag{1}$$

If a gear pair is working at center distance a with a ratio i and the tooth profile of one wheel (generally of the pinion) at the moment $\tau = 0$ is described by

$$\begin{aligned} x &= x(\varphi) \\ y &= y(\varphi) \end{aligned} \tag{2}$$

in some suitable system of coordinates (Fig. 1), where φ is a geometrical parameter, the equations describing the tooth profile of the other wheel are univocally given and the relative sliding velocity of the mating profiles can be determined as well as the normal tooth forces at the point of contact.

The *concrete* significance of the parameter φ is not essential for what is to follow in this paper; of importance is the *geometrical* character of this parameter (φ may be an angle, an arc, a distance etc.). If for describing the plane curve profile the plane vector $z = x(\varphi) + jy(\varphi)$ (complex number) is used, with j for the imaginary unit, the derivate $z' = x'(\varphi) + jy'(\varphi)$ signifies the *tangent vector* to the profile at some point, while the derivative with respect to τ of the vector $z = x(\varphi; \tau) + jy(\varphi; \tau)$ has the character of a velocity.

In the formula for the tooth friction power (1) the calculation of v_r is the simplest task. According to Eq. (26) [6]

$$|v_r| = \frac{\omega_1}{i} \sqrt{a^2 - 2a(1+i)(x \sin \omega_1 \tau + y \cos \omega_1 \tau) + (1+i)^2(x^2 + y^2)} \tag{3}$$

and corresponding to (13) [6] there shill holds

$$\tau(\varphi) = \frac{1}{\omega_1} \left[\arcsin \frac{(1+i)(xx' + yy')}{a \sqrt{x'^2 + y'^2}} - \arctan \frac{y'}{x'} \right]; \quad x' \neq 0 \tag{4}$$

(The comma denotes the derivative with respect to φ).

Eq. (4) creates a connection between the parameter φ of an arbitrary point of the given initial profile and that instant τ when the point with this parameter φ comes into the position of contact.

By combining Eqs (3) and (4), $|v_r|$ can be expressed as a function of φ only or, of τ only.

With high loads the teeth (and the other elements of the gearbox) are deformed, but these deformations have no essential influence on function $v_r(\tau)$.

The calculation of the normal tooth force F_n causes concern more. If the shape of the teeth is mathematically accurate (accurately fulfills the condition $i = \text{const}$), and if only such small loads occur or the gearbox is so rigid that there are no appreciable deformations, then the functions (2) determining the

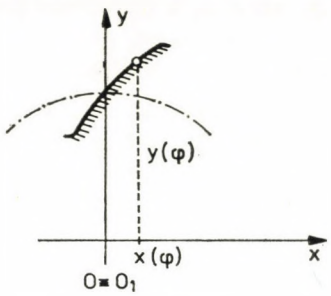

Fig. 1

tooth profile of one wheel also determines the size of force F_n. According to [6], Eq. (40),

$$F_n = M_1 \frac{\sqrt{x'^2 + y'^2}}{xx' + yy'} \tag{5}$$

and here Eq. (4) is valid too, with the aid of which F_n can be established as a function of φ only, or of τ only. It is assumed that the repartition of the tooth pressure along the tooth length is uniform.

But if due to large loads and to the design of the gearbox appreciable deformations arise on the elements of the gearbox, the repartition of the tooth pressure along the length of the tooth is far more complicated. In such cases there is also a suitable method of calculation for a good approximation of the distribution of the tooth pressure [15], but for the product $F_n|v_r|$ such a complicated expression is obtained that its practical use would be very awkward. The tooth pressure changes from point to point, only that remains true that the integral of the tooth pressure along the tooth length is equal to the forces from Eq. (5).

The complicated character of the function describing the tooth pressure makes its purely theoretical calculation with a good approximation of reality nearly impossible.

The friction coefficient depends on many variables [1, 7—10, 13]. Omitting details available in the literature only those more essential parameters are listed which strongly influence the value of the coefficient of friction:

the shape of the meshing profiles,

the roughness of the tooth surface,

the material characteristics of the teeth,
the relative sliding velocity of the teeth,
the instantaneous viscosity of the lubricant,
the state of friction (purely metallic friction, boundary layer friction, more or less hydrodynamical lubricating)
the oxide layer, dirt, which might coat the surfaces, etc.

The parameters listed are also in a very complicated mutual connections to each other, of which only the most important are mentioned:

under load the teeth are deformed — in complicated relations with the elements of the gearbox,
the deformations change the repartition of the tooth pressure,
the viscosity of the lubricant strongly varies with temperature,
because of the mechanical actions and the presence of the lubricant the material characteristics in the surface layers of the teeth change, etc.

Theoretically it would be possible to construct the function $\mu(\tau)$ or $\mu(\varphi)$ describing the change of the coefficient of friction during the engagement, based on partially empirical formulae supported by experimental results. Consequently it would be possible to establish the frictional power $P(\tau)$ or $P(\varphi)$ and to examine it from instant to instant or from profile point to profile point, and that for the most different toothings. But such a function $P(\tau)$ or $P(\varphi)$ would be extraoridinarily complicated, and if for the sake of easy calculations neglections were made, the reliability of the already relatively very small frictional loss would become totally unrealistic.

2. The tooth friction loss of the involute toothing

a) If $\omega_1 = \text{const}$, the contact point of the profiles traverses the contact length at the constant speed $r_{a1}\omega_1$ (Fig. 2). In this case the contact line can also be considered as a time axis with uniform divisions. If to the pitch point C the moment $\tau = 0$ is ordered, then

$$|v_r| = (\omega_1 + \omega_2) r_{a1} \omega_1 |\tau| \ . \tag{6}$$

If it is assumed that $\mu = \text{const}$, then on the section of single engagement $\overline{K_1K_2}$ the frictional work is according to [5]:

$$W = \mu F_n \int_{-\tau_1}^{\tau_2} |v_r| \, d\tau = \mu F_n (\omega_1 + \omega_2) \, r_{a1} \, \omega_1 \int_{-\tau_1}^{\tau_2} |\tau| \, d\tau =$$

$$= \frac{1}{2} \mu F_n (\omega_1 + \omega_2) \, r_{a1} \, \omega_1 \, (\tau_1^2 + \tau_2^2) \ .$$

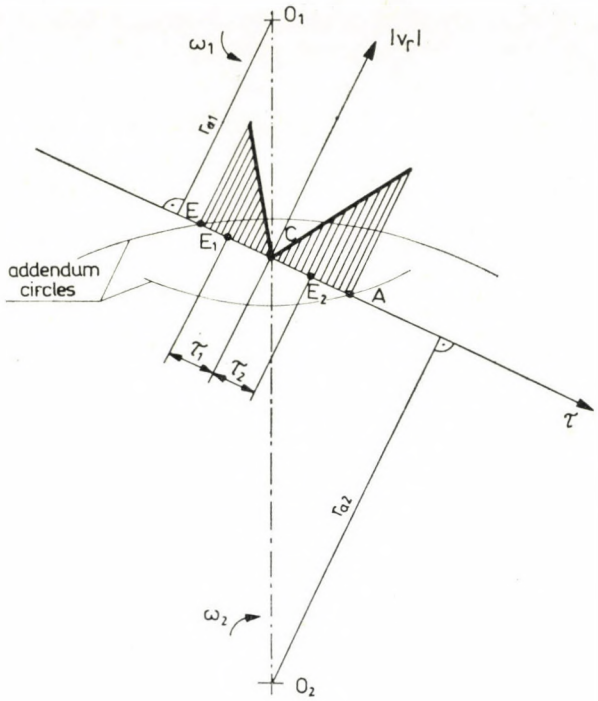

Fig. 2

Now

$$\tau_1^2 + \tau_2^2 = \left(\frac{\overline{E_1C}}{r_{a1}\,\omega_1}\right)^2 + \left(\frac{\overline{CE_2}}{r_{a1}\,\omega_1}\right)^2 = \frac{\overline{E_1C^2} + \overline{E_2C^2}}{r_{a1}^2\,\omega_1^2}$$

and with the notations

$$\overline{E_1C} = u_1\,,$$

$$\overline{E_2C} = u_2\,,$$

$$\tau_1^2 + \tau_2^2 = \frac{u_1^2 + u_2^2}{r_{a_1}^2\,\omega_1^2}\,,$$

and with this

$$W = \frac{1}{2}\,\mu\,F_n\,\frac{\omega_1 + \omega_2}{r_{a_1}\,\omega_1}\,(u_1^2 + u_2^2)\,. \tag{7}$$

If $\varepsilon = 1$, so $u_1 = e_1$ and $u_2 = e_2$, and

$$W_k = \frac{1}{2}\,\mu\,F_n\,\frac{\omega_1 + \omega_2}{r_{a1}\,\omega_1}\,(e_1^2 + e_2^2)\,. \tag{8}$$

For a constant coefficient of friction and single contact the instantaneous frictional power is from (1) proportional with $|v_r|$ (Fig. 3). The friction work according to (7) is proportional to the area below the graph.

Let us examine the case of double engagement (Fig. 4).

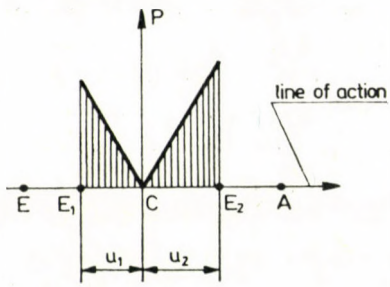

Fig. 3

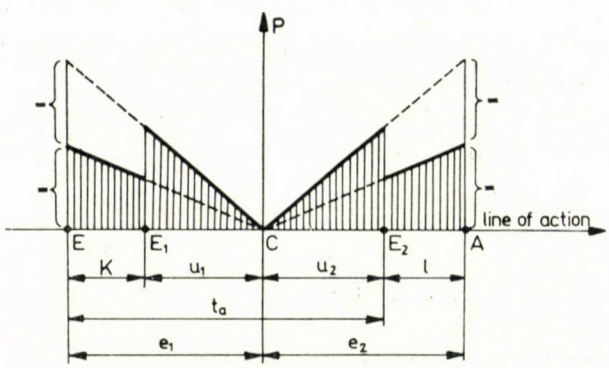

Fig. 4

Assuming provisionally that μ = const and that on the sections of double contact k and l the tooth force in normal direction F_n is divided half and half between the two teeth pairs meshing simultaneously. Then the friction power on the various sections is represented by the graph on Fig. 4; the frictional work is proportional to the area below the graph.

While the point of contact of a selected pair of teeth traverses the contact section in direction $E \rightarrow A$, the friction work consumed is given by the following — now based only on intuition:

The areas above the sections k and l of the double contact are added (while the contact point of the examined pair traverses section $\overline{EE_1}$, *simultaneously* that of the preceding pair traverses section $\overline{E_2A}$) to this sum are added the areas above sections u_1, u_2, to this sum are added again the areas above the sections k and l (because *simultaneously* with the contact on section $\overline{E_2A}$

of the examined pair of teeth the contact point of the adjacent — following — pair traverses section $\overline{EE_1}$.)

The double of areas over the the sections k and l appearing in the sum, the friction work consumed during contact of one pair of teeth is the same as if there were $\varepsilon = 1$ and on the whole section $\overline{AE}$ the whole force F_n would act on one single pair of teeth and so Eq. (8) remains correct in this case too.

In reality the friction force varies during the contact and the force F_n is not divided half and half during the double contact, therefore, in general one cannot state that for $\varepsilon \neq 1$ the friction work for the time of contact of one pair would be the same as if on the whole section $\overline{EA}$ only one pair of teeth would mesh. Therefore, Eq. (8) is true only for $\varepsilon \neq 1$ also if $\mu = \text{const}$ and F_n are equally divided between the meshing two pairs of teeth.

Incidentally let us remark — as Prof. Dr. J. MAGYAR has pointed out to the author — it is more logical to calculate the tooth friction work, not for the total contact time of one pair of teeth, but for the time required for traversing section $t_a = \overline{EE_2}$, this being the period of the function describing the periodically varying tooth friction power.

b) In his "Analytical Mechanics of Gears" BUCKINGHAM [2] gives the following formula for the friction work per unit time of hardened steel involute gears (p. 401, Eq. 19—6):

$$W_0 = \frac{F_n r_{a1} \omega_1}{\beta_1 + \beta_2} \left[\frac{\mu}{2} (\beta_1^2 + \beta_2^2) \left(1 + \frac{1}{i} \right) \right]. \tag{9}$$

Here β_1 and β_2 denote the angles marked on Fig. 5, μ is the "mean" coefficient of friction depending on the circumferential pitch circle velocity (p. 406, Eq. 19—12):

$$\mu = 0{,}05 e^{-0{,}125v} + 0{,}002 \sqrt{v} \ . \tag{10}$$

Here the dimension of v is feet/min.

Similar relations give [2] for gears made from other materials.

Remark: in the cited book the formula for the work W_0 is erroneous; after the equality sign, in the numerator of the fraction there stands $W_1 + W_2$ instead of $\beta_1 + \beta_2$, the former being, according to the symbols used in the book, the work delivered by the driving gear in the entering, resp. in the leaving section of the engagement.

Taking into account that the time required for covering the angle $\beta_1 + \beta_2$ is

$$\tau_{12} = \frac{\beta_1 + \beta_2}{\omega_1}$$

the tooth friction work of one pair of teeth in the whole range of contact is

$$W_k = W_0 \tau_{12} = \frac{F_n r_{a1} \omega_1}{\beta_1 + \beta_2} \left[\frac{\mu}{2} (\beta_1^2 + \beta_2^2) \left(1 + \frac{1}{i} \right) \right] \frac{\beta_1 + \beta_2}{\omega_1} =$$

$$= \frac{\mu}{2} F_n r_{a1} (\beta_1^2 + \beta_2^2) \left(1 + \frac{\omega_2}{\omega_1} \right) =$$

$$= \frac{\mu}{2} F_n r_{a1} \frac{\omega_1 + \omega_2}{\omega_1} (\beta_1^2 + \beta_2^2) .$$

Fig. 5 shows that

$$\beta_1^2 + \beta_2^2 = \left(\frac{\widehat{E'C'}}{r_{a1}} \right)^2 + \left(\frac{\widehat{C'A'}}{r_{a1}} \right)^2 = \frac{\overline{EC^2} + \overline{CA^2}}{r_{a1}^2} = \frac{e_1^2 + e_2^2}{r_{a1}^2} ,$$

therefore finally

$$W_K = \frac{\mu}{2} F_n \frac{\omega_1 + \omega_2}{r_{a1} \omega_1} (e_1^2 + e_2^2) ,$$

which is identical with formula (8).

According to the statements in para. a) Buckingham's formula (9) — which reflects the case of $\varepsilon = 1$ or of a force repartition $F_n|2 - F_n|2$ for $\varepsilon \neq 1$, and a constant coefficient of friction, can only be used if μ is an experimentally determined "mean" value.

c) In the SHELL Co. publication "Lubrication of Industrial Gears" [9] for the efficiency of involute gear pairs the formula

$$\eta = 100 - \mu\delta \tag{11}$$

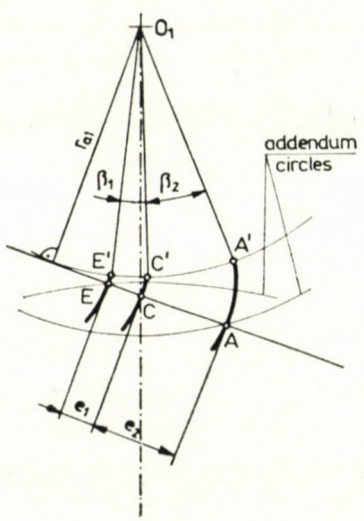

Fig. 5

is given, where μ is the "mean" coefficient of friction

$$\mu = \frac{3{,}5}{\zeta^{0,25} \sin \alpha \left(\frac{d_1 d_2}{d_1 + d_2} \right)^{0,5} \cdot v^{0,5}} . \tag{12}$$

In this formula the constants are expressed in the English system of units, ζ in centistokes, the diameters in inches, the velocity in feet/min.

The shape factor given in (11) is

$$\delta = \frac{100}{\cos \alpha} \left(\frac{1}{d_1} + \frac{1}{d_2} \right) \frac{e_1^2 + e_2^2}{e_1 + e_2} . \tag{13}$$

With suitable transformations

$$\begin{aligned}
\delta &= \frac{100}{\cos \alpha} \left(\frac{1}{d_1} + \frac{1}{d_2} \right) \frac{e_1^2 + e_2^2}{e_1 + e_2} = \\
&= 100 \left(\frac{1}{2 r_1 \cos \alpha} + \frac{1}{2 r_2 \cos \alpha} \right) \frac{e_1^2 + e_2^2}{e_1 + e_2} = \\
&= 100 \left(\frac{1}{2 r_{a1}} + \frac{1}{2 r_{a2}} \right) \frac{e_1^2 + e_2^2}{e_1 + e_2} = 100 \frac{r_{a1} + r_{a2}}{2 r_{a1} r_{a2}} \cdot \frac{e_1^2 + e_2^2}{e_1 + e_2} = \\
&= 100 \frac{\frac{r_{a1}}{r_{a2}} + 1}{2 r_{a1}} \cdot \frac{e_1^2 + e_2^2}{e_1 + e_2} = 100 \frac{\frac{\omega_2}{\omega_1} + 1}{2 r_{a1}} \cdot \frac{e_1^2 + e_2^2}{e_1 + e_2} = \\
&= 100 \frac{\omega_1 + \omega_2}{2 r_{a1} \omega_1} \cdot \frac{e_1^2 + e_2^2}{e_1 + e_2} = 100 \, F_n \frac{\omega_1 + \omega_2}{2 r_{a1} \omega_1} \cdot \frac{e_1^2 + e_2^2}{F_n (e_1 + e_2)} .
\end{aligned}$$

Here $F_n(e_1 + e_2)$, in the denominator of the last fraction, is the work *introduced* during the engagement of one pair of teeth.

Finally

$$\begin{aligned}
\eta &= 100 - \mu\delta = 100 - 100 \, \mu F_n \frac{\omega_1 + \omega_2}{2 r_{a1} \omega_1} \cdot \frac{e_1^2 + e_2^2}{F_n (e_1 + e_2)} = \\
&= 100 \left[1 - \frac{\frac{\mu}{2} F_n \frac{\omega_1 + \omega_2}{r_{a1} \omega_1} (e_1^2 + e_2^2)}{W_{\text{introduced}}} \right] .
\end{aligned}$$

This formula corresponds to the definition of the efficiency, the numerator of the fraction in the parentheses is identical with the work lost by friction according to (8).

In this formula also μ is the experimentally found "mean" value.

The Shell publication refers to the disk tests for the determination of the coefficient of friction; the same is to be found in other literature (e.g. [10]). These experiments are made with rotating discs in contact along a generatrix and pressed together. By varying the radii of the discs, the pressure, the circumferential speed of the wheels, and the viscosity of the lubricating oil, relations apt for formulating, were obtained between the coefficient of friction and its parameters.

The author thinks that the use of these formulae for the calculation of tooth friction losses is open to discussion. It is true that the variation during contact of the curvature at the point of contact and of the sliding velocity can be described with mathematical accuracy; but it is much more difficult to assess the deformations which have a great influence on the coefficient of friction, and the change of oil viscosity with temperature can greatly differ from the variations experienced at the disc tests.

3. General remarks

a) The coefficient of friction called "mean" in the preceding is *not* the mathematical mean of the function $\mu(\tau)$ calculated for the time of contact. I.e., if in (1) the notation $F_n|v_r| = \Phi(\tau)$ is used, so for the given interval

$$\tau_1 \leq \tau \leq \tau_2$$

the friction work is

$$W = \int_{\tau_1}^{\tau_2} \mu(\tau)\, \Phi(\tau)\ d\tau\,.$$

For such integrals, if in the integration interval $\mu(\tau)$ and $\Phi(\tau)$ are continuous and if the sign of $\Phi(\tau)$ is always the same (these conditions are generally fullfilled with gears), the *generalized integral mean theorem*

$$\int_{\tau_1}^{\tau_2} \mu(\tau)\, \Phi(\tau) d\tau = \mu(\tau_k) \int_{\tau_1}^{\tau_2} \Phi(\tau)\ d\tau \tag{14}$$

is valid, where $\mu(\tau_k)$ is the value of the coefficient of friction assumed in some intermediate place of the interval.

If $\Phi(\tau) \equiv 1$, then $\mu(\tau_k)$ is just the *ordinary integral mean* of μ calculated for the interval in question (arithmetic mean), but otherwise there is no guarantee for $\mu(\tau_k)$ being the *arithmetic mean* in the mathematical sense. It is better to use instead of the "mean" coefficient of friction the expression "medium" coefficient of friction; let its symbol be $\bar{\mu}$.

b) As long as it does not become technically feasible to measure with more or less accuracy the variation in time of the coefficient of friction, the

following method seems to be useful — even if not cheap — for the preliminary calculation of the tooth friction coefficient:

1. Let us manufacture a carefully machined and assembled gearbox for the given axial distance and ratio.

2. Knowing the shape of the tooth profiles for a given driving torque M_1 and angular velocity ω_1, let us *calculate* the integral

$$\int_{\tau_1}^{\tau_2} F_n |v_r| \, d\tau = G(M_1; \omega_1) \, .$$

Let us express F_n from Eqs (5) and (4), $|v_r|$ from (3) and (4) as functions of τ. In the calculation of the value $G(M_1, \omega_1)$ neither the dependency of the tooth pressure repartition from the deformation, nor the fact that for $\varepsilon \neq 1$ in the range of double contact the normally directed tooth pressure is not divided into equal parts beacuse of the deformations, are taken into account.

3. *Let us measure* experimentally, using a given lubricant, the tooth friction loss for the time interval (τ_1, τ_2) and from the equation

$$W = \mu(\tau_k) \, G(M_1; \omega_1) = \bar{\mu} G(M_1; \omega_1)$$

and let us calculate $\bar{\mu}$. This value $\bar{\mu}$ contains implicitely the influence of all factors, not considered when calculating G, W being the numerical value measured on the *real* gearbox.

4. This medium friction coefficient $\bar{\mu}$ is valid for a gearbox with a given geometry, made from a given material (and only for this) and with the assumed M_1 and ω_1.

5. With the *same* gearbox, varying M_1 and ω_1 the influence on $\bar{\mu}$ of the load and of the velocity can be measured;

6. then carrying out a similar series of measurements for an equal gearbox with a different material combination, different surface roughness, different lubricant, the influence of these factors on $\bar{\mu}$ is found.

7. Finally repeating the foregoing measurements for gearboxes with other geometry the dependence of $\bar{\mu}$ from the most characteristic parameters can be tabulated. These values of $\bar{\mu}$ already provide quite good approximations for the calculation of tooth friction losses in the design of gearboxes with a similar geometry.

Naturally, this method is very expensive and lengthy; possibly the invested work is not recovered; but it is sure that a friction coefficient determined by one given experiment only gives a very inaccurate result for the calculation of the friction losses of a completely different gearbox, material quality, surface quality, geometry of the gearbox, load, speed etc., influencing strongly the value of the coefficient of friction.

REFERENCES

1. Bowden, F. P.—Tabor, D.: The Friction and Lubrication of Solids. Clarendon Press, Oxford, 1954
2. Buckingham, E.: Analytical Mechanics of Gears. McGraw-Hill Book Corp., New York, 1949
3. Dudley, D. W.: Gear Handbook. McGraw-Hill Book Corp., New York, 1962
4. Hermann, M.: Gépelemek (Machine Elements), Németh József technikai Könyvkereskedése, Budapest 1924
5. Huszthy, L.: Súrlódási munka evolvens fogfelületeken (Friction work on involute gear surfaces), *Gép*, **(1960)** 223—230
6. Huszthy, L.: Gear Calculation by Using Complex Expressions. *Acta Techn. Hung.* **73,** (1972), 363—399
7. Kragelszkij, I. V.—Vinogwadova, I. S.: A súrlódási tényező (The coefficient of friction). Műszaki Könyvkiadó, Budapest 1961
8. Lechner, G.: Untersuchungen zur Schmierfilmbildung an Zahnrädern. *VDI-Z.* **111,** (1969), Nr. 4
9. Lubrication of Industrial Gears. Shell, London 1964
10. Niemann, G.: Schneckengetriebe mit flüssiger Reibung. *VDI-Forschungsheft*, Ausg. B, **13,** (1942), Jan-.Feb.
11. Ten Bosch, M.: Gépelemek (Machine Elements). Műszaki Könyvkiadó, Budapest 1957
12. Thomas, A. K.: Die Tragfähigkeit der Zahnräder. Karl Hanser, München, 1950
13. Vidéky, E.: A súrlódás analízise fogaskerék szempontból. *MTA Műsz. Oszt. Közleményei*, J., Nr. 2
14. Vörös, I.: Gépelemek (Machine Elements) III. Tankönyvkiadó, Budapest 1956
15. Zablonszkij, K. I.: Zsestkost Zubchatykh Peredach, Tekhnika, Kiev, 1967

Einige Bermerkungen über die Zahnreibungsverluste von Zahnradpaaren. Zahlreiche Bücher und Berichte befassen sich mit den Zahnreibungsverlusten von Zahnradpaaren. In den von den verschiedenen Verfassern abgeleiteten und im wesentlichen gleichwertigen Formeln für Evolventenzahnräderpaare ist der Reibungskoeffizient ein versuchsmäßig bestimmter Durchschnittswert. Die Arbeit strebt an die Definition des "durchschnittlichen" Reibungskoeffizienten zu präzisieren, bzw. diejenigen Bedingungen zu klären, für welche die auf die Zahnreibungsverluste bezüglichen Zusammenhänge gültig sind.

Замечания по вопросу расчета потерь от трения зубьев зубчатых колес. Вопросами потерь от трения зубьев зубчатых пар занимаются многие книги и множество статей. Выведенные различными авторами и по существу являющиеся эквивалентными формулы (действительные для зубчатых пар эвольвентного зацепления) коэффициент трения является средним значением, определенным при помощи какого-нибудь опыта. Данной статьей ставится цель уточнить толковение «среднего» коэффициента трения и, соответственно, выяснить те условия, при которых действительны зависимости, касающиеся потерь от трения зубьев.

Acta Technica Academiae Scientiarum Hungaricae, Tomus 86 (3—4), pp. 331—362 (1978)

A CLEAR ALGORITHM FOR THE CALCULATION OF THE LINEAR INDUCTION MOTOR, BASED ON FIELD THEORY

GY. TEVAN* and F. TÓTH**

CAND. OF TECHN. SCI.

[Manuscript received: 21 April 1976]

The authors discuss an (approximate) algorithm based on "field theory" consisting of relatively simple formulae for calculating the linear induction motor, which takes into account the skin effect, the transversal and longitudinal end effects and the connection between excitation and winding. It creates the connection with the equivalent circuits of the traditional induction motor, neglects the excitation of the primary iron body and the harmonics of the whole order of the travelling field, but describes the longitudinal end effect by two undamped field harmonic waves of fractional order. The calculations are compared with measurements carried out on a stationary motor and finally characteristics of linear motors are calculated with the method presented.

1. Review of the literature; Objectives

Numerous papers deal with the calculation of the linear induction eddy-current motors with nonferromagnetic secondary. They show wide variety in the creation of the model as for the method of calculation. The determination of the eddy currents in the secondary requires the calculation of the electromagnetic field, and the character of the model is essentially determined by the decision in which parts of the linear motor and with what neglections, approximations to use field theory and in what place to use traditional asynchronous-motor calculation. The neglections concern the end effects in longitudinal (movement) direction and in transversal direction, and the skineffects, thus they concern the question as to how many dimensions the partial model for the field calculation is to have. Both analytical and numerical methods occur. Amongst the papers known by the authors the most accurate analytical calculation method is published by [11], where the connection between the electromagnetic field and the excitation is correctly established as well. But these "accurate" analytical solutions are fairly complicated, reviewing the influence of the parameters is possible only by time-consuming computerized evaluation and it is hardly possible to give a clear picture with the usual asynchronous motor equivalent circuits.

* GY. TEVAN Lóránt u. 8/a, H-1125 Budapest, Hungary
** F. TÓTH Katowice u. 6, H-3526 Miskolc, Hungary

In this paper a method based on field calculation is presented which leads to an algorithm consisting of relatively simple analytical formulae, takes into consideration the skin-effect, the connection between the excitation and the electromagnetic field, approximates the longitudinal and transversal end effects, is physically easy to survey and creates the link with the usual asynchronous motor equivalent circuits, only the effect of the slot harmonics and of the excitation falling on the tooth are neglected. Finally it is to be noted that some elements of the method to be discussed can also be found in the literature [1, 2, 4, 7, 9, 13].

2. The field impedance of the secondary of the infinite linear induction motor, referred to the primary

Fig. 1 shows the outlines of a symmetrical bilateral plane linear motor and of an unilateral linear plane motor where a laminated ferromagnetic part is provided on the unexcited side of the secondary. Such an unilateral linear plane motor has a greater tractive force as compared to the case without a magnetic conductor and therefore, we shall deal only with such a motor.

For reasons of symmetry, in the symmetry plane of the bilateral linear motor the magnetic field has only a component normal to this plane and approximately likewise is the case in the boundary plane of the ferromagnetic laminated part and the secondary part.* Therefore, it is sufficient to deal only with the unilateral motor, because the relations for the unilateral motor with a secondary part thickness v are valid for both halves of a bilateral linear motor with a secondary of thickness $2v$, assumed to be cut in half by the plane of symmetry.

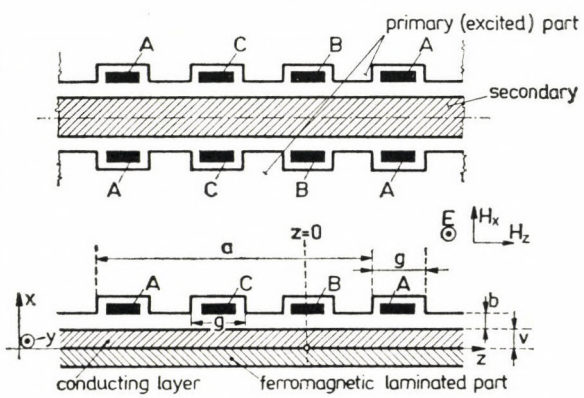

Fig. 1

* Below the conducting layer the magnetic induction is far below the saturation value.

Considering — provisionally — the plane surfaces infinite in both directions, in the system of rectangular coordinates according to Fig. 1 the magnetic field has only x- and z- components, the electrical field has only a y-component. For the conducting layer of conductivity γ of the secondary, neglecting the displacement currents, Maxwell's equations are

$$\frac{\partial H_x}{\partial z} - \frac{\partial H_z}{\partial x} = \gamma E \,, \tag{1}$$

$$\frac{\partial E}{\partial x} = -\mu_0 \frac{\partial H_z}{\partial t} \,, \tag{2}$$

$$-\frac{\partial E}{\partial z} = -\mu_0 \frac{\partial H_x}{\partial t} \,. \tag{3}$$

Calculating only with the basic harmonic of the magnetizing field travelling in the z direction, created by the three-phase excitation,

$$E = Im\left[\sqrt{2}\,\mathbf{E} e^{j\left(\omega t + \frac{\pi}{a} z\right)}\right],$$

$$H_x = Im\left[\sqrt{2}\,\mathbf{H}_x e^{j\left(\omega t + \frac{\pi}{a} z\right)}\right],$$

$$H_z = Im\left[\sqrt{2}\,\mathbf{H}_z e^{j\left(\omega t + \frac{\pi}{2} z\right)}\right],$$

where Im denotes the imaginary part of the expression in brackets, ω is the angular frequency of the secondary current, a is the pole pitch, $\mathbf{E}$, $\mathbf{H}_x$ and $\mathbf{H}_z$ the phasors depending on the variable x (the complex effective values giving also the phase position). Substituting the values E, H_x and H_2 into Eqs (1, 2, 3), the complex field characteristics (phasors) become:

$$j\frac{\pi}{a}\mathbf{H}_x - \frac{d\mathbf{H}_z}{dx} = \gamma \mathbf{E} \,, \tag{4}$$

$$\frac{d\mathbf{E}}{dx} = -j\omega\mu_0 \mathbf{H}_z, \tag{5}$$

$$j\frac{\pi}{a}\mathbf{E} = j\omega\mu_0 \mathbf{H}_x \,. \tag{6}$$

The primary three-phase current of angular frequency $\omega = 2\pi f$ excites a travelling magnetic field of velocity

$$c_0 = \frac{a}{\pi}\omega_0 = 2af \,. \tag{7}$$

If the secondary part travels with the velocity c in the same direction, the velocity of the travelling magnetic field is $c_0 - c$ with respect to this and the angular frequency of the induced currents is

$$\omega = \frac{c_0 - c}{c_0} \omega_0 = s\omega_0 \tag{8}$$

where s is the slip.

Because of the periodicity in z direction energy flows only in the x direction; the power per unit surface flowing from the primary to the secondary, i.e. in the direction opposite to the x axis, the negative complex value of the x component of the Poynting vector is

$$-\mathbf{E}\mathbf{H}_z^*,$$

where the asterisk denotes the conjugated complex value. The field impedance corresponding to this energy flow is

$$-\frac{\mathbf{E}}{\mathbf{H}_z}.$$

In the system of coordinates moving together with the primary an electric field larger by

$$\frac{c_0}{c_0 - c} = \frac{1}{s} = \frac{\omega_0}{\omega}$$

is induced, therefore, the field impedance referred to the primary is

$$\mathbf{Z} = -\frac{\omega_0}{\omega} \frac{\mathbf{E}}{\mathbf{H}_z}, \tag{9}$$

because $\mathbf{H}_z$ in the two systems is (practically) the same. From the definition equation (9)

$$\frac{d\mathbf{Z}}{dx} = \frac{\omega_0}{\omega} \left(-\frac{1}{\mathbf{H}_z} \frac{d\mathbf{E}}{dx} + \frac{\mathbf{E}}{\mathbf{H}_z^2} \frac{d\mathbf{H}_z}{dx} \right).$$

Introducing Eqs (4, 5, 6):

$$\frac{d\mathbf{Z}}{dx} = \frac{\omega_0}{\omega} \left[j\omega\mu_0 + \frac{\mathbf{E}^2}{\mathbf{H}_z^2} \left(j \frac{\pi^2}{a^2 \omega\mu_0} - \gamma \right) \right]$$

and again using Eq. (9):

$$\frac{d\mathbf{Z}}{dx} = j\omega_0 \mu_0 + \frac{\omega}{\omega_0} \mathbf{Z}^2 \left(j \frac{\pi^2}{a^2 \omega\mu_0} - \gamma \right).$$

Introducing finally the notation

$$m = \frac{a^2 \gamma \mu_0 \omega}{\pi^2} = \frac{a^2 \gamma \mu_0 \omega_0}{\pi^2} s\,, \tag{10}$$

the differential equation for $\mathbf{Z}$ takes the following form:

$$\frac{d\mathbf{Z}}{dx} = j\omega_0 \mu_0 \left[1 + \frac{\pi^2}{a^2 \omega_0^2 \mu_0^2} \mathbf{Z}^2 (1 + jm)\right]. \tag{11}$$

The general solution for this separable differential equation is

$$\mathbf{Z} = \frac{a\omega_0 \mu_0}{\pi} \frac{1}{\sqrt{1 + jm}} \tan\left(j \frac{\pi}{a} x \sqrt{1 + jm} + \mathbf{C}\right) \tag{12}$$

where $\mathbf{C}$ is an integration constant. For determining it let us take into consideration that for $x = 0$, $\mathbf{H}_z = 0$, which means that

$$\lim_{x \to 0} \mathbf{Z} = \infty.$$

On the base of this from Eq. (12), $\mathbf{C} = \pi/2$ and thus

$$\mathbf{Z} = \frac{a\omega_0 \mu_0}{\pi} \frac{1}{\sqrt{1 + jm}} \frac{1}{\tan\left(-j \sqrt{1 + jm} \frac{\pi}{a} x\right)}.$$

This is the field impedence at an arbitrary point x. The impedance of the whole secondary of the infinite linear motor is obtained by substituting $x = v$

$$\mathbf{Z}_{s\infty} = \frac{a\omega_0 \mu_0}{\pi} \mathbf{k}_\infty \tag{13}$$

where

$$\mathbf{k}_\infty = \frac{1}{\sqrt{1 + jm} \tan\left(-j \sqrt{1 + jm} \frac{\pi v}{a}\right)}. \tag{14}$$

3. Linear motor of finite width

In the real linear motor the laminated-iron primary as well as the secondary are of finite width. The currents induced in the secondary must close, therefore, the current density and thus the electric field must also have a z component. With H_x only J_y can provide a force in the z direction, therefore,

it is useful to make the secondary wider than the primary and thus the eddy currents close in the part overreaching the iron core (Fig. 2).

The modifying influence of the finite width is calculated as follows (cf. [4]):

a) in addition to the electromagnetic field discussed in Section 2), in the part of the conductor below the iron body, such an additional electromagnetic field is calculated where the magnetic field has exclusively x direction, but

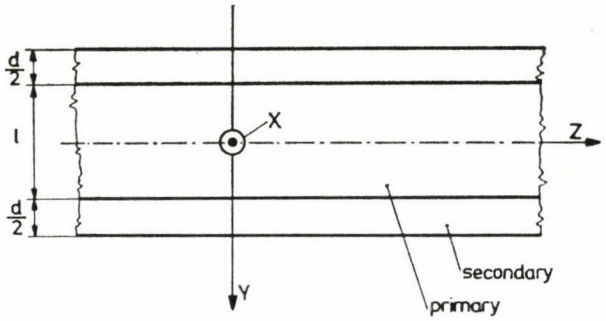

Fig. 2

the electric field has also an y and a z component, and besides from t and z these depend only on y;

b) the flux excited by the winding heads and passing through the conducting plate parts overreaching the iron body is neglected (the bulk of the flux indeed passes through the iron body);

c) in the parts of the secondary conducting plates overreaching the iron body the currents in direction x and depending on x of the field characteristics are neglected (this latter means neglecting the skin effect).

d) similar to what has been discussed in Section 2), only the basic harmonic waves are taken into consideration.

Maxwell's equations for the components

$$E_{ya} = \sqrt{2}\, Im\left\{\mathbf{E}_{ya} \exp\left[j\left(\omega t + \frac{\pi}{a} z\right)\right]\right\},$$

$$E_{za} = \sqrt{2}\, Im\left\{\mathbf{E}_{za} \exp\left[j\left(\omega t + \frac{\pi}{a} z\right)\right]\right\},$$

$$H_{xa} = \sqrt{2}\, Im\left\{\mathbf{H}_{xa} \exp\left[j\left(\omega t + \frac{\pi}{a} z\right)\right]\right\},$$

of the basic harmonic of the additional field in the part of the secondary conductor below the iron body, lead — taking into account that the phasors of the field characteristics depend only on y — to the following relations:

$$\frac{d\mathbf{E}_{za}}{dy} - j\frac{\pi}{a}\mathbf{E}_{ya} = -j\omega\mu_0\mathbf{H}_{xa}, \tag{15}$$

$$-\frac{d\mathbf{H}_{xa}}{dy} = \gamma\mathbf{E}_{za}, \tag{16}$$

$$j\frac{\pi}{a}\mathbf{H}_{xa} = \gamma\mathbf{E}_{ya}. \tag{17}$$

By derivating Eq. (15) with respect to y and making use of (16) and (17)

$$\frac{d^2\mathbf{E}_{za}}{dy^2} - j\frac{\pi}{a}\left(-j\frac{\pi}{a}\mathbf{E}_{za}\right) = j\omega\mu_0\gamma\mathbf{E}_{za}$$

which after rearranging and introducing the notation (10) takes the shape

$$\frac{d^2\mathbf{E}_{za}}{dy^2} - \frac{\pi^2}{a^2}(1+jm)\mathbf{E}_{za} = \mathbf{0}.$$

For reasons of symmetry $\mathbf{E}_{za}$ must be an impair function. Such a solution of the former differential equation is

$$\mathbf{E}_{za} = \mathbf{E}_0\sinh\left(\frac{\pi}{a}\sqrt{1+jm}\,y\right). \tag{18}$$

Eliminating $\mathbf{H}_{xa}$ from Eqs (15) and (17)

$$\mathbf{E}_{ya} = \frac{1}{j\frac{\pi}{a}(1+jm)}\frac{d\mathbf{E}_{za}}{dy},$$

substituting Eq. (18):

$$\mathbf{E}_{ya} = -\frac{j\mathbf{E}_0}{\sqrt{1+jm}}\cosh\left(\frac{\pi}{a}\sqrt{1+jm}\,y\right). \tag{19}$$

According to the approximations b) and c) in the secondary conductor part overreaching the iron body the current density and thus the electric field are potential ones, furthermore they have no x component, and do not depend on x so that

$$E = \frac{\partial V}{\partial y},\quad E_z = \frac{\partial V}{\partial z},\quad \frac{\partial^2 V}{\partial y^2} + \frac{\partial^2 V}{\partial z^2} = 0,$$

but with the conditions d)

$$V = \sqrt{2}\,Im\left[\mathbf{V}(y)e^{j\left(\omega t + \frac{\pi}{a}z\right)}\right],$$

substituting this into Laplace's equation

$$\frac{d^2\mathbf{V}}{dy^2} - \frac{\pi^2}{a^2}\mathbf{V} = 0\,,$$

and from this

$$\mathbf{V} = \mathbf{A}\,e^{\frac{\pi}{a}y} + \mathbf{B}e^{-\frac{\pi}{a}y}\,.$$

At the edge of the conductor no current emerges, therefore at $y = (l + d)/2$, $E_y = \partial V/\partial y = 0$, that is $d\mathbf{V}/dy = \mathbf{0}$, therefore

$$\frac{\pi}{a}\mathbf{A}e^{\frac{\pi}{a}\frac{l+d}{2}} - \frac{\pi}{a}\mathbf{B}e^{-\frac{\pi}{a}\frac{l+d}{2}} = \mathbf{0}\,,$$

and from this

$$\mathbf{B} = e^{\pi(l+d)/a}\,\mathbf{A}\,.$$

For this reason

$$\mathbf{V} = \mathbf{A}\left[e^{\frac{\pi}{a}y} + e^{\frac{\pi}{a}(l+d-y)}\right]. \tag{20}$$

At the junction of the parts below the iron body and those overreaching it, at $y = l/2$, the electric field must be continuous. This is simply to fulfil for the z component: in the overreaching part $E = \partial V/\partial z$ and its derivative with respect to z is $j\pi/a$ times the phasor, thus from Eqs (18) and (20)

$$j\frac{\pi}{a}\mathbf{A}\,e^{\frac{\pi}{a}\frac{l}{2}}\left(1 + e^{\pi\frac{d}{a}}\right) = \mathbf{E}_0 \sinh\left(\frac{\pi}{2}\,\frac{l}{a}\sqrt{1 + jm}\right) \tag{21}$$

The y component of the electric field under the iron body is $\mathbf{E} + \mathbf{E}_{ya}$, where $\mathbf{E}$ is the y component of the original electromagnetic field discussed in section 2, and in the part overreaching the iron body $\mathbf{E}_y = d\mathbf{V}/dy$.

$$\frac{1}{v}\int_0^v (\mathbf{E} + \mathbf{E}_{ya})_{y=l/2}\,dx = \left(\frac{d\mathbf{V}}{dy}\right)_{y=l/2}.$$

$\mathbf{E}$ does not depend on y and on the base of Eqs (19) and (20)

$$\frac{1}{v}\int_0^v \mathbf{E}dx - \frac{j\mathbf{E}_0}{\sqrt{1 + jm}}\cosh\left(\frac{\pi}{2}\,\frac{l}{a}\sqrt{1 + jm}\right) = \frac{\pi}{a}\mathbf{A}e^{\frac{\pi}{2}\frac{l}{a}}\left(1 - e^{\frac{\pi}{a}d}\right).$$

From Eqs (4) and (6), also using the notation (10)

$$\frac{\gamma}{m}(j - m)\,\mathbf{E} = \frac{d\mathbf{H}_z}{dx}$$

introducing this into the former equation and considering that $(\mathbf{H}_z)_{x=0} = \mathbf{0}$,

$$\frac{1}{v\gamma}\,\frac{m}{j-m}\,(\mathbf{H}_z)_{x=v} = \frac{j}{\sqrt{1+jm}}\,\mathbf{E}_0 \cosh\left(\frac{\pi}{2}\,\frac{l}{a}\sqrt{1+jm}\right) + \\ + \frac{\pi}{a}\,e^{\frac{\pi}{2}\,\frac{l}{a}}\left(1 - e^{\pi\frac{d}{a}}\right)\mathbf{A}.$$

Substituting from Eq. (21) the value of $\mathbf{A}$

$$\frac{1}{v\gamma}\,\frac{m}{j-m}\,(\mathbf{H}_z)_{x=v} = \mathbf{E}_0\left[\frac{j}{\sqrt{1+jm}}\cosh\left(\frac{\pi}{2}\,\frac{l}{a}\sqrt{1+jm}\right) - \right. \\ \left. - j\,\frac{1-e^{\pi\frac{d}{a}}}{1+e^{\pi\frac{d}{a}}}\sinh\left(\frac{\pi}{2}\,\frac{l}{a}\sqrt{1+jm}\right)\right]. \tag{22}$$

For calculating the additional impedance of the additional field only the correcting influence of $\mathbf{E}_{ya}$ needs to be taken into account, because with $\mathbf{H}_z$ only this furnishes power. $\mathbf{E}_{ya}$ depending on y, the mean value of the correcting field $\mathbf{E}_{ya}$ is

$$\mathbf{E}_m = \frac{1}{l}\int_{-l/2}^{l/2}\mathbf{E}_{ya}\,dy\,.$$

Using Eq. (19)

$$\mathbf{E}_m = -\frac{2a}{\pi l}\,\mathbf{E}_0\,\frac{j}{1+jm}\sinh\left(\frac{\pi}{2}\,\frac{l}{a}\sqrt{1+jm}\right). \tag{23}$$

Thus, in a similar manner as for Eq. (9) the additional impedance will be

$$\mathbf{Z}_{sa} = -\frac{\omega_0}{\omega}\,\frac{\mathbf{E}_m}{(\mathbf{H}_z)_{x=v}}$$

and thus after inserting Eqs (22) and (23), using the notation (10) and rearranging we obtain

$$\mathbf{Z}_{sa} = -\frac{\omega_0\mu_0 a}{\pi}\,\frac{j}{1+jm}\times \\ \times\frac{\frac{a}{\pi v}}{\frac{\pi}{2}\,\frac{l}{a}\sqrt{1+jm}\coth\left(\frac{\pi}{2}\,\frac{l}{a}\sqrt{1+jm}\right) + (1+jm)\,\frac{\pi}{2}\,\frac{l}{a}\,\frac{e^{\pi\frac{d}{a}}-1}{e^{\pi\frac{d}{a}}+1}}.$$

Let us introduce the notations

$$\frac{\pi}{2}\,\frac{l}{a}\sqrt{1+jm}\coth\left(\frac{\pi}{2}\,\frac{l}{a}\sqrt{1+jm}\right)=c_1+jc_2. \tag{24}$$

$$q=\frac{\pi}{2}\,\frac{l}{a}\,\frac{e^{\pi\frac{d}{a}}-1}{e^{\pi\frac{d}{a}}+1}\,. \tag{25}$$

With these

$$\mathbf{Z}_{sa}=-\frac{\omega_0\mu_0 a}{\pi}\,\mathbf{k}_a \tag{26a}$$

where

$$\mathbf{k}_a=\frac{j\dfrac{a}{\pi v}}{(1+jm)\,[c_1+q+j(c_2+mq)]}\,. \tag{26b}$$

The secondary impedance referred to the whole primary is

$$\mathbf{Z}_s=\mathbf{Z}_{s\infty}+\mathbf{Z}_{sa},$$

and so after introducing Eqs (13) and (26a)

$$\mathbf{Z}_s=\frac{a\omega_0\mu_0}{\pi}\,\mathbf{k} \tag{27a}$$

where

$$\mathbf{k}=\mathbf{k}_\infty-\mathbf{k}_a. \tag{27b}$$

Finally the electromagnetic field of the linear motor with finite width is approximated by the reduced electromagnetic field of such a linear motor with infinite width for which

$$\mathbf{E}_r=\mathbf{E}+\mathbf{E}_m, \tag{28a}$$

$$\mathbf{H}_{zr}=\mathbf{H}_z, \tag{28b}$$

$$\mathbf{H}_{xr}=\frac{\pi}{a\,\omega\mu_0}\,\mathbf{E}_r=\mathbf{H}_x+\frac{\pi}{a\omega\mu_0}\,\mathbf{E}_m\,. \tag{28c}$$

Let us remark that the second member of the right hand side of (28c) is not the mean value of $\mathbf{H}_{xa}$ because besides $\mathbf{E}_{ya}$ this also induces $\mathbf{E}_{za}$.

At the beginning of this Section we have already remarked that for increasing the traction force it is advantageous to make the secondary part wider than the primary iron body. In the formulae this appears by the absolute

value of the factor $\mathbf{k}_a$ (corresponding to the additional field according to (26b)) diminishing with increasing q; according to (25) the increase of d entrains the increase of q. Therefore, it is appropriate to make the thickness of the overreaching d as large as possible. But as for $d = 1{,}5a$ practically $q = \pi l/2a$, it is not worth while to make the secondary wider than 1,5a.

So if we do not obtain a secondary of disproportionate width —

$$d \approx 1{,}5a \tag{29a}$$

can be recommended and in this case (25) takes the more simple form

$$q = \frac{\pi}{2} \frac{l}{a} . \tag{29b}$$

4. The influence of the air gap on the impedance

The electromagnetic field of the secondary part connects through the electromagnetic field of the air gap to the electromagnetic field of the excited primary.

The field impedance also accounting for the electromagnetic field of the air gap is similarly obtained from (12) by substituting $x = b + v$, considering that in the air gap the electric conductivity $\gamma = 0$, and therefore from (10) $m = 0$. Hence

$$\mathbf{Z}_{ls} = \frac{a\omega_0 \mu_0}{\pi} \tan \left[j \frac{\pi}{a} (b + v) + \mathbf{C} \right] .$$

Because for $b = 0$, $\mathbf{Z}_{ls} = \mathbf{Z}_s$,

$$\mathbf{Z}_s = \frac{a\omega_0 \mu_0}{\pi} \tan \left(j \frac{\pi v}{a} + \mathbf{C} \right) .$$

and therefrom with regard also to (27a) a

$$\mathbf{C} = \operatorname{arc\,tan} \mathbf{k} - j \frac{\pi v}{a}$$

and re-introducing this into the formula of $\mathbf{Z}_{ls}$

$$\mathbf{Z}_{ls} = \frac{a\omega_0 \mu_0}{\pi} \tan \left(j \frac{\pi b}{a} + \operatorname{arc\,tan} \mathbf{k} \right)$$

therefore, with the additional theorem of the tangent function and the identity $\tan(jx) = j \tanh x$

$$\mathbf{Z}_{ls} = \frac{a\omega_0 \mu_0}{\pi} \mathbf{K} \tag{30}$$

where

$$\mathbf{K} = \frac{\mathbf{k} + j \tanh\left(\pi \frac{b}{a}\right)}{1 - j\mathbf{k} \tanh\left(\pi \frac{b}{a}\right)} . \tag{31}$$

So far the flux "escaping" in the y direction in the air gap has not been considered because $\mathbf{H}_y$ has been taken as being zero. Calculating the potential magnetic field of the air gap with a three-dimensional model

$$\mathbf{H}_x = \frac{\partial \mathbf{W}}{\partial x}, \quad \mathbf{H}_y = \frac{\partial \mathbf{W}}{\partial y}, \quad \mathbf{H}_z = j \frac{\pi}{a} \mathbf{W}$$

where $\mathbf{W}$ is the complex potential and according to Laplace's equation

$$\frac{\partial^2 \mathbf{W}}{\partial x^2} + \frac{\partial^2 \mathbf{W}}{\partial y^2} - \frac{\pi^2}{a^2} \mathbf{W} = \mathbf{0} .$$

But in the two-dimensional model used so far, the derivated with respect to y were zero, therefore

$$\frac{d^2 \mathbf{W}}{dx^2} - \frac{\pi^2}{a^2} \mathbf{W} = \mathbf{0} .$$

If the complex potential function in the three-dimensional model is approximated by

$$\mathbf{W} = \mathbf{W}_1(x) \cdot 1{,}17 \cos\left(2{,}34 \frac{y}{l}\right),$$

— the factor of $\mathbf{W}_1(x)$ approximates, at equal area and with minimum square error, the rectangle extending from $y = -l/2$ to $+l/2$ and unit ordinate — introducing it into Laplace's equation gives

$$\frac{d^2 \mathbf{W}_1}{dx^2} - \left[\left(\frac{2{,}34}{l}\right)^2 + \frac{\pi^2}{a^2}\right] \mathbf{W}_1 = \mathbf{0} .$$

Then $\mathbf{W}_1$ can be interpreted as the complex potential of a two-dimensional potential in which instead of π^2/a^2 takes place

$$\left[\frac{\pi}{a}\right] \sqrt{1 + \left(\frac{2{,}34}{\pi}\right)^2 \frac{a^2}{l^2}}^2 .$$

In Eq. (31) this is equivalent to increasing the air gap to the value

$$b' = b\sqrt{1 + 0{,}554\,\frac{a^2}{l^2}}\,. \tag{32a}$$

With this

$$\mathbf{K} = \frac{\mathbf{k} + j\tanh\left(\pi\dfrac{b'}{a}\right)}{1 - j\mathbf{k}\tanh\left(\pi\dfrac{b'}{a}\right)}\,. \tag{32b}$$

By rearranging

$$\mathbf{K} = \frac{j}{\tanh\left(\pi\dfrac{b'}{a}\right)}\left[1 - \frac{1 - \tanh^2\left(\dfrac{\pi b'}{a}\right)}{1 - j\mathbf{k}\tanh\left(\dfrac{\pi b'}{a}\right)}\right].$$

This shows that by increasing b'/a above 0,5 the value of th $(\pi b'/a)$ rapidly approaches one and so $\mathbf{K}$ becomes independent of $\mathbf{k}$ and so purely imaginary. No active power gets into the secondary, that is possible only if no eddy currents flow either. So by increasing the air gap the secondary currents and power strongly drop.

In the case of a plane motor of infinite length the first non-disappearing upper harmonic of the travelling wave is the fifth. Its pole pitch being the fifth of the basic harmonic, for the fifth harmonic the value b'/a is five times larger. The air gap exercises a filter action on the upper harmonic waves. This is partly the reason why we calculate with the basic harmonic waves only.

5. The total impedance of the machine referred to one slot

The impedance referred to one slot is defined by forming the ratio of half of the mean winding voltage and to the whole current flowing in the slot, where the winding voltage includes the voltages across the active resistance and that across the slot, – and the winding head leakage reactancies. First only the impedance formed with the induced voltage $\mathbf{Z}_{wi}$ is determined:

$$\mathbf{Z}_{wi} = \frac{\mathbf{U}_{wi}}{2\mathbf{I}_w}$$

where $\mathbf{U}_{wi}$ is the mean value of the induced winding voltages. Half of the induced winding voltage is, with the notations of the preceding section — also expressing the dependence on z —

$$-\,l(\mathbf{E} + \mathbf{E}_m)_{x=v+b}\,\frac{\omega_0}{\omega}\,e^{j\frac{\pi}{a}z} = l\,\mathbf{Z}_{ls}\,(\mathbf{H}_z)_{x=v+b}\,e^{j\frac{\pi}{a}z}\,.$$

If the number of slots per phase and pole is $q_1 = 1$, then with the notations of Fig. 1, half of the mean of induced winding voltage formed along the width of the slot is

$$\frac{1}{2}\mathbf{U}_{wi} = l\mathbf{Z}_{ls}(\mathbf{H}_z)_{x=v+b}\frac{1}{g}\int_{-g/2}^{g/2} e^{j\frac{\pi}{a}z}\,dz\,,$$

and thus

$$\mathbf{Z}_{wi} = l\mathbf{Z}_{ls}\frac{(\mathbf{H}_z)_{x=v+b}}{\mathbf{I}_w}\,\xi \tag{33}$$

where

$$\xi = \frac{e^{j\frac{\pi}{a}\frac{g}{2}} - e^{-j\frac{\pi}{a}\frac{g}{2}}}{j\frac{\pi}{a}g} = \frac{\sin\left(\frac{\pi}{a}\frac{g}{2}\right)}{\frac{\pi}{a}\frac{g}{2}}\,.$$

(For calculating the system of coordinates it has been assumed that the symmetry plane of the slot under examination is the plane $z = 0$).

If $q_1 \neq 1$, the above ξ is to be multiplied by the well-known winding factor and so the general form of ξ will be

$$\xi = \frac{1}{2q_1 \sin\frac{\pi}{6q_1}}\,\frac{\sin\left(\frac{\pi}{a}\frac{g}{2}\right)}{\frac{\pi}{a}\frac{g}{2}}\,. \tag{34}$$

For further developing formulae (33) the spatial distribution of H_z is represented for $x = v + b$ and for the excitation of one phase, for $q_1 = 1$ (Fig. 3).

Along the opening of the slot H_z is taken as being uniformly distributed, on the other places $H_z = 0$, because the H lines arrive perpendicularly on the surface of the primary iron body. Furthermore, for linear motors the excitation

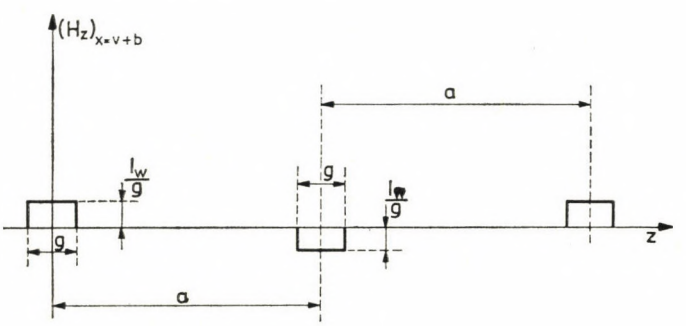

Fig. 3

of the iron part is negligible because of the large air gap (from this point of view the non ferromagnetic secondary is also considered an "air gep"). So the excitation of the slot current falls upon the opening of the slot and there $H_z = I_w/g$. The basic harmonic of this distribution is

$$H_{z1} = \frac{4}{\pi} \int_0^{\frac{g}{2}\frac{\pi}{a}} \frac{I_w}{g} \cos\left(\frac{\pi}{a} z\right) d\left(\frac{\pi}{a} z\right) = \frac{4}{\pi g} I_w \sin\left(\frac{\pi}{a} \frac{g}{2}\right).$$

If $q_1 \neq 1$, the excitation picture is regularly repeated q_1 times with a shift of $a/3q_1$ and the value of H_{z1} is multiplied by the well-known winding factor and by q_1:

$$H_{z1} = \frac{4}{\pi g} I_w \sin\left(\frac{\pi}{a} \frac{g}{2}\right) \frac{q_1}{2q_1 \sin\frac{\pi}{6q_1}}.$$

Hence with the notation (34) the basic harmonic is

$$H_{z1} = \frac{2I_w}{a} \xi q_1 .$$

The result of the single-phase excitations is a travelling basic harmonic wave H_z with a peak value of $3H_{z1}/2$. The peak of a travelling wave reaches the centre of a slot (a slot group, respectively), if in the slot (slot group) the excitation is maximum. For this reason

$$(\mathbf{H}_z)_{x=v+b} = \frac{3q_1}{a} \xi \mathbf{I}_w$$

which by introducing into Eq. (33) results in

$$\mathbf{Z}_{wi} = \frac{3lq_1}{a} \xi^2 \mathbf{Z}_{ls} ,$$

and on the base of Eq. (30) it gives

$$\mathbf{Z}_{wi} = \frac{3q_1}{\pi} \xi^2 \omega_0 \mu_0 l\mathbf{K} . \tag{35}$$

If the area of the slot filled with copper is A_1, the resistivity of the copper is ϱ_1, the length of the winding heat (at one side) is l_1, the active resistance referred to one slot will be

$$R_1 = \varrho_1 \frac{l + l_1}{A_1} .$$

Imagining the cross section "smeared" along the circumference, its thickness would be

$$\frac{3q_1 A_1}{a}.$$

Introducing the parameter

$$h = \frac{3q_1 A_1}{a} \frac{l}{l+l_1} \tag{36}$$

which has the dimension of a length,

$$R_1 = \varrho_1 \frac{l}{h \dfrac{a}{3q_1}}. \tag{37}$$

At 50 Hz the leakage reactancies of the slot and the winding head are taken as proportional to R_1 and thus

$$X_{t1} = \alpha \frac{\omega_0}{\omega_{50}} R_1 \tag{38}$$

where ω_{50} is the angular frequency belonging to 50 Hz ($= 100\pi$/sec) and α is a factor of proportionality.

The total slot impedance is now

$$\mathbf{Z}_w = R_1 + jX_{t1} + \mathbf{Z}_{wi}. \tag{39}$$

Finally let us remark that obviously for the ν-th upper harmonic wave in space Eq. (34) takes the form

$$\xi_\nu = \frac{\sin\left(\nu \dfrac{\pi}{6}\right)}{q_1 \sin\left(\nu \dfrac{\pi}{6q_1}\right)} \frac{\sin\left(\nu \dfrac{\pi}{a} \dfrac{g}{2}\right)}{\nu \dfrac{\pi}{a} \dfrac{g}{2}}. \tag{40}$$

In the case of an infinite linear motor the first non-disappearing upper harmonic is the fifth. Chiefly, because of the second factor ξ_5 is much smaller than $\xi = \xi_1$, therefore $\xi_5^2 \ll \xi_1^2$ and in connection with Eq. (35) $\mathbf{Z}_{wi}$ is influenced but little by the upper harmonic waves. This is another reason why the spatial upper harmonics can be neglected.

With a linear motor of finite length the excitation picture is not periodical (See Section 8).

6. Calculation of the tractive force and normally-directed force

If the total excitation of the slot is I_w, the air gap power referred to one slot is

$$P_{lw} = I_w^2 \, Re \, (\mathbf{Z}_{wi}) ,$$

the synchronous speed according to (7) is

$$c_0 = \frac{a}{\pi} \omega_0 ,$$

hence the tractive force for one slot is

$$F_w = \frac{P_{lw}}{c_0} = \frac{\pi}{a\omega_0} I_w^2 \, \mathrm{Re} \, (\mathbf{Z}_{wi}) .$$

This method of calculation corresponds to the model created so far: according to the condition b), Section **3**, the power penetrates into the secondary only across the iron body, and thus, from the point of view of power only the y component of the electric field is decisive. Its value in the system is moving together with the secondary s times the value of that in the system moving with the primary, and this fact justifies the above method of calculation. (If we were also to consider the power of the currents induced by the winding heads into the secondary parts protruding from the iron body, we could do this in the equivalent circuit discussed in the following Section — by imagining this loss on the primary winding and increasing R_1).

In the secondary an area

$$\frac{a}{3q_1} l$$

belongs to one slot, and so, the tractive force per unit surface is

$$\frac{F}{A} = \frac{3q_1 \, F_w}{al} = \frac{3\pi q_1}{a^2 \, l\omega_0} I_w^2 \, \mathrm{Re} \, (\mathbf{Z}_{wi}) .$$

To one slot belongs a circumference part $a/3q_1$ and thus the circumferential current is

$$d_I = \frac{3I_w q_1}{a} . \tag{41}$$

With this and formula (35) the last relation becomes

$$\frac{F}{A} = \mu_0 \, \xi^2 \, d_I^2 \, \mathrm{Re} \, (\mathbf{K}) . \tag{42}$$

This formula gives the tractive force per unit surface.

The ratio of the normal force F_n (in x direction) and the tractive force F, acting in the opposite direction to the z axis corresponding to the direction of the travelling wave, is from the Maxwell stresses

$$\frac{F_n}{F} = \frac{1}{2} \frac{(H_{xr}^2 - H_{zr}^2)_{\text{time-mean}}}{(-H_{xr} H_{zr})_{\text{time-mean}}}$$

i.e.

$$\frac{F_n}{F} = \frac{1}{2} \frac{\mathbf{H}_{xr} \mathbf{H}_{xr}^* - \mathbf{H}_{zr} \mathbf{H}_{zr}^*}{-\text{Re}\,(\mathbf{H}_{xr} \mathbf{H}_{zr}^*)} \tag{43}$$

where the "reduced" field characteristics according to Eqs (28) must be taken *on the surface of the secondary part*, at $x = v$. From Eqs (28)

$$\left(-\frac{\mathbf{H}_{xr}}{\mathbf{H}_{zr}}\right)_{x=v} = \frac{\pi}{a\omega\mu_0} \left(-\frac{\mathbf{E} + \mathbf{E}_m}{\mathbf{H}_z}\right)_{x=v} = \frac{\pi}{a\omega_0\mu_0} (\mathbf{Z}_{s\infty} + \mathbf{Z}_{sa}) = \frac{\pi}{a\omega_0\mu_0} \mathbf{Z}_s$$

finally on the base of (27a)

$$-\left(\frac{\mathbf{H}_{xr}}{\mathbf{H}_{zr}}\right)_{x=v} = \mathbf{k}\,,$$

and introducing this into (43), the ratio of the normal force and the tractive force is

$$\frac{F_n}{F} = \frac{|\mathbf{k}|^2 - 1}{2\text{Re}\,\mathbf{k}}\,. \tag{44}$$

From Eq. (44) the force in normal direction, directed along the positive x axis is positive; the force in question is that acting on the secondary, an attracting force is positive, a repulsive force is negative.

7. The equivalent circuit analogous to that of the asynchronous machine

The formulae discussed so far are suitable for determining the electrical parameters of the linear plane motor of finite width (and infinite length). The linear induction motor being after all an asynchronous machine, as a comparison with the electrical parameters of the usual asynchronous machines, it is useful to construct its equivalent circuit.

In the equivalent circuit of the traditional asynchronous machine the impedance of the secondary circuit is

$$\mathbf{Z}_2' = \frac{R_2'}{s} + jX_2'$$

where R_2' is the reduced secondary active resistance (not depending on the slip) and X_2' is the reduced secondary leakage reactance (not depending on the slip either). It is characteristic for $\mathbf{Z}_2'$ that in case of $s \to 0$ it tends towards ∞. The secondary field impedance* $\mathbf{Z}_s$ of the linear motor according to (27a) does not behave in this way, but for $s \to 0$, i.e. $m \to 0$ according to Eq. (10), on the base of Eqs (26b), (24), (14) and (27b)

$$\mathbf{k} \to \frac{j}{\tanh\left(\frac{\pi v}{a}\right)} - \frac{j\,\frac{a}{\pi v}}{\frac{\pi}{2}\,\frac{l}{a}\coth\left(\frac{\pi}{2}\,\frac{l}{a}\right)+q} \overset{\text{def}}{\equiv} \frac{j}{\tanh\frac{\pi v'}{a}}. \tag{45}$$

For the time being calculating only with the dimensionless impedancies, the impedance $\mathbf{k}$ is replaced by two such impedancies, in parallel, where one becomes ∞ for $m \to 0$. Denoting the latter by $\mathbf{k}_m$ (because of its dependence on m) it is obvious that the other impedance is just $j/\tanh(\pi v'/a)$, thus

$$\mathbf{k} = \frac{\frac{j}{\tanh\left(\frac{\pi v'}{a}\right)}\,\mathbf{k}_m}{\frac{j}{\tanh\left(\frac{\pi v'}{a}\right)} + \mathbf{k}_m},$$

and from this

$$\mathbf{k}_m = \frac{\mathbf{k}}{1 + j\tanh\left(\frac{\pi v'}{a}\right)\mathbf{k}}, \tag{46}$$

and for this $\lim_{m\to 0} \mathbf{k}_m = \infty$. [The value v' calculated from (45) tends towards v for $l \to \infty$].

The formula, taking into account the air gap (32b), is a linear fractional function with respect to $\mathbf{k}$. Such functions have three free parameters and, therefore, the effect of the air gap on the impedance K can be accounted for by a T-member (Fig. 4a).

Using in Eq. (32b) provisionally the notation $\text{th}\,(\pi b'/a) = t$ and making equal the values of K from (32b) and from the T-member, we obtain:

$$\frac{\mathbf{k} + jt}{1 - j\,\mathbf{k}\,t} = \mathbf{k}_{s1} + \frac{\mathbf{k}_p(\mathbf{k}_{s2} + \mathbf{k})}{\mathbf{k}_p + \mathbf{k}_{s2} + \mathbf{k}}$$

* The connection between the circuit impedance and the field impedance has been discussed when deriving Eqs (33) and (35);

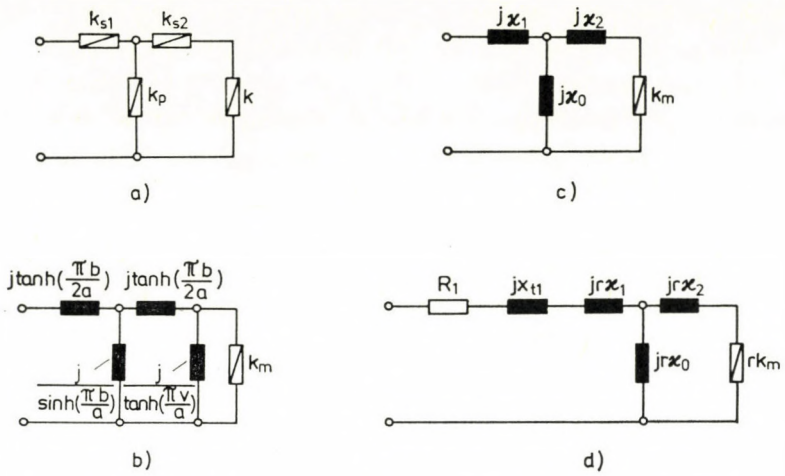

Fig. 4

and this must be true for every $\mathbf{k}$. For $\mathbf{k} \to \infty$

$$\frac{j}{t} = \mathbf{k}_{s1} + \mathbf{k}_p. \tag{47a}$$

From the identity of the pole locations

$$\frac{j}{t} = \mathbf{k}_{s2} + \mathbf{k}_p \tag{47b}$$

finally for $\mathbf{k} = 0$

$$jt = \mathbf{k}_{s1} + \frac{\mathbf{k}_p \mathbf{k}_{s2}}{\mathbf{k}_p + \mathbf{k}_{s2}} \tag{47c}$$

One solution of the system of equations (47) is

$$\mathbf{k}_p = j\sqrt{\frac{1}{t^2} - 1}; \quad \mathbf{k}_{s1} = \mathbf{k}_{s2} = j\left(\frac{1}{t} - \sqrt{\frac{1}{t^2} - 1}\right)$$

or, after reintroducing the relation $t = \text{th}\,(\pi b'/a)$

$$\mathbf{k}_p = \frac{j}{\sinh\left(\dfrac{\pi b'}{a}\right)}; \quad \mathbf{k}_{s1} = \mathbf{k}_{s2} = j\tanh\left(\frac{\pi b'}{2a}\right).$$

In accordance with this the equivalent circuit of Fig. 4b has been established, also replacing $\mathbf{k}$ by parallel branches, as was discussed at the beginning of this Section. By deltastar transformation the circuit according to Fig. 4c is

obtained where

$$\varkappa_0 = \frac{1}{\tanh\left(\frac{\pi v'}{a}\right)\cosh\left(\frac{\pi b'}{a}\right) + \sinh\left(\frac{\pi b'}{a}\right)}, \tag{48}$$

$$\varkappa_1 = \tanh\left(\frac{\pi b'}{2a}\right)\left[1 + \varkappa_0 \tanh\left(\frac{\pi v'}{a}\right)\right], \tag{49}$$

$$\varkappa_2 = \varkappa_0\left[\cosh\left(\frac{\pi b'}{a}\right) - 1\right]. \tag{50}$$

The equivalent circuit of Fig. 4c provides the dimensionless impedance $\mathbf{K}$, while the impedance for one slot $\mathbf{Z}_{wi}$ according to Eq. (35) is obtained by multiplying with the expression

$$r = \frac{3}{\pi} q_1 \xi^2 \omega_0 \mu_0 l \tag{51}$$

which has the dimension of a resistance. Thus, the equivalent circuit for the complete slot impedance according to (39) takes the shape of Fig. 4d. From this, using the traditional notations

$$\mathbf{Z}_0 = jr\varkappa_0\,,$$

$$\mathbf{Z}_1 = R_1 + j(X_{t1} + r\varkappa_1)\,,$$

$$\mathbf{Z}_2' = r\mathbf{k}_m + jr\varkappa_2\,.$$

Therefore, the main flux reactance of the linear motor will be

$$X_0 = r\varkappa_0, \tag{52}$$

its primary leakage reactance will be

$$X_1 = X_{t1} + r\varkappa_1, \tag{53}$$

its reduced secondary leakage reactance

$$X_2' = r[\varkappa_2 + \mathrm{Im}\,(\mathbf{k}_m)] \tag{54}$$

and its reduced secondary active resistance

$$R_2' = sr\ \mathrm{Re}\ (\mathbf{k}_m) \tag{55}$$

The resistance R_1 and the values in the foregoing formulae can be determined from the relations (37, 38, 27b, 45, 46, 48—51).

In the equivalent circuit Fig. 4d only the impedance $r\mathbf{k}_m$ depends on m and thus on the slip. Correspondingly only R_2' and X_2' can depend on the slip.

Finally the case merits special mention where

$$\frac{l}{a} > 5 \quad \text{and} \quad \frac{v}{a} \leqq 0{,}1 \tag{56}$$

From the first condition it follows that the value of $\mathbf{k}_a$ in (26b) can be neglected as compared to $\mathbf{k}_\infty$, and thus from (27b)

$$\mathbf{k} \cong \mathbf{k}_\infty ,$$

from the second restriction on the base of Eq. (14)

$$\mathbf{k}_\infty \cong \frac{j}{1 + jm} \frac{a}{\pi v}$$

hence on the base of Eqs (45) and (46)

$$\mathbf{k}_m \cong \frac{\dfrac{j}{1 + jm} \dfrac{a}{\pi v}}{1 + j\dfrac{\pi v}{a} \dfrac{j}{1 + jm} \dfrac{a}{\pi v}} = \frac{a}{m\pi v}$$

where $\mathbf{k}_m$ is real. With all these from (54) and (55), these formulae are deduced:

$$X_2' = r\varkappa_2 \tag{54a}$$

and

$$R_2' = \frac{s}{m} \frac{ra}{\pi v}$$

from which latter by substituting the notations (51) and (10) the relation

$$R_2' = \xi^2 \frac{1}{\gamma} \frac{l}{\dfrac{a}{3q_1} v} \tag{55a}$$

physically easy to interpret, is deduced. Thus with the conditions (56), R_2' and X_2' are independent of the slip: a circuit completely equivalent to that of the asynchronous machine is obtained, with a main flux reactance X_0 very much smaller than that of the traditional machine, assuming an equal pole pitch.

8. Linear motor of finite length

Considering its paramount importance only that case is dealt with where the primary is of finite length, but the secondary can be considered as inifinite. The magnetic field distribution $(H_z)_{x=v+b}$ due to the excitation by one phase here, differs from that shown on Fig. 3, in that it terminates at both sides (for the moment we restrain ourselves to $q_1 = 1$). Let us consider here also the fundamental harmonic of the excitation repartition, but let us terminate the sine waves of the basic harmonic from both sides, exceeding the extreme slots, at the passage through zero ! (This approximation minimizes the square error integral in the same way as the infinite sine wave the infinite excitation distribution). On those places where *there is excitation*, the excitation waves in the phases of the basic harmonic are the following (the amplitude is taken as 1):

$$\sin z' \cos t' = \frac{1}{2} \sin (z' + t') + \frac{1}{2} \sin (r' - t'),$$

$$\sin (z' - 120°) \cos (t' + 120°) = \frac{1}{2} \sin (z' + t') + \frac{1}{2} \sin (z' - t' - 240°),$$

$$\sin (z' - 240°) \cos (t' + 240°) = \frac{1}{2} \sin (z' + t') + \frac{1}{2} \sin (z' - t' - 120°),$$

where

$$z' = \frac{z}{a} 180° \text{ and } t = \omega t.$$

As the excitation on both sides is interrupted for each phase at another place, the travelling waves of negative and positive order, obtained at the right hand side, start for each phase at a different place and end at different places. Correspondingly the resulting positive and negative order waves take shape. Fig. 5 shows the distribution of a resulting travelling wave of positive order, Fig. 6 that of negative order for two poles ($p = 1$).

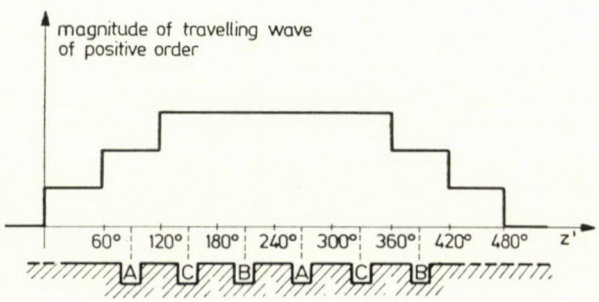

Fig. 5

(In Fig. 6 the vertical lines at 60° and 420° separate from each other the travelling waves of negative order and different phase position).

In the following the effect of the waves of negative order will be neglected; they exist only at the edges of the winding and their amplitude is smaller than that of the positive waves. Furthermore no great error is made by considering the winding of length $2ap$ infinitely repeated, with a period length $4ap$ and

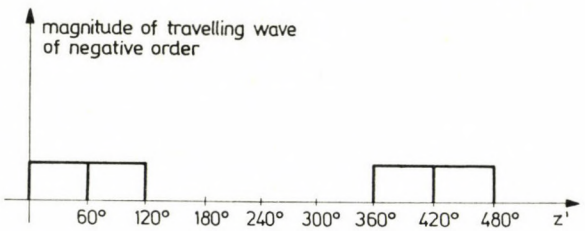

Fig. 6

taking one period of this excitation picture obtained as the appropriate model of the real situation. If $z = 0$ it is taken for the centre of the winding, then the first three members of the Fourier series for a period $4pa$ of Fig. 5, assumedly repeated are

$$b_0 + b_1 \cos\frac{\pi z}{2pa} + b_2 \cos\left(\frac{2\pi z}{2pa}\right)$$

where — taking for unit the amplitude at $z = 0$ —

$$b_0 = \frac{1}{2}\,;\; b_1 = \frac{2}{\pi}\,\frac{1 + 2\cos\left(\frac{\pi}{6p}\right)}{3} \cong \frac{2}{\pi}\left(1 - \frac{\pi^2}{108p^2}\right)\,;\; b_2 = 0;$$

(the detailed calculation is omitted).

Corresponding to the travelling wave the distribution according to Fig. 5 must still be multiplied by

$$e^{j\left(\frac{\pi}{a}z + \omega_0 t\right)}$$

and from this by omitting $e^{j\omega_0 t}$ the distribution of $(H_z)_{x=v+b}$ is obtained, expressed by the value $(3q_1/a)\,\xi\mathbf{I}_w$ from Section 5:

$$(\mathbf{H}_z)_{x=v+b} = \frac{3q_1}{a}\,\xi\mathbf{I}_w\left[b_0 + b_1\cos\frac{\pi z}{2ap}\right]e^{j\frac{\pi}{a}z} \equiv$$

$$\equiv \frac{3q_1}{a}\,\xi\mathbf{I}_w\left[b_0 e^{j\frac{\pi}{a}z} + \frac{b_1}{2}\,e^{j\frac{\pi}{a}z\left(1+\frac{1}{2p}\right)} + \frac{b_1}{2}\,e^{j\frac{\pi}{a}z\left(1-\frac{1}{2p}\right)}\right]. \qquad (57)$$

Thus *from a part of the basic harmonic wave a "fractional" harmonic wave of order* $1 + 1/2p$ *and one of order* $1-1/2p$ *are split off.* For a linear motor of infinite length, i.e. for $p \to \infty$ the fractional harmonics coincide with the basic harmonic and therefore,

$$\lim_{p\to\infty}\left(b_0 + \frac{b_1}{2} + \frac{b_1}{2}\right)$$

must be 1. But the calculation gives $1/2 + 2/\pi = 1{,}137$. The excedent is due to the omission of the neglected upper harmonics of the above Fourier series. Approximating their influence as being uniformly distributed over the three waves, finally the following weight factors are taken into account:

$$\lambda_1 = 0{,}44; \quad \lambda_{1\pm\frac{1}{2p}} = 0{,}28\left(1 - \frac{\pi^2}{108p^2}\right) . \tag{58}$$

The pole pitch of the special harmonic of ν-th order is

$$a_\nu = \frac{a}{\nu}, \tag{59}$$

and in the calculation of the harmonic impedance of order ν, a_ν must be put in the place of a in Eqs (10, 14, 24, 25, 26b, 32b).; thus an impedance factor $\mathbf{K}_\nu$ is obtained from (32b). For in Eq. (30) a_ν must be put in the place of a, but according to (57) in the unnumbered equations preceding (35) a remains, the right side of (35) must be multiplied by $a_\nu/a = 1/\nu$. The voltages induced by the progressing waves add up and hence also the impedances with the corresponding weight factors. Finally in the place of (35) one must calculate with

$$\mathbf{Z}_{wi} = \frac{3q_1}{\pi}\omega_0\mu_0 l \sum_\nu \lambda_\nu \frac{\xi_\nu^2}{\nu}\mathbf{K}_\nu \tag{60}$$

($\nu = 1,\ 1 + 1/2p,\ 1-1/2p$); the value of ξ_ν can be calculated from (40).

Similarly reasoning the place of (42) is taken by

$$\frac{F}{A} = \mu_0 d_l^2 \sum_\nu \lambda_\nu \xi_\nu^2 \operatorname{Re}(\mathbf{K}_\nu). \tag{61}$$

Introducing the factor

$$\sigma_\nu = \frac{|\mathbf{k}_\nu|^2 - 1}{2\operatorname{Re}(\mathbf{k}_\nu)} \tag{62a}$$

corresponding to the right side of (44) the ratio of the normal and tangential forces becomes

$$\frac{F_n}{F} = \frac{\sum_\nu \sigma_\nu \lambda_\nu \xi_\nu^2 \operatorname{Re}(\mathbf{K}_\nu)}{\sum_\nu \lambda_\nu \xi_\nu^2 \operatorname{Re}(\mathbf{K}_\nu)} \,. \tag{62b}$$

For all three harmonic progressing waves the equivalent circuit discussed in Section 7. can be constructed without the impedance $R_1 + jX_{f1}$; to form the resulting impedance they are connected in series with each other on the input side and the impedance $R_1 + jX_{f1}$.

The velocity of the ν-th field harmonic wave is the ν-th part of the basic harmonic, and therefore the slip referred to this wave is

$$s_\nu = \frac{\frac{c_0}{\nu} - c}{\frac{c_0}{\nu}} = 1 - \nu\frac{c}{c_0} = 1 - \nu(1 - s) \,.$$

For the fractional harmonic $\nu = 1 + 1/2\,p$ therefore

$$s_{\left(1+\frac{1}{2p}\right)} = s + \frac{1}{2p}(s - 1).$$

This shows that for $s = 0$, but also with small positive slips for this fractional harmonic, a negative slip and thus a generating force is obtained, which in fact reduces the resulting force and even this can shift it to the negative.

The method described here discusses the longitudinal end effect with *undamped travelling waves*. The solution of OBERRETL [11] consisting of undamped travelling waves is more accurate but less lucid. YAMAMURA [8, 15] and VOLDEK [5, 14] calculate with *damping travelling waves*.

9. Results of calculations and measurements

With the previously discussed calculation method the calculation and measurement results of the available motor for the state $s = 1$ are shown in Figs 7, 8 and 9. The data of the motor are:

pole pitch 0,054 m
air gap 2, 4, 6 and 10 mm
thickness of secondary 0,0025 and 0,005 m

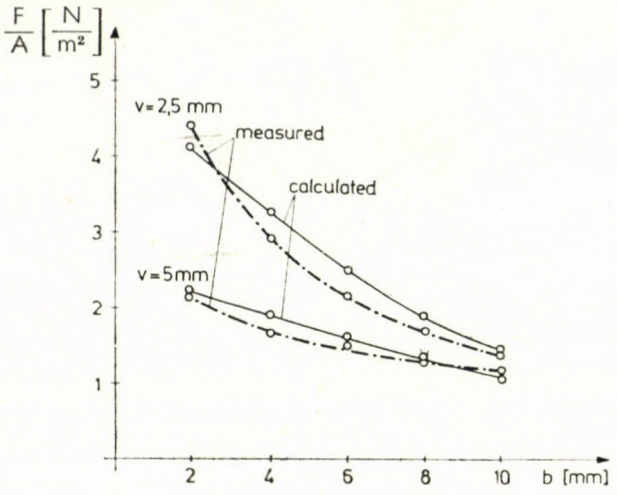

Fig. 7

overreaching of secondary 0,15 m
slot width 0,012 m
motor width 0,15 m
number of pole pairs 9
number of slots per phase and per pole 1
resistivity of secondary $0{,}303 \cdot 10^{-7}$ ohm m
primary angular frequency 314 l/s
reduced conductor height 0,0037 m
primary resistivity $0{,}2 \cdot 10^{-7}$ ohm m
leakage reactance of slot and winding head (estimated value) 1,6 R_1
nominal slip 1
nominal circumferential current 50 000 A/m.

Fig. 7 shows the tractive force per unit surface, Fig. 8 the active power per unit surface, while Fig. 9 shows the cos φ as a function of the air gap, at stationary state and under feeding with a constant terminal voltage.

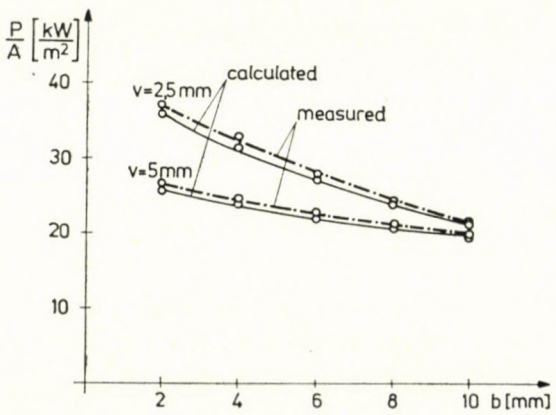

Fig. 8

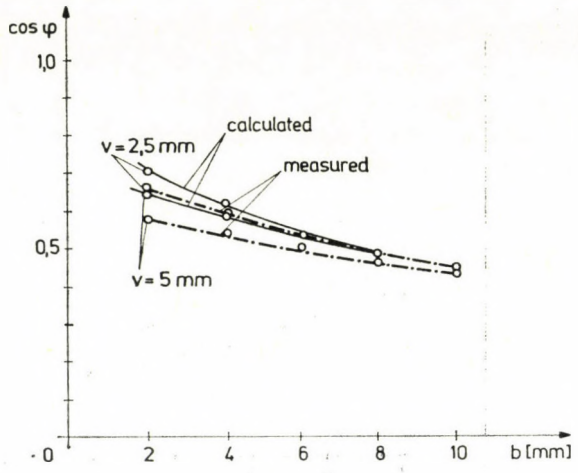

Fig. 9

Calculated traction force, current vector diagram for motors of various synchronous speeds

Fig. 10 shows the calculated traction force per unit surface of a motor with a velocity of $c_0 = 3{,}5$ m/s and its efficiency as functions of the slip.

Fig. 11 presents the current vector diagram of the same motor. In both cases the terminal voltage is constant.

In this case the calculation data where: pole pitch 0,35 m, air gap 10 mm, secondary: thickness 10 mm, overreaching 0,5 m, resistivity $0{,}35 \cdot 10^{-7}$ ohm m, slot width 0,02 m, motor width 0,2 m, number of pole pairs 7, number of slots per phase and pole 3, primary angular frequency 62,83 1/s, reduced conductor height 0,005 m, primary resistivity $3{,}5 \cdot R_1$, nominal slip 0,1, nominal circumferential current 50 000 A/m.

In the next calculation example the synchronous speed of the machine is 20 m/s. The characteristic data are: pole pitch 0,2 m, air gap 10 mm, secondary: thickness 10 mm, overreaching 0,3 m, resistivity $0{,}37 \cdot 10^{-7}$ ohm m, slot width 0,02 m, motor width 0,2 m, number of pole pairs 10, number of slots per pole and phase 2, primary angular frequency 314,2 1/s, reduced conductor height 0,005 m, primary resistivity $0{,}2 \cdot 10^{-7}$ ohm m, slot and winding head leakage reactance $3{,}5 \cdot R_1$, nominal slip 0,05 nominal circumferential current 50.000 A/m.

Fig. 12 shows the variations of the traction force and of the efficiency in motor and in generator operation ($1 \geqq s \geqq -1$) at constant terminal voltage feed.

Fig. 13 shows the current vector diagram of the machine also for constant voltage feed.

Curve 1 of Fig. 14 shows the traction force of the above machine as a function of the slip, if the current flowing through the windings is constant. Curves 2, 3 and 4 represent the traction force of the same motor at constant current feed, only the length and width dimensions of the motor change. With curve 2 the length of the machine is finite ($p = 10$) but its width is infinite; with curve 3 the length is infinite ($p = \infty$), the width is finite (0,2 m); finally with curve 4 the width of the machine as well as its length are infinite.

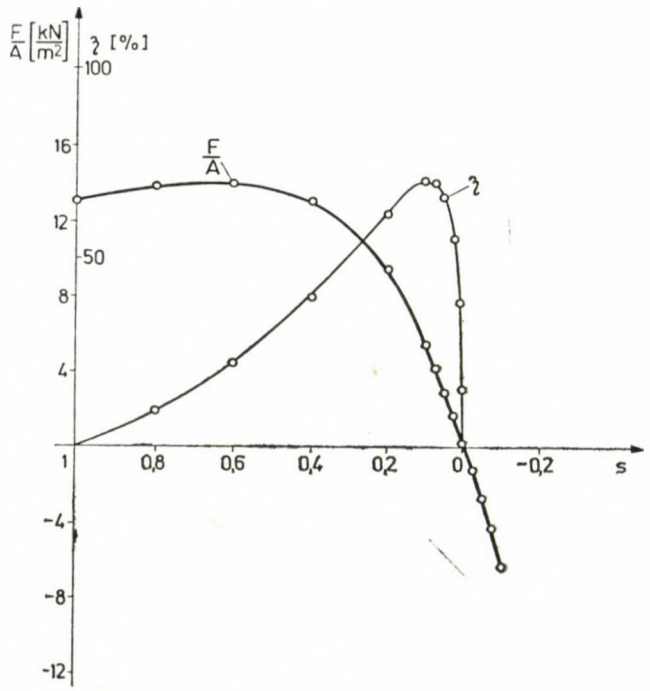
F/A [kN/m²]
η [%]
100
16
12
50
8
4
1
0,8
0,6
0,4
0,2
0
-0,2
s
-4
-8
-12
F/A
η

Fig. 10

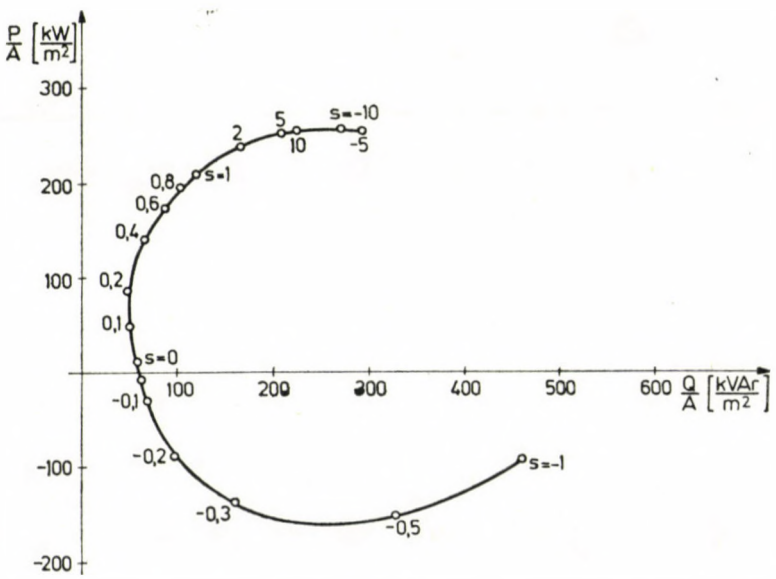
P/A [kW/m²]
300
200
100
-100
-200
100
200
300
400
500
600
Q/A [kVAr/m²]
s=-10
5
2
10
-5
0,8
s=1
0,6
0,4
0,2
0,1
s=0
-0,1
-0,2
-0,3
-0,5
s=-1

Fig. 11

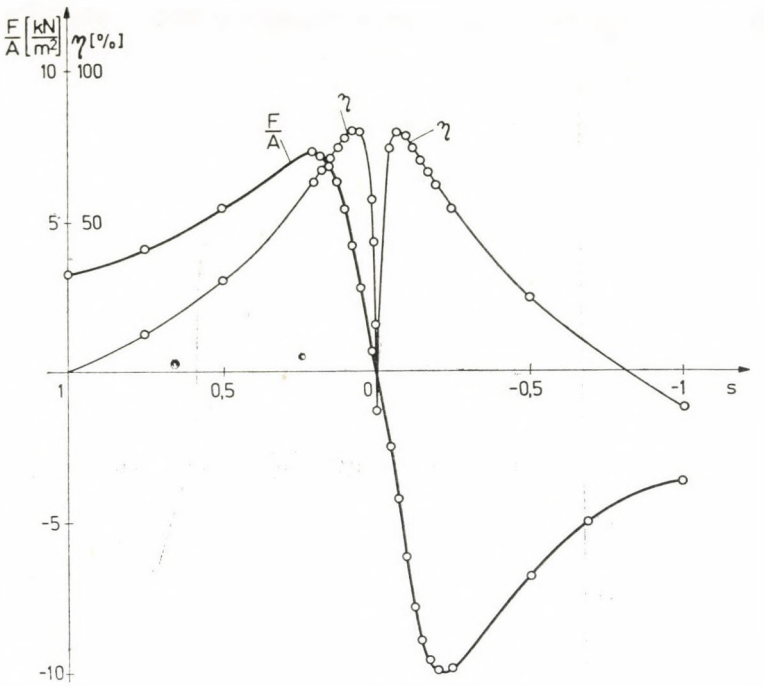
F/A [kN/m²]
η [%]
10
100
5
50
1
0,5
0
-0,5
-1
s
-5
-10
F/A
η

Fig. 12

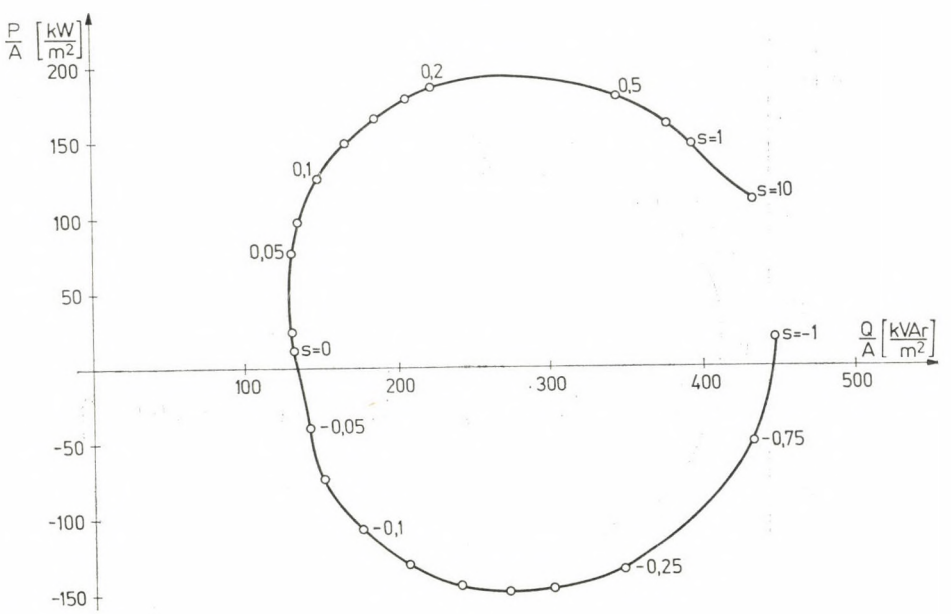
P/A [kW/m²]
200
150
100
50
-50
-100
-150
100
200
300
400
500
Q/A [kVAr/m²]
0,2
0,5
s=1
s=10
0,1
0,05
s=0
s=-1
-0,05
-0,75
-0,1
-0,25

Fig. 13

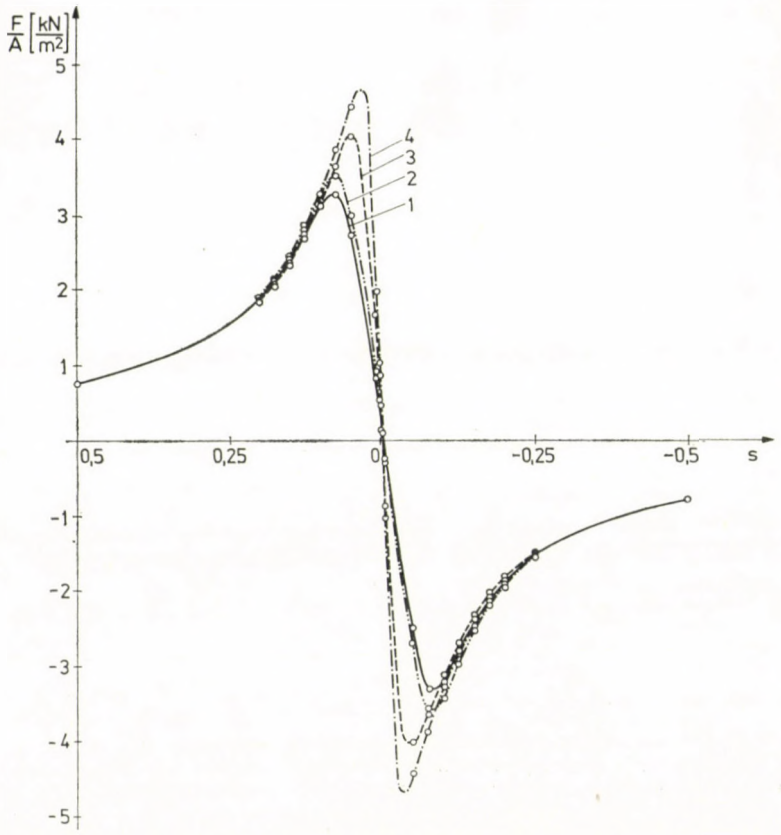

Fig. 14

REFERENCES

1. Tuschák, R.: Stromverdrängung von in kreisförmigen Nuten gebetteten massiven Leitern. *Per. Polyt. Electr. Engg.—Elektrotechn.* **1,** (1957), 27—51
2. Freeman, E. M.: Travelling Waves in Induction Machines: Input Impedance and Equaivalent Circuits. *Proc. IEE*, **115,** No. 12 (1968 dec.), 1772—1776
3. Nasar, S. A.: Electromagnetic Fields and Forces in a Linear Induction Motor, Taking into Account Edge Effects. *Proc. IEE*, **116,** (1969 april) no. 4, 605—609
4. Bolton, H.: Transverse Edge Effect in Sheet-Rotor Induction Motors. *Proc. IEE* **116,** (1969 May), No. 5, 725—731
5. Voldek, A. I.—Lazarenko, L. F.: Prodolnye kraievye effekty v linejnykh induktsionnykh magnitogidrodinamicheskykh mashinakh. *Elektrichestvo* 1970, No. 11, 26—30
6. Jufer, M.: Détermination des caractéristiques spécifiques du moteur lineáire. *R.G.E.* **80,** No. 2, (1971 Février), 105—113
7. Poloujadoff, M. et. Rey x, Ph.: Méthode intermédiaire pour l'analyse d'un moteur à induction linéaire. *R. G. E.* **80,** (Févier 1971), No. 2, 99—104
8. Yamamura, S.—Ito, H.—Ishikawa, Y.: Theories of the Linear Induction Motor and Compensated Linear Induction Motor. *IEEE Winter Meeting*, New York, 1972 Jan. 30—Febr. 4
9. Kapcsos, P.—Tevan, Gy.: Ferromágneses betétű, lineáris örvényárammotorok alkalmazása és számítása. *Elektrotechnika* **65,** (1972), No. 12, 458—465

10. SCHIEBER, D.: Principles of Operation of Linear Induction Devices. *Proc IEEE*, **61,** (1973, May) No. 5, 647–656
11. OBERRETL, K.: Dreidimensionale Berechnung des Linearmotors mit Berücksichtigung der Endeffekte und der Wicklungsverteilung. *Archiv f. Elektrotevhn.* **55,** (1973) H. 4, 181–190
12. BOON-TECK OOI: A Generalized Machine Theory of the Linear Induction Motor. *IEEE Winter Meeting*, New York 1973 Jan. 28–Febr. 2, 1252–1259
13. ALDEN, R. T. H.–NOLEN, P. I.: Transfer-Matrix Analysis of Linear Induction Machines with Finite Width and Depth. *Proc. IEEE* **121,** (1974 Nov.) No. 11. 1393–1398
14. VOLDEK, A. I.–TOLVINSKAIA, E. B.: Osnovy teorii i metodiki raschota karakteristik linejnykh asinkronnykh mashin. *Elektrichestvo*, 1975, No. 9, 29–36
15. SAKAE YAMAMURA: Theory of Linear Induction Motors. John Wiley and Sons, New York–London–Sydney–Toronto, 1972

Ein übersichtlicher Algorithmus für die Berechnung des Linearmotors aufgrund der Feldtheorie. Die Arbeit bespricht eine auf der "Feldtheorie" beruhende, aus verhältnismäßig einfachen Formeln bestehende (annähernde) Berechnungsmethode für den linearen Induktionsmotor. Die Methode berücksichtigt den Skineffekt, den Zusammenhang zwischen Erregung und Windung, schafft den Zusammenhang mit den Ersatzschaltungen des traditionellen Induktionsmotors, wobei die auf den primären Eisenkern entfallende Erregung und die ganzzahligen Harmonischen des fortschreitenden Feldes vernachlässigt werden, aber der longitudinale Endeffekt durch zwei ungedämpfte Feldharmonische von gebrochenen Ordnung beschrieben wird. Die Berechnungen werden mit Messungen an einem stehenden Motor verglichen; schließlich werden die Kennlinien der mit dieser Methode berechneten Linearmotoren vorgeführt.

Ясный расчётный алгоритм линейного индукционного двигателя основывающийся на теории поля. В статье описается (приближающий) расчётный алгоритм линейного индукционного двигателя, учитывающий поверхностный эффект, поперечный и продольный краевой эффект, связь возбуждения с обмоткой, создается связь с эквивалентной схемой традиционной асинкронной машины, пренебрегая возбуждении на первичном сердечнике и высшими гармониками целого порядка бегущего поля, но продольный краевой эффект даётся двумя (незатухащимися) пространственными гармоническими волнами дробного порядка. Расчёт сравнивается измерениями, выполнёнными на стоящей двигатели, наконец представляются характеристики линейного двигателя, вычислённого данным методом.

Acta Technica Academiae Scientiarum Hungaricae, Tomus 86 (3—4), pp. 363—394 (1978)

ELECTROMAGNETIC WAVE PROPAGATION IN INHOMOGENEOUS MEDIA

THE ANALYSIS OF THE ROTATION OF POLARIZATION, AND THE APPLICATION OF THE PRINCIPLE OF MODIFIED RAY TRACING, PART I

CS. FERENCZ*

[Manuscript received 24 May, 1977]

Part I: The propagation of monochromatic electromagnetic waves in inhomogeneous media is investigated using the "method of inhomogeneous basic modes" and the "principle of modified ray tracing". Several basic facts are obtained for the propagation in inhomogeneous media. The basic aim of the author is to explain the "W"-shape transients observed during the solar occultations of Pioneer-6 and -9 space probes. After explaining the method of investigation, in the first part, the investigations of propagation in inhomogeneous media are given in detail. In Part II, after examining the propagation is anisotropic media the "W" polarization transient is explained and the results of the investigations are summarized. It is shown that in inhomogeneous media besides the known Faraday rotation an "inhomogeneous polarisation-rotation" also occurs. This necessarily causes "W" shape polarisation transients at the time of solar occultations. Thus, new ways for investigating the structure of the front of "spreading interplanetary phenomena" are opened up.

Introduction

In the recent years in the literature "anomalous" electromagnetic wave propagation effects and their more-or-less artificial "explanations" have repeatedly been reported. Earlier we have discussed several times the question of "anomalous" redshifts [1—6]. In these works we showed that the redshifts are, in fact, not anomalous and that the effect that necessarily occurs in inhomogeneous media flowing with high velocity can be calculated by the method of relativistic ray tracing, which can be assumed to be exact for the accuracy needed here [7—12]. It is lamentable, though, that the consequences of these investigations still are not as widely appreciated as it would seem desirable and hence we still meet rather arbitrary explanations for wave propagation phenomena that are termed anomalous because they cannot be fully explained on the basis of the oversimplified models (assumption of homogeneity, etc.) that are being used.

From this point of view the question of the polarization rotation transient events observed during the solar occultation of Pioneer-6 and 9 look

* Dr. Cs. FERENCZ Government Committee on Space Research H-1369 Budapest 5, P.O.B. 315. Hungary

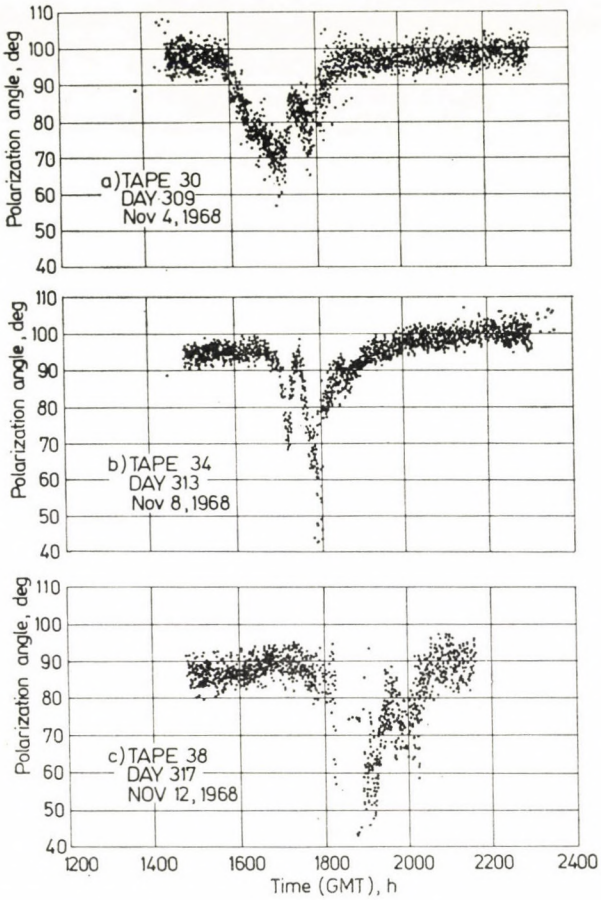

Fig. 1. Polarization transients observed during the solar occultation of Pioneer-6 in 1968 — from Ref. [13]

particularly relevant; an attempt at a rather sophisticated explanation of these phenomena has been published [13]. The transients — taken from the reference in question — can be seen in Figs. 1 and 2. However, the attempted explanation [13] does not offer a unique cause for this group of apparently identical events published by Levy et al. for Pioneer-6 (occultation: November 1968), and by Cannon et al. for Pioneer-9 (occultation: December 1970). The essence of the phenomena: superposed on the naturally occurring Faraday rotation, but in an opposite sense, polarization-rotation transients of a shape reminiscent of that of letter *W* have been observed.

Instead of invoking different, rather artificial-looking mechanisms [13] it seems self-evident to ascribe the transients to the inhomogeneity of the medium through which the waves pass; e.g. to plasma clouds ejected by the

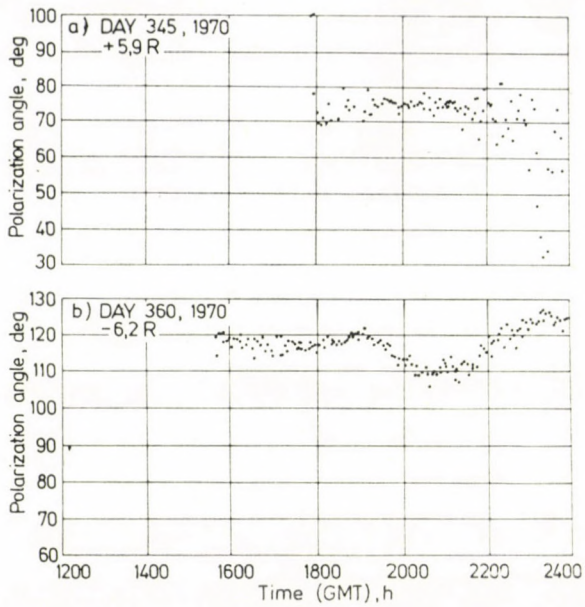

Fig. 2. Polarization transients observed during the solar occultation of Pioneer-9 in 1970 — from Ref. [13]

Sun. We know from earlier work [14—15] that such an inhomogeneity in itself gives rise to anisotropic medium characteristics (ϵ_{INH}, etc.). However, the same investigations indicated that the determination of this "inhomogeneous permittivity", etc. in the way given is almost unmanageably difficult. The exact solution of this problem can be obtained in the way hinted at by the examination of the relationship between the phase and group velocities [16] making use of the results obtained in the course of the eventual geometrica, clarification [17] of the discrepancy between the phase velocity of a plane wave and the Einsteinian velocity addition rule, which gave a unification of particle and wave descriptions on the basis of classical physics.

Until these results become immediately applicable, we may content ourselves by a suitable application of ray tracing method. So we can state the task as follows:

Let us determine for a monochromatic electromagnetic plane wave the relationships governing the passing through permittivity discontinuities and find a way for the description of the entire process of propagation from the transmitter to the receiver, with particular attention paid to the problem of polarization changes. Because of the latter requirement, we cannot neglect that the resultant signal in any individual layer is made up of infinitely many convergent reflexions.

The aim of the present investigation is twofold: to obtain general conclusions on the one hand, and some specialized statements concerning polarization changes on the other.

I. Description of the method

Of the methods described earlier, we will find useful the method of "inhomogeneous basic modes" [18] extended to take account the features appearing due to the presence of step-functions, and the "modified principle of ray tracing" which can be applied for the consideration of the compound effect of infinitely many reflexions for each layer, etc. [14, 19].

So in the present investigation in order to avoid the difficulties due to a continuously changing permittivity $\epsilon_{INH}(\bar{r}) \neq \epsilon_{HOM}(\bar{r})$ [14, 15, 19] we divide the medium into homogeneous layers as it is usual in the method of ray tracing ($\bar{r}$ is the position vector). Then we carry out the calculations with ϵ_{HOM} (denoted by ϵ in what follows) which is well-known for a number of media. We make use of the expression of permittivity of an isotropic gas consisting of neutral, polarizable particles, which is a scalar, i.e.

$$\epsilon = \varepsilon \mathbf{1} = n^2 \mathbf{1}, \tag{1}$$

where n is the refraction index and $n > 1$. Its structure is irrelevant for our purposes. We need the permittivity of the magnetized plasma as well, which is given by a well-known expression if the magnetic field ($_m\bar{B}_0$) is pointing in the $+z$-direction and the $+x$ axis is in the plane spanned by $_m\bar{B}_0$ and the wave propagation vector [20]

$$\epsilon = \begin{bmatrix} \varepsilon_\perp & -j\varepsilon_x & 0 \\ j\varepsilon_x & \varepsilon_\perp & 0 \\ 0 & 0 & \varepsilon_{||} \end{bmatrix}, \tag{2}$$

where the meaning of the individual components is well-known. (2) was chosen for the sake of application for the solar corona [13]. (For *industrial* applications $\epsilon = \mathbf{1}$ and $\mu = \mu$ (ferrite) is the right choice. However, the interested reader working in industry can work out the adaptation of the results for that case). In both (1), and (2) the permittivity $\mu = \mathbf{1}$, and the bianisotropic characteristics $\varkappa = \nu = \mathbf{0}$.

Now we have to determine the signals propagating in each homogeneous layer, the relationship between the layers, and the changes of polarization.

I/1 The method of the inhomogeneous basic modes for a medium change described by a step-function

In what follows we have to determine first of all the electromagnetic wave propagating in a medium divided into homogeneous layers, i.e. described by step-functions or distributions (generalized functions) [26] 1 $[\bar{r}(p, q)]$, where p and q are the parameters determining the surface at which the discontinuity occurs. The quantities we have chose are — according to (1) and (2)

$$\bar{D} = \epsilon \bar{E} \quad \text{and} \quad \bar{B} = \bar{H} \,, \tag{3}$$

where $\bar{E}$ is the electric field $\bar{D}$, is the electric displacement vector, $\bar{B}$ is the magnetic induction, and $\bar{H}$ is the magnetic field. As we know [21], the form of the Maxwell equations can be chosen to be, without any restrictions, the following

$$\begin{aligned} \bar{\nabla} \times \bar{H} &= \varepsilon_0 \frac{\partial \bar{D}}{\partial t} \,, \\ \bar{\nabla} \times \bar{E} &= -\mu_0 \frac{\partial \bar{B}}{\partial t} \,, \\ \bar{\nabla} \bar{B} &= 0 \,, \\ \bar{\nabla} \bar{D} &= 0 \,, \end{aligned} \tag{4}$$

where t denotes time, ε_0 and μ_0 are the permittivity and the permeability of the vacuum, respectively.

Let us assume that the medium is linear — either strictly linear, or linearly dispersive [16] — that it does not move and is stationary in time:

$$\frac{\partial \epsilon}{\partial t} \equiv 0 \,.$$

We do not analyse in general whether a solution will exist at all. A general investigation of the existence of the solution requires the consideration of boundary conditions and of the medium characteristics. In our case because of the form 1 $[\bar{r}(p, q)]$ of the variation the dispersion equation required by Floquet's theory exists, on the homogeneous intervals and so there exists a solution of the form $\bar{F}(\bar{r})e^{j\Phi i}$ — $i = 1, 2, 3$ — [22, 23], where $\bar{F}$ stands for either of the quantities $\bar{E}$, $\bar{D}$, $\bar{B}$, $\bar{H}$. However, the existence of the solution has been proven only for stationary, strictly monochromatic signals of the form [21]

$$\bar{F} = \bar{F}_0 \cdot e^{j(\omega_0 t - \varphi)} \,, \tag{5}$$

where ω_0 is the angular frequency, φ is the phase, $j^2 = -1$ and $\bar{F}_0$ is the amplitude to be interpreted in a general sense. Hence in what follows we are going to seek only *strictly monochromatic*, and consequently stationary, solutions.

Remark: It seems important here to make a comment with possibly far-reaching consequences. It is customary to study time-dependent signals by using the Fourier-transformation and characterize them by the frequency spectrum $S(\omega)$ instead of the time dependence $f(t)$. However, on the basis of [14—19, 21] and the present work we have reached the following conclusion concerning the question of stationarity and time dependence:

A fundamental revision of results obtained for so-called time-varying signals with the help of Fourier-transformation is needed. Namely, *the spectrum* $S(\omega)$, and the Fourier-transformation as a whole, represents the interference pattern as the interference of *stationary* signals having existed for an infinitely long time which is consequently also stationary in space-time, though it is propagating. (This can be shown to be true even for lumped networks.) So it is self-evident that the spectrum obtained for a pulse contains "predictions" with oscillations in front of the pulse, as it is well-known. *Really time-dependent signals* the components of which have not been in existence for an infinitely long time, *can be characterized only by a spectral function* $S(\omega, t)$. This is a fundamental difference of principle and we are going to return to this point in an other article.

It is important to notice that our investigations are valid for stationary solutions. The analysis of signals with a spectral function $S(\omega, t)$ has to be done separately.

Let us attempt to seek the solution (5) by means of the "method of inhomogeneous basic modes" [18] (which we assume the reader to be familiar with), in spite of the fact that we know, because of the occurrence of the distributions 1 $[\bar{r}(p, q)]$, if for no other reason, that for the quantities figuring here $(F_l) \not\subset f$ class of functions to which $f''_{x_1x_2} = f''_{x_2x_1}$ would be true. So we shall have to disregard those results that would follow if this condition were fulfilled. However, it is true [18] independently of this that a solution of the form (5) can be sought as

$$\bar{F} = \sum_{i=1}^{n} \sum_{l=\nu,k} (a_{il}\, e^{-j\varphi d_i}\, \bar{F}_{0il})\, e^{j(\omega_0 t - \varphi_i)} = \sum_{i,l} \bar{F}_{il} \ , \tag{6}$$

where $i = 1, 2, \ldots, n$ denote the individual inhomogeneous basic modes, φ_i are the phase functions of the inhomogeneous basic modes, $1 = \nu$ stands for real, and $1 = k$ for the imaginary part, while the rest of the notations is self-evident.

As it is well-known [18], by definition the inhomogeneous basic modes are given by the system of equations

$$\begin{aligned} \bar{K}_i \times \bar{H}_{il} &= -\omega_0 \varepsilon_0 \boldsymbol{\epsilon} \bar{E}_{il} , \\ \bar{K}_i \times \bar{E}_{il} &= \omega_0 \mu_0 \bar{H}_{il} , \\ \bar{K}_i \boldsymbol{\epsilon} \bar{E}_{il} &= 0 , \\ \bar{K}_i \bar{H}_{il} &= 0 , \end{aligned} \tag{7}$$

taking into account (3) as well, where $\bar{K}_i = \overline{\text{grad}}\ \varphi_i$. The still missing functions are obtained from the system of equations

$$\begin{aligned} &\sum_{i,l} \left[\overline{\text{grad}} (\ln a_{il} - j\varphi_{ai}) \times \bar{H}_{il} + \boldsymbol{\nabla}_{TH0il} \bar{H}_{il} \right] = 0 , \\ &\sum_{i,l} \left[\overline{\text{grad}} (\ln a_{il} - j\varphi_{ai}) \times \bar{E}_{il} + \boldsymbol{\nabla}_{TE0il} \bar{E}_{il} \right] = 0 , \\ &\sum_{i,l} \left[\overline{\text{grad}} (\ln a_{il} - j\varphi_{ai}) \boldsymbol{\epsilon} \bar{E}_{il} + \bar{\nabla}_{\varepsilon} \bar{E}_{il} + \langle \boldsymbol{\nabla}_{\varepsilon il} \bar{E}_{il} \rangle \right] = 0 , \\ &\sum_{i,l} \left[\overline{\text{grad}} (\ln a_{il} - j\varphi_{ai}) \bar{H}_{il} + \langle \boldsymbol{\nabla}_{\mu il} \bar{H}_{il} \rangle \right] = 0 , \end{aligned} \tag{8}$$

which are satisfied independently of (7), and where

$$\boldsymbol{\nabla}_{TH0il} = \begin{bmatrix} 0 & -\dfrac{\partial \ln H_{20il}}{\partial z} & \dfrac{\partial \ln H_{30il}}{\partial y} \\ \dfrac{\partial \ln H_{10il}}{\partial z} & 0 & -\dfrac{\partial \ln H_{30il}}{\partial x} \\ -\dfrac{\partial \ln H_{10il}}{\partial y} & \dfrac{\partial \ln H_{20il}}{\partial x} & 0 \end{bmatrix} ;$$

$\boldsymbol{\nabla}_{TE0il}$ is analogous to $\boldsymbol{\nabla}_{TH0il}$;

$$(\boldsymbol{\nabla}_{\varepsilon il})_{jk} = \varepsilon_{jk} \frac{\partial \ln E_{0il\,k}}{\partial x} ,$$

$$\bar{\nabla}_{\varepsilon} = \bar{\nabla} \boldsymbol{\epsilon} ;$$

$\boldsymbol{\nabla}_{\mu il}$ is analogous to $\boldsymbol{\nabla}_{\varepsilon il}$, since we know that $\boldsymbol{\mu} = \mathbf{1}$;

$$\langle \bar{u} \rangle \equiv u_1 + u_2 + u_3 .$$

However, now we have to disregard the statements that would follow for the automatic fulfilment of the equations corresponding to the div equations using

the condition for the mixed second partial derivatives. We postpone the discussion of these equations until their actual solution.

This way of solution has to be analysed considering that $\epsilon(\bar{r})$ contains, by definition, the dependence $1[\bar{r}(p, q)]$. The usefulness of the method has already been indicated by the analysis of Maxwell's equations in situations described by distributions [24], and by a couple of simple applications [19, 25]. In our case an elementary analysis of (4) immediately shows that Maxwell's equations separate into parts whose space dependences are given by

$$1[\bar{r}(p, q)] \text{ and } \delta[\bar{r}(p, q)] \text{ respectively ,}$$

and just according to the separation shown by (7), and (8). Here $\delta(\bar{r})$ is Dirac's δ-distribution. Furthermore, the system of equations (7) can be further separated, and written down for each individual layer separately, thanks to the properties of $1[\bar{r}(p, q)]$. (8) also becomes separated because of the particular features of $\delta[\bar{r}(p, q)]$, and can be written down for each surface $\bar{r}(p, q)$ separately. (We do not go into the details of the elementary proof which can be found in [26, etc.]). The result is analogous to those found in [24], only in a form specifically suitable for electromagnetic waves.

Additionally, one finds that the inhomogeneous fundamental modes, which are to be determined separately for each layer belonging to a_{il} in the total solution — though it is expedient to indicate it separately — have to be multiplied by the function

$$s_j(\bar{r}) = \{1[\bar{r}(p_{j-1}, q_{j-1})] - 1[\bar{r}(p_j, q_j)]\} \tag{9}$$

for the layer j. This amplitude-coefficient is the same for all the modes of layer j.

Taking all this into consideration, all the possible basic modes occurring in each particular layer can be obtained from the system of equations

$$\begin{aligned} \bar{K}_{ij} \times \bar{H}_{ilj} &= -\omega_0 \varepsilon_0 \epsilon_j \bar{E}_{ilj} , \\ \bar{K}_{ij} \times \bar{E}_{ilj} &= \omega_0 \mu_0 \bar{H}_{ilj} \end{aligned} \tag{(10)}$$

and from the corresponding dispersion equation

$$|\mathbf{K}_{ij} \mathbf{K}_{ij} + k_0^2 \epsilon_j| = 0 , \tag{11}$$

where

$$k_0^2 = \omega_0^2 \varepsilon_0 \mu_0 ;$$

$$\mathbf{K}_{lj} = \begin{bmatrix} 0 & -K_{ij3} & K_{ij2} \\ \mathbf{K}_{ij3} & 0 & -K_{ij1} \\ -K_{ij2} & K_{ij1} & 0 \end{bmatrix} .$$

Now the total solution summing for all components is

$$\bar{F} = \sum_j s_j(\bar{r}) \left[\sum_{i=1}^{n} \sum_{l=v,k} \bar{F}_{il} \right]_j \tag{12}$$

and for every boundary layer we have a system of equations from (8) which for the boundary of j^{th} and $(j+1)^{th}$ layers is

$$\begin{aligned}
&\sum_j^{j+1} \overline{\text{grad}}_{j,j+1}\, s_j(\bar{r}) \times \left[\sum_{i,l} \bar{H}_{il} \right]_j = 0, \\
&\sum_j^{j+1} \overline{\text{grad}}_{j,j+1}\, s_j(\bar{r}) \times \left[\sum_{i,l} \bar{E}_{il} \right]_j = 0, \\
&\sum_j^{j+1} \overline{\text{grad}}_{j,j+1}\, s_j(\bar{r}) \left\{ \epsilon_j \left[\sum_{i,l} \bar{E}_{il} \right]_j \right\} = 0, \\
&\sum_j^{j+1} \overline{\text{grad}}_{j,j+1}\, s_j(\bar{r}) \left[\sum_{i,l} \bar{H}_{il} \right]_j = 0,
\end{aligned} \tag{13}$$

and we are going to see in concrete cases that the second pair of equations in (13) is identical to a pair of components from the first pair of equations. Of course one knows that

$$\overline{\text{grad}}_{j,j+1}\, s_j(\bar{r}) = \pm \delta[\bar{r}(p_j, q_j)]\, \bar{n}_{0j} \,, \tag{9a}$$

where $\bar{n}_{0j}$ is the normal vector of the surface $\bar{r}(p_j, q_j)$. Equations (13) tell us which of the possible basic modes (10) and (11) will actually appear.

We have to proceed as described above when setting out to determine the wave pattern or its elements.

I/2. The principle of "modified ray tracing"

The principle of modified ray tracing is also known from earlier work [14, 19, 25, 27] and we also know that essentially similar methods have been worked out [28, etc.] in the theory of networks (in the theory of waveguides). The principles makes it possible to determine the full resultant wave pattern emerging as a result of infinitely many reflexions in the course of the propagation with the help of the method of ray tracing, and so enables us to carry out exactly — within the limitations of the step-function approximation of ray-tracing — the calculation of the variation of the energy, amplitude, polarization, phase, etc.

The *principle* briefly stated is the following: we follow the propagation of the signal *backwards* from that point of space, *after which certainly no more*

reflexions occur, i.e. from which no signal propagating backwards has to be considered. However, for each layer we take into account all the possible *(compatible* — to be defined later) modes. At the end we compare the initial values for the ingoing point with the initial values calculated from the parameters of the outgoing point, and iterate until the discrepancy does not exceed the limit set by the desired accuracy.

The outline of the *modified* ray tracing program is as follows:

a) We determine the most expedient way of decomposing the medium into layers. The layers can be either homogeneous or quasihomogeneous [21] (or we can even divide into layers according to inhomogeneity and medium flow — which is the "relativistic ray-tracing" [7, 8, 12, 14]).

b) Following the method described in Section I/1 we determine all the possible modes for every layer. Thereafter — with the help of (13) — on the layer boundaries we get the *compatible* fundamental modes and their relationships.

c) Making use of the results of b) we determine the set of all the *compatible* modes for the whole medium corresponding to the starting signal. This gives us the complete system of the energy parts propagating in different ways. (For this point, cf. the definition of *compatibility* and *plane-parallelism* in the given examples !).

d) We follow the signal from the receiver to the transmitter (ingoing point backwards) — i.e. opposite to the direction of the "beam" — from the border of the inhomogeneity where either all the outgoing modes of the wave leave the inhomogeneity for good — i.e. whereafter no further reflexion occurs — or from where the relationship between the forward propagating and reflected signal is determined uniquely (independently of the inhomogeneity) because of some other boundary conditions. In the case of the dispersal of energy the ultimate (relative) relationship between the individual parts is determined by the initial conditions referring to the exciting signal at the ingoing point.

We have to compare the initially given and the calculated parameters for the ingoing point, modify our assumptions for the outgoing signal according to the discrepancy found and repeat cyclically at least the operations of d) until the required accuracy is achieved.

The application of the principle is shown in detail for media characterized by (1), and (2).

I/3. Determination of the polarization changes

In the following we shall not be concerned with polarization rotation (Faraday-effect, etc.) due to well-known effects such as anisotropy, etc. We are going to determine, or at least estimate, only the additional polarization changes due to inhomogeneity, i.e. due to the variation in $s_j(\bar{r})$. For this purpose

we shoose a reference direction (plane) along the surface $\bar{r}(p_j, q_j)$ and refer the direction of the fields $\bar{E}$ and $\bar{H}$ to this. (In our case, because of (1) and (2), it is advantageous to use the field $\bar{H}$). If the cosine of reference angle is β than

$$\Delta P_{j,j+1} = \text{arc cos } \beta_{Hj+1} - \text{arc cos } \beta_{Hj}\,. \tag{14}$$

We shall go into the details of how to choose the reference direction and make the actual calculations later, when dealing with the solution of the problem. In some cases cos ΔP can be obtained by taking a scalar product.

It is *important* and can be verified by elementary means that $\Delta P_{j,j+1}$ occurs additonally to the rotation — e.g. Faraday rotation — usually considered. In the quasi-longitudinal approximation

$$\Omega_F = C_F \int N_m \bar{B}_0 \, \overline{ds}\,. \tag{15}$$

where C_F is a constant, N is the electron density, and $\overline{ds}$ the line element to be measured along the "ray-path". Then the above expression for Ω_F holds as long as the "ray path" is the same for all the propagating modes in the case corresponding to (2). The integrand of (15) does not change when passing through the discontinuity $(j, j+1)$! It is similarly accepted that no polarization-rotation occurs in isotropic media described by (1).

The examination of $\Delta P_{j,j+1}$ unambiguously shows that, on the one hand, *polarization rotation occurs in inhomogeneous isotropic media as well*, and on the other, that expressions that are like (15) but do not take into account (14), accurate as they may be, *will not suffice to describe anisotropic media*. At the same time we are going to give a *unified explanation* of the *W-shaped* polarization-rotation transients the observation of which by Pioneer-6 and 9 has been reported.

II. Analysis of isotropic inhomogemeous media

In what follows we examine the propagation of monochromatic electromagnetic waves in media, divided into homogeneous layers, and characterized by (1)

$$\bar{D} = \varepsilon \bar{E}, \quad \bar{B} = \bar{H}, \tag{16}$$

and where μ_0 and ε_0 have been incorporated into Maxwell's equations. As *usual*, let us use the planewave approximation, which is accurate enough for most practical purposes, so let the excitation be a plane wave. Hence it is expedient to use the Cartesian coordinates (x, y, z).

II/1 Determination of the basic modes

On the basis of (10), (11), and (16) the plane wave forms possible in an individual layer are given by the relationships

$$\begin{aligned} \bar{K}_{ij} \times \bar{H}_{0ilj} &= -\omega_0 \varepsilon_0 \varepsilon_j \bar{E}_{0ilj} \\ \bar{K}_{ij} \times \bar{E}_{0ilj} &= \omega_0 \mu_0 \bar{H}_{0ilj} \end{aligned} \tag{17}$$

and by

$$|\mathbf{K}_{ij}\,\mathbf{K}_{ij} + k_0^2\,\varepsilon_j\,\mathbf{1}| = 0 \tag{18}$$

(18) can be solved in an elementary manner. It entails a restriction *only* on $|\bar{K}_{ij}| \equiv K_{ij}$, but in itself does not fix any direction.

$$K_{ij} = k_0 \sqrt{\varepsilon_j}; \quad \bar{K}_{ij} = k_0 \sqrt{\varepsilon_j}\, \bar{e}_{Kij} \tag{19}$$

and

$$\varphi_{ij} = k_0 \sqrt{\varepsilon_j}(\bar{e}_{Kij}\,\bar{r}) + \varphi_{0ij}; \quad \varphi_{0ij} = \text{constant}|_{ij},$$

where $\partial\varphi_{0ij}/\partial x_l = 0$ and $\bar{e}_{Kij}$ is an arbitrary unit vector.

Thereafter, from (17) we obtain that

$$\begin{aligned} k_0 \sqrt{\varepsilon_j}\, \bar{e}_{Kij} \times \bar{H}_{0ilj} &= -\omega_0 \varepsilon_0 \varepsilon_j\, E_{0ilj} \\ k_0 \sqrt{\varepsilon_j}\, \bar{e}_{Kij} \times \bar{E}_{0ilj} &= \omega_0 \mu_0\, \bar{H}_{0ilj}. \end{aligned}$$

Hence it follows that

$$\frac{E_{0ilj}}{H_{0ilj}} = \sqrt{\frac{\mu_0}{\varepsilon_0 \varepsilon_j}} = Z_{0j} \tag{20}$$

and

$$\begin{aligned} \bar{e}_{Kij} \times \bar{H}_{0ilj} &= -\frac{1}{Z_{0j}}\, \bar{E}_{0ilj}, \\ \bar{e}_{Kij} \times \bar{E}_{0ilj} &= Z_{0j}\, \bar{H}_{0ilj}. \end{aligned} \tag{20a}$$

According to the assumptions (1) we made, let us deal with ideal, non-dissipative media for which ε_j is real. (This is only for the sake of computational convenience; losses could be included in an analogues manner without any significant change in the results, they would merely lead to attenuation). It is useful to introduce the brief notations

$$\bar{E}_{0ilj} = E_{0ilj}\, \bar{e}_{ilj}$$

and

$$\bar{H}_{0ilj} = H_{0ilj}\, \bar{h}_{ilj}, \tag{21}$$

where $\bar{e}$ and $\bar{h}$ are unit vectors.

It is known from here that

$$\bar{E}_{0ilj} \perp \bar{K}_{ij}; \quad \bar{H}_{0ilj} \perp \bar{K}_{ij} \quad \text{and} \quad \bar{E}_{0ilj} \perp \bar{H}_{0ilj}$$

follow, and the same is true for the unit vectors defining their directions: $\bar{e}_K$, $\bar{e}$, $\bar{h}$. Furthermore

$$\bar{e}_{Kij} \times \bar{h}_{ilj} = -\bar{e}_{ilj},$$
$$\bar{e}_{Kij} \times \bar{e}_{ilj} = \bar{h}_{ilj}. \tag{21a}$$

Now we have obtained the possible basic modes. Let us investigate their propagation through the boundary $(j, j+1)$.

II/2. Propagation through the surface $\bar{r}(p_j, q_j)$

Since we use the plane-wave approximation we can only deal with cases, where the boundary surface ($\mathfrak{F}$) can be replaced by the tangent plane over regions the dimensions of which are significantly larger that the wave length (λ), i.e. the surface can be replaced by a plane over areas for which

$$||\mathfrak{F}|| \gg \lambda^2.$$

In previous investigations [16, 17] it has been unambiguously concluded that for a non-plane-wave description one must attack the problem in a fundamentally new manner, and the simple $\exp j(\omega_0 t - \varphi)$ approach is basically plane-oriented. We do not aim at the solution of this problem in the present work.

In what follows we make use of the assumption $\mathfrak{F}_j \to \bar{r}(p_j, q_j) \sim$ plane and of the arrangement shown in Fig. 3. In this case $\bar{r}(p_j, q_j)$ is the coordinate plane $z = 0$ and the parameters p_j, and q_j are identical to the coordinates x and y. This choice is facilitated by the fact that in II/1. no preferred direction was found so the coordinate-system could be chosen to suit our convenience.

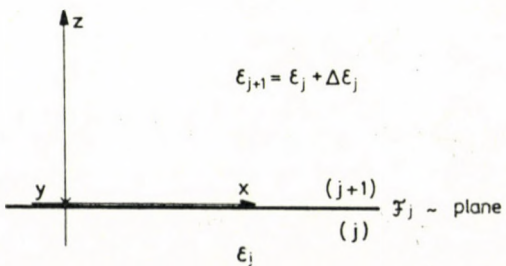

Fig. 3. The choice of the coordinate system for the boundary surface between layers $(j, j+1)$ in isotropic medium

Consequently, (9) becomes

$$s_j(\bar{r}) = s_j(z) = 1(z - z_{j-1}) - 1(z - z_j) \tag{22}$$

which is equivalent to the step-functions

$$s_j(z) = 1 - 1(z - z_j)$$

and

$$s_{j+1}(z) = 1(z - z_j) \tag{22a}$$

only at the interface $(j, j+1)$. It is well-known that from (22a) also follows that

$$\overline{\text{grad}}\, s_j(z) = -\delta(z - z_j)\,\bar{k}$$

and

$$\overline{\text{grad}}\, s_{j+1}(z) = \delta(z - z_j)\,\bar{k}\,. \tag{22b}$$

From the choice of the coordinate system it follows that (13) in this case gives rise to altogether 6 equations. For the sake of brevity we use a formal abbreviation of (6)

$$\bar{F}_j = \sum_i \bar{F}_{aij}\, e^{j(\omega_0 t - \varphi_{ij})} \tag{6a}$$

and in the layer $(j+1)$ we change the indices $i \to k$.
Then after the trivial dividing by the factor $\exp(j\omega_0 t)$ (13) becomes:

$$\delta(z - z_j)\left\{ - \sum_i H_{0ij2} e^{-jk_0 \sqrt{\varepsilon_j}\, \bar{e}_{kij}\, \bar{r}} + \right.$$

$$\left. + \sum_k H_{0kj+12}\, e^{-jk_0 \sqrt{\varepsilon_{Kj+1}}\, \bar{e}_{Kk+1}\, \bar{r}} \right\} = 0\,,$$

$$\delta(z - z_j)\left\{ - \sum_i H_{0ij1}\, e^{-jk_0 \sqrt{\varepsilon_j}\, \bar{e}_{Kij}\, \bar{r}} + \right.$$

$$\left. + \sum_k H_{0kj+11}\, e^{-jk_0 \sqrt{\varepsilon_{j+1}}\, \bar{e}_{Kkj+1}\, \bar{r}} \right\} = 0\,,$$

$$\delta(z - z_j)\left\{ \sum_i Z_{0j} (\bar{e}_{Kij} \times \bar{H}_{0ij+1})_2\, e^{-jk_0 \sqrt{\varepsilon_j}\, \bar{e}_{Kk+1}\, \bar{r}} - \right.$$

$$\left. - \sum_k Z_{0j+1}\, (\bar{e}_{Kkj} \times \bar{H}_{0kj+1})_2\, e^{-jk_0 \sqrt{\varepsilon_{+1}}\, \bar{e}_{Kkj+1}\, \bar{r}} \right\} = 0\,,$$

$$\delta(z - z_j)\left\{ \sum_i Z_{0j}\, (\bar{e}_{Kij} + \bar{H}_{0ij})_1\, e^{-jk_0 \sqrt{\varepsilon_j}\, \bar{e}_{Kij}\, \bar{r}} - \right.$$

$$
\begin{aligned}
&- \sum_k Z_{0j+1}(\bar{e}_{Kkj+1} \times \bar{H}_{0kj+1})_1 e^{-jk_0\sqrt{\varepsilon_{j+1}}\,\bar{e}_{Kkj+1}\bar{r}}\Big\} = 0,\\
\delta(z - z_j)&\Big\{- \sum_i H_{0ij3}\; e^{-jk_0\sqrt{\varepsilon_j}\,\bar{e}_{Kij}\bar{r}} +\\
&+ \sum_k H_{0kj+13} e^{-jk_0\sqrt{\varepsilon_{j+1}}\,\bar{e}_{Kkj+1}\bar{r}}\Big\} = 0,\\
\delta(z - z_j)&\Big\{\varepsilon_j \sum_i Z_{0j}(\bar{e}_{Kij} \times \bar{H}_{0ij})_3 e^{-jk_0\sqrt{\varepsilon_j}\,\bar{e}_{Kij}\bar{r}} -\\
&- \varepsilon_{j+1} \sum_k Z_{0j+1}(\bar{e}_{Kkj+1} \times \bar{H}_{0kj+1})_3\; e^{-jk_0\sqrt{\varepsilon_{j+1}}\,\bar{e}_{Kkj+1}\bar{r}}\Big\} = 0.
\end{aligned}
\tag{23}
$$

In (23), apart from $\exp(-j\bar{K}_{ij}\bar{r})$, each quantity is either constant, or known from II/1, or to be determined. Taking into account the form of the Dirac-distribution

$$
\delta(z - z_j)\, e^{-j\bar{K}_{ij}\bar{r}} \;\rightarrow\; e^{-j(K_{ij1}x + K_{ij2}\,y + K_{ij3}\,z_j)} \tag{23a}
$$

our equations must hold for any pair of values (x, y), i.e. for (p_j, q_j), independently of its choice. Let us suppose that the equations hold in the point (x_0, y_0), or (p_{j0}, q_{j0}); then with a self-evident abbreviation any of the six equations assumes the form

$$
\sum_m \mathfrak{A}_m = 0 \quad \text{or} \quad \sum_{\substack{m \\ m \neq M}} \mathfrak{A}_m = -\mathfrak{A}_M. \tag{24a}
$$

Then at the point $(x_0 + \xi, y_0)$, also with unambiguous notations,

$$
\sum_m \mathfrak{A}_m C_m^{\xi} = 0 \quad \text{or} \quad \sum_{\substack{m \\ m \neq M}} \mathfrak{A}_m C_m^{\xi} = -\mathfrak{A}_M C_M^{\xi} \tag{24b}
$$

results. However, (24a) and (24b) can be brought into a single expression by the substitution of $\mathfrak{A}_M$ and then we obtain the equality

$$
\sum_{\substack{m \\ m \neq M}} \mathfrak{A}_m C_m^{\xi} = \sum_{\substack{m \\ m \neq M}} \mathfrak{A}_m C_M^{\xi} \tag{24c}
$$

(24c) has to hold everywhere along $\mathfrak{F}$. This is the condition of the compatibility of the two sides, i.e. *the general formulation of the law of refraction and reflection* for our case. From (24c) immediately follows that

$$
C_m \equiv C_M \equiv C \tag{24d}
$$

must be true, otherwise a contradiction will result.

II/3. The refraction-reflection laws

From the comparison of (23a) and (24d) we get

$$\sqrt{\varepsilon_j}\, e_{Kij1} = \sqrt{\varepsilon_{j+1}}\, e_{Kkj+11}\,,$$
$$\sqrt{\varepsilon_j}\, e_{Kij2} = \sqrt{\varepsilon_{j+1}}\, e_{Kkj+12} \qquad 25)$$

for any i and k. Let us further have $\bar{e}_k(\cos\alpha, \cos\beta, \cos\gamma)$; then from (25) it follows that for compatible modes *within the same layer*

$\cos\alpha_j$ and $\cos\beta_j$ are identical.

For compatible modes *in the layers j and j* + 1, respectively

$$\sqrt{\varepsilon_j}\cos\alpha_j = \sqrt{\varepsilon_{j+1}}\cos\alpha_{j+1},$$
$$\sqrt{\varepsilon_j}\cos\beta_j = \sqrt{\varepsilon_{j+1}}\cos\beta_{j+1}. \qquad (25a)$$

Hence it is very simple to obtain

$$\frac{\cos\alpha_j}{\cos\beta_j} = \frac{\cos\alpha_{j+1}}{\cos\beta_{j+1}}, \qquad (26a)$$

i.e. the propagation vectors of all the modes are in the same plane containing the z axis. In an isotropic medium the plane $(\bar{k}, \bar{e}_{kij})$ cannot change. At the same time, from (25a) one obtains that

$$\frac{\sin\gamma_{j+1}}{\sin\gamma_j} = \sqrt{\frac{\varepsilon_j}{\varepsilon_{j+1}}} = \frac{n_j}{n_{j+1}} \qquad (26b)$$

being the well-known refraction-reflection law, However, (24d) still permits — while the condition (26b) remains being obeyed — the existence of

$$\cos\alpha_j, \cos\beta_j) \to \pm\cos\gamma_j. \qquad (26c)$$

Hence we have finished the characterization of all the possible *compatible* modes.

Since the plane $(\bar{k}, \bar{e}_{kij})$ cannot change, and we have no restriction on the choice of the coordinate axes x and y, we can assume without loss of generality that the x — axis lies in the plane $(\bar{k}, \bar{e}_{kij})$. Then

$$\bar{K}_{ij} \to (K_{xij},\ 0,\ K_{zij})\,.$$

Because of (25a) all the compatible K_{xij} have the same value, so let us have

$$K_{xij} = \gamma \qquad (27a)$$

and this will be the boundary condition for propagation we henceforth adopt.

So the number of the compatible "inhomogeneous basic modes" possible for each layer is 2, namely

$$\bar{K}_j = \gamma \bar{i} \pm \sqrt{k_0^2 \varepsilon_j - \gamma^2}\, \bar{k} = K_x \bar{i} \pm K_{zj} \bar{k} \,. \tag{27b}$$

Now the meaning of both (20a) and (21a) has been made unambiguous and we can continue the solution of (23).

Remark: Our previous statements are obviously true while we are working with plane-parallel layers. Also, there is no difficulty in making the $+z$ axis of our coordinate system coincide, layer-by-layer, with the normal vector, $j \to j+1$ of the tangent plane of $\mathfrak{F}_j$. Then the vectors have to be transformed, layer-by-layer, with the rotating tensor $\mathbf{T}_{j,j+1}$. This is not problematic, even numerically. However, on contemplating the situation, a few remarks are in order:

a) The actual plane-wave approximation can only be applied without hesitation of $\mathfrak{F}_j \parallel \mathfrak{F}_{j+1}$.

b) The plane-wave approximation can also be justified, if for two consecutive layers the incident planes — (26a) — do not change, or do so only to a negligibly small degree, i.e.

$$\frac{\max\left[\Delta \cos \alpha_{j,j+1};\ \ \Delta \cos \beta_{j,j+11}\right]}{\gamma / k_0 \sqrt{\varepsilon_j}} < \nu, \tag{28a}$$

where ν, which is a sufficiently small number ($\nu \ll 1$), can be deduced from the desired degree of accuracy. Moreover, the approximately infinitely many reflexions, leading to the emergence of the resultant stationary wave pattern for inhomogeneity, must take place over an interval negligible in comparison with the interlayer distance (Δz_{j+1} being the distance between $\mathfrak{F}_j$ and $\mathfrak{F}_{j+1}$). Let us denote by ${}_s\mathfrak{F}_j$ the tangent plane which, by definition, is a good substitute for $\mathfrak{F}_j$, we have

$$\frac{\mathfrak{M}(\Delta z_j \gamma / k_0 \sqrt{\varepsilon_j}) \max\left[|{}_s\bar{r}'_{pj}(p_j, q_j)|;\ |{}_s\bar{r}'_{qj}(p_j, q_j)|\right]}{\Delta z_j} < \nu, \tag{28b}$$

where, as it can be estimated from the reflection attenuation, $\mathfrak{M}$ is a sufficiently large positive number giving a lower bound on the number of reflections within the layer, that have to be considered to achieve the desired accuracy. The expression (28a) is contained in (28b).

c) In case the relationships (28) no longer apply, but the structure and geometry of the inhomogeneity are still sufficiently simple, one must keep in mind that the reflected signals do not add to the wave pattern formed by the incoming signals, but give rise to independent "bundles". Their direction

($\overline{K}_{ij}$) can be traced on the basis of what we said previously. Once we have determined all the compatible modes of the entire pattern to the desired accuracy (achieved when the energy diminishes below a preset threshold value as a result of dividing into layers, and because of the reflections), we are in the position to calculate different features (energetical, etc.) of the *scattered* wave pattern by means of the modified ray tracing. (This is, of course, merely an approximation; an accurate description becomes possible only through a fundamental change in the way of describing the propagation [17]). It is expedient to seek the independent bundles corresponding to different γ's on the "transmitter → → receiver" path, just by tracing $\overline{K}_{ij}$. Generally, in non-plane-parallel layers $\mathfrak{M}_j$ — bundles will be formed from a single bundle. In what follows, modes *belonging to the same* γ will be considered *compatible*, while the modes formed from a single incoming bundle, and belonging *to all the possible* γ*'s*, will be called the *complete system of modes of the wave pattern*.

Eventually, in connection with the relationships (27) we may mention that the signal starts from the source (transmitter) with the parameter

$$\gamma < k_0 \sqrt{\varepsilon_{\text{transmitter}}},$$

where

$$\sqrt{K_{x\,\text{transmitter}}^2 + K_{y\,\text{transmitter}}^2} = \gamma.$$

It will be propagating as long as the inequality

$$\gamma < k_0 \sqrt{\varepsilon_j}$$

holds, and if suffers *total reflection* from the boundary layer — i.e. *there will not exist a compatible mode in* $(j+1)$ — if $\gamma \geq k_0 \sqrt{\varepsilon_{j+1}}$ *becomes true*. The small uncertainty associated with the sign of equality can be avoided in the actual program by a small modification of the situation at the layer boundary. (Metals belong to this class, as well). Hence at the same time it also follows that finally the inhomogeneity will not turn the signal back on a "ray-path" to be described by a "continuous derivative" but in the case $\cos \gamma_j \neq 0$ total reflection will also occur, if the refraction index decreases. Then the ray path will have a *break point*. The conclusion will receive further corroboration later.

II/4. The electric (EM) and magnetic (HM) modes

Making use of the previous results, and of a suitable choice of the coordinate system, we can determine the form of the compatible basic modes valid in this case, which we have already used when solving (23). After some trivial

manipulations, and using the relationships and notations in (19), (20), (21), and (27), the compatible basic modes will be the following

$$E_{0iljx} = \pm \sqrt{1 - \left(\frac{\gamma}{k_0 \sqrt{\varepsilon_j}}\right)^2}\, Z_{0j}\, H_{0iljy},$$

$$E_{0iljz} = -\frac{\gamma}{k_0 \sqrt{\varepsilon_j}} Z_{0j}\, H_{0iljy},$$

$$H_{0iljy} = H_{0iljy} \equiv H_{mly}, \tag{29a}$$

and

$$H_{0iljx} = \mp \sqrt{1 - \left(\frac{\gamma}{k_0 \sqrt{\varepsilon_j}}\right)^2}\, \frac{1}{Z_{0j}} E_{0iljy},$$

$$H_{0iljz} = \frac{\gamma}{k_0 \sqrt{\varepsilon_j}} \frac{1}{Z_{0j}} E_{0iljy},$$

$$E_{0iljy} = E_{0iljy} \equiv Z_{0j}\, \mathcal{H}_{mly}. \tag{29b}$$

Furthermore, we know that

$$e_{Kj1} = \frac{\gamma}{k_0 \sqrt{\varepsilon_j}},\ e_{Kj2} \equiv 0,\ e_{Kij3} = \pm \sqrt{1 - \left(\frac{\gamma}{k_0 \sqrt{\varepsilon_j}}\right)^2} = \pm e_{Kj3}. \tag{29c}$$

If we wish to take the full signal amplitude as an independent variable, then e.g.

$$H_{ml}^2 = H_{mly}^2 + \mathcal{H}_{mly}^2 \tag{29d}$$

and then the second independent parameter appearing along with H_{ml} will be any of the direction cosines from

$$h_{ily}^2 + e_{ily}^2 = 1. \tag{29e}$$

Then it is advantageous to use the direction cosines and the amplitude H_{ml} in (29a), and (29b) as well. Choosing for example's sake, h_{ily}:

$$\begin{aligned} e_{iljx} &= e_{Klj3}\, h_{iljy}, & h_{iljx} &= -e_{Kij3} \sqrt{1 - h_{iljy}^2}, \\ e_{iljy} &= \sqrt{1 - h_{iljy}^2}, & h_{iljy} &= h_{iljy}, \\ e_{iljz} &= -e_{Kjl}\, h_{iljy}, & h_{iljz} &= e_{Kjl} \sqrt{1 - h_{iljy}^2}. \end{aligned} \tag{29f}$$

We find that we have 2—2 *compatible modes, differring* in $\pm$ signs only, *on the two sides of the plane* ${}_s\mathfrak{F}_j$. In our case this amounts to *altogether* 4 modes. This decreases to 2 (on one side only) *in the case of total reflction.* While in the

case *on the side* $(j+1)$ *the signal suffers no further reflection, i.e.* the medium is homogeneous, or when ${}_s\mathfrak{F}_{j+1}$ does not fulfill the condition of plane parallelism, and so the reflected signals generate $\mathfrak{M}$ independently propagating groups of signals (28b), *the number of compatible modes is* 3.

Furthermore, (29a) and (29b) also show that the wavemodes are inclined to separate into two independent parts, one of them depending on (H_{mly}), and the other only on $(Z_{0j}\,\mathcal{H}_{mly})$, i.e. on (E_{mly}). Since because of the inhomogeneity the y-axis will become distinguished also physically as the direction perpendicular to $\bar{K}_j$ and lying in ${}_s\mathfrak{F}_j$, we expect that the signal will really separate into two parts at the inhomogeneity.

Let us call from now on the part depending *on* (H_{mly}) the *magnetic mode*, in short HM, and the part depending *on* (E_{mly}) the *electric mode*, shortly EM. We shall see that the more intricate the medium through which the signal propagates, the clearer the separation of HM and EM is. (Section III).

Let us now expand (23) taking into account (23a), (24), (25), and (29). We immediately notice that the third equation of (23) is identical to the fifth, while its sixth equation to the first, so one of each can be omitted. The equations are written down for the, at most four possible compatible modes:

$$
\begin{aligned}
&-(H_{1vy}+jH_{1ky})\,e^{-j(\varphi_{A1}+K_{zj}z_j)}-(H_{2vy}+jH_{2ky})\,e^{-j(\varphi_{A2}-K_{zj}z_j)}+\\
&+(H_{3vy}+jH_{3ky})\,e^{-j(\varphi_{A3}+K_{zj+1}z_j)}+(H_{4vy}+jH_{4ky})\,e^{-j(\varphi_{A4}-K_{jz+1}z_j)}]=0\,,\\
&-e_{Kj3}\,[(\mathcal{H}_{1vy}+j\mathcal{H}_{1ky})\,e^{-j(\varphi_{A1}+K_{zj}z_j)}-(\mathcal{H}_{2vy}+j\mathcal{H}_{2ky})\,e^{-j(\varphi_{A2}-K_{zj}z_j)}]+\\
&+e_{Kj+13}\,[(\mathcal{H}_{3vy}+j\mathcal{H}_{3ky})\,e^{-j(\varphi_{A3}+K_{zj+1}z_j)}-(\mathcal{H}_{4vy}+j\mathcal{H}_{4ky})\,e^{-j(\varphi_{A4}-K_{zj+1}z_j)}]=0,\\
&-Z_{0j}[(\mathcal{H}_{1vy}+j\mathcal{H}_{1ky})\,e^{-j(\varphi_{A1}+K_{zj}z_j)}+(\mathcal{H}_{2vy}+j\mathcal{H}_{2ky})\,e^{-j(\varphi_{A2}-K_{zj}z_j)}]+\qquad(30)\\
&+Z_{0j+1}[(\mathcal{H}_{3vy}+j\mathcal{H}_{3ky})\,e^{-j(\varphi_{A3}+K_{zj+1}z_j)}+(\mathcal{H}_{4vy}+j\mathcal{H}_{4ky})\,e^{-j(\varphi_{A4}-K_{zj+1}z_j)}]=0,\\
&-e_{Kj3}Z_{0j}[(H_{1vy}+jH_{1ky})\,e^{-j(\varphi_{A1}-K_{zj}z_j)}-(H_{2vy}+jH_{2ky})\,e^{-j(\varphi_{A2}-K_{zj}z_j)}]+\\
&+e_{Kj+13}Z_{0j+1}[(H_{3vy}+jH_{3ky})\,e^{-j(\varphi_{A3}+K_{zj+1}z_j)}-\\
&\qquad-(H_{4vy}+jH_{4ky})\,e^{-j(\varphi_{A4}-K_{zj+1}z_j)}]=0\,,
\end{aligned}
$$

where φ_{Am} is understood to contain both φ_{ai} and φ_{0ij}; from the indices $m=1,\ \ldots,4$, 1 and 2 refer to the compatible modes in the j^{th} while 3, and 4 to those in the $(j+1)^{th}$ layer (k). We can see that at the layer boundary, i.e. in (30)

$$\varphi_{Am}\pm K_{zj}z_j=\text{constant}|_m=\varphi_{0m}\,, \tag{31}$$

i.e. it can be handled as a constant phase. From a glance at (30) it follows in an elementary manner that (30) gives only *the deviation of* φ_{0m} *from the* other φ_{0m} values; the total value has to be calculated layer-by-layer from the initial value of phase, applying (31).

It is an *important consequence* that the boundary surface ${}_s\mathfrak{F}_j$ (the $z = 0$ coordinate plane in our case) as an *inhomogneity*, *separates the wave into EM and HM modes* in a way analogous to anisotropic media! (Cf ϵ_{INH} in [15, 19], and also Section III of the present work). (30) falls into two entirely independent parts. The relationship of the two modes *within the homogeneous regions* can be obtained from (17), and (13) as

$$\overline{K}_{EMj} \equiv \overline{K}_{HMj} \quad \text{and} \quad \varphi_{AmEM} \equiv \varphi_{AmHM}.$$

However, the two pairs of equations for $\overline{H}$, and $\overline{\mathcal{H}}$ respectively, are different which proves that *within the region of inhomogeneity itself*

$$\overline{K}_{EM\,inh} \neq \overline{K}_{HM\,inh}, \quad \text{i.e.} \quad \varepsilon_{HOM}\mathbf{1} \neq \epsilon_{INH},$$

which, in point of fact, we have already verified [15, 19]. Furthermore, from (30) it is also *obvious* that $-e_{Kj3}-$ both *EM* and *HM* propagation depend on the "incidence angle" measured from the normal vector of the surface ${}_s\mathfrak{F}_j$.

Statement: From the previous discussion it transpires that there is no way of obtaining a correct result for propagation in an inhomogeneous medium assuming $\varepsilon(\overline{r})\mathbf{1}$, since the *essence of inhomogeneity* is the difference of *EM* and *HM* propagations, to be described by ϵ_{INH}.

There is an exception though, when for some direction of propagation from (29a) and (29b) we obtain $\overline{K}_{EM\,inh} = \overline{K}_{HM\,inh}$, i.e. the inhomogeneity appears isotropic [31]. Such is the case of normal incidence (parallel to-the z-axis), or the case of total reflection for both modes (metals, etc.).

Consequently, for non-ray-tracing-like description (it is understood that the modified version is better), for analytical investigations, etc., one has to give (as we shall do in another paper) the possible phenomenological $\epsilon_{INH's}$ (μ_{INH}, etc.). It may happen that only a non-linear description is feasible [19], or it may be that a linear one will suffice. Now we are going to see examples for the solution.

II/5. Emergence from inhomogeneous medium; the three-mode case

By definition, a signal leaving the inhomogeneous medium does not undergo any further reflections. So in (30) we choose

$$H_{4vy} = H_{4ky} = \mathcal{H}_{4vy} = \mathcal{H}_{4ky} = 0 \tag{32a}$$

with the exclusion of the directionswise correct, coherent, simultaneous excitation corresponding to $(m = 4)$. Since in (30) only relative phase matter, without loss of generality we can assume

$$H_{3ky} = \mathcal{H}_{3ky} = 0, \quad \varphi_{03} = 0, \quad H_{3vy} = H_0 \quad \text{and} \quad \mathcal{H}_{3vy} = \mathcal{H}_0. \tag{32b}$$

(With this we have fixed the moment $t = 0$ relative to the wave pattern). The from (30)

$$
\begin{aligned}
&-(H_{1vy} + jH_{1ky})\, e^{-j\varphi_{01}} - (H_{2vy} + jH_{2ky})\, e^{-j\varphi_{02}} + H_0 = 0 \\
&- Z_{0j}\, e_{Kj3}\,(H_{1vy} + jH_{1ky})\, e^{-j\varphi_{01}} + Z_{0j}\, e_{Kj3}(H_{2vy} + jH_{2ky})\, e^{j\varphi_{02}} + \\
&\qquad + Z_{0j+1}\, e_{Kj+1}\, H_0 = 0 \\
&e_{Kj3}\,(\mathcal{H}_{1vy} + j\mathcal{H}_{1ky})\, e^{-j\varphi_{01}} - e_{Kj3}(\mathcal{H}_{2vy} + \mathcal{H}_{2ky})\, e^{-j\varphi_{02}} - e_{Kj+13}\,\mathcal{H}_0 = 0 \\
&-Z_{0j}\,(\mathcal{H}_{1vy} + j\mathcal{H}_{1ky})\, e^{-j\varphi_{01}} - Z_{0j}\,(\mathcal{H}_{2vy} + j\mathcal{H}_{2ky})\, e^{-j\varphi_{02}} + Z_{0j+1}\,\mathcal{H}_0 = 0 \quad (33)
\end{aligned}
$$

follows. Because of (32b), (33) refers to the case when the appearing signal is polarized in plane. This means restriction to a special case, but the result will still enable us to carry out a simple analysis of polarization changes. The general case of non-planepolarized signals will be examined in the more general four-mode case.

From (33) it can be immediately seen that

$$H_{1ky} = H_{2ky} = \mathcal{H}_{1ky} = \mathcal{H}_{2ky} = 0$$

and

$$\varphi_{01} = \varphi_{02} = 0\,, \tag{34}$$

i.e. in this *special case* no phase discontinuity, or turning a plane-polarized signal into circularly polarized one, occurs.

Hence

$$
\begin{aligned}
&H_{1vy} + H_{2vy} - H_0 = 0 \\
&Z_{0j}\, e_{Kj3}\, H_{1vy} - Z_{0j}\, e_{Kj3}\, H_{2vy} - Z_{0j+1}\, e_{Kj+1\,3}\, H_0 = 0. \qquad (35a)
\end{aligned}
$$

and

$$
\begin{aligned}
&e_{Kj3}\,\mathcal{H}_{1vy} - e_{Kj3}\,\mathcal{H}_{2vy} - e_{Kj+1\ 3}\,\mathcal{H}_0 = 0 \\
&Z_{0j}\,\mathcal{H}_{1vy} + Z_{0j}\,\mathcal{H}_{2vy} - Z_{0j+1}\,\mathcal{H}_0 = 0\,. \qquad (35b)
\end{aligned}
$$

From (35) immediately follows that assuming $e_{Kj3} = e_{Kj+1\,3} = 0$ the relationships become indefinite and the problem cannot be solved. But such a case does not exist, since this assumption contradicts (27a). On the one hand this supports the remark we made in II/3/c. On the other hand, we see that the assumption of an infinite plane excitation perpendicularly to ${}_s\mathfrak{F}_j$ can never be justified. We can excite only one layer in such a way ($e_{Kj3} = 0$), and the other compatible signals, if they exist at all, have to be deduced. Hence

$$H_0 = \frac{2}{1 + \dfrac{Z_{0j+1}\, e_{Kj+13}}{Z_{0j}\, e_{K2}}}\, H_{1vy} = \frac{2}{r_{y+}}\, H_{1vy}\,,$$

$$H_{2vy} = \frac{Z_{0j}\, e_{Kj3} - Z_{0j+1}\, e_{Kj+1\,3}}{Z_{0j}\, e_{Kj3} + Z_{0j+1}\, e_{Kj+1\,3}} H_{1vy},$$

$$\mathcal{H}_0 = \frac{2}{\dfrac{Z_{0j+1}}{Z_{0j}} + \dfrac{e_{Kj+1\,3}}{e_{Kj3}}} \mathcal{H}_{1vy} = \frac{2}{r_{x+}} H_{yv1},$$

$$\mathcal{H}_{2vy} = \frac{Z_{0j+1}\, e_{Kj3} - Z_{0j}\, e_{Kj+1\,3}}{Z_{0j+1}\, e_{Nj3} + Z_{0j}\, e_{Kj+13}} \mathcal{H}_{1vy}\,. \tag{36}$$

From (36) it can be directly seen that apart from a few special cases, such as $e_{Kj3} = e_{Kj+1,3} = 1$ (normal incidence), etc., $r_{x+} \neq r_{y+}$. So, ***in general***, the two components determining the resultant polarization — ***EM and HM — have different reflection dampings***, i.e. in the course of propagation ***the polarization of the propagating signal changes.***

One must separately examine the case $r_{x+} = r_{y+}$, when there is no polarization change. The corresponding requirement from (36) is

$$Z_{0j} = Z_{0j+1}\,,$$

i.e. for "matched" layers there is no polarization rotation. In general, this requirement cannot be satisfied.

The validity of the results can be verified by writing down the equation

$$\oint_{A_{dzj}} (\bar{E} \times \bar{H})\, d\bar{A} = 0 \tag{37}$$

for a closed surface of infinitesimal width $\pm dz_j$ on ${}_s\mathfrak{F}_j$; in our case (37) is seen to be satisfied.

II/6. Propagation through an arbitrary laysr: the four-mode case

In order to see an application of the modified principle of ray tracing for *compatible* modes — after having clarified all other, even if only slightly non-routine, parts of ray tracing (plane-parallelism, energy dispersion, general features of program-building, the preliminary sorting out of all the compatible scattered mode-groups in the "transmitter-receiver" direction on the basis of (27a), etc.) — let us now *make a step back from the layer* ${}_s\mathfrak{F}^f$ *to* ${}_s\mathfrak{F}_{j-1}$.

Modes 3 and 4 for this case are already given as modes 1 and 2 of the previous case; the unknowns are modes 1 and 2 for the layer ${}_s\mathfrak{F}_{j-1}$. The layer width Δz_j, i.e. the distance between the "plane-parallel" ${}_s\mathfrak{F}_j$ and ${}_s\mathfrak{F}_{j-1}$, will be a new parameter. Applying the previous results without modification,

${}_s\mathfrak{F}_{j-1}$ is identical to the plane $z = -\Delta z_j$. The already known permittivity values are

$$\varepsilon_j = \varepsilon_{j-1} + \Delta\varepsilon_{j-1}\,\mathbf{1}\,(z + \Delta z_j),$$

$$\varepsilon_{j+1} = [\varepsilon_{j-1} + \Delta\varepsilon_{j-1}\,\mathbf{1}\,(z + \Delta z_j)] + \Delta\varepsilon_j\,\mathbf{1}\,(z).$$

However, from one point of view the previous results need generalization. As we are going to see, in general the phase changes of EM and HM will not be identical. So it was a special restriction that the EM and HM phases of the signal eventually leaving the inhomogeneity be identical — (32b). Thereforer we generalize our results from the previous condition $\mathcal{H}_{3vy} = \mathcal{H}_0$ to another one referred to ${}_s\mathfrak{F}_j$

$$\mathcal{H}_{3vy} + j\mathcal{H}_{3ky} = \mathcal{H}_0\, e^{j\varphi_{\mathcal{H}0}},$$

(36) *still remains valid*, but has to be augmented with

$$\varphi_{\mathcal{H}1} = \varphi_{\mathcal{H}2} = \varphi_{\mathcal{H}0}. \tag{36a}$$

(In a similar way φ_{H0}, etc. and can be brought in).

Now let us write down (30) for this ${}_s\mathfrak{F}_{j-1}$ case. After elementary steps in calculation one finds it expedient to intriduce the notations

$$R^{+}_{HMj} = 1 + \frac{Z_{0j+1}\, e_{Kj+1\,3}}{Z_{0j}\, e_{Kj3}},$$

$$R^{-}_{HMj} = 1 - \frac{Z_{0j+1}\, e_{Kj+1\,3}}{Z_{0j}\, e_{Kj3}}, \tag{37}$$

from which

$$R^{+}_{HMj} + R^{-}_{HMj} = 2.$$

Furthermore

$$R^{+}_{EMj} = \frac{Z_{0j+1}}{Z_{0j}} + \frac{e_{Kj+1\,3}}{e_{Kj3}},$$

$$R^{-}_{EMj} = \frac{Z_{0j+1}}{Z_{0j}} - \frac{e_{Kj+1\,3}}{e_{Kj3}}, \tag{38}$$

from where we get

$$R^{+}_{EMj} + R^{-}_{EMj} = 2\,\frac{Z_{0j+1}}{Z_{0j}}.$$

Making use of (37), and (38), (30) can be rewritten so as to assume the following analogous forms

$$H_1\, e^{j\varphi_{H1}} = \frac{R^{+}_{HMj-1}}{2}\, H_3 + \frac{R^{-}_{HMj-1}}{2}\, H_4\, e^{-j2K_{zj}\,\Delta z_j}$$

$$\mathcal{H}_1\, e^{j\varphi_{\mathcal{H}1}} = \frac{R^{+}_{EMj-1}}{2}\, \mathcal{H}_3\, e^{j\varphi_{\mathcal{H}3}} + \frac{R^{-}_{EMj-1}}{2}\, \mathcal{H}_4\, e^{j(\varphi_{\mathcal{H}4} - 2K_{zj}\,\Delta z_j)} \quad \text{etc.}$$

where, for instance

$$H_3 = \frac{R^+_{HMj}}{2} H_0, \quad H_4 = \frac{R^-_{HMj}}{2} H_0, \quad \text{etc.}$$

In this way we can obtain all the quantities we are looking for, which are the following, taking the phase of H_3 for reference:

$$H_1 = +\left[\left(\frac{R^+_{HMj-1}}{2} H_3 + \frac{R^-_{HMj-1}}{2} H_4 \cos 2K_{zj}\Delta z_j\right)^2 + \right.$$
$$\left. + \left(\frac{R^-_{HMj-1}}{2} H_4 \sin 2K_{zj}\Delta z_j\right)^2\right]^{1/2},$$

$$\varphi_{H1} = \arctan\left[\frac{-\frac{R_{HMj-1}}{2} H_4 \sin 2K_{zj}\Delta z_j}{\frac{R^+_{HMj-1}}{2} H_3 + \frac{R^-_{HMj-1}}{2} H_4 \cos 2K_{zj}\Delta z_j}\right],$$

$$H_2 = +\left[\left(\frac{R^+_{HMj-1}}{2} H_4 + \frac{R^-_{HMj-1}}{2} H_3 \cos 2K_{zj}\Delta z_j\right)^2 + \right.$$
$$\left. + \left(\frac{R^-_{HMj-1}}{2} H_3 \sin 2K_{zj}\Delta z_j\right)^2\right]^{1/2},$$

$$\varphi_{H2} = \arctan\left[\frac{+\frac{R_{HMj-1}}{2} H_3 \sin 2K_{zj}\Delta z_j}{\frac{R^+_{HMj-1}}{2} H_4 + \frac{R^-_{HMj-1}}{2} H_3 \cos 2K_{zj}\Delta z_j}\right], \qquad (39)$$

$$\mathcal{H}_1 = +\left[\left(\frac{R^+_{EMj-1}}{2} \mathcal{H}_3 \cos\varphi_{\mathcal{H}3} + \frac{R^-_{EMj-1}}{2} \mathcal{H}_4 \cos(\varphi_{\mathcal{H}4} - 2K_{zj}\Delta z_j)\right)^2 + \right.$$
$$\left. + \left(\frac{R^+_{EMj-1}}{2} \mathcal{H}_3 \sin\varphi_{\mathcal{H}3} + \frac{R^-_{EMj-1}}{2} \mathcal{H}_4 \sin(\varphi_{\mathcal{H}4} - 2K_{zj}\Delta z_j)\right)^2\right]^{1/2},$$

$$\varphi_{\mathcal{H}1} = \arctan\left[\frac{\frac{R^+_{EMj-1}}{2} \mathcal{H}_3 \sin\varphi_{\mathcal{H}3} + \frac{R^-_{EMj-1}}{2} \mathcal{H}_4 \sin(\varphi_{\mathcal{H}4} - 2K_{zj}\Delta z_j)}{\frac{R^+_{EMj-1}}{2} \mathcal{H}_3 \cos\varphi_{\mathcal{H}3} + \frac{R_{EMj-1}}{2} \mathcal{H}_4 \cos(\varphi_{\mathcal{H}4} - 2K_{zj}\Delta z_j)}\right],$$

$$\mathcal{H}_2 = +\left[\left(\frac{R^+_{EMj-1}}{2} \mathcal{H}_4 \cos\varphi_{\mathcal{H}4} + \frac{R^-_{EMj-1}}{2} \mathcal{H}_3 \cos(\varphi_{\mathcal{H}3} + 2K_{zj}\Delta z_j)\right)^2 + \right.$$
$$\left. + \left(\frac{R^+_{EMj-1}}{2} \mathcal{H}_4 \sin\varphi_{\mathcal{H}4} + \frac{R^-_{EMj-1}}{2} \mathcal{H}_3 \sin(\varphi_{\mathcal{H}3} + 2K_{zj}\Delta z_j)\right)^2\right]^{1/2}$$

$$\varphi_{\mathcal{H}2} = \arctan \left[\frac{\frac{R^{+}_{EMj-1}}{2} \mathcal{H}_4 \sin \varphi_{\mathcal{H}4} + \frac{R^{-}_{EMj-1}}{2} \mathcal{H}_3 \sin (\varphi_{\mathcal{H}3} + 2K_{zj} \Delta z_j)}{\frac{R^{+}_{EMj-1}}{2} \mathcal{H}_4 \cos \varphi_{\mathcal{H}4} + \frac{R^{-}_{EMj-1}}{2} \mathcal{H}_3 \cos (\varphi_{\mathcal{H}3} + 2K_{zj} \Delta z_j)} \right] .$$

At the following layer boundary — $_{s}\mathfrak{F}_{j-2}$ — the phases of H_3 and H_4 will no longer be identical. However, this can evidently be taken into account in (39). One can take all the phases different from zero, if necessary.

So the complete solution on the interval $z_{j-2} \leq z \leq z_{j-1}$ is

$$\mathcal{H}_1 = \bar{e}_{\mathcal{H}1} \mathcal{H}_1 e^{j\varphi_{\mathcal{H}1}} e^{j[\omega_s t - \gamma x - K_{zj-1}(z - z_{j-1})]} \cdot [1(z - z_{j-2}) - 1(z - z_{j-1})] , \quad (40)$$

where $\bar{e}_{\mathcal{H}1}$ can be obtained from (27b) and (29f). The other modes can be given in an analogous way. (39) can be checked on the basis of (37), and turns out to be correct. On the basis of the previous discussion, a *"modified ray tracing program" can be constructed*; we will not go into details here.

The only remaining task is the investigation of the polarization changes.

II/7. *The analysis of the polarization changes*

On the basis of the foregoing we are now in the position to study the polarization change ΔP given by (14).

For the investigation we choose the following *reference*:

In view of (1) we can assert that in case of accurate orientation our measuring aerial turns in the direction of $\bar{K}_{\text{receiver}}$. So it is both expedient and realistic from the point of view of measurement technology to choose as a reference plane the ($\bar{K}_{\text{receiver}}$, y-axis) plane, or in an arbitrary point of space the ($\bar{K}$, y-axis) plane.

So the direction of 0° polarization in the plane perpendicular to $\bar{K}$ is the direction of the line $(0, y, 0)$ — or, generally, the direction given by (x_0, y, z_0). $+90°$ will belong to the line of intersection of the self same plane with plane $(-x, 0, +z)$. The measured angle of polarization is then

$$P = \sphericalangle (\bar{H}_m, \; y - \text{axis}) . \quad (41)$$

This measurement instruction gives at the same time the form of ΔP-(14)-valid in the present case which is

$$\Delta P = \arccos h_{3vy} - \arccos h_{1vy} \quad (42$$

for the *plane-polarized* case (II/5). ΔP is the polarization change occurring along the direction of propagation, including the correct sign factor. In case

of *elliptic* polarization (41) cannot be so simply rewritten, so we shall stick first to the basic case of plane polarization.

a) *The case of polarization in plane*(evaluation of II/5)

$\cos \Delta P$ can be immediately given on the basis of (42), with the help of some of the previous results. From (36), (37), and (38)

$$\cos \Delta P = h_{1vy}\, h_0 + \sqrt{1 - h_{1vy}^2}\,\sqrt{1 - h_0^2} = \\ = \frac{R_{HMj}^{+}\, H_0}{\sqrt{R_{HMj}^{+2}\, H_0^2 + R_{EMj}^{+2}\, \mathcal{H}_0^2}} \cdot \frac{H_0}{\sqrt{H_0^2 + \mathcal{H}_0^2}} + \\ + \frac{R_{EMj}^{+}\, \mathcal{H}_0}{\sqrt{R_{HMj}^{+2}\, H_0^2 + R_{EMj}^{+2}\, \mathcal{H}_0^2}} \cdot \frac{\mathcal{H}_0}{\sqrt{H_0^2 + \mathcal{H}_0^2}}\,, \tag{43}$$

which after elementary manipulation becomes

$$\operatorname{tg} \Delta P = \frac{\mathfrak{X}\sqrt{1 - h_0^2}}{\mathfrak{X} h_0 + (Z_{0j}\, e_{Kj+1\,3} + Z_{0j+1}\, e_{Kj3})} \tag{44}$$

where

$$\mathfrak{X} = h_0 (Z_{0j} - Z_{0j+1})\,(e_{Kj3} - e_{Kj+13}).$$

From (44) it can be concluded that *generally*

$$\Delta P \neq 0° \tag{45}$$

The conditions of *getting* $\Delta P = 0°$

a) $h_0 = 1$, i.e. $\mathcal{H}_0 = 0$;

b) $h_0 = 0$, i.e. $H_0 = 0$; (46)

c) $e_{Kj3} = e_{Kj+13}$, which can be true only if $e_{Kj3} = e_{Kj+13} = 1$, i.e. in the case of incidence (in the direction of $+z$);

d) $Z_{0j} = Z_{0j+1}$, which generally cannot be fulfilled.

We have already met case c), and also investigated d). Cases a) and b) are pretty easy on the basis of previous results, but we are going to briefly return to them later.

For the investigation of ΔP (including its sign) in the direction of propagation we make use of $\sin \Delta P$, the form of which can be obtained in an elementary manner, analogously to previous derivations, and its value, with the notations of (36), is

$$\sin \Delta P = \frac{H_{1vy}\, \mathcal{H}_{1vy}}{r_{x+}\, r_{y+} + \sqrt{(H_{1vy}^2 + \mathcal{H}_{1vy}^2)\left(\dfrac{H_{1vy}^2}{r_{y+}^2} + \dfrac{\mathcal{H}_{1vy}^2}{r_{x+}^2}\right)}}\,(r_{y+} - r_{x+}). \tag{47}$$

To evaluate ΔP we have to examine $(r_{y+} - r_{x+})$, which is

$$(r_{y+} - r_{x+}) = \frac{(Z_{0j} - Z_{0j+1})\,(e_{Kj3} - e_{Kj+1\,3})}{z_{0j}\,e_{Kj3}} \,. \tag{48}$$

It is important to recall that in (29c), by definition, $e_{Kj3} > 0$, i.e. it does not contain sign. From (48) it can be directly seen that

$$\begin{aligned} &\text{in the case of } \Delta\varepsilon_j > 0 \qquad && (r_{y+} - r_{x+}) < 0, \\ &\text{and in the case of } \Delta\varepsilon_j < 0 \qquad && (r_{y+} - r_{x+}) < 0. \end{aligned} \tag{48a}$$

So in our case the *electric* mode *is* under any circumstances *more strongly reflected than the magnetic* mode.

$$\frac{H_0}{H_{1vy}} \geqq \frac{\mathcal{H}_0}{\mathcal{H}_{1vy}} \tag{49}$$

and the sign of equality applies only in the four cases enumerated in (46). In the energy, and in the signal propagating further, the HM component is "enriched".

Now in (47), taking into account the possible signs of H_{1vy} and $\mathcal{H}_{1vy}$, we obtain that

$$\Delta P \gtrless 0$$

according to the sign of approach to the directions of 0°, or 180°, respectively. This is determined *exclusively* by the *polarization at entering* the inhomogeneity, and thereafter in the course of propagation ΔP approaches this direction, but *it does not change sign*! (Quasi-plane-parallel case). — A separate analysis has to be done for the non-plane-parallel case, but if for instance the $+y$ direction does not change (a plasma cloud can always be modelled this way — see Fig. 4), then the $+z$ direction change leads to scattering only, and does not alter the character of change of ΔP.

By a similar analysis it can be seen that in the case of the Sun [13] e.g. the sizeable inhomogeneities which cannot be represented by ${}_s\mathcal{F}_j$ perpendicularly to the plane of the ecliptic, in the case of the Pioneer experiments lead to the scattering of the signal out of the plane of the ecliptic (very strong fading, and disruption of communication for shorter or longer time).

So in the case we wish to interpret we can *assume* that the *inhomogeneities can be characterized by a y-axis perpendicular to the plane of the ecliptic*, and so our results are applicable.

Interpretation:

Even in the simplest case possible (!) — that of a single inhomogeneity $\Delta\varepsilon$ — it is self-evident on the basis of our results that when the signal reaches the

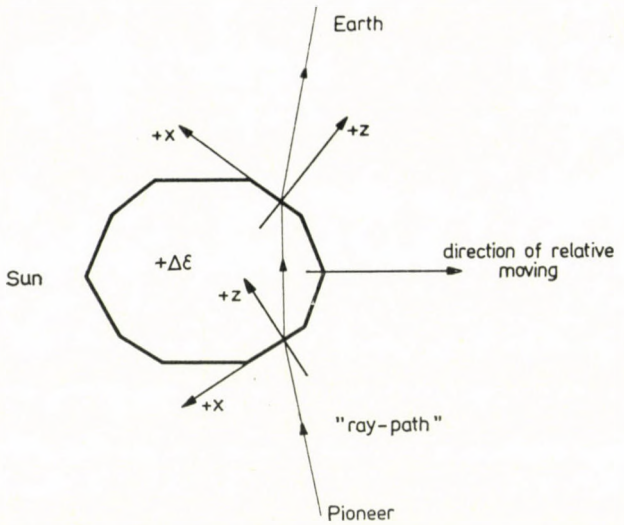

Fig. 4. A simple model of inhomogeneity for the investigation of the propagation of electromagnetic waves

inhomogeneity, e_{Kj3} is the smallest and ΔP is the largest. After this steep "jump" ΔP returns, depending on the geometry of the "front" of the inhomogeneity, to zero (!) since the centre of the inhomogeneity belongs to case c) of (46), then it again changes in the same sense as before. After the inhomogeneity leaves the beam-path, this "transient" ceases.

Then for very small values of $\Delta\varepsilon_j/\varepsilon_j$

$$\Delta P \sim 2\left(\frac{K_x}{K_z}\right)^2 \sin\alpha_0 \cos\alpha_0 \left(\frac{\Delta\varepsilon}{4\varepsilon}\right)^2,$$

where $\alpha_0 = \arccos h_0$ and $\Delta P_{\text{total}} \sim N_r \Delta P$, where N_r is the number of layers.

If, for example,

$$\frac{\Delta\varepsilon}{4\varepsilon} \sim 10^{-2} \div 10^{-4}$$

and

$$\operatorname{arc\,tg}\frac{K_x}{K_z} \sim 45^\circ \div 85^\circ,$$

then ΔP lies in the intervals

$$\Delta P \sim (0{,}6^\circ \div 0{,}006^\circ) \quad \text{and} \quad (1^\circ \div 47^\circ),$$

respectively, for passing through a single discontinuity. (For the upper limit 47° the approximate relationship is rather inaccurate). So the *occasionally*

unidirectional character and the size of ΔP can be explained even in the framework of the elementary analysis assuming isotropy.

However, *in an isotropic medium "M" and "W" shapes would be equally possible*, while in the experiments only "*W*" was found.

It is also *important* that for small, gentle inhomogeneities — whose character is very dissimilar to the one described by $1[\bar{r}(p, q)]$ — ΔP can be very small.

b) The case of *elliptical polarization* — the evaluation of II/6.

Let us define the plane of polarization as the plane containing the principal axis of the ellipse. It is given by the direction of the maximum of modulus of the space-and time-varying vector produced by the algebraic H and $\mathcal{H}$. At a given point of space — (0, 0, 0) or anything else — the analysis is identical to that of

$$(\bar{H}_1 \, e^{j\varphi}_{H1} + \bar{H}_1 \, e^{j\varphi}_{\mathcal{H}1}) \, e^{j\omega_0 t} = \bar{H}_{1\,\mathrm{tot}}.$$

Hence

$$H^2_{1\,\mathrm{tot}} = H^2_1 \sin^2(\omega_0 t + \varphi_{H1}) + \mathcal{H}^2_1 \sin^2(\omega_0 t + \varphi_{\mathcal{H}1})$$

and the maximum with respect to time — since the position is *given* — is found by solving the equation

$$\frac{\partial H^2_{1\,\mathrm{tot}}}{\partial t} = 0.$$

Introducing the notation

$$\Phi = \mathrm{arc\ tg} \frac{H^2_1 \sin 2\varphi_{H1} + \mathcal{H}^2_1 \sin 2\varphi_{\mathcal{H}1}}{H^2_1 \cos 2\varphi_{H1} + \mathcal{H}^2_1 \cos 2\varphi_{\mathcal{H}1}}$$

the *first maximum* is found at

$$t_M = \frac{1}{2\omega_0}(-\Phi + \pi); \quad t_{Mn} = \frac{1}{2\omega_0}(-\Phi \pm n\pi), \tag{50}$$

where n is a positive integer. In what follows we study how the polarization changes from the value taken at time $t = t_M$.

$$\sin \Delta P = \frac{\mathcal{H}_1(t_{M1})}{\sqrt{H^2_1(t_{M1}) + \mathcal{H}^2_1(t_{M1})}} \frac{H_3(t_{M3})}{\sqrt{H^2_3(t_{M3}) + \mathcal{H}^2_3(t_{M3})}} -$$

$$- \frac{H_1(t_{M1})}{\sqrt{H^2_1(t_{M1}) + \mathcal{H}^2_1(t_{M1})}} \frac{\mathcal{H}_3(t_{M3})}{\sqrt{H^2_3(t_{M3}) + \mathcal{H}^2_3(t_{M3})}} \tag{51}$$

$$\sin \Delta P = f^{-1}(H_i, \mathcal{H}_i, t_{Mi}) \, [\mathcal{H}_1(t_{M1}) \, H_3(t_{M3}) - H_1(t_{M1}) \, \mathcal{H}_3(t_{M3})]$$

(51) can be further discussed analytically on the basis of the foregoing; or built into the computer program as it stands. We shall not discuss it in detail, mainly in view of (48), since it can be seen from (39) that the tendency of *enrichment in HM* will persist in the course of the propagation.

REFERENCES

1. StJohn C. E.: Evidence for the Gravitational Displacement of Lines in the Solar Spectrum predicted by Einstein's Theory; *Astrophys. J.*, **57,** (1928), 195
2. Adam, M. G.: Interferometric Measurements of Solar Wavelength and an Investigation of the Einstein Gravitational Displacement; *Mon. Not. Roy. Astron. Soc.*, **108,** (1948) 446
3. Higgs, L. A.: The Solar Red-Shift; *Mon. Not. Roy. Astron. Soc.*, **121,** (1960), 421
4. Sadeh, D.—Knowles, S. H.—Yaplee, B. S.: Search for a Frequency Shift of the 21 centimeter Line from Taurus-A Near Occultation by the Sun; *Science*, **159,** (1968), 307
5. Merat, P.—Pecker, J. C.—Vigier, J. P.: Possibile Interpretation at an Anomalous Redshift Observed on the 2292 MHz Line Emitted by Pioneer-6 in the Close Vicinity of the Solar Limb; *Astr. Astrophys.*, **30,** (1974), 167
6. Jupiter Occultation Anomalies Cost Doubt on its Accuracy; *Aviat. Week & Space Techn.*, **101,** (1974) No. 25, 30
7. Ferencz, Cs.—Tarcsai, Gy.: A New Experimental Possibility of Investigating the Solar Corona: Frequency Measurements on Radio Sources when Occultated by the Sun; *Planet. Space Sci.*, **18,** (1970) 1213
8. Ferencz, Cs.—Tarcsai, Gy.: Theoretical Explanation of the Solar Limb Effect; *Planet. Space Sci.*, **19,** (1971), 659
9. Ferencz, Cs.—Tarcsai, Gy.: Interaction of Gravitational and Electromagnetic Fields or Another Effect? *Natur*, **233,** (1971), 404
10. Ferencz, Cs.—Tarcsai Gy.: Refraction Effects due to Moving Media in Doppler Measurements; Space Research *XII*, 595, Akademie-Verlag, Berlin 1972
11. Ferencz, Cs.—Tarcsai, Gy.: Redshift during Pionerr-6 Solar Occultation — Unexplained or Predicted; *Nature*, **252,** (1974), 615
12. Ferencz, Cs.—Tarcsai, Gy.: Frequency Shift Effects due to Atmospheric Motions in Interplanetary Occultational Measurements; *Space Research* XVI., 705, Akademie-Verlag, Berlin 1976
13. Bird, M. K.: Coronal Tranzient Events Observed with S-Band Faraday Rotation Measurements during Solar Occultation; *COSPAR XVIII. Plen. Meet., II.—SIP.* **1. 7.**, Varna 1975
14. Ferencz, Cs.: Electromagnetic Wave Propagation in Inhomogeneous Linear Media; Thesis submitted for the degree of Candidate of Sciences, Budapest, 1970. Library of the Hungarian Academy of Sciences (in Hungarian)
15. Ferencz, Cs.: Permittivity of Inhomogeneous Media; Proc. of the Fourth Coll. on Micr. Com.; *ET-10*, Akadémiai Kiadó, Budapest, 1970
16. Ferencz, Cs.: Electromagnetic Wave Propagation: The Analysis of the Group Velocity; *Acta Techn. Hung.*, **86,** (1978), 169
17. Ferencz, Cs.: A Geometric Resolution of the Contradiction between the Propagation of Electromagnetic Plane Waves in Moving Dielectrics and the Einsteinian Addition of Velocities; *Acta Techn. Ac. Sci. H.*, **84,** (1977), 147
18. Ferencz, Cs.: Electromagnetic Wave Propagation in Inhomogeneous Media: Method of Inhomogeneous Basic Modes; *Acta Techn. Hung.*, **86,** (1978), 79
19. Ferencz, Cs.: Wave Propagation in Inhomogeneous Linear Media; *Acta Techn. Ac. Sci. H.*, **68,** (1970), 215
20. Allis, W. P.—Buchsbaum, S. J.—Bers, A.: Waves in Anisotropic Plasmas; M.I.T. Press, Cambridge, Mass., 1963
21. Ferencz, Cs.: Electromagnetic Wave Propagation in Inhomogeneous Media: Strong and Weak Inhomogeneities; *Acta Techn. Hung.*, **85** (1977), 433
22. Kamke, E.: Differentialgleichungen, Lösungsmethoden und Lösungen I: Gewöhnliche Differentialgleichungen; Akademische Verlagsgesellschaft, Geest & Portig K. G., Leipzig 1951

23. ARNAUD, J. A.—SALEH, A. A. M.: Theorems for Bianizotropic Media; *Proc. IEEE*, **60,** (1972), 639
24. IDEMEN, M.: The Maxwell's Equations in the Sense of Distributions; IEEE Trans. *Ant. and Prop.*, **AP—21,** (1973), 736
25. FERENCZ, CS.—FERENCZ, I.—TARCSAI, GY.: Refractions Problems and Wave Propagation in Doppler Geodetical Measurements; *Nablj. I. Sz. Z.*, **9,** (1970), 361
26. CRISTESCU, R.—MARINESCU, G.: Introduction to the theory of distributions and its applications (in Hungarian). Műszaki Könyvkiadó, Budapest 1969
27. DRAHOS, D.—FERENCZ, CS.—FERENCZ, I.—HORVÁTH, F.—TARCSAI, GY.: Some Theoretical Contributions Concerning Doppler Geodetical Measurements; *Space Research* **X,** 43, North-Holland Publ. Co., Amsterdam 1970
28. FELSEN, L. B.: Rays, Modes and Equivalent Networks; *Proc. of the Fourt Coll. on Micr. Com.*, **ET—9,** Akadémiai Kiadó, Budapest 1970
29. BUDDEN, K. G.: Radio Waves in the Ionosphere; Cambridge at the Univ. Press 1966
30. PATTANTYUS, L.: Basic Studies — Material Sciences; 2; (in Hungarian) Műszaki Könyvkiadó, Budapest 1961
31. ÁRKOS, I. F.: A General Investigation of a Monochromatic Signal Propagating Along an Inhomogeneous Transmission Line; (to be published)

Fortpflanzung elektromagnetischer Wellen in inhomogenen Medien: Analyse der Drehung der Polarisation und Anwendung des Prinzips der modifizierten Verfolgung. Die Fortpflanzung der monochromatischen elektromagnetischen Wellen in inhomogenen Medien wird unter Anwendung der "Methode der inhomogenen Grundmoden" und des Prinzips der "modifizierten Strahlenverfolgung" untersucht. Der Verfasser gelangt zu mehreren grundlegenden Folgerungen in Bezug auf die Ausbreitung in inhomogenen Medien. Grundlegendes Ziel ist die Erklärung der bei der Sonnenokkultation der Raumsonden Pioneer-6 und -9 wahrgenommenen Polarisationstransienten. Nach Angabe der Untersuchungsmethode werden im I. Teil die Untersuchungen über die Ausbreitung in insotropen Medien eingehend besprochen. Im II. Teil wird nach Untersuchung der Ausbreitung in anisotropen Medien eine Erklärung für die transiente Form "W" der Polarisation erhalten und die Ergebnisse der Untersuchungen werden zusammengefaßt. Es wird nachgewiesen, daß in einem inhomogenen Medium neben dem bekannten Faraday-Rotationseffekt auch eine "inhomogene Polaristationsrotation" auftritt. Zur Zeit von Sonnenokkultationen ergibt die inhomogene Polarisationsrotation notwendigerweise "W"-förmige Transiente. Gleichzeitig wird ein neuer Weg für die Untersuchung der Frontstruktur der "sich ausbreitenden interplanetaren Erscheinungen" erschloßen.

Распространение монохроматических электромагнитных волн в негомогенной среде при применении «метода негомогенных основных модусов» и «модифицированного принципа лучевого слежения». В данной работе исследуется распространение монохроматических электромагнитных волн в негомогенной среде при применении «метода негомогенных основных модусов» и «модифицированного принципа лучевого слежения». Сделано ряд фундаментальных по своей природе заключений по вопросу распространения в негомогенной среде. Основной нашей целью является — дать объяснение «W»-образных переходных процессов поляризации, наблюдавшейся на космических зондах Пионер-6 и -9 во время оккуляции Солнца. После изложения методики исследования в 1 части дается детальное изложение исследований распространения в изотропной среде. Во II части образной переходной формы поляризации; после чего дается обобщение результатов проведенных исследований. Показано, что в негомогенной среде наряду с известным явлением ротации Фарадея возникает также «негомогенная поляризационная ротация». Доказывается, что негомогенная поляризационная ротация во время оккуляций Солнца в силу необходимости дает в результате «W»-образные переходные процессы поляризации. С этим одновременно открывается новый птуь в области исследования фронтальной структуры «распространяющихся межпланетных явлений».

Acta Technica Academiae Scientiarum Hungaricae, Tomus 86 (3—4), pp. 395—400 (1978)

AN EXAMPLE FOR CONSTRUCTING THE VARIATIONAL (ENERGETIC) ERROR PRINCIPLE

P. SCHARLE*

CANDIDATE OF TECHN. SCI.

[Manuscript received October 24, 1977]

The paper presents a less simple example for constructing the variational error functional, the idea of which was outlined previously. Starting from the governing equations of the elasticity with nonhomogeneous boundary conditions it constructs the equivalent energy expression, which proves to be the well-known form of the potential energy.

1. The error principle

In a previous paper the obviousness of conceiving the approximating methods as a couple of an approximating principle and an approximating technique has been shown ([2]). The error principles of minimizing a bilinear form of the error vectors or orthogonalizing one of them with respect to some vector space had been proved to be equivalent. Nevertheless, owing to its physical importance the energetical approximating principle is justly considered as the most suited one to the nature of the engineering problems. The paper referred to above only contains the general idea of the error principles and takes into consideration the advantage of the homogeneous boundary conditions of the given field problem. Here we present a simple example for constructing the energetic error-functional in the inhomogeneous case.

2. The non-homogeneous field problem of elasticity

Consider the general problem of linear elasticity, formulated for the domain V covered with the surface S, in the form of

$$\sigma_{ij} = \frac{1}{2} C_{ijkl}(u_{k,l} + u_{l,k}) \text{ in } V. \tag{1}$$

$$u_i = d_i \qquad \text{on } S_n \ , \tag{2}$$

* P. SCHARLE, Péterfy S. u. 44, H—1076 Budapest, Hungary

where u_i stand for the components of the displacement vector defined over V and S, d_i are the prescribed displacements on the boundary $S_u \subset S$. We restrict the class of the u_i functions allowed for those fulfilling the equations (1) and (2): the compatible displacement fields. For the exact solution u_i^0 the equations of equilibrium

$$\sigma_{ij,j} + \varrho k_i = 0, \qquad \text{in } V \tag{3}$$

$$\sigma_{ij} n_j = p_i, \qquad \text{on } S_\sigma \tag{4}$$

are fulfilled. Here ϱk_i are the components of the volume-force vector, p_i stands for the surface force components prescribed.

Following the procedure suggested by MIKHLIN ([1]) let us assume the existence of the vector ψ_i satisfying the boundary conditions (2) and (4), in the latter case in the sense of

$$\frac{1}{2} C_{ijkl}(\psi_{k,l} + \psi_{l,k}) n_j = p_i .$$

Let Ψ_i continuous and differentiable at least two times continuously in V. In other words,

$$\psi_i = d_i \mid_{S_u} \tag{5}$$

$$\sigma_{ij}^{\psi} n_j = p_i \mid_{S_\sigma} \tag{6}$$

are fulfilled.* We assume $S = S_u \cup S_\sigma$ and $S_u \cap S_\sigma = 0$.

We introduce now the transformation of

$$v_i = u_i - \psi_i \ . \tag{7}$$

This translation of u_i results in the following equations:

$$v_i = 0 \mid_{S_u} \tag{8}$$

$$\sigma_{ij}^{v} n_j = \sigma_{ij}^{u} n_j - p_i \mid_{S_\sigma} \ . \tag{9}$$

The modified problem now presents itself as constructing the vector v_i, which fulfils the equilibrium equations of

$$\sigma_{ij,j}^{v} = -\varrho k_i - \sigma_{ij,j}^{\psi}, \qquad \text{in } V \tag{10}$$

$$\sigma_{ij}^{v} n_j = 0, \qquad \text{on } S_\sigma \tag{11}$$

* In what follows we use the short conventional symbol of

$$\sigma_{ij}^{v} = \frac{1}{2} C_{ijkl}(v_{k,l} + v_{l,k}) \ ,$$

while σ_{ij}^{0} stands for the exact solution.

3. The energetic error principle

Let us restrict now the set of the functions v_i admitted for those fulfilling both (8) and (11). In this case we define for the approximating solution v_i the following error vectors:

$$g_i = v_i^0 - v_i,$$
$$h_i = -\varrho k_i - \sigma_{ij,j}^{\psi} - \sigma_{ij,j}^{v} \qquad \text{in } V, \tag{12}$$

where v_i^0 stands for the exact solution. The boundary conditions are homogeneous. The bilinear form to be minimized (in the sense of (18) — [2]) will be as follows:

$$H = \int_V g_i h_i dV = \int_V (v_i^0 - v_i)\,(-\varrho k_i - \sigma_{ij,j}^{\psi} - \sigma_{ij,j}^{v})\; dV =$$
$$= -\int_V v_i^0\, \varrho k_i\, dV - \int_V v_i^0\, \sigma_{ij,j}^{\psi}\, dV - \int_V v_i^0\, \sigma_{ij,j}^{v}\, dV +$$
$$+ \int_V v_i\, \varrho k_i\, dV + \int_V v_i\, \sigma_{ij,j}^{\psi}\, dV + \int_V v_i\, \sigma_{ij,}^{v}\, dV. \tag{13}$$

Here the first two terms contain only known or unknown constants; let

$$A_1 = -\int_V v_i^0\, \varrho k_i\, dV - \int_V v_i^0\, \sigma_{ij,j}^{\psi}\, dV. \tag{14}$$

In the third term we take the advantage of the well-known identities of the Gauss-Ostrogradski formula

$$\int_V \sigma_{ij}^{\alpha}\, \varepsilon_{ij}^{\beta} dV + \int_V \sigma_{ij,j}^{\alpha}\, \beta_i\, dV = \int_S \sigma_{ij}^{\alpha}\, n_j\, \beta_i\, dS \tag{15}$$

and the Maxwell-theorem

$$\int_V \sigma_{ij}^{\alpha}\, \varepsilon_{ij}^{\beta}\, dV = \int_V C_{ijkl}\, \varepsilon_{ij}^{\alpha}\, \varepsilon_{kl}^{\beta}\, dV = \int_V \varepsilon_{ij}^{\alpha}\, \sigma_{ij}^{\beta}\, dV. \tag{16}$$

Therefore,

$$-\int_V v_i^0\, \sigma_{ij,j}^{v}\, dV = \int_V \sigma_{ij}^{v}\, \varepsilon_{ij}^{v0}\, dV - \int_S \sigma_{ij}^{v}\, n_j\, v_i^0\, dS =$$
$$= \int_V \sigma_{ij}^{v0}\, \varepsilon_{ij}^{v}\, dV - \int_S \sigma_{ij}^{v}\, n_j\, v_i^0\, dS =$$
$$= -\int_V \sigma_{ij,j}^{v0}\, v_i\, dV + \int_S \sigma_{ij}^{v0}\, n_j v_i\, dS - \int_S \sigma_{ij}^{v}\, n_j\, v_i^0\, dS. \tag{17}$$

Here

$$\int_S (\sigma_{ij}^{v0}\, n_j\, v_i - \sigma_{ij}^{v}\, n_j\, v_i^0)\, dS = 0,$$

since

$$v_i = 0, \qquad v_i^0 = 0, \qquad \text{on } S_u$$

and

$$\sigma_{ij}^v \, n_j = 0, \qquad \sigma_{ij}^{v0} \, n_j = 0 \text{ on } S_\sigma.$$

By this transformation we obtain

$$H = A_1 + \int_V v_i \, \sigma_{ij,j}^v \, dV - 2 \int_V \sigma_{ij,j}^{v0} \, v_i \, dV \tag{18}$$

since the fourth and fifth terms in (13) may be coupled by using (10).

Let us turn back now to the u_i vector by the inverse transformation of (7), bearing in mind that the set of the compatible u_i vectors are restricted by the condition

$$\sigma_{ij}^u \, n_j = p_i. \tag{19}$$

Expanding (18) we obtain

$$H = A_1 + \int_V u_i \, \sigma_{ij,j}^u \, dV - \int_V \psi_i \, \sigma_{ij,j}^u \, dV - 2 \int u_i \sigma_{ij,j}^0 \, dV + \\ + \int_V u_i \, \sigma_{ij,j}^\psi \, dV + 2 \int_V \psi_i \, \sigma_{ij,j}^0 \, dV - \int_V \psi_i \, \sigma_{ij,j}^\psi \, dV. \tag{20}$$

In this expression the last two terms contain only known and unknown constant functions — let us note them by A_2. Therefore,

$$H = A_1 + A_2 - 2 \int_V u_i \, \sigma_{ij,j}^0 \, dV + \int_V u_i \, \sigma_{ij,j}^u \, dV + \\ + \int_V u_i \, \sigma_{ij,j}^\psi \, dV - \int_V \psi_i \, \sigma_{ij,j}^u \, dV \ . \tag{21}$$

By virtue of (3) the first integral term may be shortened here. The next term we shall expand by using the Gauss-Ostrogradski theorem, and the last two terms may be transformed into surface integrals by Green's formula. We find

$$H = A_1 + A_2 + 2 \int_V u_i \, \varrho k_i \, dV - \int_V \sigma_{ij}^u \, \varepsilon_{ij}^u \, dV + \\ + \int_S \sigma_{ij}^u \, n_j (u_i - \psi_i) \, dS + \int_S \sigma_{ij}^\psi \, n_j \, u_i \, dS. \tag{22}$$

According to the conditions given above

$$u_i = \psi_i = d_i |_{S_u} \quad \text{and} \quad \sigma_{ij}^u \, n_j = \sigma_{ij}^\psi \, n_j = p_i |_{S_\sigma} \ .$$

Therefore, we find for the surface integrals in (22) the following expression:

$$\int_S p_i (u_i - \psi_i) \, dS + \int_S \sigma_{ij}^\psi \, n_j \, d_i \, dS + \int_{S_\sigma} p_i u_i \, dS = A_3 + 2 \int_{S_\sigma} p_i \, u_i \, dS,$$

where

$$A_3 = -\int_{S_\sigma} p_i \psi_i \, dS + \int_{S_u} \sigma_{ij}^{\psi} \psi_j \, d_i \, dS ,$$

analogously to A_1 and A_2 is not to be variated.

In this manner we find

$$H = A_1 + A_2 + A_3 + 2\int_V u_i \varrho k_i \, dV - \int_V \sigma_{ij}^u \varepsilon_{ij}^u \, dV + 2\int_{S_\sigma} p_i u_i \, dS . \tag{23}$$

The quantities A_1, A_2, A_3 vanish, variating the unknown functions u_i and defining the total potential energy as

$$\Phi(u) = -\frac{1}{2} H ,$$

we obtain the well-known formula of

$$\Phi(u) = \int_V W(u) \, dV - \int_V \varrho k_i u_i \, dV - \int_{S_\sigma} p_i u_i \, dS , \tag{24}$$

where

$$W(u) = \frac{1}{2} \sigma_{ij}^u \varepsilon_{ij}^u . \tag{25}$$

The functional Φ (u) should be variated over the set of the u_i vectors fulfilling the conditions (2) and (19).

Nevertheless, the case mentioned by MIKHLIN occurs ([1], p. 119, Note 2), when the functional involves a natural boundary condition too. In particular,

$$\begin{aligned}
-\delta\Phi(u) &= -\delta\frac{1}{2}\int_V \sigma_{ij}^u \varepsilon_{ij}^u \, dV + \delta\int \varrho k_i u_i \, dV + \delta\int_{S_\sigma} p_i u_i \, dS = \\
&= -\int_V \sigma_{ij}^u (\delta u_i)_{,j} dV + \int_V \varrho k_i \, \delta u_i \, dV + \int_{S_\sigma} p_i \, \delta u_i \, dS = \\
&= \int_V \sigma_{ij,j}^u \, \delta u_i \, dV + \int_V \varrho k_i \, \delta u_i \, dV + \\
&+ \int_{S_\sigma} p_i \, \delta u_i \, dS - \int_S \sigma_{ij}^u n_j \, \delta u_i \, dS = \\
&= \int_V (\sigma_{ij,j}^u + \varrho k_i) \, \delta u_i \, dV + \\
&+ \int_{S_\sigma} (p_i - \sigma_{ij}^u n_j) \, \delta u_i \, dS - \int_{S_u} \sigma_{ij}^u n_j \, \delta u_i \, dS .
\end{aligned} \tag{26}$$

In this manner, for arbitray but compatible δu_i the condition (4) of the relative extremum is automatically realized and it is not necessary to prescribe it in advance.

REFERENCES

1. MIKHLIN, S. G.: Variational Methods in Mathematical Physics, Pergamon 1964
2. SCHARLE, P.: On the Relationship between Different Approximating Methods, *Acta Techn.* Hung. **82.** (1976). 53—59

Ein Beispiel für die konstruktive Anschreibung des (energetischen) Variationsprinzips. Die Arbeit bringt ein weniger einfaches Beispiel für die früher allgemein beschriebene Anschreibung des Variations-Fehlerfunktionals. Ausgehend von der mittels inhomogener Randbedingungen formulierten Grundaufgabe der linearen Elastizitätslehre werden die entsprechenden Energieausdrücke konstruktiv abgeleitet. Es stellt sich heraus, daß auch auf diese Weise der gut bekannte Ausdruck für die gesamte potentielle Energie abgeleitet werden kann.

Пример конструктивной записи вариационного (энергетического) принципа погрешности. В работе приводится относительно простой пример записи вариационного функционала погрешности, описанной предварительно в общих чертах. Исходя из основной задачи, сформулированной негомогенными краевыми условиями линеарной теории упругости, с помощью конструктивного метода выводятся соответствующие энергетические выражения. Выясняется, что и таким образом можно получить хорошо известное выражение полной потенциальной энергии.

Acta Technica Academiae Scientiarum Hungaricae, Tomus 86 (3—4), pp. 401—409 (1978)

ON THE ESTIMATION OF THE TORSIONAL RIGIDITY OF PRISMATIC BARS

I. ECSEDI*

[Received on June 10, 1977]

By making use of the inequalities deduced in the present paper, lower and upper limits may be produced for the numerical values of the torsional rigidity of prismatic bars of solid cross section and of homogeneous material.

1. Introduction

In this paper inequalities are presented to be used for the estimation of the torsional rigidities of prismatic bars of solid cross section and of elastic material. The estimation of the torsional rigidities of prismatic bars of elastic material by numerous reputed authors has been dealt with. The methods developed by J. B. DIAZ and A. WEINSTEIN were based mainly on the application of Schwartz's inequality. By making use of Schwartz's inequality lower and upper limits are produced for the value of Dirichlet's integral which permits the estimation of the torsional rigidity of a homogeneous prismatic bar of elastic material [1], [2], [3].

Estimations related to the minimum principle of the potential energy and complementary work were presented by C. WEBER, W. GÜNTHER [8] and A. I. LURJE [7]. J. BARTA [4] reported on a method for the estimation of the torsional rigidity, other than the methods quoted above.

The present paper exposes formulae and inequalities in connection with the torsional rigidity of prismatic bars of solid cross section of the same structure as that presented by J. BARTA. One of the results of the paper is a direct outcome of the inequalities deducted by J. BARTA to the torsional rigidity of prismatic bars of solid cross section [4]. The purpose of this paper is to deduce the formulae (20), (21), (32), (33), (34), (35). These formulae, just like J. BARTA's ones, may be used for the estimation of the torsional rigidity of prismatic bars and partly they result from those ones. However, their deduction is a simpler operation.

* Dr. I ECSEDI, Vászonfehérítő u. 24, IV/1, 3531 Miskolc, Hungary.

2. Elasticity principles

It is familiar that the torsional rigidity S of the prismatic bar of solid cross section depicted in Fig. 1 is to be determined with the aid of the formula

$$S = 2G \int_T U \, dT, \tag{1}$$

where
U = $U(x, y)$ is the stress function of the cross section (x, y being the orthogonal coordinates), and
G is the shear elasticity modulus of the bar material.

The stress function $U = U(x, y)$ satisfies in the region T determined by the cross section of the bar the differential equation of Poisson's type

$$\frac{\partial^2 U}{\partial x^2} + \frac{\partial^2 U}{\partial y^2} + 2 = 0 \tag{2}$$

and on the limiting curve γ of the cross section the homogeneous boundary condition

$$U = 0. \tag{3}$$

Often seems to be convenient to solve the the torsion problem by the determination of the function $V = V(x, y)$ interpreted by the prescription

$$V = V(x, y) = U(x, y) + \frac{x^2 + y^2}{2}. \tag{4}$$

From Eqs (2), (3) and (4) follows that the harmonic $V = V(x, y)$ satisfies in the region T and on the limiting curve γ the boundary conditions

$$\frac{\partial^2 V}{\partial x^2} + \frac{\partial^2 V}{\partial y^2} = 0 \tag{5}$$

and

$$V = \frac{x^2 + y^2}{2} \tag{6}$$

respectively.

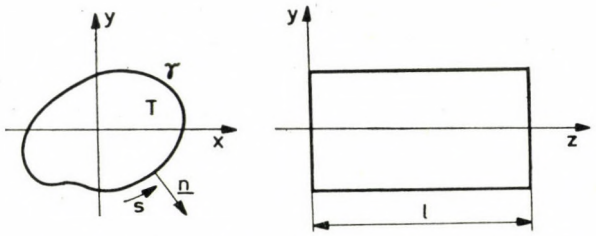

Fig. 1. Prismatic bar of solid cross section

By making use of the function $V = V(x, y)$ the torsional stiffness of the cross section may be determined by equation

$$S = G\left(2\int_T V\, dT - I\right), \tag{7}$$

where

$$I = \int_T (x^2 + y^2)\, dT\,. \tag{8}$$

Let us designate the Green's function associated with Laplace's differential operator

$$\Delta = \frac{\partial^2}{\partial x^2} + \frac{\partial^2}{\partial y^2}$$

of the region T by

$$g = g(x, y; \xi, \eta).$$

By making use of Green's function $g = g(x, y; \xi, \zeta)$ the solution to the boundary value problems designated by Eqs (2), (3) and (5), (6) may be produced in the forms

$$U(x, y) = 2\int_T g(x, y; \xi, \eta)\, dT \tag{9}$$

and

$$V(x, y) = \int_\gamma \frac{\xi^2 + \eta^2}{2} \frac{\partial}{\partial n} g(x, y; \xi, \eta)\, ds, \tag{10}$$

respectively [6], [9]. In Eqs (9) and (10) the variables of integration ξ, η, further, in Eq. (10) $\partial/\partial n$ designate the derivative calculated along the unit vector of the n normal of the limiting curva γ, and s denotes an arc coordinate on the curve γ [9].

3. Some inequalities in connection with the torsional rigidity

Be the function $F = F(x, y)$ of two variables continuously derivable through the region T which on the curve γ satisfies the homogenic boundary condition

$$F = 0. \tag{11}$$

By making use of the function $H = H(x, y)$ which satisfies the equation

$$\frac{\partial^2 F}{\partial x^2} + \frac{\partial^2 F}{\partial y^2} + H = 0 \tag{12}$$

and of Green's function $g = g(x, y; \xi, \eta)$, the function $F = F(x, y)$ may also be given in the following form

$$F(x, y) = \int_T H(\xi, \eta)\, g(x, y; \xi, \eta)\, dT. \tag{13}$$

From Eq. (13) follows

$$F(x, y) = \frac{1}{2} H(\bar{\xi}, \bar{\eta}) \int_T 2g(x, y; \xi, \eta)\, dT. \tag{14}$$

Here, $\bar{\xi} = \bar{\xi}(x, y)$, $\bar{\eta} = \bar{\eta}(x, y)$ designate a convenient "intermediate" value $[(\bar{\xi}, \bar{\eta}) \in T]$ falling in the region T, depending on the coordinates x, y according to the mean value theorem of the integral calculus. By applying the formula (9) the following result will be obtained

$$2F(x, y) = \bar{H}(x, y)\, U(x, y), \tag{15}$$

where

$$\bar{H} = \bar{H}(x, y) = H[\bar{\xi}(x, y), \bar{\eta}(x, y)]. \tag{16}$$

From Eq. (15) follows

$$4 \int_T F(x, y) dT = H^* \left(2 \int_T U(x, y)\, dT\right) = H^* S. \tag{17}$$

Here H^* denotes the value assumed in the region T for the function $\bar{H} = \bar{H}(x, y)$ on a convenient intermediate locus. Let us designate further the maximum and minimum values of the function

$$H = H(x, y) = -\left(\frac{\partial^2 F}{\partial x^2} + \frac{\partial^2 F}{\partial y^2}\right)$$

by $H_{\max}$ and $H_{\min}$, respectively.

Having $S > 0$ [1], further

$$H^* \leq H_{\max}, \quad H^* \geq H_{\min} \tag{18), (19}$$

in consequence of Eq. (17) for the torsional stiffnes S the following pair of inequalities are true

$$H_{\max} S \geq 4 \int_T F\, dT, \tag{20}$$

$$H_{\min} S \leq 4 \int_T F\, dT. \tag{21}$$

The above inequalities are obtained from the formulae (1), (2) of J. BARTA's study [4] quoted above, to the special case where the estimation is car-

ried out with the aid of such functions which vanish on the boundary curve γ. J. BARTA deduced his result with the aid of an other method.

In the following one accepts for base the function $V = V(x, y)$ in applying the above train of thought. Let $L = L(x,y)$ designate the value of the function $K = K(x, y)$ (which is harmonic in the region T), taken on the curve γ.

With the aid of Green's function $g = g(x, y; \xi, \eta)$ the function $K = K(x, y)$ may established in the form [9]:

$$K(x, y) = \int_{\gamma} L(\xi, \eta) \frac{\partial}{\partial n} g(x, y; \xi, \eta)\, ds. \tag{22}$$

From the identity

$$K(x, y) = \int_{\gamma} 2 \frac{L(\xi, \eta)}{\xi^2 + \eta^2} \frac{\xi^2 + \eta^2}{2} \frac{\partial}{\partial n} g(x, y; \xi, \eta)\, ds \tag{23}$$

by making use of the mean value theorem of the integral calculus and of the Eq. (10) one obtains

$$K(x, y) = h(\bar{\xi}, \bar{\eta})\ V(x, y)\,, \tag{24}$$

where

$$h = h(\xi, \eta) = 2 \frac{L(\xi, \eta)}{\xi^2 + \eta^2} \tag{25}$$

and $\bar{\xi} = \bar{\xi}(x, y), \bar{\eta} = \bar{\eta}(x, y)$ are coordinates which determine the "convenient point P on the curve γ depending on the coordinates x, y, $[(\bar{\xi}, \bar{\eta}) \in \gamma]$.

Eq. (24) yields by integration and by application of the mean value theorem, of the integral calculus

$$\int_T K(x, y)\, dT = h^* \int_T V(x, y)\, dT. \tag{26}$$

In the above equation h^* designates the value of the function $h(\bar{\xi}, \bar{\eta})$ assumed on a convenient locus

$$\bar{\xi} = \bar{\xi}(x^*, y^*),\ \bar{\eta} = \bar{\eta}(x^*, y^*)/(x^*, y^*) \in T,\ (\bar{\xi}, \bar{\eta}) \in \gamma)\ . \tag{26a}$$

Let us denote the maximum and minimum value of the function

$$h = h(x, y) = 2 \frac{L(x, y)}{x^2 + y^2} \tag{27}$$

interpreted on the curve γ by $h_{\max}$ and $h_{\min}$ respectively.

Since

$$\int V(x, y)\, dT > 0$$

(because $V = V(x, y)$ in the region T is harmonic and on the curve

$$V(x, y) = \frac{x^2 + y^2}{2} > 0),$$

further,

$$h^* \geq h_{\min}, \quad h^* \leq h_{\max}. \tag{28), (29}$$

In consequence of Eq. (26) the following pair of inequalities are valuable

$$\int_T K(x, y)\, dT \leq h_{\max} \int_T V(x, y)\, dT, \tag{30}$$

$$\int_T K(x, y)\, dT \geq h_{\min} \int_T V(x, y)\, dT. \tag{31}$$

Combination of formulae (30), (31) and (7) yields for the torsional rigidity S the following inequalities

$$h_{\max} S \geq G\left(2 \int_T K\, dT - h_{\max} I\right), \tag{32}$$

$$h_{\min} S \leq G\left(2 \int_T K\, dT - h_{\min} I\right). \tag{33}$$

By making use of the harmonic function $K = K(x, y) = 1$, from the above formulae we have

$$S \geq G(R^2_{\min} T - I), \tag{34}$$

$$S \leq G(R^2_{\max} T - I), \tag{35}$$

which are the lower and upper limits respectively for the estimation of the torsional rigidity S, for,

$$\int_T K(x, y)\, dT = \int_T dT = T, \tag{36}$$

$$h = h(x, y) = \frac{2}{x^2 + y^2} = \frac{2}{R^2}, \tag{37}$$

$$h_{\min} = \frac{2}{R^2_{\max}}, \quad h_{\max} = \frac{2}{R^2_{\min}}. \tag{38), (39}$$

Here $R^2_{\max}$, and $R^2_{\min}$ denote the maximum and the minimum value repectively of the function $R^2 = x^2 + y^2$ on the curve γ (Fig. 2).

[5] verifies the inequalities (34) and (35) with the aid of the maximum-minimum priciple relating to the harmonic functions.

Ex. 1. Consider the solid cross section of the form of an isosceles triangle. The equations of the sides of the triangle are as follows (Fig. 3):

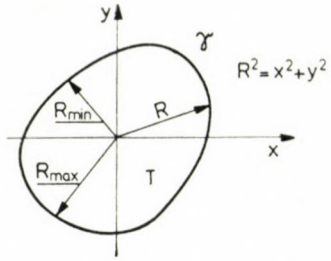

Fig. 2. Demonstration of $R^2 = x^2 + y^2$

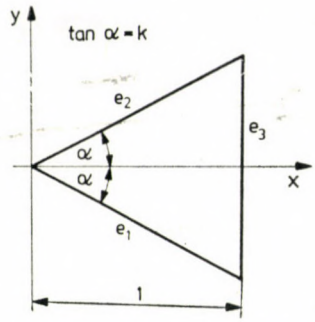

Fig. 3. Cross section of isosceles triangle

$$\begin{aligned} e_1&: \; y + kx = 0, \\ e_2&: \; y - kx = 0, \\ e_3&: \; x - 1 \; = 0. \end{aligned} \tag{a}$$

Be the $F = F(x, y)$ function needed to the application of the pair of inequalities (20), (21)

$$F(x, y) = (y^2 - k^2x^2)\,(x - 1). \tag{b}$$

Calculation with the above function yields

$$\begin{aligned} H_{\min} &= 4k^2, \\ H_{\max} &= 2 - k2^2 \end{aligned} \tag{c}$$

assuming that $0 < k \leq 1/\sqrt{3}$, further

$$\int_T F(x, y)\, dT = \frac{k^3}{15} \tag{d}$$

Calculating with the shear elasticity modulus $G = 1$ the following lower and upper limiting values may be derived for the torsional rigidity S

$$\begin{aligned} S &\leq \frac{k}{15}, \\ S &\geq \frac{2k^3}{5(1 - k^2)}, \\ &\left((0 < k \leq \frac{1}{\sqrt{3}}\right) \; . \end{aligned} \tag{e}$$

The values of the lower and upper limits $k = 1/\sqrt{3}$ (which is the case of the equilateral triangle), are the same and yield the result

$$S = \frac{1}{15\sqrt{3}} \tag{f}$$

the correctness of which may be checked [7], [8].

Ex. 2. In connection of this problem lower and upper limits are given for the torsional rigidity of the cross section of the form of isosceles triangle depicted in Fig. 3, by the application of the pair of inequalities (32) and (34).

The estimation might be carried out with the aid of the harmonic function

$$K = K(x, y) = -\frac{1}{2}(x^3 - 3xy^2) + (x^2 - y^2). \tag{g}$$

The values of the function $h = h(x, y)$ on each side of the triangle are follows (Fig. 3):

$$\begin{aligned} e_1\colon \quad & h = \frac{(3k^2 - 1)\,x + 2(1 - k^2)}{k^2 + 1}, \\ e_2\colon \quad & h = \frac{(3k^2 - 1)\,x + 2(1 - k^2)}{k^2 + 1}, \\ e_3 \quad & h = 1. \end{aligned} \tag{h}$$

Hence

$$h_{\min} = \frac{2(1 - k^2)}{1 + k^2}, \quad h_{\max} = 1 \tag{i}$$

on condition that

$$k \geq \frac{1}{\sqrt{3}}.$$

Calculating with the assumed function $K = K(x, y)$ one obtains

$$\int_T K(x, y)\, dT = \frac{3}{10}k + \frac{1}{30}k^3.$$

Replacement of the above expression into the inequalities (32), (33) yields for the torsional stiffness the following lower and upper limiting values, on condition that $G = 1$:

$$\begin{aligned} S &\geq \frac{k - k^3}{10}, \\ S &\leq \frac{3k^5 + 10k^2 - 3k}{15(1 - k^2)}, \\ &\left(k \geq \frac{1}{\sqrt{3}}\right). \end{aligned} \tag{k}$$

It is easily verifiable that in the case of the value $k = 1/\sqrt{3}$ (which is the case of the equilateral triangle) the values of the above lower and upper limits are the same, and we obtain the result

$$S = \frac{1}{15\sqrt{3}}$$

for the torsional rigidity.

REFERENCES

1. Diaz, J. B.—Weinstein, A.: The torsional Rigidity and Variational Methods. *American Journal of Mathematics*, **70,** (1948), 107
2. Diaz, J. B.: On Estimation of Torsional Rigidity and Other physical Quantities. Pro*ceedings of the First U. S. National Congress of Applied Mechanics*, (1952), p. 259
3. Weinstein, A.: New Methods for the Estimation of Torsional rigidity, *Proceedings of Symposium in Applied Mathematics.* Vol. III. (1950), 141—146
4. Barta, J.: On the Estimation of Torsional Rigidity, *KONIKL. NEDERL. Akademie. Van. Wetenschappen.* Series B. 58. No. 1. 1955. pp. 80—89
5. Ecsedi, I.: One Kind of Estimation of the Torsional Rigidity of a Prismatic Bar Having Solid Cross Section. *Gép.* **29,** (1977), 5 (In Hungarian)
6. Frank, Ph.—Mises, R.v.: Differential- und Integralgleichungen der Mechanik und Physik, Aufl. 2. Band 1
7. Лурье Л. И.: Теория упругости. Москва. Наука, 1970.
8. Weber, C.— Günther, W.: Torsionstheorie. Akademie-Verlag, Berlin 1958
9. Korn, G. A.—Korn, T. M.: Mathematical Handbook for Scientists and Engineers, McGraw Hill Book Company, 1951

Über die Schätzung der Torsionssteifheit von primatischen Stäben. Durch Anwendung der in dieser Abhandlung abgeleiteten Ungleichheiten können untere und obere Schranken für den numerischen Wert der Torsionssteifheit eines prismatischen Stabes mit Vollquerschnitt aus homogenem Material angegeben werden.

Об оценке жесткости на кручение призматических стержней. Путем применения неравенств, выведенных в данной работе, для числовых значений жесткости на кручение призматического стержня, изготовленного из гомогенного материала и имеющего сплошное сечение, можно образовать нижние и верхние ограничения.

Acta Technica Academiae Scientiarum Hungaricae, Tomus 86 (3—4), pp. 411—420 (1978)

THE EVALUATION OF THE SEPARATION OPERATIONS

PETHŐ, SZ*—ORTUTAY, M*

DOCT. OF TECHN. SCI.

[Manuscript received March 30, 1977]

The authors have examined the efficiency of the two-constitent separation. As the extreme case of separation they consider the diminuation of the specimen and the absolutely efficient separation. Relations are established for calculating the separation efficiency. Several separation operations can be evaluated by the efficiency indexes even if the separation parameters and the mass yields are different.

Symbols

B	mass of raw material
$f(x)$	density function
$F(x)$	distribution function
H, M	mass of products
M_{hm}	error moment
m	mass yield
T	faulty mass fraction
x	physical characteristic of material
$\bar{x}$	average quality
$[x_{max}, x_{min}]$	interval of raw material distribution
x_a, x_f	limits of separation range
$\bar{X}$	equalizing parameter
z	separation zone
Subscripts:	
m	value referring to product M
h	value referring to product H
Superscripts:	
t	value referring to the theoretical separation
i	value referring to the absolutely inefficient separation

1. Introduction

The measure of separation of the concrete separation operation is the equalizing parameter. The most useful characteristic for the sharpness of separation is the fraction of faulty material and its first moment sum with respect to the equalizing parameter. Several tests for the sharpness of separation, using this characteristic, can be compared only if the separation has been made for the same equalizing parameter.

* Dr. PETHŐ, Sz. } Nehézipari Műszaki Egyetem, Miskolc Egyetemváros, Hungary
ORTUTAY, M. }

In the following the authors deal with the evaluation of the separation operations. With the evaluation indexes separation tests of different sizes can also be compared and the quality of the separation can be decided. The basis of the evaluation is by comparing the sharpness factors of the actual, the absolutely efficient and the absolutely inefficient separation operations.

The material to be separated is considered as being granular although the general model also refers to the separation of non-granular material — e.g. the distillation of a complex mixture.

2. Parameters of real separation operation

Fig. 1 shows the theoretical diagram of a real separation process, Fig. 2 shows the probability distribution and probability density functions of the mass flows in the separation operation. The physical characteristic of the grains to be separated is x, the distribution and probability density functions of the raw material are $F(x)$ and $f(x)$. Fig. (2) shows the distribution and probabilite density functions $F_h(x)$ and $f_h(x)$, and $F_m(x)$ and $f_m(x)$ of the separation products multiplied by the mass yields.

The range of the feed material is $x_{\max} - x_{\min}$. The range of the separation is z, where x_a is the lower and x_f the upper limit, $z = x_f - x_a$. Both separation products contain grains with the characteristic $x_a < x < x_f$.

The mass yield m_h can be determined from the input and output mass flows B, H, M of the installation:

$$m_h = \frac{H}{B}, \quad m_m = \frac{M}{B} = 1 - m_h \, . \tag{1}$$

Knowing the density and distribution functions the average quality of the raw material and of the products can be calculated by

$$\bar{x} = \int_{x_{\min}}^{x_{\max}} f(x)\, x dx = x_{\min} + \int_{x_{\min}}^{x_{\max}} [1 - (Fx)]\, dx, \tag{2}$$

$$\bar{x}_h = \int_{x_{\min}}^{x_f} f_h(x)\, x dx = x_{\min} + \int_{x_{\min}}^{x_f} [1 - F_h(x)]\, dx \, , \tag{3}$$

$$\bar{x}_m = \int_{x_a}^{x_{\max}} f_m(x)\, x dx = x_a + \int_{x_a}^{x_{\max}} [1 - F_m(x)]\, dx \, . \tag{4}$$

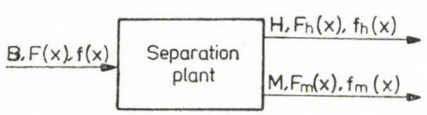

Fig. 1. Scheme of two-component separation

The characteristic of the separation is the equalizing parameter $\overline{X}$. It can be proved [2, 4] that the mass T_h of the grains of product H with a quality larger than $\overline{X}$ and the mass T_m of the garins of product M with a qualty below $\overline{X}$ are equal: $T_h = T_m = T_{hm}$. These defective material fractions characterizing the sharpness of the separation can be calculated from (5):

$$T_{hm} = m_m \int_{x_a}^{\overline{X}} f_m(x)\, dx = m_h \int_{\overline{X}}^{x_f} f_h(x)\, dx. \tag{5}$$

The proportions of the products of the faulty material are shown on the density functions of Fig. 2 by hatched areas;

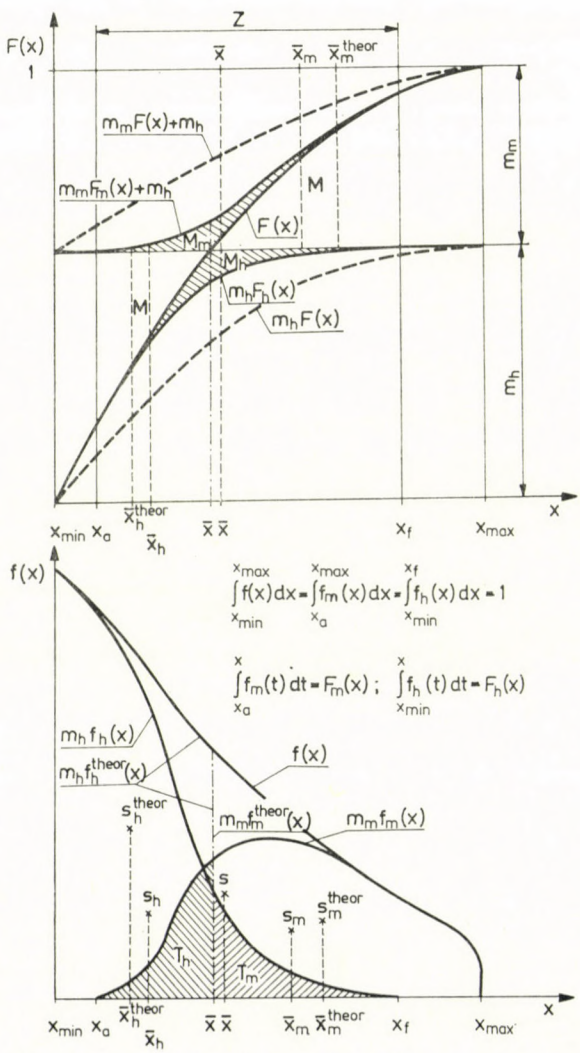

Fig. 2. Distribution and density functions of two-product separation

The absolute sum of the first moments of the mass fraction smaller than $x(x_a < x < x_f)$ of the product H and that of the product M greater than x are minimum for the equalizing paramter $\bar{X}$. Correspondingly, the first moments without the sign of the faulty mass fraction according to (5) for the equalizing parameter are a criterion of separation sharpness

$$M_{hm} = m_h \int_{\bar{X}}^{x_f} f_h(x)\,(x - \bar{X})\,dx + m_m \int_{x_a}^{\bar{X}} f_m(x)\,(\bar{X} - x)\,dx =$$

$$= m_h \int_{\bar{X}}^{x_f} [1 - F(x)]\,dx + m_m \int_{x_a}^{\bar{X}} F_m(x)\,dx\,. \qquad (6)$$

The doctorate dissertation of ENGEL contains many measuring results referring to separation. Table I. and Fig. 3 have been made by using one of

Table 1

Interval [mm]	$F(x)$	$m_h F_h(x)$	$m_m F_m(x)$
1—2	1,0000	—	0,5252
0,75—1	0,9072	0,4748	0,4324
0,5—0,75	0,8359	0,4742	0,3617
0,3—0,5	0,6563	0,4423	0,2140
0,1—0,3	0,2276	0,1967	0,0309
0—0,1	0,0029	0,0029	—

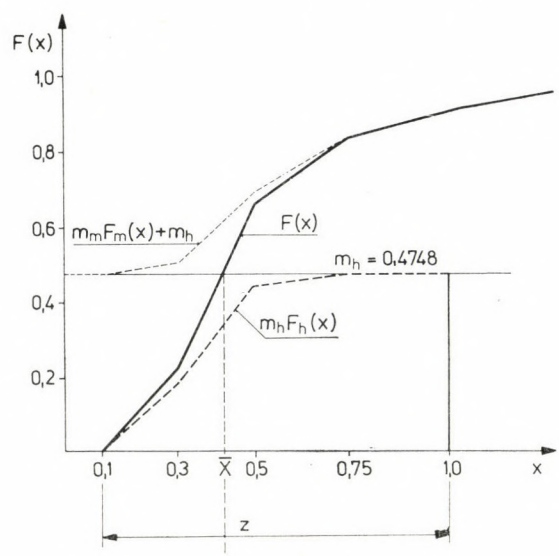

Fig. 3. Distribution functions of experimental separation

his results. From the experiments the following values have been calculated:

$\bar{X} = 0{,}415325$ mm, $\bar{x} = 0{,}530402$ mm, $\bar{x}_h = 0{,}331945$ mm,

$\bar{x}_m = 0{,}709815$ mm, $m_h = 0{,}4748$, $m_m = 0{,}5252$,

$T_{hm} = 0{,}13648$, $M_{hm} = 0{,}024108$.

3. The parameters of absolutely efficient and of absolutely inefficient separation

However be the separation, for unchanged mass yield the separation parameter also remains unchanged. Theoretically the separation may have two extreme cases. In one case the separation is absolutely efficient, in the other it is absolutely inefficient.

With an absolutely efficient separation at the equalizing parameter $\bar{X}$ the result is mass yields equal to that of the real operation and the products do not contain grains with equal properties. The average qualities $\bar{x}_h^t$ and $\bar{x}_m^t$ of the separated products can be directly determined from the density and distribution functions of the raw material.

$$\bar{x}_h^t = \frac{1}{m_h}\int_{x_{\min}}^{\bar{X}} f(x)\, x dx = x_{\min} + \int_{x_{\min}}^{\bar{X}} \left[1 - \frac{1}{m_h} F(x)\right] dx\,, \tag{7}$$

$$\bar{x}_m^t = \frac{1}{m_m}\int_{\bar{X}}^{x_{\max}} f(x)\, x dx = \bar{X} + \frac{1}{m_m}\int_{\bar{X}}^{x_{\max}} [1 - F(x)]\, dx\,. \tag{8}$$

Because of the absolutely efficient separation for the product H, $m_h f_h^t(x) = f(x)$, if $x_{\min} < x < \bar{X}$ and it is $f_h^t(x) = 0$, if $x > \bar{X}$. For the product M, $m_m f_h^t(x) = f(x)$, if $\bar{X} < x < x_{\max}$, and $f_m^t(x) = 0$, if $x < \bar{X}$. The density functions of the absolutely efficient separation are shown in Fig 2. If the raw material of Table I. with a distribution function $F(x)$ could be separated perfectely the average grain sizes of the product would be:

$$\bar{x}_h^t = 0{,}281169; \quad \bar{x}_m^t = 0{,}755718.$$

As the products do not contain defective material parts, the values of the parameters, which can be determined from (5) and (6), are zero, i.e.

$$T_{hm}^t = 0 \quad \text{and} \quad M_{hm}^t = 0.$$

It is also possible to divide the raw material in accordance with the reduction of the sample, inproportion with the mass yields. If the sample reduction is perfect, i.e. the separation zone is equal to the range of the raw material and

there is no separation according to the quality of the grains, the density and distribution functions of the separation products and also their average quality are exactly the same as those of the raw material. Such a separation is qualified as absolutely inefficient. The value of the distribution functions multiplied by the mass yield are also conatined in Fig. 2.

In the case of an absolutely inefficient deparation the laws concerning the equalization parameters hold as well, from (5) and (6) the faulty material quality and the sum of the moments can also be determined in this case.

The defective material proportion of the products is

$$T_{hm}^{i} = m_m \int_{x_{\min}}^{\overline{X}} f(x)\, dx = m_h \int_{\overline{X}}^{x_{\max}} f(x)\, dx .$$

Considering that $\int_{x_{\min}}^{\overline{X}} f(x)\, dx = m_h$, the faulty material fraction can be calculated directly from the yields:

$$T_{hm}^{i} = m_m m_h = m_h(1 - m_h) . \tag{9}$$

The sum of the first moments with respect to the equalizing parameter can be determined for absolutely inefficient separation with the aid of (10):

$$M_{hm}^{i} = m_h(x_{\max} - \overline{X}) + \int_{x_{\min}}^{\overline{X}} F(x)\, dx - m_h \int_{x_{\min}}^{x_{\max}} F(x)\, dx = m_m m_h(\overline{x}_m^t - \overline{x}_h^t) . \tag{10}$$

For a sample reduction of the raw material according to Table I. the following parameters, characterizing the products can be calculated:

$$T_{hm}^{i} = 0{,}249365,$$

$$M_{hm}^{i} = 0{,}118336 \text{ mm}^2.$$

4. Evaluation of the separation operation

The efficiency characteristics must comply with several requirements. According to BARSKIJ [1] and SCHULZ [3] it is basically important that this efficiency should

- be applicable to any physical separation and not depend on the machinery used;
- result in 1 or 100% values for perfect separation, while for a mere sampling process it should give 0, or 0%;
- be a function of the quantity and the composition of the raw material and the products;
- have a physical meaning. Its calculation should cause no difficulties.

The real separation can be evaluated on the basis of the parameters of the separation possibilities discussed in paras. 3 and 4, because in the sense of Fig. 4 its position is uniquely defined between the extreme limits.

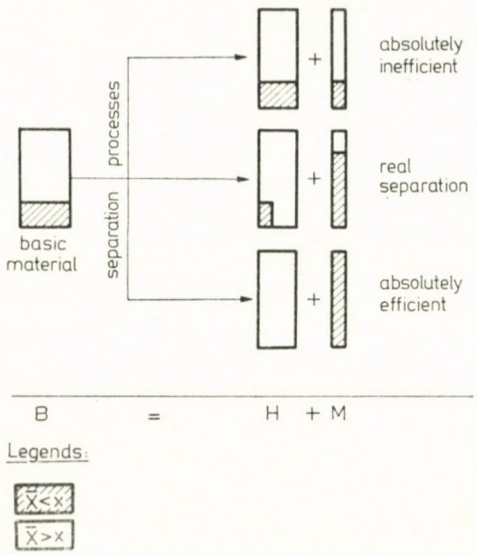

Fig. 4. Comparison of separation possibilities

The given separation operation can be evaluated by comparing its sharpness parameters to those of an absolutely efficient and of an absolutely inefficient separation.

The separation operation is the more efficient, the more it approaches the theoretically obtainable one and is the less efficient, the nearer it is to sample reduction. This definition can be formulated by Eq. (11) as follows:

$$\text{Efficiency index} = \frac{\begin{pmatrix}\text{real separation}\\ \text{parameter}\end{pmatrix} - \begin{pmatrix}\text{parameter of absolutely}\\ \text{inefficient separation}\end{pmatrix}}{\begin{pmatrix}\text{parameter of absolutely}\\ \text{efficient separation}\end{pmatrix} - \begin{pmatrix}\text{parameter of absolutely}\\ \text{innefficient separation}\end{pmatrix}} . \tag{11}$$

By using the examined parameters the following indexes indicating the efficiency of the separation can be calculated:

$$\alpha = \frac{T_{hm} - T^i_{hm}}{T^t_{hm} - T^i_{hm}} = 1 - \frac{T_{hm}}{T^i_{hm}} = 1 - \frac{T_{hm}}{m_h m_m}, \tag{12}$$

$$\beta = \frac{M_{hm} - M^i_{hm}}{M^t_{hm} - M^i_{hm}} = 1 - \frac{M_{hm}}{M^i_{hm}}, \tag{13}$$

$$T^t_{hm} = 0 \quad \text{and} \quad M^t_{hm} = 0.$$

Starting out from the faultless material fraction of any product, the index given by Eq. (12) can be deduced. For the product H the perfect material fractions of the real, the absolutely efficient and the absolutely inefficient separations are $m_h - T_{hm}$, m_h and $m_h - T^i_{hm}$. For the product M the same are $m_m - T_{hm}$, m_m and $m_m - T^i_{hm}$. The same indexes also are obtained, if the sum of the perfect mass fractions are taken, because the perfect mass fractions are in the former order $1 - 2\,T_{hm}$, 1 and $1 - 2\,T^i_{hm}$. The refore the index α is the complimentary yield of the defective material of the separation products referred to the absolutely inefficient separation and at the same time α is the yield of the real perfect mass fraction related to the absolutely efficient separation. In the case of an absolutely efficient separation the mass yield is in both cases 1.

For the separation according to Table I. the efficiency index α is in both cases 0,452688. This means that after separation the defective mass fraction has dropped by 45% and by eliminating further 55% the separation would be inefficient altogether. The yield of the perfect mass fraction of the real separation related to the absolutely efficient separation is also 0,452688.

The starting point for establishing Eq. (13) was the sum of the first moments with respect to the equalizing parameter of the defective mass fractions (6), which in the literature in accordance with the denomination given by MAYER [2, 7] are taken as the error moment of separation. Although this parameter does not entirely fulfill the prelimarily discussed requirements, it frequently occurs in qualifications.

By re-arranging Eq. (6) an expression (4) can be obtained which permits a new interpretation of the sums of first moments, not known so far in the literature.

$$M_{hm} = (\bar{x}_h - x_i)\, m_h - (\bar{x}^t_h - x_i)\, m_h,$$
$$M_{hm} = (\bar{x}^t_m - x_i)\, m_m - (x_i - \bar{x}^t_m)\, m_m,$$

x_i of Eqs. (14) is arbitrarily chosen, but after the choice is made, it remains constant.

M_{hm} is the difference of the first moments with respect to x_i, which moments also take into account the average qualities of the real and of the absolutely efficient separations. Therefore, M_{hm} is not only the (separation) error moment characterizing the given separation, but permits the comparison with the absolutely efficient separation for any separation product.

In connection with the efficiency index β (13) it is useful also to express the moment sums (6) and (14) as follows:

$$M_{hm} = m_h(\bar{x}_h - \bar{x}^t_h), \tag{15a}$$
$$M_{hm} = m_m(\bar{x}^t_m - \bar{x}_m)\,, \tag{15b}$$
$$M^i_{hm} = m_h(\bar{x} - \bar{x}^t_h)\,, \tag{16a}$$
$$M^i_{hm} = m_m(\bar{x}^t_m - \bar{x})\,. \tag{16b}$$

By these relations the irregular areas in the corresponding distribution function diagrams become rectangles. The vertical sides of the rectangles are the mass yields, their horizontal sides are the differences of the average qualities. Therefore, the moment sums M_{hm} and M^i_{hm} are the losses of the real and of the absolutely inefficient separation of the valuable component (e.g. metal loss, in classification the products of the mass yield and the differences of the mean grain sizes) as compared with the absolutely efficient separation. These valuable component masses are obtained from the product H (Eqs (15a) and (16a) (into the product M (Eqs. (15b) and (16b)). and spoil the quality of both separation products.

Introducing the former moment sums into (13), the efficiency index can be directly calculated from the qualities:

$$\beta = \frac{\bar{x} - \bar{x}_h}{\bar{x} - \bar{x}^t_h} = \frac{\bar{x} - \bar{x}_m}{\bar{x} - \bar{x}^t_m} . \tag{17}$$

Starting from this efficiency index the average quality of the raw material can be given by

$$\bar{x} = \frac{\bar{x}_h \bar{x}^t_m - \bar{x}_m \bar{x}^t_h}{(\bar{x}_h + \bar{x}^t_m) - (\bar{x}_m + \bar{x}^t_h)} .$$

Eq. (17) points out that the efficiency index β also describes the ratio of the changes in the average qualities. (13) and (17) also show that the sums of the first moments of the faulty mass fractions result in the same efficiency parameters as those calculated from the qualities of the products.

In the examined numerical example $\beta = 0{,}796272$. This efficiency parameter points out that the change in the moment sums of the faulty material fractions of the products and in the compositions of the products is approx. 80% of the possibilities.

REFERENCES

1. Barskij—Plakozin: Kriterii optimizacii razdelitelnykh procesov. Izd. Nauka, Moskva 1967
2. Leschonski, K.: Kennzeichnung einer Trennung. Ullmanns Enzyklopädie, 4 Aufl. Bd. 3, 1972
3. Schulz, N. F.: *Trans. Society of Mining Engrs.*, AIME, **247**, (1970), 81—87
4. Pethő, Sz.: Szétválasztási és homogenizálási műveletek (Separation and homogeneization operations; D. Sci. techn. dissertation), Manuscript, 1975
5. Pethő—Ortutay: Über die Beurteilungsmöglichkeiten einer Zweiproduktentrennung. Proc. of II. Vegyipari Gépészeti Konferencia (IInd Conference on Chemical Engineering), GTE Budapest, 1975, 63—70
6. Mayer, F. V.: Allgemeine Grundlagen der T-Kurven. *Aufbereitungs-Technik* 1967, Nr. 8, 429—440, Nr. 12, 673—678, 1968 Nr. 1, 14—23
7. Mayer, F. V.: Berechnung der neuen Trennschärfe-Kennwerte (Trennfehlermoment) aus der Teilungszahlen. 1. Teil, *Aufbereitungs-Technik* 1971, Nr. 2, 82—90

Qualifizierung der Trennverfahren. Die Verfasser untersuchen den Wirkungsgrad der Zweiproduktentrennung. Als extreme Fälle der Trennung werden die Musterverkleinerung und die absolut wirksame Trennung angesehen. Zusammenhänge werden abgeleitet, mit deren Hilfe die Wirksamkeit der Trennung festgestellt werden kann. Mehrere Trennverfahren können mittels der Wirksamkeitsindices auch dann qualifiziert werden, wenn die Trennparameter und die Massenausbeuten verschieden sind.

Классификация процессов разделения. Авторы в своей статье исследуют эффективность разделения с двумя продуктами. В качестве крайних случаев разделения считаются разделение с уменьшением модели и с абсолютно эффективным разделением. Выведены зависимости с помощью которых можно определить эффективность разделения. Ряд процессов разделения можно классифицировать с помощью показателей эффективности даже в том случае, когда параметры разделения и массовые выходы являются различными.

Acta Technica Academiae Scientiarum Hungaricae, Tomus 86 (3—4), pp. 421—464 (1978)

ANALYTICAL TREATMENT OF DISCRETE MODELS FOR REINFORCED AND PRESTRESSED CONCRETE MEMBERS

G. TASSI*
DOCTOR OF TECHN. SCI.

[Manuscript received January 12, 1978]

A one-dimensional model of reinforced and prestressed concrete members, composed of elements simulating the concrete, the steel and their bond has been analyzed. Analytic treatment of the equation system for the discrete model is facilitated by the possibility to invert in closed form the coefficient matrix of the system. Cracks are taken into consideration by modifying the coefficient matrix by one diade for each. Also a method for reckoning with plastic deformations will be outlined. The obtained closed formulae show how this phenomenon related to cracking develops for one, two or more cracks. — Applicability of the relationships is demonstrated by examples. Formulae of internal forces, deformations and crack width involving also the mesh of the discrete model, the effect of selecting the mesh can be weighed.

1. Introduction

The analysis of limit states of deformation and cracking ([16], [25]), gains increasingly more importance in the development of limit state design of reinforced and prestressed concrete beams. Several problems are inapplicable to the classic theory of reinforced concrete, reducing the problems to relationships of elementary methods of the strength of materials. Analysis of local forces in deep girders, at crack surroundings, etc. require computations taking general plane (or spatial) strees state into consideration.

To solve bi- and tri-dimensional problems, finite elements methods are increasingly gaining ground ([1], [5], [10], [11], [26]), some of them specify reckoning with the effect of reinforcement, cracking and non-linearity. The theory based on framework analogy makes it possible to produce a comprehensive, uniform model of reinforced and prestressed concrete units in stress states I and II, possibly with the consideration of certain non-linearities ([18]). The bi- or tri-dimensional discrete problem can, however, be demonstrated not to be solvable in closed form even with a suitably chosen grid, just as no closed analytic solution of continuum problems is possible even in special cases ([20]).

The one dimensional finite model even composite, or having discontinuities will be shown to be suitable for analysis provided, of course, equidistant nodes have been assumed.

* Prof. Dr. G. Tassi, Veres Péter út 181. H-1165 Budapest, Hungary

2. Field of applications and purpose of one-dimensional models

One-dimensional models are expedient for examining local stresses in units with force transfer between two units in truly equidistant points, such as in welded fabric- or ladder-reinforced units ([3], [7]) or multiple Dmitriev-loops ([4], [6]). The models also lend themselves for examining the interaction between two different units continuously joined. A given problem involving the model of a linear bar of two connected units has been demonstrated ([22]) to be accessible to matrix analysis, and so are problems inexpressible by *one* linear equation system. Formulae of total elongation due to axial forces, of stresses in concrete and reinforcement, as well as of bond have been established. Other possibilites are to determine the effect of cracking and the arising non-linearity of the relationship between bond and the relative displacement on the stress and deformation states.

There are some truly one-dimensional problems (ties and stays, etc.) that are continuous or really discrete. Calculated characteristics of the forces and reactions of models for bi- and tri-dimensional problems depend on the mesh, the more so if the quantities are related to effective discontinuities, cracks, local plastic deformations. Closed solutions of the one-dimensional problem directly or indirectly contain the mesh distance, facilitating the evaluation of results of problems solved by numerical methods. One-dimensional experimental models lend themselves for testing the type of bond between concrete to steel, the stiffness of reinforced or prestressed concrete members, the cracking conditions (*e.g.* [2], [12], [23]) and development of suitable computation methods will permit tracing and evaluating these tests.

3. One-dimensional model analysis of reinforced and prestressed concrete members

Several fundamental cases will be presented which will help in deducing some general conclusions.

3.1. Principle and basic forms of models

In the model — in elastic, uncracked condition — the concrete unit is represented by a bar of given stiffness, and the reinforcing or prestressing steel by another. Bond is represented by bars of given mechanical properties connecting the two elements. This is in harmony with the concept that the bond force is a function of relative displacement ([17]). In the model the axes of elements simulating the concrete, the steel and the bond coincide in the rectilinear axis of the composite bar, and it is plotted only for the sake of demostration as in Fig. 1 and simplified in Fig. 2.

3.2. Model of reinforced or prestressed concrete unit varieties in the case of concrete and steel in elastic condition

Let us consider first the build-up of the models, to be followed by the solution of actual problems.

3.21. Consideration of bond type in a coaxial bar of steel and concrete units

The bond is rather complex, to be spoken of as a strength characteristic of some structural material only by analogy.

3.211. Rigid connection

With no relative displacement between originally common points of concrete and steel, the model of the unit is that in Fig. 3. Let be b the stiffness of the model section for the concrete, and vb that for the steel, then the stiffness matrix of the member may be written as

$$\mathbf{K} = b(1+v)\begin{bmatrix} 1 & -1 & & & & & \\ -1 & 2 & -1 & & & & \\ & \cdot & \cdot & \cdot & & & \\ & & \cdot & \cdot & \cdot & & \\ & & & \cdot & \cdot & \cdot & \\ & & & & -1 & 2 & -1 \\ & & & & & -1 & 2 \end{bmatrix}$$

Without entering into details of the rigid connection, notice that matrix **K** is non-singular (supported structure) symmetric, tri-diagonal with a so-called one-pair matrix as its inverse ([9], [13]). The peculiarity of this special case is pointed out by the remark that — considering the bonding force as unknown — the coefficient matrix of the set of equations written according to the method of forces is a one-pair matrix.

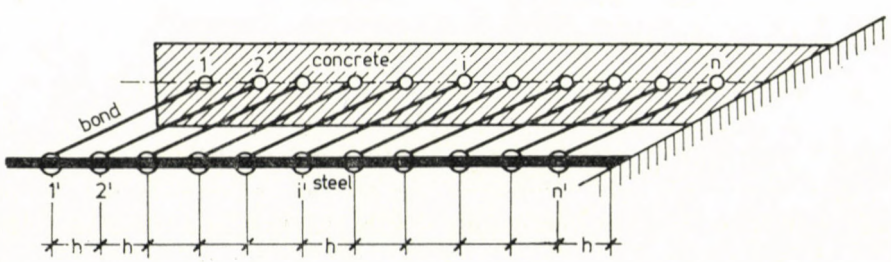

Fig. 1

3.212. Rigid elastic connection

Considering relative displacement to be zero up to a given value of bond stress, and thereafter to vary linearly, a section of the model has to be assumed to be of rigid connection, thereafter the bars simulating the linear connection (Fig. 4) of stiffness γb will have the stiffness matrix

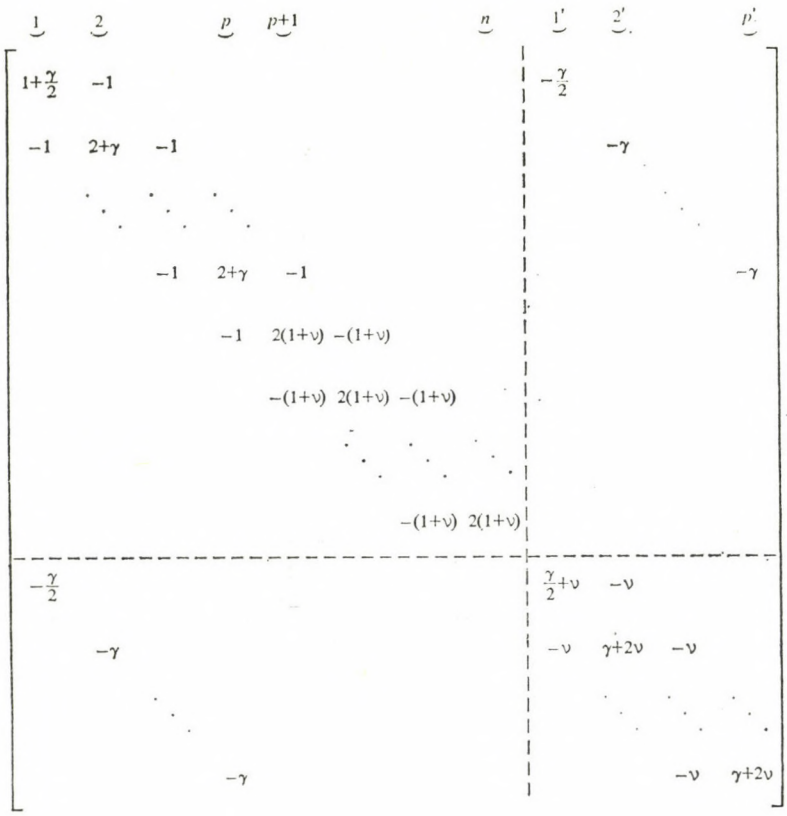

3.213. Elastic connection

The assumption of an initially linear connection between bond force and relative displacement results in model of Fig. 5. Particulars of the coefficient matrix of the set of equations written according to the displacement method — the stiffness matrix — will be found in item 4.1.

Here again it is only pointed out for the sake of interest that the coefficient matrix of the set of equations written by the force method — again with bond forces as unknowns — is a linear combination of a one-pair matrix and of the unit matrix modified in its element of subscript 1,1.

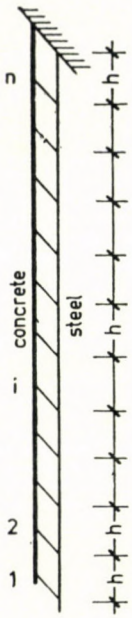

Fig. 2

Fig. 3

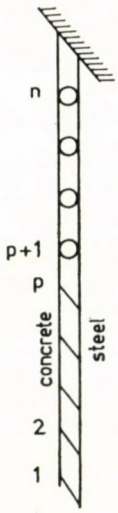

Fig. 4

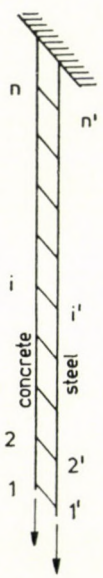

Fig. 5

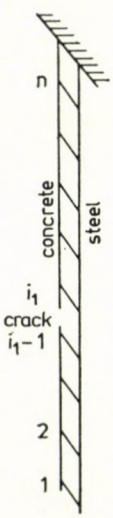

Fig. 6

3.214. Elastic-plastic connection

Assuming an initially linear relation between the bond force and the relative displacement, and a constant force after a certain displacement, the connection bar has to be considered an elastic-plastic material. The fictitious connection bar is elongated by

$$\Delta l = u_i - u_{n+i} = u_{bi} - u_{ai}.$$

For one connection bar yielded, vector $\mathbf{q}_m$ in the equation (see [14], [18])

$$\mathbf{K}''\mathbf{u}'' = q\mathbf{q} + \mathbf{q}_m$$

becomes

$$\mathbf{q}_m = \begin{bmatrix} 0 \\ \vdots \\ 0 \\ T_F \\ 0 \\ \vdots \\ 0 \\ \hline 0 \\ \vdots \\ 0 \\ -T_F \\ 0 \\ \vdots \\ 0 \end{bmatrix} \begin{matrix} \\ \\ \\ (i \\ \\ \\ \\ \\ \\ \\ \\ (n+i \\ \\ \\ \end{matrix} = T_F \left[\begin{array}{c} \mathbf{e}_i \\ \hline -\mathbf{e}_i \end{array}\right] = T_F \mathbf{v},$$

where $\mathbf{e}_i$ is a n-th order i-th unit vector, hence $\mathbf{v}$ has $2n$ elements. Modified coefficient matrix $\mathbf{K}''$ is obtained by cancelling the element for the yielded bar stiffness. If one connecting bar yields, the coefficient matrix valid before the bar yield is modified by a diade, hence the matrix

$$b\gamma\mathbf{v}\mathbf{v}^*$$

has to be subtracted.

3.22. Consideration of the crack in the elastic model

Considering the concrete as a linearly elastic material of tensile stiffness, or if there is an a priori cracked element, model in item *3.2* will of course change. Obviously, omission of a bar (item *3.14* in [18]) corresponds to the modification of the stiffness matrix by a diade. In case of the rupture of the

concrete section between points with subscripts $i_1 - 1$ and i_1 (Fig. 6) the original coefficient matrix has to be diminished by a diade producible from vectors corresponding to the modification of the nodal stiffnesses of two neighbouring concrete points. The diade to be subtracted for the concrete cracking $b\mathbf{ww}^*$ will later be explained to be with

$$\mathbf{w} = \begin{bmatrix} \mathbf{e}_{i_1-1} - \mathbf{e}_{i_1} \\ \hline 0 \end{bmatrix},$$

and so can the subsequent cracks be reckoned with.

3.3. The load

Producing the inverse of the original or modified coifficient matrix in closed form for an arbitrary load, model nodal displacements are obtained by multiplication. The internal forces can be calculated from the displacements. The one-parameter load can be written in the form of $q\mathbf{q}$ in the general case, where the vector of $2n$ elements

$$\mathbf{q} = \begin{bmatrix} q_1 \\ q_2 \\ \vdots \\ q_n \\ \hline q_{n+1} \\ q_{n+2} \\ \vdots \\ q_{2n} \end{bmatrix} = q \begin{bmatrix} c_1 \\ c_2 \\ \vdots \\ c_n \\ \hline c_{n+1} \\ c_{n+2} \\ \vdots \\ c_{2n} \end{bmatrix}$$

applies to the case described in item *3.213*. In the case of item *3.211* the vector may have n elements, the transitory case being that of the rigid-elastic connection (item *3.212*). The purpose of analysis is met by determining the forces in the model exclusively for those in the free end, although neither the general case has theoretical hindrances. In general, the unit end load is

$$\mathbf{l} = c \begin{bmatrix} c_b \\ 0 \\ \vdots \\ 0 \\ \hline c_a \\ 0 \\ \vdots \\ 0 \end{bmatrix} : \begin{bmatrix} c_b\ \mathbf{e}_1 \\ \hline c_a\ \mathbf{e}_1 \end{bmatrix},$$

with q in terms of N(or kp), c_b and c_a in pure numbers or vice versa.

Let us consider now some peculiar load cases. In case of perfect anchorage in the prestressed bar ([24]), the concrete unit is subject to force

$$P_b = -\frac{P_f}{1+\nu},$$

and the steel to

$$P_a = \frac{P_f}{1+\nu},$$

P_f being the prestressing force. Thus, applying load

$$\mathbf{q} = q\begin{bmatrix} \mathbf{e}_1 \\ \hline \nu\mathbf{e}_1 \end{bmatrix}, \quad q = \frac{P_f}{1+\nu}$$

in the case of the elastic crack-free member is required to develop a strain condition homogeneous along its length, and identical to that due to the fully anchored force P_f, and, obviously, in this case the connection force will be zero throughout (see[24]). Of course, the prestressing steel force is obtained by modifying the prestressing force by the steel force given by the solution.

To analyze the tendon anchorage, the load vector may be assumed according to the following considerations. For a linear relation between the bond force and the relative displacement, calculation shows impossibility of full anchorage over a finite length ([24]). Force transfer characteristics are obtained by applying the load

$$\mathbf{q} = q\begin{bmatrix} 0 \\ \hline \mathbf{e}_1 \end{bmatrix}, \quad q = P_f \,.$$

In a cracking condition test, if the free end of the steel bar is loaded, load vector

$$\mathbf{q} = q\begin{bmatrix} 0 \\ \hline \mathbf{e}_1 \end{bmatrix},$$

and clamping the concrete end vector

$$\mathbf{q} = q\begin{bmatrix} \mathbf{e}_1 \\ \hline 0 \end{bmatrix}$$

have to be applied.

Different structural designs of stays and ties involve different cases of c_b and c_a.

4. Detailed analysis of the elastic crack-free model

Let us consider the model seen in Fig. 7 for the case of linearly elastic concrete, steel and their bond.

4.1. The coefficient matrix and its inverse

With the introduced notations, the coefficient matrix becomes

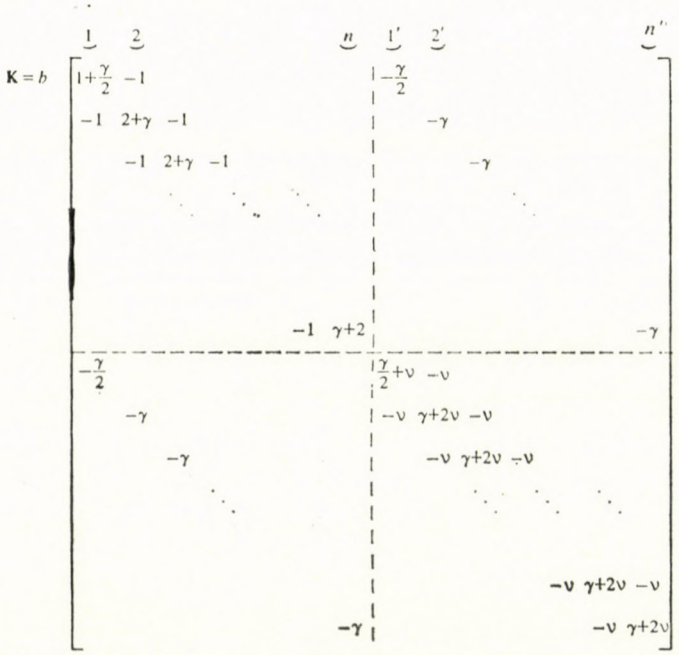

demonstrable to be a special case of the plane reinforced unit model (item *3.24* in [18]).

To need as few basic type blocks for writing the coefficient matrix as possible, take the form

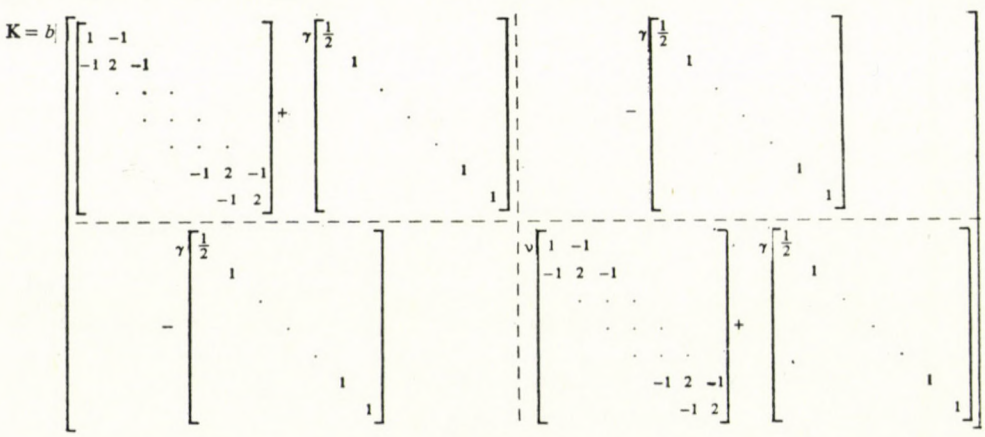

Let $D = \gamma \begin{bmatrix} \frac{1}{2} & & & \\ & 1 & & \\ & & \ddots & \\ & & & \frac{1}{2} \end{bmatrix}$ and $G = \begin{bmatrix} 1 & -1 & & & \\ -1 & 2 & -1 & & \\ & \ddots & \ddots & \ddots & \\ & & & -1 & 2 \end{bmatrix}$,

giving the coefficient matrix in the form

$$\mathbf{K} = b \begin{bmatrix} \mathbf{G} + \mathbf{D} & -\mathbf{D} \\ -\mathbf{D} & \nu\mathbf{G} + \mathbf{D} \end{bmatrix}. \tag{2}$$

Inverse of this matrix partitioned to four blocks can be written in the known, also partitioned form ([13]).

G being a non-singular, symmetric tri-diagonal matrix, its inverse is known to be a one-pair matrix ([9], [13]). A simple calculation proves

$$G^{-1} = B = \begin{bmatrix} n & n-1 & n-2 & n-3 & \cdot & 1 \\ n-1 & n-1 & n-2 & n-3 & \cdot & 1 \\ n-2 & n-2 & n-2 & n-3 & \cdot & 1 \\ n-3 & n-3 & n-3 & n-3 & \cdot & 1 \\ \cdot & \cdot & \cdot & \cdot & \cdot & \cdot \\ 1 & 1 & 1 & 1 & \cdot & 1 \end{bmatrix} \tag{3}$$

with elements possible in the form

$$B_{ij} = \begin{cases} n+1-j, & \text{ha} \quad i \leq j, \\ n+1-i, & \text{ha} \quad i \geq j. \end{cases}$$

Hence, the inverse sought for can be written as

$$\frac{1}{b}\mathbf{K}^{-1} = \frac{1}{b} \begin{bmatrix} \mathbf{B}(\mathbf{E} - \mathbf{DC}) & \frac{1}{\nu}\mathbf{BDC} \\ \frac{1}{\nu}\mathbf{BDC} & \frac{1}{\nu}\mathbf{B}\left(\mathbf{E} - \frac{1}{\nu}\mathbf{DC}\right) \end{bmatrix}, \tag{4}$$

where

$$\mathbf{C} = \left[\mathbf{G} + \frac{1+\nu}{\nu}\mathbf{D}\right]^{-1}.$$

Since the resulting C is the inverse of a tri-diagonal matrix again, hence a one-pair matrix, its elements will be obtained by means of parameter introduced by the transformation.

$$2 + \frac{1+\nu}{\nu}\gamma = 2 \operatorname{ch}\vartheta; \quad i.e. \quad 4 \operatorname{sh}^2\frac{\vartheta}{2} = \frac{1+\nu}{\nu}\gamma$$

in the form

$$C_{ij} = \begin{cases} \dfrac{\operatorname{ch}(i-1)\vartheta}{\operatorname{ch} n\vartheta} \dfrac{\operatorname{sh}(n+1-j)\vartheta}{\operatorname{sh}\vartheta}; & \text{if} \quad i \leq j \\ \dfrac{\operatorname{ch}(j-1)\vartheta}{\operatorname{ch} n\vartheta} \dfrac{\operatorname{sh}(n+1-i)\vartheta}{\operatorname{sh}\vartheta}; & \text{if} \quad i \geq j. \end{cases}$$

In particular,

$$\operatorname{sh}\vartheta \operatorname{ch} n\vartheta \mathbf{C} =$$

$$= \begin{bmatrix} \operatorname{sh} n\vartheta & \operatorname{sh}(n-1)\vartheta & \operatorname{sh}(n-2)\vartheta & \dots \operatorname{sh}2\vartheta & \operatorname{sh}\vartheta \\ \operatorname{sh}(n-1)\vartheta & \operatorname{sh}(n-1)\vartheta\operatorname{ch}\vartheta & \operatorname{sh}(n-2)\vartheta\operatorname{ch}\vartheta & \dots \operatorname{sh}2\vartheta\operatorname{ch}\vartheta & \operatorname{sh}\vartheta\operatorname{ch}\vartheta \\ \operatorname{sh}(n-2)\vartheta & \operatorname{sh}(n-2)\vartheta\operatorname{ch}\vartheta & \operatorname{sh}(n-2)\vartheta\operatorname{ch}2\vartheta & \dots \operatorname{sh}2\vartheta\operatorname{ch}2\vartheta & \operatorname{sh}\vartheta\operatorname{ch}2\vartheta \\ \cdot & \cdot & \cdot & \cdots \cdot & \cdot \\ \cdot & \cdot & \cdot & \cdots \cdot & \cdot \\ \cdot & \cdot & \cdot & \cdots \cdot & \cdot \\ \operatorname{sh}2\vartheta & \operatorname{sh}2\vartheta \cdot \operatorname{ch}\vartheta & \operatorname{sh}2\vartheta \cdot \operatorname{ch}2\vartheta & \dots \operatorname{sh}2\vartheta\operatorname{ch}(n-2)\vartheta & \operatorname{sh}\vartheta\operatorname{ch}(n-2)\vartheta \\ \operatorname{sh}\vartheta & \operatorname{sh}\vartheta \cdot \operatorname{ch}\vartheta & \operatorname{sh}\vartheta \cdot \operatorname{ch}2\vartheta & \dots \operatorname{sh}2\vartheta\operatorname{ch}(n-2)\vartheta & \operatorname{sh}\vartheta\operatorname{ch}(n-1)\vartheta \end{bmatrix}. \tag{5}$$

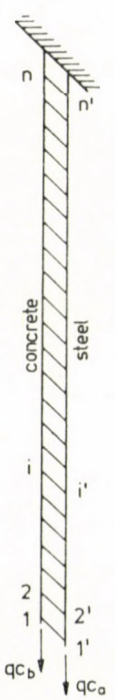

Fig. 7

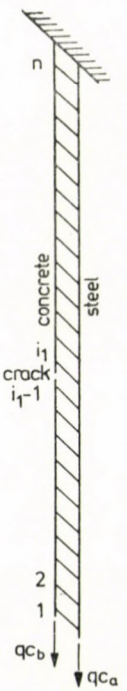

Fig. 8

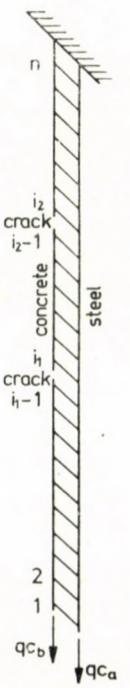

Fig. 9

The inverse will be transformed from (4) to the clear form

$$\frac{1}{b}(1-\nu)\,\mathbf{K}^{-1}=\frac{1}{b}\begin{bmatrix}\mathbf{B}+\nu\mathbf{C} & \mathbf{B}-\mathbf{C}\\ \mathbf{B}-\mathbf{C} & \mathbf{B}+\dfrac{1}{\nu}\mathbf{C}\end{bmatrix}. \tag{6}$$

4.2. The load and the nodal displacements quantities needed for determining internal forces

Since elements of the inverse (6) can be written in closed form, the problem can be solved for any load case. For examining reinforced or prestressed concrete bar behaviour phenomena, it is sufficient to consider loads on free member ends. Partitioning **K** as in (1) in the equation system of the displacement method,

$$\mathbf{u}=\begin{bmatrix}\mathbf{u}_b\\ \hline \mathbf{u}_b\end{bmatrix}=\frac{1}{b}\mathbf{K}^{-1}\mathbf{q}=\frac{1}{b}\mathbf{K}^{-1}q\begin{bmatrix}c_b\,\mathbf{e}_1\\ \hline c_a\,\mathbf{e}_1\end{bmatrix}, \tag{7}$$

q being the load parameter and $\mathbf{e}_1$ a first unit vector with n elements. Utilizing blocks in (6) of the inverse $\mathbf{K}^{-1}$

$$\frac{q}{b}\mathbf{K}^{-1}\begin{bmatrix}c_b\,\mathbf{e}_1\\ \hline c_a\,\mathbf{e}_1\end{bmatrix}=\frac{q}{b}\frac{1}{1+\nu}\cdot$$

$$\cdot\begin{bmatrix}\left\{(c_b+c_a)\,(n+1-i)+(c_b\nu-c_a)\,\dfrac{\operatorname{sh}(n+1-i)\,\vartheta}{\operatorname{sh}\vartheta\operatorname{ch}n\vartheta}\right\}\\ \left\{(c_b+c_a)\,(n+1-i)-\dfrac{c_b\nu-c_a}{\nu}\,\dfrac{\operatorname{sh}(n+1-i)\,\vartheta}{\operatorname{sh}\vartheta\operatorname{ch}n\vartheta}\right\}\end{bmatrix}. \tag{8}$$

The entire bar stiffnes is characterized by $u_{b1}^{(0)}u_{a1}^{(0)}$; (index $(^0)$ refers to crackless-ness),

$$u_{b1}^{(0)}=\frac{q}{b}\frac{1}{1+\nu}\left\{n(c_b+c_a)+(c_b\nu-c_a)\,\frac{\operatorname{sh}n\vartheta}{\operatorname{sh}\vartheta\operatorname{ch}n\vartheta}\right\},$$

$$u_{a1}^{(0)}=\frac{q}{b}\frac{1}{1+\nu}\left\{n(c_b+c_a)-\frac{c_b\nu-c_a}{\nu}\,\frac{\operatorname{sh}n\vartheta}{\operatorname{sh}\vartheta\operatorname{ch}n\vartheta}\right\}. \tag{9}$$

Internal forces can be determined from the relative displacement of neighbouring nodes, in concrete

$$\Delta u_{bi}^{(0)} = u_{bi}^{(0)} - u_{bi+1}^{(0)};\ (u_{bn+1} = 0),$$

and in steel

$$\Delta u_{ai}^{(0)} = u_{ai}^{(0)} - u_{ai+1}^{(0)};\ (u_{a_{n+1}} = 0).$$

Introducing a matrix forming differences

$$\mathbf{N} = \begin{bmatrix} 1 & -1 & & & & \\ & 1 & -1 & & & \\ & & \cdot & \cdot & & \\ & & & \cdot & \cdot & \\ & & & & 1 & -1 \\ & & & & & 1 \end{bmatrix} (n$$

the vector of relative displacements can be written as

$$\begin{bmatrix} \Delta \mathbf{u}_b \\ \hline \Delta \mathbf{u}_a \end{bmatrix} = \begin{bmatrix} \mathbf{N} & \mathbf{0} \\ \hline \mathbf{0} & \mathbf{N} \end{bmatrix} \begin{bmatrix} \mathbf{u}_b \\ \hline \mathbf{u}_a \end{bmatrix}. \tag{10}$$

Using relationship (7), elements of the hypervector made of relative displacements are expressed by

$$\begin{bmatrix} \Delta u_{bi}^{(0)} \\ \hline \Delta u_{ai}^{(0)} \end{bmatrix} = \frac{1}{1+\nu} \frac{q}{b} \begin{bmatrix} c_b + c_a + (c_b \nu - c_a) \dfrac{\operatorname{ch}\left(n - i + \frac{1}{2}\right)\vartheta}{\operatorname{ch} n\vartheta \operatorname{ch}^3 \frac{\vartheta}{2}} \\ \\ c_b + c_a - \dfrac{c_b \nu - c_a}{\nu} \dfrac{\operatorname{ch}\left(n - i + \frac{1}{2}\right)\vartheta}{\operatorname{ch} \vartheta \operatorname{ch} \frac{\vartheta}{2}} \end{bmatrix} \begin{matrix} (n \\ \cdot \\ (2n \end{matrix} \tag{11}$$

Elements of the relative displacements for determining the bond model bar forces, hence of the difference vector

$$\Delta u_{bai}^{(0)} = u_{bi}^{(0)} - u_{ai}^{(0)}$$

are

$$u_{bi}^{(0)} - u_{ai}^{(0)} = \frac{q}{b} \frac{1}{\nu} (c_b \nu - c_a) \frac{\operatorname{sh}(n - i + 1)\vartheta}{\operatorname{ch} n\vartheta \operatorname{sh} \vartheta}. \tag{12}$$

5. Model of the elastic, cracked member

As referred to in *3.22*, concrete cracking can be simulated in the model by modifying the stiffness matrix by a diade.

5.1. Case of a single crack

Rupture of the bar connecting points $i_1 - 1$ and i_1 (Fig. 8) involves subtraction of matrix of rank 1 from the original matrix

$$b \begin{bmatrix} & & \\ & 1 & -1 \\ & -1 & 1 \\ & & \end{bmatrix} \begin{matrix} \\ (i_1 \\ (i_1 \\ \\ (2n \end{matrix}$$

The matrix to be subtracted is equivalent to the diade

$$b\mathbf{w}\mathbf{w}^* = b \left[\begin{array}{c} \mathbf{e}_{i_1-1} - \mathbf{e}_{i_1} \\ \hline 0 \end{array}\right] [\mathbf{e}^*_{i_1-1} - \mathbf{e}^*_{i_1} \underbrace{|}_{n} \underbrace{0}_{2n}] . \tag{13}$$

The equation system of modified coefficient matrix is solved by using the theorem by SHERMAN and and MORRISON ([13], [15]), producing the inverse of the matrix modified by a diade by modifying the original inverse by a diade

$$\frac{1}{b}\left\{\left[\begin{array}{c} \mathbf{K} \\ \\ \end{array}\right] - \left[\begin{array}{c} \mathbf{w} \\ \\ \end{array}\right] [\mathbf{w}^* \ ]\right\}^{-1} = \frac{1}{b}\left\{\mathbf{K}^{-1} + \frac{\mathbf{K}^{-1}\mathbf{w}\mathbf{w}^*\mathbf{K}^{-1}}{1 - \mathbf{w}^*\mathbf{K}^{-1}\mathbf{w}}\right\} . \tag{14}$$

Multiplied by the load vector, the vector (7) $\mathbf{u} = \mathbf{u}^{(0)}$ has to be increased by the vector

$$\mathbf{m}^{(1)} = \left[\begin{array}{c} \mathbf{m}^{(1)}_b \\ \hline \mathbf{m}^{(1)}_a \end{array}\right] = \frac{1}{b} \frac{\mathbf{K}^{-1}\mathbf{w}\mathbf{w}^*\mathbf{K}^{-1}\mathbf{q}}{1 - \mathbf{w}^*\mathbf{K}^{-1}\mathbf{w}} \tag{15}$$

expediently calculated by multiplying the vector

$$\mathbf{K}^{-1}\mathbf{w} = \frac{1}{1 + v}\left[\begin{array}{c} (\mathbf{B} + v\mathbf{C})(\mathbf{e}_{i_1-1} - \mathbf{e}_{i_1}) \\ \hline (\mathbf{B} - \mathbf{C})(\mathbf{e}_{i_1-1} - \mathbf{e}_{i_1}) \end{array}\right] \begin{matrix} (n \\ (2n \end{matrix} \tag{16}$$

by the scalar value

$$\frac{1}{b} \frac{\mathbf{w}^*\mathbf{K}^{-1}\mathbf{q}}{1 - \mathbf{w}^*\mathbf{K}^{-1}\mathbf{w}} . \tag{17}$$

Substituting elements (3) and (5) of matrices **B** and **C** and using them to produce vectors

$$\mathbf{B}(\mathbf{e}_{i_1-1} - \mathbf{e}_{i_1}) = \begin{bmatrix} 1 \\ 1 \\ \vdots \\ 1 \\ 0 \\ \vdots \\ 0 \end{bmatrix} \begin{matrix} (1 \\ (2 \\ \\ (i_1 - 1 \\ (i_1 \\ \\ (n \end{matrix}$$

and

$$\operatorname{ch} n\vartheta \operatorname{sh} \vartheta \mathbf{C}(\mathbf{e}_{i_1-1} - \mathbf{e}_{i_1}) =$$

$$\begin{bmatrix} \operatorname{sh}(n+2-i_1)\vartheta - \operatorname{sh}(n+1-i_1)\vartheta \\ [\operatorname{sh}(n+2-i_1)\vartheta - \operatorname{sh}(n+1+i_1)\vartheta] \operatorname{ch}\vartheta \\ \vdots \\ [\operatorname{sh}(n+2-i_1)\vartheta - \operatorname{sh}(n+1-i_1)\vartheta] \operatorname{ch}(i_1-2)\vartheta \\ \hline \operatorname{sh}(n+1-i_1)\vartheta[\operatorname{ch}(i_1-2)\vartheta - \operatorname{ch}(i_1-1)\vartheta] \\ \operatorname{sh}(n-i_1)\vartheta[\operatorname{ch}(i_1-2)\vartheta - \operatorname{ch}(i_1-1)\vartheta] \\ \vdots \\ \operatorname{sh}\vartheta[\operatorname{ch}(i_1-2)\vartheta - \operatorname{ch}(i_1-1)\vartheta] \end{bmatrix} \begin{matrix} (1 \\ (2 \\ \\ (i_1-1 \\ (i_1 \\ (i_1+1 \\ \\ (n \end{matrix}$$

resp. permits to calculate elements of the model part simulating the concrete or the steel — either $i \leq i_1 - 1$ or $i \geq i_1 -$ constituting vector (17). Writing this latter in the form $\begin{bmatrix} \varphi^{(1)} \\ \hline \psi^{(1)} \end{bmatrix}$, denoting its elements for the concrete and the steel by $\varphi_i^{(1)}$ and $\psi_i^{(1)}$ respectively, results in terms

$$[(\mathbf{B} + \nu\mathbf{C})(\mathbf{e}_{i_1-1} - \mathbf{e}_{i_1})]_i = \varphi_i^{(1)} =$$

$$= \begin{cases} 1 + \dfrac{\nu \operatorname{ch}\left(n + \dfrac{3}{2} - i_1\right)\vartheta}{\operatorname{ch} n\vartheta \operatorname{ch}\dfrac{\vartheta}{2}} \operatorname{ch}(i-1)\vartheta; & \text{if} \quad i \leq i_1 - 1\,, \\ \\ -\dfrac{\nu \operatorname{sh}\left(i_1 - \dfrac{3}{2}\right)\vartheta}{\operatorname{ch} n\vartheta \operatorname{ch}\dfrac{\vartheta}{2}} \operatorname{sh}(n+1-i)\vartheta; & \text{if} \quad i \geq i_1\,, \end{cases} \tag{18}$$

$$[(\mathbf{B}-\mathbf{C})\,(\mathbf{e}_{i_1-1}-\mathbf{e}_{i_1})]_i = \psi_i^{(1)} =$$

$$= \begin{cases} 1 - \dfrac{\operatorname{ch}\left(n+\dfrac{3}{2}-i_1\right)\vartheta}{\operatorname{ch} n\vartheta \operatorname{ch}\dfrac{\vartheta}{2}} \operatorname{ch}(i-1)\vartheta; & \text{if} \quad i \leq i_1 - 1\ , \\ \dfrac{\operatorname{sh}\left(i_1-\dfrac{3}{2}\right)\vartheta}{\operatorname{ch} n\vartheta \operatorname{ch}\dfrac{\vartheta}{2}} \operatorname{sh}(n+1-i)\vartheta; & \text{if} \quad i \geq i_1 . \end{cases}$$

The determined $\varphi_i^{(1)}$ $\psi_i^{(1)}$ help to obtain the scalar multiplier (15) by a simple calculation as follows (for the case where the one-parameter load acts at the bar end alone)

$$\frac{1}{b}\frac{\mathbf{w}^*\mathbf{K}^{-1}\mathbf{q}}{1-\mathbf{w}^*\mathbf{K}^{-1}\mathbf{w}} = \frac{q}{b}\frac{1}{1+\nu}\frac{c_b\varphi_1^{(1)}+c_a\psi_1^{(1)}}{1-\dfrac{1}{1+\nu}(\varphi_{i_1-1}^{(1)}-\varphi_{i_1}^{(1)})}\ . \tag{19}$$

Eqs (18) permit to replace (19) by

$$\frac{q}{b}\frac{1}{\nu}\frac{c_b+c_a+(c_b\nu-c_a)\dfrac{\operatorname{ch}\left(n+\dfrac{3}{2}-i_1\right)\vartheta}{\operatorname{ch} n\vartheta \operatorname{ch}\vartheta\dfrac{1}{2}\vartheta}}{1+\dfrac{\operatorname{sh}(n-1)\vartheta-\operatorname{sh} n\vartheta-2\operatorname{sh}^2\dfrac{\vartheta}{2}\operatorname{sh}(n-2i_1+3)\vartheta}{\operatorname{ch} n\vartheta \operatorname{sh}\vartheta}}$$

which, multiplied by vector (17) and considering (18) leads to vector $\mathbf{m}^{(1)}$ according to (15). From among absolute displacements, only that at the free bar end is of importance, of values $u_{b1}^{(1)}$ and $u_{a1}^{(1)}$. Bar end displacements are obtained as sum of $u_{b1}^{(0)}$ and $u_{a1}^{(0)}$ for the crack-free case, and of $m_{b1}^{(1)}$ and $m_{a1}^{(1)}$ from crack modifications. After substitutions

$$m_{b1}^{(1)} = \frac{q}{b}\frac{1}{(1+\nu)\,2\operatorname{sh}\left(i_1-\dfrac{3}{2}\right)\vartheta \operatorname{sh}\vartheta}\left\{c_b+c_a+\right.$$

$$\left.+(c_b\nu-c_a)\frac{\operatorname{ch}\left(n+\dfrac{3}{2}-i_1\right)\vartheta}{\operatorname{ch} n\vartheta \operatorname{ch}\dfrac{\vartheta}{2}}+\frac{c_b\nu-c_a}{\nu}+\frac{c_b+c_a}{\nu}\frac{\operatorname{ch} n\vartheta \operatorname{ch}\dfrac{\vartheta}{2}}{\operatorname{ch}\left(n+\dfrac{3}{2}-i_1\right)\vartheta}\right\};$$

and so $m_{a1}^{(1)}$. Increasing the modification by the displacement for a crack-free bar (9) yields

$$u_{b1}^{(1)} = \frac{q}{b}\frac{1}{1+\nu}\left\{n(c_b + c_a) + (c_b\nu - c_a)\frac{\operatorname{th} n\vartheta}{\operatorname{sh}\vartheta} + \right.$$

$$+ \frac{1}{2\operatorname{sh}\left(i_1 - \frac{3}{2}\right)\vartheta \operatorname{sh}\vartheta}\left[(c_b + c_a)\left(1 + \frac{1}{\nu}\frac{\operatorname{ch} n\vartheta \operatorname{ch}\frac{\vartheta}{2}}{\operatorname{ch}\left(n + \frac{3}{2} - i_1\right)\vartheta}\right) + \right.$$

$$\left.\left. + (c_b\nu - c_a)\left(\frac{1}{\nu} + \frac{\operatorname{ch}\left(n + \frac{3}{2} - i_1\right)\vartheta}{\operatorname{ch} n\vartheta \operatorname{ch}\frac{\vartheta}{2}}\right)\right]\right\},$$

and so $u_{a1}^{(1)}$ can be written

The vector of displacement modification due to cracking under arbitrary load is obtained according to (14) by multiplying the load vector by the second term in (14). Making use of quantities $\varphi_i^{(1)}$ and $\psi_i^{(1)}$ introduced in (18), reducing and simplifying yields the modifiying matrix, a single diade, in the form

$$\frac{1}{b}\frac{1}{\nu}\frac{1}{1+\nu}\frac{1}{\operatorname{ch} n\vartheta \operatorname{sh}\vartheta \operatorname{ch}\left(n + \frac{3}{2} - i_1\right)\vartheta \operatorname{sh}\left(i_1 - \frac{3}{2}\right)\vartheta}\begin{bmatrix}\Phi_i^{(1)} \\ \hline \Psi_i^{(1)}\end{bmatrix}[\Phi_j^{(1)} \mid \Psi_j^{(1)}],$$

where

$$\Phi_i^{(1)} = \begin{cases} \operatorname{ch} n\vartheta \operatorname{ch}\frac{\vartheta}{2} + \nu \operatorname{ch}\left(n + \frac{3}{2} - i_1\right)\vartheta \operatorname{ch}(i-1)\vartheta; & \text{if} \quad i \leq i_1 - 1, \\ -\nu \operatorname{sh}\left(i_1 - \frac{3}{2}\right)\vartheta \operatorname{sh}(n+1-i)\vartheta; & \text{if} \quad i \geq i_1, \end{cases}$$

$$\Psi_i^{(1)} = \begin{cases} \operatorname{ch} n\vartheta \operatorname{ch}\frac{\vartheta}{2} - \operatorname{ch}\left(n + \frac{3}{2} - i_1\right)\vartheta \operatorname{ch}(i-1)\vartheta; & \text{if} \quad i \leq i_1 - 1\ , \\ \operatorname{sh}\left(i_1 - \frac{3}{2}\right)\vartheta \operatorname{sh}(n+1-i)\vartheta; & \text{if} \quad i \geq i_1. \end{cases}$$

Of course, now the absolute displacement vector will be obtained by adding the modification vector to (8) defined by the given q. The vector of relative

displacements between neighbouring nodes, needed for computing internal forces in each bar section is obtained by forming product

$$\left[\begin{array}{c|c} \mathbf{N} & 0 \\ \hline 0 & \mathbf{N} \end{array}\right]\left[\begin{array}{c} \mathbf{m}_b^{(1)} \\ \hline \mathbf{m}_a^{(1)} \end{array}\right]$$

and adding it to vector (10)

$$\Delta u_{bi}^{(1)} = \frac{q}{b}\frac{1}{1+\nu}\left\{(c_b + c_a)\left(1 - \frac{\operatorname{sh}\left(i-\frac{1}{2}\right)\vartheta}{\operatorname{sh}\left(i_1-\frac{3}{2}\right)\vartheta}\right) + \right.$$

$$\left. + \frac{c_b\nu - c_a}{\operatorname{ch} n\vartheta \operatorname{ch}\frac{\vartheta}{2}}\left[\operatorname{ch}\left(n - i + \frac{1}{2}\right)\vartheta - \frac{\operatorname{ch}\left(n - i_1 + \frac{3}{2}\right)\vartheta \operatorname{sh}\left(i_1 - \frac{1}{2}\right)\vartheta}{\operatorname{sh}\left(i_1 - \frac{3}{2}\right)\vartheta}\right]\right\};$$

$$\text{if } i \leq i_1 - 2,$$

$$\Delta u_{bi}^{(1)} = \frac{q}{b}\frac{c_b + c_a}{1+\nu}\left(1 - \frac{\operatorname{ch}\left(n + \frac{1}{2} - i\right)\vartheta}{\operatorname{ch}\left(n + \frac{3}{2} - i_1\right)\vartheta}\right); \quad \text{if} \quad i \geq i_1,$$

and for $i = i_1 - 1$ hence the relative displacement between two concrete points adjacent to the crack cross section (the crack width) is

$$\Delta u_{bi_1-1}^{(1)} = \frac{q}{b}\frac{1}{2\nu \operatorname{sh}\frac{\vartheta}{2}\operatorname{sh}\left(i_1 - \frac{3}{2}\right)\vartheta}\left\{(c_a + c_b)\frac{\operatorname{ch} n\vartheta \operatorname{ch}\frac{\vartheta}{2}}{\operatorname{ch}\left(n + \frac{3}{2} - i_1\right)\vartheta} + (c_b\nu - c_a)\right\}.$$

Elongation of reinforcement intervals

$$\Delta u_{ai}^{(1)} = \frac{q}{b}\left\{\frac{c_b + c_a}{1+\nu}\left(1 + \frac{1}{\nu}\frac{\operatorname{sh}\left(i-\frac{1}{2}\right)\vartheta}{\operatorname{sh}\left(i_1 - \frac{3}{2}\right)\vartheta}\right) - \right.$$

$$\left. - \frac{c_b\nu - c_a}{(1+\nu)\nu}\frac{\operatorname{sh}(i_1 - 1 - i)\vartheta}{\operatorname{sh}\left(i_1 - \frac{3}{2}\right)\vartheta \operatorname{ch}\frac{\vartheta}{2}}\right\},$$

$$\text{if } i \leq i_1 - 2,$$

$$\Delta u_{ai}^{(1)} = \frac{q}{b} \frac{c_b + c_a}{1 + \nu} \left(1 + \frac{1}{\nu} \frac{\operatorname{ch}\left(n + \frac{1}{2} - i\right)\vartheta}{\operatorname{ch}\left(n + \frac{3}{2} - i_1\right)\vartheta} \right), \quad \text{if} \quad i \geq i_1$$

and in the crack cross section, hence for $i = i_1 - 1$ obviously,

$$\Delta u_{ai_1-1}^{(1)} = \frac{q}{b} \frac{c_b + c_a}{\nu}.$$

Relative displacement $\Delta \mathbf{u}_{ba}^{(1)} = \mathbf{u}_a^{(1)} - \mathbf{u}_b^{(1)}$ needed for determining forces in the bar simulating the bond results from adding the corresponding modification to (12) to yield

$$\Delta u_{bai}^{(1)} = \frac{q}{b} \left(\frac{c_b + c_a}{2\vartheta \operatorname{sh} \frac{\vartheta}{2}} \frac{\operatorname{ch}(i-1)\vartheta}{\operatorname{sh}\left(i_1 - \frac{3}{2}\right)\vartheta} + \frac{c_b \nu - c_a}{\nu \operatorname{sh} \vartheta} \frac{\operatorname{ch}\left(i - i_1 + \frac{1}{2}\right)\vartheta}{\operatorname{sh}\left(i_1 - \frac{3}{2}\right)\vartheta} \right);$$

$$\text{if} \quad i \leq i_1 - 1,$$

$$\Delta u_{bai}^{(1)} = -\frac{q}{b} \frac{c_b + c_a}{2\nu \operatorname{sh} \frac{\vartheta}{2}} \frac{\operatorname{sh}(n + 1 - i)\vartheta}{\operatorname{ch}\left(n + \frac{3}{2} - i_1\right)\vartheta}; \quad \text{if} \quad i \geq i_1. \tag{20}$$

5.2. Case of two cracks

Let us consider now the case where two cracks develop, hence the concrete stiffness vanishes between nodes $i_1 - 1$, i_1 and $i_2 - 1$, i_2 (Fig. 9). Stiffness matrix of the bar with two cracks is obtained by modifying the original coefficient matrix (1) by two diades.

In this case, the modification will be by a matrix of rank 2, written as the sum of two diades, to be factorized out by analogy to (13) as

$$b \begin{bmatrix} \mathbf{w}_1 & \mathbf{w}_2 \\ & \\ & \end{bmatrix} \begin{bmatrix} \mathbf{w}_1^* \\ \mathbf{w}_2^* \end{bmatrix} = b \left[\begin{array}{c|c} \mathbf{e}_{i_1-1} - \mathbf{e}_{i_1} & \mathbf{e}_{i_2-1} - \mathbf{e}_{i_2} \\ \hline 0 & 0 \end{array}\right] \left[\begin{array}{c|c} \mathbf{e}_{i_1-1}^* - \mathbf{e}_{i_1}^* & 0 \\ \hline \mathbf{e}_{i_2-1}^* - \mathbf{e}_{i_2}^* & 0 \end{array}\right].$$

Generalizing the theorem apllied for one crack, the inverse of the matrix modifed by two diades can be written as

$$\left\{ \mathbf{K} - \begin{bmatrix} \mathbf{w}_1 & \mathbf{w}_2 \\ & \\ & \end{bmatrix} \begin{bmatrix} \mathbf{w}_1^* \\ \mathbf{w}_2^* \end{bmatrix} \right\}^{-1} =$$

$$= \mathbf{K}^{-1} + \mathbf{K}^{-1} \begin{bmatrix} \mathbf{w}_1 & \mathbf{w}_2 \\ & \\ & \end{bmatrix} \left\{ \mathbf{E} - \begin{bmatrix} \mathbf{w}_1^* \\ \mathbf{w}_2^* \end{bmatrix} \mathbf{K}^{-1} \begin{bmatrix} \mathbf{w}_1 & \mathbf{w}_2 \\ & \\ & \end{bmatrix} \right\}^{-1} \begin{bmatrix} \mathbf{w}_1^* \\ \mathbf{w}_2^* \end{bmatrix} \mathbf{K}^{-1}. \tag{21}$$

Utilizing relationships for one crack in item *5.1* [see. (17) and (18)], now we obtain

$$\begin{bmatrix} \mathbf{w}_1^* \\ \mathbf{w}_2^* \end{bmatrix} \mathbf{K}^{-1} = \frac{1}{1+\nu} \begin{bmatrix} \mathbf{e}_{i_1-1}^* - \mathbf{e}_{i_1}^* \\ \mathbf{e}_{i_2-1}^* - \mathbf{e}_{i_2}^* \end{bmatrix} [\mathbf{B} + \nu\mathbf{C} \mid \mathbf{B} - \mathbf{C}] = \frac{1}{1+\nu} \left[\begin{array}{c|c} \varphi_j^{(1)} & \psi_j^{(1)} \\ \hline \varphi_j^{(2)} & \psi_j^{(2)} \end{array}\right] =$$

$$= \frac{1}{1+\nu} \cdot \qquad j \leq i_1 - 1 \qquad\qquad j \geq i_1$$

$$\cdot \left[\begin{array}{c|c} 1 + \nu \dfrac{\operatorname{ch}\left(n + \frac{3}{2} - i_1\right)\vartheta \operatorname{ch}(j-1)\vartheta}{\operatorname{ch} n\vartheta \operatorname{ch}\frac{\vartheta}{2}} & -\nu \dfrac{\operatorname{sh}\left(i_1 - \frac{3}{2}\right)\vartheta \operatorname{sh}(n+1-j)\vartheta}{\operatorname{ch} n\vartheta \operatorname{ch}\frac{\vartheta}{2}} \\ \hline 1 + \nu \dfrac{\operatorname{ch}\left(n + \frac{3}{2} - i_2\right)\vartheta \operatorname{ch}(j-1)\vartheta}{\operatorname{ch} n\vartheta \operatorname{ch}\frac{\vartheta}{2}} & -\nu \dfrac{\operatorname{sh}\left(i_2 - \frac{3}{2}\right)\vartheta \operatorname{sh}(n+1-j)\vartheta}{\operatorname{ch} n\vartheta \operatorname{ch}\frac{\vartheta}{2}} \end{array}\right]$$

$$j \leq i_2 - 1 \qquad\qquad j \geq i_2$$

$$j \leq i_1 - 1 \qquad\qquad j \geq i_1$$

$$\left[\begin{array}{c|c} 1 - \dfrac{\operatorname{ch}\left(n + \frac{3}{2} - i_1\right)\vartheta \operatorname{ch}(j-1)\vartheta}{\operatorname{ch} n\vartheta \operatorname{ch}\frac{\vartheta}{2}} & \dfrac{\operatorname{sh}\left(i_1 - \frac{3}{2}\right)\vartheta \operatorname{sh}(n+1-j)\vartheta}{\operatorname{ch} n\vartheta \operatorname{ch}\frac{\vartheta}{2}} \\ \hline 1 - \dfrac{\operatorname{ch}\left(n + \frac{3}{2} - i_2\right)\vartheta \operatorname{ch}(j-1)\vartheta}{\operatorname{ch} n\vartheta \operatorname{ch}\frac{\vartheta}{2}} & \dfrac{\operatorname{sh}\left(i_2 - \frac{3}{2}\right)\vartheta \operatorname{sh}(n+1-j)\vartheta}{\operatorname{ch} n\vartheta \operatorname{ch}\frac{\vartheta}{2}} \end{array}\right]$$

$$j \leq i_2 - 1 \qquad\qquad j \geq i_2 \qquad (22)$$

leading simply to a matrix of order two in (21)

$$\mathbf{E} - \begin{bmatrix} \mathbf{w}_1^* \\ \mathbf{w}_2^* \end{bmatrix} \mathbf{K}^{-1} \begin{bmatrix} \mathbf{w}_1 & \mathbf{w}_2 \\ & \end{bmatrix} = \frac{\gamma}{\operatorname{ch} n\vartheta \operatorname{sh}\vartheta} \cdot$$

$$\cdot \left[\begin{array}{c|c} \operatorname{sh}\left(i_1 - \frac{3}{2}\right)\vartheta \operatorname{ch}\left(n + \frac{3}{2} - i_1\right)\vartheta & \operatorname{sh}\left(i_1 - \frac{3}{2}\right)\vartheta \operatorname{ch}\left(n + \frac{3}{2} - i_2\right)\vartheta \\ \hline \operatorname{sh}\left(i_1 - \frac{3}{2}\right)\vartheta \operatorname{ch}\left(n + \frac{3}{2} - i_2\right)\vartheta & \operatorname{sh}\left(i_2 - \frac{3}{2}\right)\vartheta \operatorname{ch}\left(n + \frac{3}{2} - i_2\right)\vartheta \end{array}\right]$$

to be inverted into

$$\left\{\mathbf{E} - \begin{bmatrix} \mathbf{w}_1^* \\ \mathbf{w}_2^* \end{bmatrix} \mathbf{K}^{-1} \begin{bmatrix} \mathbf{w}_1 & \mathbf{w}_2 \end{bmatrix}\right\}^{-1} =$$

$$= \frac{\operatorname{sh} \vartheta}{\gamma \operatorname{sh} (i_2 - i_1)\,\vartheta} \begin{bmatrix} \dfrac{\operatorname{sh}\left(i_2 - \dfrac{3}{2}\right)\vartheta}{\operatorname{sh}\left(i_1 - \dfrac{3}{2}\right)\vartheta} & -1 \\ -1 & \dfrac{\operatorname{ch}\left(n + \dfrac{3}{2} - i_1\right)\vartheta}{\operatorname{ch}\left(n + \dfrac{3}{2} - i_2\right)\vartheta} \end{bmatrix} . \quad (23)$$

By analogy to the case of one crack, in the following the only case of a load vector

$$\mathbf{q} = q \begin{bmatrix} c_b & \mathbf{e}_1 \\ c_a & \mathbf{e}_1 \end{bmatrix} \begin{matrix} (n \\ (2n \end{matrix}$$

will be considered. Multiplying modified inverse (21) by load vector $\mathbf{q}$ and utilizing (22) yields

$$\begin{bmatrix} \mathbf{w}_1^* \\ \mathbf{w}_2^* \end{bmatrix} \mathbf{K}^{-1}\mathbf{q} = \frac{q}{1+\nu} \begin{bmatrix} c_b\varphi_1^{(1)} + c_a\psi_1^{(1)} \\ c_b\varphi_1^{(2)} + c_a\psi_1^{(2)} \end{bmatrix} . \quad (24)$$

Similarly to vector (15), vector $\mathbf{m}^{(2)}$ modifying the displacement vector $\mathbf{u}^{(2)}$ of the member with two cracks compared to the crackfree case is obtained on the basis of (21) by post-multiplying the inverse (23) by the two-element vector (24) and pre-multiplying by the transpose of (22), by the bi-column matrix

$$\mathbf{K}^{-1} \left[\begin{array}{c:c} \mathbf{w}_1 & \mathbf{w}_2 \end{array}\right] = \frac{1}{1+\nu} \left[\begin{array}{c:c} \varphi^{(1)} & \varphi^{(2)} \\ \psi^{(1)} & \psi^{(2)} \end{array}\right] =$$

$$= \frac{1}{1+\nu} \left[\begin{array}{cc:cc} 1 + \nu \dfrac{\operatorname{ch}\left(n + \frac{3}{2} - i_1\right)\vartheta}{\operatorname{ch} n\vartheta \operatorname{ch} \frac{\vartheta}{2}} \operatorname{ch}(i-1)\vartheta;\ i \leqslant i_1 & & \nu \dfrac{\operatorname{ch}\left(n + \frac{3}{2} - i_2\right)\vartheta}{\operatorname{ch} n\vartheta \operatorname{ch} \frac{\vartheta}{2}} \operatorname{ch}(i-1)\vartheta;\ i \leqslant i_2 - 1 & \\ & -\nu \dfrac{\operatorname{sh}\left(i_1 - \frac{3}{2}\right)\vartheta}{\operatorname{ch} n\vartheta \operatorname{ch} \frac{\vartheta}{2}} \operatorname{sh}(n+1-i)\vartheta;\ i \geqslant i_1 & & -\nu \dfrac{\operatorname{sh}\left(i_2 - \frac{3}{2}\right)\vartheta}{\operatorname{ch} n\vartheta \operatorname{ch} \frac{\vartheta}{2}} \operatorname{sh}(n+1-i)\vartheta;\ i \geqslant i_2 \\ \hdashline 1 - \dfrac{\operatorname{ch}\left(n + \frac{3}{2} - i_1\right)\vartheta}{\operatorname{ch} n\vartheta \operatorname{ch} \frac{\vartheta}{2}} \operatorname{ch}(i-1)\vartheta;\ i \leqslant i_1 - 1 & & -\dfrac{\operatorname{ch}\left(n + \frac{3}{2} - i_2\right)\vartheta}{\operatorname{ch} n\vartheta \operatorname{ch} \frac{\vartheta}{2}} \operatorname{ch}(i-1)\vartheta;\ i \leqslant i_2 - 1 & \\ & \dfrac{\operatorname{sh}\left(i_1 - \frac{3}{2}\right)\vartheta}{\operatorname{ch} n\vartheta \operatorname{ch} \frac{\vartheta}{2}} \operatorname{sh}(n+1-i)\vartheta;\ i \geqslant i_1 & & \dfrac{\operatorname{sh}\left(i_2 - \frac{3}{2}\right)\vartheta}{\operatorname{ch} n\vartheta \operatorname{ch} \frac{\vartheta}{2}} \operatorname{sh}(n+1-i)\vartheta;\ i \geqslant i_2 \end{array}\right]$$

Multiplication by this latter involves the following considerations. Assume $i_2 > i_1$. Terms $\varphi_i^{(1)}$ and $\varphi_i^{(2)}$ and $\psi_i^{(1)}$ and $\psi_i^{(2)}$ resp. are obviously [see (18)] subject to different analytic formulae, depending on whether

$$i \leq i_1 - 1 \text{ or } i \geq i_1 \text{ and } i \leq i_2 - 1 \text{ or } i \geq i_2 \text{ resp.}$$

Thus, in multiplying by matrix (25), there are three different analytic formulae to express modification of the displacement vector $\mathbf{m}^{(2)}$, depending on whether

$$\begin{aligned} i &\leq i_1 - 1, \\ i_1 &\leq i \leq i_2 - 1, \\ i_2 &\leq i. \end{aligned}$$

Among elements of vector

$$\mathbf{u}^{(2)} = \begin{bmatrix} \mathbf{u}_b^{(2)} \\ \mathbf{u}_a^{(2)} \end{bmatrix}$$

only elements $u_{b1}^{(2)}$ and $u_{a1}^{(2)}$ characterizing the bar stiffness are wanted.

By analogy to the one-crack case, these are obtained by increasing crack-free bar end displacements $u_{b1}^{(0)}$ and $u_{a1}^{(0)}$ by modifications $\mathrm{m}_{b1}^{(2)}$ and $m_{a1}^{(2)}$. Making use of (25), (23) and (24)

$$m_{b1}^{(2)} = \frac{q}{b(1+\nu)^2} \frac{\operatorname{sh}\vartheta}{\gamma \operatorname{sh}(i_2 - i_1)\vartheta} \left[\varphi_1^{(1)} \middle| \varphi_1^{(2)} \right] \cdot$$

$$\cdot \begin{bmatrix} \dfrac{\operatorname{sh}\left(i_2 - \frac{3}{2}\right)\vartheta}{\operatorname{sh}\left(i_1 - \frac{3}{2}\right)\vartheta} & -1 \\ -1 & \dfrac{\operatorname{ch}\left(n + \frac{3}{2} - i_1\right)\vartheta}{\operatorname{ch}\left(n + \frac{3}{2} - i_2\right)\vartheta} \end{bmatrix} \begin{bmatrix} c_b \varphi_1^{(1)} + c_a \psi_1^{(1)} \\ \hline c_b \varphi_1^{(2)} + c_a \psi_1^{(2)} \end{bmatrix};$$

$$m_{a1}^{(2)} = \frac{q}{b(1+\nu)^2} \frac{\operatorname{sh}\vartheta}{\gamma \operatorname{sh}(i_2 - i_1)\vartheta} \left[\psi_1^{(1)} \middle| \psi_1^{(2)} \right] \cdot$$

$$\cdot \begin{bmatrix} \dfrac{\operatorname{sh}\left(i_2 - \frac{3}{2}\right)\vartheta}{\operatorname{sh}\left(i_1 - \frac{3}{2}\right)\vartheta} & -1 \\ -1 & \dfrac{\operatorname{ch}\left(n + \frac{3}{2} - i_1\right)\vartheta}{\operatorname{ch}\left(n + \frac{3}{2} - i_2\right)\vartheta} \end{bmatrix} \begin{bmatrix} c_b \varphi_1^{(1)} + c_a \psi_1^{(1)} \\ \hline c_b \varphi_1^{(2)} + c_a \psi_1^{(2)} \end{bmatrix}.$$

Adding to the crack-free bar end displacement (9) results in

$$u_{b1}^{(2)} = \frac{q}{b}\frac{1}{1+\nu}\left\{n(c_b + c_a) + (c_b\,\nu - c_a)\frac{\coth\left(i_1 - \frac{3}{2}\right)\vartheta}{\operatorname{sh}\vartheta} + \right.$$

$$+ \frac{2c_b\nu + c_a(\nu - 1)}{2\nu \operatorname{sh}\left(i_1 - \frac{3}{2}\right)\vartheta \operatorname{sh}\frac{\vartheta}{2}} + \frac{c_b + c_a}{\nu} \cdot$$

$$\left. \cdot \left[\frac{\coth\left(i_1 - \frac{3}{2}\right)\vartheta + \operatorname{th}\left(n + \frac{3}{2} - i_2\right)\vartheta}{2 \operatorname{th}\frac{\vartheta}{2}} + \frac{\operatorname{th}(i_2 - i_1)\vartheta}{\operatorname{th}\frac{\vartheta}{2}}\right]\right\}$$

and so will $u_{a1}^{(2)}$ be similarly.

Relative displacements needed for determining internal forces in each interval of the member can be computed similarly to the case of one crack, by adding vector (10) to product

$$\left[\begin{array}{c|c} \mathbf{N} & 0 \\ \hline 0 & \mathbf{N} \end{array}\right]\left[\begin{array}{c} \mathbf{m}_b^{(2)} \\ \hline \mathbf{m}_a^{(2)} \end{array}\right]. \tag{16}$$

Multiplication by matrix $\mathbf{N}$ yields the difference between elements of vector $m_b^{(2)}$ and $m_a^{(2)}$. Considering expressions (25) five different formulae each are obtained for the product elements, depending on whether

1. $i \leq i_1 - 2$,
2. $i = i_1 - 1$,
3. $i_1 \leq i \leq i_2 - 2$,
4. $i = i_2 - 1$,
5. $i_2 \leq 1$. ,

In the case of concrete, cases *2* and *4* are those of crack width, while for steel it necessarily leads to a formula differing from $c_b + c_a$ by a constant multiplier alone. Multiplication (26) is advisably done by multiplying the inverse (25) post-multiplied by the two-element vector (24) now by the two-column matrix

$$\frac{1}{1+\nu}\left[\begin{array}{c|c} \mathbf{N}\,\varphi^{(1)} & \mathbf{N}\,\varphi^{(2)} \\ \hline \mathbf{N}\,\psi^{(1)} & \mathbf{N}\,\psi^{(2)} \end{array}\right]$$

obtained from (25).

Performing the operations we obtain vectors $\Delta\mathbf{m}_b^{(2)}$ and $\Delta\mathbf{m}_a^{(2)}$ modifying the elongation of crack-free bar lengths. Adding it to vector (11) yields:

Concrete interval elongations

$$\Delta u_{bi}^{(2)} = \frac{q}{b}\,\frac{1}{1+\nu}\left\{(c_b + c_a)\left(1 - \frac{\operatorname{sh}\left(i-\frac{1}{2}\right)\vartheta}{\operatorname{sh}\left(i_1-\frac{3}{2}\right)\vartheta}\right) + \frac{c_b\,\nu - c_a}{\operatorname{ch} n\vartheta\,\operatorname{ch}\frac{\vartheta}{2}}\cdot\right.$$

$$\left.\cdot\left[\operatorname{ch}\left(n-i+\frac{1}{2}\right)\vartheta - \frac{\operatorname{ch}\left(n-i_1+\frac{3}{2}\right)\vartheta\,\operatorname{sh}\left(i-\frac{1}{2}\right)\vartheta}{\operatorname{sh}\left(i_1-\frac{3}{2}\right)\vartheta}\right]\right\} =$$

$$= \Delta u_{bi}^{(1)};\quad \text{if}\quad i \le i_1 - 2,$$

$$\Delta u_{bi_1-1}^{(2)} = \frac{q}{b}\left\{\frac{c_b + c_a}{\nu}\,\frac{\operatorname{ch}\frac{\vartheta}{2}}{2\,\operatorname{sh}\frac{\vartheta}{2}}\,\frac{\operatorname{ch}(i_1+i_2-3)\frac{\vartheta}{2}}{\operatorname{sh}\left(i_1-\frac{3}{2}\right)\vartheta\,\operatorname{ch}(i_2-i_1)\frac{\vartheta}{2}} + \right.$$

$$\left. + \frac{c_b\,\nu - c_a}{2\nu\,\operatorname{sh}\frac{\vartheta}{2}\,\operatorname{sh}\left(i_1-\frac{3}{2}\right)\vartheta}\right\},$$

giving the width of the crack nearer to the beam free end;

$$\Delta u_{bi}^{(2)} = \frac{q}{b}\,\frac{c_b + c_a}{1+\nu}\left(1 - \frac{\operatorname{ch}\left(i+1-\frac{i_2+i_1}{2}\right)\vartheta}{\operatorname{ch}(i_2-i_1)\frac{\vartheta}{2}}\right);\quad \text{if}\quad i_1 \le i \le i_2 - 2,$$

$$\Delta u_{bi_2-1}^{(2)} = \frac{q}{b}\,\frac{c_b + c_a}{\nu}\,\frac{\operatorname{ch}\frac{\vartheta}{2}\operatorname{sh}(2n+3-i_2-i_1)\frac{\vartheta}{2}}{2\,\operatorname{sh}\frac{\vartheta}{2}\operatorname{ch}(i_2-i_1)\frac{\vartheta}{2}\operatorname{ch}\left(n+\frac{3}{2}-i_2\right)\vartheta},$$

being the crack width nearer to the clamping, and

$$\Delta u_{bi}^{(2)} = \frac{q}{b}\,\frac{c_b + c_a}{1+\nu}\left(1 - \frac{\operatorname{ch}\left(n+\frac{1}{2}-i\right)\vartheta}{\operatorname{ch}\left(n+\frac{3}{2}-i_2\right)\vartheta}\right);\quad \text{if}\quad i \ge i_2\,.$$

Steel interval elongations

$$\Delta u_{ai}^{(2)} = \frac{q}{b}\left\{\frac{c_b + c_a}{1+\nu}\left(1 + \frac{1}{\nu}\,\frac{\operatorname{sh}\left(i-\frac{1}{2}\right)\vartheta}{\operatorname{sh}\left(i_1-\frac{3}{2}\right)\vartheta}\right) - \right.$$

$$\left. - \frac{c_b\,\nu - c_a}{(1+\nu)\,\nu}\,\frac{\operatorname{sh}\,(i_1-1-i)\,\vartheta}{\operatorname{sh}\left(i_1-\frac{3}{2}\right)\vartheta\,\operatorname{ch}\frac{\vartheta}{2}}\right\} = \Delta u_{ai}^{(1)};\ \text{if}\quad i \le i_1 - 2\,,$$

$$\Delta u_{ai}^{(2)} = \frac{q}{b}\,\frac{c_b + c_a}{1+\nu}\left(1 + \frac{1}{\nu}\,\frac{\operatorname{ch}\left(i+1-\frac{i_2+i_1}{2}\right)\vartheta}{\operatorname{ch}\,(i_2-i_1)\,\frac{\vartheta}{2}}\right);\ \text{if}\ i_1 \le i \le i_2 - 2,$$

$$\Delta u_{ai}^{(2)} = \frac{q}{b}\,\frac{c_b + c_a}{1+\nu}\left(1 + \frac{1}{\nu}\,\frac{\operatorname{ch}\left(n+\frac{1}{2}-i\right)\vartheta}{\operatorname{ch}\left(n+\frac{3}{2}-i_2\right)\vartheta}\right);\ \text{if}\ i \ge i_2.$$

At both cracks, *i.e.* for $i = i_1 - 1$ and $i = i_2 - 1$ it is

$$\Delta u_{ai}^{(2)} = \frac{q}{b}\,\frac{c_b + c_a}{\nu}\,.$$

Elongation of the bar simulating the bond

$$\Delta u_{ba}^{(2)} = \mathbf{u}_b^{(2)} - \mathbf{u}_a^{(2)}$$

is obtained by increasing (12) by the corresponding modification

$$\Delta u_{bai}^{(2)} = \frac{q}{b}\left(\frac{c_b + c_a}{2\nu\operatorname{sh}\frac{\vartheta}{2}}\,\frac{\operatorname{ch}\,(i-1)\,\vartheta}{\operatorname{sh}\left(i_1-\frac{3}{2}\right)\vartheta} + \right.$$

$$\left. + \frac{c_b\nu - c_a}{\nu\operatorname{sh}\vartheta}\,\frac{\operatorname{ch}\left(i-i_1+\frac{1}{2}\right)\vartheta}{\operatorname{sh}\left(i_1-\frac{3}{2}\right)\vartheta}\right) = \Delta u_{bai}^{(1)};\ i \le i_1 - 1\,,$$

$$\Delta u_{bai}^{(2)} = \frac{q}{b} \frac{c_b + c_a}{2\nu \operatorname{sh} \frac{\vartheta}{2}} \frac{\operatorname{sh}\left(i + \frac{1}{2} - \frac{i_2 - i_1}{2}\right)\vartheta}{\operatorname{ch}\,(i_2 - i_1)\frac{\vartheta}{2}}; \quad i_1 \leq i \leq i_2 - 1,$$

$$\Delta u_{bai}^{(2)} = -\frac{q}{b} \frac{c_b + c_a}{2\nu \operatorname{sh} \frac{\vartheta}{2}} \frac{\operatorname{sh}\,(n + 1 - i)\,\vartheta}{\operatorname{ch}\left(n + \frac{3}{2} - i_2\right)\vartheta}; \quad i \geq i_2 .$$

5.3. Case of an arbitrary number of cracks

Now the general case of k cracks in the concrete will be considered (Fig. 10) where stiffness of the element simulating the concrete vanishes between nodes $i_r - 1$ and i_r ($r = 1, 2, \ldots, k$). By analogy to the one or two crack cases, blocks $\mathbf{G} + \mathbf{D}$ of the original matrix [see (2)] pertaining to the crack-free case have to be reduced by the matrix

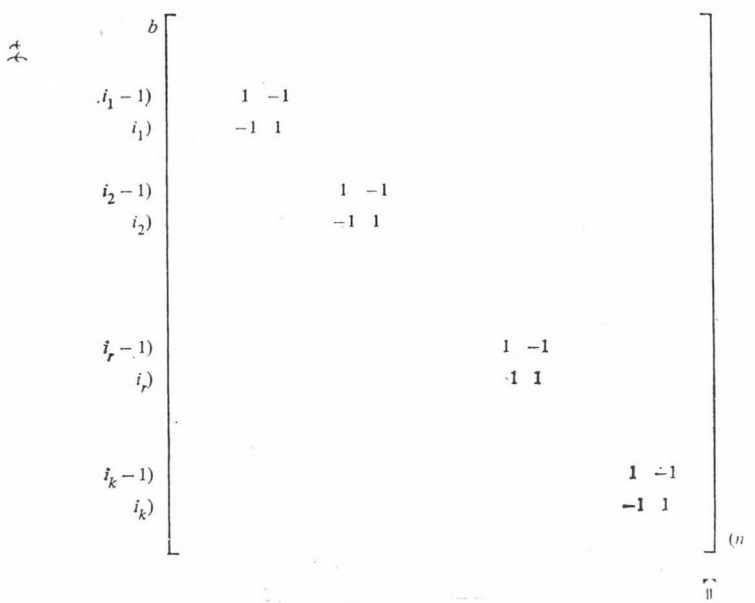

of rank r, hence written as the sum of r diades, in the factorized form

$$b \begin{bmatrix} \mathbf{w}_1 & \mathbf{w}_2 & \dots & \mathbf{w}_r & \dots & \mathbf{w}_k \\ & & & & & \\ & & & & & \\ & & & & & \end{bmatrix} \begin{bmatrix} \mathbf{w}_1^* & & & \\ \mathbf{w}_2^* & & & \\ \vdots & & & \\ \mathbf{w}_r^* & & & \\ \vdots & & & \\ \mathbf{w}_k^* & & & \end{bmatrix} =$$

$$= b \begin{bmatrix} \mathbf{e}_{i_1-1} - \mathbf{e}_{i_1} & \mathbf{e}_{i_2-1} - \mathbf{e}_{i_2} & \dots & \mathbf{e}_{i_r-1} - \mathbf{e}_{i_r} & \dots & \mathbf{e}_{i_k-1} - \mathbf{e}_{i_k} \\ & & & & & \\ \hline & & & & & \\ 0 & 0 & \dots & 0 & \dots & 0 \\ & & & & & \end{bmatrix} \begin{bmatrix} \mathbf{e}_{i_1-1}^* - \mathbf{e}_{i_1}^* & 0 \\ \mathbf{e}_{i_2-1}^* - \mathbf{e}_{i_2}^* & 0 \\ \vdots & \\ \mathbf{e}_{i_r-1}^* - \mathbf{e}_{i_r}^* & 0 \\ \vdots & \\ \mathbf{e}_{i_k-1}^* - \mathbf{e}_{i_k}^* & 0 \end{bmatrix}.$$

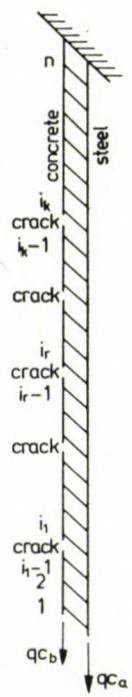

Fig. 10

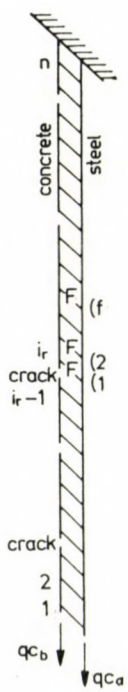

Fig. 11

Let us introduce notation

$$= \begin{bmatrix} \mathbf{w}_1 & \mathbf{w}_2 \dots \mathbf{w}_r \dots \mathbf{w}_k \end{bmatrix} \text{ and } \mathbf{w}^* = \begin{bmatrix} \mathbf{w}_1^* \\ \mathbf{w}_2^* \\ \vdots \\ \mathbf{w}_r^* \\ \vdots \\ \mathbf{w}_k^* \end{bmatrix}.$$

Generalizing (14) for (21) yields for the inverse of the matrix modified by k diade

$$\{\mathbf{K} - \mathbf{W}\mathbf{W}^*\}^{-1} = \mathbf{K}^{-1} + \mathbf{K}^{-1}\mathbf{W}\{\mathbf{E} - \mathbf{W}^*\mathbf{K}^{-1}\mathbf{W}\}^{-1}\mathbf{W}^*\mathbf{K}^{-1}. \quad (27)$$

Thus, under the considered modified conditions, displacements are given according to Eq. $\mathbf{K}\mathbf{u} = \mathbf{q}$ by

$$\mathbf{u} = (\mathbf{K} - \mathbf{W}\mathbf{W}^*)^{-1}\mathbf{q}\ .$$

Substituting (27) yields

$$\mathbf{u}^{(k)} = \mathbf{K}^{-1}\mathbf{q} + \mathbf{K}^{-1}\mathbf{W}\{\mathbf{E} - \mathbf{W}^*\mathbf{K}^{-1}\mathbf{W}\}^{-1}\mathbf{W}\mathbf{W}^*\mathbf{K}^{-1}\mathbf{q},$$

meaning that vector $\mathbf{u}^{(k)}$ of displacements at k cracking is obtained by increasing vector $\mathbf{u}^{(0)}$ for the crack-free case by the modification $\mathbf{m}^{(k)}$ of the displacements due to cracking, where

$$\mathbf{m}^{(k)} = \mathbf{K}^{-1}\mathbf{W}\{\mathbf{E} - \mathbf{W}^*\mathbf{K}^{-1}\mathbf{W}\}^{-1}\mathbf{W}^*\mathbf{K}^{-1}\mathbf{q}.$$

Let us determine first the sub-vectors $\mathbf{m}_b^{(k)}$ and $\mathbf{m}_a^{(k)}$ of vector $\mathbf{m}^{(k)}$. Utilizing (17), (18) and (22)

$$\mathbf{W}^*\mathbf{K}^{-1} = \frac{1}{1+\nu}\begin{bmatrix} \mathbf{e}_{i_1-1}^* - \mathbf{e}_{i_1}^* \\ \mathbf{e}_{i_2-1}^* - \mathbf{e}_{i_2}^* \\ \vdots \\ \mathbf{e}_{ik-1}^* - \mathbf{e}_{ik}^* \end{bmatrix}\left[\mathbf{B} + \nu\mathbf{C} \,\middle|\, \mathbf{B} - \mathbf{C}\right] =$$

$$= \frac{1}{1+\nu}\left[\begin{array}{c|c} \varphi_j^{(1)} & \psi_j^{(1)} \\ \varphi_j^{(2)} & \psi_j^{(2)} \\ \vdots & \vdots \\ \varphi_j^{(k)} & \psi_j^{(k)} \end{array}\right], \quad (28)$$

where

$$\varphi_j^{(r)} = \begin{cases} 1 + v \dfrac{\operatorname{ch}\left(n + \dfrac{3}{2} - i_r\right)\vartheta \operatorname{ch}(j-1)\vartheta}{\operatorname{ch} n\vartheta \operatorname{ch}\dfrac{\vartheta}{2}}, & \text{if} \quad j \leq i_r - 1, \\ -v \dfrac{\operatorname{sh}\left(i_r - \dfrac{3}{2}\right)\vartheta \operatorname{sh}(n+1-j)\vartheta}{\operatorname{ch} n\vartheta \operatorname{ch}\dfrac{\vartheta}{2}}, & \text{if} \quad j \geq i_r, \end{cases}$$

$$\psi_j^{(r)} = \begin{cases} 1 - \dfrac{\operatorname{ch}\left(n + \dfrac{3}{2} - i_r\right)\vartheta \operatorname{ch}(j-1)\vartheta}{\operatorname{ch} n\vartheta \operatorname{ch}\dfrac{\vartheta}{2}}, & \text{if} \quad j \leq i_r - 1, \\ \dfrac{\operatorname{sh}\left(i_r - \dfrac{3}{2}\right)\vartheta \operatorname{sh}(n+1-j)\vartheta}{\operatorname{ch} n\vartheta \operatorname{ch}\dfrac{\vartheta}{2}}, & \text{if} \quad j \geq i_r, \end{cases} \tag{29}$$

and $r = 1, 2, \ldots, k$.

By this means r-th order matrix in (27) to be inverted becomes

$$\mathbf{E} - \mathbf{W}^* \mathbf{K}^{-1} \mathbf{W} = \frac{\gamma}{\operatorname{ch} n\vartheta \operatorname{sh}\vartheta} [z_{st}]; \quad s, t = 1, 2, \ldots, r, \ldots, k,$$

where

$$z_{st} = \begin{cases} \chi_s \omega_t, & \text{if} \quad s \leq t, \\ \omega_s \chi_t, & \text{if} \quad s \geq t, \end{cases}$$

furthermore

$$\chi_s = \operatorname{sh}\left(i_s - \frac{3}{2}\right)\vartheta$$

and

$$\omega_s = \operatorname{ch}\left(n - \frac{3}{2} - i_s\right)\vartheta.$$

The obtained k-th order matrix to be inverted is seen to be a one-pair matrix, hence its inverse is a symmetric tri-diagonal. With reference to item *4.1*, a simple calculation shows the inverse to be

$$\{\mathbf{E} - \mathbf{W}^* \mathbf{K}^{-1} \mathbf{W}\}^{-1} =$$

$$= \frac{\operatorname{sh} \vartheta}{\gamma} \begin{bmatrix} \dfrac{\operatorname{sh}\left(i_2 - \frac{3}{2}\right)\vartheta}{\operatorname{sh}\left(i_1 - \frac{3}{2}\right)\vartheta \operatorname{sh}(i_2 - i_1)\vartheta} & -\dfrac{1}{\operatorname{sh}(i_2 - i_1)\vartheta} & & \\ -\dfrac{1}{\operatorname{sh}(i_2 - i_1)\vartheta} & \dfrac{\operatorname{sh}(i_3 - i_1)\vartheta}{\operatorname{sh}(i_3 - i_2)\vartheta \operatorname{sh}(i_2 - i_1)\vartheta} & -\dfrac{1}{\operatorname{sh}(i_3 - i_2)\vartheta} & \\ & \cdot & \cdot & \\ & & -\dfrac{1}{\operatorname{sh}(i_k - i_{k-1})\vartheta} & \dfrac{\operatorname{ch}\left(n + \frac{3}{2} - i_{k-1}\right)\vartheta}{\operatorname{ch}\left(n + \frac{3}{2} - i_k\right)\vartheta \operatorname{sh}(i_k - i_{k-1})\vartheta} \end{bmatrix}$$

This is a general case of cracking to be considered for one-parameter load $\mathbf{q}$ acting at the bar end. Multiplying the modified inverse (27) by $\mathbf{q}$, the column vector of k elements becomes

$$\mathbf{W}^* \mathbf{K}^{-1} \mathbf{q} = \frac{q}{1 + v} [c_b \varphi_1^{(r)} + c_a \psi_1^{(r)}], \quad r = 1, 2, \ldots, k. \tag{31}$$

According to (27), vector $\mathbf{m}^{(k)}$ of the modification the displacement vector $\mathbf{u}^{(k)}$ of the unit with k cracks compared to the crack-free unit is obtained by post-multiplying inverse (30) by vector (31) and pre-multiplying by the transpose of (28), a matrix with k columns

$$\mathbf{K}^{-1}\mathbf{W} = \frac{1}{1 + v} \begin{bmatrix} \varphi^{(1)} \varphi^{(2)} & \ldots & \varphi^{(r)} & \ldots & \varphi^{(k)} \\ \psi^{(1)} \psi^{(2)} & \ldots & \psi^{(r)} & \ldots & \psi^{(k)} \end{bmatrix}. \tag{32}$$

Previous considerations for two cracks will be completed by the following: $i_k > i_{k-1} > \ldots > i_r > \ldots > i_2 > i_1$. From (29) of $\varphi_i^{(r)}$ and $\psi_i^{(r)}$ ($i = 1, 2, \ldots n$; $r = 1, 2, \ldots, k$) results in fact that upon multiplying by matrix (32), modification $\mathbf{m}^{(k)}$ of the displacement vector can be given in $k + 1$ different analytic forms, depending on whether

$$\begin{aligned} & i \leq i_1 - 1, \\ i_{r-1} \leq\ & i \leq i_r - 1, \quad r = 2, \ldots, k \\ & \vdots \\ & i_k \leq i\,. \end{aligned}$$

Among elements of vector

$$\mathbf{u}^{(k)} = \begin{bmatrix} \mathbf{u}_b^{(k)} \\ \hline \mathbf{u}_a^{(k)} \end{bmatrix}$$

again those expressing member end point displacements $\mathbf{u}_{b1}^{(k)}$; $\mathbf{u}_{a1}^{(k)}$ alone are needed

$$m_{b1}^{(k)} = \frac{q}{b(1+\nu)^2} \frac{\operatorname{sh}\vartheta}{\gamma} [\varphi_1^{(1)}, \varphi_1^{(2)}, \ldots, \varphi_1^{(k)}] \cdot$$

$$\begin{bmatrix} \dfrac{\operatorname{sh}\left(i_2 - \frac{3}{2}\right)\vartheta}{\operatorname{sh}\left(i_1 - \frac{3}{2}\right)\vartheta \operatorname{sh}(i_2 - i_1)\vartheta} & -\dfrac{1}{\operatorname{sh}(i_2 - i_1)\vartheta} & & \\ -\dfrac{1}{\operatorname{sh}(i_2 - i_1)\vartheta} & \dfrac{\operatorname{sh}(i_3 - i_1)\vartheta}{\operatorname{sh}(i_3 - i_2)\vartheta \operatorname{sh}(i_2 - i_1)\vartheta} & -\dfrac{1}{\operatorname{sh}(i_3 - i_2)\vartheta} & \\ & \ddots & \ddots & \\ & & -\dfrac{1}{\operatorname{sh}(i_k - i_{k-1})\vartheta} & \dfrac{\operatorname{ch}\left(n + \frac{3}{2} - i_{k-1}\right)\vartheta}{\operatorname{ch}\left(n + \frac{3}{2} - i_k\right)\vartheta \operatorname{sh}(i_k - i_{k-1})\vartheta} \end{bmatrix} \cdot$$

$$\cdot \begin{bmatrix} c_b\varphi_1^{(1)} + c_a\psi_1^{(1)} \\ c_b\varphi_1^{(2)} + c_a\psi_1^{(2)} \\ \vdots \\ c_b\varphi_1^{(k)} + c_a\psi_1^{(k)} \end{bmatrix},$$

and so $m_{a1}^{(k)}$ can be calculated. Adding displacements (9) of the crackless bar end to the modification yields

$$u_{b1}^{(k)} = \frac{q}{b} \frac{1}{1+\nu} \left\{ n(c_b + c_a) + (c_b\nu + c_a) \frac{\coth\left(i_1 - \frac{3}{2}\right)\vartheta}{\operatorname{sh}\vartheta} + \right.$$

$$+ \frac{2c_b\nu + c_a(\nu - 1)}{2\nu \operatorname{sh}\left(i_1 - \frac{3}{2}\right)\vartheta \operatorname{sh}\frac{\vartheta}{2}} + \frac{c_b + c_a}{\nu} \cdot$$

$$\left. \cdot \left[\frac{\coth\left(i_1 - \frac{3}{2}\right)\vartheta + \operatorname{th}\left(n + \frac{3}{2} - i_k\right)\vartheta}{2 \operatorname{th}\frac{\vartheta}{2}} + \sum_{j=2}^{k} \frac{\operatorname{th}(i_j - i_{j-1})\frac{\vartheta}{2}}{\operatorname{th}\frac{\vartheta}{2}} \right] \right\},$$

and so $u_{a1}^{(k)}$ *i.e.* $(u_{a1}^{(k)} = u_{b1}^{(k)} - \Delta u_{ba1}^{(k)}$ will be obtained. Elongation of sections of bar cracked at k places is obtained by adding vector (10) for the crack-free case to the product

$$\left[\begin{array}{c|c} \mathbf{N} & 0 \\ \hline 0 & \mathbf{N} \end{array}\right] \left[\begin{array}{c} \mathbf{m}_b^{(k)} \\ \mathbf{m}_a^{(k)} \end{array}\right]. \tag{33}$$

Multiplication by matrix **N** now yields the difference between elements of vectors $\mathbf{m}_b^{(k)}$ and $\mathbf{m}_a^{(k)}$. Taking expressions $\varphi_i^{(r)}$, $\psi_i^{(r)}$ [see (29)] into consideration, the elements of the products will have $2k + 1$ different formulae, depending on whether

$$\begin{aligned} & i \leq i_1 - 2 \\ & i = i_1 - 1 \\ & \vdots \\ i_r - 1 \leq i \leq i_r - 2 \quad & r = 2, \ldots, k \\ i = i_r - 1 \quad & r = 2, \ldots, k-1 \\ & \vdots \\ & i = i_k - 1 \\ i_k \leq i. & \end{aligned}$$

Also now, multiplication (33) is advisably done by post-multiplying inverse (30) by vector (31) pre-multiplied by matrix

$$\frac{1}{1+\nu} \left[\begin{array}{c|c|c|c} \mathbf{N}\varphi^{(1)} & \mathbf{N}\varphi^{(2)} & \ldots & \mathbf{N}\varphi^{(k)} \\ \hline \mathbf{N}\psi^{(1)} & \mathbf{N}\psi^{(2)} & \ldots & \mathbf{N}\psi^{(k)} \end{array}\right]$$

obtained from (32). Performing these operations, results in vectors $\Delta\mathbf{m}_b^{(2)}$ and $\Delta\mathbf{m}_a^{(k)}$ modifying the elongation of crackfree bar sections. Adding it to vector (10), yields for the elongation of concrete and steel sections

$$\Delta u_{bi}^{(k)} = \frac{q}{b} \left\{ \frac{c_b + c_a}{1+\nu} \left(1 - \frac{\operatorname{sh}\left(i - \frac{1}{2}\right)\vartheta}{\operatorname{sh}\left(i_1 - \frac{3}{2}\right)\vartheta} \right) + \frac{c_b \nu - c_a}{1+\nu} \frac{1}{\operatorname{ch} n\vartheta \operatorname{ch} \frac{\vartheta}{2}} \cdot \right.$$

$$\left. \operatorname{ch}\left(n - 1 + \frac{1}{2}\right)\vartheta - \frac{\operatorname{ch}\left(n - i_1 + \frac{3}{2}\right)\vartheta \operatorname{sh}\left(i - \frac{1}{2}\right)\vartheta}{\operatorname{sh}\left(i_1 - \frac{3}{2}\right)\vartheta} \right\} = \Delta u_{bi}^{(1)},$$

$$\text{if} \quad i \leq i_1 - 2\,;$$

$$\Delta u_{bi}^{(k)} = \frac{q}{b}\left\{\frac{c_b + c_a}{\nu}\,\frac{\operatorname{ch}\frac{\vartheta}{2}}{2\operatorname{sh}\frac{\vartheta}{2}}\,\frac{\operatorname{ch}(i_1 + i_2 - 3)\frac{\vartheta}{2}}{\operatorname{sh}\left(i_1 - \frac{3}{2}\right)\vartheta \operatorname{ch}(i_2 - i_1)\frac{\vartheta}{2}} + \right.$$

$$\left. + \frac{c_b \nu - c_a}{2\nu \operatorname{sh}\frac{\vartheta}{2}\operatorname{sh}\left(i_1 - \frac{3}{2}\right)\vartheta}\right\}, \quad \text{if} \quad i = i_1 - 1\,,$$

which represents the crack width next to the free beam end,

$$\Delta u_{bi}^{(k)} = \frac{q}{b}\,\frac{c_b + c_a}{1 + \nu}\left(1 - \frac{\operatorname{ch}\left(i + 1 - \frac{i_r + i_{r-1}}{2}\right)\vartheta}{\operatorname{ch}(i_r - i_{r-1})\frac{\vartheta}{2}}\right), \quad \text{if } i_{r-1} \leq i \leq i_r - 2\,,$$

$$\Delta u_{bi}^{(k)} = \frac{q}{b}\,\frac{c_b + c_a}{\nu}\,\frac{\operatorname{ch}\frac{\vartheta}{2}}{2\operatorname{sh}\frac{\vartheta}{2}}\left[\operatorname{th}(i_r - i_{r-1})\frac{\vartheta}{2} + \operatorname{th}(i_{r-1} - i_r)\frac{\vartheta}{2}\right], \quad \text{if } i = i_r - 1,$$

latter being the width of the r-th crack,

$$\Delta u_{bi}^{(k)} = \frac{q}{b}\,\frac{c_b + c_a}{\nu}\,\frac{\operatorname{ch}\frac{\vartheta}{2}\operatorname{sh}(2n + 3 - i_k - i_{k-1})\frac{\vartheta}{2}}{2\operatorname{sh}\frac{\vartheta}{2}\operatorname{ch}(i_k - i_{k-1})\frac{\vartheta}{2}\operatorname{ch}\left(n + \frac{3}{2} - i_k\right)\vartheta}, \quad \text{if } i = i_k - 1,$$

which is equal to the width of the crack next to the clamping,

$$\Delta u_{ai}^{(k)} = \frac{q}{b}\,\frac{c_b + c_a}{1 + \nu}\left(1 - \frac{\operatorname{ch}\left(n + \frac{1}{2} - i\right)\vartheta}{\operatorname{ch}\left(n + \frac{3}{2} - i_k\right)\vartheta}\right), \quad \text{if} \quad i_k \leq i\,.$$

$$\Delta u_{ai}^{(k)} = \frac{q}{b}\left(\frac{c_b + c_a}{1 + \nu}\left(1 + \frac{1}{\nu}\,\frac{\operatorname{sh}\left(i - \frac{1}{2}\right)\vartheta}{\operatorname{sh}\left(i_1 - \frac{3}{2}\right)\vartheta}\right) - \right.$$

$$\left. - \frac{c_b \nu - c_a}{(1 + \nu)\nu}\,\frac{\operatorname{sh}(i_1 - 1 - i)\vartheta}{\operatorname{sh}\left(i_1 - \frac{3}{2}\right)\vartheta \operatorname{ch}\frac{\vartheta}{2}}\right) = \Delta u_{ai}^{(1)}, \quad \text{if} \quad i \leq i_1 - 2\,;$$

$$\Delta u_{ai}^{(k)} = \frac{q}{b}\,\frac{c_b + c_a}{1+\nu}\left(1 + \frac{1}{\nu}\,\frac{\operatorname{ch}\left(i+1-\dfrac{i_r+i_{r-1}}{2}\right)\vartheta}{\operatorname{ch}\,(i_r - i_{r-1})\,\dfrac{\vartheta}{2}}\right), \text{ if } i_{r-1} \leq i \leq i - 2_r;$$

$$\Delta u_{ai}^{(k)} = \frac{q}{b}\,\frac{c_b + c_a}{1+\nu}\left(1 + \frac{1}{\nu}\,\frac{\operatorname{ch}\left(n+\dfrac{1}{2}-i\right)\vartheta}{\operatorname{ch}\left(n+\dfrac{3}{2}-i_k\right)\vartheta}\right), \quad \text{if} \quad i_k \leq i.$$

To the analogy of items *5.1* and *5.2*, steel elongation across the cracks

$$\Delta u_{ai}^{(k)} = \frac{q}{b}\,\frac{c_b + c_a}{\nu}, \qquad \text{if} \quad i = i_r - 1, \quad r = 1, 2, \ldots, k\,.$$

Elongation of the bar simulating the bond

$$\Delta u_{ba}^{(k)} = \mathbf{u}_b^{(\eta)} - \mathbf{u}_a^{(k)}$$

is obtained by increasing (12) by the corresponding modification

$$\Delta u_{bai}^{(k)} = \frac{q}{b}\left(\frac{c_b + c_a}{2\nu \operatorname{sh}\dfrac{\vartheta}{2}}\,\frac{\operatorname{ch}\,(i-1)\,\vartheta}{\operatorname{sh}\left(i_1 - \dfrac{3}{2}\right)\vartheta} + \frac{c_b\nu - c_a}{\nu \operatorname{sh}\vartheta}\,\frac{\operatorname{ch}\left(i - i_1 + \dfrac{1}{2}\right)\vartheta}{\operatorname{sh}\left(i_1 - \dfrac{3}{2}\right)\vartheta}\right) = \Delta u_{abi}^{(b)},$$

$$i \leq i_1 - 1;$$

$$\Delta u_{bai}^{(k)} = \frac{q}{b}\,\frac{c_b + c_a}{2\nu \operatorname{sh}\dfrac{\vartheta}{2}}\,\frac{\operatorname{sh}\left(i + \dfrac{1}{2} - \dfrac{i_r - i_{r-1}}{2}\right)\vartheta}{\operatorname{ch}\,(i_r - i_{r-1})\,\dfrac{\vartheta}{2}}\;; \quad 1 < r \leq k; \quad i_{r-1} \leq i \leq i_r - 1,$$

$$\Delta u_{abi}^{(k)} = -\frac{q}{b}\,\frac{c_b + c_a}{2\nu \operatorname{sh}\dfrac{\vartheta}{2}}\,\frac{\operatorname{sh}\,(n+1-i)\,\vartheta}{\operatorname{ch}\left(n+\dfrac{3}{2}-i_k\right)\vartheta}, \qquad i \geq i_k\,.$$

6. Effect of the yield of the bar simulating the bond

In course of concrete cracking, relative displacement of concrete and steel points originally in the same cross section abruptly gets a value over a longer section where there is no more bond stresses increase. This case is rather difficult to analyze — especially if at a point the bond stress does not increase monotonously or changes its sign. The forces and reactions and the deformation condition in the model may be written in more detail than will be seen here in the case of the bond described under *3.214*, here simply the computation principle will be outlined. For a load arranged as under *5.* with a parameter q_0 in the former, fixed condition, increased now to q, concomitant to the assumed yield at f places of the connecting bar one side of an intermediate crack (Fig. 11), denoting displacements in the actual case by $\mathbf{u}'' = \mathbf{u}^{(f)}$ yields the equation system

$$\mathbf{K}''\mathbf{u}^{(f)} = q\mathbf{c} + \mathbf{q}_m = q\begin{bmatrix} c_b \\ 0 \\ \vdots \\ 0 \\ \hline c_a \\ 0 \\ \vdots \\ 0 \end{bmatrix} + T_F \left[\begin{array}{c|l} & \\ 1 & (i \\ 1 & (i_r + 1 \\ \vdots & \vdots \\ 1 & (i_r + f - 1 \\ \hline & \\ -1 & (i_r \\ -1 & (i_r + 1 \\ \vdots & \vdots \\ -1 & (i_r + f - 1 \end{array}\right]$$

For the sake of comprehension, let us write the stiffness matrix for a concrete cracked between modes $i_r - 1$ and i_r and for the yield of a bar joining node i_r at the crack edge. Taking (1), (27) and the connecting bar yieldinto consideration, the coefficient becomes

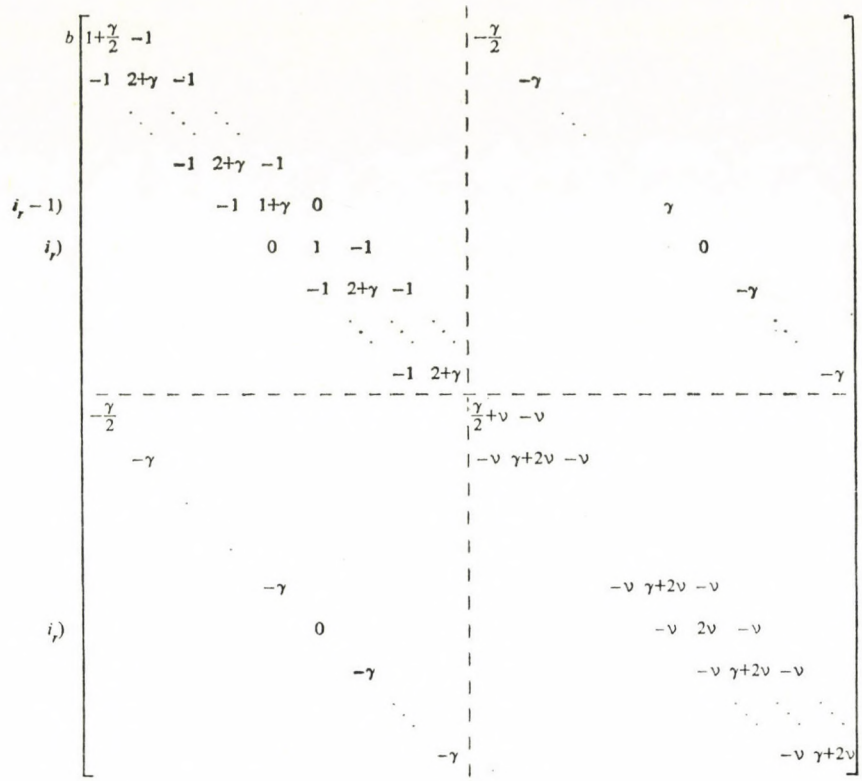

Hence, the original coefficient matrix for the elastic crack-free case has to be reduced by a matrix $\mathbf{K} - \mathbf{W}\,\mathbf{W}^*$ multiplied by $\mathbf{v}$, and by a matrix

$$\begin{matrix} b\gamma \\ i_r) \\ \\ \\ i_r) \end{matrix} \begin{bmatrix} & \\ 1 & -1 \\ \hdashline & \\ -1 & 1 \end{bmatrix}. \tag{35}$$

Matrix (35) is a diade which, by means of the vector of $2n$ elements

$$\mathbf{v}_1 = \begin{bmatrix} \mathbf{e}_{i_r} \\ \hdashline -\mathbf{e}_{i_r} \end{bmatrix}$$

can be written in the form

$$b\gamma\,\mathbf{v}_1\,\mathbf{v}_1^* = b\sqrt{\gamma}\,\mathbf{v}_1\sqrt{\gamma}\,\mathbf{v}_1^*.$$

Coefficient matrix $\mathbf{K}''$ for the case of yield of the connecting bar joining node $i_r, i_r+1, \ldots, i_r+f-1$ and is obtained by deducing from matrix $\mathbf{K} - \mathbf{W}\,\mathbf{W}^*$ the product $\sqrt{\gamma}\,\mathbf{V}\,\sqrt{\gamma}\,\mathbf{V}^*$ for yielded bonds, where

$$\mathbf{V} = \begin{bmatrix} \mathbf{e}_{i_r} & \mathbf{e}_{i_r+1} & \cdots & \mathbf{e}_{i_r+f-1} \\ -\mathbf{e}_{i_r} & -\mathbf{e}_{i_r+1} & \cdots & -\mathbf{e}_{i_r+f-1} \end{bmatrix}. \tag{36}$$

Thus

$$\mathbf{K}'' = \mathbf{K} - \mathbf{W}\mathbf{W}^* - \sqrt{\gamma}\,\mathbf{V}\sqrt{\gamma}\,\mathbf{V}^*.$$

More detailed treatment will be now omitted, examples in item 7 refer to the elastic case only.

7. Some results of the analytic solution of one-dimensional problems

As an example for the crack analysis of reinforced and prestressed concrete structures resp., the common case of axially reinforced or prestressed bars will be considered. Omitting the control of the tensile strength of concrete, we do not have to differentiate according to whether the member is a fully anchored prestressed or a normally reinforced one, cracking has been assumed empirically.

Calculations are essentially aimed at internal forces, deformations, crack widths for different mesh. Our examples will refer to concrete, steel and bond with alinear function (item 4.).

7.1 Characteristics of the examined members

Published data ([2]) were applied in analyzing a member of 160 cm length. Because of symmetry considerations, calculations applied for a bar clamped at one end $L = 80$ cm in length. The examined concrete bar has a cross-sectional area of 192 cm^2, and a modulus of elasticity of 35 000 MPa (350 000 kp/cm^2), hence $b[0{,}1\ \text{MPa}] = b[\text{kp/cm}^2] = 8 \times 10^7/h$ (h being the mesh). Reinforcement of 2 cm^2 cross-sectional area has a stiffness of round $4 \times 10^6/h$, resulting in the ratio $v = 0{,}05$. The bond characteristic coefficient is $\gamma = 1{,}25 \times 10^{-8}\ h^2\ p_d/\Lambda$, where p_d/Λ has two different characteristics, 4×10^2 MPa (4×10^3 kp/cm^2) and 12×10^2 MPa (12×10^3 kp/cm^2) taken of our tests ([23]). Here p_d is the perimeter of the reinforcing steel and Λ the reciprocal slope of the linear bond shear stress versus relative displacement function. Load parameter has uniformly been taken as 4×10^3, irrelevant in the actual case.

Nodal points outside the clamping cross section amount to $n = L/h$. Indicating the place of cracks as the abscissa y_r measured from the free end, with notations in Fig. 12

$$i_r = 2 + \text{entier}\,\frac{y_r}{h}.$$

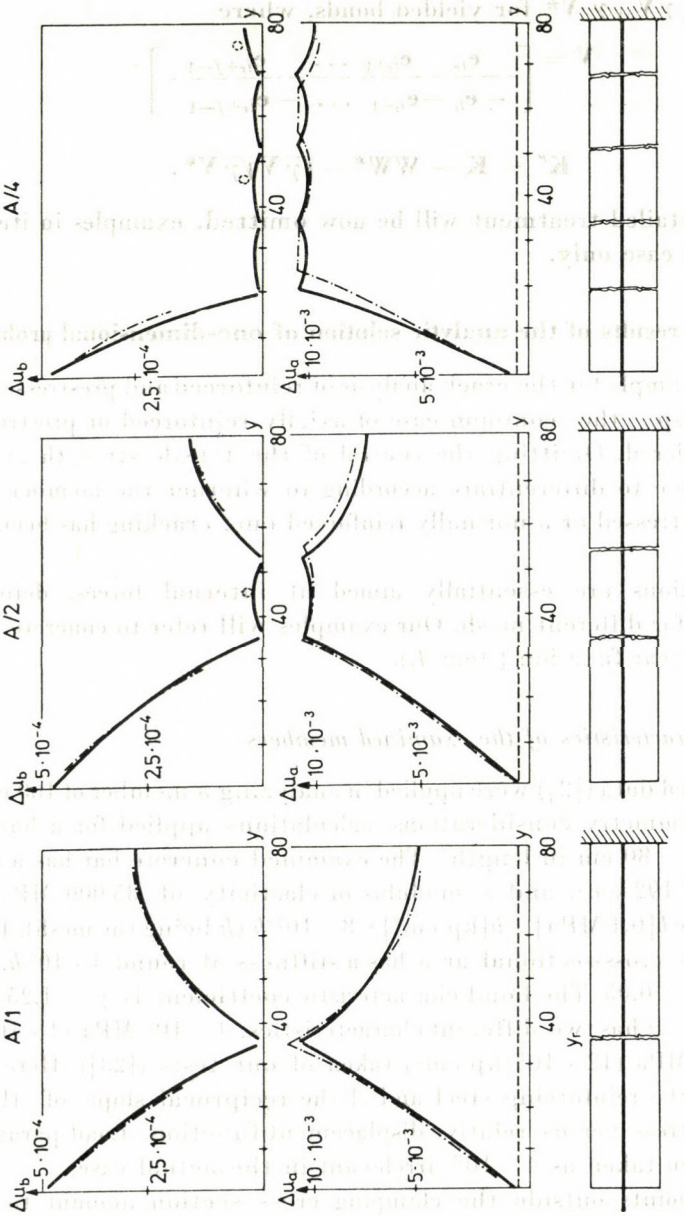
A/4
A/2
A/1
y
80
40
Δu_b
Δu_a
$2{,}5\cdot10^{-4}$
$5\cdot10^{-4}$
$10\cdot10^{-3}$
$5\cdot10^{-3}$
y_r

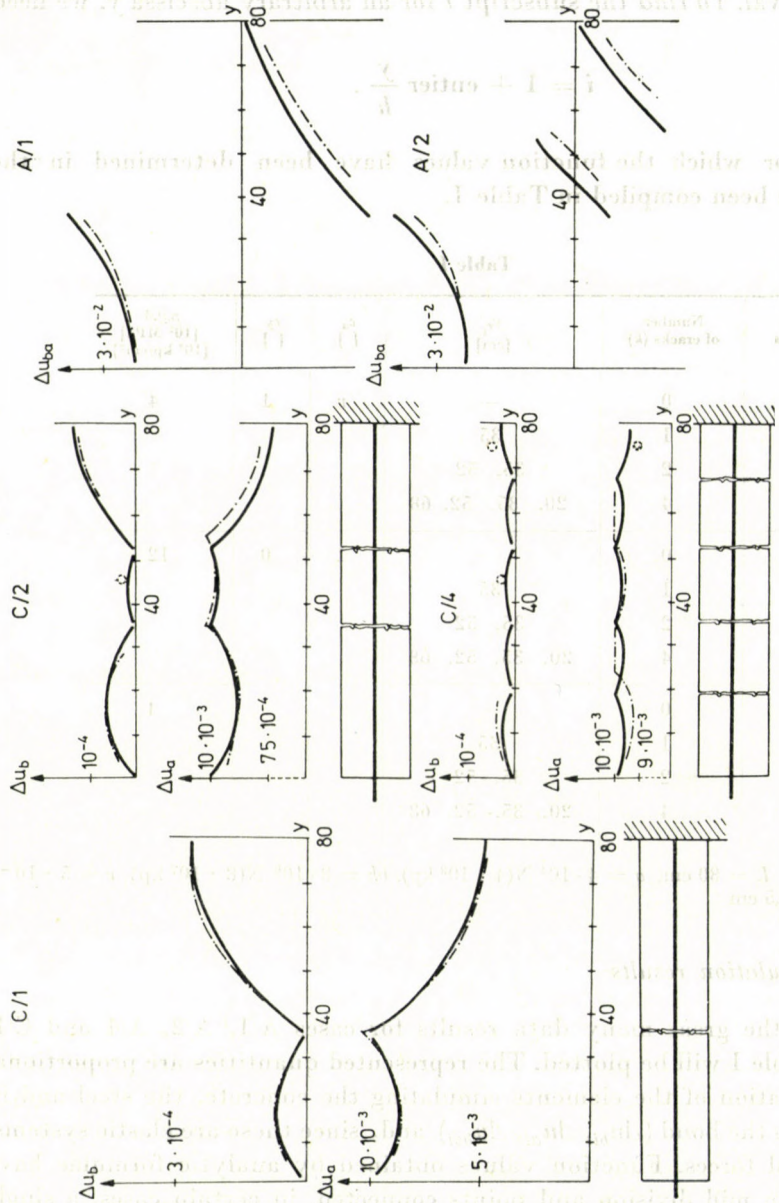
A/1
A/2
C/2
C/4
C/1
y
80
40
Δu_{ba}
Δu_b
Δu_a
$3 \cdot 10^{-2}$
10^{-4}
$10 \cdot 10^{-3}$
$75 \cdot 10^{-4}$
$9 \cdot 10^{-3}$
$3 \cdot 10^{-4}$
$5 \cdot 10^{-3}$

Fig. 12

If the obtained $i_r = i_{r+1} = i_{r+2} = \ldots = i_{r+s}$, then the cracks i_{r+1}, i_{r+2}, $\ldots$, i_{r+s} are left out of consideration by the calculation since the cracks are within the same interval. To find the subscript i for an arbitrary abscissa y, we need to apply

$$i = 1 + \text{entier}\,\frac{y}{h}\,.$$

Parameters for which the function values have been determined in the examples have been compiled in Table I.

Table I

Sign of series	Number of cracks (k)	y_{r_i} [cm]	c_a [ ]	c_b [ ]	p_d/A [10^2 MPa] [10^3 kp/cm^2]
A	0	—	ν	1	4
	1	35			
	2	35, 52			
	4	20, 35, 52, 68			
B	0	—	1	0	12
	1	35			
	2	35, 52			
	4	20, 35, 52, 68			
C	0	—			4
	1	35			
	2	35, 52			
	4	20, 35,- 52, 68			

In all the cases $L = 80$ cm, $q = 4 \cdot 10^4$ N($4 \cdot 10^3$ kp), $bh = 8 \cdot 10^8$ N($8 \cdot 10^7$ kp), $\nu = 5 \cdot 10^{-2}$, $h = 10{,}5$, 1 and 0,5 cm

7.2. *Calculation results*

Among the great many data results for cases A/1, A/2, A/4 and C/1, C/2, C/4 in Table I will be plotted. The represented quantities are proportional to the deformation of the elements simulating the concrete, the steel and in some examples the bond (Δu_{bi}, Δu_{ai}, Δu_{bai}) and, since these are elastic systems, to the internal forces. Function values obtained by analytic formulae have been plotted in mid division and points connected, in certain cases, a single point could be plotted (Fig. 12).

To visualize the mesh effect, values obtained for $h = 0{,}5$ cm have been traced in full line, and for $h = 10$ cm with dashed line, both reduced to $h = 10$ cm.

Elongation values characterizing the member stiffnes (u_{b1}) have been determined for different cases of cracking. The increase of the overall elongation with each crack under constant load is quite conspicuous. For instance, in example *A*, in cases of one, two, four cracks, the calculated stiffness ratio compared to the crack-free bar was, for a mesh $h = 10$ cm ($h = 5$ cm in brackets): 0,0566 (0,0564); 0,0476 (0,0488); 0,0376 (0,0336).

The stiffness of the tested tension member was seen to abruptly decrease after the first crack but to vary less after subsequent cracks, pointing to the necessity of prestress in stays or tie rods of huge structures (*e.g.* [21]), and to the important change of forces and reactions due to stay cracking. The example shows the effect of mesh to be moderate. On the contrary, different mesh would be disturbing. Thus, apparently, there is no unambiguous dependence between calculated stiffness and mesh. Relative deviations between overall elongations, calculated with otherwise equal data, as a function of the mesh, ranged from 1,1% to 11,2%. Results of examples *B* and *C* demonstrated the effect of bond characteristics.

Also the calculated crack width depends on Λ and γ, and on the crack position. Related to the series in *B*, for γ modified according to examples *C*, relations of crack widths calulated with other-wise equal parameters for mesh of $h = 10$ cm (in brackets $h = 5$ cm) are, in case of one crack, 1,371 (1,402), for four cracks 1,057 (1,054); 1,029 (1,043); 1,058 (1,046); 1,082 (1,069) in this order. Several comparisons showed the crack width not to depend typically on the mesh. Note that in the investigated cases, the relative deviation between crack widths ranged from 1,6% to 7,4% according to the mesh. The examples included no case where the calulcation would refer to one, rather than two or more cracks because of increased mesh. Obviously, it would cause a rough error, to be absolutely avoided by chosing a mesh incomparable with the crack distance.

7.3 Conclusions drawn from calculation results

The elaborated relationships lend themselves also to the quantitative analysis of one-dimensional reinforced or prestressed concrete models. For a given crack condition stiffness characteristics of the member can be calculated. The relationships are suitable to exactly determine internal forces of elements of an actually discrete behaviour based on the starting data, or to apply the discrete model formulae — aptly selecting the mesh — as a fair approximation of the continuous bond.

Selection of the mesh involves the following conclusions: In two different models, even if the ratio of interval lengths is as much as 20, but there are sufficient mesh intervals in the given domain or between the cracks — calculation accuracy is little affected by the mesh size. Also, if mesh distances are

comparable to crack spacings, the calculation is somewhat meaningless. Thus, mesh intervals are advisably assumed as lower by an order than the expected crack width. It is easy to understand that the accuracy of a result does not depend exclusively or primarily on the mesh. Namely, if in a continuous member some crack is situated nearer to a node of a discrete model belonging to a coarser mesh than to that of a finer one then calculation for a coarser mesh will better approximate the continuum conditions in the surroundings of the investigated spot (see *e.g.* the surroundings of both cracks of example $C/2$ in Fig. 12). Of course, the deviation is more likely to be greater for a coarser mesh as compared to the exact case for the continuum, but the other case is only possible, as exemplified by the calculation values referred to. It is typical that in a cracking case, stiffness or crack width, as a function of the mesh could be represented by a monotonously increasing, monotonously decreasing function or such showing intermediate extreme values.

To increase the accuracy, reducing the mesh in subsequent calculations for the selected system, and desirous to avoid the case referred to — where reducing the mesh hence adding to the calculation work did not result in any increased accuracy — mesh had to be reduced according to increasing powers of 1/3. Namely, in this concept, odd multiples of half interval h will yield abscissae to which characteristics determined from the relative displacements between neighbouring nodes will be assigned. These mesh halves exactly coincide with halving points obtained from a finer mesh if the new interval is $(1/3)^k$ times the original one ($k = 1, 2, \ldots$).

8. Conclusions

Analytic treatment of the system of equations for one-dimensional discrete reinforced or prestressed concrete model analyses written according to the displacement method was facilitated by the recognition that it is possible and advantageous to partition the coefficient matrix into four blocks, by correctly selecting the order of unknowns .

Although within this problem, blocks of the coefficient matrix are not commutative even in the simple case — that of an elastic, crack-free member — blocks of the inverse could be written. Calculations are centered around the thesis of the matrix theory stating that the inverse of any tri-diagonal matrix is a one-pair matrix, and vice versa.

Consideration of cracks modified the coefficient matrix, so that each crack was affected by one diade of modification. Thereby the theorem for producing the inverse of modified matrices could be applied. Its practical application in the given case was again permitted by the quoted reciprocity between one-pair and tri-diagonal matrices. The applied principle and the

developed method permit us to determine, for an arbitrary load, the forces and the deformed condition, here, however, formulae were only given for the practical case where external forces act only at the free end of the member simulating the concrete and the steel, of arbitary ratio.

The obtained formulae demonstrate modification of the phenomenon upon one, two or more cracks. The analysis is much complicated by the yield of the bond model. The mathematical treatment is again made possible by the recognition of the need to modify the coefficient matrix already modified because of the cracks by as many further diades as there are yielded bars.

The example shows the suitability of the developed relationships for the exact analysis of axially reinforced or prestressed units with really equidistance load transfer intervals. Formulae for the discrete model truly illustrate the replacement of a continuous model by a finite one, the obtained analytic relationships are essentially contributions to the evaluation of the mesh applied in the finite model.

REFERENCES

1. Almási, J.: Wieviel Spaltzugbewehrung ist nötig? *IVBH Abhandlungen* **35**-II. (1975) 15—27
2. Avram, C.—Filimon, J.—Capatu, Ch.: Aspects concernant la fissuration des éléments en béton precontraint. *6^e Congrès de la FIP*, Praha 1970
3. Bodó, L.: Betonacélok és feszítőacélok technológiája (Technology of Reinforcing and Prestressing Steels). Műszaki Könyvkiadó Bp. 1968
4. Bogin, N. M.: Tekhnologiya predvaritel'no napryazhennogo zhelezobetona. Gosstroyizdat Moscow 1960
5. Cedolin, L.—Dei Poli, S.: Finite Element Nonlinear Analysis of Reinforced Concrete Bidimensional Structures. *Inst. di Sc. e Techn. delle Constr.* Milano N° 40, 1974
6. Dimitriev, S. A.—Kalaturov, B. A.: Raschet predvaritel'no napryazhennykh zhelezobetonnykh konstruktsiy. Stroyizdat, Moscow 1965
7. Fogarasi, Gy.—Adamik, M.: Hegesztett betonacél vázak (Welded Skeletons of Reinforcing Steel). Műszaki Könyvkiadó Budapest, 1976
8. Fujii, M.: Shear Design of Prestressed Concrete Stepped Beams. *Journal of Japan P. C. Engineering Association* 16 (1974) 5. 33—40
9. Gantmakher, F. R.—Kreyn, M. G.: Ostsillatsionnye matritsy i yadra i malye kolebaniya mekhanicheskikh sistem. Gostekhizdat, Moscow 1960
10. Guyon, Y.: Béton précontraint. Etude théorique et expérimentale. Eyrolles, Paris, 1951
11. Nilson, A. H.: Nonlinear Analysis of Reinforced Concrete by Finite Element Method. *ACI Journal* (1968), 757—766
12. Robinson, J. R.—Morisset, A.: Paramètres fondamentaux de la fissuration des tirants en béton armé. *Annales de l'Institut Technique du Bâtiment et des Travaux Publics* **254**, (1969), 2
13. Rózsa, P.: Lineáris algebra és alkalmazásai (Linear Algebra and its Applications). Műszaki Könyvkiadó, Budapest, 1974
14. Rózsa, P.—Tassi, G.: Eine Matrizenmethode zur Lösung statisch unbestimmter Systeme im elasto-plastischen Bereich. *Wissenschaftliche Zeitschrift der Technischen Universität Dresden.* **10,** (1961), 1329—1332
15. Sherman, J.—Morrison, W. J.: Adjustment of an Inverse Matrix Corresponding to Changes in a given Column or a Given Row of the Original Matrix. *The Annals of Mathematical Statistics* **21,** (1949), 124
16. Szalai, K.—Almási, J.—Hegedűs, I.—Kovács, B.: A vasbeton szerkezetek új tervezési szabványának műszaki-gazdasági következményei (Technical-Economical Consequences

of the New Standard for Reinforced Concrete Structures). *Magyar Építőipar* **32,** (1974), 89—96
17. TASSI, G.: A feszített betét betonban való lehorgonyzódásának elmélete (The theory of Anchorage of Prestressed Reinforcement in Concrete). *Építés- és Közlekedéstudományi Közlemények* (1959) 1—2, 217—218
18. TASSI, G.: Analogy-Based Mathematical Model of Reinforced and Prestressed Concrete Members. *Periodica Polytechnica*, **22** (1978), 3—4. 169—204
19. TASSI, G.: Experimentelle Forschungen und Berechnungsmethoden zur Prüfung der Grenzzustände von Spannbetonbalken. *Periodica Polytechnica* **18,** (1974), 189—207
20. TASSI, G.: Feszített vasbeton tartók feszültségi és alakváltozási állapotai (Stress-Strain Conditions of Prestressed Concrete Members). Thesis, Academy of Sc. Hung. 1975
21. TASSI, G.: Függesztett és szabadon szerelt feszítettbeton hídszerkezetek. (Stayed and Cantilever Mounted Prestressed Concrete Bridge Structures). *Mélyépítéstudományi Szemle.* **23,** (1973), 522—526
22. TASSI, G.: Két kapcsolt elemből álló rúd egydimenziós számítási modelljének vizsgálata. (Analysis of a Onedimensional Mathematical Model of a Bar of Two Connected Elements). *BME Építőmérnöki Kar Építőanyagok Tanszék Tudományos Közlemények* **21,** (1975), 141—166
23. TASSI, G.: Kísérleti kutatások a feszített betét lehorgonyzódásának vizsgálatára (Experimental Research on the Investigation of Self-Anchorage of the Prestressing Steel.). *Építés- és Közlekedéstudományi Közlemények* (1960), 235—265
24. TASSI, G.: The Possibility of Anchorage on Finite Length in Pretensioned Prestressed Concrete. *Sc. Publ. of the Techn, Univ. of Arch. Buildg. Civ. and Transp. Engineering* (1957), 41—50
25. TASSI, G.—WINDISCH, A.: A feszített vasbeton szerkezetek új szabványának műszaki-gazdasági következményei (Technical-Economical Consequences of the New Standard for Prestressed Concrete Structures). *Magyar Építőipar* **23,** (1974), 97—103
26. TASSI, G.—WINDISCH, A.: Analysis and Model Testing of the Anchorage Zone of Post-tensioned Beams. *FIP VII. Congress*, New York (1974)

Analytische Untersuchung der diskreten Modelle von Stahlbeton- und Spannbetonelementen. Es wird das aus den Beton, die Bewehrung und die Verbindung repräsentierenden Elementen zusammengesetzte, eindimensionale Modell von Stahlbeton- und Spannbetonstäben analytisch untersucht. Eine analytische Behandlung des für das diskrete Modell angeschriebenen Gleichungssystems wird dadurch ermöglicht, daß die Koeffizientenmatrix des Systems in geschlossener Form invertierbar ist. Die Berücksichtigung der Risse ergibt sich als die Modifikation um je eine Dyade der Koeffizientenmatrix. Die Arbeit zeigt auch eine Methode zur Berücksichtigung gewisser plastischer Fromänderungen. Die erhaltenen geschlossenen Formeln zeigen, wie sich die Erscheinung in Verbindung mit der Rißbildung im Falle eines, zweier oder weiterer Risse beliebiger Anzahl gestaltet. Die Anwendbarkeit der Beziehungen wird an Beispielen gezeigt. Da die Formeln der inneren Kräfte, der Formänderungen und der Rißbreiten auch das Teilungsintervall des diskreten Modells enthalten, läßt sich die Wirkung der Wahl des Teilungsintervalls gut beurteilen.

Аналитическое исследование дискретных моделей элементов из железобетона и предварительно напряженного железобетона. В работе рассматривается аналитическим путем одномерная модель железнобетонных и преднапряженно-железобетонных стержней, составленная из элементов, представляющих бетон, сталь и связь. Трактовка аналитическим путем системы уравнений, записанной для дискретной модели возможна благодаря тому, что матрица коэффициентов системы может быть инвертирована в законченной форме. Учет трещин получается как модификация матрицы коэффициентов по диаду. В работе показывается и метод для учета некоторых пластичных деформаций. Получение связанное с трещиноватостью в случае одной, двух или больше — любого числа — трещин. Примеры доказывают применимость зависимостей. Так как формулы внутренних сил, деформаций и ширин трещин заключают в себе и шаг дискретной модели, влияние выбора шага хорошо оценимо.

BOOK REVIEW

G. Ammelburg

KONFERENZTECHNIK

VDI-Verlag GmbH Düsseldorf, 1976, 176 S.

Jetzt, wo auch in Ungarn eine neue Form des Unterrichts der Führungstechnik in den Vordergrund trat, kann diese in der BRD erschienene, für Ingenieure zusammengestellte Arbeit von Interesse sein.

Der Verfasser geht davon aus, daß im Verhältnis zu anderen Mitteln der Führung die verschiedenen Konferenzen einen relativ schlechten Wirkungsgrad haben. In der Einleitung faßt das Buch sofort die tatsächliche Situation der Konferenzen zusammen und es hat eine niederschmetternde Meinung von der Organisation, der Vorbereitung, der Leitung, dem Ablauf, dem Wirkungsgrad und dem Erfolg der heutigen Konferenzen. Da jedoch die Konferenzen unverändert nützliche Mittel der Information, Motivierung, Kommunikation sein können, behandelt der Verfasser der Reihe nach die damit zusammenhängenden Probleme, Schwierigkeiten und Lösungsmöglichkeiten. Solche sind z. B. der Führungsstil und die Führungstechnik, die diesbezüglichen Kenntnisse aus Psychologie und Soziologie; die Gruppengespräche als Führungsmittel; die Persönlichkeit des Konferenzleiters; die Vorbereitung und Regulierung; viele Eigenarten der Konferenzleitung und des Konferenzablaufs; die Rückkopplung (feed back), schließlich die auf der Konferenz sich ergebenden mehrerlei besonderen Situationen.

Das Buch schließt mit der Zusammenfassung der Benennung der Konferenzarten, Wiederholung der 17 Thesen der Konferenztechnik und dem Literaturverzeichnis mit 24 Hinweisen.

Es ist der Mühe Wert als Geschmacksprobe die bald deutschen, bald englischen Ausdrücke der Nomenklatur der Konferenzarten im Original zu zitieren: Besprechung, Brainstorming, Case-method, Demonstration, Forum, Hearing, Kollege, Kollektiv, Kolloquium, Meeting, Metaplan, Panel discussion, Presentation, Pressekonferenz, Runde, Rundgespräch, Seminar, Sit-in, Teach-in, Sitzung, Symposion, Tagung, Teamwork, Versammlung, Lehrkonferenz.

Im Gegensatz zu dieser ausführlichen (und auf Einzelheiten nicht eingehenden) Aufzählung beschränken sich die praktischen Ratschläge auf eine ausgesprochene Art der Unternehmenskonferenz mit nur 8—12 Teilnehmern.

Die 17 Thesen fassen auch viele nützliche Ratschläge zusammen und charakterisieren zugleich den wesentlichen Inhalt des Buches, deswegen zählen wir sie hier auf:

1. Konferenzleiter sollte nicht der höchste anwesende Vorgesetzte und auch nicht der beste Fachmann der anstehenden Thematik sein, sondern ein Könner in Konferenztechnik.
2. Wer sich in einer Konferenz manipuliert fühlt, sollte zunächst einmal sich selbst überprüfen, ob er nicht Vorurteilen unterliegt, und dann freimütig versuchen diese abzubauen.
3. Wenn eine Konferenz nicht mehr erbringt als die Summe der Einzelleistungen der Teilnehmer, dann sollte sie besser unterbleiben.
4. Bei Routinekonferenzen oder häufig sich wiederholenden Konferenzen der gleichen Gruppe sollte ein turnusmäßiger Wechsel der Konferenzleitung grundsätzlich angestrebt werden.
5. Vertrauen muss als Basis jeglicher Kommunikation zwischen Menschen auch in der Konferenz angestrebt werden.
6. Konferenzzeit ist Arbeitszeit eines jeden einzelnen, multipliziert mit der Anzahl der Teilnehmer.
7. Je besser die Arbeitsvorbereitung, desto mehr Erfolgserwartung für eine rationell ablaufende Konferenz.
8. Cliquenbildung jeglicher Art wird stets zum Tod einer Konferenz führen.
9. Die Gegebenheiten des Konferenzraums tragen entscheidend zum Ablauf und zum Ergebnis einer Konferenz bei.

10. Eine optische Demonstrationsmöglichkeit gehört unabdingbar zur Ausstattung eines Konferenzraums.

11. Pünktlicher Beginn und pünktlicher Schluß sind des A und Ω jeder guten Konferenz.

12. Jeder Konferenzteilnehmer sollte — nach Möglichkeit — ausreichend Vorinformationen erhalten und ist verpflichtet, sich intensiv auf die Konferenz vorzubereiten.

13. Der Konferenzleiter greift in die Diskussion der Konferenz nur ein zwecks Steuerung und Regelung der Ordnung. Die eigene Meinung hat er unbedingt zurückzustellen.

14. Namenschilder (Tischkarten) sind eine wichtige Kommunikationshilfe; auf diese sollte auch nicht verzichtet werden, wenn die Teilnehmer einander gut kennen.

15. Abstimmung sollten bei Konferenzen nur dann praktiziert werden, wenn keinerlei Chance mehr für eine Kompromisslösung vorhanden ist.

16. Jeder Konferenzteilnehmer darf sich in der Konferenz so gut blamieren, wie er kann. Nur der Konferenzleiter darf auf keinen Fall einen Teilnehmer vor der Gruppe bloß stellen oder lächerlich machen.

17. Ein allseits befriedigender Konferenzabschluß ist die beste Voraussetzung für eine positive Einstellung der Teilnehmer zur nächsten Konferenz.

Es ist zweifellos ein Wert des Buches daß es die mit der kompletten Abwicklung der Konferenzen verbundenen Begriffe zusammenfaßt, erläutert und zweckmäßige Ordnungsprinzipien aufstellt.

Z. Terplán

BETONTECHNISCHE BERICHTE, 1976

Beton Verlag GmbH Düsseldorf

Die Publikation enthält acht Abhandlungen, die über die neuesten Ergebnisse de Forschungsinstitute der Bundesrepublik Deutschland berichten.

Die Stuttgarter Forscher beantworten auf Grund ihrer Forschungen die Frage, ob die Schalldämmung der Betonbauwerke den Anforderungen entspricht.

Die Schalldämmung der aus normalen Beton (Schwerbeton) errichteten Bauwerke ist bei den durch die üblichen Abmessungen bedingten Gewichte bzw. Massenverhältnisse ausreichend.

Die in den aus Schichten bestehenden Elementen der Plattenbauten angeordneten Wärmedämmschichten steigern die Schalldämmung dieser Konstruktionen. Im Beton ist die Verbreitung des Körperschalls bedeutend, doch ist sein Dämpfungsvermögen nicht minderwertiger, als das der Ziegelbauten. Die Düsseldorfer Versuchsserie lieferte wertvolle Anhaltspunkte zur Planung von Spannbetonreaktoren. Die Änderungen der mechanischen Kennwerte des Betons infolge von Neutronbestrahlung sind unbedeutend. Die Verminderung der Druckfestigkeit ist erst nach Überschreitung des Wertes von etwa $3 \cdot 10^{19}$ Neutron/cm^2, die der Zugfestigkeit bei mehr els etwa $1 \cdot 10^{19}$ Neurron/cm^2 zu beobachten. Bei richtiger Wahl des Zuschlagstoffes erträgt der Beton eine Temperatur von 200 ÷ 300 °C ohne jede Verminderung der Festigkeit. Für diesen Zweck eignete sich Kalksteinsplitt am besten. Beim Bau von Reaktoren erwies sich der im Volumenverhältnis von 3% angefertigte "Stahlfaden-, Stahlfaserbeton" als sehr vorteilhaft.

Die gute Wärmeisolierung der Gebäude bildet eine bedeutende Grundlage der Energieeinsparung. Die diesbezüglichen minimalen Anforderungen sind in DIN 4108 unter Berücksichtigung der Wohnungshygiene bereits festgelegt, doch hat die Ermittlung der tatsächlichen Wärmeverluste der Gebäude eine weitere Verschärfung der Vorschriften erfordert. Im Rahmen dieser Bestimmungen wurde der Wärmedurchgang nicht nur der Fenster und Türen, sondern auch der Decken (Kellerdecke und Dachdecke) eingeschränkt. Der Wärmeschutz erstreckt sich auf die bauphysikalischen Zusammenhänge zwischen der Wärmedämmung, den Temperaturschwankungen und der klimatischen Feuchtigkeit.

Bekanntlich sind die wärmetechnischen Eigenschaften des Betons günstig. Der Autor bietet einige Beispiele für die Anordung der Wärme- und Dampfsperrschichten. Die richtige Wahl der zur Verfügung stehenden und in großem Ausmaß angewandten technischen Lösungen ermöglichen die Befriedigung der Anforderungen der bestehenden Vorschriften.

Die Abhandlung von WALY analysiert, gestützt auf deutsche und amerikanische Untersuchungsergebnisse, die mechanischen Eigenschaften 30- und 50-jähriger Betone und kommt zum Schluß, daß die Druckfestigkeit des im Freien gelagerten Portlanzementbetons nach 30 Jahren 2,3mal und nach 50 Jahren 2,5mal größer ist, als die 28tägige Druckfestigkeit. Die Steigerung des Elastizitätsmoduls kann mit 15 ÷ 20% angenommen werden.

Die beschränkte oder hohe Frostbeständigkeit des Betons gewährleisten die frostbeständigen Zuschlagstoffe. Die den diesbezüglichen Vorschriften von DIN 4226 entsprechend vorgenommen Untersuchungen erwiesen sich als unzulänglich, weshalb fünf große Forschungsinstitute der Budesrepublik Deutschland auf Grund von 130 Untersuchungen eine neue Qualifizierungsmethode ausgearbeitet haben, die den jeweiligen an den Beton gestellten Anforderungen (Frostbeständigkeitsgrad) unter seiner Bestimmung (z.B. Sichtbetonfläche, Straßenbelag usw.) entsprechend, die anzuwendende Untersuchungsmethode und ihre Auswertung vorschreibt.

Die Abhandlung LOCHERS befaßt sich mit den die Druckfestigkeit der Zemente betreffenden Fragen. Anhand von fachliterarischen Daten und auf Grund seiner eigenen Versuchsergebnisse hat er festgestellt, daß die mittlere (spezifische) Druckfestigkeit des Zementsteins 2000 kp/cm^2 beträgt. Dieser Wert vermindert sich gesetzmäßig mit dem Maß der kapillaren Porosität. Auch der Erhärtungsprozeß und die Zusammensetzung des Zements wirken sich auf die spezifische Druckfestigkeit aus. Durch Druck bei hoher Temperatur kann eine spezifische Festigkeit von 6000 kp/cm^2 erzielt werden. Der Erhärtunsprozeß nimmt nach einer "Ruhepause" von 6 Stunden seinen Anfang. Dieser Vorgang kann durch Zugabe von Chemikalien oder durch Wärmebehandlung beschleunigt werden. Das Feinmahlen des Zementes ist nur innerhalb gewisser Grenzen vorteilhaft, da der zu fein gemahlene Zement im Interesse der Verarbeitbarkeit des Betons die erhöhte Zugabe von Wasser erfordert, was die Verminderung der Festigkeit des Betons zur Folge hat.

Gegenstand der Düsseldorfer Versuche war die Wirkung der verschiedenen Zemente auf die Stabilität der Zementsuspension und der Verflüssigung zu ermitteln. Es können lückenlose Zusammenhänge zwischen den physikalischen, chemischen und mineralogischen Kennwerten, sowie den rheologoschen Eigenschaften der Zementsuspension festgestellt werden. Zu den Versuchen wurden 19 Zementarten mit Wasserzementfaktoren von 0,6 bis 2,0 verwendet. Das Resultat wurde mit elektronischer Datenverarbeitung nach dem Regressionsverfahren ermittelt. Die Stabilität der Zementsuspension kann in Funktion der Viskosität und des Wasserzementfaktors ausgedrückt werden.

Die Absetzgeschwindigkeit bestimmen vor allem der Wasserzementfaktor und die Kornverteilung.

Die letzte Abhandlung der Ausgabe behandelt die derzeitige Lage und die künftigen Aufgaben der Betontechnologie.

Die Eigenschaften des Betons sind bekannt und sein Verhalten verschiedenen Einflüssen gegenüber können als bereinigte Fragen erachtet werden. In Kenntniss dieser ist es stets möglich die technisch und wirtschaftlich entsprechendste Lösung zu wählen.

Die Abhandlungen enthalten reiche literarische Informationen. Die Ausgabe '76 schließt ein Verzeichnis der bisher veröffentlichten Abhandlungen ab.

B. Goschy

Aurel A. Beleș—Mircea V. Soare

ELLIPTIC AND HYPERBOLIC PARABOLOIDAL SHELLS USED IN CONSTRUCTIONS

Editura Academie Române -Christie and Partners, Boucharest—London 1971, 750 pages, 230 figures, 95 tables, autor's index

The book entitled "Elliptic and Hyperbolic Paraboloidal Shells Used in Constructions" is the expanded translation of the one published in 1964 in Roumanian. It was formarly translated into French (Dunod Paris, 1967) and also into German (VEB Verlag für Bauwesen, Berlin 1971).

The work is divided in to three parts and into 16 chapters, complimented by 8 appendices.

The first part discusses the principle rules and solution methods of the theory of shell structures. The second part deals with the membrane theory of elliptic and hyperbolic paraboloidal shells, including the deformation problems of the membrane-like state of stresses. The third part treats the bending theory of elliptic and hyperbolic paraboloidal shells. The appendices contain different kinds of useful function tables.

The book collects in one framework all those knowledges which have been widely discussed on pages of different international periodicals and congress proceedings. In this framework

a considerable part is devoted to the important research results achieved by the authors themselves. These contributed to a great extent to the clarification of the state of stresses and deformations of elliptic and hyperbolic paraboloidal shells.

All the problems treated in the book are discussed in detail. The form of the discussions is comprehensible and clear, the statements are convincing. The whole work is well-illustrated by figures and diagrams, giving a true insight into the subjects under discussion. All the chapters are complemented by a detailed list of references. Through these the possibility is given for the further study of the treated problems.

The English version of the book assures that this prominent work would become known is a wider circle than up till now. It will be a useful aid for all those who, all over the world, are dealing with theoretical and practical problems of shell structures. The book could also be excellently used as an text book for university students.

P. Csonka

O. Föllinger

LINEARE ATASTSYSTEME

R. Oldenbourg Verlag München, Wien 1974, 329 Seiten, 113 Bilder, 2 Tabellen

Prof. Dr. rer. nat. Otto FÖLLINGER schreibt im Vorwort seines Buches: " . . . Demnach sind die Methoden zur Behandlung von Abtastsystemen bis her nicht in der gleichen weise Allegemeingut geworden wie die Methoden für kontinuirlichen Systeme, obgleich durch die Verwendung von Prozessrechnern zur Steuerung und Regelung ein sehr aktuelles Interesse an derartigen Systemen besteht. Aus diesen Grund wurde das Thema in die Reihe "Methoden der Regelungstechnik" aufgenommen. Entsprechend der Zielsetzung der Reihe beschränkt sich der Text auf die wesentlichen Züge der Theorie und versucht, diese anschaulich und anwendungsnah darzustellen".

Das Buch beschäftigt sich mit den Grundprinzipen der linearen Abtastsystemen, behandelt die diskrete z-Transformation, gibt Bedingungen für die Stabilität geschlossener Regelkreisen, entwirft ein Algorithm für endliche Einstellzeit und schlieslich führt in die Theorie des Zustandsraums ein.

Nachden im Kapitel 1. das Abtastvorgang durch Beispiele deutlich erklärt wurde, wird der Direkter Digitaler Kontrolle (DDC) am Hand einer konkreten Regelstrecke erklärt. Zwei — in den Prozessrechnern übliche Algorithmen — die PI Positons- und Geschwindigkeits — Algorithmen werden abgeleitet.

Kapitel 2 ist die mathematische Beschreibung des Abtastvorganges. Die Erzeugung einer Treppenfunktion aus einer kontinuirlichen Funktion kann auf zwei Weisen implementiert und aus einfachen mathematischen Operationen aufgebaut werden. Physikalisch teilt es sich auf Abtastung und Speicherung über die Abtastzeit. Die mathematische Zerlegung der Treppenfunktion führt zu der Reihenschaltung von Impulsabtäster und Halteglied. Aus der allgemeinen Beschreibung eines Haltegliedes werden die Impulsantworten der üblichen Halteglieder O-ter und 1. Ordnung hergeleitet.

Kapitel 3 ist die mathematische Behandlung von Abtastsystemen in der Zeitbereich und in Form der z-Transformation. Die Rechnenregeln wie Verschiebungs-, Dämpfungs-, Differenzbildungs-, Summations-, Faltungs- und Grenzwertregeln, sowie die Methoden der z-Transformation rationaler Laplace Funktionen und die Rücktransformation der z-Transformierten werden ausfühlich abgeleitet. Die Transformierten häufig vorkommener Funktionen sind in Tafeln zusammengefasst.

Im Kapitel 4 wird die z-Übertragungsfunktion zur mathematischen Beschreibung von Abtastsystemen eingeleitet. Mit deren Hilfe werden die Führungs — und Störübertragungsfunktionen geschlossener Regelkreisen abgeleitet.

Kapitel 5 ist dem Problem der Stabilität gewidmet. Nach der Definition der Stabilität werden notwendige und hinreichende Stabilitätsbedingungen in Zeit und z-Bereich hergeleitet. Aus den vielen algebraischen Stabilitätsuntersuchungen werden die bilineare Transformation, die Methode von Schur-Cohn-Jury, und das Reduktionsverfahren ausführlich behandelt. Um Stabilität, oder Labilität schnell zu bestimmen werden nur notwendige und nur hinreichende Bedingungen auch gegeben. Stabilitätsungleichungen für Polinome niedrigen Grades, welche in der Praxis häufig vorkommen, sind auch presentiert. Als graphische Stabilitätsuntersuchungen wurden das Wurzelortverfahren, das Nyquist -Verfahren, die Verwendung der Abtast-Ortskurve und Frequenzkennlinien dargestellt.

Im Kapitel 6 wird ein Syntheseverfahren behandelt, das es bei kontinuirlichen Systemen nicht gibt, der Entwurf auf endliche Einstellzeit. Es ist von besonderen Bedeutung, weil man den mit dem Führungswert vorgeschriebenen Wert mit konventionellen diskreten Regeln in kurzer Zeit nicht erreichen kann. Um eine endliche Einstellzeit zu erreichen, kann es sinnvoll sein auch in ein ursprünglich kontinuirliches System einen Abtaster stellen. Die Synthesegleichungen werden hergeleitet und durch Beispiele erklärt. Der optimale Eingangssygnal der Strecke ist im geschlossenene Regelkreis als Ausgang eines Reglers herstellbar, die Parameter des diskreten Reglers werden gegeben. Der Regler ist durch Abtast-Halteglieder oder mit Hilfe von rationalen kontinuirlichen Übertragungsgliedern realisierbar.

Im Kapitel 7 wird die Beschreibung der Abtastsysteme im Zustandsraum presentiert. Nach der Behandlung der Grundbegriffe, der Transformationen, der Steuerbarkeit und der Beobachbarkeit wird der Regler auf endliche Einstellzeit im Zustandsraum entworfen und durch ein Beispiel ausführlich erklärt.

Das Buch entspricht den Zielen entsetzt bei dem Author. Es ist eine gute Einleitung in die Theorie linearer Abtastsysteme. Sein Vorteil verglichen mit anderen Büchern ist, daß das ganze Thema zuerst in der Zeitbereich und nur später mit Hilfe der z-Transformierten behandelt wird, so verliert der Leser den Kontakt mit dem ursprünglichen Regelproblem nicht, das in der zeitbereich abgefasst wurde.

Das Buch, wie andere Monographie der Reihe "Methoden der Regelungstechnik", ist als Textbuch für Studenten sowie für Ingenieure, die das Thema Abtastregelungen kennenlernen möchten, vorgeschlagen.

R. Haber

G. Franz (Schriftleiter)

BETON-KALENDER 1977

Verlag von Wilhelm Ernst u. Sohn, Berlin—München—Düsseldorf 1977. Teil I.: 1085 Seiten, Teil II.: 1135 S

Dieses Werk ist nun der 66. Jahrgang des von Jahr zu Jahr verjüngt erscheinenden vorzüglichen Taschenbuches.

Der erste Band enthält 10 Kapitel. Unter diesen sind die bedeutendsten jene, die sich mit den Stahlbetonkonstruktionen (W. SCHUHMACHER), mit der Festigkeitslehre (Prof. N. DIMITROV), Statik der Stabtragwerke (H. AHRENS—Prof. H. DUDECK), Bemessung der Stahlbetonkonstruktionen und Stabilitätsproblemen (G. GRASSNER, Prof. K. KORDINA—Prof. U. QUEST), sowie mit der Bemessung der Spannbetonbauteile (Prof. H. RÜSCH—Prof. H. KUPFER) befassen.

Der zweite Band des Werkes enthält 6 Kapitel. Von diesen ist die für den Ingenieur der Theorie und Praxis unentbehrliche Sammlung der Bestimmungen am weitläufigsten behandelt (H. GOFFIN). Wiederholt erscheinen einige aus den vorherigen Jahrgängen schon bekannte Kapitel: die Abdichtung von Bauwerken (R. LINDER), die Frage des Erddruckes, sowie die Teile, die sich mit der Gründung beschäftigen (N. KLÖCKNER—H. G. SCHMIDT).

Erwähnenswert ist noch unter den neuen Kapiteln derjenige Teil, der sich mit der Lagerung und den Lagern der Bauwerke befaßt, und diese so äußerst wichtige und oft vernachlässigte Frage des Stahlbetonbauens durch die scharfe Gegenüberstellung der richtigen und fehlerhaften Lösungen erklärt.

Als neues Kapitel erschien im Taschenbuch der Beitrag über Silos (G. TIM-WINDELS). Hier werden sämtliche Fragen in Bezug auf die Planung, Ausführung und Benutzung der Silos eingehend behandelt, und anhand von lehrreichen Bildern und Diagrammen werden alle Kenntnisse, die auf diesem Gebiet wichtig sind, zusammengefaßt.

Der Schriftleiter Prof. G. FRANZ, und die Verfasser der einzelnen Kapitel haben sorgfältig geachtet darauf, daß dieses Buch über den derzeitigen Stand, resp. über die aktuellen Probleme des Stahlbetonbauens einen kurzgefaßten, aber klaren und ausführlichen Bericht gibt. Der Text wurde durch zahlreiche Bilder, nützliche Tafeln, Diagramme und Formeln ergänzt. Sehr wertvoll sind die am Ende der einzelnen Kapitel befindlichen Literaturverzeichnisse, die zum weiteren Studium der verschiedenen behandelten Fragen dienen.

Alles zusammengefaßt, ist festzustellen, daß der neue Jahrgang dieses Handbuches von langjährigen Vergangenheit, der alten Tradition getreu, den Interessen des Stahlbetonbauens nicht nur auf deutschem Sprachgebiet, sondern auch über dessen Grenzen gute Dienste leisten wird.

P. Csonka

V. I. Karpman

NICHTLINEARE WELLEN IN DISPERSIVEN MEDIEN

Akademie — Verlag Berlin 1977, 235 Seiten, 25 Abbildungen. Übersetzung aus dem Russischen

Das vorliegende Buch gehört zur Serie "Wissenschaftliche Taschenbücher", Reihe Mathematik/Physik. Es ist die überarbeitete und erweiterte Fassung eines Vorlesungszyklus, den der Autor an der Staatlichen Universität in Nowosibirsk gehalten hat. In einigen Fällen wurde die Auswahl des Stoffes bis zu einem gewissen Grade von den eigenen Interessen des Verfassers diktiert, auf der anderen Seite hat man sich bemüht, die Grundgedanken und -ergebnisse möglichst vollständig wiederzugeben.

Das Buch enthält fünf Kapitel. Das erste Kapitel beschäftigt sich mit der linearen Näherung, das zweite gibt Beispiele für dispersive Medien. In dem dritten Kapitel werden die Fragen der nichtlinearen stationären Wellen, dabei im vierten die Theorie der nichtlinearen Wellen in Medien mit schwacher Dispersion behandelt. Das fünfte Kapitel beschreibt die "Enveloppen"-Wellen. Im Anhang werden die Probleme nichtlinearer Wellen mit langsam veränderlichen Parametern, die Entwicklung elektroakustischer Wellen im Plasma mit negativer Dielektrizitätskonstante, die ponderomotorische Kraft eines hochfrequenten Wellenfeldes im magnetoaktiven Plasma und der Kollaps von Plasmawellen behandelt.

Die Benutzung des Buches ist durch Inhalt-, Literatur- und Sachverzeichnis erleichtert.

Das Studieren des Buches erhebt Anspruch auf mathematischen und physischen Vorkentnisse von hoher Niveau. Das Buch ist für mit dem Problemkreis befassenden Studenten, Physiker und Ingenieure zu empfehlen.

F. Csáki

Á. Kézdi

FRAGEN DER BODENPHYSIK

Akadémiai Kiadó Bp. 1976. 148 Seiten, 215 Photos und Bilder, 6 Tafeln

Das Buch von Prof. KÉZDI herausgegeben vom Akadémie-Verlag im Jahre 1976 im Auftrag von dem Verein Deutscher Ingenieure (VDI) ist ein wertvoller Band des vielseitigen fachliterarischen Wirkens des Autors auf dem Gebiet der Bodenphysik, der Bodenmechanik und der Geotechnik. Das Buch beschäftigt sich mit einigen hervorgehobenen Fragen der Bodenphysik und beantwortet dieselben aufgrund von neuen Angaben, die im Zusammenhang mit der Verteilung der Körner und Poren nach dem Rauminhalt, mit der Verdichtbarkeit der Sande und der sog. Übergangsböden, mit dem hydraulischen Bodenbruch, der Suffosion und Erosion, der Phasenänderungen, die in den Sandböden auftreten, und mit der Schubfestgkeit und Zugfestigkeit der bindigen Böden sowie mit den anderen bezüglichen Problemen entstehen.

Kennzeichnend für das Buch ist, daß es die Wechselwirkungen der im Boden anwesenden drei Phasen (die Bodenteilchen, das Wasser und die Luft) untersucht. Der Autor führt für den zwischen den körnigen und bindigen Böden befindlichen Boden eine neue Definition ein und teilt die auf denselben bezüglichen und aufgrund von Experimenten erhaltenen Kenntnisse mit. Auch im Zusammenhang mit den Phasenbewegungen wird über neue Kenntnisse berichtet, und zwar in Zusammenhang mit der Möglichkeit der Versandung der Entnahmebrunnen und mit der in den Dreiphasenzonen auftretenden Wasserbewegungen. Im Zusammenhang mit dem Verhalten wird der sog. Selbstfiltereffekt ausführlich analysiert. Ein besonderes Verdienst des Buches ist, daß es eine einheitliche Untersuchungsmethode durchführt; die Auswirkungen der Phasenänderungen wurden mit Hilfe des Dreiecksdiagramms analysiert.

In dem Einleitungskapitel gibt der Autor die Untersuchungsgründe der Phasenänderungen bekannt. Abschnitt II behandelt die bodenphysische Analyse der Bodenteilchen und der Teilchenmengen, und zwar die Verteilung der Grobkörner, der Porengrößen im feinkörnigen Material, den Zusammenhang zwischen der Kornverteilung und der Verdichtbarkeit, die Eigenschaften der körnigen Mischungen und die Verdichtbarkeit der Übergangsböden. Abschnitt III erörtert die Fragen dier Festigkeit, und zwar der Festigkeit der Sande, der Übergangsböden und der bindigen Böden, den Sprödbruch der Böden, und die Schubfestigkeit der bindigen Böden. Einige Fälle der Phasenbewegungen werden im Abschnitt IV behandelt, wo nach der Zusammenfassung der grundsätzlichen Gesetzmäßigkeiten der Wasserbewegung in den gesättigten Sanden der hydraulische Bodenbruch, die Suffosion und Erosion, die in den Drei-

phasenzonen auftretenden Phasenbewegungen, weiters, in den bindigen Böden stattfindenden Bewegungen erörtert werden.

Das Literaturverzeichnis umfaßt 87 Werke und Abhandlungen. Es ist bedauerlich, daß die auf den Zwei- und Dreiphasensickerungen bezügliche heimische und ausländische (besonders die neueste) Wasserbau-Fachliteratur im Verzeichnis kaum erwähnt wird.

Das Fachbuch, welches die neuesten Ergebnisse der Bodenphysik und darunter in erster Linie die Versuchsergebnisse der Autors und des Geotechnischen Laboratoriums der Budapester Technischen Universität darstellt, kann in den Kreisen der sich mit der Bodenmechanik und Geotechnik beschäftigenden Ingenieure mit voller Anerkennung rechnen. Auch die in der Praxis arbeitenden Fachleute können in diesem Buch Lösungen zu Problemen finden, mit denen sie sich seit langem beschäftigen.

Ő. Starosolszky

Miklós Kozák

BERECHNUNG DER NICHT PERMANENTEN WASSERBEWEGUNGEN BEI FREIER OBERFLÄCHE

Akadémiai Kiadó, 1977. 410 Seiten

Das Buch befaßt sich im I. Teil mit der Theorie, im II. Teil mit der praktischen Berechnung der nicht permanenten Wasserbewegungen bei freier Oberfläche.

Die Wahl des Themas ist ungemein zeitgemäß, da die Mehrzahl der in der Natur auftretenden Wasserbewegungen temporär veränderlich, also nicht permanent ist. In der Praxis des Wasserbauingenieurs ergeben sich zahlreiche Aufgaben, wo es unerläßlich ist, den zeitweise wechselnden Charakter der Wasserbewegung in Betracht zu ziehen. Solche sind z.B. die Ansammlung der Wasser im Zuflußgebiet, das Abziehen der Flutwellen und die Möglichkeit ihrer Vorhersage, Untersuchung des Wasserhaushaltsgleichgewichtes von See, Speichern, die Berechnung von, in Kanälen und Flüssen entstehenden nicht permanenten Strömungen, ferner die tägliche Regulierung von Staustufen und Spitzenkraftwerken, die planmäßige Sicherung der Vorbedingungen der Schiffahrt, die planmäßige Inbetriebhaltung des komplizierten, geregelten Betriebes von Bewässerungskanalsystemen, Betriebsproben von Durchflußbauwerken und Wasserstandregulierungswerken usw. In allen angeführten Fällen kann es erforderlich sein allgemeine hydraulische Berechnungen vorzunehmen, deren Zweck es ist, die wichtigsten hydraulisch-technischen Kennwerte des Systems für die ganze Dauer des Vorganges zu bestimmen. Die Berechnungen können mit Hilfe der Theorie der nicht permanenten Strömungen durchgeführt werden.

Zur Lösung solcher Aufgaben bietet das Buch theoretische Grundlagen und zahlreiche praktische Anleitungen.

Im ersten Teil des Buches hat der Autor die theoretischen Grundlagen des Problems bei eingehender Bearbeitung der internationalen Fachliteratur festgelegt und mit seinen eigenen Forschungsergebnissen ergänzt, die sich vornehmlich auf die Berechnung der, in Betten mit zusammengesetzten Profilen entstehenden, nicht permanenten Wasserbewegungen beziehen. Das Verdienst des Verfassers besteht in der Einfachheit, Verständlichkeit und in der klaren, deutlichen Fassung des Stoffes. Im Interesse der Verständlichkeit ist die der Hydraulik entsprechende, ingenieurmäßige Denkungsweise in den Vordergrund gestellt.

Die sehr reiche Fachliteratur hat der Autor richtig verarbeitet und in Betracht gezogen und war hauptsächlich darauf bedacht, für die Berechnungsverfahren der eindimensionalen Strömungen gut brauchbare theoretische Grundlagen zu schaffen.

Ein besonderes Verdienst des Buches besteht in der Fortentwicklung zahlreicher Einzelheiten des Themas, besonders in der ausführlichen Bearbeitung und Lösung von praktischen Aufgaben, wie die Berechnung von Flutwellen, das ergänzende Oberflächengefälle, Theorie der Charakteristiken, Berechnung und Bemessung der komplexen Speicher, Kanalsysteme und Betten zusammengesetzter Profile, der Dammbrüche usw.

Im zweiten Teil des Buches löst der Autor ausschließlich praktische Beispiele, denen er komplette in FORTRAN-IV. verfaßte Programmlisten beifügt.

Es ist den Fachleuten allgemein bekannt, daß die nicht permanenten Wasserbewegungen bei freier Oberfläche — praktisch — nur mit einem Digitalautomaten berechnet werden können. Der Autor gibt deshalb für alle wichtigeren Berechnungsverfahren das vollständige

in FORTRAN-IV verfaßte mathematische Programm an. Die Programme sind im Subrutinsystem angefertigt und eignen sich — in entsprechender Weise zusammengestellt — zur Lösung zahlreicher Aufgaben. Detaillierte Beschreibungen und Beispiele erleichtern das Verständnis der Programme.

Das Wesen der auf dem Subrutinsystem beruhenden Berechnungen besteht darin, daß die Berechnung der einzelnen Phasen der nicht permanenten Strömungen (die Berechnung der Profilkennwerte, Gleichungskonstanten, Phasenkonstanten, Anfangs- und Grenzbedingungen usw.) in je einer selbstständigen Algorithmengruppe und diese dann in FORTRAN IV angegebenen Subrutinen zusammengefaßt sind. Hiermit hat der Autor einen neuen Weg in der Hydraulik eröffnet, namentlich die Normung der Berechnung der nicht permanenten Wasserbewegungen, ihre Vereinfachung und Mechanisierung. Die Uneigennützigkeit des Verfassers bezeugt der Umstand, daß er im Buch zahlreiche, vollständige Programme angibt, die unmittelbar abgeschrieben werden können und die vielerorts noch als Amtsgeheimnisse behandelt werden.

Die in Buchform erfolgte Veröffentlichung solcher, detaillierter Programme, die sofort kopiert werden können, ist heute noch ungewohnt. Der Autor wollte auch hiermit die Lösung zahlreicher hydraulischer Aufgaben mit Hilfe von Rechenautomaten und die raschere Verbreitung solcher Verfahren fördern.

Hinsichtlich der hydraulischen Berechnungen ist es ein langentbehrtes Werk, das sowohl Forscher, als auch praktisch tätige Ingenieure gut gebrauchen können. Einen besonderen Vorteil bietet das Buch dadurch, daß es auch zu Lehrzwecken geeignet ist.

J. Bogárdi

László Rétházi

GRUNDWASSER IM TIEFBAU

In der ungarischen Fachliteratur ist dies das erste Buch, welches die technischen und wirtschaftlichen Probleme des Grundwassers in allen seinen Zusammenhänge ausführlich umfaßt. Es handelt sich nicht um "technische Literatur", denn dieses Buch kann nicht nur von den Fachleuten des Tiefbaus, sondern auch von denselben der Geologie, Hydrologie, Meteorologie, und auch der Landwirtschaftskunde mit Erfolg entweder als Sammlung von Informationsbelegen und Richtlinien für eine Methodologie oder zu deren wissenschaftlichen Forschungen, sowie zur Lösung ihrer praktischen Aufgaben benutzt werden. Dies soll zugleich ein Hinweis darauf sein, daß dieses Werk auch die Forschungsergebnisse aller zugeordneten Disziplinen (der anderen Wissenschaftszweigen wie Physik, Chemie, Mathematik, usw. miteinbegriffen), die mit dem Auftreten des Grundwassers, mit seinem Vorkommen, seinen Eigenschaften und mit seiner Behandelbarkeit in Beziehung gebracht und in diesem Zusammenhang verwertet werden können.

In einem Sonderabschnitt beschreibt der Autor die mathematischen Methoden, mit deren Hilfe die mit Beobachtungen und Datenmengen arbeitende semiempirische Geophydrologie erfolgreiche Voraussagen machen kann. Dazu gehören der Bestand der Dichte- und Verteilungsfunktionen, die Aufstellung der stochastischen Zusammenhänge, wie auch die Untersuchung der Periodizität.

Dieses Werk ist eine Monographie, in welcher die Forschungsergebnisse der Verfasser der im Literaturverzeichnis angeführten 342 Abhandlungen und Bücher zu finden sind und wozu der Autor besondere Auswertungen, Grenzwerte und Feststellungen im Zusammenhang mit deren Zuverlässigkeit hinzufügt. Der Autor hat auch den Stoff seiner eigenen 26 Aufsätze benutzt, wodurch das Werk die eigenen technischen Erfahrungen und Kentnisse des Autors als des besten Fachmanns der Disziplin in Ungarn dem Leser mitteilt.

Das Werk gliedert sich in zwei Teile. Der erste Teil behandelt theoretische und methodische Probleme, während der zweite sich mit den praktischen Fragen beschäftigt. Diese beiden Teile sind im Verhältnis zueinander und die einzigen Abschnitte untereinander harmonisch proportional aufgebaut. Die Abfassung ist nicht wortreich, sondern klar und folgerichtig. Die Abbildungen erklären in entsprechender Zahl und mit gehöriger Kraft den Text, und die in dem Anhang von 20 Seiten zusammengestellten Tabellen beeinsträchtigen in keiner Weise die Lesbarkeit.

Der erste Teil enthält die folgenden Kapitel: die Entstehung und Klassifikation der Grundwasser; die physischen, chemischen und biologischen Kennwerte des Grundwassers;

Wärme- und Wasserhaushalt und Kapillarität der oberen Bodenschicht; die atmosphärischen Erscheinungen, der Niederschlag, die Verdunstung; die räumlichen und zeitlichen Änderungen des Grundwasserstandes; die Voraussage des Grundwasserstandes und der damit zusammenhängende mathematische Apparat.

Der Inhalt des zweiten Teils ist: die Vorbereitung der Tiefbauarbeiten; Aufklärung der Grundwasserverhältnisse; Wirkung der natürlichen und künstlichen Faktoren (der Wasserläufe, Verhältnisse der Geländeobefläche, der technischen Einwirkungen, usw.); Ermittelung der Grenzwerte des Grundwasserstandes; der Wasserentzug und die Lösungen von weiteren Tiefbauproblemen; Analyse von Gebäudeschäden.

Zusammenfassend kann festgestellt werden daß das Werk eine Menge von während eines Lebens angehäuften gründlichen Kentnissen eines hochgebildeten Wissenschaftlers enthält.

H. Héjj

G. Franz (Schriftleiter):

BETON-KALENDER 1978

TASCHENBUCH FÜR BETON- ,STAHLBETON- UND SPANNBETONBAU, SOWIE DIE VERWANDTEN FÄCHER

Verlag von Wilhelm Ernst u. Sohn, Berlin—München—Düsseldorf 1978

Der BETON-KALENDER das zweibändige Standardwerk des Betonbaues steht nun in seiner 67. Auflage den Experten des Faches zur Verfügung.

Der erste Band des Werkes besteht aus 12 Kapiteln in einem Umfang von 1165 Seiten. Diese befassen sich unter anderen eingehend mit den Eigenschaften der Stahlbetongrundstoffe (Prof. J. Bonzel, W. Schumacher), mit dem Kräftespiel der drei- und vierseitig gelagerten Rechteckplatten (Prof. F. Czerny), mit den wichtigen Aufgaben der Festigkeitslehre im Ingenieur-Bauwesen (Prof. N. Dimitrov), mit der Statik der Stabtragwerke (H. Ahrens, Prof. H. Duddeck), mit den gültigen Bemessungsnormen der Stahlbetonkonstruktionen. (E. Grasser), mit den Bemessungsproblemen der Stahlbetonbauteile (Prof. K. Kordina, Prof. U. Quast), sowie mit dem Problem der Spannbetonkonstruktionen (Prof. H. Rüsch, Prof. H. Kupfer).

Der zweite Band enthält 1006 Seiten, deren Hälfte ungefähr über die in der BRD gültigen Bestimmungen und Normen eingehend berichtet (H. Goffin). Sehr gründlich wird die Berechnung der Bauteile mit zweiachsigen Spannungszustand (Scheiben) (W. Schleeh), sowie die Fragen des Betonstraßenbaues behandelt (J. Schlums, Prof. D. Schwär).

In der neuen Ausgabe wurden die aus den vorigen übernommenen Kapitel vollständig umgearbeitet. Das war besonders von dem Umstand begründet, daß ab 1. Jänner 1978 in der BRD anstatt der früheren Messeinheiten das neue SI-Mess-System eingeführt wurde, und infolge dessen auch die Benennung einiger Baustoffe sich änderte.

Im Vorwort des Buches wird ein schönes Andenken dem unlängst im Alter von 88 Jahren verstorbenen Prof. E. Rausch gestellt und auch dessen ungarische Herkunft erwähnt (hervorragender Autor des Kapitels »Maschinenfundamente«). In der neuen Ausgabe wurde dieser Problemenkreis (F. P. Müller) mit den Bemessungsfragen der Baudynamik erweitert. Neu ist weiterhin das Kapitel, welches die Niederländischen Stahlbetonbestimmungen weitgehend behandelt (W. Hof).

Diesen reichen und abwechslungsvollen Stoff des Taschenbuches überblickend ist eindeutig festzustellen, daß der bekannte Redaktor Prof. G. Franz die sich gut bewährte Tradition treu bewahrt hat: die neue Ausgabe — den bisherigen ähnlich — den Interessen des Betonbaues vorzüglich dient, und als solche, auch weitaus über die Landesgrenzen, eine bedeutende Hilfe für die Fachkreise sein wird.

P. Csonka

A. Mälmeisters, V. Tamuzs, G. Teters

MECHANIK DER POLYMERWERKSTOFFE

Akademie-Verlag, Berlin, 1977, 597 Seiten

Die rasche Entwicklung der chemischen Industrie ermöglicht die massenhafte und verhältnismäßig billige Herstellung von Kunststoffen verschiedenster Eigenschaften. Diese Stoffe können aber in der Maschinen-, Fahrzeug- und Bauindustie nur dann Anwendung finden, wenn genügende und verläßliche Theorien und Verfahren zur Beschreibung der Festigkeitseigenschaften dieser Stoffe und des mechanischen Verhaltens der aus diesen angefertigten Konstruktionen und Bestandteilen zur Verfügung stehen.

Bekanntlich weichen die Festigkeitseigenschaften der Kunststoffe wesentlich von jenen der herkömmlichen Stoffe ab. Die Kunststoffe sind im allgemeinen anisotrop, auf Temperaturänderungen sehr empfindlich, ihre Schubsteifigkeit ist gering und sie neigen sehr zu bedeutenden plastischen und viskosen Formänderungen. Daher eignen sich die herkömmlichen Theorien der Mechanik nicht zur Untersuchung von, aus Kunststoffen hergestellten Konstruktionen. Statt denen sind solche allgemein gültige Theorien erforderlich, die auch die erwähnten besonderen Eigenschaften der Kunststoffe in Betracht zu ziehen geeignet sind.

Der großen technischen und wirtschaftlichen Bedeutung der Kunststoffe entsprechend nimmt die Anzahl der Werke und Aufsätze, die ihr mechanisches Verhalten behandeln, laufend zu. Die von A. Mälmeisters, V. Tamuzs und G. Teters 1972 in russischer Sprache verfaßte und 1977 auch in deutscher Übersetzung erschienene Monographie ist von besonderer Bedeutung. In diesem Werk veröffentlichen die Autoren in einer einheitlichen Form die zur Untersuchung von Kunststoffkonstruktionen geeigneten Theorien und Berechnungsverfahren und führen diese, an der Lösung von zahlreichen Beispielen der Ingenieurpraxis vor. Das Werk enthält die folgenden wichtigsten Kapitel: Beschreibung des Spannungs- und Formänderungszustandes; Zusammenhang zwischen Spannungen und Formänderungen bei elastischen Körpern; Stoffe mit rheologischen Eigenschaften; Plastische Körper; Bruchtheorien; Steifigkeits- und Stabilitätsuntersuchungen von Stäben, Platten und Schalen.

Wie aus obiger Aufzählung ersichtlich, behandelt das Buch von den Grundbegriffen angefangen alle wichtigeren Theorien der Festigkeitslehre; befaßt sich besonders mit der Wirkung der durch Temperaturänderung und Schub verursachten Formänderungen, ferner mit den viskosen, plastischen und nicht linear elastische Stoffen, da diese Fragen im Zusammenhang mit Kunststoffkonstruktionen von grundlegender Bedeutung sind. Für die Praxis sind besonders die beiden letzten Kapitel interessant, weil sie anhand der Lösung zahlreicher Beispiele aufzeigen, in welcher Weise die angeführten besonderen Wirkungen und Materialeigenschaften der Kunststoffe bei den Festigkeits-, Steifigkeits- und Stabilitätsuntersuchungen von Stäben, Balken, Platten und Schalen in Rechnung zu Stellen sind.

Die Verfasser behandeln den Stoff auf einem hohen theoretischen Niveau in einheitlicher, übersichtlicher Form, wo sie mit Indizes versehene Tensorzeichen verwenden. Die verschiedenen Aufgaben sind analytisch gelöst, die Möglichkeit der Anwendung numerischer Methoden ist nicht erwähnt. Die in Literaturverzeichnis angeführten 350 Bücher und Abhandlungen sind vornehmlich der sowjetischen Fachliteratur entnommen und bieten eine vorteilhafte Übersicht der erzielten wissenschaftlichen Ergebnisse.

Das in theoretischer und didaktischer Beziehung gleichermaßen vorzüglich verfaßte Werk von A. Mälmeisters, V. Tamuzs und G. Teters befriedigt vor allem die auf den neuen Gebieten der Festigkeitslehre tätigen Forscher, Lehrer, sowie die Hörer postgradualer Fortbildungskurse, doch bietet es auch den in der Industrie und in Konstruktionsbüros tätigen Technologen und Konstrukteuren wertvolle Hilfe.

S. Kaliszky

Stiller, Th.

GROSSE FORSCHER UND ERFINDER. LEBEN UND WERK

SCHÄTZE IM DEUTSCHEN MUSEUM

VDI Verlag — Verlag des Vereines Deutscher Ingenieure. Düsseldorf 1978

Unlängst wurde die 75. Jahreswende der Gründung des Münchener Deutschen Museums, eines der ältesten und reichsten fachgeschichtlichen Museen der Welt, gefeiert. Anläßlich dieser Feier hat die Direktion in neuer und schmucker Ausstellung den Band erscheinen lassen, welcher das dort aufbewahrte, äußerst wertvolle Gedenkmaterial demonstriert.

Dieses Werk enthält das Porträt, die kurze Beschreibung des Lebens und Lebenswerkes von 77 ausgezeichneten Wissenschaftlern, deren bedeutendstes Werk im Museum bewahrt blieb. Unter diesen werden erwähnt NEWTON, LEIBNIZ, BERNOULLI, EULER, EINSTEIN, HEISENBERG und unter den berühmten Erfindern WATT, STEPHENSON, SIEMENS, EDISON und unter den berühmten Erfindern WATT, STEPHENSBON, SIEMENS, EDISON und die Brüder WRIGHT. Jedem Forscher, resp. Erfinder werden im Buch nur je zwei Seiten gewidmet, und auch deren großer Teil ist vom Bildmaterial besetzt. Infolgedessen sind die Textteile, die über die einzelnen Gelehrten berichten, äußerst kurz gefaßt, doch zeigen sie sehr treffend und überzeugend ihre Tätigkeit und ihre Bedeutung.

Das Werk ist durch sein reiches und schönes Bildmaterial, sowie durch seinen wertvollen Inhalt eine besonders interessante Lektüre und zugleich auch ein schöner Beweis von dem außerordentlich wertvollen und reichen Gedenkmaterial, das im Deutschen Museum bewahrt blieb.

P. Csonka

INDEX

Printed in Hungary

A kiadásért felel az Akadémiai Kiadó igazgatója — Műszaki szerkesztő: Zacsik Annamária
A kézirat nyomdába érkezett: 1978. V. 9. — Terjedelem: 21,70 (A/5) ív, 74 ábra (1 melléklet)

79.5848 Akadémiai Nyomda, Budapest — Felelős vezető: Bernát György

Acta Techn. Hung. **86** (1978), pp. 237—269

POLINSZKY et al.: *A Logic Theory of Hazards and its Application to Combustion Processes*

The aim of the present paper is to introduce a theory of hazards, and an actual application thereof. This theory describes the idea of hazards by logic rather than by an algebraic quantity. The introduction informs on how to model the hazards of any actually operating plant. As an application of the theory of hazards, a study on combustion processes using the method of stationary thermal conditons will be described. Then, on this basis the coefficients of combustion process hazards are determined. With these factors known, the hazards of all the elementary events feasible in the area associated with the combustion processes will be theoretically calculated, by taking into full account the preconditons of hazards.

Acta Techn. Hung. **86** (1978), pp. 271—285

BARTA, J.: *Survey of Some Variational Theorems in Elastostatics*

Variational theorems will be examined to show whether these are minimal theorems at the same time. The proofs will be carried out by applying the influence numbers as is usual in the theory of structures. A numerically elaborated example elucidates the application of the different theorems.

Acta Techn. Hung. **86** (1978), pp. 287—300

WEBER, J.—LEOPOLD, J.: *An Investigation of Chip Forming Based on the Theory of Elasticity*

The paper presents a model for calculating the stresses on the cutting surface of a cutting tool based on the theory of sliding lines. The sliding line fields known since LEE and SHAFFER, are extended ad for the coefficient of friction, the possible chip angle and a realistic cutting edge radius. Some results of numerical calculations are discussed; they show the great influence of the cutting edge radius on the stress distribution.

Acta Techn. Hung. **86** (1978), pp. 301—316

KALINSZKY, S.: *Simple, Discrete Models of the Elastic Subgrade*

Paper presents the pyramid and the shear models of subgrade which both can be used for the numerical analysis of elastically supported structures and the subgrade, as well. Containing two independent parameters the shear model is quite general, since as special cases the Winkler—Zimmermann and the pyramid models are also included in it. The application of the two discrete models is illustrated by a numerical example.

Acta Techn. Hung. **86** (1978), pp. 317—329

HUSZTHY, K.: *Remarks on the Calculation of the Tooth Friction Losses of Gears*

Numerous books and papers have dealt with the tooth friction losses of gear pairs. In the basically equivalent formulae deduced by different authors the coefficient of friction is a mean value determined by some experiment. The present paper aims at a more accurate definition of the "mean" friction coefficient and at clarifying the conditions under which the relation for tooth friction are valid.

Acta Techn. Hung. **86** (1978), pp. 331—362

TEVAN, GY.—TÓTH, F.: *A Clear Algorithm for the Calculation of the Linear Induction Motor, Based on Field Theory*

The authors discuss an (approximate) algorithm based on "field theory" consisting of relatively simple formulae for calculating the linear induction motor, which takes into account the skin effect, the transversal and longitudinal effects and the connection between excitation and winding. It creates the connection with the equivalent circuits of the traditional induction motor, neglects the excitation of the primary iron body and the harmonics of the whole order of the travelling field, but describes the longitudinal effect by two undamped field harmonic waves of fractional order. The calculations are compared with measurements carried out on a stationary motor and finally characteristics of linear motors are calculated with the method presented.

Acta Techn. Hung. **86** (1978), pp. 363—394

FERENCZ, CS.: *Electromagnetic Wave Propagation in Inhomogeneous Media: The Analysis of the Rotation of Polarization, and the Application of the Principle of Modified Ray Tracing Part. I.*

The propagation of monochromatic electromagnetic waves in inhomogeneous media is investigated using the "method of inhomogeneous basic modes" and the "principle of modified ray tracing". Several basic facts are obtained for the propagation in inhomogeneous media. The basic aim of the author is to explain the "W"-shape transients observed during the solar occultations of Pioneer-6 and -9 space probes. After explaining the method of investigation, in the first part, the investigations of propagation in inhomogeneous media are given in detail. In Part II, after examining the propagation is anisotopic media the "W" polarisation transient is explained and the results of the investigations are summarized. It is shown that in inhomogeneous media besides the known Faraday rotation an "inhomogeneous polarisation-rotation" also occurs. This necessarily causes "W" shape polarisation transients at the time of solar occultations. Thus, new ways for investigating the structure of the front of spreading interplanetary phenomena" are opened up.

Acta Techn. Hung. **86** (1978), pp. 395—400

SCHARLE, P.: *An Example for Constructing the Variational (Energetic) Error Principle*

The paper presents a less simple example for constructing the variational error functional, the idea of which was outlined previously. Starting from the governing equations of the elasticity with nonhomogeneous boundary conditions it constructs the equivalent energy expression, which proves to be the well-known form of the potential energy.

Acta Techn. Hung. **86** (1978), pp. 401—409

ECSEDI, I.: *On the Estimation of tde Torsional Rigidity of Prismatic Bars*

By making use of the inequalities deduced in the present paper, lower and upper limits may be produced for the numerical values of the torsional rigidity of prismatic bars of solid cross section and of homogeneous material.

Acta Techn. Hung. **86** (1978), pp. 411—420

PERHŐ, SZ.—ORTUTAY, M.: *The Evaluation of the Separation Operations*

The authors have examined the efficiency of the two-constituent separation. As the extreme case of separation they consider the diminuation of the specimen and the absolutely efficient separation. Relations are established for calculating the separation efficiency. Several separation operations can be evaluated by the efficiency indexes even, if the separation parameters and the mass yields are different.

Acta Techn. Hung. **86** (1978), pp. 421—464

TASSI, G.: *Analytical Treatment of Discrete Models for Reinforced and Prestressed Concrete Members*

A one-dimensional model of reinforced and prestressed concrete members, composed of elements simulating the concrete, the steel and their bond has been analyzed. Analytic treatment of the equation system for the discrete model is facilitated by the possibility to invert in closed from the coefficient matrix of the system. Craks are taken into consideration by modifying the coefficient matrix by one diade for each. Also a method for reckoning with plastic deformations will be outlined. The obtained closed formulae show how this phenomenon related to cracking develops for one, two or more cracks. — Applicability of the relationships is demonstrated by examples. Formulae of internal forces, deformations and crack width involving also the mesh of the discrete model, the effect of selecting the mesh can be weighed.

The *Acta Technica* publish papers on technical subjects in English, French, German and Russian.

The *Acta Technica* appear in parts of varying size, making up one volume.

Manuscripts should be addressed to

Acta Technica
H-1051 Budapest
Münnich Ferenc u. 7.
Hungary

Correspondence with the editors and publishers should be sent to the same address.

Subscription rate: $ 36.00 a volume.

Orders may be placed with "Kultura" Foreign Trading Company (H-1389 Budapest 62, P. O. B. 149. Account No. 218-10990) or its representatives abroad.

Les *Acta Technica* paraissent en français, allemand, anglais et russe et publient des travaux du domaine des sciences techniques.

Les *Acta Technica* sont publiés sous forme de fascicules qui seront réunis en volumes.

On est prié d'envoyer les manuscrits destinés à la rédaction à l'adresse suivante:

Acta Technica
H-1051 Budapest
Münnich Ferenc u. 7.
Hongrie

Toute correspondance doit être envoyée à cette même adresse.

Le prix de l'abonnement: $ 36.00 par volume.

On peut s'abonner à l'Entreprise du Commerce Extérieur «Kultura» (H-1389 Budapest 62, P. O. B. 149. Compte courant No. 218-10990) on chez représentants à l'étranger.

«*Acta Technica*» публикуют трактаты из области технических наук на русском, не ецком, английском и французском языках.

«*Acta Technica*» выходяг отдельными выпусками разного объема. Несколько выпусков составляют один том.

Предназначенные для публикации рускописи следует направлять по адресу:

Acta Technica
H-1051 Budapest
Münnich Ferenc u. 7.
Венгрия

По этому же адресу направлять всякую корреспонденцию для редакции и администрации.

Подписная цена — $ 36.00 за том. Заказы принимает предприятие по внешней торговле «Kultura» (H-1389 Budapest 62, P. O. B. 149 Текущий счет № 218-10990) или его заграничные представительства и уполномоченные.

Reviews of the Hungarian Academy of Sciences are obtainable at the following addresses:

AUSTRALIA
C.B.D. LIBRARY AND SUBSCRIPTION SERVICE, Box 4886, G.P.O., *Sydney N.S.W. 2001*
COSMOS BOOKSHOP, 135 Ackland Street, *St. Kilda (Melbourne), Victoria 3182*

AUSTRIA
GLOBUS, Höchstädtplatz 4, *1200 Wien* XX

BELGIUM
OFFICE INTERNATIONAL DE LIBRAIRIE, 30 Avenue Marnix, *1050 Bruxelles*
LIBRAIRIE DU MONDE ENTIER, 162 Rue du Midi, *1000 Bruxelles*

BULGARIA
HEMUS, Bulvar Ruszki 6, *Sofia*

CANADA
PANNONIA BOOKS, P.O. Box 1017, Postal Station "B", *Toronto, Ontario M5T 2T8*

CHINA
CNPICOR, Periodical Department, P.O. Box 50, *Peking*

CZECHOSLOVAKIA
MAD'ARSKÁ KULTURA, Národní třida 22, *115 66 Praha*
PNS DOVOZ TISKU, Vinohradská 46, *Praha 2*
PNS DOVOZ TLAČE, *Bratislava 2*

DENMARK
EJNAR MUNKSGAARD, Norregade 6, *1165 Copenhagen*

FINLAND
AKATEEMINEN KIRJAKAUPPA, P.O. Box 128, *SF-00101 Helsinki 10*

FRANCE
EUROPERIODIQUES S. A., 31 Avenue de Versailles, *78170 La Celle St. Cloud*
LIBRAIRIE LAVOISIER, 11 rue Lavoisier, *75008 Paris*
OFFICE INTERNATIONAL DE DOCUMENTATION ET LIBRAIRIE, 38 rue Gay-Lussac, *75240 Paris Cedex 05*

GERMAN DEMOCRATIC REPUBLIC
HAUS DER UNGARISCHEN KULTUR, Karl-Liebknecht-Strasse 9, *DDR-102 Berlin*
DEUTSCHE POST ZEITUNGSVERTRIEBSAMT, Strasse der Pariser Kommüne 3—4, *DDR-104 Berlin*

GERMAN FEDERAL REPUBLIC
KUNST UND WISSEN ERICH BIEBER, Postfach 46, *7000 Stuttgart 1*

GREAT BRITAIN
BLACKWELL'S PERIODICALS DIVISION, Hythe Bridge Street, *Oxford OX1 2ET*
BUMPUS, HALDANE AND MAXWELL LTD., Cower Works, *Olney, Bucks MK46 4BN*
COLLET'S HOLDINGS LTD., Denington Estate, *Wellingborough, Northants NN8 2QT*
W.M. DAWSON AND SONS LTD., Cannon House, *Folkestone, Kent CT19 5EE*
H. K. LEWIS AND CO., 136 Gower Street, *London WCIE 6BS*

GREECE
KOSTARAKIS BROTHERS, International Booksellers, 2 Hippokratous Street, *Athens-143*

HOLLAND
MEULENHOFF-BRUNA B.V., Beulingstraat 2, *Amsterdam*
MARTINUS NIJHOFF B.V., Lange Voorhout 9—11, *Den Haag*
SWETS SUBSCRIPTION SERVICE, 347b Heereweg, *Lisse*

INDIA
ALLIED PUBLISHING PRIVATE LTD., 13/14 Asaf Ali Road, *New Delhi 110001*
150 B-6 Mount Road, *Madras 600002*
INTERNATIONAL BOOK HOUSE PVT. LTD Madame Cama Road, *Bombay 400039*
THE STATE TRADING CORPORATION OF INDIA LTD., Books Import Division, Chandralok 36 Janpath, *New Delhi 110001*

ITALY
EUGENIO CARLUCCI, P.O. Box 252, *70100 Bari*
INTERSCIENTIA, Via Mazzé 28, *10149 Torino*
LIBRERIA COMMISSIONARIA SANSONI, Via Lamarmora 45, *50121 Firenze*
SANTO VANASIA, Via M. Macchi 58, *20124 Milano*
D. E. A., Via Lima 28, *00198 Roma*

JAPAN
KINOKUNIYA BOOK-STORE CO. LTD., 17-7 Shinjuku-ku 3 chome, Shinjuku-ku, *Tokyo 160-91*
MARUZEN COMPANY LTD., Book Department, P.O. Box 5056 Tokyo International, *Tokyo 100-31*
NAUKA LTD. IMPORT DEPARTMENT, 2-30 19 Minami Ikebukuro, Toshima-ku, *Tokyo 171*

KOREA
CHULPANMUL, *Phenjan*

NORWAY
TANUM-CAMMERMEYER, Karl Johansgatan 41—43, *1000 Oslo*

POLAND
WĘGIERSKI INSTYTUT KULTURY, Marszałkowska 80, *Warszawa*
CKP I W ul. Towarowa 28 *00-958 Warsaw*

ROMANIA
D. E. P., *Bucureşti*
ROMLIBRI, Str. Biserica Amzei 7, *Bucureşti*

SOVIET UNION
SOJUZPETCHATJ — IMPORT, *Moscow*
and the post offices in each town
MEZHDUNARODNAYA KNIGA, *Moscow G-200*

SPAIN
DIAZ DE SANTOS, Lagasca 95, *Madrid 6*

SWEDEN
ALMQVIST AND WIKSELL, Gamla Brogatan 26, *101 20 Stockholm*
GUMPERTS UNIVERSITETSBOKHANDEL AB Box 346, *401 25 Göteborg 1*

SWITZERLAND
KARGER LIBRI AG, Petersgraben 31, *4011 Basel*

USA
EBSCO SUBSCRIPTION SERVICES, P.O. Box 1943, *Birmingham, Alabama 65201*
F. W. FAXON COMPANY, INC., 15 Southwest Park, *Westwood, Mass, 02090*
THE MOORE-COTTRELL SUBSCRIPTION AGENCIES, *North Cohocton, N. Y. 14838*
READ-MORE PUBLICATIONS, INC., 140 Cedar Street, *New York, N. Y. 10003*
STECHERT-MACMILLAN, INC., 7250 Westfield Avenue, *Pennsauken* N. J. 08110

VIETNAM
XUNHASABA, 32, Hai Ba Trung, *Hanoi*

YUGOSLAVIA
JUGOSLAVENSKA KNJIGA, Terazije 27, *Beograd*
FORUM, Vojvode Mišića 11, *21000 Novi Sad*

15. III. 1979 HU ISSN 0001—7035 Index: 26.025